ISSN 1007-9327 (print)
ISSN 2219-2840 (online)

World Journal of *Gastroenterology*

World J Gastroenterol 2016 May 28; 22(20): 4789-4962

Published by Baishideng Publishing Group Inc

World Journal of Gastroenterology

A peer-reviewed, online, open-access journal of gastroenterology and hepatology

Editorial Board

2014-2017

The *World Journal of Gastroenterology* Editorial Board consists of 1376 members, representing a team of worldwide experts in gastroenterology and hepatology. They are from 68 countries, including Algeria (2), Argentina (7), Australia (31), Austria (9), Belgium (11), Brazil (20), Brunei Darussalam (1), Bulgaria (2), Cambodia (1), Canada (26), Chile (4), China (164), Croatia (2), Cuba (1), Czech (6), Denmark (2), Egypt (9), Estonia (2), Finland (6), France (20), Germany (58), Greece (31), Guatemala (1), Hungary (15), Iceland (1), India (33), Indonesia (2), Iran (10), Ireland (9), Israel (18), Italy (194), Japan (149), Jordan (1), Kuwait (1), Lebanon (7), Lithuania (1), Malaysia (1), Mexico (11), Morocco (1), Netherlands (5), New Zealand (4), Nigeria (3), Norway (6), Pakistan (6), Poland (12), Portugal (8), Puerto Rico (1), Qatar (1), Romania (10), Russia (3), Saudi Arabia (2), Singapore (7), Slovenia (2), South Africa (1), South Korea (69), Spain (51), Sri Lanka (1), Sudan (1), Sweden (12), Switzerland (5), Thailand (7), Trinidad and Tobago (1), Tunisia (2), Turkey (55), United Kingdom (49), United States (180), Venezuela (1), and Vietnam (1).

Gordon Stanley Howarth, *Roseworthy*
Seungha Kang, *Brisbane*
Alfred King Lam, *Gold Coast*
Ian C Lawrance, *PerthFremantle*
Barbara Anne Leggett, *Brisbane*
Daniel A Lemberg, *Sydney*
Rupert W Leong, *Sydney*
Finlay A Macrae, *Victoria*
Vance Matthews, *Melbourne*
David L Morris, *Sydney*
Reme Mountifield, *Bedford Park*
Hans J Netter, *Melbourne*
Nam Q Nguyen, *Adelaide*
Liang Qiao, *Westmead*
Rajvinder Singh, *Adelaide*
Ross Cyril Smith, *StLeonards*
Kevin J Spring, *Sydney*
Debbie Trinder, *Fremantle*
Daniel R van Langenberg, *Box Hill*
David Ian Watson, *Adelaide*
Desmond Yip, *Garran*
Li Zhang, *Sydney*

Austria

Felix Aigner, *Innsbruck*
Gabriela A Berlakovich, *Vienna*
Herwig R Cerwenka, *Graz*
Peter Ferenci, *Wien*
Alfred Gangl, *Vienna*
Kurt Lenz, *Linz*
Markus Peck-Radosavljevic, *Vienna*
Markus Raderer, *Vienna*
Stefan Riss, *Vienna*

Belgium

Michael George Adler, *Brussels*
Benedicte Y De Winter, *Antwerp*
Mark De Ridder, *Jette*
Olivier Detry, *Liege*
Denis Dufrane Dufrane, *Brussels*
Sven M Francque, *Edegem*
Nikos Kotzampassakis, *Liège*
Geert KMM Robaeys, *Genk*
Xavier Sagaert, *Leuven*
Peter Starkel, *Brussels*
Eddie Wisse, *Keerbergen*

Brazil

SMP Balzan, *Santa Cruz do Sul*
JLF Caboclo, *Sao jose do rio preto*
Fábio Guilherme Campos, *Sao Paulo*
Claudia RL Cardoso, *Rio de Janeiro*
Roberto J Carvalho-Filho, *Sao Paulo*
Carla Daltro, *Salvador*
José Sebastiao dos Santos, *Ribeirao Preto*
Eduardo LR Mello, *Rio de Janeiro*
Sthela Maria Murad-Regadas, *Fortaleza*
Claudia PMS Oliveira, *Sao Paulo*
Júlio C Pereira-Lima, *Porto Alegre*
Marcos V Perini, *Sao Paulo*
Vietla Satyanarayana Rao, *Fortaleza*
Raquel Rocha, *Salvador*
AC Simoes e Silva, *Belo Horizonte*
Mauricio F Silva, *Porto Alefre*
Aytan Miranda Sipahi, *Sao Paulo*
Rosa Leonôra Salerno Soares, *Niterói*
Cristiane Valle Tovo, *Porto Alegre*
Eduardo Garcia Vilela, *Belo Horizonte*

Brunei Darussalam

Vui Heng Chong, *Bandar Seri Begawan*

Bulgaria

Tanya Kirilova Kadiyska, *Sofia*
Mihaela Petrova, *Sofia*

Cambodia

Francois Rouet, *Phnom Penh*

Canada

Brian Bressler, *Vancouver*
Frank J Burczynski, *Winnipeg*
Wangxue Chen, *Ottawa*
Francesco Crea, *Vancouver*
Mirko Diksic, *Montreal*
Jane A Foster, *Hamilton*
Hugh J Freeman, *Vancouver*
Shahrokh M Ghobadloo, *Ottawa*
Yuewen Gong, *Winnipeg*
Philip H Gordon, *Quebec*
Rakesh Kumar, *Edmonton*
Wolfgang A Kunze, *Hamilton*
Patrick Labonte, *Laval*
Zhikang Peng, *Winnipeg*
Jayadev Raju, *Ottawa*
Maitreyi Raman, *Calgary*
Giada Sebastiani, *Montreal*
Maida J Sewitch, *Montreal*
Eldon A Shaffer, *Alberta*
Christopher W Teshima, *Edmonton*
Jean Sévigny, *Québec*
Pingchang Yang, *Hamilton*
Pingchang Yang, *Hamilton*
Eric M Yoshida, *Vancouver*
Bin Zheng, *Edmonton*

Chile

Marcelo A Beltran, *La Serena*
Flavio Nervi, *Santiago*
Adolfo Parra-Blanco, *Santiago*
Alejandro Soza, *Santiago*

China

Zhao-Xiang Bian, *Hong Kong*
San-Jun Cai, *Shanghai*
Guang-Wen Cao, *Shanghai*
Long Chen, *Nanjing*
Ru-Fu Chen, *Guangzhou*
George G Chen, *Hong Kong*
Li-Bo Chen, *Wuhan*
Jia-Xu Chen, *Beijing*
Hong-Song Chen, *Beijing*
Lin Chen, *Beijing*
Yang-Chao Chen, *Hong Kong*
Zhen Chen, *Shanghai*
Ying-Sheng Cheng, *Shanghai*
Kent-Man Chu, *Hong Kong*
Zhi-Jun Dai, *Xi'an*
Jing-Yu Deng, *Tianjin*
Yi-Qi Du, *Shanghai*
Zhi Du, *Tianjin*
Hani El-Nezami, *Hong Kong*
Bao-Ying Fei, *Hangzhou*
Chang-Ming Gao, *Nanjing*
Jian-Ping Gong, *Chongqing*
Zuo-Jiong Gong, *Wuhan*
Jing-Shan Gong, *Shenzhen*
Guo-Li Gu, *Beijing*
Yong-Song Guan, *Chengdu*
Mao-Lin Guo, *Luoyang*
Jun-Ming Guo, *Ningbo*
Yan-Mei Guo, *Shanghai*
Xiao-Zhong Guo, *Shenyang*
Guo-Hong Han, *Xi'an*
Ming-Liang He, *Hong Kong*
Peng Hou, *Xi'an*
Zhao-Hui Huang, *Wuxi*
Feng Ji, *Hangzhou*
Simon Law, *Hong Kong*
Yu-Yuan Li, *Guangzhou*
Meng-Sen Li, *Haikou*
Shu-De Li, *Shanghai*
Zong-Fang Li, *Xi'an*
Qing-Quan Li, *Shanghai*
Kang Li, *Lasa*
Han Liang, *Tianjin*
Xing'e Liu, *Hangzhou*
Zheng-Wen Liu, *Xi'an*
Xiao-Fang Liu, *Yantai*
Bin Liu, *Tianjin*
Quan-Da Liu, *Beijing*
Hai-Feng Liu, *Beijing*
Fei Liu, *Shanghai*
Ai-Guo Lu, *Shanghai*
He-Sheng Luo, *Wuhan*
Xiao-Peng Ma, *Shanghai*
Yong Meng, *Shantou*
Ke-Jun Nan, *Xi'an*
Siew Chien Ng, *Hong Kong*
Simon SM Ng, *Hong Kong*
Zhao-Shan Niu, *Qingdao*
Di Qu, *Shanghai*
Ju-Wei Mu, *Beijing*
Rui-Hua Shi, *Nanjing*
Bao-Min Shi, *Shanghai*
Xiao-Dong Sun, *Hangzhou*
Si-Yu Sun, *Shenyang*
Guang-Hong Tan, *Haikou*
Wen-Fu Tang, *Chengdu*
Anthony YB Teoh, *Hong Kong*
Wei-Dong Tong, *Chongqing*
Eric Tse, *Hong Kong*
Hong Tu, *Shanghai*

Stavros Gourgiotis, *Athens*
Leontios J Hadjileontiadis, *Thessaloniki*
Thomas Hyphantis, *Ioannina*
Ioannis Kanellos, *Thessaloniki*
Stylianos Karatapanis, *Rhodes*
Michael Koutsilieris, *Athens*
Spiros D Ladas, *Athens*
Theodoros K Liakakos, *Athens*
Emanuel K Manesis, *Athens*
Spilios Manolakopoulos, *Athens*
Gerassimos John Mantzaris, *Athens*
Athanasios D Marinis, *Piraeus*
Nikolaos Ioannis Nikiteas, *Athens*
Konstantinos X Papamichael, *Athens*
George Sgourakis, *Athens*
Konstantinos C Thomopoulos, *Patras*
Konstantinos Triantafyllou, *Athens*
Christos Triantos, *Patras*
Georgios Zacharakis, *Athens*
Petros Zezos, *Alexandroupolis*
Demosthenes E Ziogas, *Ioannina*

Guatemala

Carlos Maria Parellada, *Guatemala*

Hungary

Mihaly Boros, *Szeged*
Tamás Decsi, *Pécs*
Gyula Farkas, *Szeged*
Andrea Furka, *Debrecen*
Y vette Mandi, *Szeged*
Peter L Lakatos, *Budapest*
Pal Miheller, *Budapest*
Tamás Molnar, *Szeged*
Attila Olah, *Gyor*
Maria Papp, *Debrecen*
Zoltan Rakonczay, *Szeged*
Ferenc Sipos, *Budapest*
Miklós Tanyi, *Debrecen*
Tibor Wittmann, *Szeged*

Iceland

Tryggvi Bjorn Stefánsson, *Reykjavík*

Indiad

Brij B Agarwal, *New Delhi*
Deepak N Amarapurkar, *Mumbai*
Shams ul Bari, *Srinagar*
Sriparna Basu, *Varanasi*
Runu Chakravarty, *Kolkata*
Devendra C Desai, *Mumbai*
Nutan D Desai, *Mumbai*
Suneela Sunil Dhaneshwar, *Pune*
Radha K Dhiman, *Chandigarh*
Pankaj Garg, *Mohali*
Uday C Ghoshal, *Lucknow*
Kalpesh Jani, *Vadodara*
Premashis Kar, *New Delhi*
Jyotdeep Kaur, *Chandigarh*
Rakesh Kochhar, *Chandigarh*
Pradyumna K Mishra, *Mumbai*
Asish K Mukhopadhyay, *Kolkata*
Imtiyaz Murtaza, *Srinagar*
P Nagarajan, *New Delhi*
Samiran Nundy, *Delhi*
Gopal Pande, *Hyderabad*
Benjamin Perakath, *Vellore*
Arun Prasad, *New Delhi*
D Nageshwar Reddy, *Hyderabad*
Lekha Saha, *Chandigarh*
Sundeep Singh Saluja, *New Delhi*
Mahesh Prakash Sharma, *New Delhi*
Sadiq Saleem Sikora, *Bangalore*
Sarman Singh, *New Delhi*
Rajeev Sinha, *Jhansi*
Rupjyoti Talukdar, *Hyderabad*
Rakesh Kumar Tandon, *New Delhi*
Narayanan Thirumoorthy, *Coimbatore*

Indonesia

David Handojo Muljono, *Jakarta*
Andi Utama, *Jakarta*

Iran

Arezoo Aghakhani, *Tehran*
Seyed Mohsen Dehghani, *Shiraz*
Ahad Eshraghian, *Shiraz*
Hossein Khedmat, *Tehran*
Sadegh Massarrat, *Tehran*
Marjan Mohammadi, *Tehran*
Roja Rahimi, *Tehran*
Farzaneh Sabahi, *Tehran*
Majid Sadeghizadeh, *Tehran*
Farideh Siavoshi, *Tehran*

Ireland

Gary Alan Bass, *Dublin*
David J Brayden, *Dublin*
Ronan A Cahill, *Dublin*
Glen A Doherty, *Dublin*
Liam J Fanning, *Cork*
Barry Philip McMahon, *Dublin*
RossMcManus, *Dublin*
Dervla O'Malley, *Cork*
Sinead M Smith, *Dublin*

Israel

Dan Carter, *Ramat Gan*
Jorge-Shmuel Delgado, *Metar*
Eli Magen, *Ashdod*
Nitsan Maharshak, *Tel Aviv*
Shaul Mordechai, *Beer Sheva*
Menachem Moshkowitz, *Tel Aviv*
William Bahij Nseir, *Nazareth*
Shimon Reif, *Jerusalem*
Ram Reifen, *Rehovot*
Ariella Bar-Gil Shitrit, *Jerusalem*
Noam Shussman, *Jerusalem*
Igor Sukhotnik, *Haifa*
Nir Wasserberg, *Petach Tiqwa*
Jacob Yahav, *Rehovot*
Doron Levi Zamir, *Gedera*
Shira Zelber-Sagi, *Haifa*
Romy Zemel, *Petach-Tikva*

Italy

Ludovico Abenavoli, *Catanzaro*
Luigi Elio Adinolfi, *Naples*
Carlo Virginio Agostoni, *Milan*
Anna Alisi, *Rome*
Piero Luigi Almasio, *Palermo*
Donato Francesco Altomare, *Bari*
Amedeo Amedei, *Florence*
Pietro Andreone, *Bologna*
Imerio Angriman, *Padova*
Vito Annese, *Florence*
Paolo Aurello, *Rome*
Salavtore Auricchio, *Naples*
Gian Luca Baiocchi, *Brescia*
Gianpaolo Balzano, *Milan*
Antonio Basoli, *Rome*
Gabrio Bassotti, *San Sisto*
Mauro Bernardi, *Bologna*
Alberto Biondi, *Rome*
Ennio Biscaldi, *Genova*
Massimo Bolognesi, *Padua*
Luigi Bonavina, *Milano*
Aldo Bove, *Chieti*
Raffaele Bruno, *Pavia*
Luigi Brusciano, *Napoli*
Giuseppe Cabibbo, *Palermo*
Carlo Calabrese, *Bologna*
Daniele Calistri, *Meldola*
Vincenza Calvaruso, *Palermo*
Lorenzo Camellini, *Reggio Emilia*
Marco Candela, *Bologna*
Raffaele Capasso, *Naples*
Lucia Carulli, *Modena*
Renato David Caviglia, *Rome*
Luigina Cellini, *Chieti*
Giuseppe Chiarioni, *Verona*
Claudio Chiesa, *Rome*
Michele Cicala, *Roma*
Rachele Ciccocioppo, *Pavia*
Sandro Contini, *Parma*
Gaetano Corso, *Foggia*
Renato Costi, *Parma*
Alessandro Cucchetti, *Bologna*
Rosario Cuomo, *Napoli*
Giuseppe Currò, *Messina*
Paola De Nardi, *Milano*
Giovanni D De Palma, *Naples*
Raffaele De Palma, *Napoli*
Giuseppina De Petro, *Brescia*
Valli De Re, *Aviano*
Paolo De Simone, *Pisa*
Giuliana Decorti, *Trieste*
Emanuele Miraglia del Giudice, *Napoli*
Isidoro Di Carlo, *Catania*
Matteo Nicola Dario Di Minno, *Naples*
Massimo Donadelli, *Verona*
Mirko D'Onofrio, *Verona*
Maria Pina Dore, *Sassari*
Luca Elli, *Milano*
Massimiliano Fabozzi, *Aosta*

Massimo Falconi, *Ancona*
Ezio Falletto, *Turin*
Silvia Fargion, *Milan*
Matteo Fassan, *Verona*
Gianfranco Delle Fave, *Roma*
Alessandro Federico, *Naples*
Francesco Feo, *Sassari*
Davide Festi, *Bologna*
Natale Figura, *Siena*
Vincenzo Formica, *Rome*
Mirella Fraquelli, *Milan*
Marzio Frazzoni, *Modena*
Walter Fries, *Messina*
Gennaro Galizia, *Naples*
Andrea Galli, *Florence*
Matteo Garcovich, *Rome*
Eugenio Gaudio, *Rome*
Paola Ghiorzo, *Genoa*
Edoardo G Giannini, *Genova*
Luca Gianotti, *Monza*
Maria Cecilia Giron, *Padova*
Alberto Grassi, *Rimini*
Gabriele Grassi, *Trieste*
Francesco Greco, *Bergamo*
Luigi Greco, *Naples*
Antonio Grieco, *Rome*
Fabio Grizzi, *Rozzano*
Laurino Grossi, *Pescara*
Simone Guglielmetti, *Milan*
Tiberiu Hershcovici, *Jerusalem*
Calogero Iacono, *Verona*
Enzo Ierardi, *Bari*
Amedeo Indriolo, *Bergamo*
Raffaele Iorio, *Naples*
Paola Iovino, *Salerno*
Angelo A Izzo, *Naples*
Loreta Kondili, *Rome*
Filippo La Torre, *Rome*
Giuseppe La Torre, *Rome*
Giovanni Latella, *L'Aquila*
Salvatore Leonardi, *Catania*
Massimo Libra, *Catania*
Anna Licata, *Palermo*
C armela Loguercio, *Naples*
Amedeo Lonardo, *Modena*
Carmelo Luigiano, *Catania*
Francesco Luzza, *Catanzaro*
Giovanni Maconi, *Milano*
Antonio Macrì, *Messina*
Mariano Malaguarnera, *Catania*
Francesco Manguso, *Napoli*
Tommaso Maria Manzia, *Rome*
Daniele Marrelli, *Siena*
Gabriele Masselli, *Rome*
Sara Massironi, *Milan*
Giuseppe Mazzarella, *Avellino*
Michele Milella, *Rome*
Giovanni Milito, *Rome*
Antonella d'Arminio Monforte, *Milan*
Fabrizio Montecucco, *Genoa*
Giovanni Monteleone, *Rome*
Mario Morino, *Torino*
Vincenzo La Mura, *Milan*
Gerardo Nardone, *Naples*
Riccardo Nascimbeni, *Brescia*
Gabriella Nesi, *Florence*
Giuseppe Nigri, *Rome*
Erica Novo, *Turin*
Veronica Ojetti, *Rome*
Michele Orditura, *Naples*
Fabio Pace, *Seriate*
Lucia Pacifico, *Rome*
Omero Alessandro Paoluzi, *Rome*
Valerio Pazienza, *San Giovanni Rotondo*
Rinaldo Pellicano, *Turin*
Adriano M Pellicelli, *Rome*
Nadia Peparini, *Ciampino*
Mario Pescatori, *Rome*
Antonio Picardi, *Rome*
Alberto Pilotto, *Padova*
Alberto Piperno, *Monza*
Anna Chiara Piscaglia, *Rome*
Maurizio Pompili, *Rome*
Francesca Romana Ponziani, *Rome*
Cosimo Prantera, *Rome*
Girolamo Ranieri, *Bari*
Carlo Ratto, *Tome*
Barbara Renga, *Perugia*
Alessandro Repici, *Rozzano*
Maria Elena Riccioni, *Rome*
Lucia Ricci-Vitiani, *Rome*
Luciana Rigoli, *Messina*
Mario Rizzetto, *Torino*
Ballarin Roberto, *Modena*
Roberto G Romanelli, *Florence*
Claudio Romano, *Messina*
Luca Roncucci, *Modena*
Cesare Ruffolo, *Treviso*
L ucia Sacchetti, *Napoli*
Rodolfo Sacco, *Pisa*
Lapo Sali, *Florence*
Romina Salpini, *Rome*
Giulio Aniello, *Santoro Treviso*
Armando Santoro, *Rozzano*
Edoardo Savarino, *Padua*
Marco Senzolo, *Padua*
Annalucia Serafino, *Rome*
Giuseppe S Sica, *Rome*
Pierpaolo Sileri, *Rome*
Cosimo Sperti, *Padua*
Vincenzo Stanghellini, *Bologna*
Cristina Stasi, *Florence*
Gabriele Stocco, *Trieste*
Roberto Tarquini, *Florence*
Mario Testini, *Bari*
Guido Torzilli, *Milan*
Guido Alberto Massimo, *Tiberio Brescia*
Giuseppe Toffoli, *Aviano*
Alberto Tommasini, *Trieste*
Francesco Tonelli, *Florence*
Cesare Tosetti Porretta, *Terme*
Lucio Trevisani, *Cona*
Guglielmo M Trovato, *Catania*
Mariapia Vairetti, *Pavia*
Luca Vittorio Valenti, *Milano*
Mariateresa T Ventura, *Bari*
Giuseppe Verlato, *Verona*
Marco Vivarelli, *Ancona*
Giovanni Li Volti, *Catania*
Giuseppe Zanotti, *Padua*
Vincenzo Zara, *Lecce*
Gianguglielmo Zehender, *Milan*
Anna Linda Zignego, *Florence*
Rocco Antonio Zoccali, *Messina*
Angelo Zullo, *Rome*

Japan

Yasushi Adachi, *Sapporo*
Takafumi Ando, *Nagoya*
Masahiro Arai, *Tokyo*
Makoto Arai, *Chiba*
Takaaki Arigami, *Kagoshima*
Itaru Endo,*Yokohama*
Munechika Enjoji, *Fukuoka*
Shunji Fujimori, *Tokyo*
Yasuhiro Fujino, *Akashi*
Toshiyoshi Fujiwara, *Okayama*
Yosuke Fukunaga, *Tokyo*
Toshio Fukusato, *Tokyo*
Takahisa Furuta, *Hamamatsu*
Osamu Handa, *Kyoto*
Naoki Hashimoto, *Osaka*
Yoichi Hiasa, *Toon*
Masatsugu Hiraki, *Saga*
Satoshi Hirano, *Sapporo*
Keiji Hirata, *Fukuoka*
Toru Hiyama, *Higashihiroshima*
Akira Hokama, *Nishihara*
Shu Hoteya, *Tokyo*
Masao Ichinose, *Wakayama*
Tatsuya Ide, *Kurume*
Masahiro Iizuka, *Akita*
Toshiro Iizuka, *Tokyo*
Kenichi Ikejima, *Tokyo*
Tetsuya Ikemoto, *Tokushima*
Hiroyuki Imaeda, *Saitama*
Atsushi Imagawa, *Kan-onji*
Hiroo Imazu, *Tokyo*
Shuji Isaji, *Tsu*
Toru Ishikawa, *Niigata*
Toshiyuki Ishiwata, *Tokyo*
Soichi Itaba, *Kitakyushu*
Yoshiaki Iwasaki, *Okayama*
Tatehiro Kagawa, *Isehara*
Satoru Kakizaki, *Maebashi*
Naomi Kakushima, *Shizuoka*
Terumi Kamisawa, *Tokyo*
Akihide Kamiya, *Isehara*
Osamu Kanauchi, *Tokyo*
Tatsuo Kanda, *Chiba*
Shin Kariya, *Okayama*
Shigeyuki Kawa, *Matsumoto*
Takumi Kawaguchi, *Kurume*
Takashi Kawai, *Tokyo*
Soo Ryang Kim, *Kobe*
Shinsuke Kiriyama, *Gunma*
Tsuneo Kitamura, *Urayasu*
Masayuki Kitano, *Osakasayama*
Hirotoshi Kobayashi, *Tokyo*
Hironori Koga, *Kurume*
Takashi Kojima, *Sapporo*
Satoshi Kokura, *Kyoto*
Shuhei Komatsu, *Kyoto*
Tadashi Kondo, *Tokyo*
Yasuteru Kondo, *Sendai*
Yasuhiro Kuramitsu, *Yamaguchi*
Yukinori Kurokawa, *Osaka*
Shin Maeda, *Yokohama*
Koutarou Maeda, *Toyoake*

Hitoshi Maruyama, *Chiba*
Atsushi Masamune, *Sendai*
Hiroyuki Matsubayashi, *Suntogun*
Akihisa Matsuda, *Inzai*
Hirofumi Matsui, *Tsukuba*
Akira Matsumori, *Kyoto*
Yoichi Matsuo, *Nagoya*
Y Matsuzaki, *Ami*
Toshihiro Mitaka, *Sapporo*
Kouichi Miura, *Akita*
Shinichi Miyagawa, *Matumoto*
Eiji Miyoshi, *Suita*
Toru Mizuguchi, *Sapporo*
Nobumasa Mizuno, *Nagoya*
Zenichi Morise, *Nagoya*
Tomohiko Moriyama, *Fukuoka*
Kunihiko Murase, *Tusima*
Michihiro Mutoh, *Tsukiji*
Akihito Nagahara, *Tokyo*
Hikaru Nagahara, *Tokyo*
Hidenari Nagai, *Tokyo*
Koichi Nagata, *Shimotsuke-shi*
Masaki Nagaya, *Kawasaki*
Hisato Nakajima, *Nishi-Shinbashi*
Toshifusa Nakajima, *Tokyo*
Hiroshi Nakano, *Kawasaki*
Hiroshi Nakase, *Kyoto*
Toshiyuki Nakayama, *Nagasaki*
Takahiro Nakazawa, *Nagoya*
Shoji Natsugoe, *Kagoshima City*
Tsutomu Nishida, *Suita*
Shuji Nomoto, *Naogya*
Sachiyo Nomura, *Tokyo*
Takeshi Ogura, *Takatsukishi*
Nobuhiro Ohkohchi, *Tsukuba*
Toshifumi Ohkusa, *Kashiwa*
Hirohide Ohnishi, *Akita*
Teruo Okano, *Tokyo*
Satoshi Osawa, *Hamamatsu*
Motoyuki Otsuka, *Tokyo*
Michitaka Ozaki, *Sapporo*
Satoru Saito, *Yokohama*
Naoaki Sakata, *Sendai*
Ken Sato, *Maebashi*
Toshiro Sato, *Tokyo*
Tomoyuki Shibata, *Toyoake*
Tomohiko Shimatani, *Kure*
Yukihiro Shimizu, *Nanto*
Tadashi Shimoyama, *Hirosaki*
Masayuki Sho, *Nara*
Ikuo Shoji, *Kobe*
Atsushi Sofuni, *Tokyo*
Takeshi Suda, *Niigata*
M Sugimoto, *Hamamatsu*
Ken Sugimoto, *Hamamatsu*
Haruhiko Sugimura, *Hamamatsu*
Shoichiro Sumi, *Kyoto*
Hidekazu Suzuki, *Tokyo*
Masahiro Tajika, *Nagoya*
Hitoshi Takagi, *Takasaki*
Toru Takahashi, *Niigata*
Yoshihisa Takahashi, *Tokyo*
Shinsuke Takeno, *Fukuoka*
Akihiro Tamori, *Osaka*
Kyosuke Tanaka, *Tsu*
Shinji Tanaka, *Hiroshima*
Atsushi Tanaka, *Tokyo*
Yasuhito Tanaka, *Nagoya*
Shinji Tanaka, *Tokyo*
Minoru Tomizawa, *Yotsukaido City*
Kyoko Tsukiyama-Kohara, *Kagoshima*
Takuya Watanabe, *Niigata*
Kazuhiro Watanabe, *Sendai*
Satoshi Yamagiwa, *Niigata*
Takayuki Yamamoto, *Yokkaichi*
Hiroshi Yamamoto, *Otsu*
Kosho Yamanouchi, *Nagasaki*
Ichiro Yasuda, *Gifu*
Yutaka Yata, *Maebashi-city*
Shin-ichi Yokota, *Sapporo*
Norimasa Yoshida, *Kyoto*
Hiroshi Yoshida, *Tama-City*
Hitoshi Yoshiji, *Kashihara*
Kazuhiko Yoshimatsu, *Tokyo*
Kentaro Yoshioka, *Toyoake*
Nobuhiro Zaima, *Nara*

Jordan
Khaled Ali Jadallah, *Irbid*

Kuwait
Islam Khan, *Kuwait*

Lebanon
Bassam N Abboud, *Beirut*
Kassem A Barada, *Beirut*
Marwan Ghosn, *Beirut*
Iyad A Issa, *Beirut*
Fadi H Mourad, *Beirut*
AIa Sharara, *Beirut*
Rita Slim, *Beirut*

Lithuania
Antanas Mickevicius, *Kaunas*

Malaysia
Huck Joo Tan, *Petaling Jaya*

Mexico
Richard A Awad, *Mexico City*
Carlos R Camara-Lemarroy, *Monterrey*
Norberto C Chavez-Tapia, *Mexico City*
Wolfgang Gaertner, *Mexico City*
Diego Garcia-Compean, *Monterrey*
Arturo Panduro, *Guadalajara*
OT Teramoto-Matsubara, *Mexico City*
Felix Tellez-Avila, *Mexico City*
Omar Vergara-Fernandez, *Mexico City*
Saúl Villa-Trevino, *Cuidad de México*

Morocco
Samir Ahboucha, *Khouribga*

Netherlands
Robert J de Knegt, *Rotterdam*
Tom Johannes Gerardus Gevers, *Nijmegen*
Menno Hoekstra, *Leiden*
BW Marcel Spanier, *Arnhem*
Karel van Erpecum, *Utrecht*

New Zealand
Leo K Cheng, *Auckland*
Andrew Stewart Day, *Christchurch*
Jonathan Barnes Koea, *Auckland*
Max Petrov, *Auckland*

Nigeria
Olufunmilayo Adenike Lesi, *Lagos*
Jesse Abiodun Otegbayo, *Ibadan*
Stella Ifeanyi Smith, *Lagos*

Norway
Trond Berg, *Oslo*
Trond Arnulf Buanes, *Krokkleiva*
Thomas de Lange, *Rud*
Magdy El-Salhy, *Stord*
Rasmus Goll, *Tromso*
Dag Arne Lihaug Hoff, *Aalesund*

Pakistan
Zaigham Abbas, *Karachi*
Usman A Ashfaq, *Faisalabad*
Muhammad Adnan Bawany, *Hyderabad*
Muhammad Idrees, *Lahore*
Saeed Sadiq Hamid, *Karachi*
Yasir Waheed, *Islamabad*

Poland
Thomas Brzozowski, *Cracow*
Magdalena Chmiela, *Lodz*
Krzysztof Jonderko, *Sosnowiec*
Anna Kasicka-Jonderko, *Sosnowiec*
Michal Kukla, *Katowice*
Tomasz Hubert Mach, *Krakow*
Agata Mulak, *Wroclaw*
Danuta Owczarek, *Kraków*
Piotr Socha, *Warsaw*
Piotr Stalke, *Gdansk*
Julian Teodor Swierczynski, *Gdansk*
Anna M Zawilak-Pawlik, *Wroclaw*

Portugal
Marie Isabelle Cremers, *Setubal*
Ceu Figueiredo, *Porto*
Ana Isabel Lopes, *LIsbon*
M Paula Macedo, *Lisboa*
Ricardo Marcos, *Porto*
Rui T Marinho, *Lisboa*
Guida Portela-Gomes, *Estoril*

Filipa F Vale, *Lisbon*

Puerto Rico

Caroline B Appleyard, *Ponce*

Qatar

Abdulbari Bener, *Doha*

Romania

Mihai Ciocirlan, *Bucharest*
Dan LucianDumitrascu, *Cluj-Napoca*
Carmen Fierbinteanu-Braticevici, *Bucharest*
Romeo G Mihaila, *Sibiu*
Lucian Negreanu, *Bucharest*
Adrian Saftoiu, *Craiova*
Andrada Seicean, *Cluj-Napoca*
Ioan Sporea, *Timisoara*
Letiţia Adela Maria Streba, *Craiova*
Anca Trifan, *Iasi*

Russia

Victor Pasechnikov, *Stavropol*
Vasiliy Ivanovich Reshetnyak, *Moscow*
Vitaly Skoropad, *Obninsk*

Saudi Arabia

Abdul-Wahed N Meshikhes, *Dammam*
M Ezzedien Rabie, *Khamis Mushait*

Singapore

Brian KP Goh, *Singapore*
Richie Soong, *Singapore*
Ker-Kan Tan, *Singapore*
Kok-Yang Tan, *Singapore*
Yee-Joo Tan, *Singapore*
Mark Wong, *Singapore*
Hong Ping Xia, *Singapore*

Slovenia

Matjaz Homan, *Ljubljana*
Martina Perse, *Ljubljana*

South Korea

Sang Hoon Ahn, *Seoul*
Seung Hyuk Baik, *Seoul*
Soon Koo Baik, *Wonju*
Soo-Cheon Chae, *Iksan*
Byung-Ho Choe, *Daegu*
Suck Chei Choi, *Iksan*
Hoon Jai Chun, *Seoul*
Yeun-Jun Chung, *Seoul*
Young-Hwa Chung, *Seoul*
Ki-Baik Hahm, *Seongnam*
Sang Young Han, *Busan*
Seok Joo Han, *Seoul*
Seung-Heon Hong, *Iksan*
Jin-Hyeok Hwang, *Seoungnam*
Jeong Won Jang, *Seoul*
Jin-Young Jang, *Seoul*
Dae-Won Jun, *Seoul*
Young Do Jung, *Kwangju*
Gyeong Hoon Kang, *Seoul*
Sung-Bum Kang, *Seoul*
Koo Jeong Kang, *Daegu*
Ki Mun Kang, *Jinju*
Chang Moo Kang, *Seodaemun-gu*
Gwang Ha Kim, *Busan*
Sang Soo Kim, *Goyang-si*
Jin Cheon Kim, *Seoul*
Tae Il Kim, *Seoul*
Jin Hong Kim, *Suwon*
Kyung Mo Kim, *Seoul*
Kyongmin Kim, *Suwon*
Hyung-Ho Kim, *Seongnam*
Seoung Hoon Kim, *Goyang*
Sang Il Kim, *Seoul*
Hyun-Soo Kim, *Wonju*
Jung Mogg Kim, *Seoul*
Dong Yi Kim, *Gwangju*
Kyun-Hwan Kim, *Seoul*
Jong-Han Kim, *Ansan*
Sang Wun Kim, *Seoul*
Ja-Lok Ku, *Seoul*
Kyu Taek Lee, *Seoul*
Hae-Wan Lee, *Chuncheon*
Inchul Lee, *Seoul*
Jung Eun Lee, *Seoul*
Sang Chul Lee, *Daejeon*
Song Woo Lee, *Ansan-si*
Hyuk-Joon Lee, *Seoul*
Seong-Wook Lee, *Yongin*
Kil Yeon Lee, *Seoul*
Jong-Inn Lee, *Seoul*
Kyung A Lee, *Seoul*
Jong-Baeck Lim, *Seoul*
Eun-Yi Moon, *Seoul*
SH Noh, *Seoul*
Seung Woon Paik, *Seoul*
Won Sang Park, *Seoul*
Sung-Joo Park, *Iksan*
Kyung Sik Park, *Daegu*
Se Hoon Park, *Seoul*
Yoonkyung Park, *Gwangju*
Seung-Wan Ryu, *Daegu*
Il Han Song, *Cheonan*
Myeong Jun Song, *Daejeon*
Yun Kyoung Yim, *Daejeon*
Dae-Yeul Yu *Daejeon*

Spain

Mariam Aguas, *Valencia*
Raul J Andrade, *Málaga*
Antonio Arroyo, *Elche*
Josep M Bordas, *Barcelona*
Lisardo Boscá, *Madrid*
Ricardo Robles Campos, *Murcia*
Jordi Camps, *Reus*
Carlos Cervera *Barcelona*
Alfonso Clemente, *Granada*
Pilar Codoner-Franch, *Valencia*
Fernando J Corrales, *Pamplona*
Fermin Sánchez de Medina, *Granada*
Alberto Herreros de Tejada, *Majadahonda*
Enrique de-Madaria, *Alicante*
JE Dominguez-Munoz, *Santiago de Compostela*
Vicente Felipo, *Valencia*
CM Fernandez-Rodriguez, *Madrid*
Carmen Frontela-Saseta, *Murcia*
Julio Galvez, *Granada*
Maria Teresa García, *Vigo*
MI Garcia-Fernandez, *Málaga*
Emilio Gonzalez-Reimers, *La Laguna*
Marcel Jimenez, *Bellaterra*
Angel Lanas, *Zaragoza*
Juan Ramón Larrubia, *Guadalajara*
Antonio Lopez-Sanroman, *Madrid*
Vicente Lorenzo-Zuniga, *Badalona*
Alfredo J Lucendo, *Tomelloso*
Vicenta Soledad Martinez-Zorzano, *Vigo*
José Manuel Martin-Villa, *Madrid*
Julio Mayol, *Madrid*
Manuel Morales-Ruiz, *Barcelona*
Alfredo Moreno-Egea, *Murcia*
Albert Pares, *Barcelona*
Maria Pellise, *Barcelona*
José Perea, *Madrid*
Miguel Angel Plaza, *Zaragoza*
María J Pozo, *Cáceres*
Enrique Quintero, *La Laguna*
Jose M Ramia, *Madrid*
Francisco Rodriguez-Frias, *Barcelona*
Silvia Ruiz-Gaspa, *Barcelona*
Xavier Serra-Aracil, *Barcelona*
Vincent Soriano, *Madrid*
Javier Suarez, *Pamplona*
Carlos Taxonera, *Madrid*
M Isabel Torres, *Jaén*
Manuel Vazquez-Carrera, *Barcelona*
Benito Velayos, *Valladolid*
Silvia Vidal, *Barcelona*

Sri Lanka

Arjuna Priyadarsin De Silva, *Colombo*

Sudan

Ishag Adam, *Khartoum*

Sweden

Roland G Andersson, *Lund*
Bergthor Björnsson, *Linkoping*
Johan Christopher Bohr, *Örebro*
Mauro D'Amato, *Stockholm*
Thomas Franzen, *Norrkoping*
Evangelos Kalaitzakis, *Lund*
Riadh Sadik, *Gothenburg*
Per Anders Sandstrom, *Linkoping*
Ervin Toth, *Malmö*
Konstantinos Tsimogiannis, *Vasteras*
Apostolos V Tsolakis, *Uppsala*

Switzerland

Gieri Cathomas, *Liestal*
Jean Louis Frossard, *Geneve*
Christian Toso, *Geneva*
Stephan Robert Vavricka, *Zurich*
Dominique Velin, *Lausanne*

Thailand

Thawatchai Akaraviputh, *Bangkok*
P Yoysungnoen Chintana, *Pathumthani*
Veerapol Kukongviriyapan, *Muang*
Vijittra Leardkamolkarn, *Bangkok*
Varut Lohsiriwat, *Bangkok*
Somchai Pinlaor, *Khaon Kaen*
D Wattanasirichaigoon, *Bangkok*

Trinidad and Tobago

B Shivananda Nayak, *Mount Hope*

Tunisia

Ibtissem Ghedira, *Sousse*
Lilia Zouiten-Mekki, *Tunis*

Turkey

Inci Alican, *Istanbul*
Mustafa Altindis, *Sakarya*
Mutay Aslan, *Antalya*
Oktar Asoglu, *Istanbul*
Yasemin Hatice Balaban, *Istanbul*
Metin Basaranoglu, *Ankara*
Yusuf Bayraktar, *Ankara*
Süleyman Bayram, *Adiyaman*
Ahmet Bilici, *Istanbul*
Ahmet Sedat Boyacioglu, *Ankara*
Züleyha Akkan Cetinkaya, *Kocaeli*
Cavit Col, *Bolu*
Yasar Colak, *Istanbul*
Cagatay Erden Daphan, *Kirikkale*
Mehmet Demir, *Hatay*
Ahmet Merih Dobrucali, *Istanbul*
Gülsüm Ozlem Elpek, *Antalya*
Ayse Basak Engin, *Ankara*
Eren Ersoy, *Ankara*
Osman Ersoy, *Ankara*
Yusuf Ziya Erzin, *Istanbul*
Mukaddes Esrefoglu, *Istanbul*
Levent Filik, *Ankara*
Ozgur Harmanci, *Ankara*
Koray Hekimoglu, *Ankara*
Abdurrahman Kadayifci, *Gaziantep*
Cem Kalayci, *Istanbul*
Selin Kapan, *Istanbul*
Huseyin Kayadibi, *Adana*
Sabahattin Kaymakoglu, *Istanbul*
Metin Kement, *Istanbul*
Mevlut Kurt, *Bolu*
Resat Ozaras, *Istanbul*
Elvan Ozbek, *Adapazari*
Cengiz Ozcan, *Mersin*
Hasan Ozen, *Ankara*
Halil Ozguc, *Bursa*
Mehmet Ozturk, *Izmir*
Orhan V Ozkan, *Sakarya*
Semra Paydas, *Adana*
Ozlem Durmaz Suoglu, *Istanbul*
Ilker Tasci, *Ankara*
Müge Tecder-ünal, *Ankara*
Mesut Tez, *Ankara*
Serdar Topaloglu, *Trabzon*
Murat Toruner, *Ankara*
Gokhan Tumgor, *Adana*
Oguz Uskudar, *Adana*
Mehmet Yalniz, *Elazig*
Mehmet Yaman, *Elazig*
Veli Yazisiz, *Antalya*
Yusuf Yilmaz, *Istanbul*
Ozlem Yilmaz, *Izmir*
Oya Yucel, *Istanbul*
Ilhami Yuksel, *Ankara*

United Kingdom

Nadeem Ahmad Afzal, *Southampton*
Navneet K Ahluwalia, *Stockport*
Yeng S Ang, *Lancashire*
Ramesh P Arasaradnam, *Coventry*
Ian Leonard Phillip Beales, *Norwich*
John Beynon, *Swansea*
Barbara Braden, *Oxford*
Simon Bramhall, *Birmingham*
Geoffrey Burnstock, *London*
Ian Chau, *Sutton*
Thean Soon Chew, *London*
Helen G Coleman, *Belfast*
Anil Dhawan, *London*
Sunil Dolwani, *Cardiff*
Piers Gatenby, *London*
Anil T George, *London*
Pasquale Giordano, *London*
Paul Henderson, *Edinburgh*
Georgina Louise Hold, *Aberdeen*
Stefan Hubscher, *Birmingham*
Robin D Hughes, *London*
Nusrat Husain, *Manchester*
Matt W Johnson, *Luton*
Konrad Koss, *Macclesfield*
Anastasios Koulaouzidis, *Edinburgh*
Simon Lal, *Salford*
John S Leeds, *Aberdeen*
JK K Limdi, *Manchester*
Hongxiang Liu, *Cambridge*
Michael Joseph McGarvey, *London*
Michael Anthony Mendall, *London*
Alexander H Mirnezami, *Southampton*
J Bernadette Moore, *Guildford*
Claudio Nicoletti, *Norwich*
Savvas Papagrigoriadis, *London*
Sylvia LF Pender, *Southampton*
David Mark Pritchard, *Liverpool*
James A Ross, *Edinburgh*
Kamran Rostami, *Worcester*
Xiong Z Ruan, *London*
Frank I Tovey, *London*
Dhiraj Tripathi, *Birmingham*
Vamsi R Velchuru, *Great Yarmouth*
Nicholas T Ventham, *Edinburgh*
Diego Vergani, *London*
Jack Westwood Winter, *Glasgow*
Terence Wong, *London*
Ling Yang, *Oxford*

United States

Daniel E Abbott, *Cincinnati*
Ghassan K Abou-Alfa, *New York*
Julian Abrams, *New York*
David William Adelson, *Los Angeles*
Jonathan Steven Alexander, *Shreveport*
Tauseef Ali, *Oklahoma City*
Mohamed R Ali, *Sacramento*
Rajagopal N Aravalli, *Minneapolis*
Hassan Ashktorab, *Washington*
Shashi Bala, *Worcester*
Charles F Barish, *Raleigh*
P Patrick Basu, *New York*
Robert L Bell, *Berkeley Heights*
David Bentrem, *Chicago*
Henry J Binder, *New Haven*
Joshua Bleier, *Philadelphia*
Wojciech Blonski, *Johnson City*
Kenneth Boorom, *Corvallis*
Brian Boulay, *Chicago*
Carla W Brady, *Durham*
Kyle E Brown, *Iowa City*
Adeel A Butt, *Pittsburgh*
Weibiao Cao, *Providence*
Andrea Castillo, *Cheney*
Fernando J Castro, *Weston*
Adam S Cheifetz, *Boston*
Xiaoxin Luke Chen, *Durham*
Ramsey Cheung, *Palo Alto*
Parimal Chowdhury, *Little Rock*
Edward John Ciaccio, *New York*
Dahn L Clemens, *Omaha*
Yingzi Cong, *Galveston*
Laura Iris Cosen-Binker, *Boston*
Joseph John Cullen, *Lowa*
Mark J Czaja, *Bronx*
Mariana D Dabeva, *Bronx*
Christopher James Damman, *Seattle*
Isabelle G De Plaen, *Chicago*
Punita Dhawan, *Nashville*
Hui Dong, *La Jolla*
Wael El-Rifai, *Nashville*
Sukru H Emre, *New Haven*
Paul Feuerstadt, *Hamden*
Josef E Fischer, *Boston*
Laurie N Fishman, *Boston*
Joseph Che Forbi, *Atlanta*
Temitope Foster, *Atlanta*
Amy E Foxx-Orenstein, *Scottsdale*
Daniel E Freedberg, *New York*
Shai Friedland, *Palo Alto*
Virgilio George, *Indianapolis*
Ajay Goel, *Dallas*
Oliver Grundmann, *Gainesville*
Stefano Guandalini, *Chicago*
Chakshu Gupta, *St. Joseph*
Grigoriy E Gurvits, *New York*

Xiaonan Han, *Cincinnati*
Mohamed Hassan, *Jackson*
Martin Hauer-Jensen, *Little Rock*
Koichi Hayano, *Boston*
Yingli Hee, *Atlanta*
Samuel B Ho, *San Diego*
Jason Ken Hou, *Houston*
Lifang Hou, *Chicago*
K-Qin Hu, *Orange*
Jamal A Ibdah, *Columbia*
Robert Thomas Jensen, *Bethesda*
Huanguang "Charlie" Jia, *Gainesville*
Rome Jutabha, *Los Angeles*
Andreas M Kaiser, *Los Angeles*
Avinash Kambadakone, *Boston*
David Edward Kaplan, *Philadelphia*
Randeep Kashyap, *Rochester*
Rashmi Kaul, *Tulsa*
Ali Keshavarzian, *Chicago*
Amir Maqbul Khan, *Marshall*
Nabeel Hasan Khan, *New Orleans*
Sahil Khanna, *Rochester*
Kusum K Kharbanda, *Omaha*
Hyun Sik Kim, *Pittsburgh*
Joseph Kim, *Duarte*
Jae S Kim, *Gainesville*
Miran Kim, *Providence*
Timothy R Koch, *Washington*
Burton I Korelitz, *New York*
Betsy Kren, *Minneapolis*
Shiu-Ming Kuo, *Buffalo*
Michelle Lai, *Boston*
Andreas Larentzakis, *Boston*
Edward Wolfgang Lee, *Los Angeles*
Daniel A Leffler, *Boston*
Michael Leitman, *New York*
Suthat Liangpunsakul, *Indianapolis*
Joseph K Lim, *New Haven*
Elaine Y Lin, *Bronx*
Henry C Lin, *Albuquerque*
Rohit Loomba, *La Jolla*
James David Luketich, *Pittsburgh*
Li Ma, *Stanford*
Mohammad F Madhoun, *Oklahoma City*
Thomas C Mahl, *Buffalo*
Ashish Malhotra, *Bettendorf*
Pranoti Mandrekar, *Worcester*
John Marks, *Wynnewood*
Wendy M Mars, *Pittsburgh*
Julien Vahe Matricon, *San Antonio*
Craig J McClain, *Louisville*
Tamir Miloh, *Phoenix*
Ayse Leyla Mindikoglu, *Baltimore*
Huanbiao Mo, *Denton*
Klaus Monkemuller, *Birmingham*
John Morton, *Stanford*
Adnan Muhammad, *Tampa*
Michael J Nowicki, *Jackson*
Patrick I Okolo, *Baltimore*
Giusepp Orlando, *Winston Salem*
Natalia A Osna, *Omaha*
Virendra N Pandey, *Newark*
Mansour A Parsi, *Cleveland*
Michael F Picco, *Jacksonville*
Daniel S Pratt, *Boston*
Xiaofa Qin, *Newark*
Janardan K Reddy, *Chicago*
Victor E Reyes, *Galveston*
Jon Marc Rhoads, *Houston*
Giulia Roda, *New York*
Jean-Francois Armand Rossignol, *Tampa*
Paul A Rufo, *Boston*
Madhusudana Girija Sanal, *New York*
Miguel Saps, *Chicago*
Sushil Sarna, *Galveston*
Ann O Scheimann, *Baltimore*
Bernd Schnabl, *La Jolla*
Matthew J Schuchert, *Pittsburgh*
Ekihiro Seki, *La Jolla*
Chanjuan Shi, *Nashville*
David Quan Shih, *Los Angeles*
Shadab A Siddiqi, *Orlando*
William B Silverman, *Iowa City*
Shashideep Singhal, *New York*
Bronislaw L Slomiany, *Newark*
Steven F Solga, *Bethlehem*
Byoung-Joon Song, *Bethesda*
Dario Sorrentino, *Roanoke*
Scott R Steele, *Fort Lewis*
Branko Stefanovic, *Tallahassee*
Arun Swaminath, *New York*
Kazuaki Takabe, *Richmond*
Naoki Tanaka, *Bethesda*
Hans Ludger Tillmann, *Durham*
George Triadafilopoulos, *Stanford*
John Richardson Thompson, *Nashville*
Andrew Ukleja, *Weston*
Miranda AL van Tilburg, *Chapel Hill*
Gilberto Vaughan, *Atlanta*
Vijayakumar Velu, *Atlanta*
Gebhard Wagener, *New York*
Kasper Saonun Wang, *Los Angeles*
Xiangbing Wang, *New Brunswick*
Daoyan Wei, *Houston*
Theodore H Welling, *Ann Arbor*
C Mel Wilcox, *Birmingham*
Jacqueline Lee Wolf, *Boston*
Laura Ann Woollett, *Cincinnati*
Harry Hua-Xiang Xia, *East Hanover*
Wen Xie, *Pittsburgh*
Guang Yu Yang, *Chicago*
Michele T Yip-Schneider, *Indianapolis*
Sam Zakhari, *Bethesda*
Kezhong Zhang, *Detroit*
Huiping Zhou, *Richmond*
Xiao-Jian Zhou, *Cambridge*
Richard Zubarik, *Burlington*

Venezuela

Miguel Angel Chiurillo, *Barquisimeto*

Vietnam

Van Bang Nguyen, *Hanoi*

World Journal of Gastroenterology

Contents

Weekly Volume 22 Number 20 May 28, 2016

Contents

World Journal of Gastroenterology
Volume 22 Number 20 May 28, 2016

NAME OF JOURNAL
World Journal of Gastroenterology

ISSN
ISSN 1007-9327 (print)
ISSN 2219-2840 (online)

LAUNCH DATE
October 1, 1995

FREQUENCY
Weekly

EDITORIAL OFFICE
Jin-Lei Wang, Director
Xiu-Xia Song, Vice Director
World Journal of Gastroenterology
Room 903, Building D, Ocean International Center,
No. 62 Dongsihuan Zhonglu, Chaoyang District,
Beijing 100025, China
Telephone: +86-10-59080039
Fax: +86-10-85381893
E-mail: editorialoffice@wjgnet.com
Help Desk: http://www.wjgnet.com/esps/helpdesk.aspx
http://www.wjgnet.com

PUBLISHER
Baishideng Publishing Group Inc
8226 Regency Drive,
Pleasanton, CA 94588, USA
Telephone: +1-925-223-8242
Fax: +1-925-223-8243
E-mail: bpgoffice@wjgnet.com
Help Desk: http://www.wjgnet.com/esps/helpdesk.aspx
http://www.wjgnet.com

PUBLICATION DATE
May 28, 2016

INSTRUCTIONS TO AUTHORS
Full instructions are available online at http://www.wjgnet.com/bpg/g_info_20160116143427.htm

ONLINE SUBMISSION
http://www.wjgnet.com/esps/

World Journal of Gastroenterology

Submit a Manuscript: http://www.wjgnet.com/esps/
Help Desk: http://www.wjgnet.com/esps/helpdesk.aspx
DOI: 10.3748/wjg.v22.i20.4789

World J Gastroenterol 2016 May 28; 22(20): 4789-4793
ISSN 1007-9327 (print) ISSN 2219-2840 (online)

EDITORIAL

When a liver transplant recipient goes back to alcohol abuse: Should we be more selective?

Monica Leon, Joseph Varon, Salim Surani

Monica Leon, Facultad de Medicina, Universidad Popular Autonoma del Estado de Puebla, Puebla, Puebla 72410, Mexico

Joseph Varon, Foundation Surgical Hospital of Houston, Houston, TX 77054, United States

Salim Surani, Texas A and M University, Corpus Christi, TX 78405, United States

Salim Surani, Pulmonary Associates, Corpus Christi, TX 78336, United States

Author contributions: All authors have contributed in preparation and review of the manuscript.

Conflict-of-interest statement: All authors declare no conflict of interest related to this publication.

Correspondence to: Salim Surani, MD, MPH, MSHM, FACP, FCCP, FAASM, Texas A and M University, 1177 West Wheeler, Avenue, Aransas Pass Texas, Corpus Christi, TX 78405, United States. srsurani@hotmail.com
Telephone: +1-361-8857722
Fax: +1-361-8507563

Received: February 9, 2016
Peer-review started: February 9, 2016
First decision: March 21, 2016
Revised: April 2, 2016
Accepted: May 4, 2016
Article in press: May 4, 2016
Published online: May 28, 2016

Abstract

Alcoholic liver disease (ALD) is one of the most common indications for liver transplantation (LT). However, it has always remained as a complicated topic from both medical and ethical grounds, as it is seen for many a "self-inflicted disease". Over the years, the survival rate of transplanted patients has significantly improved. The allocation system and the inclusion criteria for LT has also undergone some modifications. Early LT for acute alcoholic hepatitis has been subject to recent clinical studies with encouraging results in highly selected patients. We have learned from studies the importance of a multidisciplinary evaluation of candidates for LT. Complete abstinence should be attempted to overcome addiction issues and to allow spontaneous liver recovery. Risk factors for relapse include the presence of anxiety or depressive disorder, short duration of sobriety pre-LT and lack of social support. The identification of risk factors and the strengthen of social support system may decrease relapse among these patients. Family counseling of candidates is highly encouraged to prevent relapse to alcohol. Relapse has been associated with different histopathological changes, graft damage, graft loss and even decrease in survival among some studies. Therefore, each patient should be carefully selected and priority is to continue to lean on patients with high probability of success. The ethical issue remains as to the patient returning to drinking after the LT, hindering the way for other patients who could have received the same organ.

Key words: Liver transplantation; Alcoholic liver disease; Alcoholic cirrhosis; Selection criteria; Relapses

Core tip: Alcoholic liver disease is one of the most common indications for liver transplantation (LT). The selection criteria of the majority of transplant programs require 6-mo of complete abstinence, with the aim to allow spontaneous liver recovery and to overcome addiction issues. The evaluation of LT candidates should be multidisciplinary with a strong emphasis in family and social support and a strong patient commitment of abstinence to prevent relapses.

Leon M, Varon J, Surani S. When a liver transplant recipient goes back to alcohol abuse: Should we be more selective? *World J Gastroenterol* 2016; 22(20): 4789-4793 Available from: URL: http://www.wjgnet.com/1007-9327/full/v22/i20/4789.htm DOI: http://dx.doi.org/10.3748/wjg.v22.i20.4789

Liver transplantation (LT) has become an accepted therapy for some patients with end-stage liver disease. The use of LT for alcoholic liver disease (ALD) continues to be controversial from both medical and ethical point of view[1,2]. However, it remains a common indication for LT worldwide[1,3,4].

One of the strongest ethical arguments against LT for ALD is the probability of relapse. For a patient to be listed as candidate for LT, 6 mo of abstinence must be achieved in most liver transplantation centers. Studies differ in the validation of this "6-mo rule" as well as in the real impact that relapse to drinking could have on the transplanted liver[5-8]. Recent studies have shown similar survival rates among LT for ALD and other chronic causes of end-stage liver disease recipients[1]. Early transplantation for acute alcoholic hepatitis (AAH), for example, has promising results[9,10]. However, a special multidisciplinary approach for alcoholic patients pre- and post-LT should be pursue with a goal of complete abstinence when possible.

Ever since Starzl *et al*[11], reported in 1963 the first three successful cases of liver transplantations in humans, an interest in increasing the use of life-saving intervention has evolved. By 1968, these investigators, reported the results of seven patients, one of them with 1-year post-transplant survival[12]. The next decade was characterized by important advances in tissue preservation, surgical techniques, control of infections and advances in immunosuppressive therapy with decrease in tissue rejection[13]. By 1979 there were about 318 human LT reported worldwide. The majority of them, performed at the University of Colorado (United States) and at the University Hospital at Cambridge and King's College Hospital (United Kingdom)[14]. In 1979, 15 years after the first LT, the 1-year survival rate had improved from to 28% to 50%[13]. Years later, the Organ Procurement and Transplantation Network was established by the United States government in 1987, operating under the United Network for Organ Sharing (UNOS)[15].

After the experimental years and over the last decades, there have been several changes in liver transplant indications and allocation system (UNOS). Initially, priority allocation was established based on "sickest first", meaning ICU's patients with acute complications - acute esophageal varices, hepatorenal syndrome or portosystemic encephalopathy[15]. The original allocation system was based on the Child-Turcotte-Pugh score. This was later proven to be sub-optimal in predicting the mortality and prioritization of patients[15]. In 2002, the national UNOS adopted the model for end stage liver disease (MELD) allocation system[16]. The MELD was developed to screen for short-term prognosis, and prioritize candidates according to disease severity, based on serum creatinine, serum bilirubin, international normalized ratio of prothrombin time (INR) and serum sodium[17].

Given the geographical disparity in organ allocation as seen by the disparities in waiting list and differences between units of organ, in 2013, the "Share 35" policy was implemented. Such policy instructs to give priority to candidate recipients for LT with MELD > 35[18]. Following this implementation, the waiting list for patients with MELD > 35 decreased from 18 d to 9 d in the last 2 years[19].

Currently, the accepted indications for LT are: acute liver failure, cirrhosis (with complications), liver metabolic diseases with systemic manifestations and systemic complications of chronic liver disease[20]. The latest guidelines for LT emphasize the importance of a multidisciplinary evaluation process; hepatology evaluation, surgical evaluation, laboratory testing, cardiac evaluation, hepatic imaging, psychiatry, psychology or mental health professional consultation, social work evaluation, financial and insurance counseling and nutritional evaluation[20].

As noted, ALD accounts for the second most common indication for LT[3,21]. ALD comprises subclinical biochemical damage, fatty liver, steatohepatitis, fibrosis and cirrhosis that can end up in end stage liver disease[21,22]. Other alcohol-induced entities include AAH and hepatocellular carcinoma[3,21,22]. On alcohol-induced injuries, the current guidelines continue to enforce the minimum of 6-mo of abstinence, this time is required to allow addiction issues to be addressed and helps in allowing spontaneous liver recovery. For patients with cirrhosis, LT is recommended once complications (ascites, hepatic encephalopathy, variceal hemorrhage or hepatocellular dysfunction) results in a MELD score > 15[20]. An entity that requires special consideration is AAH, a syndrome presenting with abdominal pain, fever, jaundice and acute hepatic decompensation[3]. Without transplantation, the probability of death in this group of patients is high and 70%-80% die within 6 mo[9,23,24].

Significant controversy on LT for alcoholic hepatitis exist[9]. Mathurin and coworkers examined patients that were not responding to medical treatment and that underwent an early liver transplant. Those pati-

ents that received an early LT had a significant higher survival than the patients in the medical therapy group[9]. Despite the favorable results, it should be noted that all the patients in this study were carefully selected and that 90% of non-responders to medical treatment were excluded due to a predisposition to addiction or unfavorable social or familial profiles. One of the key inclusion criteria for the enrollment in this pilot study, was the patient agreement to adhere to total alcohol abstinence. After LT, 3 out of 26 had alcohol consumption (11.5%). The authors concluded that the low rate of alcohol relapse was probably related to the carefully selection of recipients. More recently, Im and associates conducted a similar study in the United States, where early LT, in highly selected patients with severe alcoholic hepatitis, resulted in improved outcomes[10].

The main concerns remain the high chance of alcohol intake relapse after LT, which has been reported from 7%-95%[25]. The significant differences among data can be explained by differences in the use of terms "recidivism" and "relapse", which some studies utilize to define any alcohol intake, and in others to define heavy drinking[1,3,26-28]. Relapse to "harmful drinking" has been reported in 8%-21% of LT recipients[7,8,29-31]. Occasional drinks "slips", may not cause a significant graft damage, but with a history of alcoholism, it would be difficult to predict if these so called "slips", could end up in complete relapse and harmful alcohol abuse[1,32,33].

In an attempt to predict this risk, several analyses have been done[29,34-36]. Yates and coworkers used the high-risk alcoholism relapse (HRAR) scale, which consisted of evaluating the duration of heavy drinking, usual number of daily drinks, and inpatient treatment due to alcohol consumption[37]. In another study, 387 LT recipients were retrospectively analyzed by De Gottardi *et al*[29], finding an 11.9% relapse (harmful alcohol consumption). The presence of anxiety or depressive disorder, duration of sobriety of less than 6 mo, elevated HRAR score and age, were among the factors associated with increased risk of alcohol relapse[29].

Alcohol-induced injuries to allografts have been well documented[8,28,38]. In a retrospective study, Rice and coworkers evaluated the association between relapse and graft damage[28]. In this study, any alcoholic relapse was associated with increased risk of damage to the transplanted liver and particularly heavy drinking was associated with allograft loss (P = 0.008)[28]. Although most studies have found evidence of liver damage among relapse patients, they differ in reference to alcohol relapse and mortality rates[27,38].

Despite the established criteria regarding the 6-mo rule of abstinence, the sobriety time before LT is a strong predictor of relapse among recipients[6]. While on the waiting list, mandatory blood alcohol levels, urinary ethyl glucuronide and assistance to alcohol addiction units (AAU) could be used as strategies to prevent relapses[26,39,40]. In addition, the support of an AAU within the LT center has showed to decrease the prevalence of alcohol relapse. Carbonneau *et al*[40] studied the incidence of drinking while on the LT waiting list. They randomly checked blood alcohol levels, and 17% of them were found to relapse on drinking alcohol while on the LT waiting list. The time of relapse ranged from 2-23 mo. Interestingly, the increase of random blood alcohol level measurements was related to a decrease in alcohol use. Patients may have had lower alcohol ingestion by the fear of being caught and withdrawn from the list[40].

Addolorato *et al*[26] implemented the presence of an AUU in the LT center. Patients who were follow-up at the AUU had a lower relapse than the patients who were not seen by this unit (16.4% *vs* 35.1% respectively).

LT as a therapeutic option for alcoholic liver disease continues to be controversial. Different ethical and medical opinions preclude it to be fully accepted. Organ allocation for patients in whom the liver damage is considered to be self-inflicted may not be well accepted[2,29,41]. Yet, this practice continues. This may be causing conflict with the public opinion and may result in an unfavorable change in willingness to donate[2,5].

In an effort to assess the opinion on allocation priorities for LT, Neuberger *et al*[42] conducted a survey based study among general public, family doctors and gastroenterologists. Among groups a hypothetical alcoholic man and a prisoner were found to have lower priority for liver transplant allocation[42].

It is clear that given the current organ shortage, priority should be given to patients with high probability of success. For ALD, complete abstinence should be sought to allow possible liver repair and avoid unnecessary LT. Abstinence pre and post LT may be reinforced by the implementation of strict clinical and laboratory screening for alcohol relapses and strong support groups. AAU and strong social support system along with closer follow-up post transplant may help in preventing relapse on alcohol. The selection criteria should play a strong emphasis of the family environment and social structure and family counseling and alcohol abstinence should be also sought from family members prior to transplanting the patient with alcoholic liver disease to prevent future relapse. In cases of AAH, more multi-center studies with larger samples are needed to make solid conclusions.

REFERENCES

1 **Ursic-Bedoya J**, Faure S, Donnadieu-Rigole H, Pageaux GP. Liver transplantation for alcoholic liver disease: Lessons learned and unresolved issues. *World J Gastroenterol* 2015; **21**: 10994-11002 [PMID: 26494956 DOI: 10.3748/wjg.v21.i39.10994]

2 **Ubel PA**, Jepson C, Baron J, Mohr T, McMorrow S, Asch DA. Allocation of transplantable organs: do people want to punish patients for causing their illness? *Liver Transpl* 2001; **7**: 600-607 [PMID: 11460227 DOI: 10.1053/jlts.2001.25361]

3 **Singal AK**, Chaha KS, Rasheed K, Anand BS. Liver transplantation

in alcoholic liver disease current status and controversies. *World J Gastroenterol* 2013; **19**: 5953-5963 [PMID: 24106395 DOI: 10.3748/wjg.v19.i36.5953]
4 **Younossi ZM**, Stepanova M, Afendy M, Fang Y, Younossi Y, Mir H, Srishord M. Changes in the prevalence of the most common causes of chronic liver diseases in the United States from 1988 to 2008. *Clin Gastroenterol Hepatol* 2011; **9**: 524-530.e1; quiz e60 [PMID: 21440669 DOI: 10.1016/j.cgh.2011.03.020]
5 **Shawcross DL**, O'Grady JG. The 6-month abstinence rule in liver transplantation. *Lancet* 2010; **376**: 216-217 [PMID: 20656110 DOI: 10.1016/S0140-6736(10)60487-4]
6 **Bravata DM**, Olkin I, Barnato AE, Keeffe EB, Owens DK. Employment and alcohol use after liver transplantation for alcoholic and nonalcoholic liver disease: a systematic review. *Liver Transpl* 2001; **7**: 191-203 [PMID: 11244159 DOI: 10.1053/jlts.2001.22326]
7 **Pfitzmann R**, Schwenzer J, Rayes N, Seehofer D, Neuhaus R, Nüssler NC. Long-term survival and predictors of relapse after orthotopic liver transplantation for alcoholic liver disease. *Liver Transpl* 2007; **13**: 197-205 [PMID: 17205563 DOI: 10.1002/lt.20934]
8 **Pageaux GP**, Bismuth M, Perney P, Costes V, Jaber S, Possoz P, Fabre JM, Navarro F, Blanc P, Domergue J, Eledjam JJ, Larrey D. Alcohol relapse after liver transplantation for alcoholic liver disease: does it matter? *J Hepatol* 2003; **38**: 629-634 [PMID: 12713874 DOI: 10.1016/S0168-8278(03)00088-6]
9 **Mathurin P**, Moreno C, Samuel D, Dumortier J, Salleron J, Durand F, Castel H, Duhamel A, Pageaux GP, Leroy V, Dharancy S, Louvet A, Boleslawski E, Lucidi V, Gustot T, Francoz C, Letoublon C, Castaing D, Belghiti J, Donckier V, Pruvot FR, Duclos-Vallée JC. Early liver transplantation for severe alcoholic hepatitis. *N Engl J Med* 2011; **365**: 1790-1800 [PMID: 22070476 DOI: 10.1056/NEJMoa1105703]
10 **Im GY**, Kim-Schluger L, Shenoy A, Schubert E, Goel A, Friedman SL, Florman S, Schiano TD. Early Liver Transplantation for Severe Alcoholic Hepatitis in the United States-A Single-Center Experience. *Am J Transplant* 2016; **16**: 841-849 [PMID: 26710309 DOI: 10.1111/ajt.13586]
11 **Starzl TE**, Marchioro TL, Vonkaulla KN, Hermann G, Brittain RS, Waddell WR. Homotransplantation of the liver in humans. *Surg Gynecol Obstet* 1963; **117**: 659-676 [PMID: 14100514]
12 **Starzl TE**, Groth CG, Brettschneider L, Penn I, Fulginiti VA, Moon JB, Blanchard H, Martin AJ, Porter KA. Orthotopic homotransplantation of the human liver. *Ann Surg* 1968; **168**: 392-415 [PMID: 4877589 DOI: 10.1097/00000658-196809000-00009]
13 **Starzl TE**, Koep LJ, Halgrimson CG, Hood J, Schroter GP, Porter KA, Weil R. Fifteen years of clinical liver transplantation. *Gastroenterology* 1979; **77**: 375-388 [PMID: 376395]
14 **Russell PS**, Cosimi AB. Transplantation. *N Engl J Med* 1979; **301**: 470-479 [PMID: 111125 DOI: 10.1056/NEJM197908303010904]
15 **Wiesner RH**. Patient selection in an era of donor liver shortage: current US policy. *Nat Clin Pract Gastroenterol Hepatol* 2005; **2**: 24-30 [PMID: 16265097 DOI: 10.1038/ncpgasthep0070]
16 **Freeman RB**, Wiesner RH, Edwards E, Harper A, Merion R, Wolfe R. Results of the first year of the new liver allocation plan. *Liver Transpl* 2004; **10**: 7-15 [PMID: 14755772 DOI: 10.1002/lt.20024]
17 **Wiesner R**, Edwards E, Freeman R, Harper A, Kim R, Kamath P, Kremers W, Lake J, Howard T, Merion RM, Wolfe RA, Krom R. Model for end-stage liver disease (MELD) and allocation of donor livers. *Gastroenterology* 2003; **124**: 91-96 [PMID: 12512033 DOI: 10.1053/gast.2003.50016]
18 **Feng S**, O'Grady J. Share 35: a liver in time saves lives? *Am J Transplant* 2015; **15**: 581-582 [PMID: 25693468 DOI: 10.1111/ajt.13102]
19 **Kim WR**, Lake JR, Smith JM, Skeans MA, Schladt DP, Edwards EB, Harper AM, Wainright JL, Snyder JJ, Israni AK, Kasike BL. OPTN/ SRTR 2014 annnual data report: Liver. *Am J Transplant* 2016; **16** Suppl S2: 69-98 [DOI: 10.1111/ajt.13668]
20 **Martin P**, DiMartini A, Feng S, Brown R, Fallon M. Evaluation for liver transplantation in adults: 2013 practice guideline by the American Association for the Study of Liver Diseases and the American Society of Transplantation. *Hepatology* 2014; **59**: 1144-1165 [PMID: 24716201 DOI: 10.1002/hep.26972]
21 **Testino G**, Burra P, Bonino F, Piani F, Sumberaz A, Peressutti R, Giannelli Castiglione A, Patussi V, Fanucchi T, Ancarani O, De Cerce G, Iannini AT, Greco G, Mosti A, Durante M, Babocci P, Quartini M, Mioni D, Aricò S, Baselice A, Leone S, Lozer F, Scafato E, Borro P. Acute alcoholic hepatitis, end stage alcoholic liver disease and liver transplantation: an Italian position statement. *World J Gastroenterol* 2014; **20**: 14642-14651 [PMID: 25356027 DOI: 10.3748/wjg.v20.i40.14642]
22 **Testino G**, Leone S, Borro P. Alcohol and hepatocellular carcinoma: a review and a point of view. *World J Gastroenterol* 2014; **20**: 15943-15954 [PMID: 25473148 DOI: 10.3748/wjg.v20.i43.15943]
23 **Neuberger J**, Schulz KH, Day C, Fleig W, Berlakovich GA, Berenguer M, Pageaux GP, Lucey M, Horsmans Y, Burroughs A, Hockerstedt K. Transplantation for alcoholic liver disease. *J Hepatol* 2002; **36**: 130-137 [PMID: 11804676 DOI: 10.1016/S0168-8278(01)00278-1]
24 **Nguyen-Khac E**, Thevenot T, Piquet MA, Benferhat S, Goria O, Chatelain D, Tramier B, Dewaele F, Ghrib S, Rudler M, Carbonell N, Tossou H, Bental A, Bernard-Chabert B, Dupas JL. Glucocorticoids plus N-acetylcysteine in severe alcoholic hepatitis. *N Engl J Med* 2011; **365**: 1781-1789 [PMID: 22070475 DOI: 10.1056/NEJMoa1101214]
25 **Lim JK**, Keeffe EB. Liver transplantation for alcoholic liver disease: current concepts and length of sobriety. *Liver Transpl* 2004; **10**: S31-S38 [PMID: 15382288 DOI: 10.1002/lt.20267]
26 **Addolorato G**, Mirijello A, Leggio L, Ferrulli A, D'Angelo C, Vassallo G, Cossari A, Gasbarrini G, Landolfi R, Agnes S, Gasbarrini A. Liver transplantation in alcoholic patients: impact of an alcohol addiction unit within a liver transplant center. *Alcohol Clin Exp Res* 2013; **37**: 1601-1608 [PMID: 23578009 DOI: 10.1111/acer.12117]
27 **Cuadrado A**, Fábrega E, Casafont F, Pons-Romero F. Alcohol recidivism impairs long-term patient survival after orthotopic liver transplantation for alcoholic liver disease. *Liver Transpl* 2005; **11**: 420-426 [PMID: 15776421 DOI: 10.1002/lt.20386]
28 **Rice JP**, Eickhoff J, Agni R, Ghufran A, Brahmbhatt R, Lucey MR. Abusive drinking after liver transplantation is associated with allograft loss and advanced allograft fibrosis. *Liver Transpl* 2013; **19**: 1377-1386 [PMID: 24115392 DOI: 10.1002/lt.23762]
29 **De Gottardi A**, Spahr L, Gelez P, Morard I, Mentha G, Guillaud O, Majno P, Morel P, Hadengue A, Paliard P, Scoazec JY, Boillot O, Giostra E, Dumortier J. A simple score for predicting alcohol relapse after liver transplantation: results from 387 patients over 15 years. *Arch Intern Med* 2007; **167**: 1183-1188 [PMID: 17563028 DOI: 10.1001/archinte.167.11.1183]
30 **Conjeevaram HS**, Hart J, Lissoos TW, Schiano TD, Dasgupta K, Befeler AS, Millis JM, Baker AL. Rapidly progressive liver injury and fatal alcoholic hepatitis occurring after liver transplantation in alcoholic patients. *Transplantation* 1999; **67**: 1562-1568 [PMID: 10401763]
31 **DiMartini A**, Dew MA, Day N, Fitzgerald MG, Jones BL, deVera ME, Fontes P. Trajectories of alcohol consumption following liver transplantation. *Am J Transplant* 2010; **10**: 2305-2312 [PMID: 20726963 DOI: 10.1111/j.1600-6143.2010.03232.x]
32 **Vaillant GE**. A 60-year follow-up of alcoholic men. *Addiction* 2003; **98**: 1043-1051 [PMID: 12873238 DOI: 10.1046/j.1360-0443.2003.00422.x]
33 **Fuller RK**. Definition and diagnosis of relapse to drinking. *Liver Transpl Surg* 1997; **3**: 258-262 [PMID: 9346749 DOI: 10.1002/lt.500030311]
34 **Tandon P**, Goodman KJ, Ma MM, Wong WW, Mason AL, Meeberg G, Bergsten D, Carbonneau M, Bain VG. A shorter duration of pre-transplant abstinence predicts problem drinking after liver transplantation. *Am J Gastroenterol* 2009; **104**: 1700-1706 [PMID: 19471253 DOI: 10.1038/ajg.2009.226]
35 **Miguet M**, Monnet E, Vanlemmens C, Gache P, Messner M, Hruskovsky S, Perarnau JM, Pageaux GP, Duvoux C, Minello A, Hillon P, Bresson-Hadni S, Mantion G, Miguet JP. Predictive factors of alcohol relapse after orthotopic liver transplantation for alcoholic

liver disease. *Gastroenterol Clin Biol* 2004; **28**: 845-851 [PMID: 15523219 DOI: 10.1016/S0399-8320(04)95146-9]

36 **Mackie J**, Groves K, Hoyle A, Garcia C, Garcia R, Gunson B, Neuberger J. Orthotopic liver transplantation for alcoholic liver disease: a retrospective analysis of survival, recidivism, and risk factors predisposing to recidivism. *Liver Transpl* 2001; **7**: 418-427 [PMID: 11349262 DOI: 10.1053/jlts.2001.23789]

37 **Yates WR**, Booth BM, Reed DA, Brown K, Masterson BJ. Descriptive and predictive validity of a high-risk alcoholism relapse model. *J Stud Alcohol* 1993; **54**: 645-651 [PMID: 8271799 DOI: 10.15288/jsa.1993.54.645]

38 **Burra P**, Mioni D, Cecchetto A, Cillo U, Zanus G, Fagiuoli S, Naccarato R, Martines D. Histological features after liver transplantation in alcoholic cirrhotics. *J Hepatol* 2001; **34**: 716-722 [PMID: 11434618]

39 **Staufer K**, Andresen H, Vettorazzi E, Tobias N, Nashan B, Sterneck M. Urinary ethyl glucuronide as a novel screening tool in patients pre- and post-liver transplantation improves detection of alcohol consumption. *Hepatology* 2011; **54**: 1640-1649 [PMID: 21809364 DOI: 10.1002/hep.24596]

40 **Carbonneau M**, Jensen LA, Bain VG, Kelly K, Meeberg G, Tandon P. Alcohol use while on the liver transplant waiting list: a single-center experience. *Liver Transpl* 2010; **16**: 91-97 [PMID: 19866447 DOI: 10.1002/lt.21957]

41 **Ratcliffe J**. Public preferences for the allocation of donor liver grafts for transplantation. *Health Econ* 2000; **9**: 137-148 [PMID: 10721015]

42 **Neuberger J**, Adams D, MacMaster P, Maidment A, Speed M. Assessing priorities for allocation of donor liver grafts: survey of public and clinicians. *BMJ* 1998; **317**: 172-175 [PMID: 9665895]

P- Reviewer: Kapoor S, Schemmer P, Zeng Z **S- Editor**: Qi Y
L- Editor: A **E- Editor**: Wang CH

World Journal of Gastroenterology

Submit a Manuscript: http://www.wjgnet.com/esps/
Help Desk: http://www.wjgnet.com/esps/helpdesk.aspx
DOI: 10.3748/wjg.v22.i20.4794

World J Gastroenterol 2016 May 28; 22(20): 4794-4801
ISSN 1007-9327 (print) ISSN 2219-2840 (online)

TOPIC HIGHLIGHT

2016 Inflammatory Bowel Disease: Global view

Inflammatory bowel disease and cancer: The role of inflammation, immunosuppression, and cancer treatment

Jordan E Axelrad, Simon Lichtiger, Vijay Yajnik

Jordan E Axelrad, Simon Lichtiger, Department of Medicine, Division of Digestive and Liver Diseases, Columbia University Medical Center, New York, NY 10032, United States

Vijay Yajnik, Department of Medicine, Division of Gastroenterology, The Massachusetts General Hospital, Boston, MA 02445, United States

Author contributions: Axelrad JE, Lichtiger S and Yajnik V wrote the paper.

Conflict-of-interest statement: Authors declare no conflict of interests for this article.

Correspondence to: Vijay Yajnik, MD, PhD, Department of Medicine, Division of Gastroenterology, The Massachusetts General Hospital, Crohn's and Colitis Center, 165 Cambridge Street 9th Floor, Boston, MA 02445, United States. vyajnik@mgh.harvard.edu
Telephone: +1-617-7246005
Fax: +1-617-7263080

Received: February 11, 2016
Peer-review started: February 11, 2016
First decision: March 21, 2016
Revised: March 25, 2016
Accepted: April 7, 2016
Article in press: April 7, 2016
Published online: May 28, 2016

Abstract

In patients with inflammatory bowel disease (IBD), chronic inflammation is a major risk factor for the development of gastrointestinal malignancies. The pathogenesis of colitis-associated cancer is distinct from sporadic colorectal carcinoma and the critical molecular mechanisms underlying this process have yet to be elucidated. Patients with IBD have also been shown to be at increased risk of developing extra-intestinal malignancies. Medical therapies that diminish the mucosal inflammatory response represent the foundation of treatment in IBD, and recent evidence supports their introduction earlier in the disease course. However, therapies that alter the immune system, often used for long durations, may also promote carcinogenesis. As the population of patients with IBD grows older, with longer duration of chronic inflammation and longer exposure to immunosuppression, there is an increasing risk of cancer development. Many of these patients will require cancer treatment, including chemotherapy, radiation, hormonal therapy, and surgery. Many patients will require further treatment for their IBD. This review seeks to explore the characteristics and risks of cancer in patients with IBD, and to evaluate the limited data on patients with IBD and cancer, including management of IBD after a diagnosis of cancer, the effects of cancer treatment on IBD, and the effect of IBD and medications for IBD on cancer outcomes.

Key words: Inflammatory bowel disease; Cancer; Anti-tumor necrosis factor; Immunosuppression; Chemotherapy; Radiation

Core tip: Patients with inflammatory bowel disease (IBD) and cancer represent a challenging population. Gastroenterologists and oncologists caring for patients with IBD and cancer are increasingly confronted with questions regarding the management of IBD after a diagnosis of cancer, and conversely, the management of cancer in patients with IBD. This review seeks to explore the characteristics, risks, and pathogenesis of cancer in patients with IBD, and to evaluate the data on patients with IBD and cancer, including the interaction between IBD and cancer treatment.

Axelrad JE, Lichtiger S, Yajnik V. Inflammatory bowel disease and cancer: The role of inflammation, immunosuppression, and cancer treatment. *World J Gastroenterol* 2016; 22(20): 4794-4801 Available from: URL: http://www.wjgnet.com/1007-9327/full/v22/i20/4794.htm DOI: http://dx.doi.org/10.3748/wjg.v22.i20.4794

INTRODUCTION

Crohn's disease (CD) and ulcerative colitis (UC) are chronic inflammatory conditions of the gastrointestinal tract. Although the disease pathogenesis is not fully understood, inflammatory bowel disease (IBD) is characterized by chronic inflammation of the gastrointestinal tract in genetically susceptible individuals exposed to environmental risk factors. Together, IBD is estimated to affect more than 0.4% of Europeans and North Americans, a number that is expected to increase over time[1]. It is well recognized that patients with IBD are at an increased risk of developing colorectal cancer (CRC), primarily the result of chronic intestinal inflammation[2-4]. More recently, patients with IBD have also been shown to be at increased risk of developing extra-intestinal malignancies, thought to be a consequence of immunosuppressive therapies and an underlying inflammatory state[5].

As the population of patients with IBD grows and ages, there is an inevitable increase in the risk of cancer development. Moreover, many of these patients may require cancer treatment, including chemotherapy, radiation, and immunotherapy, and many may require further treatment for their IBD. The focus of this review is to evaluate the characteristics, pathogenesis, and risks of cancer in patients with IBD, and to explore the relationship between IBD and cancer treatment.

IBD AND RISK OF CANCER

Cancer secondary to chronic intestinal inflammation

In patients with IBD, chronic intestinal inflammation is the primary risk factor for the development of gastrointestinal malignancy. Cancers as a result of chronic intestinal inflammation include CRC, small bowel adenocarcinoma, intestinal lymphoma, anal cancer, and cholangiocarcinoma (Table 1)[6].

Table 1 Cancer secondary to chronic intestinal inflammation

Cancer type	Standardized incidence ratio
Colorectal cancer[3]	5.7 (95%CI: 4.6-7.0)
Small bowel adenocarcinoma[20]	27.1 (95%CI: 14.9-49.2)
Intestinal lymphoma[36]	17.51 (95%CI: 6.43-38.11)
Anal cancer[60]	Data not available
Cholangiocarcinoma[23]	916.63 (95%CI: 297.88-2140.99) in UC

UC: Ulcerative colitis.

The risk and pathogenesis of inflammation-associated cancer has chiefly been described in colitis-associated CRC. In a meta analysis, quantitative estimates of CRC risk in UC have been reported to be 2% after 10 years, 8% after 20 years, and 18% after 30 years of disease[3]. Moreover, studies of CRC in UC have noted a high concordance between CRC risk with the location and extent of disease, with a standardized incidence ratio (SIR) of 1.7 for proctitis, 2.8 for left-sided colitis, and 14.8 for pancolitis[7]. All of these studies support the strong association between inflammation and cancer development.

Patients with IBD develop colon cancer in a manner similar to well described sporadic molecular mechanisms including mutations in the adenomatous polyposis coli (*APC*) gene, aneuploidy, DNA methylation, microsatellite instability (MSI), activation of the oncogene *k-ras*, activation of *COX-2*, and mutation in tumor suppressor genes *DCC/DPC4*, and eventual loss of *p53* function[8]. However, underlying colonic inflammation changes the timing and sequence of these genomic changes, yielding a process of carcinogenesis that is faster and multifocal[4]. Contrary to sporadic cancers in which the dysplastic precursor is the adenomatous polyp, dysplasia in patients with IBD can be localized, diffuse, or multifocal[4,9].

Studies mapping genomic instability secondary to DNA aneuploidy in patients with IBD indicate that these cell populations became more widely distributed, occupying larger areas of colonic mucosa[9]. Over time, further subpopulations with increasingly unstable genomics arise and expand, representing a whole field change, marking the entire colon at risk for further carcinogenesis[9,10].

In terms of specific molecular mechanisms that differ between colitis-associated cancer and sporadic cancer, early mutation in p53 is thought to play a fundamental role. Changes in p53 have been found in up to 85% of colitis-associated cancers[11]. Furthermore, alterations in p53 have been observed in biopsies from inflamed mucosa in more than 50% of patients with UC who did not have cancer, indicating a significant role of inflammation in these mutations[12]. In addition, loss of APC, an early event in the development of

Table 2 Cancer secondary to immunosuppression

Increased risk under anti-metabolites	Increased risk under anti-TNFα	Increased risk under anti-metabolite with anti-TNFα
Non-Hodgkin lymphoma[33-35]	Melanoma[42]	Hepatosplenic T-cell lymphoma[38]
Acute myeloid leukemia and Myelodysplastic syndromes[61]		
Non-melanoma skin cancers (basal and squamous cell carcinomas)[39-41]		
Urinary tract cancers[62]		

TNF-α: Tumor necrosis factor alpha.

sporadic CRC, is less frequent and tends to occur later in colitis-associated cancer[13]. DNA methylation also differs with increased hypermethylation of several genes, including *hMLH1* and *p16*, occurring earlier and contributing to microsatellite instability[14].

The immune response and oxidative stress play a critical role in the initiation and progression of carcinogenesis, contributing to the aforementioned molecular mechanisms leading to cancer. The inflammatory microenvironment of IBD, consisting of a variety of immune cells, epithelial cells, stromal cells, cytokines, and chemokines, has many similarities to the microenvironment of cancers, suggesting similar inflammatory mediators and mechanisms that promote both IBD and cancer development[15]. These mediators, produced by inflammatory cells, include tumor necrosis factor alpha (TNF-α), ILs-1, 6, 12, 13, 17, 22, and 23[15]. The interaction between the signaling of these cytokines and immune response play a major role in inflammation and colitis-associated cancer.

The increased expression of several inflammation-associated genes in IBD, such as cyclooxygenase-2 (COX-2) and nitric oxide synthase-2 (NOS-2), have also been noted in colonic neoplasia[12]. It is thought that reactive oxygen and nitrogen species produced by inflammatory cells expressing these genes not only directly damage colonic epithelium, but also contribute to the genetic alterations driving carcinogenesis[9].

In addition, alterations in the microbiota contribute to colitis-associated cancer. In mouse models of colitis-associated cancer susceptible to inflammation or cancer, cancer did not develop when the mice were germ-free or treated with antibiotics[16,17]. Studies of the microbiota in patients with CRC have demonstrated varying populations of bacteria that differ from cancer-free controls, suggesting that the complex interaction between the host genome, colonic epithelial-cell receptors, and the luminal microbiota create an environment conducive to carcinogenesis. Stool samples derived from CRC patients had higher levels of *Fusobacterium*, *Enterococcus*, *Escherichia*, *Shigella*, *Klebsiella*, *Streptococcus*, and *Peptostreptococcus*, *Firmicutes*, *Bacteroidetes*, and a depletion of bacteria belonging to *Lachnospiraceae* family compared to controls[18,19]. Although we are just beginning to understand the association between specific gastrointestinal microbes and cancer, much remains unknown regarding the causes and effects of these relationships and how manipulating the microbiome may have therapeutic potential.

In addition to CRC, small-bowel adenocarcinoma, specifically ileal carcinoma, has been shown to be significantly associated with the severity and duration of CD, and it is 20 to 30 fold more common in patients with CD compared to the general population[20]. Moreover, it is often found in areas with previous or synchronous ileal dysplasia, suggesting that it may evolve in a similar manner to the molecular and immune mechanisms of CRC described above[21]. In addition, cholangiocarcinoma, when associated with UC-primary sclerosing cholangitis (PSC), yields a risk nearly 160 fold greater than controls, suggesting the inflammatory state of IBD-PSC may contribute to biliary carcinogenesis[22,23].

Cancer secondary to immunosuppression

Given that chronic inflammation underlies the disease state of IBD, medications that mitigate inflammation by suppression of the immune system represent the cornerstone of treatment. In addition to treating IBD, it is postulated that these medications, such as immunomodulators [thiopurines (azathioprine or mercaptopurine) or methotrexate] and biologic agents (TNF-α antagonists), may reduce the incidence of inflammation-associated cancer. However, given that immunomodulators and biologic agents act on the immune system, they may also promote carcinogenesis.

Thiopurines and methotrexate promote the development of cancer by a variety of mechanisms including direct alteration in DNA, activation of oncogenes, reduction in physiologic immunosurveillance of malignant cells, and impaired immune control of oncogenic viruses[24-26]. Less is known about the carcinogenic potential of biologic therapies that block TNF-α and existing molecular data is inconsistent. TNF-α has been shown to exhibit anti-tumor effects by initiating cellular apoptosis of malignant cells, but it is secreted by most tumors to facilitate cellular survival and enhance neoplastic proliferation as a pro-tumor inflammatory cytokine[27-29].

Several studies have indicated a risk of therapy-associated malignancies in IBD patients. Population-based cohort and meta-analyses have demonstrated that current use of thiopurines for IBD is associated with a 1.3 to 1.7 overall relative risk of cancer, which is reversible after withdrawal[30,31]. Current exposure to TNF-α antagonists has not been shown to be associated with an overall excess risk of cancer, but data is very limited[32]. Specific cancers thought secondary to long-standing immunosuppression in the setting of IBD include lymphomas, acute myeloid leukemia, myelodysplastic syndromes, skin cancers, and urinary tract cancers (Table 2).

For lymphoma, multiple studies have demonstrated incidence ratios of non-Hodgkin lymphoma following thiopurine exposure ranging from 1.6 to 37.5, with no excess risk attributed to IBD itself[33-35]. The exception to this is primary intestinal lymphoma, where duration and severity of CD play a primary role[36]. In the setting of thiopurines, most lymphoma is Epstein-Barr virus (EBV)-associated and thought to result from the loss of immune control of EBV-infected B lymphocytes[37]. Furthermore, there have been several cases of fatal early postmononucleosis lymphoma in young men who are previously seronegative for EBV[33]. In addition, Hepatosplenic T-cell Lymphoma, though very rare, is primarily associated with thiopurine exposure in combination with TNF-α antagonists in both adolescent and young males[38]. However, recent data suggests that there is no excess risk of lymphoma in patients with IBD exposed to TNF-α antagonists[32].

In a study from the Cancers Et Surrisque Associé aux Maladies inflammatoires intestinales En France (CESAME) cohort, the risk of myeloid disorders was not increased among patients with IBD or ongoing thiopurine treatment (SIR = 1.54, 95%CI: 0.05-8.54), but patients with past exposures to thiopurines had an increased risk of myeloid disorders (SIR = 6.98; 95%CI: 1.44-20.36)[31].

For skin cancers, there is substantial evidence that thiopurines increase the risk of basal cell and squamous cell carcinomas, collectively known as nonmelanoma skin cancers (NMSC)[39-41]. In another study from the CESAME group, an increased risk of NMSC was observed in the patients with IBD and associated with ongoing thiopurine exposure (HR = 5.9; 95%CI: 2.1-16.4) and past thiopurine exposure (HR = 3.9; 95%CI: 1.3-12.1)[41]. However, in a large retrospective cohort of patients with IBD, there was no excess risk of nonmelanoma skin cancer attributable to TNF-α antagonists[40]. In addition, studies have demonstrated an increased risk of melanoma in patients with IBD, with no increased risk associated with thiopurine exposure[40-42]. Conversely, patients exposed to TNF-α antagonists have been found to be 1.5 to 2 times more likely to develop melanoma to patients with IBD who were not exposed to TNF-α antagonists[32]. As such, thiopurines increase the risk of NMSC whereas TNF-α antagonists increase the risk of melanoma.

Secondary or recurrent cancer in patients with a history of cancer

Given the above-mentioned risks of immunomodulator and biologic-associated malignancy, patients with a history of cancer were excluded from clinical trials of TNF-α antagonists. Additionally, there is substantial data within the transplant literature indicating that immunosuppression, such as thiopurines and calcineurin inhibitors, increases the risk of new and recurrent malignancies in patients with a history of cancer[43,44]. As such, oncologists and gastroenterologists generally suspend immunosuppression for IBD after a diagnosis of cancer, both while undergoing cancer treatment and during remission from cancer. This approach may worsen IBD and even complicate appropriate cancer management. Although there is little data on patients with IBD and a history of cancer, there is emerging data regarding the management of IBD after a diagnosis of cancer.

In 17047 patients in the CESAME prospective observational cohort, exposure to immunosuppression was independently associated with the development of cancer with an adjusted HR of 1.9 (95%CI: 1.2-3.0)[31]. However, it did not increase the risk of new or recurrent cancer in patients with a history of cancer[31]. Given the limited number of patients with IBD and a history of cancer with subsequent exposure to immunosuppression in the cohort, this conclusion only applied to thiopurine exposure and no conclusions were drawn on anti-TNF-α therapies[31].

A similar study from the New York Crohn's and Colitis Organization (NYCCO) representing a consortium of 8 academic medical centers found that nearly 30% of patients with IBD and a history of cancer developed new or recurrent cancer[45]. However, exposure to TNF-α antagonists, antimetabolites, or the combination was not associated with an increased risk of new or recurrent cancer within 5 years following a diagnosis of cancer (Log-rank P = 0.14)[45]. Furthermore, after adjusting for the risk of recurrence of prior cancer, there was still no difference in risk of new or recurrent cancer between exposure groups (anti-TNF-α HR = 0.32, 95%CI: 0.09-1.09; anti-TNF-α with an antimetabolite HR = 0.64, 95%CI: 0.26-1.59; antimetabolite HR = 1.08, 95%CI: 0.54-2.15)[45].

In addition, data from NYCCO showed that duration of anti-TNF-α after a diagnosis of cancer was not associated with the risk or type of new or recurrent cancer[45]. Studies within the rheumatoid arthritis literature corroborate these findings with data demonstrating no difference in the development of new or recurrent cancer in patients with a history of cancer who were subsequently exposed to anti-TNF-α agents compared with those receiving disease-modifying anti-rheumatic drugs alone[46,47]. However, given small sample sizes, these studies often grouped different types of cancers together. In the NYCCO study for example, all solid malignancies, such as breast, prostate, and lung, were grouped together. This statistical approach may not reflect the natural biologic activity of carcinogenesis and the direct effects of immunosuppression on cancer development, limiting the ability to draw conclusions on specific cancers.

CANCER TREATMENT AND IBD

While data on the risk of new or recurrent cancer under immunosuppression in patients with IBD and

a history of cancer is limited, though increasing, considerably less is known regarding the effects of cancer treatment on IBD, and the effect of IBD and medications for IBD on important cancer outcomes.

Effect of cancer treatment on IBD

In a study from the Massachusetts General Hospital, 84 patients with IBD and extra-intestinal cancer were assessed for the effect of cancer treatment on the course of IBD[48]. The authors found that 66.7% of patients with active IBD at their cancer diagnosis experienced remission from IBD thought secondary to cytotoxic chemotherapy. Conversely, 17.4% of patients in remission from IBD at their cancer diagnosis experienced a flare during or within 5 years after their cancer treatment[48]. In the remission group, the authors found the risk of flare to be greatest among patients who received hormonal therapies (combination cytotoxic chemotherapy with adjuvant hormone therapy HR = 12.25, 95%CI: 1.51-99.06; hormone monotherapy HR = 11.56, 95%CI: 1.39-96.43). This suggests that hormonal therapies for cancer, such as breast and prostate, may increase the risk of IBD reactivation or counter the protective effects of cytotoxic chemotherapy[48]. A majority of patients with active IBD at their cancer diagnosis appeared to benefit from cancer treatment in the form of IBD remission, which was much more likely if the cancer treatment included cytotoxic chemotherapeutics and less likely if patients were treated with hormonal monotherapy[48].

In this cohort, there was no appreciable modification in IBD medications after a diagnosis of cancer. TNF-α antagonists were continued in three patients and the proportion of patients maintained on immunomodulators decreased slightly from 22% to 14% after a cancer diagnosis[48]. These data, however, were not compared to a control group of patients without chemotherapy or without cancer to assess whether patients with IBD and extra-intestinal cancer experienced a course of IBD different from patients without chemotherapy or cancer.

However, other studies have demonstrated a major modification in IBD medications after a diagnosis of cancer. In a study from a French clinical prospective database, a diagnosis of extra-intestinal cancer had a marked impact on the management of IBD, but was not associated with significant modifications in activity of IBD[49]. A diagnosis of extra-intestinal cancer led to some changes in therapeutic strategy, with a lesser use of thiopurines (19% *vs* 25%, $P < 0.001$) and an increased use of intestinal surgery (4% *vs* 2.5%, $P = 0.05$)[49].

Effect of IBD on cancer

Little is known regarding specific cancer outcomes in patients with IBD. Oncologists have generally been reluctant to administer pelvic irradiation in the setting of IBD, as the tolerance of pelvic irradiation in these patients is largely unknown. There exists only one study in the literature from Green *et al*[50] which retrospectively examined 47 patients with IBD and rectal cancer treated over a 34-year period (1960-1994) from the Mount Sinai Hospital, New York. The authors found a five-year overall survival rate of 42% and disease-free survival of 43%, which were comparable to results published for non-IBD-associated rectal cancer at that time, however, patients with high-grade tumors had statistically lower rates[50]. Complications, such as gastrointestinal morbidity or small bowel obstruction, were comparable to those reported in several large randomized trials of adjuvant chemoradiation therapy in rectal cancer arising in the general population[50].

In terms of chemotherapy and associated cancer outcomes, a small study on 8 patients with IBD and gastrointestinal malignancy showed that the most common gastrointestinal adverse event was diarrhea, with 38% of patients experiencing greater than 7 stools per day over baseline and/or fecal incontinence, all of which occurred in patients with CD[51]. Several studies have examined the effect of IBD medications on cancer outcomes. Multiple studies have demonstrated a role of anti-TNF-α in improving cachexia and increasing chemotherapy tolerance in patients with non-small cell lung cancer, renal cell carcinoma, and pancreatic cancer[52-54]. Moreover, in patients treated with TNF-α antagonists, the occurrence of cancer during treatment was not associated with a worse prognosis, and may even have a protective effect by reducing aggressive metastatic breast cancers at a cellular level[55,56].

Immunotherapies for cancer and immune-related colitis

Immunotherapy for cancer has shown promise in cases refractory to conventional treatment. However, unguided immune stimulation in cancer patients presents its own challenges. There are several reports of anti-cytotoxic T-lymphocyte-associated protein-4 antibodies used for melanoma, such as ipilimumab, and programmed cell death-1 receptor inhibitors used for melanoma and non-small cell lung cancer, such as and nivolumab, producing an immune-related colitis that is remarkably similar to IBD[57,58]. These medications, particularly when used in combination, result in clinical symptoms, endoscopic manifestations, and pathologic cellular infiltrates that emulate IBD. Fortunately, the majority of these cases respond to conventional treatments for IBD such as systemic corticosteroids, budesonide, and infliximab[57,58].

In a recent study, 50% of patients with advanced melanoma and baseline autoimmune disease, such as rheumatoid arthritis, IBD, and psoriasis, experienced either autoimmune exacerbations or immune-related adverse reactions when treated with ipilimumab[59]. These reactions were generally manageable with standard treatment including corticosteroids and infliximab[59]. As the field of immunotherapy for cancer

evolves, we may see an increase in immune mediated colitis, which highlights the important role for T-cell checkpoint inhibitors in exacerbating IBD or causing an IBD-like colitis.

CONCLUSION

Patients with IBD are at an increased risk of cancer secondary to long-standing intestinal inflammation and secondary to immunosuppressive therapies. As the population of patients with IBD ages, there is an increasing risk of cancer development. Many of these patients will require cancer treatment and many will require further treatment for their IBD.

Much research is being devoted to exploring the role of chronic intestinal inflammation from IBD in carcinogenesis, and the role of immunosuppressive medications used to treat IBD in the promotion and prevention of cancer. Despite these efforts, much remains unknown regarding the interaction between IBD, medications for IBD, and cancer treatment, and the risk of cancer recurrence in patients with IBD and a history of cancer.

Understanding the effects of chemotherapy, hormonal therapies, radiation, and surgery for cancer on IBD may help identify patients at the highest risk for disease exacerbation during and after specific cancer treatments, especially in those who may require re-initiation of immunosuppressive therapies for IBD. In addition, while retrospective data has demonstrated some evidence for the safety of immunosuppression in patients with IBD and a history of cancer, prospective data are needed to validate these findings. Furthermore, data is lacking regarding specific cancers, treatments, and risk of recurrence under varying immunosuppressive medications for IBD. More data will permit the development of evidence-based, quantitative risk-benefit models including cancer and IBD-related variables to assist clinicians in managing this complex patient population.

REFERENCES

1 **Molodecky NA**, Soon IS, Rabi DM, Ghali WA, Ferris M, Chernoff G, Benchimol EI, Panaccione R, Ghosh S, Barkema HW, Kaplan GG. Increasing incidence and prevalence of the inflammatory bowel diseases with time, based on systematic review. *Gastroenterology* 2012; **142**: 46-54.e42; quiz e30 [PMID: 22001864 DOI: 10.1053/j.gastro.2011.10.001]

2 **Rutter MD**, Saunders BP, Wilkinson KH, Rumbles S, Schofield G, Kamm MA, Williams CB, Price AB, Talbot IC, Forbes A. Thirty-year analysis of a colonoscopic surveillance program for neoplasia in ulcerative colitis. *Gastroenterology* 2006; **130**: 1030-1038 [PMID: 16618396 DOI: 10.1053/j.gastro.2005.12.035]

3 **Eaden JA**, Abrams KR, Mayberry JF. The risk of colorectal cancer in ulcerative colitis: a meta-analysis. *Gut* 2001; **48**: 526-535 [PMID: 11247898]

4 **Ullman TA**, Itzkowitz SH. Intestinal inflammation and cancer. *Gastroenterology* 2011; **140**: 1807-1816 [PMID: 21530747 DOI: 10.1053/j.gastro.2011.01.057]

5 **Pedersen N**, Duricova D, Elkjaer M, Gamborg M, Munkholm P, Jess T. Risk of extra-intestinal cancer in inflammatory bowel disease: meta-analysis of population-based cohort studies. *Am J Gastroenterol* 2010; **105**: 1480-1487 [PMID: 20332773 DOI: 10.1038/ajg.2009.760]

6 **Beaugerie L**, Itzkowitz SH. Cancers complicating inflammatory bowel disease. *N Engl J Med* 2015; **372**: 1441-1452 [PMID: 25853748 DOI: 10.1056/NEJMra1403718]

7 **Ekbom A**, Helmick C, Zack M, Adami HO. Ulcerative colitis and colorectal cancer. A population-based study. *N Engl J Med* 1990; **323**: 1228-1233 [PMID: 2215606 DOI: 10.1056/NEJM199011013231802]

8 **Vogelstein B**, Papadopoulos N, Velculescu VE, Zhou S, Diaz LA, Kinzler KW. Cancer genome landscapes. *Science* 2013; **339**: 1546-1558 [PMID: 23539594 DOI: 10.1126/science.1235122]

9 **Itzkowitz SH**, Yio X. Inflammation and cancer IV. Colorectal cancer in inflammatory bowel disease: the role of inflammation. *Am J Physiol Gastrointest Liver Physiol* 2004; **287**: G7-G17 [PMID: 15194558 DOI: 10.1152/ajpgi.00079.2004]

10 **Rubin CE**, Haggitt RC, Burmer GC, Brentnall TA, Stevens AC, Levine DS, Dean PJ, Kimmey M, Perera DR, Rabinovitch PS. DNA aneuploidy in colonic biopsies predicts future development of dysplasia in ulcerative colitis. *Gastroenterology* 1992; **103**: 1611-1620 [PMID: 1426881]

11 **Yin J**, Harpaz N, Tong Y, Huang Y, Laurin J, Greenwald BD, Hontanosas M, Newkirk C, Meltzer SJ. p53 point mutations in dysplastic and cancerous ulcerative colitis lesions. *Gastroenterology* 1993; **104**: 1633-1639 [PMID: 8500720]

12 **Hussain SP**, Amstad P, Raja K, Ambs S, Nagashima M, Bennett WP, Shields PG, Ham AJ, Swenberg JA, Marrogi AJ, Harris CC. Increased p53 mutation load in noncancerous colon tissue from ulcerative colitis: a cancer-prone chronic inflammatory disease. *Cancer Res* 2000; **60**: 3333-3337 [PMID: 10910033]

13 **Aust DE**, Terdiman JP, Willenbucher RF, Chang CG, Molinaro-Clark A, Baretton GB, Loehrs U, Waldman FM. The APC/beta-catenin pathway in ulcerative colitis-related colorectal carcinomas: a mutational analysis. *Cancer* 2002; **94**: 1421-1427 [PMID: 11920497]

14 **Fleisher AS**, Esteller M, Harpaz N, Leytin A, Rashid A, Xu Y, Liang J, Stine OC, Yin J, Zou TT, Abraham JM, Kong D, Wilson KT, James SP, Herman JG, Meltzer SJ. Microsatellite instability in inflammatory bowel disease-associated neoplastic lesions is associated with hypermethylation and diminished expression of the DNA mismatch repair gene, hMLH1. *Cancer Res* 2000; **60**: 4864-4868 [PMID: 10987299]

15 **Francescone R**, Hou V, Grivennikov SI. Cytokines, IBD, and colitis-associated cancer. *Inflamm Bowel Dis* 2015; **21**: 409-418 [PMID: 25563695 DOI: 10.1097/MIB.0000000000000236]

16 **Abreu MT**, Peek RM. Gastrointestinal malignancy and the microbiome. *Gastroenterology* 2014; **146**: 1534-1546.e3 [PMID: 24406471 DOI: 10.1053/j.gastro.2014.01.001]

17 **Irrazábal T**, Belcheva A, Girardin SE, Martin A, Philpott DJ. The multifaceted role of the intestinal microbiota in colon cancer. *Mol Cell* 2014; **54**: 309-320 [PMID: 24766895 DOI: 10.1016/j.molcel.2014.03.039]

18 **Castellarin M**, Warren RL, Freeman JD, Dreolini L, Krzywinski M, Strauss J, Barnes R, Watson P, Allen-Vercoe E, Moore RA, Holt RA. Fusobacterium nucleatum infection is prevalent in human colorectal carcinoma. *Genome Res* 2012; **22**: 299-306 [PMID: 22009989 DOI: 10.1101/gr.126516.111]

19 **Wang T**, Cai G, Qiu Y, Fei N, Zhang M, Pang X, Jia W, Cai S, Zhao L. Structural segregation of gut microbiota between colorectal cancer patients and healthy volunteers. *ISME J* 2012; **6**: 320-329 [PMID: 21850056 DOI: 10.1038/ismej.2011.109]

20 **Jess T**, Gamborg M, Matzen P, Munkholm P, Sørensen TI. Increased risk of intestinal cancer in Crohn's disease: a meta-analysis of population-based cohort studies. *Am J Gastroenterol* 2005; **100**: 2724-2729 [PMID: 16393226 DOI: 10.1111/j.1572-0241.2005.00287.x]

21 **Svrcek M**, Piton G, Cosnes J, Beaugerie L, Vermeire S, Geboes K, Lemoine A, Cervera P, El-Murr N, Dumont S, Scriva A, Lascols O, Ardizzone S, Fociani P, Savoye G, Le Pessot F, Novacek G, Wrba F, Colombel JF, Leteurtre E, Bouhnik Y, Cazals-Hatem D, Cadiot G, Diebold MD, Rahier JF, Delos M, Fléjou JF, Carbonnel F. Small bowel adenocarcinomas complicating Crohn's disease are associated

with dysplasia: a pathological and molecular study. *Inflamm Bowel Dis* 2014; **20**: 1584-1592 [PMID: 25029614 DOI: 10.1097/MIB.0000000000000112]
22 **Singh S**, Talwalkar JA. Primary sclerosing cholangitis: diagnosis, prognosis, and management. *Clin Gastroenterol Hepatol* 2013; **11**: 898-907 [PMID: 23454027 DOI: 10.1016/j.cgh.2013.02.016]
23 **Manninen P**, Karvonen AL, Laukkarinen J, Aitola P, Huhtala H, Collin P. Colorectal cancer and cholangiocarcinoma in patients with primary sclerosing cholangitis and inflammatory bowel disease. *Scand J Gastroenterol* 2015; **50**: 423-428 [PMID: 25636976 DOI: 10.3109/00365521.2014.946085]
24 **Münz C**, Moormann A. Immune escape by Epstein-Barr virus associated malignancies. *Semin Cancer Biol* 2008; **18**: 381-387 [PMID: 18996483 DOI: 10.1016/j.semcancer.2008.10.002]
25 **O'Donovan P**, Perrett CM, Zhang X, Montaner B, Xu YZ, Harwood CA, McGregor JM, Walker SL, Hanaoka F, Karran P. Azathioprine and UVA light generate mutagenic oxidative DNA damage. *Science* 2005; **309**: 1871-1874 [PMID: 16166520 DOI: 10.1126/science.1114233]
26 **Zitvogel L**, Tesniere A, Kroemer G. Cancer despite immunosurveillance: immunoselection and immunosubversion. *Nat Rev Immunol* 2006; **6**: 715-727 [PMID: 16977338 DOI: 10.1038/nri1936]
27 **Balkwill F**. Tumour necrosis factor and cancer. *Nat Rev Cancer* 2009; **9**: 361-371 [PMID: 19343034 DOI: 10.1038/nrc2628]
28 **Beaugerie L**. Inflammatory bowel disease therapies and cancer risk: where are we and where are we going? *Gut* 2012; **61**: 476-483 [PMID: 22157331 DOI: 10.1136/gutjnl-2011-301133]
29 **Danial NN**, Korsmeyer SJ. Cell death: critical control points. *Cell* 2004; **116**: 205-219 [PMID: 14744432]
30 **Pasternak B**, Svanström H, Schmiegelow K, Jess T, Hviid A. Use of azathioprine and the risk of cancer in inflammatory bowel disease. *Am J Epidemiol* 2013; **177**: 1296-1305 [PMID: 23514635 DOI: 10.1093/aje/kws375]
31 **Beaugerie L**, Carrat F, Colombel JF, Bouvier AM, Sokol H, Babouri A, Carbonnel F, Laharie D, Faucheron JL, Simon T, de Gramont A, Peyrin-Biroulet L. Risk of new or recurrent cancer under immunosuppressive therapy in patients with IBD and previous cancer. *Gut* 2014; **63**: 1416-1423 [PMID: 24162591 DOI: 10.1136/gutjnl-2013-305763]
32 **Nyboe Andersen N**, Pasternak B, Basit S, Andersson M, Svanström H, Caspersen S, Munkholm P, Hviid A, Jess T. Association between tumor necrosis factor-α antagonists and risk of cancer in patients with inflammatory bowel disease. *JAMA* 2014; **311**: 2406-2413 [PMID: 24938563 DOI: 10.1001/jama.2014.5613]
33 **Beaugerie L**, Brousse N, Bouvier AM, Colombel JF, Lémann M, Cosnes J, Hébuterne X, Cortot A, Bouhnik Y, Gendre JP, Simon T, Maynadié M, Hermine O, Faivre J, Carrat F. Lymphoproliferative disorders in patients receiving thiopurines for inflammatory bowel disease: a prospective observational cohort study. *Lancet* 2009; **374**: 1617-1625 [PMID: 19837455 DOI: 10.1016/S0140-6736(09)61302-7]
34 **Korelitz BI**, Mirsky FJ, Fleisher MR, Warman JI, Wisch N, Gleim GW. Malignant neoplasms subsequent to treatment of inflammatory bowel disease with 6-mercaptopurine. *Am J Gastroenterol* 1999; **94**: 3248-3253 [PMID: 10566724 DOI: 10.1111/j.1572-0241.1999.01530.x]
35 **Lewis JD**, Bilker WB, Brensinger C, Deren JJ, Vaughn DJ, Strom BL. Inflammatory bowel disease is not associated with an increased risk of lymphoma. *Gastroenterology* 2001; **121**: 1080-1087 [PMID: 11677199]
36 **Sokol H**, Beaugerie L, Maynadié M, Laharie D, Dupas JL, Flourié B, Lerebours E, Peyrin-Biroulet L, Allez M, Simon T, Carrat F, Brousse N. Excess primary intestinal lymphoproliferative disorders in patients with inflammatory bowel disease. *Inflamm Bowel Dis* 2012; **18**: 2063-2071 [PMID: 22271569 DOI: 10.1002/ibd.22889]
37 **Pietersma F**, Piriou E, van Baarle D. Immune surveillance of EBV-infected B cells and the development of non-Hodgkin lymphomas in immunocompromised patients. *Leuk Lymphoma* 2008; **49**: 1028-1041 [PMID: 18452077 DOI: 10.1080/10428190801911662]
38 **Kotlyar DS**, Osterman MT, Diamond RH, Porter D, Blonski WC, Wasik M, Sampat S, Mendizabal M, Lin MV, Lichtenstein GR. A systematic review of factors that contribute to hepatosplenic T-cell lymphoma in patients with inflammatory bowel disease. *Clin Gastroenterol Hepatol* 2011; **9**: 36-41.e1 [PMID: 20888436 DOI: 10.1016/j.cgh.2010.09.016]
39 **Long MD**, Herfarth HH, Pipkin CA, Porter CQ, Sandler RS, Kappelman MD. Increased risk for non-melanoma skin cancer in patients with inflammatory bowel disease. *Clin Gastroenterol Hepatol* 2010; **8**: 268-274 [PMID: 20005977 DOI: 10.1016/j.cgh.2009.11.024]
40 **Long MD**, Martin CF, Pipkin CA, Herfarth HH, Sandler RS, Kappelman MD. Risk of melanoma and nonmelanoma skin cancer among patients with inflammatory bowel disease. *Gastroenterology* 2012; **143**: 390-399.e1 [PMID: 22584081 DOI: 10.1053/j.gastro.2012.05.004]
41 **Peyrin-Biroulet L**, Khosrotehrani K, Carrat F, Bouvier AM, Chevaux JB, Simon T, Carbonnel F, Colombel JF, Dupas JL, Godeberge P, Hugot JP, Lémann M, Nahon S, Sabaté JM, Tucat G, Beaugerie L. Increased risk for nonmelanoma skin cancers in patients who receive thiopurines for inflammatory bowel disease. *Gastroenterology* 2011; **141**: 1621-1628.e1-5 [PMID: 21708105 DOI: 10.1053/j.gastro.2011.06.050]
42 **Singh S**, Nagpal SJ, Murad MH, Yadav S, Kane SV, Pardi DS, Talwalkar JA, Loftus EV. Inflammatory bowel disease is associated with an increased risk of melanoma: a systematic review and meta-analysis. *Clin Gastroenterol Hepatol* 2014; **12**: 210-218 [PMID: 23644389 DOI: 10.1016/j.cgh.2013.04.033]
43 **Gutierrez-Dalmau A**, Campistol JM. Immunosuppressive therapy and malignancy in organ transplant recipients: a systematic review. *Drugs* 2007; **67**: 1167-1198 [PMID: 17521218]
44 **Penn I**. Kidney transplantation in patients previously treated for renal carcinomas. *Transpl Int* 1993; **6**: 350 [PMID: 8297466]
45 **Axelrad J**, Bernheim O, Colombel JF, Malerba S, Ananthakrishnan A, Yajnik V, Hoffman G, Agrawal M, Lukin D, Desai A, McEachern E, Bosworth B, Scherl E, Reyes A, Zaidi H, Mudireddy P, DiCaprio D, Sultan K, Korelitz B, Wang E, Williams R, Chen L, Katz S, Itzkowitz S. Risk of New or Recurrent Cancer in Patients With Inflammatory Bowel Disease and Previous Cancer Exposed to Immunosuppressive and Anti-Tumor Necrosis Factor Agents. *Clin Gastroenterol Hepatol* 2016; **14**: 58-64 [PMID: 26247164 DOI: 10.1016/j.cgh.2015.07.037]
46 **Dixon WG**, Watson KD, Lunt M, Mercer LK, Hyrich KL, Symmons DP. Influence of anti-tumor necrosis factor therapy on cancer incidence in patients with rheumatoid arthritis who have had a prior malignancy: results from the British Society for Rheumatology Biologics Register. *Arthritis Care Res* (Hoboken) 2010; **62**: 755-763 [PMID: 20535785 DOI: 10.1002/acr.20129]
47 **Strangfeld A**, Hierse F, Rau R, Burmester GR, Krummel-Lorenz B, Demary W, Listing J, Zink A. Risk of incident or recurrent malignancies among patients with rheumatoid arthritis exposed to biologic therapy in the German biologics register RABBIT. *Arthritis Res Ther* 2010; **12**: R5 [PMID: 20064207 DOI: 10.1186/ar2904]
48 **Axelrad JE**, Fowler SA, Friedman S, Ananthakrishnan AN, Yajnik V. Effects of cancer treatment on inflammatory bowel disease remission and reactivation. *Clin Gastroenterol Hepatol* 2012; **10**: 1021-1027.e1 [PMID: 22732273 DOI: 10.1016/j.cgh.2012.06.016]
49 **Rajca S**, Seksik P, Bourrier A, Sokol H, Nion-Larmurier I, Beaugerie L, Cosnes J. Impact of the diagnosis and treatment of cancer on the course of inflammatory bowel disease. *J Crohns Colitis* 2014; **8**: 819-824 [PMID: 24439392 DOI: 10.1016/j.crohns.2013.12.022]
50 **Green S**, Stock RG, Greenstein AJ. Rectal cancer and inflammatory bowel disease: natural history and implications for radiation therapy. *Int J Radiat Oncol Biol Phys* 1999; **44**: 835-840 [PMID: 10386640]
51 **Naito A**, Mizushima T, Takeyama H, Sakai D, Uemura M, Kudo T, Nishimura J, Shinzaki S, Hata T, Sato T, Takemasa I, Nakajima K, Iijima H, Yamamoto H, Doki Y, Mori M. Feasibility of Chemotherapy in Patients with Inflammatory Bowel Disease-Related Gastrointestinal Cancer. *Hepatogastroenterology* 2014; **61**: 942-946 [PMID: 26158146]

52 **Harrison ML**, Obermueller E, Maisey NR, Hoare S, Edmonds K, Li NF, Chao D, Hall K, Lee C, Timotheadou E, Charles K, Ahern R, King DM, Eisen T, Corringham R, DeWitte M, Balkwill F, Gore M. Tumor necrosis factor alpha as a new target for renal cell carcinoma: two sequential phase II trials of infliximab at standard and high dose. *J Clin Oncol* 2007; **25**: 4542-4549 [PMID: 17925549 DOI: 10.1200/JCO.2007.11.2136]

53 **Jatoi A**, Ritter HL, Dueck A, Nguyen PL, Nikcevich DA, Luyun RF, Mattar BI, Loprinzi CL. A placebo-controlled, double-blind trial of infliximab for cancer-associated weight loss in elderly and/or poor performance non-small cell lung cancer patients (N01C9). *Lung Cancer* 2010; **68**: 234-239 [PMID: 19665818 DOI: 10.1016/j.lungcan.2009.06.020]

54 **Wiedenmann B**, Malfertheiner P, Friess H, Ritch P, Arseneau J, Mantovani G, Caprioni F, Van Cutsem E, Richel D, DeWitte M, Qi M, Robinson D, Zhong B, De Boer C, Lu JD, Prabhakar U, Corringham R, Von Hoff D. A multicenter, phase II study of infliximab plus gemcitabine in pancreatic cancer cachexia. *J Support Oncol* 2008; **6**: 18-25 [PMID: 18257397]

55 **Hamaguchi T**, Wakabayashi H, Matsumine A, Sudo A, Uchida A. TNF inhibitor suppresses bone metastasis in a breast cancer cell line. *Biochem Biophys Res Commun* 2011; **407**: 525-530 [PMID: 21414299 DOI: 10.1016/j.bbrc.2011.03.051]

56 **Raaschou P**, Simard JF, Neovius M, Askling J. Does cancer that occurs during or after anti-tumor necrosis factor therapy have a worse prognosis? A national assessment of overall and site-specific cancer survival in rheumatoid arthritis patients treated with biologic agents. *Arthritis Rheum* 2011; **63**: 1812-1822 [PMID: 21305513 DOI: 10.1002/art.30247]

57 **Weber J**. Ipilimumab: controversies in its development, utility and autoimmune adverse events. *Cancer Immunol Immunother* 2009; **58**: 823-830 [PMID: 19198837 DOI: 10.1007/s00262-008-0653-8]

58 **Weber JS**, Dummer R, de Pril V, Lebbé C, Hodi FS. Patterns of onset and resolution of immune-related adverse events of special interest with ipilimumab: detailed safety analysis from a phase 3 trial in patients with advanced melanoma. *Cancer* 2013; **119**: 1675-1682 [PMID: 23400564 DOI: 10.1002/cncr.27969]

59 **Johnson DB**, Sullivan RJ, Ott PA, Carlino MS, Khushalani NI, Ye F, Guminski A, Puzanov I, Lawrence DP, Buchbinder EI, Mudigonda T, Spencer K, Bender C, Lee J, Kaufman HL, Menzies AM, Hassel JC, Mehnert JM, Sosman JA, Long GV, Clark JI. Ipilimumab Therapy in Patients With Advanced Melanoma and Preexisting Autoimmune Disorders. *JAMA Oncol* 2016; **2**: 234-240 [PMID: 26633184 DOI: 10.1001/jamaoncol.2015.4368]

60 **Slesser AA**, Bhangu A, Bower M, Goldin R, Tekkis PP. A systematic review of anal squamous cell carcinoma in inflammatory bowel disease. *Surg Oncol* 2013; **22**: 230-237 [PMID: 24050823 DOI: 10.1016/j.suronc.2013.08.002]

61 **Lopez A**, Mounier M, Bouvier AM, Carrat F, Maynadié M, Beaugerie L, Peyrin-Biroulet L. Increased risk of acute myeloid leukemias and myelodysplastic syndromes in patients who received thiopurine treatment for inflammatory bowel disease. *Clin Gastroenterol Hepatol* 2014; **12**: 1324-1329 [PMID: 24582568 DOI: 10.1016/j.cgh.2014.02.026]

62 **Bourrier A**, Carrat F, Colombel JF, Bouvier AM, Abitbol V, Marteau P, Cosnes J, Simon T, Peyrin-Biroulet L, Beaugerie L. Excess risk of urinary tract cancers in patients receiving thiopurines for inflammatory bowel disease: a prospective observational cohort study. *Aliment Pharmacol Ther* 2016; **43**: 252-261 [PMID: 26549003 DOI: 10.1111/apt.13466]

P- Reviewer: Felix K, Gonzalez-Perez RR, Kanat O **S- Editor**: Qi Y
L- Editor: A **E- Editor**: Wang CH

World Journal of Gastroenterology

Submit a Manuscript: http://www.wjgnet.com/esps/
Help Desk: http://www.wjgnet.com/esps/helpdesk.aspx
DOI: 10.3748/wjg.v22.i20.4802

World J Gastroenterol 2016 May 28; 22(20): 4802-4811
ISSN 1007-9327 (print) ISSN 2219-2840 (online)

TOPIC HIGHLIGHT

2016 Inflammatory Bowel Disease: Global view

Hydradenitis suppurativa and inflammatory bowel disease: An unusual, but existing association

Mariabeatrice Principi, Nicoletta Cassano, Antonella Contaldo, Andrea Iannone, Giuseppe Losurdo, Michele Barone, Mario Mastrolonardo, Gino Antonio Vena, Enzo Ierardi, Alfredo Di Leo

Mariabeatrice Principi, Antonella Contaldo, Andrea Iannone, Giuseppe Losurdo, Michele Barone, Enzo Ierardi, Alfredo Di Leo, Gastroenterology Section, Department of Emergency and Organ Transplantation, University of Bari, 70124 Bari, Italy

Nicoletta Cassano, Gino Antonio Vena, Dermatology and Venereology Private Practice, 70124 Bari/76121 Barletta, Italy

Mario Mastrolonardo, Dermatology Unit, Department of Medical and Surgical Sciences, University of Foggia, 71122 Foggia, Italy

Author contributions: Principi M, Ierardi E and Di Leo A designed the study, revised the manuscript and approved the final version; Cassano N, Contaldo A, Iannone A, Losurdo G and Mastrolonardo M collected the data and wrote the manuscript; Barone M and Vena GA revised the final version before approval.

Conflict-of-interest statement: No conflict of interest is declared by authors.

Correspondence to: Dr. Enzo Ierardi, Professor, Gastroenterology Section, Department of Emergency and Organ Transplantation, University of Bari, 70124 Bari, Italy. ierardi.enzo@gmail.com
Telephone: +39-80-5594034
Fax: +39-80-5593088

Received: March 18, 2016
Peer-review started: March 21, 2016
First decision: March 31, 2016
Revised: April 11, 2016
Accepted: May 4, 2016
Article in press: May 4, 2016
Published online: May 28, 2016

Abstract

Inflammatory bowel disease (IBD) could be associated with several extra-intestinal manifestations (EIMs) involving musculoskeletal, hepatopancreatobiliary, ocular, renal, and pulmonary systems, as well as the skin. In the last years, hidradenitis suppurativa (HS) is acquiring an increasing interest. IBD, especially Crohn's disease (CD), is among the most reported associated diseases in HS patients. The aim of this paper is to give a brief overview of data showing a possible epidemiologic and pathogenetic association between IBD and HS. We performed a pooled-data analysis of four studies and pooled prevalence of HS in IBD patients was 12.8%, with a 95%CI of 11.7%-13.9%. HS was present in 17.3% of subjects with CD (95%CI: 15.5%-19.1%) and in 8.5% of UC patients (95%CI: 7.0%-9.9%). Some items, especially altered immune imbalance, are generally involved in IBD pathogenesis as well as invoked by HS. Smoking is one of the most relevant risk factors for both disorders, representing a predictor of their severity, despite, actually, there being a lack of studies analyzing a possible shared pathway. A role for inheritance in HS and CD pathogenesis has been supposed. Despite a genetic susceptibility having been demonstrated for both diseases, further studies are needed to investigate a genetic mutual route. Although the pathogenesis of IBD and HS is generally linked to alterations of the immune response, recent findings suggest a role for intestinal and skin microbiota, respectively. In detail, the frequent finding of *Staphylococcus aureus* and coagulase-negative staphylococci on HS cutaneous lesions suggests a

bacterial involvement in disease pathogenesis. Moreover, microflora varies in the different cutaneous regions of the body and, consequently, two different profiles of HS patients have been identified on these bases. On the other hand, it is well-known that intestinal microbiota may be considered as "the explosive mixture" at the origin of IBD despite the exact relationship having not been completely clarified yet. A better comprehension of the role that some bacterial species play in the IBD pathogenesis may be essential to develop appropriate management strategies in the near future. A final point is represented by some similarities in the therapeutic management of HS and IBD, since they may be controlled by immunomodulatory drugs. In conclusion, an unregulated inflammation may cause the lesions typical of both HS and IBD, particularly when they coexist. However, this is still a largely unexplored field.

Key words: Hydradenitis suppurativa; Inflammatory bowel disease; Crohn's disease; Ulcerative colitis; Intestinal microbiota; Skin microbiota; Immunosuppressant drugs

Core tip: The present topic outlines the main data regarding a possible association between hydradenitis suppurativa and inflammatory bowel disease with particular attention to epidemiology, etiopathogenetic factors, genetic susceptibility, intestinal/skin microbiota and therapeutic analogies. Finally, an unregulated inflammation leading to microscopic granulomatous wounds may cause the lesions typical of both diseases, particularly when they coexist. However, this is still a largely unexplored field, and further studies are required.

Principi M, Cassano N, Contaldo A, Iannone A, Losurdo G, Barone M, Mastrolonardo M, Vena GA, Ierardi E, Di Leo A. Hydradenitis suppurativa and inflammatory bowel disease: An unusual, but existing association. *World J Gastroenterol* 2016; 22(20): 4802-4811 Available from: URL: http://www.wjgnet.com/1007-9327/full/v22/i20/4802.htm DOI: http://dx.doi.org/10.3748/wjg.v22.i20.4802

INTRODUCTION

Inflammatory bowel disease (IBD) is a group of chronic inflammatory conditions of the alimentary tract, that are mainly represented by Crohn's disease (CD) and ulcerative colitis (UC)[1]. These disorders could be associated with several extra-intestinal manifestations (EIMs) involving musculoskeletal, hepatopancreatobiliary, ocular, renal, and pulmonary systems, as well as the skin. In particular, joint, liver, eye, and skin EIMs are considered the most relevant and frequent manifestations[2].

Joint involvement is the most common EIM of IBD[2] and includes peripheral arthropathy, subclassified in pauciarticular, polyarticular forms, and axial arthropathy, such as sacroileitis and spondilitis. Primary sclerosing cholangitis represents the most common cause of hepatobiliary involvement in IBD patients, especially in UC[3,4]. Ocular complications, including episcleritis, scleritis and uveitis, occur more frequently in patients with isolated small intestinal CD[2].

Different dermatological manifestations may arise during the course of IBD. Indeed, pyoderma gangrenosum, psoriasis, Sweet's syndrome, aphthous stomatitis can be observed, even if erythema nodosum represents the most common IBD-associated dermatological disease. Moreover, in recent years, hydradenitis suppurativa (HS) has been acquiring an increasing interest, even though it may be frequently misdiagnosed as a consequence of an inadequate expertise[5].

HS[2] is defined as "a chronic inflammatory, recurrent, debilitating follicular skin disease that usually presents after puberty with painful deep seated inflamed lesions in the apocrine gland-bearing areas of the body, most commonly the axillae, inguinal and anogenital regions"[3]. HS diagnosis is based on the following clinical criteria: (1) the presence of typical lesions, (2) their characteristic sites, and (3) the chronic course of disease, showing recurring flares[5]. Hurley classification identifies three progressive stages of disease severity: (1) abscess formation, single or multiple, without sinus tract and scarring; (2) recurrent abscesses, with tract formation and healing wound, as well as single or multiple widely separated lesions; and (3) diffuse or multiple interconnected tracts and abscesses across entire area[4].

IBD, especially CD, is among the most reported comorbid diseases in HS patients[5].

Patients with HS and CD have more often been found to be smokers, and more likely to develop perianal disease, and to show an increased need for immunosuppressants and surgical resections[6]. Moreover, on the basis of recent evidence supporting the role of immune imbalance in both conditions[1-3,5-8], a shared pathogenesis between IBD and HS may be presumed. Indeed, multiple predisposing factors could influence the onset and progression of both diseases, *i.e.*, gut luminal agents, genetics and environmental factors[2].

The aim of this paper is to give a brief overview of data showing a possible epidemiologic and pathogenetic association between IBD and HS.

EPIDEMIOLOGY AND POOLED-DATA ANALYSIS OF LITERATURE

The first series of patients with both CD and HS was described by Church *et al*[9]. Twenty-four patients were recruited. The diagnosis of CD pre-dated that of

Table 1 Case reports about the association Crohn's disease-hydradenitis suppurativa

Ref.	*n*	Localization of CD	Localization of HS	CD predates HS
Ostlere *et al*[11], 1991	3	Colon	Anogenital	NR
Burrows *et al*[12], 1992	2	Colon	Anogenital, axillae, groin	NR
Gower-Rousseau *et al*[13], 1992	1	Ileo-colon	Perineum	NR
Attanoos *et al*[14], 1993	3	Colon, ileo-colon, colon-jejunum	Anogenital, axillae, perineum	Yes
Tsianos *et al*[15], 1995	1	Colon	Anogenital, axillae, sternum	Yes
Roy *et al*[16], 1997	1	Ileo-colon	Axillae	NR
Martínez *et al*[17], 2001	1	Ileo-colon	Axillae	Yes
Roussomoustakaki *et al*[18], 2003	1	Ileo-colon	Anogenital, axillae, groin	No
Yazdanyar *et al*[19], 2010	2	Colon	Axillae, groin, submammary	No
Goertz *et al*[20], 2008	1	Colon	Perianal	Yes
dos Santos *et al*[21], 2012	1	Rectum	Perianal	Yes
Hiraiwa *et al*[22], 2013	1	Ulcerative colitis	Groin	Yes

CD: Crohn's disease; HS: Hydradenitis suppurativa.

HS by an average of 3.5 years. More recently, other 15 patients with CD and HS followed at Mount Sinai Medical Center in the period 2003-2013 have been reported[10]. Apart from these few cohort studies, only case reports about association of IBD-HS have been published. Such single cases are summarized in Table 1[11-22].

Currently, the prevalence of HS in IBD has been investigated in four studies[23-26]. In the pilot one[23], 158 patients with IBD were asked by a standardized questionnaire about the presence of symptoms suggestive of HS, such as recurrent painful boils in the axillae and/or groin[27]. Further, a picture representing a classical HS skin lesion was shown to the patients in order to have a visual comparison with the injury they were suffering from. On the basis of this method, HS prevalence of 16% in patients with IBD was detected (17% and 14% in CD and in UC patients, respectively). The same authors replicated this study in a larger sample (1093 IBD patients), with an overall prevalence of 23%, in detail 26.3% for CD and 18.3% for UC[24]. A female predominance and a correlation between smoking and severe HS course were recorded. More recently, two other epidemiological studies were carried out. In a cohort study performed in the Olmsted county in Minnesota[25], 679 IBD patients were followed up over a median period of 19.8 years. In such patients, the clinical diagnosis of HS was directly established by dermatologists. HS was found in 8 patients (1.8%), 5 with CD and 3 with UC. A significant association with obesity, female sex and perianal CD disease was found. Two out of 3 subjects with UC had undergone ileal pouch-anal anastomosis. Compared with the control group, the incidence rate ratio of HS in IBD was 8.9 [95% confidence interval (CI): 3.6-17.5]. The 10- and 30-year cumulative incidence of HS was 0.85% and 1.55%, respectively. Axillae, groin, and thighs were the most common sites of involvement. Finally, Janse *et al*[26] showed an HS prevalence of 10.6% (134 out of 1260) in their IBD cohort, with a higher association with CD (15.1%) than with UC (6.1%). In this study, the diagnosis was achieved using a questionnaire validated for HS[27].

We performed a pooled-data analysis of the four cited studies, as shown in Figure 1. The pooled prevalence of HS in IBD patients was 12.8%, with a 95%CI of 11.7%-13.9%. HS was present in 17.3% of subjects with CD (95%CI: 15.5%-19.1%) and in 8.5% of UC patients (95%CI: 7.0%-9.9%), thus confirming a stronger association with CD. In three out of four studies, the diagnosis of HS was established by means of a questionnaire, and these three studies showed the highest prevalence rates. This detail may lead to the conclusion that such diagnostic strategy, despite validated, could overestimate the prevalence of HS in comparison to the clinician direct evaluation.

The clinical pattern of the IBD-HS association appears to be characterized by female predominance, increased frequency of tobacco smoking and by the fact that intestinal disease foregoes skin involvement. Clinical and pathogenetic features of HS and IBD association are summarized in Table 2.

PATHOGENETIC FACTORS

The pathogenesis of HS is still obscure. Ever-growing attention has been focused on the role of the immune system, and recent findings suggest the involvement of the interleukin (IL)-23/Th17 pathway in HS-related inflammatory response[28].

HS is characterized by epidermal alterations such as psoriasiform epidermal hyperplasia and keratin pluggings. In HS lesions, the epidermis is an active source of proinflammatory cytokines. It shows inflammasome activation and can be stimulated by IL-17$^+$ cells. The inflammatory process in HS involves the recruitment of innate immune cells, particularly IL-17-expressing neutrophils[29].

Impaired Notch signalling has been proposed to be a crucial pathomechanism of HS, capable of compromising apocrine gland homoeostasis and leading to subsequent stimulation of TLR-mediated innate immunity[30]. This mechanism has been hypothesized not only as an inducer of inflammation in

Table 2 Main clinical and pathogenesis features of hydradenitis suppurativa and inflammatory bowel disease (adapted from van der Zee *et al*[23])

	CD	UC	HS
Localization	Entire alimentary tract	Colon	Inverse areas of the skin
Layer of inflammation	Transmural	Mucosa	Deep derm
Confluency of lesions	No (skip lesions)	Yes	Yes
Fistulae	Yes	No	Yes
Influence of smoking	Aggravates	No (or improvement)	Aggravates
Disease chronicity	Yes	Yes	Yes
Genetic predisposition	Yes	Yes	Yes
Influence of microbiota	Yes	Yes	Yes
Female predominance	↑	↑	↑↑
Response to anti-TNFα therapy	Yes	Yes	Yes

CD: Crohn's disease; UC: Ulcerative colitis; HS: Hydradenitis suppurativa; TNFα: Tumor necrosis factor alpha.

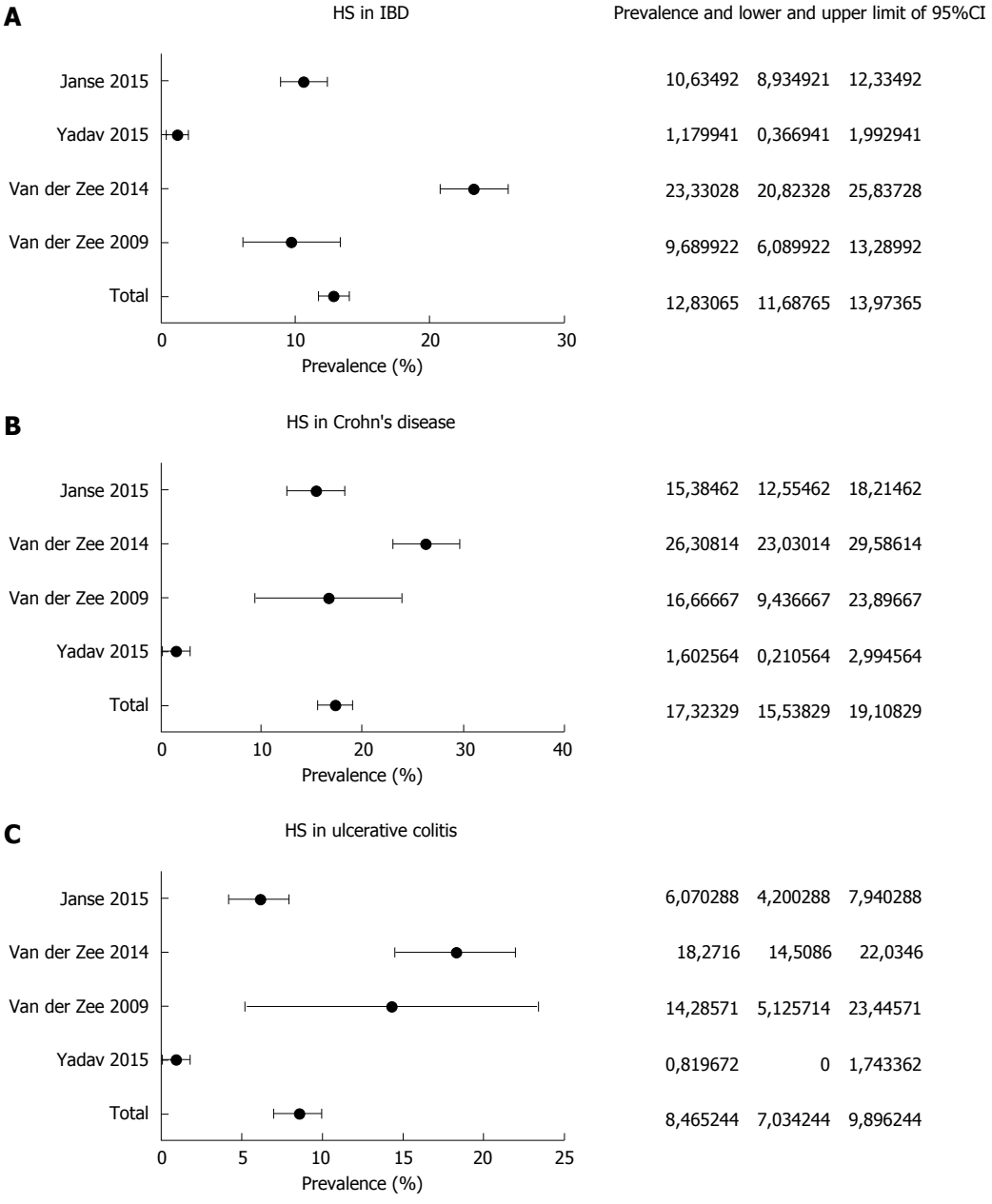

Figure 1 Pooled-data analysis of studies exploring the prevalence of Hydradenitis suppurativa in subjects with inflammatory bowel disease (A), either Crohn's disease (B) and ulcerative colitis (C). CD: Crohn's disease; IBD: Inflammatory bowel disease; HS: Hydradenitis suppurativa.

HS but also as responsible for an insufficient feedback regulation of overstimulated innate immunity, linking HS to other Th17-driven comorbidities.

On the other hand, an alteration of immune imbalance with a prevalence of inflammatory cytokines has been clearly stated for inflammatory bowel disease and, at the moment, strongly affects therapeutic approach[1-4].

Some items, generally involved in IBD pathogenesis, are invoked also for HS.

Smoking

Smoking is one of the most relevant risk factors for both HS and CD, representing a predictor of their severity[4,6].

In a recent meta-analysis enclosing 33 cohort studies[31], CD smoker patients showed increased risks of disease activity flares [odds ratio (OR) = 1.97; 95%CI: 1.21-2.01], post-surgical flares (OR = 1.97; 95%CI: 1.36-2.85), need for both first surgery (OR = 1.68; 95%CI: 1.33-2.12) and second surgery (OR = 2.17; 95%CI: 1.63-2.89). Conversely, the risk of such events was significantly reduced by smoking discontinuation[31-33]. Moreover, smoking has been reported as a well-established risk factor in HS by the European S1 guidelines for the treatment of HS/acne inversa[34]. An association between prevalence of HS and current smoking was found in a French cohort comprising about 10000 subjects (OR = 12.55; 95%CI: 8.58-18.38). This association was not demonstrated in former smokers[35]. Despite this evidence, some aspects of the correlation between HS severity and smoking remain controversial. Indeed, Sartorius *et al*[36] demonstrated a more severe course in active smokers as compared to non-smokers (P = 0.03), even though no statistical difference with former smokers was observed. Conversely, no effect of smoking on disease severity was found in a cohort study enclosing 268 HS patients[37].

Although the relationship between smoking and both diseases is supported by evidence, a hypothetical shared pathogenetic mechanism remains unclear and may be different for HS and CD. Indeed, nicotine may act in HS by multiple pathways, *i.e.,* over-stimulation of the sweat gland with a possible duct obstruction and consequent inflammation, chemotaxis for neutrophils, over-expression of tumor necrosis factor (TNF) alpha in keratinocytes and thickening of epidermidis by means of non-neuronal acetylcholine[38]. Simultaneously, in CD nicotine determines a more aggressive disease pattern, probably causing ischemia of microvessels, due to the implementation of carbon monoxide concentration, and by decreasing the expression of anti-inflammatory cytokines[37]. Finally, smoking cessation improves CD course, however this topic has not been largely investigated in HS[36].

On the other hand, it is well known that smoking does not affect UC course. In detail, nicotine may modulate the immune system by means of its binding to nicotine acetylcholine receptor α7 subunit expressed on macrophage, leading to a reduction of TNF-alpha and inflammation[39].

In conclusion, even if smoking represents a crucial pathogenic factor for both CD and HS, there is currently a lack of studies analyzing a possible shared pathway.

Genetic susceptibility

A role for inheritance in HS and CD pathogenesis has been supposed. Up to 40% of patients with HS show a familial history and an autosomal dominant pattern of inheritance has been observed in some familial cases[6]. Two loci on chromosome 6 and 19, and another one on chromosome 1 (1p21.1-1q25.3) have been linked to HS[6,40,41]. However, a recent report by Al-Ali *et al*[42] did not report any association between the locus 1p21.1-1q25.3 and this disease. Additionally, mutations involving presenilin-1 (PSEN1), presenilin enhancer-2 (PSENEN) and nicastrin (NCSTN) genes, which determine the inactivation of the gamma-secretase enzyme complex, have also been related to HS. The mutation of this enzyme complex is involved in HS pathogenesis via aberrant trichilemmal keratinization[6,41-44].

As for CD, the nucleotide-binding oligomerization domain containing 2 (*NOD2*) gene has been described as a possible inherited factor. Three different mutations have been identified in Caucasian CD patients: one frameshift and two missense mutations[45,46]. This gene is involved in intestinal homeostasis by detecting peptidoglycan released from the gut microbiota and driving a nuclear factor-κB (NF-κB)-mediated inflammatory response. The alteration of this process is supposed to play a role in the development of chronic intestinal inflammation[46].

A recent study by Janse *et al*[26] tried to identify a genetic link between HS and CD. The authors evaluated three different genes, *i.e.,* ELOVL fatty acid elongase 7 (*ELOVL7*) gene on chromosome 5, sulfotransferase family cytosolic 1B member 1 (*SULT1B1*) and sulfotransferase family 1E member 1(*SULT1E1*) genes on chromosome 4. These genes on chromosome 4 originate from the sulfotransferase family, encoding for enzymes that catalyze the sulphate conjugation of hormones, drugs, neurotransmitters and xenobiotic compounds. *SULT1E1* encodes for an enzyme regulating estrogen homeostasis[47]. These hormones seem to be involved in HS clinical course. Indeed, the reactivation of the disease usually occurs during hypoestrogenic states, thus estrogens seem to play a protective role[48]. Additionally, since adiposity is another supposed risk factor for HS, the expression of SULT1E1 in the abdominal subcutaneous tissue of obese people may be considered further evidence of the role of obesity[6]. Moreover, Ahima *et al*[47] demonstrated the co-expression of estrogen

sulfotransferase and TNF-alpha in abdominal adipose tissue of obese subjects. This last pro-inflammatory cytokine has a role in HS and CD pathogenesis as well as representing a therapeutic target for both diseases[49].

However, further studies are needed to investigate the genetic association between HS and CD.

Microbiota

Although the pathogenesis of IBD and HS is generally linked to alterations of the immune response[4,42], recent findings suggest a role for intestinal and skin microbiota, respectively[50,51].

The frequent finding of *Staphylococcus aureus* (*S. aureus*) and coagulase-negative staphylococci (CoNS) on HS cutaneous lesions suggests a bacterial involvement in disease pathogenesis[49].

Kurzen *et al*[52] supposed that nicotine may stimulate the growth of *S. aureus*. Jemec *et al*[53] suggested that *S. aureus* could induce the initial development process of HS, since it influences a series of anatomical alterations in the hair follicles facilitating inflammation and necrosis.

CoNS, in particular *Staphylococcus epidermidis* (*S. epidermidis*), usually are non-pathogenic microorganisms and commensals of the normal skin flora[54]. Lapins *et al*[55] found CoNS in 21 patients with HS. Sixteen out of the 21 patients showed CoNS in the deep levels of the skin, and in 9 of them CoNS were the only bacteria isolated, thus presuming a promoting activity for these germs in HS inflammation. A histological retrospective study analyzing 27 patients with HS showed the presence of *S. epidermidis*-related biofilm (*i. e.*, an extracellular matrix used by bacteria as a protective cover against host defense mechanisms and antimicrobial agents) in one-fifth of the samples located in hair follicles and sinus tracts[56].

Since microflora varies in the different cutaneous regions of the body, in relation to different distributions of hair follicles and glands, two different profiles of HS patients have been identified in a recent report by Guet-Revillet *et al*[57]. *Staphylococcus lugdunensis* was cultured from 58% of HS lesions, that were almost exclusively Hurley stage 1 lesions and more frequently located on the buttocks and the breasts, whereas a polymicrobial flora (strict anaerobes and/or anaerobic actinomycetes and/or streptococci of the milleri group) was predominantly associated with Hurley stage 2 and stage 3 lesions, especially in the axilla, and inguinal and gluteal folds.

Finally, antibiotics represent a treatment option for HS. In this regard, both topic and oral administrations act by killing involved bacteria and determining an indirect immunomodulation with reduction of pro-inflammatory cytokines and induction of neutrophil apoptosis[6].

With regard to IBD pathogenesis, modification of intestinal microflora, including about 1000 bacterial species, has been proposed as a promoting factor. Moreover, different bacterial compositions affect different sites of digestive system inflammation in animal models[51]. Indeed, in germ IL-10-/-germ free mice, bacterial colonization of *Escheria coli* or *Bilophila wadworthia* led to cecum or distal colon involvement, respectively[58]. Couturier-Maillard *et al*[59] described a potential link between genetic factors and microbiome modulation. They transplanted fecal microbiota from healthy wild-type mice to NOD2 deficient ones, obtaining a reduction of IBD risk. Conversely, disease risk rose in wild-type mice that received fecal microbiota from NOD2-deficient ones.

Smoking, as previously described for HS, could determine microbiota alterations, also in the gut with a reduction of Firmicutes and Actinobacteria and an increase of Proteobacteria and Bacteroides[60,61].

The modulation of gut microbiota is a potential therapeutic target in IBD and antibiotics, such as metronidazole and ciprofloxacin, which are currently used in Crohn's colitis, ileocolitis and pouchitis[3,51]. Nevertheless, tetracyclines, antibiotics largely used for HS, showed a Hazard Ratio for developing IBD, for any exposure to these drugs, of 1.39 (95%CI: 1.02-1.90) even if no clear explanation of the mechanism was found[62]. Additionally, a meta-analysis[63] of 11 observational studies, including 7208 IBD patients, demonstrated an OD of 1.57 (95%CI: 1.27-1.94) for IBD development after the exposure to any antibiotic. This risk was higher for CD (OR = 1.74; 95%CI: 1.35-2.23), metronidazole (OR = 5.01, 95%CI: 1.65-15.25), fluoroquinolones (OR = 1.79, 95%CI: 1.03-3.12) and in children (OR = 2.75; 95%CI: 1.72-4.38). Only the penicillin class was not associated with IBD onset.

THERAPEUTIC ANALOGIES

IBD and HS may show some similarities in the therapeutic management, since they may be controlled by some immunomodulatory drugs.

Indeed, HS may benefit from anti-TNF-alpha biologic therapy, similarly to IBD. Numerous case reports have demonstrated that infliximab improves skin lesions in patients with both CD and HS[18, 20,21,64,65]. On these bases, patients suffering from HS have been treated off-label with infliximab and etanercept, with a remission rate of about 35% and a decrease in HS activity of 50%[49,66]. In a systematic review by Haslund *et al*[67], almost all HS treated patients experienced a positive effect. Infliximab therapy is indicated in moderate-severe HS and is well tolerated, reduces skin pain, decreases disease severity and improves quality of life[49]. However, the long-term results are rather poor. Adalimumab has been recently approved by Food and Drug Administration for HS treatment. This FDA approval is based on the results of two pivotal Phase 3 studies, PIONEER I and PIONEER II[68-70].

Additionally, Ustekinumab is a monoclonal antibody

that selectively targets IL-12 and IL-23, which has been proposed for both IBD and HS treatment. In a setting of 17 HS patients, Ustekinumab allowed, after 40 wk, a moderate improvement in the 82% and a complete clinical response in the 47%[71]. A similar success rate, ranging from 46% to 65%, has been found in patients affected by CD who did not benefit from other anti-TNF alpha biologic agents[72,73].

Finally, other immunomodulators, such as corticosteroids and cyclosporine, have been proven to be effective for HS[73-76], similarly to IBD, thus supporting a possible link. However, the general level of evidence for these drugs is very low, given the small number of HS patients described in the literature so far and the lack of randomized controlled studies.

CONCLUSIVE REMARKS

IBD and HS share a chronic inflammatory trait. Despite an association between these two conditions having been reported only anecdotally, in recent years novel clinical investigations performed on large scale have shed new light on their association. The link between HS and IBD - CD in particular - could be stronger than expected. However, epidemiologic data is not supported by strong basic studies. Despite some evidence having shown that immune dysregulation, alteration of microbiota, genetic factors and tobacco smoking may underlie both diseases[52,59,77], a convincing *in vivo* proof has not yet been found. Additionally, the common therapeutic scenario described for IBD and HS might be another clue for their association.

CONCLUSION

An unregulated inflammation leading to microscopic granulomatous wounds may cause the lesions typical of both diseases, particularly when they coexist. However, this is still a largely unexplored field, and further studies are required to elucidate their pathogenesis and possible therapeutic approaches, as well as the interconnection between the disorders and the consequent practical implications. Indeed, despite the association between HS and IBD having been under-evaluated up to now, our pooled results show that the mean prevalence of HS in IBD is 12.8%, with a peak for CD (17.3%). Therefore, an existent link between these two conditions may be argued. On these bases, a careful skin examination should usually be performed in IBD patients, since the association CD-HS may be very disabling. Therefore, an early detection of HS in IBD could prevent the worsening of the skin disorder, thus avoiding the need ~~of~~ for some toxic medications.

REFERENCES

1 **Baumgart DC**, Sandborn WJ. Inflammatory bowel disease: clinical aspects and established and evolving therapies. *Lancet* 2007; **369**: 1641-1657 [PMID: 17499606 DOI: 10.1016/S0140-6736(07)60751-X]

2 **Levine JS**, Burakoff R. Extraintestinal manifestations of inflammatory bowel disease. *Gastroenterol Hepatol* (N Y) 2011; **7**: 235-241 [PMID: 21857821]

3 **Van Assche G**, Dignass A, Bokemeyer B, Danese S, Gionchetti P, Moser G, Beaugerie L, Gomollón F, Häuser W, Herrlinger K, Oldenburg B, Panes J, Portela F, Rogler G, Stein J, Tilg H, Travis S, Lindsay JO. Second European evidence-based consensus on the diagnosis and management of ulcerative colitis part 3: special situations. *J Crohns Colitis* 2013; **7**: 1-33 [PMID: 23040453 DOI: 10.1016/j.crohns.2012.09.005]

4 **Van Assche G**, Dignass A, Reinisch W, van der Woude CJ, Sturm A, De Vos M, Guslandi M, Oldenburg B, Dotan I, Marteau P, Ardizzone A, Baumgart DC, D'Haens G, Gionchetti P, Portela F, Vucelic B, Söderholm J, Escher J, Koletzko S, Kolho KL, Lukas M, Mottet C, Tilg H, Vermeire S, Carbonnel F, Cole A, Novacek G, Reinshagen M, Tsianos E, Herrlinger K, Oldenburg B, Bouhnik Y, Kiesslich R, Stange E, Travis S, Lindsay J. The second European evidence-based Consensus on the diagnosis and management of Crohn's disease: Special situations. *J Crohns Colitis* 2010; **4**: 63-101 [PMID: 21122490 DOI: 10.1016/j.crohns.2009.09.009]

5 **Dessinioti C**, Katsambas A, Antoniou C. Hidradenitis suppurrativa (acne inversa) as a systemic disease. *Clin Dermatol* 2014; **32**: 397-408 [PMID: 24767187 DOI: 10.1016/j.clindermatol.2013.11.006]

6 **Nazary M**, van der Zee HH, Prens EP, Folkerts G, Boer J. Pathogenesis and pharmacotherapy of Hidradenitis suppurativa. *Eur J Pharmacol* 2011; **672**: 1-8 [PMID: 21930119 DOI: 10.1016/j.ejphar.2011.08.047]

7 **Danby FW**, Margesson LJ. Hidradenitis suppurativa. *Dermatol Clin* 2010; **28**: 779-793 [PMID: 20883920 DOI: 10.1016/j.det.2010.07.003]

8 **Alikhan A**, Lynch PJ, Eisen DB. Hidradenitis suppurativa: a comprehensive review. *J Am Acad Dermatol* 2009; **60**: 539-561; quiz 562-563 [PMID: 19293006 DOI: 10.1016/j.jaad.2008.11.911]

9 **Church JM**, Fazio VW, Lavery IC, Oakley JR, Milsom JW. The differential diagnosis and comorbidity of hidradenitis suppurativa and perianal Crohn's disease. *Int J Colorectal Dis* 1993; **8**: 117-119 [PMID: 8245664 DOI: 10.1007/BF00341181]

10 **Kamal N**, Cohen BL, Buche S, Delaporte E, Colombel JF. Features of Patients With Crohn's Disease and Hidradenitis Suppurativa. *Clin Gastroenterol Hepatol* 2016; **14**: 71-79 [PMID: 25956836 DOI: 10.1016/j.cgh.2015.04.180]

11 **Ostlere LS**, Langtry JA, Mortimer PS, Staughton RC. Hidradenitis suppurativa in Crohn's disease. *Br J Dermatol* 1991; **125**: 384-386 [PMID: 1954129 DOI: 10.1111/j.1365-2133.1991.tb14178.x]

12 **Burrows NP**, Jones RR. Crohn's disease in association with hidradenitis suppurativa. *Br J Dermatol* 1992; **126**: 523 [PMID: 1610696 DOI: 10.1111/j.1365-2133.1992.tb11830.x]

13 **Gower-Rousseau C**, Maunoury V, Colombel JF, Coulom P, Piette F, Cortot A, Paris JC. Hidradenitis suppurativa and Crohn's disease in two families: a significant association? *Am J Gastroenterol* 1992; **87**: 928 [PMID: 1615957]

14 **Attanoos RL**, Appleton MA, Hughes LE, Ansell ID, Douglas-Jones AG, Williams GT. Granulomatous hidradenitis suppurativa and cutaneous Crohn's disease. *Histopathology* 1993; **23**: 111-115 [PMID: 8406382 DOI: 10.1111/j.1365-2559.1993.tb00468.x]

15 **Tsianos EV**, Dalekos GN, Tzermias C, Merkouropoulos M, Hatzis J. Hidradenitis suppurativa in Crohn's disease. A further support to this association. *J Clin Gastroenterol* 1995; **20**: 151-153 [PMID: 7769199 DOI: 10.1097/00004836-199503000-00018]

16 **Roy MK**, Appleton MA, Delicata RJ, Sharma AK, Williams GT, Carey PD. Probable association between hidradenitis suppurativa and Crohn's disease: significance of epithelioid granuloma. *Br J Surg* 1997; **84**: 375-376 [PMID: 9117312 DOI: 10.1002/bjs.1800840331]

17 **Martínez F**, Nos P, Benlloch S, Ponce J. Hidradenitis suppurativa and Crohn's disease: response to treatment with infliximab. *Inflamm Bowel Dis* 2001; **7**: 323-326 [PMID: 11720323 DOI: 10.1097/00054725-200111000-00008]

18 **Roussomoustakaki M**, Dimoulios P, Chatzicostas C, Kritikos HD, Romanos J, Panayiotides JG, Kouroumalis EA. Hidradenitis suppurativa associated with Crohn's disease and spondyloarthropathy: response to anti-TNF therapy. *J Gastroenterol* 2003; **38**: 1000-1004 [PMID: 14614610 DOI: 10.1007/s00535-003-1185-9]

19 **Yazdanyar S**, Miller IM, Jemec GB. Hidradenitis suppurativa and Crohn's disease: two cases that support an association. *Acta Dermatovenerol Alp Pannonica Adriat* 2010; **19**: 23-25 [PMID: 20976417]

20 **Goertz RS**, Konturek PC, Naegel A, Janka R, Amann K, Maennlein G, Wein A, Hahn EG, Boxberger F. Experiences with a long-term treatment of a massive gluteal acne inversa with infliximab in Crohn' s disease. *Med Sci Monit* 2009; **15**: CS14-CS18 [PMID: 19114971]

21 **dos Santos CH**, Netto PO, Kawaguchi KY, Parreira Alves JA, de Alencar Souza VP, Reverdito S. Association and management of Crohn's disease plus hidradenitis suppurativa. *Inflamm Bowel Dis* 2012; **18**: E801-E802 [PMID: 21993924 DOI: 10.1002/ibd.21897]

22 **Hiraiwa T**, Hanami Y, Yamamoto T. Hidradenitis suppurativa and multiple dermatofibromas in a patient with ulcerative colitis. *J Dermatol* 2013; **40**: 1071-1072 [PMID: 24330184 DOI: 10.1111/1346-8138.12316]

23 **van der Zee HH**, van der Woude CJ, Florencia EF, Prens EP. Hidradenitis suppurativa and inflammatory bowel disease: are they associated? Results of a pilot study. *Br J Dermatol* 2010; **162**: 195-197 [PMID: 19681876 DOI: 10.1111/j.1365-2133.2009.09430.x]

24 **van der Zee HH**, de Winter K, van der Woude CJ, Prens EP. The prevalence of hidradenitis suppurativa in 1093 patients with inflammatory bowel disease. *Br J Dermatol* 2014; **171**: 673-675 [PMID: 24673289 DOI: 10.1111/bjd.13002]

25 **Yadav S**, Singh S, Edakkanambeth Varayil J, Harmsen WS, Zinsmeister AR, Tremaine WJ, Davis MD, Wetter DA, Colombel JF, Loftus EV. Hidradenitis Suppurativa in Patients With Inflammatory Bowel Disease: A Population-Based Cohort Study in Olmsted County, Minnesota. *Clin Gastroenterol Hepatol* 2016; **14**: 65-70 [PMID: 25952308 DOI: 10.1016/j.cgh.2015.04.173]

26 **Janse IC**, Koldijk MJ, Spekhorst LM, Vila AV, Weersma RK, Dijkstra G, Horváth B. Identification of Clinical and Genetic Parameters Associated with Hidradenitis Suppurativa in Inflammatory Bowel Disease. *Inflamm Bowel Dis* 2016; **22**: 106-113 [PMID: 26422515 DOI: 10.1097/MIB.0000000000000579]

27 **Esmann S**, Dufour DN, Jemec GB. Questionnaire-based diagnosis of hidradenitis suppurativa: specificity, sensitivity and positive predictive value of specific diagnostic questions. *Br J Dermatol* 2010; **163**: 102-106 [PMID: 20331444 DOI: 10.1111/j.1365-2133.2010.09773.x]

28 **Schlapbach C**, Hänni T, Yawalkar N, Hunger RE. Expression of the IL-23/Th17 pathway in lesions of hidradenitis suppurativa. *J Am Acad Dermatol* 2011; **65**: 790-798 [PMID: 21641076 DOI: 10.1016/j.jaad.2010.07.010]

29 **Melnik BC**, Plewig G. Impaired Notch-MKP-1 signalling in hidradenitis suppurativa: an approach to pathogenesis by evidence from translational biology. *Exp Dermatol* 2013; **22**: 172-177 [PMID: 23489419 DOI: 10.1111/exd.12098]

30 **Lima AL**, Karl I, Giner T, Poppe H, Schmidt M, Presser D, Goebeler M, Bauer B. Keratinocytes and neutrophils are important sources of proinflammatory molecules in hidradenitis suppurativa. *Br J Dermatol* 2016; **174**: 514-521 [PMID: 26436522 DOI: 10.1111/bjd.14214]

31 **To N**, Gracie DJ, Ford AC. Systematic review with meta-analysis: the adverse effects of tobacco smoking on the natural history of Crohn's disease. *Aliment Pharmacol Ther* 2016; **43**: 549-561 [PMID: 26749371 DOI: 10.1111/apt.13511]

32 **Johnson GJ**, Cosnes J, Mansfield JC. Review article: smoking cessation as primary therapy to modify the course of Crohn's disease. *Aliment Pharmacol Ther* 2005; **21**: 921-931 [PMID: 15813828 DOI: 10.1111/j.1365-2036.2005.02424.x]

33 **Nunes T**, Etchevers MJ, Domènech E, García-Sánchez V, Ber Y, Peñalva M, Merino O, Nos P, Garcia-Planella E, Casbas AG, Esteve M, Taxonera Samsó C, Montoro Huguet M, Gisbert JP, Martín Arranz MD, García-Sepulcre MF, Barreiro-de Acosta M, Beltrán B, Alcaide Suárez N, Saro Gismera C, Cabriada JL, Cañas-Ventura A, Gomollón F, Panés J. Smoking does influence disease behaviour and impacts the need for therapy in Crohn's disease in the biologic era. *Aliment Pharmacol Ther* 2013; **38**: 752-760 [PMID: 23980933 DOI: 10.1111/apt.12440]

34 **Zouboulis CC**, Desai N, Emtestam L, Hunger RE, Ioannides D, Juhász I, Lapins J, Matusiak L, Prens EP, Revuz J, Schneider-Burrus S, Szepietowski JC, van der Zee HH, Jemec GB. European S1 guideline for the treatment of hidradenitis suppurativa/acne inversa. *J Eur Acad Dermatol Venereol* 2015; **29**: 619-644 [PMID: 25640693 DOI: 10.1111/jdv.12966]

35 **Revuz JE**, Canoui-Poitrine F, Wolkenstein P, Viallette C, Gabison G, Pouget F, Poli F, Faye O, Roujeau JC, Bonnelye G, Grob JJ, Bastuji-Garin S. Prevalence and factors associated with hidradenitis suppurativa: results from two case-control studies. *J Am Acad Dermatol* 2008; **59**: 596-601 [PMID: 18674845 DOI: 10.1016/j.jaad.2008.06.020]

36 **Sartorius K**, Emtestam L, Jemec GB, Lapins J. Objective scoring of hidradenitis suppurativa reflecting the role of tobacco smoking and obesity. *Br J Dermatol* 2009; **161**: 831-839 [PMID: 19438453 DOI: 10.1111/j.1365-2133.2009.09198.x]

37 **Vazquez BG**, Alikhan A, Weaver AL, Wetter DA, Davis MD. Incidence of hidradenitis suppurativa and associated factors: a population-based study of Olmsted County, Minnesota. *J Invest Dermatol* 2013; **133**: 97-103 [PMID: 22931916 DOI: 10.1038/jid.2012.255]

38 **Kelly G**, Sweeney CM, Tobin AM, Kirby B. Hidradenitis suppurativa: the role of immune dysregulation. *Int J Dermatol* 2014; **53**: 1186-1196 [PMID: 24961484 DOI: 10.1111/ijd.12550]

39 **Wang H**, Yu M, Ochani M, Amella CA, Tanovic M, Susarla S, Li JH, Wang H, Yang H, Ulloa L, Al-Abed Y, Czura CJ, Tracey KJ. Nicotinic acetylcholine receptor alpha7 subunit is an essential regulator of inflammation. *Nature* 2003; **421**: 384-388 [PMID: 12508119 DOI: 10.1038/nature01339]

40 **Yazdanyar S**, Jemec GB. Hidradenitis suppurativa: a review of cause and treatment. *Curr Opin Infect Dis* 2011; **24**: 118-123 [PMID: 21192260 DOI: 10.1097/QCO.0b013e3283428d07]

41 **Gao M**, Wang PG, Cui Y, Yang S, Zhang YH, Lin D, Zhang KY, Liang YH, Sun LD, Yan KL, Xiao FL, Huang W, Zhang XJ. Inversa acne (hidradenitis suppurativa): a case report and identification of the locus at chromosome 1p21.1-1q25.3. *J Invest Dermatol* 2006; **126**: 1302-1306 [PMID: 16543891 DOI: 10.1038/sj.jid.5700272]

42 **Al-Ali FM**, Ratnamala U, Mehta TY, Naveed M, Al-Ali MT, Al-Khaja N, Sheth JJ, Master DC, Maiti AK, Chetan GK, Nath SK, Radhakrishna U. Hidradenitis suppurativa (or Acne inversa) with autosomal dominant inheritance is not linked to chromosome 1p21.1-1q25.3 region. *Exp Dermatol* 2010; **19**: 851-853 [PMID: 20698881 DOI: 10.1111/j.1600-0625.2010.01088.x]

43 **Pink AE**, Simpson MA, Brice GW, Smith CH, Desai N, Mortimer PS, Barker JN, Trembath RC. PSENEN and NCSTN mutations in familial hidradenitis suppurativa (Acne Inversa). *J Invest Dermatol* 2011; **131**: 1568-1570 [PMID: 21412258 DOI: 10.1038/jid.2011.42]

44 **Pan Y**, Lin MH, Tian X, Cheng HT, Gridley T, Shen J, Kopan R. gamma-secretase functions through Notch signaling to maintain skin appendages but is not required for their patterning or initial morphogenesis. *Dev Cell* 2004; **7**: 731-743 [PMID: 15525534 DOI: 10.1016/j.devcel.2004.09.014]

45 **Hugot JP**, Laurent-Puig P, Gower-Rousseau C, Olson JM, Lee JC, Beaugerie L, Naom I, Dupas JL, Van Gossum A, Orholm M, Bonaiti-Pellie C, Weissenbach J, Mathew CG, Lennard-Jones JE, Cortot A, Colombel JF, Thomas G. Mapping of a susceptibility locus for Crohn's disease on chromosome 16. *Nature* 1996; **379**: 821-823 [PMID: 8587604 DOI: 10.1038/379821a0]

46 **Sartor RB**. Mechanisms of disease: pathogenesis of Crohn's disease and ulcerative colitis. *Nat Clin Pract Gastroenterol Hepatol* 2006; **3**: 390-407 [PMID: 16819502 DOI: 10.1038/ncpgasthep0528]

47 **Ahima RS**, Stanley TL, Khor VK, Zanni MV, Grinspoon SK. Estrogen sulfotransferase is expressed in subcutaneous adipose tissue

of obese humans in association with TNF-alpha and SOCS3. *J Clin Endocrinol Metab* 2011; **96**: E1153-E1158 [PMID: 21543429 DOI: 10.1210/jc.2010-2903]
48 **Harrison BJ**, Read GF, Hughes LE. Endocrine basis for the clinical presentation of hidradenitis suppurativa. *Br J Surg* 1988; **75**: 972-975 [PMID: 3219545 DOI: 10.1002/bjs.1800751011]
49 **Grant A**, Gonzalez T, Montgomery MO, Cardenas V, Kerdel FA. Infliximab therapy for patients with moderate to severe hidradenitis suppurativa: a randomized, double-blind, placebo-controlled crossover trial. *J Am Acad Dermatol* 2010; **62**: 205-217 [PMID: 20115947 DOI: 10.1016/j.jaad.2009.06.050]
50 **Loftus EV**. Clinical epidemiology of inflammatory bowel disease: Incidence, prevalence, and environmental influences. *Gastroenterology* 2004; **126**: 1504-1517 [PMID: 15168363 DOI: 10.1053/j.gastro.2004.01.063]
51 **Bringiotti R**, Ierardi E, Lovero R, Losurdo G, Di Leo A, Principi M. Intestinal microbiota: The explosive mixture at the origin of inflammatory bowel disease? *World J Gastrointest Pathophysiol* 2014; **5**: 550-559 [PMID: 25400998 DOI: 10.4291/wjgp.v5.i4.550]
52 **Kurzen H**, Kurokawa I, Jemec GB, Emtestam L, Sellheyer K, Giamarellos-Bourboulis EJ, Nagy I, Bechara FG, Sartorius K, Lapins J, Krahl D, Altmeyer P, Revuz J, Zouboulis CC. What causes hidradenitis suppurativa? *Exp Dermatol* 2008; **17**: 455-456; discussion 457-472 [PMID: 18400064 DOI: 10.1111/j.1600-0625.2008.00712_1.x]
53 **Jemec GB**, Faber M, Gutschik E, Wendelboe P. The bacteriology of hidradenitis suppurativa. *Dermatology* 1996; **193**: 203-206 [PMID: 8944341 DOI: 10.1159/000246246]
54 **Ring HC**, Riis Mikkelsen P, Miller IM, Jenssen H, Fuursted K, Saunte DM, Jemec GB. The bacteriology of hidradenitis suppurativa: a systematic review. *Exp Dermatol* 2015; **24**: 727-731 [PMID: 26119625 DOI: 10.1111/exd.12793]
55 **Lapins J**, Jarstrand C, Emtestam L. Coagulase-negative staphylococci are the most common bacteria found in cultures from the deep portions of hidradenitis suppurativa lesions, as obtained by carbon dioxide laser surgery. *Br J Dermatol* 1999; **140**: 90-95 [PMID: 10215774 DOI: 10.1046/j.1365-2133.1999.02613.x]
56 **Jahns AC**, Killasli H, Nosek D, Lundskog B, Lenngren A, Muratova Z, Emtestam L, Alexeyev OA. Microbiology of hidradenitis suppurativa (acne inversa): a histological study of 27 patients. *APMIS* 2014; **122**: 804-809 [PMID: 24475943 DOI: 10.1111/apm.12220]
57 **Guet-Revillet H**, Coignard-Biehler H, Jais JP, Quesne G, Frapy E, Poirée S, Le Guern AS, Le Flèche-Matéos A, Hovnanian A, Consigny PH, Lortholary O, Nassif X, Nassif A, Join-Lambert O. Bacterial pathogens associated with hidradenitis suppurativa, France. *Emerg Infect Dis* 2014; **20**: 1990-1998 [PMID: 25418454 DOI: 10.3201/eid2012.140064]
58 **Kim SC**, Tonkonogy SL, Albright CA, Tsang J, Balish EJ, Braun J, Huycke MM, Sartor RB. Variable phenotypes of enterocolitis in interleukin 10-deficient mice monoassociated with two different commensal bacteria. *Gastroenterology* 2005; **128**: 891-906 [PMID: 15825073 DOI: 10.1053/j.gastro.2005.02.009]
59 **Couturier-Maillard A**, Secher T, Rehman A, Normand S, De Arcangelis A, Haesler R, Huot L, Grandjean T, Bressenot A, Delanoye-Crespin A, Gaillot O, Schreiber S, Lemoine Y, Ryffel B, Hot D, Nùñez G, Chen G, Rosenstiel P, Chamaillard M. NOD2-mediated dysbiosis predisposes mice to transmissible colitis and colorectal cancer. *J Clin Invest* 2013; **123**: 700-711 [PMID: 23281400 DOI: 10.1172/JCI62236]
60 **Biedermann L**, Zeitz J, Mwinyi J, Sutter-Minder E, Rehman A, Ott SJ, Steurer-Stey C, Frei A, Frei P, Scharl M, Loessner MJ, Vavricka SR, Fried M, Schreiber S, Schuppler M, Rogler G. Smoking cessation induces profound changes in the composition of the intestinal microbiota in humans. *PLoS One* 2013; **8**: e59260 [PMID: 23516617 DOI: 10.1371/journal.pone.0059260]
61 **Matsuoka K**, Kanai T. The gut microbiota and inflammatory bowel disease. *Semin Immunopathol* 2015; **37**: 47-55 [PMID: 25420450 DOI: 10.1007/s00281-014-0454-4]
62 **Margolis DJ**, Fanelli M, Hoffstad O, Lewis JD. Potential association between the oral tetracycline class of antimicrobials used to treat acne and inflammatory bowel disease. *Am J Gastroenterol* 2010; **105**: 2610-2616 [PMID: 20700115 DOI: 10.1038/ajg.2010.303]
63 **Ungaro R**, Bernstein CN, Gearry R, Hviid A, Kolho KL, Kronman MP, Shaw S, Van Kruiningen H, Colombel JF, Atreja A. Antibiotics associated with increased risk of new-onset Crohn's disease but not ulcerative colitis: a meta-analysis. *Am J Gastroenterol* 2014; **109**: 1728-1738 [PMID: 25223575 DOI: 10.1038/ajg.2014.246]
64 **Lebwohl B**, Sapadin AN. Infliximab for the treatment of hidradenitis suppurativa. *J Am Acad Dermatol* 2003; **49**: S275-S276 [PMID: 14576652 DOI: 10.1016/S0190-9622(03)01132-0]
65 **Katsanos KH**, Christodoulou DK, Tsianos EV. Axillary hidradenitis suppurativa successfully treated with infliximab in a Crohn's disease patient. *Am J Gastroenterol* 2002; **97**: 2155-2156 [PMID: 12190206 DOI: 10.1111/j.1572-0241.2002.05950.x]
66 **Pelekanou A**, Kanni T, Savva A, Mouktaroudi M, Raftogiannis M, Kotsaki A, Giamarellos-Bourboulis EJ. Long-term efficacy of etanercept in hidradenitis suppurativa: results from an open-label phase II prospective trial. *Exp Dermatol* 2010; **19**: 538-540 [PMID: 19758320 DOI: 10.1111/j.1600-0625.2009.00967.x]
67 **Haslund P**, Lee RA, Jemec GB. Treatment of hidradenitis suppurativa with tumour necrosis factor-alpha inhibitors. *Acta Derm Venereol* 2009; **89**: 595-600 [PMID: 19997689 DOI: 10.2340/00015555-0747]
68 **Abbvie**. Drug molecule: Adalimumab (Humira). 2015 Available from: URL: https://dailymed.nlm.nih.gov/dailymed/drugInfo.cfm?setid=608D4F0D-B19F-46D3-749A-7159AA5F933D
69 **Kimball AB**, Kerdel F, Adams D, Mrowietz U, Gelfand JM, Gniadecki R, Prens EP, Schlessinger J, Zouboulis CC, van der Zee HH, Rosenfeld M, Mulani P, Gu Y, Paulson S, Okun M, Jemec GB. Safety and Efficacy of Adalimumab in Patients with Moderate to Severe Hidradenitis Suppurativa: Results from First 12 Weeks of PIONEER I, a Phase 3, Randomized, Placebo-Controlled Trial. Abstract #210 44th. Copenhagen, Denmark: Annual Meeting of the European Society for Dermatological Research (ESDR), 2014
70 **Kimball AB**, Kerdel F, Adams D, Mrowietz U, Gelfand JM, Gniadecki R, Prens EP, Schlessinger J, Zouboulis CC, van der Zee HH, Rosenfeld M, Mulani P, Gu Y, Paulson S, Okun M, Jemec GB. Efficacy and Safety of Adalimumab in Patients with Moderate to Severe Hidradenitis Suppurativa: Results from PIONEER II, a Phase 3, Randomized, Placebo-Controlled Trial. Abstract FC08.2. 22nd. Amsterdam, Netherlands: Congress of the European Dermatology and Venereology (EADV) Meeting, 2014
71 **Blok JL**, Li K, Brodmerkel C, Horvátovich P, Jonkman MF, Horváth B. Ustekinumab in hidradenitis suppurativa: clinical results and a search for potential biomarkers in serum. *Br J Dermatol* 2016; **174**: 839-846 [PMID: 26641739 DOI: 10.1111/bjd.14338]
72 **Harris KA**, Horst S, Gadani A, Nohl A, Annis K, Duley C, Beaulieu D, Ghazi L, Schwartz DA. Patients with Refractory Crohn's Disease Successfully Treated with Ustekinumab. *Inflamm Bowel Dis* 2016; **22**: 397-401 [PMID: 26752468 DOI: 10.1097/MIB.0000000000000624]
73 **Wils P**, Bouhnik Y, Michetti P, Flourie B, Brixi H, Bourrier A, Allez M, Duclos B, Grimaud JC, Buisson A, Amiot A, Fumery M, Roblin X, Peyrin-Biroulet L, Filippi J, Bouguen G, Abitbol V, Coffin B, Simon M, Laharie D, Pariente B. Subcutaneous Ustekinumab Provides Clinical Benefit for Two-Thirds of Patients With Crohn's Disease Refractory to Anti-Tumor Necrosis Factor Agents. *Clin Gastroenterol Hepatol* 2016; **14**: 242-250.e2 [PMID: 26432476 DOI: 10.1016/j.cgh.2015.09.018]
74 **Buckley DA**, Rogers S. Cyclosporin-responsive hidradenitis suppurativa. *J R Soc Med* 1995; **88**: 289P-290P [PMID: 7636825]
75 **Gupta AK**, Ellis CN, Nickoloff BJ, Goldfarb MT, Ho VC, Rocher LL, Griffiths CE, Cooper KD, Voorhees JJ. Oral cyclosporine in the treatment of inflammatory and noninflammatory dermatoses. A clinical and immunopathologic analysis. *Arch Dermatol* 1990; **126**: 339-350 [PMID: 2178558 DOI: 10.1001/archderm.1990.01670270071012]

76 **Danto JL**. Preliminary studies of the effect of hydrocortisone on hidradenitis suppurativa. *J Invest Dermatol* 1958; **31**: 299-300 [PMID: 13611353 DOI: 10.1038/jid.1958.124]
77 **Giudici F**, Maggi L, Santi R, Cosmi L, Annunziato F, Nesi G, Barra G, Bassotti G, De Palma R, Tonelli F. Perianal Crohn's disease and hidradenitis suppurativa: a possible common immunological scenario. *Clin Mol Allergy* 2015; **13**: 12 [PMID: 26203298 DOI: 10.1186/s12948-015-0018-8]

P- Reviewer: Actis GC, Ahluwalia NK, Capasso R, Zezos P
S- Editor: Gong ZM **L- Editor**: A **E- Editor**: Wang CH

World Journal of Gastroenterology

Submit a Manuscript: http://www.wjgnet.com/esps/
Help Desk: http://www.wjgnet.com/esps/helpdesk.aspx
DOI: 10.3748/wjg.v22.i20.4812

World J Gastroenterol 2016 May 28; 22(20): 4812-4823
ISSN 1007-9327 (print) ISSN 2219-2840 (online)

REVIEW

Current and emerging therapies in unresectable and recurrent gastric cancer

Erin Jou, Lakshmi Rajdev

Erin Jou, Lakshmi Rajdev, Department of Oncology, Montefiore Medical Center/Albert Einstein College of Medicine, Bronx, NY 10467, United States

Author contributions: Jou E and Rajdev L contributed equally to this work.

Conflict-of-interest statement: The authors declare that they have no conflict of interest.

Correspondence to: Lakshmi Rajdev, MD, Department of Oncology, Montefiore Medical Center/Albert Einstein College of Medicine, 1695 Eastchester Road, Bronx, NY 10467, United States. lrajdev@montefiore.org
Telephone: +1-718-4058404
Fax: +1-718-4058433

Received: February 25, 2016
Peer-review started: February 25, 2016
First decision: March 31, 2016
Revised: April 8, 2016
Accepted: April 20, 2016
Article in press: April 20, 2016
Published online: May 28, 2016

Abstract

Gastric cancer is one of the most lethal cancers worldwide despite many advances and options in therapy. As it is often diagnosed at an advanced stage, prognosis is poor with a median overall survival of less than twelve months. Chemotherapy remains the mainstay of treatment for these patients but it confers only a moderate survival advantage. There remains a need for new targeted treatment options and a way to better define patient populations who will benefit from these agents. In the past few years, there has been a better understanding of the biology, molecular profiling, and heterogeneity of gastric cancer. Our increased knowledge has led to the identification of gastric cancer subtypes and to the development of new targeted therapeutic agents. There are now two new targeted agents, trastuzumab and ramucirumab, that have recently been approved for the treatment of advanced and metastatic gastric cancer. There are also many other actively investigated targets, including epidermal growth factor receptor, the phosphatadylinositol 3-kinase/protein kinase B/mammalian target of rapamycin pathway, c-Met, poly ADP-ribose polymerase, and immune checkpoint inhibition. In this review, we discuss the current management of advanced gastric cancer as well as emerging targeted therapies and immunotherapy.

Key words: Advanced gastric cancer; Immunotherapy; Human epidermal growth factor receptor type 2; Targeted therapy; Vascular endothelial growth factor receptor

Core tip: Despite many advances in medical and surgical treatments, gastric cancer remains the second leading cause of cancer deaths. There is a greater understanding of the molecular heterogeneity of gastric cancer in recent years, resulting in the development and clinical investigation of different targeted agents. This review will discuss current treatment strategies and highlight targeted therapies and emerging drugs for advanced gastric cancer.

Jou E, Rajdev L. Current and emerging therapies in unresectable and recurrent gastric cancer. *World J Gastroenterol* 2016;

22(20): 4812-4823 Available from: URL: http://www.wjgnet.com/1007-9327/full/v22/i20/4812.htm DOI: http://dx.doi.org/10.3748/wjg.v22.i20.4812

INTRODUCTION

Gastric cancer is the fourth most common cancer and second leading cause of cancer deaths worldwide[1-3]. Gastric cancer is commonly diagnosed at an advanced stage and those patients with advanced disease have a median survival of less than 1 year[4]. Incidence rates and location of the tumor vary considerably between geographic regions. The highest incidence is in East Asia, Eastern Europe and parts of South and Central America where adenocarcinomas of the distal stomach are more prevalent. Cancers located in the proximal stomach or at the gastroesophageal junction (GEJ) are more prevalent in Western Europe and North America[5].

For patients with locally advanced and metastatic disease, chemotherapy remains the mainstay of treatment. Treatment options include platinums, irinotecan, epirubicin, fluoropyrimidines, and taxanes. The addition of a third drug to a two agent regimen increases the response rate with a modest survival improvement but at the expense of increased toxicity[6].

In recent years, advances in the understanding of the biology and molecular profiling of gastric cancer have led to the development of targeted treatments and to a better survival in select patients with advanced disease. There are now two new targeted agents, trastuzumab and ramucirumab, that have been approved in the last 5 years for the treatment of advanced or metastatic gastric cancer. Many more targeted therapies are currently being actively investigated.

In this review, we discuss the management of advanced gastric cancer and the progress in recent years in targeted therapy and immunotherapy.

CHEMOTHERAPY

Gastric cancer is a chemotherapy-sensitive disease with multiple active agents, including fluoropyrimidines, anthracyclines, platinum agents, taxanes, and irinotecan. Treatment of advanced gastric cancer with chemotherapy confers a moderate survival advantage and is primarily palliative. Combination therapy is associated with a higher response rate and increased survival when compared to single agents. The combination of cisplatin and fluorouracil (CF), or with epirubicin in a triple-drug regimen (ECF), has been the most commonly used doublet and triplet regimens. Newer agents were added to these regimens to try to improve response rate (RR), time to progression (TTP) and overall survival (OS). These trials are listed in Table 1.

The addition of docetaxel to cisplatin and fluorouracil (DCF) was shown to be associated with improvement of RR (37% *vs* 25%, $P = 0.01$), TTP (5.6 mo *vs* 3.7 mo, $P < 0.001$), and OS (9.2 mo *vs* 8.6 mo, $P = 0.02$); however there were significant grade 3 to 4 toxicities, including a high rate of febrile neutropenia[7]. These toxicities limited the adoption of this regimen into clinical practice.

Oxaliplatin (O) and oral fluoropyrimidines - capecitabine (X) and S-1 - have been substituted for cisplatin and fluorouracil (5-FU) respectively, and found to be noninferior and less toxic[8-10]. The phase Ⅲ REAL-2 study evaluated the efficacy of oxaliplatin and capecitabine in a 2 × 2 noninferiority trial with four regimens: ECF (control arm), ECX, EOF, and EOX. The median survival times were 9.9 mo, 9.9 mo, 9.3 mo and 11.2 mo respectively[9]. Progression free survival (PFS) and RR did not differ significantly between the different regimens. This study has led to the widespread use of oxaliplatin-based regimens in the frontline treatment of advanced gastric and GEJ cancer.

In Japan, the SPIRITS trial showed that the combination of cisplatin and S-1 (CS) significantly improved OS when compared to S-1 monotherapy (13 mo *vs* 11 mo), leading to this doublet being considered standard first-line in Japan[11]. However, in the United States and Europe, the FLAGS study showed no improvement in outcome when substituting S-1 for 5-FU in combination with cisplatin, so S-1 remains unlicensed in these areas[12].

Irinotecan has also been evaluated in combination with fluorouracil in patients with advanced gastric cancer with no significant differences in response rate, progression free and overall survival compared to the standard care[13,14]. This regimen was found to be less toxic so irinotecan has now been incorporated into the treatment approach.

Although most patients receive first-line chemotherapy, patients who progress after treatment usually have a worsened performance status, which limits treatment options. However, recent studies assessed the administration of irinotecan or docetaxel monotherapy as second-line therapy compared to best supportive care and demonstrated a survival advantage with chemotherapy[15-17]. Therefore, it is now considered standard of care for appropriate patients with a preserved performance status to receive second-line chemotherapy although no standard regimen has been established. A recent trial reported that irinotecan and taxanes have similar survival outcomes[18].

Despite all these treatments, however, the median survival is less than 1 year. There remains a need for new treatment options with targeted therapy and a way to identify which patients would benefit from these new agents.

Table 1 First line chemotherapy completed trials

Ref.	Arms	*n*	TTP/PFS (mo)	OS (mo)
Van Cutsem *et al*[7]	DCF *vs* CF	445	TTP: 5.6 *vs* 3.7 *P* < 0.001	9.2 *vs* 8.6 *P* = 0.02
Al-Batran *et al*[8]	FLO *vs* FLP	220	PFS: 5.8 *vs* 3.9 *P* = 0.077	10.7 *vs* 8.8
REAL-2[9]	ECF *vs* ECX *vs* EOF *vs* EOX	1002	PFS: 6.2 *vs* 6.7 *vs* 6.5 *vs* 7.0	9.9 *vs* 9.9 *vs* 9.3 *vs* 11.2
Kang *et al*[10]	XP *vs* FP	316	PFS: 5.6 *vs* 5.0	10.5 *vs* 9.3
SPIRITS[11]	CS *vs* S-1	298	PFS: 6.0 *vs* 4.0 *P* < 0.0001	13.0 *vs* 11.0 *P* = 0.04
FLAGS[12]	CS *vs* CF	1053	PFS: 4.8 *vs* 5.5 *P* = 0.920	8.6 *vs* 7.9 *P* = 0.20
Dank *et al*[13]	IF *vs* CF	333	TTP: 5.0 *vs* 4.2 *P* = 0.088	9.0 *vs* 8.7
Guimbaud *et al*[14]	FOLFIRI *vs* ECX	416	PFS: 5.3 *vs* 5.8 *P* = 0.960	9.5 *vs* 9.7 *P* = 0.95

DCF: Docetaxel/cisplatin/fluorouracil; CF: Cisplatin/fluorouracil; FLO: Fluorouracil/leucovorin/oxaliplatin; FLP: Fluorouracil/leucovorin/cisplatin; ECF: Epirubicin/cisplatin/fluorouracil; ECX: Epirubicin/cisplatin/capecitabine; EOF: Epirubicin/oxaliplatin/fluorouracil; EOX: Epirubicin/oxaliplatin/capecitabine; XP: Cisplatin/capecitabine; FP: Cisplatin/fluorouracil; CS: Cisplatin/S-1; SOX: S-1/oxaliplatin; IF: Irinotecan/fluorouracil; FOLFIRI: Fluorouracil/leucovorin/irinotecan.

MOLECULAR CLASSIFICATION

Gastric cancer is a heterogeneous disease; however, it wasn't until recently that we developed a better understanding of the molecular and genomic basis of gastric cancer. The Cancer Genome Atlas proposed four molecularly unique subtypes of gastric cancer: tumors positive for Epstein-Barr virus (EBV), microsatellite unstable (MSI) tumors, genomically stable tumors and tumors with chromosomal instability[19].

Tumors associated with EBV were predominantly in the fundus or body and were shown to have a higher prevalence of mutations in *PIK3CA* (approximately 80%), extensive DNA hypermethylation, overexpression of PD-L1 and PD-L2, and EBV-CpG island methylator phenotype (CIMP) expression. MSI tumors were diagnosed at a relatively older age (median age 72 years) and showed elevated mutation rates, gastric CIMP and *MLH1* silencing but generally lacked targetable amplifications. Unlike in colorectal cancer, BRAF mutations were not seen in gastric MSI tumors. Genomically stable tumors tended to be diagnosed at an earlier age (median age 59 years) and were enriched for diffuse histology, associated with *CDH1* and *RHOA* mutations and CLDN18-ARHGAP fusion, which is implicated in cell motility. Almost half of gastric tumors demonstrated chromosomal instability, which was predominantly intestinal histology with an elevated frequency in the GEJ and cardia and showed marked aneuploidy. They were associated with *TP53* mutation with RTK-RAS activation.

This study showed distinct genomic features in the different molecular subtypes that provide a guide to targeted therapy and allow for development of clinical trials to explore therapies in defined sets of patients.

TARGETED THERAPIES

Human epidermal growth factor receptor 2 inhibitors

Human epidermal growth factor receptor 2 (HER2) is a transmembrane tyrosine kinase receptor belonging to the epidermal growth factor receptor (EGFR) family. Activation of the HER2 receptor activates downstream signals in the Ras/Raf/mitogen-activated protein kinase (MAPK) and phosphatadylinositol 3-kinase (PI3K)/protein kinase B (Akt)/mammalian target of rapamycin (mTOR) pathways that are responsible for regulating a variety of tumor biology, such as cell growth, differentiation, and survival[20-22]. The reported HER2 positivity in patients with gastric cancer ranges widely from 6% to 34% depending on the histologic subtype and location with the highest rates of expression observed in intestinal type tumors and in cancers located in the GEJ[23-25]. Unlike in breast cancer where overexpression of HER2 associates with a more aggressive tumor[26], the prognostic role of HER2 in gastric cancer is less clear. Also HER2 testing in gastric cancer differs from that in breast cancer because of inherent differences in tumor biology - gastric cancer more frequently shows tumor heterogeneity and incomplete membrane staining due to its high frequency of glandular formation[27]. There are several different strategies for targeting HER2: anti-HER2 monoclonal antibodies or small-molecule tyrosine kinase inhibitors (TKIs). Table 2 summarizes the completed trials with targeted agents in advanced gastric cancer and Table 3 outlines the ongoing trials.

The first targeted agent approved in gastric cancer was trastuzumab, which acts on the extracellular domain of the HER2 receptor and inhibits HER2-mediated signaling. Trastuzumab for gastric cancer (ToGA) was a phase Ⅲ, randomized controlled trial

Table 2 Targeted therapy completed trials

Ref.	Name Phase	Indication	Line	Arms	*n*	PFS (mo)	OS (mo)
HER2							
[28]	ToGA Phase Ⅲ	HER2(+) Adv/Met GC and GEJ	1st	Fluoropyrimidine/cisplatin ± trastuzumab	594	6.7 *vs* 5.5 *P* = 0.0002	13.8 *vs* 11.1 *P* = 0.0050
[29]	LOGiC Phase Ⅲ	HER2(+) Adv/Met GC and GEJ	1st	CapeOx ± lapatinib	545	6.4 *vs* 5.4 p = 0.1000	12.2 *vs* 10.5 *P* = 0.3492
[30]	TyTAN Phase Ⅲ	HER2(+) Adv/Met GC and GEJ	2nd	Paclitaxel ± lapatinib	261	5.4 *vs* 4.4 *P* = 0.2441	11.0 *vs* 8.9 *P* = 0.2088
EGFR							
[36]	EXPAND Phase Ⅲ	Adv/Met GC and GEJ	1st	Capecitabine/cisplatin ± cetuximab	904	4.4 *vs* 5.9 *P* = 0.3200	9.4 *vs* 10.7 *P* = 0.9500
[37]	REAL3 Phase Ⅲ	Adv/Met GC and GEJ	1st	EOX *vs* modified EOX + panitumumab	553	6.0 *vs* 7.4 *P* = 0.0680	8.8 *vs* 11.3 *P* = 0.013
VEGFR							
[48]	Sunitinib Phase Ⅱ	Adv GC and GEJ	2nd	Sunitinib	78	2.3	6.8
[49]	Sunitinib Phase Ⅱ	Adv GC and GEJ	2nd or 3rd	FOLFIRI ± sunitinib	91	3.6 *vs* 3.3 *P* = 0.6600	10.5 *vs* 9.0 *P* = 0.2100
[50]	Sorafenib Phase Ⅱ	Adv/Met GC and GEJ	1st	Docetaxel/cisplatin + sorafenib	44	5.8	13.6
[51]	Sorafenib Phase Ⅱ	Adv GC and GEJ	2nd	Oxaliplatin + sorafenib	40	3	6.5
[53]	Regorafenib Phase Ⅱ	Adv GC and GEJ	2nd or 3rd	Regorafenib *vs* placebo	152	11.1 wk *vs* 3.9 wk *P* < 0.0001	25 wk *vs* 19.4 wk *P* = 0.1100
[41]	AVAGAST Phase Ⅲ	Adv GC and GEJ	1st	Capecitabine/cisplatin ± bevacizumab	774	6.7 *vs* 5.3 *P* = 0.0037	12.1 *vs* 10.1 *P* = 0.1002
[43]	REGARD Phase Ⅲ	Met GC and GEJ	2nd	BSC ± ramucirumab	355	2.1 *vs* 1.3 *P* < 0.0001	5.2 *vs* 3.8 *P* = 0.0473
[44,45]	RAINBOW Phase Ⅲ	Met GC and GEJ	2nd	Paclitaxel ± ramucirumab	665	4.4 *vs* 2.86 *P* < 0.0001	9.63 *vs* 7.36 *P* = 0.0169
[47]	Apatinib Phase Ⅲ	Adv GC and GEJ	3rd	Apatinib *vs* placebo	270	78 d *vs* 53 d *P* < 0.0001	195 d *vs* 140 d *P* < 0.016
mTOR							
[58]	GRANITE-1 Phase Ⅲ	Adv GC and GEJ	2nd or 3rd	BSC ± everolimus	656	1.7 *vs* 1.4 *P* = 0.0010	5.4 *vs* 4.3 *P* = 0.124

Adv: Advanced; Met: Metastatic; GC: Gastric cancer; GEJ: Gastroesophageal junction; CapeOx: Capecitabine/oxaliplatin; EOX: Epirubicin/oxaliplatin/capecitabine; FOLFIRI: Fluorouracil/leucovorin/irinotecan; BSC: Best supportive care; HER2: Human epidermal growth factor receptor 2; EGFR: Epidermal growth factor receptor; VEGFR: Vascular endothelial growth factor receptor; mTOR: Mammalian target of rapamyin.

involving 584 treatment naïve patients with metastatic or locally advanced unresectable HER2-overexpressing (defined as IHC3+ or FISH positive) gastric or GEJ adenocarcinoma[28]. The addition of trastuzumab to standard chemotherapy demonstrated a significant clinical benefit with higher response rate (47% *vs* 35%), improved progression-free survival (PFS) (6.7 mo *vs* 5.5 mo) and improved OS (13.8 mo *vs* 11.1 mo) compared to the chemotherapy alone arm. In an exploratory analysis, trastuzumab had the greatest survival benefit in patients with IHC3+ tumors, and with FISH+/IHC2+ tumors and ineffective in those with FISH positive but IHC 0 or 1+ tumors. Based on this data, trastuzumab was approved in combination with chemotherapy for the treatment of patients with metastatic HER2-overexpressing gastric or GEJ adenocarcinoma who have not received prior treatment. The ongoing HELOISE trial is evaluating whether a higher dose of trastuzumab in patients with a high tumor burden will have improved OS compared to the standard dosing [NCT01450696].

Given these significant results from the ToGA study, other strategies to target HER2 have been evaluated. Lapatinib is a tyrosine kinase inhibitor of EGFR and HER2 that binds to the intracellular ATP binding site of these kinases and interferes with their activation. However, unlike with trastuzumab, the trials with lapatinib failed to meet their primary endpoints. The phase Ⅲ LOGiC trial evaluated the addition of lapatinib to capecitabine and oxaliplatin as first line therapy in 545 patients with HER2 positive advanced gastric and GEJ adenocarcinomas[29]. Median OS was 12.2 *vs* 10.5 mo in the lapatinib arm compared to the placebo arm with a hazard ratio (HR) of 0.91 (95%CI: 0.73-1.12, *P* = 0.35). However, subgroup analysis showed that certain subgroups - Asian patients (median OS 16.5 mo *vs* 10.9 mo, HR = 0.91) and those under 60 years (median OS 12.9 mo *vs* 9 mo, HR = 0.69) - had significant improvements in OS. Similar negative results were seen in the second line setting: the TyTAN trial compared weekly paclitaxel with or without lapatinib and although the median OS was prolonged by two months (11.0 mo *vs* 8.9 mo, HR = 0.84), it was not statistically significant[30]. The subgroup of

Table 3 Ongoing trials

Name Phase	Indication	Line	Agent	ClinicalTrials.gov Identifier
HER2				
HELOISE Phase Ⅲ	HER2(+) Met GC and GEJ	1st	Trastuzumab	NCT01450696
JACOB Phase Ⅲ	HER2(+) Met GC and GEJ	1st	Pertuzumab	NCT01774786
VEGFR				
RAINFALL Phase Ⅲ	HER2(-) Met GC and GEJ	1st	Ramucirumab	NCT02314117
PARP				
Olaparib Phase Ⅲ	Adv GC and GEJ	2nd	Olaparib	NCT01924533
Immune checkpoints				
KEYNOTE-059 Phase Ⅱ	Adv GC and GEJ		Pembrolizumab	NCT02335411
KEYNOTE-061 Phase Ⅲ	Adv GC and GEJ	2nd	Pembrolizumab	NCT02370498
KEYNOTE-062 Phase Ⅲ	Adv GC and GEJ	1st	Pembrolizumab	NCT02494583
MEDI4736 Phase Ⅰ/Ⅱ	Advanced solid tumors		MEDI4736	NCT01693562
JAVELIN Gastric 100 Phase Ⅲ	Adv/Met GC and GEJ	1st	Avelumab	NCT02625610
JAVELIN Gastric 300 Phase Ⅲ	Met/recurrent GC and GEJ	3rd	Avelumab	NCT02625623
Phase Ⅰ/Ⅱ	Met/recurrent GC and GEJ		MEDI4736 + Tremelimumab *vs* MEDI4736 *vs* Tremelimumab	NCT02340975
Phase Ⅰ/Ⅱ	Advanced solid tumors		Nivolumab +/- Ipilimumab	NCT01928394

Adv: Advanced; Met: Metastatic; GC: Gastric cancer; GEJ: Gastroesophageal junction; HER2: Human epidermal growth factor receptor 2; VEGFR: Vascular endothelial growth factor receptor; PARP: Poly ADP-ribose polymerase.

patients with IHC3+, however, did have a significant benefit in both PFS (5.6 mo *vs* 4.2 mo) and OS (14 mo *vs* 7.6 mo).

Two other drugs that have been FDA approved for the treatment of patients with metastatic HER2 positive breast cancer are being investigated in HER2 positive gastric cancer. Pertuzumab is an antibody that binds to a different site on HER2 than trastuzumab and inhibits the dimerization of HER2. The phase Ⅲ JACOB trial will evaluate the efficacy and safety of pertuzumab in combination with trastuzumab, fluoropyrimidine and cisplatin [NCT01774786]. TDM-1 is an antibody-drug conjugate of trastuzumab and a potent microtubule inhibitor DM1. The multicenter phase Ⅱ/Ⅲ GATSBY trial to evaluate TDM-1 *vs* a taxane in advanced gastric cancer as second line did not show an efficacy benefit of TDM-1 over taxane[31].

EGFR inhibitors

EGFR (HER1) is a member of the same family of tyrosine kinase receptors as HER2 and it activates the same intracellular signaling pathways that are responsible for regulating cell growth, differentiation, and survival[32,33]. EGFR overexpression occurs in 30%-60% of gastric cancer and is associated with a worse prognosis[34,35]. However, studies evaluating antibody inhibitors of EGFR have failed to demonstrate a survival advantage.

Cetuximab is a chimeric monoclonal IgG1 antibody that binds to the extracellular domain of EGFR and competitively inhibits the binding of EGF and other ligands. The phase Ⅲ trial EXPAND randomized 904 patients to capecitabine and cisplatin with or without cetuximab and did not find progression free or overall survival benefit for the cetuximab group (4.4 mo *vs* 5.6 mo and 9.4 mo *vs* 10.7 mo, respectively)[36]. Response rates were comparable between the two arms (30% *vs* 29%) but the cetuximab arm resulted in a higher rate of grade 3 and 4 toxicity (88% *vs* 77%).

Panitumumab is a fully humanized monoclonal IgG2 antibody targeting EGFR. The phase Ⅱ/Ⅲ REAL3 trial evaluated the efficacy of epirubicin, oxaliplatin, and capecitabine with or without panitumumab as first line therapy[37]. The phase Ⅲ study did not show any benefit and actually showed a lower survival in the experimental arm at a preplanned interim analysis (median OS 8.8 mo *vs* 11.3 mo) so it was discontinued prematurely.

Vascular endothelial growth factor receptor inhibitors

Pathological angiogenesis is crucial for tumor growth, survival and metastases. VEGF is an important regulator of angiogenesis and acts on its vascular endothelial growth factor receptor (VEGFR) to stimulate endothelial cells to divide and migrate to form new blood vessels or sprout from existing ones and to help newly formed

blood vessels survive[38]. VEGFR is overexpressed in 30%-60% of gastric cancer and is a predictor of poor prognosis[39,40]. Trials evaluating anti-VEGF agents are listed in Table 2.

Bevacizumab is a recombinant humanized IgG1 monoclonal antibody against VEGF. AVAGAST was a large randomized phase Ⅲ study evaluating the addition of bevacizumab to capecitabine and cisplatin[41]. Median PFS (6.7 mo *vs* 5.3 mo) and overall response rate (ORR) (46% *vs* 37.4%) was significantly improved in the bevacizumab arm but the primary endpoint of OS was not met (12.1 mo *vs* 10.1 mo, $P = 0.1002$). In subgroup analysis, patients from North and South America showed survival benefit from the addition of bevacizumab (11.5 mo *vs* 6.8 mo, HR = 0.63, 95%CI: 0.43-0.94), patients from Europe showed a trend toward benefit (HR = 0.85, 95%CI: 0.63-1.14), and patients from Asia had no benefit (HR = 0.97, 95%CI: 0.75-1.25), further suggesting heterogeneity of this disease worldwide. Similar negative results were seen in the AVATAR study where bevacizumab was added to capecitabine and cisplatin in Asian patients with advanced gastric cancer[42].

Ramucirumab is a fully humanized monoclonal antibody against VEGFR-2. The phase Ⅲ REGARD trial compared ramucirumab monotherapy with best supportive care in the second line[43]. The study showed improved median PFS (2.1 mo *vs* 1.3 mo, $P < 0.001$) and median OS (5.2 mo *vs* 3.8 mo, $P = 0.047$). In the phase Ⅲ RAINBOW study, advanced gastric or GEJ adenocarcinoma patients were randomized to paclitaxel with or without ramucirumab in the second line setting[44,45]. The addition of ramucirumab showed improved OS of 9.6 mo *vs* 7.4 mo compared to paclitaxel alone ($P = 0.0169$) and improved PFS (4.4 mo *vs* 2.9 mo). Based on these trial results, ramucirumab was approved as a single agent for treatment of patients with advanced gastric or GEJ cancer after progressing on prior treatment, as well as in combination with paclitaxel. This is the first approval of a biologic agent in an unselected population with gastric and GEJ cancers. Ramucirumab was also tested in the first line setting in combination with FOLFOX, but it did not show an improvement in the primary endpoint of PFS or median[46]. It is also being studied in the phase Ⅲ RAINFALL trial comparing PFS in patients with HER2-negative, metastatic gastric or GEJ adenocarcinoma receiving ramucirumab with cisplatin and fluoropyrimidine *vs* cisplatin and fluoropyrimidine as first line treatment [NCT02314117].

A phase Ⅲ trial assessing a TKI against VEGFR, apatinib, with a two-to-one randomization to apatinib *vs* placebo in the third line setting in advanced gastric cancer showed that median OS was significantly prolonged in the apatinib group of 195 d *vs* 140 d ($P < 0.016$), as was median PFS of 78 d *vs* 53 d ($P < 0.0001$)[47].

Sunitinib and sorafenib are multitargeted TKIs that inhibit VEGFR as well as other kinases. Phase Ⅱ trials have been conducted both as monotherapy and in combination with chemotherapy and have shown mixed results[48-51]. These results are summarized in Table 2. Pazopanib, another multitargeted TKI that inhibits angiogenesis, showed marginal efficacy in a phase Ⅱ trial as first line with 5-FU/oxaliplatin[52]. Data on a phase Ⅱ trial of regorafenib, a multi-kinase inhibitor, following progression after 1st or 2nd line chemotherapy demonstrated significantly improved PFS in the regorafenib arm[53]. Pre-specified analyses found the effect of regorafenib to be greater in South Korea than in Australia, New Zealand and Canada.

mTOR inhibitors

PI3K/Akt/mTOR pathway is a major downstream cascade of tyrosine kinase signaling and one of the most frequently altered pathways in malignancies. mTOR, an intracellular key serine/threonine protein kinase, regulates cell growth, motility, cellular metabolism and angiogenesis[54,55]. Dysregulation of this pathway is associated with poor survival and may contribute to resistance to chemotherapy[56,57].

Everolimus, an oral mTOR inhibitor, was evaluated in the phase Ⅲ GRANITE-1 trial where it was compared to best supportive care in advanced gastric cancer that progressed after previous chemotherapy[58]. The trial randomly assigned 656 patients in a 2:1 ratio to everolimus or placebo. Although median PFS was improved (1.68 mo *vs* 1.41 mo, $P < 0.001$), the trial did not meet its primary endpoint of improved OS (5.39 *vs* 4.3 mo, $P = 0.124$). Everolimus is currently being evaluated in combination with paclitaxel as second line treatment in a phase Ⅲ trial [NCT01248403].

c-MET inhibitors

MET is a tyrosine kinase receptor and signals through RAS-MAPK and PI3K-AKT pathways to mediate cell migration, survival, invasion and angiogenesis. Aberrant HGF/MET signaling triggers multiple intracellular signals that lead to tumor growth, proliferation and metastasis[59]. In addition to oncogenesis, aberrant MET signaling has been associated with *in vitro* resistance to cytotoxic agents[60]. c-MET amplification is associated with a higher tumor stage, a more aggressive phenotype and a significantly diminished survival[61,62].

Crizotinib is a small molecule inhibitor of anaplastic lymphoma kinase and MET tyrosine kinase that is approved in non-small cell lung cancer. In a study of patients with gastroesophageal cancer, of the 489 tumors screened, 10 patients (2%) harbored MET amplification (> 5 copies)[63]. These tumors were more likely to be high-grade and present at advanced stages. Two out of these four patients had a clinical response with a delay in tumor progression. However the responses were transient and time to progression in these two patients was 3.7 mo and 3.5 mo.

Rilotumumab is a fully humanized monoclonal IgG2

against HGF that inhibits the binding of HGF to the MET receptor. A phase Ⅱ trial evaluating rilotumumab in combination with ECX in patients with untreated advanced gastroesophageal cancer showed minimally improved median PFS and median OS but an exploratory analysis showed that patients with high MET expression appeared to experience marked clinical benefit from addition of rilotumumab to ECX with improvement in median OS from 5.7 to 11.1 mo (HR = 0.29)[64,65]. These results led to 2 phase Ⅲ studies: RILOMET-1 (rilotumumab in combination with ECX as first-line treatment for advanced MET-positive gastroesophageal cancer) and RILOMET-2 (rilotumumab with cisplatin and capecitabine as first-line therapy in gastric cancer). However, data from RILOMET-1 showed that OS, PFS and ORR were statistically worse in the rilotumumab arm[66]. No subgroups seemed to benefit with rilotumumab, including those with higher percentages of cells with ⩾ 1+ MET expression.

Onartuzumab is a monovalent humanized monoclonal antibody against the MET receptor and prevents HGF binding to MET. Onartuzumab in combination with mFOLFOX6 was evaluated in patients with untreated metastatic gastroesophageal cancer that were HER2-negative and MET-positive (Ⅲ 50% of tumor with moderate-strong intensity staining by IHC based on central review) in a phase Ⅲ trial, MetGastric. The trial showed that the addition of onartuzumab to mFOLFOX6 did not improve PFS in the unselected population or in the MET-positive subgroup[67,68]. Monoclonal antibodies that target c-MET have limited activity as seen in the phase Ⅲ trials with rilotumumab and onartuzumab, and better biomarkers are needed to select patients for trials with c-MET inhibitors.

Poly ADP-ribose polymerase inhibitors

Poly ADP-ribose polymerase (PARP) is a family of proteins that are critical for the function of base excision repair (BER). BER repairs single strand DNA breaks. If these single strand breaks are not repaired, they become double strand breaks which leads to cell death[69]. PARP inhibitors interfere with BER and prevent this repair mechanism which may ultimately lead to death of tumor cells[70].

Olaparib was studied in a second line phase Ⅱ trial for metastatic or recurrent gastric cancer in combination with paclitaxel *vs* paclitaxel alone[71]. The trial found a statistically significant improvement in OS, but not PFS. Initial preclinical data suggested that responsiveness of gastric cancer cell lines to olaparib was associated with low ataxia telangiectasia mutated (ATM) protein levels, so the study performed a subset analysis and found that patients with low ATM showed a larger improvement in OS with olaparib. These results led to a phase Ⅲ trial of olaparib in combination with paclitaxel compared with paclitaxel monotherapy in patients with advanced gastric cancer who have progressed following first line therapy [NCT01924533]. Another PARP inhibitor, veliparib, is currently being studied in a phase I trial with FOLFIRI in patients with advanced gastric cancer [NCT01123876].

IMMUNOTHERAPY

Tumor cells have developed mechanisms in which they modulate the immune system, allowing them to escape the immune cells and provide a shield for which the tumor is able to invade, migrate, and grow[72,73]. Immune checkpoints are inhibitory pathways that maintain self-tolerance and protect tissues from damage when the immune system is active. The expression of immune-checkpoint proteins can be dysregulated by tumors, making this an important immune resistance mechanism[74]. This has led to increasing interest in immunotherapy as a treatment option in multiple solid malignancies.

Cytotoxic T-lymphocyte-associated antigen 4 (CTLA4) was the first immune checkpoint receptor to be clinically targeted. It is expressed exclusively on T cells and is a negative regulator of T-cell activation. There are two fully humanized CTLA4 antibodies, ipilimumab and tremelimumab. After ipilimumab became the first therapy to improve overall survival in patients with advanced melanoma[75], it is now being evaluated in other advanced cancers including gastric cancer. A phase Ⅱ trial to evaluate the efficacy of ipilimumab after first-line chemotherapy in the treatment of unresectable or metastatic gastric or GEJ adenocarcinomas was just completed and awaiting results [NCT01585987]. Tremelimumab was investigated in a phase Ⅱ trial as second-line treatment for patients with metastatic gastric cancer but had an ORR of only 5% and median OS similar to that of second-line chemotherapy[76].

Another immune-checkpoint protein which is expressed on T cells, programmed cell death protein 1 (PD-1), inhibits the activity of the T cell when bound to its ligands PD-L1 and PD-L2 on the surface of a cell. Tumor cells often overexpress PD-L1 or PD-L2 resulting in T cell anergy and escape from immunosurveillance. The KEYNOTE-012 phase Ib study of pembrolizumab, a monoclonal antibody that blocks PD-1 interaction with its ligands, in patients with recurrent and metastatic gastric cancer with PD-L1 tumor positivity based on a prototype IHC assay showed an ORR of 31.6% in Asia Pacific and 30% in the rest of world[77]. These results present an exciting novel strategy in the treatment of advanced gastric cancer. The phase Ⅱ KEYNOTE-059 of pembrolizumab with cisplatin and 5-FU as first-line is currently enrolling [NCT02335411]. Also, two phase Ⅲ trials, KEYNOTE-061 [NCT02370498] of pembrolizumab *vs* paclitaxel as second line therapy and KEYNOTE-062 [NCT02494583] of pembrolizumab alone or in combination with cisplatin and fluoropyrimidine *vs* chemotherapy as first line therapy, are currently ongoing.

There was preliminary evidence of an association

between PD-L1 expression and PFS (P = 0.032) and ORR (P = 0.071) in the KEYNOTE-012 study. This relationship between PD-L1 expression and clinical outcomes was further explored and found that PD-L1 expression level was associated with ORR (1-sided P = 0.10) and ORR was 22% (95%CI: 10-39) by central review and 33% (95%CI: 19-50) by investigator review[78]. The 6-mo PFS rate was 24% and the 6-mo OS rate was 69%. Another biomarker that may be predictive of anti-PD-1 therapy is mismatch repair-deficiency. A phase Ⅱ trial of pembrolizumab for the treatment of colorectal and other GI tumors, including gastric cancer, with mismatch repair-deficiency, or high microsatellite instability (MSI-H), demonstrated high ORR and prolonged PFS [immune-related ORR 71% (5 of 7 patients); immune-related PFS 67% (4 of 6 patients)] when treated with pembrolizumab, supporting the hypothesis that mismatch repair-deficient tumors are more responsive to PD-1 blockade than are mismatch repair-proficient tumors[79].

MEDI4736, a PD-L1 IgG1 antibody, is being studied in a phase Ⅰ/Ⅱ trial in patients with advanced solid tumors including gastric cancer and the results of the phase Ⅰ showed good clinical activity with tumor shrinkage and durable responses[80]. Expansion in multiple cancers is ongoing [NCT01693562]. Another PD-L1 inhibitor, Avelumab (MSB0010718C), is being investigated in phase I trials in advanced cancers [NCT01943461, NCT01772004] and in phase Ⅲ trials in the first line [NCT02625610] and third line [NCT02625623] settings. The combination of CTLA-4 and PDL-1 inhibitors is also being evaluated [NCT01975831, NCT02340975, NCT01928394]. These ongoing trials are outlined in Table 3.

CONCLUSION

Chemotherapy has long been the standard treatment for advanced gastric cancer. Current combination cytotoxic regimens are associated with response rates of ⩾ 40% but median survival is still less than one year. To improve on this outcome, we have made many advances in our knowledge of the molecular etiology and heterogeneity of gastric cancer, which has led to the development of different targeted therapies. The ToGA trial has established trastuzumab as a new standard of care for patients with HER2 positive (IHC3+ or IHC2+/FISH positive) advanced or metastatic gastric cancer, but this benefit is limited to only approximately 20% of patients with advanced disease. Ramucirumab has also been approved recently for treatment in the second line setting and offers a valuable alternative or addition to chemotherapy. Despite these advances, standard therapy for advanced gastric cancer in the first line setting for patients who are not HER2 positive is still combination chemotherapy with either a doublet or triplet of a platinum and a fluoropyrimidine. Second line options are still limited and include irinotecan, docetaxel, paclitaxel with or without ramucirumab or ramucirumab monotherapy.

There remains a need to better define patient populations who will benefit from targeted therapy and predict the response to drugs. The Cancer Genome Atlas Research Network has recently classified four molecular subtypes of gastric cancer and identified other possible targets for future clinical research. This will allow for the development of clinical trials in the future to explore therapies in defined sets of patients. Better use of biomarkers to select these sets of patients to improve outcomes will be crucial. Also, as our understanding of the complex interplay between the tumor, the tumor microenvironment and the immune system expand, use of immunotherapy will continue to grow. Although the optimal use of these agents is not yet defined, they may provide an unmet need for patients who did not benefit or unable to tolerate traditional chemotherapy. Further work is necessary to determine the role of targeted therapy and the combination of targeted agents with cytotoxic agents that will translate into improved survival but the future looks optimistic.

REFERENCES

1 **Siegel R**, Ma J, Zou Z, Jemal A. Cancer statistics, 2014. *CA Cancer J Clin* 2014; **64**: 9-29 [PMID: 24399786 DOI: 10.3322/caac.21208]

2 **Jemal A**, Bray F, Center MM, Ferlay J, Ward E, Forman D. Global cancer statistics. *CA Cancer J Clin* 2011; **61**: 69-90 [PMID: 21296855 DOI: 10.3322/caac.20107]

3 **Ferlay J**, Shin HR, Bray F, Forman D, Mathers C, Parkin DM. Estimates of worldwide burden of cancer in 2008: GLOBOCAN 2008. *Int J Cancer* 2010; **127**: 2893-2917 [PMID: 21351269 DOI: 10.1002/ijc.25516]

4 **Cunningham D**, Okines AF, Ashley S. Capecitabine and oxaliplatin for advanced esophagogastric cancer. *N Engl J Med* 2010; **362**: 858-859 [PMID: 20200397 DOI: 10.1056/NEJMc0911925]

5 **Kamangar F**, Dores GM, Anderson WF. Patterns of cancer incidence, mortality, and prevalence across five continents: defining priorities to reduce cancer disparities in different geographic regions of the world. *J Clin Oncol* 2006; **24**: 2137-2150 [PMID: 16682732 DOI: 10.1200/JCO.2005.05.2308]

6 **Wagner AD**, Grothe W, Haerting J, Kleber G, Grothey A, Fleig WE. Chemotherapy in advanced gastric cancer: a systematic review and meta-analysis based on aggregate data. *J Clin Oncol* 2006; **24**: 2903-2909 [PMID: 16782930 DOI: 10.1200/JCO.2005.05.0245]

7 **Van Cutsem E**, Moiseyenko VM, Tjulandin S, Majlis A, Constenla M, Boni C, Rodrigues A, Fodor M, Chao Y, Voznyi E, Risse ML, Ajani JA. Phase III study of docetaxel and cisplatin plus fluorouracil compared with cisplatin and fluorouracil as first-line therapy for advanced gastric cancer: a report of the V325 Study Group. *J Clin Oncol* 2006; **24**: 4991-4997 [PMID: 17075117 DOI: 10.1200/JCO.2006.06.8429]

8 **Al-Batran SE**, Hartmann JT, Probst S, Schmalenberg H, Hollerbach S, Hofheinz R, Rethwisch V, Seipelt G, Homann N, Wilhelm G, Schuch G, Stoehlmacher J, Derigs HG, Hegewisch-Becker S, Grossmann J, Pauligk C, Atmaca A, Bokemeyer C, Knuth A, Jäger E. Phase III trial in metastatic gastroesophageal adenocarcinoma with fluorouracil, leucovorin plus either oxaliplatin or cisplatin: a study of the Arbeitsgemeinschaft Internistische Onkologie. *J Clin Oncol* 2008; **26**: 1435-1442 [PMID: 18349393 DOI: 10.1200/JCO.2007.13.9378]

9 **Cunningham D**, Starling N, Rao S, Iveson T, Nicolson M, Coxon

F, Middleton G, Daniel F, Oates J, Norman AR. Capecitabine and oxaliplatin for advanced esophagogastric cancer. *N Engl J Med* 2008; **358**: 36-46 [PMID: 18172173 DOI: 10.1056/NEJMoa073149]

10 **Kang YK**, Kang WK, Shin DB, Chen J, Xiong J, Wang J, Lichinitser M, Guan Z, Khasanov R, Zheng L, Philco-Salas M, Suarez T, Santamaria J, Forster G, McCloud PI. Capecitabine/cisplatin versus 5-fluorouracil/cisplatin as first-line therapy in patients with advanced gastric cancer: a randomised phase III noninferiority trial. *Ann Oncol* 2009; **20**: 666-673 [PMID: 19153121 DOI: 10.1093/annonc/mdn717]

11 **Koizumi W**, Narahara H, Hara T, Takagane A, Akiya T, Takagi M, Miyashita K, Nishizaki T, Kobayashi O, Takiyama W, Toh Y, Nagaie T, Takagi S, Yamamura Y, Yanaoka K, Orita H, Takeuchi M. S-1 plus cisplatin versus S-1 alone for first-line treatment of advanced gastric cancer (SPIRITS trial): a phase III trial. *Lancet Oncol* 2008; **9**: 215-221 [PMID: 18282805 DOI: 10.1016/S1470-2045(08)70035-4]

12 **Ajani JA**, Rodriguez W, Bodoky G, Moiseyenko V, Lichinitser M, Gorbunova V, Vynnychenko I, Garin A, Lang I, Falcon S. Multicenter phase III comparison of cisplatin/S-1 with cisplatin/infusional fluorouracil in advanced gastric or gastroesophageal adenocarcinoma study: the FLAGS trial. *J Clin Oncol* 2010; **28**: 1547-1553 [PMID: 20159816 DOI: 10.1200/JCO.2009.25.4706]

13 **Dank M**, Zaluski J, Barone C, Valvere V, Yalcin S, Peschel C, Wenczl M, Goker E, Cisar L, Wang K, Bugat R. Randomized phase III study comparing irinotecan combined with 5-fluorouracil and folinic acid to cisplatin combined with 5-fluorouracil in chemotherapy naive patients with advanced adenocarcinoma of the stomach or esophagogastric junction. *Ann Oncol* 2008; **19**: 1450-1457 [PMID: 18558665 DOI: 10.1093/annonc/mdn166]

14 **Guimbaud R**, Louvet C, Ries P, Ychou M, Maillard E, André T, Gornet JM, Aparicio T, Nguyen S, Azzedine A, Etienne PL, Boucher E, Rebischung C, Hammel P, Rougier P, Bedenne L, Bouché O. Prospective, randomized, multicenter, phase III study of fluorouracil, leucovorin, and irinotecan versus epirubicin, cisplatin, and capecitabine in advanced gastric adenocarcinoma: a French intergroup (Fédération Francophone de Cancérologie Digestive, Fédération Nationale des Centres de Lutte Contre le Cancer, and Groupe Coopérateur Multidisciplinaire en Oncologie) study. *J Clin Oncol* 2014; **32**: 3520-3526 [PMID: 25287828 DOI: 10.1200/JCO.2013.54.1011]

15 **Ford HE**, Marshall A, Bridgewater JA, Janowitz T, Coxon FY, Wadsley J, Mansoor W, Fyfe D, Madhusudan S, Middleton GW, Swinson D, Falk S, Chau I, Cunningham D, Kareclas P, Cook N, Blazeby JM, Dunn JA. Docetaxel versus active symptom control for refractory oesophagogastric adenocarcinoma (COUGAR-02): an open-label, phase 3 randomised controlled trial. *Lancet Oncol* 2014; **15**: 78-86 [PMID: 24332238 DOI: 10.1016/S1470-2045(13)70549-7]

16 **Kang JH**, Lee SI, Lim do H, Park KW, Oh SY, Kwon HC, Hwang IG, Lee SC, Nam E, Shin DB, Lee J, Park JO, Park YS, Lim HY, Kang WK, Park SH. Salvage chemotherapy for pretreated gastric cancer: a randomized phase III trial comparing chemotherapy plus best supportive care with best supportive care alone. *J Clin Oncol* 2012; **30**: 1513-1518 [PMID: 22412140 DOI: 10.1200/JCO.2011.39.4585]

17 **Thuss-Patience PC**, Kretzschmar A, Bichev D, Deist T, Hinke A, Breithaupt K, Dogan Y, Gebauer B, Schumacher G, Reichardt P. Survival advantage for irinotecan versus best supportive care as second-line chemotherapy in gastric cancer--a randomised phase III study of the Arbeitsgemeinschaft Internistische Onkologie (AIO). *Eur J Cancer* 2011; **47**: 2306-2314 [PMID: 21742485 DOI: 10.1016/j.ejca.2011.06.002]

18 **Hironaka S**, Ueda S, Yasui H, Nishina T, Tsuda M, Tsumura T, Sugimoto N, Shimodaira H, Tokunaga S, Moriwaki T, Esaki T, Nagase M, Fujitani K, Yamaguchi K, Ura T, Hamamoto Y, Morita S, Okamoto I, Boku N, Hyodo I. Randomized, open-label, phase III study comparing irinotecan with paclitaxel in patients with advanced gastric cancer without severe peritoneal metastasis after failure of prior combination chemotherapy using fluoropyrimidine plus platinum: WJOG 4007 trial. *J Clin Oncol* 2013; **31**: 4438-4444 [PMID: 24190112 DOI: 10.1200/JCO.2012.48.5805]

19 **Cancer Genome Atlas Research Network**. Comprehensive molecular characterization of gastric adenocarcinoma. *Nature* 2014; **513**: 202-209 [PMID: 25079317 DOI: 10.1038/nature13480]

20 **Hsieh AC**, Moasser MM. Targeting HER proteins in cancer therapy and the role of the non-target HER3. *Br J Cancer* 2007; **97**: 453-457 [PMID: 17667926 DOI: 10.1038/sj.bjc.6603910]

21 **Okines A**, Cunningham D, Chau I. Targeting the human EGFR family in esophagogastric cancer. *Nat Rev Clin Oncol* 2011; **8**: 492-503 [PMID: 21468131 DOI: 10.1038/nrclinonc.2011.45]

22 **Li SG**, Li L. Targeted therapy in HER2-positive breast cancer. *Biomed Rep* 2013; **1**: 499-505 [PMID: 24648975 DOI: 10.3892/br.2013.95]

23 **Gravalos C**, Jimeno A. HER2 in gastric cancer: a new prognostic factor and a novel therapeutic target. *Ann Oncol* 2008; **19**: 1523-1529 [PMID: 18441328 DOI: 10.1093/annonc/mdn169]

24 **Yano T**, Doi T, Ohtsu A, Boku N, Hashizume K, Nakanishi M, Ochiai A. Comparison of HER2 gene amplification assessed by fluorescence in situ hybridization and HER2 protein expression assessed by immunohistochemistry in gastric cancer. *Oncol Rep* 2006; **15**: 65-71 [PMID: 16328035 DOI: 10.3892/or.15.1.65]

25 **Sheng WQ**, Huang D, Ying JM, Lu N, Wu HM, Liu YH, Liu JP, Bu H, Zhou XY, Du X. HER2 status in gastric cancers: a retrospective analysis from four Chinese representative clinical centers and assessment of its prognostic significance. *Ann Oncol* 2013; **24**: 2360-2364 [PMID: 23788757 DOI: 10.1093/annonc/mdt232]

26 **Carey LA**, Perou CM, Livasy CA, Dressler LG, Cowan D, Conway K, Karaca G, Troester MA, Tse CK, Edmiston S, Deming SL, Geradts J, Cheang MC, Nielsen TO, Moorman PG, Earp HS, Millikan RC. Race, breast cancer subtypes, and survival in the Carolina Breast Cancer Study. *JAMA* 2006; **295**: 2492-2502 [PMID: 16757721 DOI: 10.1001/jama.295.21.2492]

27 **Hofmann M**, Stoss O, Shi D, Büttner R, van de Vijver M, Kim W, Ochiai A, Rüschoff J, Henkel T. Assessment of a HER2 scoring system for gastric cancer: results from a validation study. *Histopathology* 2008; **52**: 797-805 [PMID: 18422971 DOI: 10.1111/j.1365-2559.2008.03028.x]

28 **Bang YJ**, Van Cutsem E, Feyereislova A, Chung HC, Shen L, Sawaki A, Lordick F, Ohtsu A, Omuro Y, Satoh T, Aprile G, Kulikov E, Hill J, Lehle M, Rüschoff J, Kang YK. Trastuzumab in combination with chemotherapy versus chemotherapy alone for treatment of HER2-positive advanced gastric or gastro-oesophageal junction cancer (ToGA): a phase 3, open-label, randomised controlled trial. *Lancet* 2010; **376**: 687-697 [PMID: 20728210 DOI: 10.1016/S0140-6736(10)61121-X]

29 **Hecht JR**, Bang YJ, Qin SK, Chung HC, Xu JM, Park JO, Jeziorski K, Shparyk Y, Hoff PM, Sobrero A, Salman P, Li J, Protsenko SA, Wainberg ZA, Buyse M, Afenjar K, Houé V, Garcia A, Kaneko T, Huang Y, Khan-Wasti S, Santillana S, Press MF, Slamon D. Lapatinib in Combination With Capecitabine Plus Oxaliplatin in Human Epidermal Growth Factor Receptor 2-Positive Advanced or Metastatic Gastric, Esophageal, or Gastroesophageal Adenocarcinoma: TRIO-013/LOGiC-A Randomized Phase III Trial. *J Clin Oncol* 2016; **34**: 443-451 [PMID: 26628478 DOI: 10.1200/JCO.2015.62.6598]

30 **Satoh T**, Xu RH, Chung HC, Sun GP, Doi T, Xu JM, Tsuji A, Omuro Y, Li J, Wang JW, Miwa H, Qin SK, Chung IJ, Yeh KH, Feng JF, Mukaiyama A, Kobayashi M, Ohtsu A, Bang YJ. Lapatinib plus paclitaxel versus paclitaxel alone in the second-line treatment of HER2-amplified advanced gastric cancer in Asian populations: TyTAN--a randomized, phase III study. *J Clin Oncol* 2014; **32**: 2039-2049 [PMID: 24868024 DOI: 10.1200/JCO.2013.53.6136]

31 **Kang YK**, Shah MA, Ohtsu A, Van Cutsem E, Ajani JA, van der Horst T, Harle-Yge M, Piao Y, Althaus B, Thuss-Patience PC. A randomized, open-label, multicenter, adaptive phase 2/3 study of trastuzumab emtansine (T-DM1) versus a taxane (TAX) in patients

(pts) with previously treated HER2-positive locally advanced or metastatic gastric/gastroesophageal junction adenocarcinoma (LA/MGC/GEJC). *J Clin Oncol* 2016; **34**: 5

32 **Herbst RS**. Review of epidermal growth factor receptor biology. *Int J Radiat Oncol Biol Phys* 2004; **59**: 21-26 [PMID: 15142631]

33 **Oda K**, Matsuoka Y, Funahashi A, Kitano H. A comprehensive pathway map of epidermal growth factor receptor signaling. *Mol Syst Biol* 2005; **1**: 2005.0010 [PMID: 16729045 DOI: 10.1038/msb4100014]

34 **Wang KL**, Wu TT, Choi IS, Wang H, Resetkova E, Correa AM, Hofstetter WL, Swisher SG, Ajani JA, Rashid A, Albarracin CT. Expression of epidermal growth factor receptor in esophageal and esophagogastric junction adenocarcinomas: association with poor outcome. *Cancer* 2007; **109**: 658-667 [PMID: 17211865 DOI: 10.1002/cncr.22445]

35 **Lieto E**, Ferraraccio F, Orditura M, Castellano P, Mura AL, Pinto M, Zamboli A, De Vita F, Galizia G. Expression of vascular endothelial growth factor (VEGF) and epidermal growth factor receptor (EGFR) is an independent prognostic indicator of worse outcome in gastric cancer patients. *Ann Surg Oncol* 2008; **15**: 69-79 [PMID: 17896140 DOI: 10.1245/s10434-007-9596-0]

36 **Lordick F**, Kang YK, Chung HC, Salman P, Oh SC, Bodoky G, Kurteva G, Volovat C, Moiseyenko VM, Gorbunova V, Park JO, Sawaki A, Celik I, Götte H, Melezínková H, Moehler M. Capecitabine and cisplatin with or without cetuximab for patients with previously untreated advanced gastric cancer (EXPAND): a randomised, open-label phase 3 trial. *Lancet Oncol* 2013; **14**: 490-499 [PMID: 23594786]

37 **Waddell T**, Chau I, Cunningham D, Gonzalez D, Okines AF, Okines C, Wotherspoon A, Saffery C, Middleton G, Wadsley J, Ferry D, Mansoor W, Crosby T, Coxon F, Smith D, Waters J, Iveson T, Falk S, Slater S, Peckitt C, Barbachano Y. Epirubicin, oxaliplatin, and capecitabine with or without panitumumab for patients with previously untreated advanced oesophagogastric cancer (REAL3): a randomised, open-label phase 3 trial. *Lancet Oncol* 2013; **14**: 481-489 [PMID: 23594787 DOI: 10.1016/S1470-2045(13)70096-2]

38 **Ferrara N**, Gerber HP, LeCouter J. The biology of VEGF and its receptors. *Nat Med* 2003; **9**: 669-676 [PMID: 12778165 DOI: 10.1038/nm0603-669]

39 **Prins MJ**, Verhage RJ, ten Kate FJ, van Hillegersberg R. Cyclooxygenase isoenzyme-2 and vascular endothelial growth factor are associated with poor prognosis in esophageal adenocarcinoma. *J Gastrointest Surg* 2012; **16**: 956-966 [PMID: 22258871 DOI: 10.1007/s11605-011-1814-1]

40 **Shi H**, Xu JM, Hu NZ, Xie HJ. Prognostic significance of expression of cyclooxygenase-2 and vascular endothelial growth factor in human gastric carcinoma. *World J Gastroenterol* 2003; **9**: 1421-1426 [PMID: 12854133 DOI: 10.3748/wjg.v9.i7.1421]

41 **Ohtsu A**, Shah MA, Van Cutsem E, Rha SY, Sawaki A, Park SR, Lim HY, Yamada Y, Wu J, Langer B, Starnawski M, Kang YK. Bevacizumab in combination with chemotherapy as first-line therapy in advanced gastric cancer: a randomized, double-blind, placebo-controlled phase III study. *J Clin Oncol* 2011; **29**: 3968-3976 [PMID: 21844504]

42 **Shen L**, Li J, Xu J, Pan H, Dai G, Qin S, Wang L, Wang J, Yang Z, Shu Y, Xu R, Chen L, Liu Y, Yu S, Bu L, Piao Y. Bevacizumab plus capecitabine and cisplatin in Chinese patients with inoperable locally advanced or metastatic gastric or gastroesophageal junction cancer: randomized, double-blind, phase III study (AVATAR study). *Gastric Cancer* 2015; **18**: 168-176 [PMID: 24557418 DOI: 10.1007/s10120-014-0351-5]

43 **Fuchs CS**, Tomasek J, Yong CJ, Dumitru F, Passalacqua R, Goswami C, Safran H, dos Santos LV, Aprile G, Ferry DR, Melichar B, Tehfe M, Topuzov E, Zalcberg JR, Chau I, Campbell W, Sivanandan C, Pikiel J, Koshiji M, Hsu Y, Liepa AM, Gao L, Schwartz JD, Tabernero J. Ramucirumab monotherapy for previously treated advanced gastric or gastro-oesophageal junction adenocarcinoma (REGARD): an international, randomised, multicentre, placebo-controlled, phase 3 trial. *Lancet* 2014; **383**: 31-39 [PMID: 24094768 DOI: 10.1016/S0140-6736(13)61719-5]

44 **Wilke H**, Van Cutsem E, Oh SC, Bodoky G, Shimada Y, Hironaka S, Sugimoto N, Lipatov ON, Kim TY, Cunningham D, Ohtsu A, Rougier P, Emig M, Carlesi R, Chandrawansa K, Muro K. RAINBOW: A global, phase 3, randomized, double-blind study of ramucirumab plus paclitaxel versus placebo plus paclitaxel in the treatment of metastatic gastric adenocarcinoma following disease progression on first-line platinum- and fluoropyrimidine-containing combination therapy: Results of a multiple Cox regression analysis adjusting for prognostic factors. *J Clin Oncol* 2014; **32**: 4076

45 **Wilke H**, Muro K, Van Cutsem E, Oh SC, Bodoky G, Shimada Y, Hironaka S, Sugimoto N, Lipatov O, Kim TY, Cunningham D, Rougier P, Komatsu Y, Ajani J, Emig M, Carlesi R, Ferry D, Chandrawansa K, Schwartz JD, Ohtsu A. Ramucirumab plus paclitaxel versus placebo plus paclitaxel in patients with previously treated advanced gastric or gastro-oesophageal junction adenocarcinoma (RAINBOW): a double-blind, randomised phase 3 trial. *Lancet Oncol* 2014; **15**: 1224-1235 [PMID: 25240821 DOI: 10.1016/S1470-2045(14)70420-6]

46 **Yoon HH**, Bendell JC, Braiteh FS, Firdaus I, Philip PA, Cohn AL, Lewis N, Anderson DM, Arrowsmith E, Schwartz JD, Xu Y, Koshiji M, Alberts SR, Wainberg ZA. Ramucirumab (RAM) plus FOLFOX as front-line therapy (Rx) for advanced gastric or esophageal adenocarcinoma (GE-AC): Randomized, double-blind, multicenter phase 2 trial. *J Clin Oncol* 2014; **32**: 4004

47 **Qin S**. Phase III study of apatinib in advanced gastric cancer: A randomized, double-blind, placebo-controlled trial. *J Clin Oncol* 2014; **32**: 4003

48 **Bang YJ**, Kang YK, Kang WK, Boku N, Chung HC, Chen JS, Doi T, Sun Y, Shen L, Qin S, Ng WT, Tursi JM, Lechuga MJ, Lu DR, Ruiz-Garcia A, Sobrero A. Phase II study of sunitinib as second-line treatment for advanced gastric cancer. *Invest New Drugs* 2011; **29**: 1449-1458 [PMID: 20461441 DOI: 10.1007/s10637-010-9438-y]

49 **Moehler MH**, Thuss-Patience PC, Schmoll HJ, Hegewisch-Becker S, Wilke H, Al-Batran SE, Weissinger F, Kullmann F, Fischer Von Weikersthal L, Siveke JT, Kanzler S, Schimanski CC, Otte M, Schollenberger L, Koenig J, Galle PR. FOLFIRI plus sunitinib versus FOLFIRI alone in advanced chemorefractory esophagogastric cancer patients: a randomized placebo-controlled multicentric AIO phase II trial. *J Clin Oncol* 2013; **31**: 4086

50 **Sun W**, Powell M, O'Dwyer PJ, Catalano P, Ansari RH, Benson AB. Phase II study of sorafenib in combination with docetaxel and cisplatin in the treatment of metastatic or advanced gastric and gastroesophageal junction adenocarcinoma: ECOG 5203. *J Clin Oncol* 2010; **28**: 2947-2951 [PMID: 20458043 DOI: 10.1200/JCO.2009.27.7988]

51 **Martin-Richard M**, Gallego R, Pericay C, Garcia Foncillas J, Queralt B, Casado E, Barriuso J, Iranzo V, Juez I, Visa L, Saigi E, Barnadas A, Garcia-Albeniz X, Maurel J. Multicenter phase II study of oxaliplatin and sorafenib in advanced gastric adenocarcinoma after failure of cisplatin and fluoropyrimidine treatment. A GEMCAD study. *Invest New Drugs* 2013; **31**: 1573-1579 [PMID: 24077981 DOI: 10.1007/s10637-013-0020-2]

52 **Thuss-Patience PC**, Al-Batran SE, Siveke JT, Homann N, Malfertheiner P, Glaeser D, Stein A, Tamm I, Daum S, Potenberg J, Florschütz A, Vogel A, Ridwelski K, Ritgen M, Geissler M, Schmalenberg H, Schlattmann P, Lorenz M, Breithaupt K, Pichlmeier U. Pazopanib and 5-FU/oxaliplatin as first-line treatment in advanced gastric cancer: PaFLO, a randomized phase II study from the AIO (Arbeitsgemeinschaft Internistische Onkologie). *J Clin Oncol* 2015; **33**: 4033

53 **Pavlakis N**, Sjoquist KM, Tsobanis E, Martin AJ, Kang YK, Bang YJ, O'Callaghan CJ, Tebbutt NC, Rha SY, Lee J, Cho JY, Lipton LR, Burnell MJ, Alcindor T, Strickland A, Kim JW, Yip S, Simes J, Zalcberg JR, Goldstein D. INTEGRATE: A randomized, phase II, double-blind, placebo-controlled study of regorafenib in refractory advanced oesophagogastric cancer (AOGC): A study by the Australasian Gastrointestinal Trials Group (AGITG)-Final overall and subgroup results. *J Clin Oncol* 2015; **33**: 4003

54 **Guertin DA**, Sabatini DM. Defining the role of mTOR in cancer. *Cancer Cell* 2007; **12**: 9-22 [PMID: 17613433 DOI: 10.1016/j.ccr.2007.05.008]

55 **Bjornsti MA**, Houghton PJ. The TOR pathway: a target for cancer therapy. *Nat Rev Cancer* 2004; **4**: 335-348 [PMID: 15122205 DOI: 10.1038/nrc1362]

56 **Shi J**, Yao D, Liu W, Wang N, Lv H, He N, Shi B, Hou P, Ji M. Frequent gene amplification predicts poor prognosis in gastric cancer. *Int J Mol Sci* 2012; **13**: 4714-4726 [PMID: 22606006 DOI: 10.3390/ijms13044714]

57 **Yu HG**, Ai YW, Yu LL, Zhou XD, Liu J, Li JH, Xu XM, Liu S, Chen J, Liu F, Qi YL, Deng Q, Cao J, Liu SQ, Luo HS, Yu JP. Phosphoinositide 3-kinase/Akt pathway plays an important role in chemoresistance of gastric cancer cells against etoposide and doxorubicin induced cell death. *Int J Cancer* 2008; **122**: 433-443 [PMID: 17935137 DOI: 10.1002/ijc.23049]

58 **Ohtsu A**, Ajani JA, Bai YX, Bang YJ, Chung HC, Pan HM, Sahmoud T, Shen L, Yeh KH, Chin K, Muro K, Kim YH, Ferry D, Tebbutt NC, Al-Batran SE, Smith H, Costantini C, Rizvi S, Lebwohl D, Van Cutsem E. Everolimus for previously treated advanced gastric cancer: results of the randomized, double-blind, phase III GRANITE-1 study. *J Clin Oncol* 2013; **31**: 3935-3943 [PMID: 24043745 DOI: 10.1200/JCO.2012.48.3552]

59 **Gherardi E**, Birchmeier W, Birchmeier C, Vande Woude G. Targeting MET in cancer: rationale and progress. *Nat Rev Cancer* 2012; **12**: 89-103 [PMID: 22270953 DOI: 10.1038/nrc3205]

60 **Yashiro M**, Nishii T, Hasegawa T, Matsuzaki T, Morisaki T, Fukuoka T, Hirakawa K. A c-Met inhibitor increases the chemosensitivity of cancer stem cells to the irinotecan in gastric carcinoma. *Br J Cancer* 2013; **109**: 2619-2628 [PMID: 24129235 DOI: 10.1038/bjc.2013.638]

61 **Nakajima M**, Sawada H, Yamada Y, Watanabe A, Tatsumi M, Yamashita J, Matsuda M, Sakaguchi T, Hirao T, Nakano H. The prognostic significance of amplification and overexpression of c-met and c-erb B-2 in human gastric carcinomas. *Cancer* 1999; **85**: 1894-1902 [PMID: 10223227]

62 **Graziano F**, Galluccio N, Lorenzini P, Ruzzo A, Canestrari E, D' Emidio S, Catalano V, Sisti V, Ligorio C, Andreoni F, Rulli E, Di Oto E, Fiorentini G, Zingaretti C, De Nictolis M, Cappuzzo F, Magnani M. Genetic activation of the MET pathway and prognosis of patients with high-risk, radically resected gastric cancer. *J Clin Oncol* 2011; **29**: 4789-4795 [PMID: 22042954 DOI: 10.1200/JCO.2011.36.7706]

63 **Lennerz JK**, Kwak EL, Ackerman A, Michael M, Fox SB, Bergethon K, Lauwers GY, Christensen JG, Wilner KD, Haber DA, Salgia R, Bang YJ, Clark JW, Solomon BJ, Iafrate AJ. MET amplification identifies a small and aggressive subgroup of esophagogastric adenocarcinoma with evidence of responsiveness to crizotinib. *J Clin Oncol* 2011; **29**: 4803-4810 [PMID: 22042947 DOI: 10.1200/JCO.2011.35.4928]

64 **Oliner KS**, Tang R, Anderson A, Lan Y, Iveson T, Donehower RC, Jiang Y, Dubey S, Loh E. Evaluation of MET pathway biomarkers in a phase II study of rilotumumab (R, AMG 102) or placebo (P) in combination with epirubicin, cisplatin, and capecitabine (ECX) in patients (pts) with locally advanced or metastatic gastric (G) or esophagogastric junction (EGJ) cancer. *J Clin Oncol* 2012; **30**: 4005

65 **Iveson T**, Donehower RC, Davidenko I, Tjulandin S, Deptala A, Harrison M, Nirni S, Lakshmaiah K, Thomas A, Jiang Y, Zhu M, Tang R, Anderson A, Dubey S, Oliner KS, Loh E. Rilotumumab in combination with epirubicin, cisplatin, and capecitabine as first-line treatment for gastric or oesophagogastric junction adenocarcinoma: an open-label, dose de-escalation phase 1b study and a double-blind, randomised phase 2 study. *Lancet Oncol* 2014; **15**: 1007-1018 [PMID: 24965569 DOI: 10.1016/S1470-2045(14)70023-3]

66 **Cunningham D**, Tebbutt NC, Davidenko I, Murad AM, Al-Batran SE, Ilson DH, Tjulandin S, Gotovkin E, Karaszewska B, Bondarenko I, Tejani MA, Udrea AA, Tehfe MA, Baker N, Oliner KS, Zhang Y, Hoang T, Sidhu R, Catenacci DVT. Phase III, randomized, double-blind, multicenter, placebo (P)-controlled trial of rilotumumab (R) plus epirubicin, cisplatin and capecitabine (ECX) as first-line therapy in patients (pts) with advanced MET-positive (pos) gastric or gastroesophageal junction (G/GEJ) cancer: RILOMET-1 study. *J Clin Oncol* 2015; **33**: 4000

67 **Shah MA**, Cho JY, Huat ITB, Tebbutt NC, Yen CJ, Kang A, Shames DS, Bu L, Kang YK. Randomized Phase II Study of FOLFOX /- MET Inhibitor, Onartuzumab (O), in Advanced Gastroesophageal Adenocarcinoma (GEC). *J Clin Oncol* 2015; **33**: 2

68 **Shah MA**, Bang YJ, Lordick F, Tabernero J, Chen M, Hack SP, Phan SC, Shames DS, Cunningham D. METGastric: A phase III study of onartuzumab plus mFOLFOX6 in patients with metastatic HER2-negative (HER2-) and MET-positive (MET) adenocarcinoma of the stomach or gastroesophageal junction (GEC). *J Clin Oncol* 2015; **33**: 4012

69 **Javle M**, Curtin NJ. The role of PARP in DNA repair and its therapeutic exploitation. *Br J Cancer* 2011; **105**: 1114-1122 [PMID: 21989215 DOI: 10.1038/bjc.2011.382]

70 **Rouleau M**, Patel A, Hendzel MJ, Kaufmann SH, Poirier GG. PARP inhibition: PARP1 and beyond. *Nat Rev Cancer* 2010; **10**: 293-301 [PMID: 20200537 DOI: 10.1038/nrc2812]

71 **Bang YJ**, Im SA, Lee KW, Cho JY, Song EK, Lee KH, Kim YH, Park JO, Chun HG, Zang DY, Fielding A, Rowbottom J, Hodgson D, O'Connor MJ, Yin X, Kim WH. Randomized, Double-Blind Phase II Trial With Prospective Classification by ATM Protein Level to Evaluate the Efficacy and Tolerability of Olaparib Plus Paclitaxel in Patients With Recurrent or Metastatic Gastric Cancer. *J Clin Oncol* 2015; **33**: 3858-3865 [PMID: 26282658 DOI: 10.1200/JCO.2014.60.0320]

72 **Dunn GP**, Bruce AT, Ikeda H, Old LJ, Schreiber RD. Cancer immunoediting: from immunosurveillance to tumor escape. *Nat Immunol* 2002; **3**: 991-998 [PMID: 12407406 DOI: 10.1038/ni1102-991]

73 **Schreiber RD**, Old LJ, Smyth MJ. Cancer immunoediting: integrating immunity's roles in cancer suppression and promotion. *Science* 2011; **331**: 1565-1570 [PMID: 21436444 DOI: 10.1126/science.1203486]

74 **Pardoll DM**. The blockade of immune checkpoints in cancer immunotherapy. *Nat Rev Cancer* 2012; **12**: 252-264 [PMID: 22437870 DOI: 10.1038/nrc3239]

75 **Hodi FS**, O'Day SJ, McDermott DF, Weber RW, Sosman JA, Haanen JB, Gonzalez R, Robert C, Schadendorf D, Hassel JC, Akerley W, van den Eertwegh AJ, Lutzky J, Lorigan P, Vaubel JM, Linette GP, Hogg D, Ottensmeier CH, Lebbé C, Peschel C, Quirt I, Clark JI, Wolchok JD, Weber JS, Tian J, Yellin MJ, Nichol GM, Hoos A, Urba WJ. Improved survival with ipilimumab in patients with metastatic melanoma. *N Engl J Med* 2010; **363**: 711-723 [PMID: 20525992 DOI: 10.1056/NEJMoa1003466]

76 **Ralph C**, Elkord E, Burt DJ, O'Dwyer JF, Austin EB, Stern PL, Hawkins RE, Thistlethwaite FC. Modulation of lymphocyte regulation for cancer therapy: a phase II trial of tremelimumab in advanced gastric and esophageal adenocarcinoma. *Clin Cancer Res* 2010; **16**: 1662-1672 [PMID: 20179239 DOI: 10.1158/1078-0432.CCR-09-2870]

77 **Muro K**, Bang Y, Shankaran V, Geva R, Catenacci DVT, Gupta S, Eder JP, Berger R, Gonzalez EJ, Pulini J, Ray AB, Dolled-Filhart M, Emancipator K, Pathiraja K, Shu X, Koshiji MR, Cheng J, Chung HC. LBA15 A phase 1b study of pembrolizumab (PEMBRO; MK-3475) in patients (PTS) with advanced gastric cancer. *Ann Oncol* 2014; **25**: v1-v41 [DOI: 10.1093/annonc/mdu438.15]

78 **Muro K**, Bang YJ, Shankaran V, Geva R, Catenacci DVT, Gupta S, Eder JP, Berger R, Gonzalez EJ, Ray A, Dolled-Filhart M, Emancipator K, Pathiraja K, Lunceford JK, Cheng JD, Koshiji M, Chung HC. Relationship between PD-L1 expression and clinical outcomes in patients (Pts) with advanced gastric cancer treated with the anti-PD-1 monoclonal antibody pembrolizumab (Pembro; MK-3475) in KEYNOTE-012. *J Clin Oncol* 2015; **33**: 3

79 **Le DT**, Uram JN, Wang H, Bartlett BR, Kemberling H, Eyring AD, Skora AD, Luber BS, Azad NS, Laheru D, Biedrzycki B,

Donehower RC, Zaheer A, Fisher GA, Crocenzi TS, Lee JJ, Duffy SM, Goldberg RM, de la Chapelle A, Koshiji M, Bhaijee F, Huebner T, Hruban RH, Wood LD, Cuka N, Pardoll DM, Papadopoulos N, Kinzler KW, Zhou S, Cornish TC, Taube JM, Anders RA, Eshleman JR, Vogelstein B, Diaz LA. PD-1 Blockade in Tumors with Mismatch-Repair Deficiency. *N Engl J Med* 2015; **372**: 2509-2520 [PMID: 26028255 DOI: 10.1056/NEJMoa1500596]

80 **Lutzky J**, Antonia SJ, Blake-Haskins A, Li X, Robbins PB, Shalabi AM, Vasselli J, Ibrahim RA, Khleif S, Segal NH. A phase 1 study of MEDI4736, an anti-PD-L1 antibody, in patients with advanced solid tumors. *J Clin Oncol* 2014; **32**: 3001

P- Reviewer: Gu GL, Korkeila E, Luo HS, Nomura S
S- Editor: Ma YJ **L- Editor**: A **E- Editor**: Ma S

World Journal of Gastroenterology

Submit a Manuscript: http://www.wjgnet.com/esps/
Help Desk: http://www.wjgnet.com/esps/helpdesk.aspx
DOI: 10.3748/wjg.v22.i20.4824

World J Gastroenterol 2016 May 28; 22(20): 4824-4834
ISSN 1007-9327 (print) ISSN 2219-2840 (online)

REVIEW

Multiplex qPCR for serodetection and serotyping of hepatitis viruses: A brief review

Mohammad Irshad, Priyanka Gupta, Dhananjay Singh Mankotia, Mohammad Ahmad Ansari

Mohammad Irshad, Priyanka Gupta, Dhananjay Singh Mankotia, Mohammad Ahmad Ansari, Clinical Biochemistry Division, Department of Laboratory Medicine, All India Institute of Medical Sciences, New Delhi 110029, India

Author contributions: Gupta P collected the information from published literature; Mankotia DS and Ansari MA categorized it under different sub-headings and prepared the manuscript; Irshad M edited the manuscript and corrected/modified the language.

Conflict-of-interest statement: There is no conflict of interest among the authors of this study.

Correspondence to: Dr. Mohammad Irshad, Professor, Clinical Biochemistry Division, Department of Laboratory Medicine, All India Institute of Medical Sciences, Ansari Nagar, New Delhi 110029, India. drirshad54@yahoo.com
Telephone: +91-11-26594981
Fax: +91-11-26588663

Received: February 9, 2016
Peer-review started: February 9, 2016
First decision: March 7, 2016
Revised: March 9, 2016
Accepted: March 30, 2016
Article in press: March 30, 2016
Published online: May 28, 2016

Abstract

The present review describes the current status of multiplex quantitative real time polymerase chain reaction (qPCR) assays developed and used globally for detection and subtyping of hepatitis viruses in body fluids. Several studies have reported the use of multiplex qPCR for the detection of hepatitis viruses, including hepatitis A virus (HAV), hepatitis B virus (HBV), hepatitis C virus (HCV), hepatitis D virus (HDV), and hepatitis E virus (HEV). In addition, multiplex qPCR has also been developed for genotyping HBV, HCV, and HEV subtypes. Although a single step multiplex qPCR assay for all six hepatitis viruses, *i.e.*, A to G viruses, is not yet reported, it may be available in the near future as the technologies continue to advance. All studies use a conserved region of the viral genome as the basis of amplification and hydrolysis probes as the preferred chemistries for improved detection. Based on a standard plot prepared using varying concentrations of template and the observed threshold cycle value, it is possible to determine the linear dynamic range and to calculate an exact copy number of virus in the specimen. Advantages of multiplex qPCR assay over singleplex or other molecular techniques in samples from patients with co-infection include fast results, low cost, and a single step investigation process.

Key words: Co-infection; Viral genome; Quantitative real-time polymerase chain reaction; Genotyping techniques; Serotyping; Hepatitis viruses

Core tip: The present review describes the worldwide application and the significance of multiplex quantitative real time polymerase chain reaction (qPCR) for simultaneous detection of hepatitis viruses and their subtypes in serum. The published literature has demonstrated that the multiplex qPCR assay is a fast, easy, cost-effective, and sensitive technique for the early diagnosis of hepatitis co-infections. Use of this technique, in comparison to other diagnostic procedures, is increasing in diagnostic laboratories.

Irshad M, Gupta P, Mankotia DS, Ansari MA. Multiplex qPCR for serodetection and serotyping of hepatitis viruses: A brief review. *World J Gastroenterol* 2016; 22(20): 4824-4834 Available from: URL: http://www.wjgnet.com/1007-9327/full/v22/i20/4824.htm DOI: http://dx.doi.org/10.3748/wjg.v22.i20.4824

INTRODUCTION

Viral hepatitis is a serious public health problem requiring early diagnosis and timely treatment. There are a number of hepatitis viruses that have already been characterized based on their molecular structure and named alphabetically as hepatitis viruses A, B, C, D, E, and G (HAV, HBV, HCV, HDV, HEV, and HGV), respectively. These are hepatotropic and non-cytopathic in nature and cause liver damage by immune mediated cell lysis[1]. There is an additional group of viruses that cause hepatitis but are not yet characterized. These viruses have been put under the category of non A-G hepatitis viruses. HAV infects mainly the pediatric age group, occurs both sporadically as well as in epidemics, and accounts for an estimated 1.4 million cases annually[2]. Two billion people are suspected to be infected with HBV globally, and approximately 350 million of them suffer from chronic hepatitis B infection[3]. About 25% of adults infected with HBV during childhood are reported to die from hepatocellular carcinoma (HCC) or liver cirrhosis[4]. In addition, 3-4 million people are infected with HCV each year, and a high proportion of them develop chronic HCV infection. A large population infected with HCV dies from serious liver diseases annually[5]. Similarly, reports are also available on HEV infection. In addition to individual viral infection, there are cases of co-infections reported from various parts of the world. Hepatitis A and E infections usually run a benign course of disease and resolve in due course of time without developing chronic diseases. In contrast, hepatitis B and C infections cause severe liver diseases, developing chronicity in a significant number of patients. Interestingly, hepatitis A and E infections in patients with pre-existing HBV or HCV infections lead to the development of serious diseases with a significant rise in morbidity and mortality[6].

The diagnosis of hepatitis viral infections is usually done with serological markers in blood. However, there are situations where serology loses its credibility. For example, serological markers can not differentiate between past and present infections. In addition, serological tests do not address the problem of antigenic variations in viruses, infections with different genotypes, presence of silent carriers, and absence of antibody in early phase of infection[7]. Moreover, the presence of maternal antibodies makes it impossible to detect infections in newborns[8]. In order to have an alternate system, the nucleic acid tests (NAT) based methods were developed for detecting the viral genome in serum for the diagnosis of viral hepatitis. NAT based methods have the benefit of direct examination of the infectious agent's genome in serum[9,10].

The conventional polymerase chain reaction (PCR) is one such NAT based method that has been in practice in some laboratories for the diagnosis of viral hepatitis in the last few years[11]. However, conventional PCR is a lengthy procedure with several technical and operational problems, and so, it is of limited use. In addition, each marker needs to be investigated separately by PCR, and it takes a very long time to reach a final diagnosis. Because of these limitations of conventional PCR, the use of real time PCR was supposed to be a better option for early diagnosis of viral hepatitis in both sporadic and epidemic cases. Real time PCR is one of the latest techniques frequently used for the diagnosis of various infectious diseases, including viral hepatitis. It can detect causative pathogen-related nucleic acid in body fluids in a very short time period. It can also be used to determine different molecular forms and variant molecular species of pathogens, including bacteria, viruses, and several parasites[12,13]. Real time PCR is a specific and sensitive technique and uses specific probes and primers to detect target sequences in the genome. Moreover, this technique is performed on an automated machine without the need of post PCR procedures, thus minimizing cross contamination between samples, simultaneously accelerating the analysis[14].

The recent development of molecular technologies has relayed a strong message to medical researchers to explore ways to further improve the diagnostic procedures. Those researchers working in the area of medical virology have switched from traditional approaches of virus detection in clinical samples to multiplexing for simultaneous detection of multiple pathogens in a single assay[15]. Recently, several PCR based assays coupled with oligonucleotide microarray technology have been designed to allow for the simultaneous detection and genotyping of several viruses, including blood borne pathogens[16], respiratory viruses[17], and adenoviruses[18]. These assays show a significant increase in the sensitivity of detection, reaching 10-100 copies of target RNA/DNA in a sample[19]. Given the ease of performance, short reaction time, low cost, and the ability to monitor the results on a screen, these assays have proved attractive to all diagnostic laboratories furnished with minimal essential facilities. After surveying the literature on the use of PCR based multiplex assays for detecting and genotyping hepatitis viruses, we noticed several attempts to develop multiplex real time PCR assays for hepatitis in the last few years. Here, we provide an up to date review on the development, use, and significance of multiplex qPCR in the field of viral hepatitis.

Table 1 Conserved genomic regions used as templates for amplification of hepatitis viruses in qPCR assays

Virus	Conserved region	Ref.
HAV	5′ UTR	[4,15,20,22]
HBV	S-gene	[4, 19-21]
	X-gene	[15]
HCV	5′ UTR	[4,15,19-21]
HDV	Ribozyme-1	[20]
HEV	ORF2	[15,22]
	ORF3	[20]
HGV	5′ UTR	[20]

HAV: Hepatitis A virus; HBV: Hepatitis B virus; HCV: Hepatitis C virus; HDV: Hepatitis D virus; HEV: Hepatitis E virus; UTR: Untranslated region; ORF: Open reading frame.

EXPERIMENTAL APPROACH FOR MULTIPLEX qPCR

Search for conserved regions

In order to develop a multiplex qPCR assay for multiple pathogens, the first and foremost step is to explore and locate the target region on each pathogen's genome for amplification purpose. Since variation in the genome is a dynamic process, it is necessary that a multiplex assay uses the most conserved region representing all the strains/variants for detection of the pathogen in body fluid. In the case of hepatitis viral infections, studies have reported a distinct conserved region that has been used as a target for amplification of each individual viral genome[4,20,21]. Table 1 shows the list of target regions used in various studies on multiplex qPCR assays developed for hepatitis viruses. The 5′ untranslated region (UTR) was reported to be the main target template in HAV, HCV, and HGV[20,22]. It was based on the availability of most conserved sequence in the 5′ UTR for amplification purpose. Similarly, S-gene or X-gene was used for HBV, ribozyme-1 gene for HDV, and open reading frame (ORF)-2 or ORF-3 region for HEV. Different studies have reported different sequences as templates in these selected conserved regions, though, there was very little information provided about the exact location of the sequences used.

Designing of primers and probes

After deciding which conserved region and location of the sequence were to be used as template, it is important to design the primers and probes for their use in the development of qPCR[23]. The selection of the primer is based on its specificity with the target template. At the same time, its length, melting temperature, GC content, 3′ end stability, sequence complexity, and location in the target sequence determine the length and melting temperature of the amplicon produced and the amplification efficiency of the assay[23,24]. Notably, the choice of chemistry and probe design are at the liberty of the user's interest, with numerous options available to them[24]. During selection of chemistry and probe, one needs to determine whether to quantify DNA, profile mRNA, or perform allelic discrimination assays[25].

Real-time PCR and melting curve analysis (MCA) are good techniques for quantifying nucleic acids, detecting mutations, and conducting genotyping analysis. These methods often use TaqMan probes[26], Molecular beacons[27], Sunrise primers[28], Scorpion primers[29], and Light-up probes[30]. An alternative to probe-based methods is the use of DNA intercalating dyes that bind to double-stranded DNA. These dyes include ethidium bromide[31] and SYBR Green I[32,33]. However, certain drawbacks limit the use of SYBR Green I for resolving multiplex PCR based on MCA[34]. Other alternative dyes, such as BEBO[35], YO-PRO-1[36], LC Green[37], and SYTO-9[38,39] have also been tried for use in real time PCR. Table 2 provides a brief review of various chemistries/dyes offering several options for their use in qPCR assay developed for different purposes. Studies for detecting and genotyping hepatitis viruses with qPCR have reported different sets of dyes based on choice and their availability[40]. However, most of the studies conducted have reported a frequent use of hydrolysis probes despite many options available. This information is available in the data[41-71] compiled in Table 3.

The probe-based assays (*e.g.,* TaqMan assays)[72] began to gain attention in mid-1990s with the development of quenched, fluorescent probes[73,74] and the commercialization of real-time thermal cyclers[26,75]. TaqMan (also known as Fluorogenic 5′ nuclease assay) probes contain two dyes, a reporter dye (*e.g.,* 6-FAM) at the 5′ end and an acceptor dye at 3′ end, usually tetramethyl rhodamine (TAMRA). Recently, TAMRA fluorescent acceptor quencher dye was substituted with a non-fluorescent quencher, *e.g*., Black Hole Quencher[76]. The proximity of the quencher to the reporter in an intact probe quenches the fluorescence signal of the reporter dye through fluorescence resonance energy transfer. During amplification, the 5′ to 3′ nucleolytic activity of Taq polymerase cleaves the probe between the reporter and the quencher only if the probe hybridizes to the target. The probe fragments get displaced from the target, separating the reporter dye from the quencher dye, resulting in increased emission of fluorescence. Floating TaqMan probes are quenched due to random coiling in solution, where fluorophore- and quencher-labeled ends come together[77]. In contrast, Molecular Beacon probes are oligonucleotides designed in a way to induce hairpin formation and produce the quenched state[78]. TaqMan and Molecular Beacon probes have been shown to be less effective in discriminating closely related targets, as in single nucleotide polymorphisms, drug-resistant mutants, and somatic cancer mutations[79,80]. However, molecular beacons are useful in situations where it is not possible to isolate probe-target hybrids from

Table 2 Chemistries/Dyes used in qPCR assays

S. NO.	Class	Types	Structure	Mechanism of action	Advantages	Applications
1	DNA binding dyes	Ethidium Bromide, SYBR Green, SYBR Gold, YO-PRO-1, SYTO, BEBO, BOXTO, EvaGreen	Intercalating dyes	Bind to the minor groove of dsDNA during amplification	Inexpensive Easily available	Pathogen detection Gene expression SNP detection Genotyping
2	Fluorophore labeled oligonucleotide	*Primer probes*				
		Hairpins: Scorpions, Ampliflour, LUX	Loop based oligonucleotides	Bind to target during denaturation with emission of fluorescence	Inexpensive, Prevent formation of primer dimer, Less background signals	Pathogen detection Genotyping SNP allelic discrimination Mutation detection
		Cyclicons	Cyclic structure with reporter at 3′ end and quencher at 5′ end	Reporter and quencher in close proximity with energy transfer *via* FRET quenching. Their separation results in fluorescence emission during amplification	Inexpensive Less contamination Less background signals	Pathogen detection Genotyping SNP allelic discrimination Mutation detection
		Angler	Probe with DNA sequence bound to reverse primer through a HEG linker	During annealing step, DNA polymerase does extension of 3′ end reverse primer. Later on, SYBR Gold dye intercalates in dsDNA emitting fluorescence	Highly specific	Gene expression Pathogen detection SNP detection Genotyping
		Probes				
		Hydrolysis Probes: TaqMan probes, MGB-TaqMan, Snake assay	Oligonucleotide with reporter at 5′ and quencher at 3′ end	Probe is degraded by 5′ to 3′ exonuclease activity of DNA polymerase generating fluorescence during extension	Design and synthesis easy	Microarray validation Pathogen detection SNP allelic discrimination Mutation detection
		Hybridization probes: Hybprobes, Molecular Beacon, HyBeacon, MGB Probes	A pair of oligonucleotides having reporter dye on first and quencher on second oligonucleotide	Binding to target during hybridization and annealing brings fluorophore into proximity producing fluorescence by FRET	Design and synthesis quick and easy	Microarray validation Pathogen detection Viral/Bacterial genotyping SNP allelic discrimination Mutation detection
		Nucleic acid analogues				
		PNAs, LNAs, ZNAs Non-natural bases	Intercalating/inserting dyes	Identical to conventional oligonucleotides	Resistant to nuclease and proteases activity	Discriminate between DNA and cDNA in prokaryotes

All above details were collected from report published in *Clinica Chimica Acta* 2015; **439**: 231-250[25]. SNP: Single nucleotide polymorphisms.

an excess of the hybridization probes, for example in sealed tubes or within living cells[81]. An effective probe requires a careful balancing act based on melting temperature (Tm) and, therefore, repeated design and testing are needed to develop an effective probe[82]. Available evidence suggests that the use of TaqMan probes in qPCR assays for hepatitis viruses provide a good balancing act.

Designing tools

Today, several designing tools are available to guide the design of qPCR assays and analyze resulting quantitative data. Many of them are available online, and some are provided with qPCR instruments from different manufacturers[83]. Some important tools include Primer3, Primer-BLAST, PerlPrimer, FastPCR software, IDTSciTools, and UniPrime[84-89]. In addition, some of them have programming to analyze the secondary structure of primers. MP primer is used to design primers for multiplex PCR assays[90]. The Minimum Information for Publication of qPCR Experiments (MIQE) guidelines also provide clear instructions on the steps that are important for qPCR assay design[91]. Several research companies offer help for designing primers and probes with use of their designing tools. The studies reported in this article demonstrate a liberal use of tools without any specific need or choice affecting the results.

Instruments used in multiplex qPCR assay

Various types of advanced technology-based equipment for multiplex qPCR assays with analysis of amplified products are available globally. A list of the instruments used with their brands in various studies conducted on qPCR for viral hepatitis is shown in Table 3. With increasing advances in technology, the number of filters and, accordingly, the resolution of the amplification curve during the PCR assay have also increased. Now it is possible to detect/discriminate more pathogens or allelic/mutational changes[92,93] in a

Table 3 Global status of multiplex qPCR developed for hepatitis viral infections with and without other pathogens

No.	Assay systems	Instruments used	Group of pathogens detected		Types of chemistries/ detection methods used	Ref.
			Hepatitis viruses	Other pathogens		
1	Multiplex real time PCR	Mx4000 (Stratagene)	HBV, HCV	HIV type-1, T. pallidum	TaqMan-LNA probe	[21]
2	Multiplex real time PCR	Light cycler 480 (Roche)	HEV genotypes	-	N.A.	[41]
3	Real time PCR assay	ABI 7500 (Applied Biosystems)	HAV, HBV, HCV, HDV, HEV	-	TaqMan Array card	[42]
4	Multiplex qPCR assay	Light cycler 480 (Roche)	HBV, HDV	-	TaqMan probe	[43]
5	Multiplex qPCR assay	ABI 7500 (Applied Biosystems)	HAV, HEV	-	Hydrolysis probe	[22]
6	Multiplex qRT-PCR	N.A.	HAV	Norovirus genotypes 1 and 2	TaqMan probe	[44]
7	Multiplex ligation dependent probe real time PCR	Rotor-GeneQ (Qiagen)	HBV mutants	-	TaqMan probe MLPA probe	[45]
8	Multiplex real time RT-PCR	N.A.	HEV genotypes	-	N.A.	[46]
9	Multiplex qPCR	N.A.	HBV genotypes	-	SYBR Green	[47]
10	Multiplex Real time PCR	N.A.	HAV	Norovirus, Rotavirus, Coxsackievirus	TaqMan probe	[48]
11	Multiplex Real time PCR	Light cycler 2.0 (Roche)	HAV, HBV, HCV and HEV	-	FRET probe	[15]
12	Multiplex RT-PCR	ABI 2720 (Applied Biosystems)	HCV	HIV type-1	SYBR Green I	[8]
13	Multiplex qPCR	N.A.	HAV, HEV	Entero and Adeno-viruses	N.A.	[49]
14	Multiplex Real-Time PCR Assay	CFX96 (Bio-Rad)	HAV, HBV, HCV	-	READ technology based fluorophore	[4]
15	RT PCR assay	Smart cycler Ⅱ (Cepheid)	HBV, HCV	-	TaqMan probe	[50]
16	Duplex real time PCR	ABI 7500 (Applied Biosystems)	HBV variants	-	Hydrolysis probe	[51]
17	Multiplex RT PCR	N.A.	HCV subtyping	-	Electrophoresis	[52]
18	Multiplex qPCR	N.A.	HBV genotypes	-	N.A.	[53]
19	Multiplex qPCR	N.A.	HCV	HIV type-1	SYBR Green I	[54]
20	Duplex real-time RT-PCR	ABI Prism system (Applied Biosystems)	HCV variants	-	Hydrolysis probe	[55]
21	Multiplex real time PCR	N.A.	HAV	Norovirus genotypes 1 and 2	N.A.	[56]
22	Duplex real-time qRT-PCR	ABI Prism 7000 (Applied Biosystems)	HAV	MS2 bacteriophage	MGB-TaqMan probe	[57]
23	Multiplex TaqMan RT-qPCR system	MX30005P (Stratagene)	HEV	FCV	TaqMan probe	[58]
24	Multiplex real time PCR	ABI 7300 (Applied Biosystems)	HBV genotypes	-	TaqMan probe	[59]
25	Real time PCR	N.A.	HBV genotypes	-	TaqMan probe	[60]
26	Multiplex real time PCR	Mx3005P (Stratagene)	HEV	FCV	TaqMan probe	[61]
27	Multiplex RT PCR assay	ABI Prism 7500 (Applied Biosystems)	HCV	PDV	MGB hybridization probe	[62]
28	Multiplex qPCR assay	N.A.	HBV	B19, HHV-8, EBV, CMV, VZV	N.A.	[63]
29	Multiplex qPCR	N.A.	HBV, HCV	HIV type-1	SYBR Green I	[16]
30	Multiplex Real Time PCR	ABI 7500 (Applied Biosystems)	HBV mutants	-	LNA probes with SYBR Green I	[64]
31	Microarray multiplex assay	ABI Prism 7700 (Applied Biosystems)	HBV, HCV	HIV type-1	Oligonucleotide array labeled with Cy5 and Cy3	[65]
32	Real time multiplex PCR	N.A.	HAV	Entero and Adeno-viruses	Probes labeled with FAM, R6G, ROX, Cy5	[66]
33	Multiplex real time RT-PCR	LightCycler (Roche)	HCV	HIV type-1	SYBR Green	[67]
34	Real time multiplex PCR	icycler iQ (Bio-Rad)	HCV variants	-	TaqMan probes	[68]
35	Multiplex real-time RT PCR	ABI 7000 (Applied Biosystems)	HCV genotypes	-	Primer probes	[69]
36	Multiplex real-time qPCR	Mx4000 (Stratagene)	HBV, HCV	HIV type-1	TaqMan probes	[70]
37	Automated multiplex PCR	ABI Prism 7700 (Applied Biosystems)	HBV, HCV	HIV type-1	TaqMan probes	[71]

single step multiplex assay. The choice of instrument is more a function of availability, without much difference in their analytical qualities. Multiplex qPCR assays developed for hepatitis viruses may use any brand, depending on a match between the number of component pathogens to be detected and the filters

available for detection. Other features of equipment do not seem to affect the results.

Optimization of protocol

For each pathogen used as a component in the multiplex assay, a carefully developed singleplex assay is needed. The design of primers and probes is dictated purely by the nature of the target template and clear guidelines for amplification. This exercise is followed in order to prepare a record of common amplification conditions noted in singleplex assays and for their application as such in multiplex assays. The multiplex protocol is reframed in a way to have minimum possible deviations from the working protocol of the singleplex assay. During the multiplex assay, the possibility of cross interaction/interference among different molecules is quite likely and may cause unsuccessful amplification. This interaction may or may not occur, but it has to be worked out cautiously in each multiplex assay.

There have been reports on singleplex as well as multiplex assays developed for detection of some hepatitis viruses and their genotypes[16] (Table 3). Such a study was conducted at our research center where a multiplex assay was developed for simultaneous detection of hepatitis virus A, B, C, and E[15]. These viruses are frequently prevalent in India, posing a serious problem, causing incidences of both sporadic and epidemic hepatitis from time to time[94,95]. The use of singleplex followed by the development of multiplex assay in these cases does not show many changes in the experimental protocol. This implies that the amplification protocol of individual viruses is not influenced during multiplex assays. We noted a clear amplification curve on the screen during multiplex assay that was the same exact pattern noted during singleplex assay[15].

Table 3 shows the global status of multiplex assays used for analyzing hepatitis viruses with or without other pathogens[41-71]. In all these assays, viral amplification by the simultaneous presence of other pathogenic genomes was indicated. An overall survey of the experimental designs reported in multiplex assays indicated that standard conditions of reverse transcription, denaturation, annealing, and extension temperature were followed without much deviation from the singleplex protocol.

MIQE guidelines

The guidelines published by Bustin *et al*[91] in 2009 clearly defined the terms used and steps necessary to design the experiments for developing qPCR assay. Since 2009, many published reports in the area of viral hepatitis on multiplex qPCR were found to follow these guidelines and give interpretation of results referring to terminology and definitions outlined there. The guidelines state that multiplexing expands power of qPCR analysis but needs documentation for accurate quantification of multiple targets in a single tube assay.

ASSESSMENT OF SENSITIVITY AND SPECIFICITY

Generation of standard curve

In order to generate a standard curve for each hepatitis virus, the standard control that includes the conserved region targeted for amplification/ detection is synthesized artificially and cloned into a suitable vector (*e.g.,* pUC 57)[15] using cloning kits. These standards are used as a template for standardization of amplifications. The copy number of standard plasmids is calculated using their concentration and the size of linearized plasmids. Each standard template is added to PCR mix (Tris-HCl, KCl, $MgCl_2$, four dNTPs, primers, and Taq DNA polymerase in a suitable concentration ratio), and PCR is performed under standardized conditions. For generation of the standard curve, a 10-fold serial dilution of each standard plasmid (10^1-10^8 copies/μL) is prepared and run in triplicate. At the end, data are analyzed by an automatic system that generates a standard curve[21]. The standard curves are used to quantify the amplification product and to assess the linear dynamic range using 10-fold dilution series of standard plasmid of each individual virus. One specimen standard plot is shown in Figure 1, which was prepared during development of quadruplex qPCR for hepatitis virus A, B, C, and E. Such plots are used to calculate copy number of individual template using correlation coefficient and Y-intercept value based on regression analysis.

Standard curve showing amplification plots of 10-fold serial dilution of HAV template using standard cloned plasmids. Such standard curves are generated from the amplification plots run in triplicate and show a linear dynamic range. The correlation coefficient and the slope of each standard plot are shown in the figure.

Assessment of sensitivity

Using the standard curve prepared above, now it is possible to assess the sensitivity and determine the linear dynamic range of an individual virus. Moreover, observed Ct values may be used to calculate the exact copy number of virus in an unknown specimen[96,97]. Based on the data collected from various studies, including our study[15], it has been noticed that the linear dynamic range of each individual hepatitis virus usually falls in the range 10^1-10^8 copies/μL.

Assessment of specificity

The specificity of qPCR assay is assessed by evaluating sera from healthy controls and patients with unrelated diseases negative for hepatitis markers by serology and all other NAT based techniques. Negative results from these sera and clear positive signals from serologically positive hepatitis sera demonstrate the high level of specificity of qPCR. To date, all studies on qPCR demonstrate the assay to be specific[15,22]. In

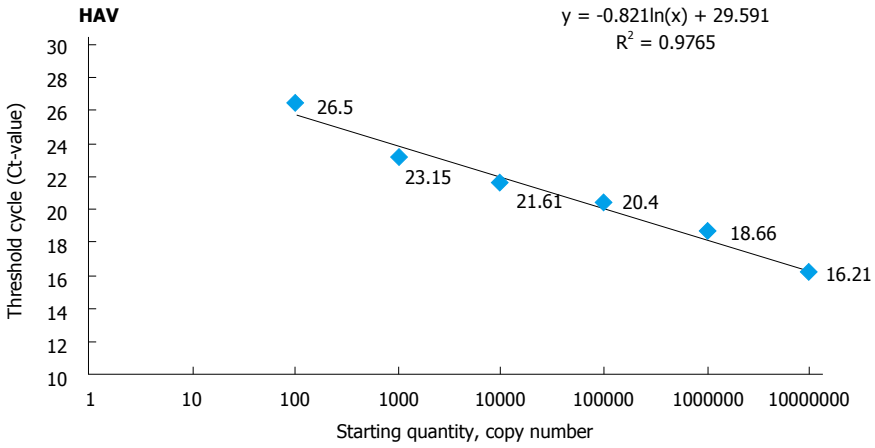

Figure 1 Standard curve showing amplification of hepatitis A virus[15]. HAV: Hepatitis A virus.

reports on viral hepatitis, qPCR assays demonstrated high specificity with a very low chance of false positive results[19,71].

MULTIPLEX qPCR IN RELATION TO OTHER ASSAYS

The multiplex qPCR assays were developed and used both for comparison as well as in combination with other molecular technologies to improve the sensitivity for detection of the viral genome[16,98]. Various other assay systems were also developed for simultaneous detection of HBV, HCV, and human immunodeficiency virus in addition to multiplex qPCR. The status of multiplex qPCR assay was assessed in comparison to other molecular techniques used for detection and genotyping of viruses, including hepatitis viruses. The other assay systems included flowcytometric microsphere based hybridization assay[99], transcription-mediated amplification (TMA)[100], and nucleic acid sequence based amplification (NASBA)[101]. Comparatively, TMA was reported to be an equally sensitive technique. However, when comparing qPCR with NASBA and TMA for the detection of hepatitis viruses, the level of sensitivity of TMA was found to be associated closely with qPCR[100]. Of course, qPCR assay was reported to be faster, more economic, and easier to perform compared to all other assays evaluated.

FUTURE AND LIMITATIONS OF MULTIPLEX qPCR

Multiplex qPCR assays are proving to be very good analytical and diagnostic procedures in medicine. Recently, these assays have been successfully used for both basic research and clinical applications[42,102]. Although the practice of doing separate assays for separate pathogens, including hepatitis viral markers, are still in place, the use of the multiplex assay is seen to be beneficial in terms of time and overall cost involved. Moreover, multiplex assays, when used for quantification of HCV- RNA, were found to resolve many problems with real time monitoring of the amplification process. In fact, in multiplex qPCR assays, real time PCR makes quantification of DNA and RNA of different organism more precisely and with better reproducibility because it depends on the threshold cycle value determined during the exponential phase of PCR rather than on end points[103]. In addition, these assays report a direct relationship between starting template copy number and the number of cycles required to get a positive signal. In this manner, real time qPCR appears to be a good option for laboratory diagnosis of viral hepatitis, both for screening as well as for the final diagnosis of suspected cases of viral hepatitis infections.

CONCLUSION

Based on the information compiled in the present review, there is an increasing trend/interest in the diagnostic area towards the development and use of multiplex qPCR assay for the simultaneous detection of hepatitis viruses or their subtypes in sera samples. Several studies have been conducted in last few years that clearly demonstrate the preferable use of qPCR over other techniques in the area of viral hepatitis. This technique has been used to detect hepatitis viruses in combination with various other viral and non-viral pathogens and reported to be a sensitive, fast, and cost-effective technique compared to other multi-step assay procedures. The use of multiplex qPCR in genotyping of hepatitis viral subtypes also provides great help in serotype detection. To date, multiplex qPCR has been successfully employed for the simultaneous detection of hepatitis virus A, B, C, D, and E and genotyping of their strains. It appears to be a good tool for screening blood donor samples in blood banks for hepatitis viruses. Moreover, a single step multiplex qPCR assay allows for an early diagnosis

and timely treatment of patients with viral hepatitis. Several studies in this field are in progress, with more important information likely to be available until the next such update is necessary.

ACKNOWLEDGMENTS

We appreciate the infrastructure provided by All India Institute of Medical Sciences, New Delhi, India, for conduct of this study.

REFERENCES

1 **Oh IS**, Park SH. Immune-mediated Liver Injury in Hepatitis B Virus Infection. *Immune Netw* 2015; **15**: 191-198 [PMID: 26330805 DOI: 10.4110/in.2015.15.4.191]

2 **Hadler S**. Global impact of hepatitis A virus infection; changing patterns. In: Lemon S, Margolis H, Editors. Viral hepatitis and liver disease. Baltimore: Williams and Wilkins, 1991: 4-20

3 **Custer B**, Sullivan SD, Hazlet TK, Iloeje U, Veenstra DL, Kowdley KV. Global epidemiology of hepatitis B virus. *J Clin Gastroenterol* 2004; **38**: S158-S168 [PMID: 15602165]

4 **Park Y**, Kim BS, Choi KH, Shin DH, Lee MJ, Cho Y, Kim HS. A novel multiplex real-time PCR assay for the concurrent detection of hepatitis A, B and C viruses in patients with acute hepatitis. *PLoS One* 2012; **7**: e49106 [PMID: 23145085 DOI: 10.1371/journal.pone.0049106]

5 **Lozano R**, Naghavi M, Foreman K, Lim S, Shibuya K, Aboyans V, Abraham J, Adair T, Aggarwal R, Ahn SY, Alvarado M, Anderson HR, Anderson LM, Andrews KG, Atkinson C, Baddour LM, Barker-Collo S, Bartels DH, Bell ML, Benjamin EJ, Bennett D, Bhalla K, Bikbov B, Bin Abdulhak A, Birbeck G, Blyth F, Bolliger I, Boufous S, Bucello C, Burch M, Burney P, Carapetis J, Chen H, Chou D, Chugh SS, Coffeng LE, Colan SD, Colquhoun S, Colson KE, Condon J, Connor MD, Cooper LT, Corriere M, Cortinovis M, de Vaccaro KC, Couser W, Cowie BC, Criqui MH, Cross M, Dabhadkar KC, Dahodwala N, De Leo D, Degenhardt L, Delossantos A, Denenberg J, Des Jarlais DC, Dharmaratne SD, Dorsey ER, Driscoll T, Duber H, Ebel B, Erwin PJ, Espindola P, Ezzati M, Feigin V, Flaxman AD, Forouzanfar MH, Fowkes FG, Franklin R, Fransen M, Freeman MK, Gabriel SE, Gakidou E, Gaspari F, Gillum RF, Gonzalez-Medina D, Halasa YA, Haring D, Harrison JE, Havmoeller R, Hay RJ, Hoen B, Hotez PJ, Hoy D, Jacobsen KH, James SL, Jasrasaria R, Jayaraman S, Johns N, Karthikeyan G, Kassebaum N, Keren A, Khoo JP, Knowlton LM, Kobusingye O, Koranteng A, Krishnamurthi R, Lipnick M, Lipshultz SE, Ohno SL, Mabweijano J, MacIntyre MF, Mallinger L, March L, Marks GB, Marks R, Matsumori A, Matzopoulos R, Mayosi BM, McAnulty JH, McDermott MM, McGrath J, Mensah GA, Merriman TR, Michaud C, Miller M, Miller TR, Mock C, Mocumbi AO, Mokdad AA, Moran A, Mulholland K, Nair MN, Naldi L, Narayan KM, Nasseri K, Norman P, O'Donnell M, Omer SB, Ortblad K, Osborne R, Ozgediz D, Pahari B, Pandian JD, Rivero AP, Padilla RP, Perez-Ruiz F, Perico N, Phillips D, Pierce K, Pope CA, Porrini E, Pourmalek F, Raju M, Ranganathan D, Rehm JT, Rein DB, Remuzzi G, Rivara FP, Roberts T, De León FR, Rosenfeld LC, Rushton L, Sacco RL, Salomon JA, Sampson U, Sanman E, Schwebel DC, Segui-Gomez M, Shepard DS, Singh D, Singleton J, Sliwa K, Smith E, Steer A, Taylor JA, Thomas B, Tleyjeh IM, Towbin JA, Truelsen T, Undurraga EA, Venketasubramanian N, Vijayakumar L, Vos T, Wagner GR, Wang M, Wang W, Watt K, Weinstock MA, Weintraub R, Wilkinson JD, Woolf AD, Wulf S, Yeh PH, Yip P, Zabetian A, Zheng ZJ, Lopez AD, Murray CJ, AlMazroa MA, Memish ZA. Global and regional mortality from 235 causes of death for 20 age groups in 1990 and 2010: a systematic analysis for the Global Burden of Disease Study 2010. *Lancet* 2012; **380**: 2095-2128 [PMID: 23245604 DOI: 10.1016/S0140-6736(12)61728-0]

6 **Tandon BN**, Gupta H, Irshad M, Joshi YK, Chawla TC. Associated infection with non-A, non-B virus as possible cause of liver failure in Indian HBV carriers. *Lancet* 1984; **2**: 750-751 [PMID: 6148498]

7 **Allain JP**. Genomic screening for blood-borne viruses in transfusion settings. *Clin Lab Haematol* 2000; **22**: 1-10 [PMID: 10762297 DOI: 10.1046/j.1365-2257.2000.00265.x]

8 **Paryan M**, Forouzandeh MM, Kia V, Mohammadi-Yeganeh S, Abbasali RA, Mirab SS. Design and development of an in-house multiplex RT-PCR assay for simultaneous detection of HIV-1 and HCV in plasma samples. *Iran J Microbiol* 2012; **4**: 8-14 [PMID: 22783455 DOI: 10.1007/s12088-012-0271-1]

9 **Mine H**, Emura H, Miyamoto M, Tomono T, Minegishi K, Murokawa H, Yamanaka R, Yoshikawa A, Nishioka K. High throughput screening of 16 million serologically negative blood donors for hepatitis B virus, hepatitis C virus and human immunodeficiency virus type-1 by nucleic acid amplification testing with specific and sensitive multiplex reagent in Japan. *J Virol Methods* 2003; **112**: 145-151 [PMID: 12951223 DOI: 10.1016/S0166-0934(03)00215-5]

10 **Candotti D**, Richetin A, Cant B, Temple J, Sims C, Reeves I, Barbara JA, Allain JP. Evaluation of a transcription-mediated amplification-based HCV and HIV-1 RNA duplex assay for screening individual blood donations: a comparison with a minipool testing system. *Transfusion* 2003; **43**: 215-225 [PMID: 12559017 DOI: 10.1046/j.1537-2995.2003.00308.x]

11 **Heiat M**, Ranjbar R, Alavian SM. Classical and modern approaches used for viral hepatitis diagnosis. *Hepat Mon* 2014; **14**: e17632 [PMID: 24829586 DOI: 10.5812/hepatmon.17632]

12 **Fukumoto H**, Sato Y, Hasegawa H, Saeki H, Katano H. Development of a new real-time PCR system for simultaneous detection of bacteria and fungi in pathological samples. *Int J Clin Exp Pathol* 2015; **8**: 15479-15488 [PMID: 26823918]

13 **Wong AA**, Pabbaraju K, Wong S, Tellier R. Development of a multiplex real-time PCR for the simultaneous detection of herpes simplex and varicella zoster viruses in cerebrospinal fluid and lesion swab specimens. *J Virol Methods* 2016; **229**: 16-23 [PMID: 26711555 DOI: 10.1016/j.jviromet.2015.12.009]

14 **Kubista M**, Andrade JM, Bengtsson M, Forootan A, Jonák J, Lind K, Sindelka R, Sjöback R, Sjögreen B, Strömbom L, Ståhlberg A, Zoric N. The real-time polymerase chain reaction. *Mol Aspects Med* 2006; **27**: 95-125 [PMID: 16460794 DOI: 10.1016/j.mam.2005.12.007]

15 **Irshad M**, Ansari MA, Irshad K, Lingaiah R. Novel single-step multiplex real-time polymerase chain reaction assay for simultaneous quantification of hepatitis virus A, B, C, and E in serum. *J Gastroenterol Hepatol* 2013; **28**: 1869-1876 [PMID: 23800094 DOI: 10.1111/jgh.12302]

16 **Khodakov DA**, Zakharova NV, Gryadunov DA, Filatov FP, Zasedatelev AS, Mikhailovich VM. An oligonucleotide microarray for multiplex real-time PCR identification of HIV-1, HBV, and HCV. *Biotechniques* 2008; **44**: 241-246, 248 [PMID: 18330353 DOI: 10.2144/000112628]

17 **Kodani M**, Yang G, Conklin LM, Travis TC, Whitney CG, Anderson LJ, Schrag SJ, Taylor TH, Beall BW, Breiman RF, Feikin DR, Njenga MK, Mayer LW, Oberste MS, Tondella ML, Winchell JM, Lindstrom SL, Erdman DD, Fields BS. Application of TaqMan low-density arrays for simultaneous detection of multiple respiratory pathogens. *J Clin Microbiol* 2011; **49**: 2175-2182 [PMID: 21471348 DOI: 10.1128/JCM.02270-10]

18 **Lin B**, Vora GJ, Thach D, Walter E, Metzgar D, Tibbetts C, Stenger DA. Use of oligonucleotide microarrays for rapid detection and serotyping of acute respiratory disease-associated adenoviruses. *J Clin Microbiol* 2004; **42**: 3232-3239 [PMID: 15243087 DOI: 10.1128/JCM.42.7.3232-3239.2004]

19 **Pripuzova N**, Wang R, Tsai S, Li B, Hung GC, Ptak RG, Lo SC. Development of real-time PCR array for simultaneous detection of eight human blood-borne viral pathogens. *PLoS One* 2012; **7**: e43246 [PMID: 22912836 DOI: 10.1371/journal.pone.0043246]

20 **Ito K**, Shimizu N, Watanabe K, Saito T, Yoshioka Y, Sakane E, Tsunemine H, Akasaka H, Kodaka T, Takahashi T. Analysis of viral

infection by multiplex polymerase chain reaction assays in patients with liver dysfunction. *Intern Med* 2013; **52**: 201-211 [PMID: 23318849 DOI: 10.2169/internalmedicine.52.8206]
21 **Zhou L**, Gong R, Lu X, Zhang Y, Tang J. Development of a Multiplex Real-Time PCR Assay for the Detection of Treponema pallidum, HCV, HIV-1, and HBV. *Jpn J Infect Dis* 2015; **68**: 481-487 [PMID: 25866106 DOI: 10.7883/yoken.JJID.2014.416]
22 **Qiu F**, Cao J, Su Q, Yi Y, Bi S. Multiplex hydrolysis probe real-time PCR for simultaneous detection of hepatitis A virus and hepatitis E virus. *Int J Mol Sci* 2014; **15**: 9780-9788 [PMID: 24886818 DOI: 10.3390/ijms15069780]
23 **Wang X**, Seed B. High-throughput primer and probe design. In: Dorak MT, editor. Real-time PCR. Taylor and Francis Group, 2006: 93-106
24 **Bustin SA**, Nolan T. Primers and probes. In: Bustin SA, editor. A-Z of quantitative PCR. La Jolla, CA: International University Line, 2004: 279-326
25 **Navarro E**, Serrano-Heras G, Castaño MJ, Solera J. Real-time PCR detection chemistry. *Clin Chim Acta* 2015; **439**: 231-250 [PMID: 25451956 DOI: 10.1016/j.cca.2014.10.017]
26 **Heid CA**, Stevens J, Livak KJ, Williams PM. Real time quantitative PCR. *Genome Res* 1996; **6**: 986-994 [PMID: 8908518 DOI: 10.1101/gr.6.10.986]
27 **Kostrikis LG**, Tyagi S, Mhlanga MM, Ho DD, Kramer FR. Spectral genotyping of human alleles. *Science* 1998; **279**: 1228-1229 [PMID: 9508692 DOI: 10.1126/science.279.5354.1228]
28 **Nazarenko IA**, Bhatnagar SK, Hohman RJ. A closed tube format for amplification and detection of DNA based on energy transfer. *Nucleic Acids Res* 1997; **25**: 2516-2521 [PMID: 9171107 DOI: 10.1093/nar/25.12.25161107]
29 **Whitcombe D**, Theaker J, Guy SP, Brown T, Little S. Detection of PCR products using self-probing amplicons and fluorescence. *Nat Biotechnol* 1999; **17**: 804-807 [PMID: 10429248 DOI: 10.1038/11751]
30 **Isacsson J**, Cao H, Ohlsson L, Nordgren S, Svanvik N, Westman G, Kubista M, Sjöback R, Sehlstedt U. Rapid and specific detection of PCR products using light-up probes. *Mol Cell Probes* 2000; **14**: 321-328 [PMID: 11040096 DOI: 10.1006/mcpr.2000.0321]
31 **Higuchi R**, Dollinger G, Walsh PS, Griffith R. Simultaneous amplification and detection of specific DNA sequences. *Biotechnology* (N Y) 1992; **10**: 413-417 [PMID: 1368485]
32 **Wittwer CT**, Herrmann MG, Moss AA, Rasmussen RP. Continuous fluorescence monitoring of rapid cycle DNA amplification. *Biotechniques* 1997; **22**: 130-131, 134-138 [PMID: 8994660]
33 **Ririe KM**, Rasmussen RP, Wittwer CT. Product differentiation by analysis of DNA melting curves during the polymerase chain reaction. *Anal Biochem* 1997; **245**: 154-160 [PMID: 9056205 DOI: 10.1006/abio.1996.9916]
34 **Giglio S**, Monis PT, Saint CP. Demonstration of preferential binding of SYBR Green I to specific DNA fragments in real-time multiplex PCR. *Nucleic Acids Res* 2003; **31**: e136 [PMID: 14602929 DOI: 10.1093/nar/gng135]
35 **Bengtsson M**, Karlsson HJ, Westman G, Kubista M. A new minor groove binding asymmetric cyanine reporter dye for real-time PCR. *Nucleic Acids Res* 2003; **31**: e45 [PMID: 12682380 DOI: 10.1093/nar/gng045]
36 **Ishiguro T**, Saitoh J, Yawata H, Yamagishi H, Iwasaki S, Mitoma Y. Homogeneous quantitative assay of hepatitis C virus RNA by polymerase chain reaction in the presence of a fluorescent intercalater. *Anal Biochem* 1995; **229**: 207-213 [PMID: 7485974 DOI: 10.1006/abio.1995.1404]
37 **Wittwer CT**, Reed GH, Gundry CN, Vandersteen JG, Pryor RJ. High-resolution genotyping by amplicon melting analysis using LCGreen. *Clin Chem* 2003; **49**: 853-860 [PMID: 12765979 DOI: 10.1373/49.6.853]
38 **Monis PT**, Giglio S, Saint CP. Comparison of SYTO9 and SYBR Green I for real-time polymerase chain reaction and investigation of the effect of dye concentration on amplification and DNA melting curve analysis. *Anal Biochem* 2005; **340**: 24-34 [PMID: 15802126 DOI: 10.1016/j.ab.2005.01.046]
39 **Giglio S**, Monis PT, Saint CP. Legionella confirmation using real-time PCR and SYTO9 is an alternative to current methodology. *Appl Environ Microbiol* 2005; **71**: 8944-8948 [PMID: 16332896 DOI: 10.1128/AEM.71.12.8944-8948.2005]
40 **Gudnason H**, Dufva M, Bang DD, Wolff A. Comparison of multiple DNA dyes for real-time PCR: effects of dye concentration and sequence composition on DNA amplification and melting temperature. *Nucleic Acids Res* 2007; **35**: e127 [PMID: 17897966 DOI: 10.1093/nar/gkm671]
41 **Gruhn CC**, Wedemeyer H, Bremer B, Heckmann M, Steimer M, Carman WF. Clinical evaluation of a novel Fast-track diagnostics multiplex real-time PCR assay for detection and quantification of Hepatitis E virus. *J Clin Virol* 2015; **70**: S124-S125 [DOI: 10.1016/j.jcv.2015.07.289]
42 **Kodani M**, Mixson-Hayden T, Drobeniuc J, Kamili S. Rapid and sensitive approach to simultaneous detection of genomes of hepatitis A, B, C, D and E viruses. *J Clin Virol* 2014; **61**: 260-264 [PMID: 25081939 DOI: 10.1016/j.jcv.2014.06.027]
43 **Taranta A**, Rogalska-Taranta M, Gutierrez R, Manns MP, Bock M, Wursthorn K. Rapid hepatitis B and hepatitis Delta virus RNA quantification from small-sized liver tissue samples. *J Clin Virol* 2014; **61**: 286-288 [PMID: 25151628 DOI: 10.1016/j.jcv.2014.07.016]
44 **Fuentes C**, Guix S, Pérez-Rodriguez FJ, Fuster N, Carol M, Pintó RM, Bosch A. Standardized multiplex one-step qRT-PCR for hepatitis A virus, norovirus GI and GII quantification in bivalve mollusks and water. *Food Microbiol* 2014; **40**: 55-63 [PMID: 24549198 DOI: 10.1016/j.fm.2013.12.003]
45 **Jia S**, Wang F, Li F, Chang K, Yang S, Zhang K, Jiang W, Shang Y, Deng S, Chen M. Rapid detection of hepatitis B virus variants associated with lamivudine and adefovir resistance by multiplex ligation-dependent probe amplification combined with real-time PCR. *J Clin Microbiol* 2014; **52**: 460-466 [PMID: 24478474 DOI: 10.1128/JCM.02554-13]
46 **Zhang X**, Li A, Shuai J, Dai Y, Zhu Z, Wu S, He Y. Validation of an internally controlled multiplex real time RT-PCR for detection and typing of HEV genotype 3 and 4. *J Virol Methods* 2013; **193**: 432-438 [PMID: 23850697 DOI: 10.1016/j.jviromet.2013.07.007]
47 **Becker CE**, Kretzmann NA, Mattos AA, Veiga AB. Melting curve analysis for the screening of hepatitis B virus genotypes A, D and F in patients from a general hospital in southern Brazil. *Arq Gastroenterol* 2013; **50**: 219-225 [PMID: 24322195 DOI: 10.1590/S0004-28032013000200039]
48 **Kang LH**, Oh SH, Park JW, Won YJ, Ryu S, Paik SY. Simultaneous detection of waterborne viruses by multiplex real-time PCR. *J Microbiol* 2013; **51**: 671-675 [PMID: 24037661 DOI: 10.1007/s12275-013-3199-1]
49 **Marova AA**, Oksanich AS, Kaira AN, Meskina ER, Medvedeva EA, Ivanova OE, Lukashev AN, Kyuregian KK, Kalinkina MA, Egorova OV, Zverev VV, Faĭzuloev EV. [Experience of application of multiplex qPCR for differential diagnostics of intestinal viral infections]. *Zh Mikrobiol Epidemiol Immunobiol* 2012; (**6**): 39-45 [PMID: 23297630]
50 **Ynk Y**, Rahmathulla S, Madhavi C, Ramachandra VV, Vishnupriya S, Habeeb MA, Khaja MN. Simultaneous detection of Hepatitis B virus and Hepatitis C virus in human plasma using Taq-man chemistry. *J Med Allied Sci* 2011; **1**: 69-73
51 **Sun S**, Meng S, Zhang R, Zhang K, Wang L, Li J. Development of a new duplex real-time polymerase chain reaction assay for hepatitis B viral DNA detection. *Virol J* 2011; **8**: 227 [PMID: 21569595 DOI: 10.1186/1743-422X-8-227]
52 **Lee YM**, Chen YJ, Lee CM, Kuo LH, Wong WW, Chen YM. Detection of hepatitis C virus subtypes 6a, 6n, 6w and mixed infections using a modified multiplex real-time polymerase chain reaction protocol. *J Formos Med Assoc* 2011; **110**: 762-767 [PMID: 22248830 DOI: 10.1016/j.jfma.2011.11.006]
53 **Désiré N**, Sanchis T, Ben Moussa F, Stitou H, Katlama C, Thibault V. [Development and validation of a specific method for relative HBV-genotype G (G-HBV) quantification in the context of co-infection with other genotypes]. *Pathol Biol* (Paris) 2011; **59**:

e13-e19 [PMID: 20822865 DOI: 10.1016/j.patbio.2010.07.005]
54 **De Crignis E**, Re MC, Cimatti L, Zecchi L, Gibellini D. HIV-1 and HCV detection in dried blood spots by SYBR Green multiplex real-time RT-PCR. *J Virol Methods* 2010; **165**: 51-56 [PMID: 20045028 DOI: 10.1016/j.jviromet.2009.12.017]
55 **Meng S**, Li J. A novel duplex real-time reverse transcriptase-polymerase chain reaction assay for the detection of hepatitis C viral RNA with armored RNA as internal control. *Virol J* 2010; **7**: 117 [PMID: 20529244 DOI: 10.1186/1743-422X-7-117]
56 **Morales-Rayas R**, Wolffs PF, Griffiths MW. Simultaneous separation and detection of hepatitis A virus and norovirus in produce. *Int J Food Microbiol* 2010; **139**: 48-55 [PMID: 20223543 DOI: 10.1016/j.ijfoodmicro.2010.02.011]
57 **Blaise-Boisseau S**, Hennechart-Collette C, Guillier L, Perelle S. Duplex real-time qRT-PCR for the detection of hepatitis A virus in water and raspberries using the MS2 bacteriophage as a process control. *J Virol Methods* 2010; **166**: 48-53 [PMID: 20188760 DOI: 10.1016/j.jviromet.2010.02.017]
58 **Leblanc D**, Poitras E, Gagné MJ, Ward P, Houde A. Hepatitis E virus load in swine organs and tissues at slaughterhouse determined by real-time RT-PCR. *Int J Food Microbiol* 2010; **139**: 206-209 [PMID: 20206394 DOI: 10.1016/j.ijfoodmicro.2010.02.016]
59 **Malmström S**, Berglin-Enquist I, Lindh M. Novel method for genotyping hepatitis B virus on the basis of TaqMan real-time PCR. *J Clin Microbiol* 2010; **48**: 1105-1111 [PMID: 20107090 DOI: 10.1128/JCM.01442-09]
60 **Tanic N**, Stanojevic B, Tanic N, Schaefer S, Niesters HG, Bozic M, Dimitrijevic B. Concurrent quantitation of the A and D genotypes of hepatitis B virus. *J Virol Methods* 2009; **161**: 265-270 [PMID: 19591875 DOI: 10.1016/j.jviromet.2009.06.022]
61 **Ward P**, Poitras E, Leblanc D, Letellier A, Brassard J, Plante D, Houde A. Comparative analysis of different TaqMan real-time RT-PCR assays for the detection of swine Hepatitis E virus and integration of Feline calicivirus as internal control. *J Appl Microbiol* 2009; **106**: 1360-1369 [PMID: 19187137 DOI: 10.1111/j.1365-2672.2008.04104.x]
62 **Clancy A**, Crowley B, Niesters H, Herra C. The development of a qualitative real-time RT-PCR assay for the detection of hepatitis C virus. *Eur J Clin Microbiol Infect Dis* 2008; **27**: 1177-1182 [PMID: 18551325 DOI: 10.1007/s10096-008-0556-9]
63 **Compston LI**, Sarkobie F, Li C, Candotti D, Opare-Sem O, Allain JP. Multiplex real-time PCR for the detection and quantification of latent and persistent viral genomes in cellular or plasma blood fractions. *J Virol Methods* 2008; **151**: 47-54 [PMID: 18479760 DOI: 10.1016/j.jviromet.2008.03.023]
64 **Sun Z**, Zhou L, Zeng H, Chen Z, Zhu H. Multiplex locked nucleic acid probes for analysis of hepatitis B virus mutants using real-time PCR. *Genomics* 2007; **89**: 151-159 [PMID: 16935466 DOI: 10.1016/j.ygeno.2006.07.011]
65 **Hsia CC**, Chizhikov VE, Yang AX, Selvapandiyan A, Hewlett I, Duncan R, Puri RK, Nakhasi HL, Kaplan GG. Microarray multiplex assay for the simultaneous detection and discrimination of hepatitis B, hepatitis C, and human immunodeficiency type-1 viruses in human blood samples. *Biochem Biophys Res Commun* 2007; **356**: 1017-1023 [PMID: 17407765 DOI: 10.1016/j.bbrc.2007.03.087]
66 **Oksanich AS**, Faĭzuloev EB, Nikonova AA, Kashirin VI, Lotte VD, Ivanova OE, Zverev VV. [Real-time multiplex PCR for rapid detection of enteroviruses, adenoviruses and hepatitis A virus in clinical specimens]. *Zh Mikrobiol Epidemiol Immunobiol* 2007; (**5**): 65-70 [PMID: 18038551]
67 **Gibellini D**, Gardini F, Vitone F, Schiavone P, Furlini G, Re MC. Simultaneous detection of HCV and HIV-1 by SYBR Green real time multiplex RT-PCR technique in plasma samples. *Mol Cell Probes* 2006; **20**: 223-229 [PMID: 16537101 DOI: 10.1016/j.mcp.2005.12.005]
68 **Pugnale P**, Latorre P, Rossi C, Crovatto K, Pazienza V, Gottardi AD, Negro F. Real-time multiplex PCR assay to quantify hepatitis C virus RNA in peripheral blood mononuclear cells. *J Virol Methods* 2006; **133**: 195-204 [PMID: 16384611 DOI: 10.1016/j.jviromet.2005.11.007]
69 **Cook L**, Sullivan K, Krantz EM, Bagabag A, Jerome KR. Multiplex real-time reverse transcription-PCR assay for determination of hepatitis C virus genotypes. *J Clin Microbiol* 2006; **44**: 4149-4156 [PMID: 16988019 DOI: 10.1128/JCM.01230-06]
70 **Candotti D**, Temple J, Owusu-Ofori S, Allain JP. Multiplex real-time quantitative RT-PCR assay for hepatitis B virus, hepatitis C virus, and human immunodeficiency virus type 1. *J Virol Methods* 2004; **118**: 39-47 [PMID: 15158067 DOI: 10.1016/j.jviromet.2004.01.017]
71 **Meng Q**, Wong C, Rangachari A, Tamatsukuri S, Sasaki M, Fiss E, Cheng L, Ramankutty T, Clarke D, Yawata H, Sakakura Y, Hirose T, Impraim C. Automated multiplex assay system for simultaneous detection of hepatitis B virus DNA, hepatitis C virus RNA, and human immunodeficiency virus type 1 RNA. *J Clin Microbiol* 2001; **39**: 2937-2945 [PMID: 11474017 DOI: 10.1128/JCM.39.8.2937-2945.2001]
72 **Holland PM**, Abramson RD, Watson R, Gelfand DH. Detection of specific polymerase chain reaction product by utilizing the 5'----3' exonuclease activity of Thermus aquaticus DNA polymerase. *Proc Natl Acad Sci USA* 1991; **88**: 7276-7280 [PMID: 1871133]
73 **Lee LG**, Connell CR, Bloch W. Allelic discrimination by nick-translation PCR with fluorogenic probes. *Nucleic Acids Res* 1993; **21**: 3761-3766 [PMID: 8367293 DOI: 10.1093/nar/21.16.3761]
74 **Livak KJ**, Flood SJ, Marmaro J, Giusti W, Deetz K. Oligonucleotides with fluorescent dyes at opposite ends provide a quenched probe system useful for detecting PCR product and nucleic acid hybridization. *PCR Methods Appl* 1995; **4**: 357-362 [PMID: 7580930]
75 **Gibson UE**, Heid CA, Williams PM. A novel method for real time quantitative RT-PCR. *Genome Res* 1996; **6**: 995-1001 [PMID: 8908519]
76 **Crisalli P**, Kool ET. Multi-path quenchers: efficient quenching of common fluorophores. *Bioconjug Chem* 2011; **22**: 2345-2354 [PMID: 22034828 DOI: 10.1021/bc200424r]
77 **Tyagi S**, Kramer FR. Molecular beacons: probes that fluoresce upon hybridization. *Nat Biotechnol* 1996; **14**: 303-308 [PMID: 9630890 DOI: 10.1038/nbt0396-303]
78 **Bonetta L**. Prime time for real-time PCR. *Nat Methods* 2005; **2**: 305-312 [DOI: 10.1038/nmeth0405-305]
79 **Cheng J**, Zhang Y, Li Q. Real-time PCR genotyping using displacing probes. *Nucleic Acids Res* 2004; **32**: e61 [PMID: 15087493 DOI: 10.1093/nar/gnh055]
80 **Zhang DY**, Chen SX, Yin P. Optimizing the specificity of nucleic acid hybridization. *Nat Chem* 2012; **4**: 208-214 [PMID: 22354435 DOI: 10.1038/nchem.1246]
81 **Tyagi S**, Marras SAE, Vet JAM, Kramer FR. Molecular beacons: Hybridization probes for detection of nucleic acids in homogeneous solutions. In: Kessler C, editor. Nonradioactive Analysis of Biomolecules. 2nd ed. Berlin: Springer-Verlag, 2000: 606-616
82 **Murray JL**, Hu P, Shafer DA. Seven novel probe systems for real-time PCR provide absolute single-base discrimination, higher signaling, and generic components. *J Mol Diagn* 2014; **16**: 627-638 [PMID: 25307756 DOI: 10.1016/j.jmoldx.2014.06.008]
83 **Bustin S**, Bergkvist A, Nolan T. In silico tools for qPCR assay design and data analysis. *Methods Mol Biol* 2011; **760**: 283-306 [PMID: 21780004 DOI: 10.1007/978-1-61779-176-5_18]
84 **Rozen S**, Skaletsky H. Primer3 on the WWW for general users and for biologist programmers. *Methods Mol Biol* 2000; **132**: 365-386 [PMID: 10547847]
85 **Kalendar R**, Lee D, Schulman AH. FastPCR software for PCR, in silico PCR, and oligonucleotide assembly and analysis. *Methods Mol Biol* 2014; **1116**: 271-302 [PMID: 24395370 DOI: 10.1007/978-1-62703-764-8_18]
86 **Marshall OJ**. PerlPrimer: cross-platform, graphical primer design for standard, bisulphite and real-time PCR. *Bioinformatics* 2004; **20**: 2471-2472 [PMID: 15073005 DOI: 10.1093/bioinformatics/bth254]
87 **Owczarzy R**, Tataurov AV, Wu Y, Manthey JA, McQuisten KA,

Almabrazi HG, Pedersen KF, Lin Y, Garretson J, McEntaggart NO, Sailor CA, Dawson RB, Peek AS. IDT SciTools: a suite for analysis and design of nucleic acid oligomers. *Nucleic Acids Res* 2008; **36**: W163-W169 [PMID: 18440976 DOI: 10.1093/nar/gkn198]

88 **Bekaert M**, Teeling EC. UniPrime: a workflow-based platform for improved universal primer design. *Nucleic Acids Res* 2008; **36**: e56 [PMID: 18424794 DOI: 10.1093/nar/gkn191]

89 **Ye J**, Coulouris G, Zaretskaya I, Cutcutache I, Rozen S, Madden TL. Primer-BLAST: a tool to design target-specific primers for polymerase chain reaction. *BMC Bioinformatics* 2012; **13**: 134 [PMID: 22708584 DOI: 10.1186/1471-2105-13-134]

90 **Shen Z**, Qu W, Wang W, Lu Y, Wu Y, Li Z, Hang X, Wang X, Zhao D, Zhang C. MPprimer: a program for reliable multiplex PCR primer design. *BMC Bioinformatics* 2010; **11**: 143 [PMID: 20298595 DOI: 10.1186/1471-2105-11-143]

91 **Bustin SA**, Benes V, Garson JA, Hellemans J, Huggett J, Kubista M, Mueller R, Nolan T, Pfaffl MW, Shipley GL, Vandesompele J, Wittwer CT. The MIQE guidelines: minimum information for publication of quantitative real-time PCR experiments. *Clin Chem* 2009; **55**: 611-622 [PMID: 19246619 DOI: 10.1373/clinchem.2008.112797]

92 **Balashov SV**, Gardiner R, Park S, Perlin DS. Rapid, high-throughput, multiplex, real-time PCR for identification of mutations in the cyp51A gene of Aspergillus fumigatus that confer resistance to itraconazole. *J Clin Microbiol* 2005; **43**: 214-222 [PMID: 15634974 DOI: 10.1128/JCM.43.1.214-222.2005]

93 **Tuffaha MSA**. Phenotypic and genotypic diagnosis of malignancies: An immunohistochemical and molecular approach. Wiley-Blackwell, 2008 [DOI: 10.1002/9783527621521]

94 **Acharya SK**, Madan K, Dattagupta S, Panda SK. Viral hepatitis in India. *Natl Med J India* 2006; **19**: 203-217 [PMID: 17100109]

95 **Irshad M**, Acharya SK. Hepatitis D virus (HDV) infection in severe forms of liver diseases in north India. *Eur J Gastroenterol Hepatol* 1996; **8**: 995-998 [PMID: 8930565]

96 **Schmittgen TD**, Livak KJ. Analyzing real-time PCR data by the comparative C(T) method. *Nat Protoc* 2008; **3**: 1101-1108 [PMID: 18546601 DOI: 10.1038/nprot.2008.73]

97 **Caraguel CG**, Stryhn H, Gagné N, Dohoo IR, Hammell KL. Selection of a cutoff value for real-time polymerase chain reaction results to fit a diagnostic purpose: analytical and epidemiologic approaches. *J Vet Diagn Invest* 2011; **23**: 2-15 [PMID: 21217022 DOI: 10.1177/104063871102300102]

98 **McCormick MK**, Dockter J, Linnen JM, Kolk D, Wu Y, Giachetti C. Evaluation of a new molecular assay for detection of human immunodeficiency virus type 1 RNA, hepatitis C virus RNA, and hepatitis B virus DNA. *J Clin Virol* 2006; **36**: 166-176 [PMID: 16427802 DOI: 10.1016/j.jcv.2005.12.003]

99 **Defoort JP**, Martin M, Casano B, Prato S, Camilla C, Fert V. Simultaneous detection of multiplex-amplified human immunodeficiency virus type 1 RNA, hepatitis C virus RNA, and hepatitis B virus DNA using a flow cytometer microsphere-based hybridization assay. *J Clin Microbiol* 2000; **38**: 1066-1071 [PMID: 10698998]

100 **Stramer SL**, Krysztof DE, Brodsky JP, Fickett TA, Reynolds B, Dodd RY, Kleinman SH. Comparative analysis of triplex nucleic acid test assays in United States blood donors. *Transfusion* 2013; **53**: 2525-2537 [PMID: 23550838 DOI: 10.1111/trf.12178]

101 **Deiman B**, Jay C, Zintilini C, Vermeer S, van Strijp D, Venema F, van de Wiel P. Efficient amplification with NASBA of hepatitis B virus, herpes simplex virus and methicillin resistant Staphylococcus aureus DNA. *J Virol Methods* 2008; **151**: 283-293 [PMID: 18514336 DOI: 10.1016/j.jviromet.2008.04.009]

102 **Parker J**, Fowler N, Walmsley ML, Schmidt T, Scharrer J, Kowaleski J, Grimes T, Hoyos S, Chen J. Analytical Sensitivity Comparison between Singleplex Real-Time PCR and a Multiplex PCR Platform for Detecting Respiratory Viruses. *PLoS One* 2015; **10**: e0143164 [PMID: 26569120 DOI: 10.1371/journal.pone.0143164]

103 **Pabinger S**, Rödiger S, Kriegner A, Vierlinger K, Weinhäusel A. A survey of tools for the analysis of quantitative PCR (qPCR) data. *Biomol Detect Quantif* 2014; **1**: 23-33 [DOI: 10.1016/j.bdq.2014.08.002]

P- Reviewer: da Silva NM, Pokorska-Spiewak M **S- Editor**: Qi Y
L- Editor: Filipodia **E- Editor**: Ma S

World Journal of Gastroenterology

Submit a Manuscript: http://www.wjgnet.com/esps/
Help Desk: http://www.wjgnet.com/esps/helpdesk.aspx
DOI: 10.3748/wjg.v22.i20.4835

World J Gastroenterol 2016 May 28; 22(20): 4835-4847
ISSN 1007-9327 (print) ISSN 2219-2840 (online)

REVIEW

Advanced imaging techniques in the therapeutic response of transarterial chemoembolization for hepatocellular carcinoma

Ke Yang, Xiao-Ming Zhang, Lin Yang, Hao Xu, Juan Peng

Ke Yang, Xiao-Ming Zhang, Lin Yang, Hao Xu, Juan Peng, Sichuan Key Laboratory of Medical Imaging, Department of Radiology, Affiliated Hospital of North Sichuan Medical College, Nanchong 637000, Sichuan Province, China

Author contributions: Yang K and Yang L wrote the paper; Zhang XM designed the research; Xu H and Peng J collected the data.

Supported by Projects of Department of Science and Technology of Sichuan Province, No. 2016JY0105.

Conflict-of-interest statement: Authors declare no conflict of interests for this article.

Correspondence to: Lin Yang, MD, Sichuan Key Laboratory of Medical Imaging, Department of Radiology, Affiliated Hospital of North Sichuan Medical College, Wenhua Road No. 63, Nanchong 637000, Sichuan Province, China. linyangmd@163.com
Telephone: +86-817-2262223
Fax: +86-817-2222856

Received: February 26, 2016
Peer-review started: February 28, 2016
First decision: March 21, 2016
Revised: March 29, 2016
Accepted: April 20, 2016
Article in press: April 20, 2016
Published online: May 28, 2016

Abstract

Hepatocellular carcinoma (HCC) is one of the major causes of morbidity and mortality in patients with chronic liver disease. Transarterial chemoembolization (TACE) can significantly improve the survival rate of patients with HCC and is the first treatment choice for patients who are not suitable for surgical resections. The evaluation of the response to TACE treatment affects not only the assessment of the therapy efficacy but also the development of the next step in the treatment plan. The use of imaging to examine changes in tumor volume to assess the response of solid tumors to treatment has been controversial. In recent years, the emergence of new imaging technology has made it possible to observe the response of tumors to treatment prior to any morphological changes. In this article, the advances in studies reporting the use of computed tomography perfusion imaging, diffusion-weighted magnetic resonance imaging (MRI), intravoxel incoherent motion, diffusion kurtosis imaging, magnetic resonance spectroscopy, magnetic resonance perfusion-weighted imaging, blood oxygen level-dependent MRI, positron emission tomography (PET)/computed tomography and PET/MRI to assess the TACE treatment response are reviewed.

Key words: Blood oxygen level-dependent; Computed tomography perfusion imaging; Chemoembolization; Diffusion kurtosis imaging; Diffusion-weighted imaging; Hepatocellular carcinoma; Magnetic resonance perfusion-weighted imaging; Intravoxel incoherent motion; Magnetic resonance spectroscopy

Core tip: Imaging studies play an important role in the evaluation of the response to transarterial chemoembolization treatment. The use of imaging to examine changes in tumor size to assess the response of solid tumors to treatment has been controversial. In recent years, the emergence of new imaging technologies has made it possible to observe the response of tumors to treatment prior to any morphological changes. In this article, we present a summary of the most recent information on the role of imaging in assessing the treatment response in hepatocellular carcinomas.

Yang K, Zhang XM, Yang L, Xu H, Peng J. Advanced imaging techniques in the therapeutic response of transarterial chemoembolization for hepatocellular carcinoma. *World J Gastroenterol* 2016; 22(20): 4835-4847 Available from: URL: http://www.wjgnet.com/1007-9327/full/v22/i20/4835.htm DOI: http://dx.doi.org/10.3748/wjg.v22.i20.4835

INTRODUCTION

Hepatocellular carcinoma (HCC) is one of the major causes of morbidity and mortality in patients with chronic liver disease. Due to the undetected onset of liver cancer, the majority of patients receiving treatment are already in the advanced stage and are no longer candidates for surgical resection. Transarterial chemoembolization (TACE) involves the local infusion of a mixture of chemotherapeutic agents, blocks the blood supply to cancerous lesions and induces ischemia and necrosis in the tumor tissue, thereby significantly improving the survival rate of patients with liver cancer[1-4]. Currently, TACE has been recommended as the standard treatment for patients with stage B (Barcelona Clinic Liver Cancer staging) HCC[5,6]. The assessment of the response of HCC to TACE treatment affects not only the evaluation of the therapeutic efficacy but also the development of the next step in the treatment plan, including the time and frequency of repeated chemoembolization[7]. The previous World Health Organization and Response Evaluation Criteria in Solid Tumors criteria for evaluating the response of solid tumors to treatment depended on the measurement of tumor size[8]. The use of conventional imaging techniques to examine changes in tumor size to assess the response of solid tumors to treatment has been controversial, as many HCC treatments act by inducing tumor necrosis or by reducing vascularity, which is not necessarily accompanied by tumor shrinkage even when response occurs; notably, some tumors clearly respond to treatment but show no remarkable changes in size[9,10]. In recent years, the assessment of tumor viability has attracted increasing attention. The modified Response Evaluation Criteria in Solid Tumors criteria recommended by the European Association for the Study of the Liver consider the treatment factors leading to tumor necrosis and define the lesions that uptake a contrasting agent in the arterial phase as the surviving tumor after treatment[11]. In recent years, the emergence of new imaging technologies has made it possible to observe the response of tumors to treatment prior to any morphological changes. In this article, studies reporting advances in the use of computed tomography perfusion imaging (CTPI), diffusion-weighted magnetic resonance imaging (DWI), intravoxel incoherent motion (IVIM), diffusion kurtosis imaging (DKI), magnetic resonance spectroscopy (MRS), magnetic resonance perfusion-weighted imaging (MR PWI), blood oxygen level-dependent magnetic resonance imaging (BOLD MRI), positron emission tomography/computed tomography (PET/CT) and PET/MRI to assess the response to TACE treatment are reviewed.

COMPUTED TOMOGRAPHY PERFUSION IMAGING

Lipiodol is an ideal embolic agent commonly used in TACE treatment for HCC, and studies have shown that the deposition of lipiodol in the lesions is correlated with antitumor effects[12]. Conventional CT scanning has been widely used in the evaluation and follow-up of the efficacy of TACE treatment for HCC. Though CT can be used to visualize the distribution of lipiodol within the lesions, the high density deposition of lipiodol in tumor tissue can significantly affect the judgment of the viability of the tumor by CT.

CTPI not only clearly shows anatomy of the liver but also reflects changes in liver hemodynamics by allowing the quantitative analysis of blood perfusion in the liver tissue. CTPI performs continuous dynamic scans on selected slices while a contrast agent is intravenously injected, resulting in a curve that reflects the density changes of each pixel within the slice over time (time-density curve). A variety of mathematical models are then used to calculate the various perfusion parameters of the tissues and organs to evaluate the blood perfusion status[13-16] (Figure 1). The main parameters measured by CTPI include hepatic arterial perfusion (HAP), hepatic portal perfusion (HPP), total liver perfusion (TLP), hepatic arterial perfusion index (HAPI), hepatic portal perfusion index (HPPI), blood volume (BV) and mean transit time (MTT). Early CTPI scans used a single-slice continuous dynamic scan mode, but with progress in the development of multi-slice CT and software technology, CTPI has advanced from single-slice perfusion scans to multi-slice and same slice dynamic CT perfusion scans. Currently, spiral CT involving 64 or more slices can be used to conduct full-size liver perfusion scans with greatly improved temporal and spatial resolutions, which allows for the acquisition of more comprehensive hemodynamic information in a single scan. Moreover,

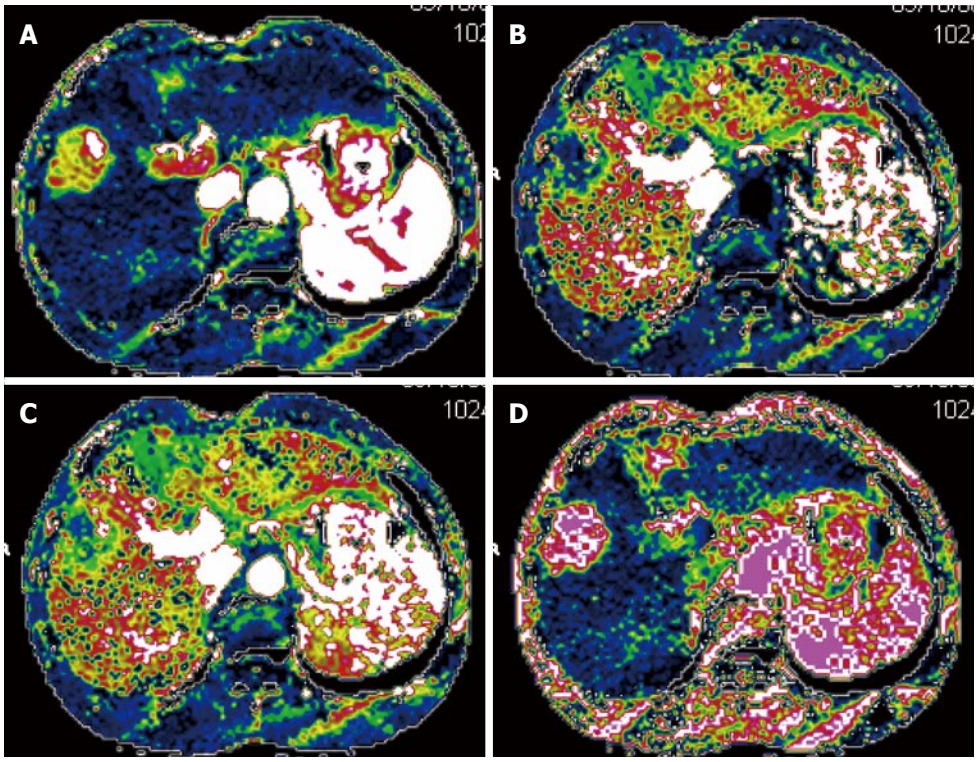

Figure 1 Seventy-year-old male patient with hepatocellular carcinoma. Axial perfusion images of the tumor before transarterial chemoembolization were created by maximum slope method. The tumor showed an increased hepatic arterial perfusion and decreased hepatic portal perfusion compared with the normal parenchyma. The values of hepatic arterial perfusion, hepatic portal perfusion, total liver perfusion and hepatic arterial perfusion index were 0.512 mL/min.mL, 0.226 mL/min.mL, 0.738 mL/min.mL and 69.4%, respectively. A: Image of hepatic arterial perfusion; B: Image of hepatic portal perfusion; C: Image of total liver perfusion; D: Image of hepatic arterial perfusion index.

lesions distant from the hilum can also be measured using CTPI, which has further promoted the clinical application of this technique[17-19].

The blood supply to HCC is one of the main factors affecting the efficacy of TACE treatment[20]. Increased blood supply to the HCC is associated with greater lipiodol accumulation after TACE treatment, whereas reduced blood supply to the HCC results in rather small amounts of lipiodol deposition in the treated lesions[21].

Many investigators have examined the effectiveness of CTPI in evaluating the response of HCC to TACE treatment, suggesting that CT perfusion imaging can accurately measure blood perfusion to the tumor and thus could be used to evaluate the response to TACE therapy[22-27]. Chen *et al*[22] assessed the changes in the CT perfusion parameters pre- and post-TACE in thirty-nine HCC patients in different treatment response groups. In the partial response (PR) treatment response group, the HAP, hepatic arterial fracture (HAF) and hepatic blood volume (HBV) of viable tumors post-TACE were reduced compared with their pre-TACE values. In the stable disease (SD) group, however, none of the CT perfusion parameters were significantly different pre- and post-TACE. In the progressive disease (PD) group, the post-TACE values for HAP, HAF, portal vein perfusion (PVP) and hepatic blood flow (HBF) of viable tumors were significantly increased compared to the pre-TACE values. These results indicated that changes in the CT perfusion parameters of viable tumors are correlated with responses of HCC to TACE, which can be feasibly monitored using CTPI. Reiner *et al*[23] studied sixteen patients with HCC who received CT liver perfusion during the treatment planning stage prior to transarterial radioembolization with Yttrium-90 (90Y) microspheres. The results showed that when responders were compared to non-responders, the 50th and 75th percentiles of arterial perfusion were significantly different and that the response to therapy could be predicted with a sensitivity of 88% and specificity of 75%. Our own studies[9,21] have shown that the CT perfusion parameters of HCC (HAP, TLP and HAPI) significantly decreased after TACE treatment[9] and that the blood perfusion parameters of the HCC lesions were correlated with post-TACE lipiodol deposition. Moreover, increased amounts of blood perfusion were associated with the increased deposition of lipiodol, and vice versa[21]. On the CT perfusion images, the areas with densely deposited lipiodol in the residual lesions in cases with complete or partial response (PR) displayed the complete absence of blood perfusion[9].

These results show that CTPI can be used to accurately measure the changes in perfusion parameters after TACE treatment for HCC and to evaluate the response to TACE therapy prior to changes in tumor size. CTPI can also be used to predict the efficacy of TACE therapy for HCC, to help select appropriate patients for TACE therapy and to develop individualized

treatment programs.

C-arm CT has emerged in recent years and can quantitatively measure the blood volume (BV) changes in tumor tissues. This technique has dramatically increased the convenience of assessing the response to TACE therapy[28-30]. Peynircioğlu *et al*[30] performed radioembolization (n = 21) or TACE (n = 13) treatment on thirty-four patients with HCC and used C-arm CT to measure the tumor BV before and after treatment. These cases were compared to ten cases in which perfusion imaging was performed using multidetector computed tomography (MDCT). The results showed that the mean BV of fourteen tumor lesions in the ten MDCT perfusion patients was highly correlated with the BV values obtained with C-arm CT. After treatment with TACE or radioembolization, the BV values decreased significantly, suggesting that the quantitative BV measurements obtained using C-arm CT are well-correlated with those obtained using MDCT; thus, C-arm CT is a promising tool for monitoring perfusion changes during hepatic arterial embolization. Currently, C-arm CT is mainly used to measure BV, but with the further development of this method, additional parameters can be used in the evaluation of TACE in the clinical treatment of HCC.

The main shortcoming of CTPI is that perfusion CT studies increase radiation exposure. In the future, with improvements to the equipment and technology, the radiation dose will be reduced.

DIFFUSION-WEIGHTED MRI

DWI is currently the only non-invasive imaging technique that can detect the free diffusion motion (Brownian motion) of water molecules in living tissue. Detecting the free diffusion motion of water molecules in the human body enables magnetic resonance at the molecular level. DWI not only reflects the dispersion characteristics of various tissues but also enables quantitative analyses of the microscopic structures and functional changes of tissues and organs. Though DWI has mainly been used in studies of central nervous system diseases[31-33], this technique is increasingly being applied to abdominal examinations[34-42]. At present, the commonly used single-time spin echo-echo planar imaging (SE-EPI) can image in rapid sequence and only takes 20-30 s to complete a liver scan[43], prompting the application of SE-EPI in the diagnosis and treatment of liver diseases.

DWI enables quantitative analyses by measuring the apparent diffusion coefficient (ADC) value. Thus, this technique can be used in assessing the effectiveness of TACE treatment for HCC[44-47]. After TACE therapy for HCC, the tumor cells undergo necrosis and decrease in number, the gaps between cells enlarge, and structures such as the cell membranes are damaged or dissolved, leading to enhanced water diffusion capacity and an increased ADC value. When the tumor survives or recurs, however, the ADC value does not increase or decrease. Bonekamp[44] used TACE therapy to treat seventy-one HCC lesions in forty-eight patients and performed MRI scans before the TACE treatment and one and six months after the treatment to monitor the ADC and venous enhancement (VE) as the tumor changed in size. The results demonstrated that thirty HCC lesions showed PR, thirty-five showed SD, and six showed PD 6 mo after TACE. Increase in ADC and decrease in VE 1 mo after TACE were significantly different between PR, SD, and PD. Yu *et al*[45] used enhanced MRI and DWI scans in twenty-three patients with liver cancer who had received TACE treatment, finding a total of twenty-three recurrent nodules in sixteen cases; the overall sensitivity in DWI was increased from 85.0% to 92.0%, though the specificity was decreased from 65.0% to 50.0%. The pre-TACE tumor ADC can be used to predict the response of HCC to TACE treatment. Mannelli *et al*[47] conducted DWI scans on thirty-six patients receiving TACE treatment for HCC and found that HCCs with poor and incomplete responses to TACE had significantly lower pre-treatment values of ADC and lower post-TACE values of ADC compared to HCCs with good or complete responses.

The shortcomings of DWI include EPI-related artifacts, such as deformation artifacts. Moreover, the ADC values of benign and malignant nodules in the liver overlap to some extent, and discriminating between these values requires a combination of medical history and other test results. Many factors that influence the ADC value, including the MR device, scan parameters (TR and TE), the b-value and the ROI, should be investigated in the future.

INTRAVOXEL INCOHERENT MOTION MR IMAGING

During DWI imaging, the b-value (a gradient factor) determines the sensitivity of the diffusion motion of water molecules in the tissue under analysis while affecting the accuracy of the ADC value. A low b-value enables the acquisition of images with a high SNR but lowers the sensitivity to the diffusion motion, resulting in a higher impact exerted by the blood perfusion on the DWI imaging. Under a high b-value, blood perfusion only has a small impact on DWI imaging, but the tissue contrast is decreased, leading to poor image quality[35,48-50].

IVIM, a multi-b-value diffusion-weighted imaging approach based on the principle of DWI, uses quantitative indicators to show the molecular diffusion and microperfusion of the local capillary network in lesions. The commonly used parameters include the true molecular-diffusion coefficient (D), the perfusion-related diffusion coefficient (D*) and the perfusion fraction (f). Compared with DWI, IVIM better reveals the diffusion effect of water molecules within a lesion

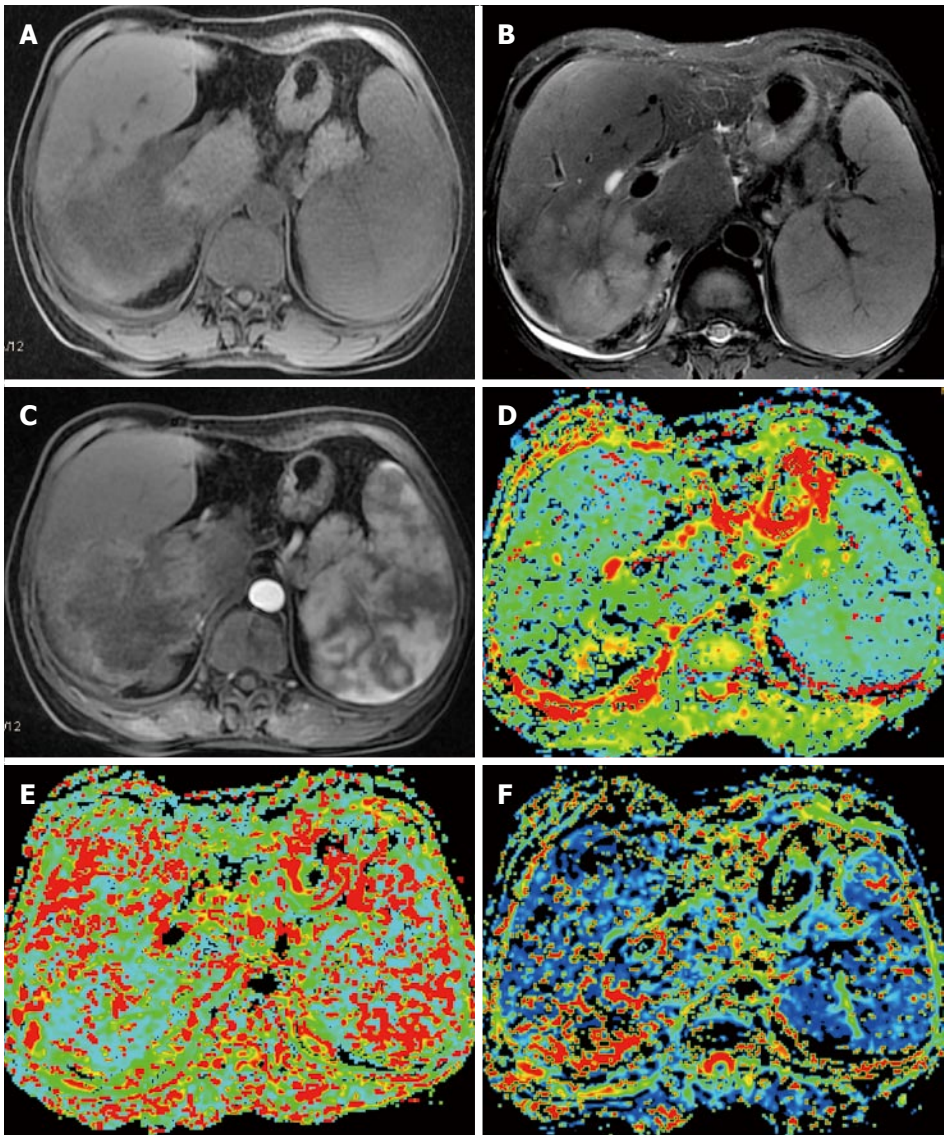

Figure 2 Fifty-three-year-old female patient with hepatocellular carcinoma in the right lobe of the liver. A: Axial T1-weighted image shows a hypointense mass lesion; B: Axial T2-weighted image shows a hyperintense mass lesion; C: Contrast-enhanced MRI during the arterial phase showing lesion enhancement; D: Mapping of the estimated value of the *D* parameter. The average value in the lesion ROI was $D = 1.22 \times 10^{-3}$ mm^2/s; E: Mapping of the estimated value of the *D** parameter. The average value in the lesion ROI was $D^* = 20.6 \times 10^{-3}$ mm^2/s; F: Mapping of the perfusion fraction (f) with a value of 19.6%.

and is thus more conducive to making judgments regarding the nature of liver lesions[51-55]. Watanabe *et al*[51] performed IVIM imaging on a total of 120 liver lesions (including 34 metastases, 32 HCC, 33 hemangiomas and 21 liver cysts) in seventy-four patients and showed that the mean D and ADC values of the benign lesions were greater than those of malignant lesions. The area under the ROC curve for the ADC values was significantly greater than that for the D values, which enabled the differentiation between benign and malignant lesions. When an ADC cut-off value of 1.40 was applied, the sensitivity and specificity for the detection of malignant lesions were 89% and 98%, respectively. Other studies have shown similar results[52-55] (Figure 2).

The applications of IVIM in cancer treatment evaluation have mainly focused on radiotherapy or chemotherapy in head and neck cancers and in breast cancer[56-67]. In recent years, some investigators have applied IVIM in the anti-angiogenesis therapy of liver cancer (including metastatic liver cancer) or radiofrequency ablation therapy[68-73]. Guo *et al*[71] investigated the use of IVIM-DWI to monitor the responses of VX2 tumors to radiofrequency ablation (RF Ablation) therapy in 10 VX2 tumor-bearing rabbits, showing that the IVIM-DWI derived f, D and D* parameters have the potential to indicate the response to therapy immediately after the RF ablation treatment. Shirota *et al*[72] evaluated the association between the therapeutic outcomes of sorafenib for advanced HCC and the parameters of IVIM. Though the true diffusion coefficient (DC) of responders at baseline was significantly higher than that of the non-responders, no significant differences were found in the

other parameters between these two groups. These results indicated that the DC before treatment may be a useful parameter for predicting the therapeutic outcome of using sorafenib to treat advanced HCC.

The use of IVIM to assess the response to TACE treatment in liver cancer has rarely been reported. Park *et al*[74] performed IVIM-DWI and Gd-EOB-DTPA-enhanced MRI scans before TACE therapy in forty-four cases of HCC and conducted CT scans after the TACE treatment. The patients were divided into two groups, the lipiodol good uptake (LGU) group and the lipiodol poor uptake (LPU) group, based on lipiodol deposition, and the results showed that both the arterial enhancement ratio derived from the contrast enhanced MRI and the D* values derived from IVIM-DWI were significantly higher in the LGU group than in the LPU group, indicating that the parameters of IVIM could help to predict lipiodol uptake.

DIFFUSION KURTOSIS IMAGING

The theoretical basis of the DWI and IVIM technologies is that the diffusion of water molecules *in vivo* assumes a normal distribution. In fact, due to the differences in structures and functions of local tissues and cells, the diffusion of water molecules *in vivo* is often a non-normal distribution. DKI is based on the non-normal distribution diffusion of water molecules *in vivo*, and the parameters of DKI measurements include the S, K and D values. DKI is still largely in the research phase, but this technique is being explored in wider clinical studies primarily focused on central nervous system diseases[75-83]. It is encouraging that some investigators have recently begun to use DKI in experiments to investigate its applications in liver diseases both *in vitro* and *in vivo*. Rosenkrantz *et al*[84] performed DKI and DWI scans on *in vitro* samples from twelve HCC cases and showed that the DKI model may provide additional value in characterizing HCC compared to a standard monoexponential model of DWI. Filli *et al*[85] also found that whole-body DKI is technically feasible and may reflect the tissue microstructure more meaningfully than whole-body DWI. Goshima *et al*[86] studied sixty-two consecutive patients with HCC to compare the use of DKI and conventional DWI in assessing the response to treatment. They found that compared to the non-viable group, the mean kurtosis (MK) value and mean ADC value in the viable group were significantly higher and lower, respectively. The sensitivity, specificity and AUC of the ROC curve for the assessment of HCC viability were greater using MK compared to ADC. These results indicated that DKI can be a new option for assessing the post-therapeutic response in HCC.

The results described above indicate that in the near future, DKI will play an important role in evaluating the response of liver cancer to TACE treatment.

MAGNETIC RESONANCE SPECTROSCOPY

Based on chemical shift effects and MRI principles, MRS uses a Fourier transform to process free induction decay signals to convert them into spectra with distributed frequencies. The areas under different metabolic peaks along the MRS frequency axis reflect the different concentrations of different compounds and can be quantitatively measured and analyzed. Thus, MRS not only truly reflects the molecular and chemical compositions of a tissue but also indirectly depicts the metabolism in the tissue[87].

The commonly used nuclei in MRS measurements of the liver are mainly ^{31}P and ^{1}H. By using ^{1}H-MRS to determine the amounts and ratios of choline and its derivatives after TACE treatment for liver cancer, it is possible to know whether HCC survives or relapses after TACE therapy. Studies have shown significant decreases in the choline/lipid values and the absolute value of choline complexes after TACE treatment for liver cancer. Kuo *et al*[88] investigated the use of proton MRS to assess hepatic lesions *in vivo* and the use of a 3.0-T scanner to measure the changes in metabolites related to HCC after TACE treatment. Their study included forty-three consecutive patients with hepatic tumors. Among the patients with proven HCC, eight lesions were evaluated before TACE and two to five days after TACE. A significant difference was achieved in the mean choline/lipid ratio between the malignant and benign tumors, and the mean choline/lipid ratios were significantly decreased after TACE. Wu *et al*[89] also reached similar conclusions. Taken together, those studies indicated that MRS has the potential for use in the detection of early metabolite changes in HCC after TACE[90-92].

The shortcomings of MRS mainly include its rather low sensitivity and specificity in differentiating between small nodules in the liver.

MAGNETIC RESONANCE PERFUSION-WEIGHTED IMAGING

MR PWI is an MRI technology that can reflect the microvascular distribution and blood perfusion in tissues. In MR PWI, a contrast agent is intravenously injected to increase the magnetic sensitivity of local capillaries and induce local magnetic field changes, leading to reduced signals derived from shortened transverse relaxation time by proton spin dephasing in tissues. The fast scanning imaging sequence generates a series of dynamic images; based on these images, the changes in signal intensity of the contrast agent when passing the hepatic parenchyma over time are used to generate the time-intensity curve (TIC), and semi-quantitative parameters such as maximal enhancement (MaxEn), initial enhancement rate (ER)

and initial area under the curve are calculated to indirectly reflect the vascularity and perfusion in the tumor[93]. Quantitative indicators calculated using the Tofts model include K (trans), k (ep) and v (e)[94,95]. The commonly used PWI sequences include enhanced spin labeling MRI (arterial spin labeling, ASL), T2*-weighted contrast-enhanced dynamic magnetic susceptibility MRI (dynamic susceptibility contrast, DSC) and T1-weighted dynamic contrast-enhanced MRI (dynamic contrast enhancement, DCE). ASL-MRI and DSC-MRI have been mostly used in PWI studies of the brain, whereas the DCE-MRI sequence has been frequently used in PWI studies of the liver[93]. PWI is a new technology that can improve the sensitivity and specificity of liver disease diagnoses. With its high temporal and spatial resolutions, PWI can directly reflect the blood perfusion of the subject tissue and indirectly reflect the tissue's microvascular distribution. This technique better displays the lesions and tremendously helps facilitate the analysis of the disease, the identification of benign and malignant lesions and the assessment of the response to TACE treatment[96-102]. Xu *et al*[96] investigated the value of perfusion-weighted MRI in the evaluation of the intranodular hemodynamic characteristics of dysplastic nodules (DNs) and HCCs in an experimental rat model. A total of 40 rats with chemically induced DNs and HCCs were investigated. Time to peak (Tp), maximal relative signal enhancement (REmax) and the initial slope of the signal intensity (SI) *vs* the time curves of the nodules and cirrhotic liver tissues were evaluated. The nodules that precisely corresponded to the MRI were examined histologically, and the results showed that HCCs had a significantly higher REmax, a shorter Tp and a higher slope than the adjacent cirrhotic liver. The REmax and slope of DNs were significantly lower than the adjacent cirrhotic liver parenchyma. Chen *et al*[97] performed MR PWI scans in thirty-five cases of HCC 24-48 h before and 48-168 h after TACE treatment, finding that in thirty-four of the HCC patients, the time-signal intensity curve (TSC) before TACE quickly decreased and then slowly increased in the tumor region of interest. After TACE, the fluctuating range of the TSC was significantly reduced in thirty-one patients, slightly reduced in three and not significantly changed in one. These results show that MR PWI is highly useful in the clinical evaluation of the efficacy of TACE in treating HCC.

Compared with CTPI, MR PWI has a higher temporal resolution, requires a smaller dose of contrast agent and poses no risk of radiation injury. However, this spectroscopic imaging technique requires more specialized equipment, has a longer imaging time and is thus more affected by environmental factors (*e.g.*, respiratory motion and the shifts caused by respiratory motion of the target lesions, *etc.*). Moreover, the heavy load on data processing has limited the clinical application and promotion of PWI.

BLOOD OXYGEN LEVEL DEPENDENT MRI

Ogawa *et al*[103] believed that paramagnetic deoxyhemoglobin could be used as a natural contrast agent in MRI scans and that deoxyhemoglobin might have contrast effects that could be observed using a gradient echo sequence in high-magnetic field. Based on these effects, these authors investigated whether determining the microvascular blood oxygen content could be used to reflect the dynamics and pathophysiology of blood flow in organs and tissues[103,104]. *In vivo*, paramagnetic deoxyhemoglobin forms a small magnetic field and a magnetic field gradient in its surroundings, causing heterogeneity in the magnetic field within the local tissue and shortening the T2*-weighted signal. The blood oxyhemoglobin and deoxyhemoglobin have opposite magnetic properties, and when the blood flow in the local tissue and the relative amount of oxygenated hemoglobin increase, the T2*-shortening effect of deoxygenated hemoglobin weakens, causing elongated local T2*, and vice versa. Because the value of the transverse relaxation rate (R2*) and the deoxyhemoglobin concentration in the tissue are correlated, in practice, the R2* value is used as an indicator for the quantitative evaluation of changes in the oxygen content in the local tissue.

The BOLD MRI technique, which has been successfully applied in studies of the central nervous system and urogenital system[105-112], is still in the exploratory stage for the diagnosis and treatment of liver cancer. Choi *et al*[113] studied the feasibility of using carbogen-challenge BOLD MRI to assess the early response of liver tumors to chemoembolization in a rat hepatoma model. Their results demonstrated that there was a significant difference between the pre-chemoembolization and post-chemoembolization percentages by which the R2* values of the tumors changed. Zhang *et al*[114] evaluated the feasibility of performing carbogen gas-challenge BOLD MRI measurements in patients with HCC and found that in two cases, the R2* values were significantly decreased one day after TACE. These findings indicated the feasibility of using BOLD MRI to evaluate the response of liver cancer to TACE treatment.

The shortcomings of BOLD MRI are that the technology is susceptible to influences of plasma proteins, molecular diffusion, pH, temperature, pixels, blood flow and vascular course. The iron stored in the liver may also affect the results. Plotting the ROI and analyzing the R2* value are susceptible to the influences of factors such as partial volume effects, blood vessels, necrosis, and bleeding. In future research, BOLD MRI technology will play an important role in evaluating the use of TACE to treat liver cancer.

PET/CT AND PET/MRI

PET/CT can reveal the metabolic information of

tumor tissues at the molecular level and can be used to diagnose malignant cancer with high sensitivity and specificity. Fluoro-deoxy-glucose (18F-FDG) is a glucose analogue that can reflect glucose metabolism in the tissue. Because changes in tissue metabolism always precede changes in tissue structure, PET/CT can be used to assess the early response after TACE treatment and to show residual, recurring and metastasized lesions by quantitatively analyzing the changes in the standardized uptake value (SUV) of the HCC lesions before and after TACE treatment[115-120]. Kim *et al*[115] performed PET/CT and enhanced CT scans on thirty-eight liver cancer lesions in thirty-six patients after TACE therapy and found that for the viable residual lesions, the diagnostic sensitivities of PET/CT and contrast-enhanced CT in the early postembolic period were 100% and 94%, respectively; in the late postembolic period, these values were 93% and 79%, respectively. When the multiphasic CT was normal, the 18F-FDG PET/CT could clearly reveal intrahepatic tumor recurrence and/or extrahepatic metastases in patients with elevated AFP after TACE treatment for HCC[119,120].

Due to the high cost of PET/CT examination and the high radiation dose, this method is not suitable for use in the routine evaluation of TACE treatment.

PET/MRI combines the advantages of PET and MRI. This method not only provides a better soft tissue contrast than PET/CT, thus providing richer information on molecular function and form, but also overcomes the body damage caused by CT irradiation during a PET/CT examination and the false positives found in PET/CT images. Although PET/MRI is a very recent technology, preliminary studies have already shown that PET/MRI has a great potential for applications in the nervous system, cardiovascular system and neoplastic diseases[121-125]. Yu *et al*[126] reported that the additional value of functional MRI techniques in combination with PET must be considered; MR DWI, for example, has been demonstrated to significantly improve the detection of sub-centimeter sized intrahepatic HCC metastases compared with conventional liver MRI alone (84% *vs* 69%). Tsouana *et al*[127] employed hybrid 18F-Fluroethyl-Choline (FEC) PET)/MRI to evaluate the treatment response of four cases of intracranial non-germinomatous germ cell tumors, and the results showed that in two patients, faint or absent choline avidity correlated with negative histology, whereas in two other patients, persistent choline avidity in the residual mass suggested the presence of a viable tumor, which was subsequently confirmed histologically.

Currently, the use of PET/MRI to evaluate interventional treatment for HCC has been rarely reported. Fowler *et al*[128] studied the relationship between dose deposition measured by PET/MRI and the response of individual lesions to radioembolization with 90Y microspheres. Twenty-six patients undergoing lobar treatment with 90Y microspheres underwent PET/MRI within 66 h of treatment and had follow-up imaging available. The results showed that the average dose could be used to predict the responses of responders and non-responders for all lesion types. PET/MRI of the 90Y microsphere distribution in patients with colorectal metastases showed significantly higher dose volume histograms (DVHs) values for responders than non-responders. A DVH analysis of the 90Y microsphere distribution following treatment may be an important predictor of response and could be used to guide future adaptive therapy trials. With the development of PET/MRI, this technology will provide more useful information for the evaluation of interventional liver cancer treatments.

CONCLUSION

In recent years, emerging imaging techniques such as new functional imaging have been effectively used to evaluate the early response of HCC to TACE treatment. Because different imaging techniques have their own advantages and disadvantages, to detect cancer lesions as early as possible and to provide accurate information regarding the diagnosis, staging and treatment evaluation, clinical applications should combine multiple imaging techniques according to the specific circumstances such that the advantages of each technique can compensate for the shortcomings of other techniques, thereby providing a comprehensive evaluation of the lesion[129,130]. With the rapid development of medical imaging, imaging technology will play an increasingly important role in cancer diagnosis and the evaluation of the treatment response.

REFERENCES

1 **Lo CM**, Ngan H, Tso WK, Liu CL, Lam CM, Poon RT, Fan ST, Wong J. Randomized controlled trial of transarterial lipiodol chemoembolization for unresectable hepatocellular carcinoma. *Hepatology* 2002; **35**: 1164-1171 [PMID: 11981766 DOI: 10.1053/jhep.2002.33156]

2 **Song do S**, Nam SW, Bae SH, Kim JD, Jang JW, Song MJ, Lee SW, Kim HY, Lee YJ, Chun HJ, You YK, Choi JY, Yoon SK. Outcome of transarterial chemoembolization-based multi-modal treatment in patients with unresectable hepatocellular carcinoma. *World J Gastroenterol* 2015; **21**: 2395-2404 [PMID: 25741147 DOI: 10.3748/wjg.v21.i8.2395]

3 **Marelli L**, Stigliano R, Triantos C, Senzolo M, Cholongitas E, Davies N, Tibballs J, Meyer T, Patch DW, Burroughs AK. Transarterial therapy for hepatocellular carcinoma: which technique is more effective? A systematic review of cohort and randomized studies. *Cardiovasc Intervent Radiol* 2007; **30**: 6-25 [PMID: 17103105 DOI: 10.1007/s00270-006-0062-3]

4 **Llovet JM**, Real MI, Montaña X, Planas R, Coll S, Aponte J, Ayuso C, Sala M, Muchart J, Solà R, Rodés J, Bruix J. Arterial embolisation or chemoembolisation versus symptomatic treatment in patients with unresectable hepatocellular carcinoma: a randomised controlled trial. *Lancet* 2002; **359**: 1734-1739 [PMID: 12049862 DOI: 10.1016/s0140-6736(02)08649-x]

5 **European Association For The Study Of The Liver, European Organisation For Research And Treatment Of Cancer**. EASL-EORTC clinical practice guidelines: management of hepatocellular carcinoma. *J Hepatol* 2012; **56**: 908-943 [PMID: 22424438 DOI:

10.1016/j.jhep.2011.12.001]
6 **Bruix J**, Sherman M. Management of hepatocellular carcinoma: an update. *Hepatology* 2011; **53**: 1020-1022 [PMID: 21374666 DOI: 10.1002/hep.24199]
7 **Lim HK**, Han JK. Hepatocellular carcinoma: evaluation of therapeutic response to interventional procedures. *Abdom Imaging* 2002; **27**: 168-179 [PMID: 11847576 DOI: 10.1007/s00261-001-0093-9]
8 **Therasse P**, Arbuck SG, Eisenhauer EA, Wanders J, Kaplan RS, Rubinstein L, Verweij J, Van Glabbeke M, van Oosterom AT, Christian MC, Gwyther SG. New guidelines to evaluate the response to treatment in solid tumors. European Organization for Research and Treatment of Cancer, National Cancer Institute of the United States, National Cancer Institute of Canada. *J Natl Cancer Inst* 2000; **92**: 205-216 [PMID: 10655437 DOI: 10.1093/jnci/92.3.205]
9 **Yang L**, Zhang XM, Tan BX, Liu M, Dong GL, Zhai ZH. Computed tomographic perfusion imaging for the therapeutic response of chemoembolization for hepatocellular carcinoma. *J Comput Assist Tomogr* 2012; **36**: 226-230 [PMID: 22446364 DOI: 10.1097/RCT.0b013e318245c23c]
10 **Kamel IR**, Liapi E, Reyes DK, Zahurak M, Bluemke DA, Geschwind JF. Unresectable hepatocellular carcinoma: serial early vascular and cellular changes after transarterial chemoembolization as detected with MR imaging. *Radiology* 2009; **250**: 466-473 [PMID: 19188315 DOI: 10.1148/radiol.2502072222]
11 **Arora A**, Kumar A. Treatment Response Evaluation and Follow-up in Hepatocellular Carcinoma. *J Clin Exp Hepatol* 2014; **4**: S126-S129 [PMID: 25755604 DOI: 10.1016/j.jceh.2014.05.005]
12 **Kanematsu T**, Furuta T, Takenaka K, Matsumata T, Yoshida Y, Nishizaki T, Hasuo K, Sugimachi K. A 5-year experience of lipiodolization: selective regional chemotherapy for 200 patients with hepatocellular carcinoma. *Hepatology* 1989; **10**: 98-102 [PMID: 2544499 DOI: 10.1002/hep.1840100119]
13 **Miles KA**, Hayball M, Dixon AK. Colour perfusion imaging: a new application of computed tomography. *Lancet* 1991; **337**: 643-645 [PMID: 1671994 DOI: 10.1016/0140-6736(91)92455-B]
14 **Miles KA**. Measurement of tissue perfusion by dynamic computed tomography. *Br J Radiol* 1991; **64**: 409-412 [PMID: 2036562 DOI: 10.1259/0007-1285-64-761-409]
15 **Miles KA**, Hayball MP, Dixon AK. Functional images of hepatic perfusion obtained with dynamic CT. *Radiology* 1993; **188**: 405-411 [PMID: 8327686 DOI: 10.1148/radiology.188.2.8327686]
16 **Miles KA**, Hayball MP, Dixon AK. Measurement of human pancreatic perfusion using dynamic computed tomography with perfusion imaging. *Br J Radiol* 1995; **68**: 471-475 [PMID: 7788231 DOI: 10.1259/0007-1285-68-809-471]
17 **Singh J**, Sharma S, Aggarwal N, Sood RG, Sood S, Sidhu R. Role of Perfusion CT Differentiating Hemangiomas from Malignant Hepatic Lesions. *J Clin Imaging Sci* 2014; **4**: 10 [PMID: 24744967 DOI: 10.4103/2156-7514.127959]
18 **Thaiss WM**, Haberland U, Kaufmann S, Spira D, Thomas C, Nikolaou K, Horger M, Sauter AW. Iodine concentration as a perfusion surrogate marker in oncology: Further elucidation of the underlying mechanisms using Volume Perfusion CT with 80 kVp. *Eur Radiol* 2015; Epub ahead of print [PMID: 26679179 DOI: 10.1007/s00330-015-4154-9]
19 **Kaufmann S**, Horger T, Oelker A, Kloth C, Nikolaou K, Schulze M, Horger M. Characterization of hepatocellular carcinoma (HCC) lesions using a novel CT-based volume perfusion (VPCT) technique. *Eur J Radiol* 2015; **84**: 1029-1035 [PMID: 25816994 DOI: 10.1016/j.ejrad.2015.02.020]
20 **Vogl TJ**, Schaefer P, Lehnert T, Nour-Eldin NE, Ackermann H, Mbalisike E, Hammerstingl R, Eichler K, Zangos S, Naguib NN. Intraprocedural blood volume measurement using C-arm CT as a predictor for treatment response of malignant liver tumours undergoing repetitive transarterial chemoembolization (TACE). *Eur Radiol* 2016; **26**: 755-763 [PMID: 26123407 DOI: 10.1007/s00330-015-3869-y]
21 **Yang L**, Zhang XM, Zhou XP, Tang W, Guan YS, Zhai ZH, Dong GL. Correlation between tumor perfusion and lipiodol deposition in hepatocellular carcinoma after transarterial chemoembolization. *J Vasc Interv Radiol* 2010; **21**: 1841-1846 [PMID: 20980165 DOI: 10.1016/j.jvir.2010.08.015]
22 **Chen G**, Ma DQ, He W, Zhang BF, Zhao LQ. Computed tomography perfusion in evaluating the therapeutic effect of transarterial chemoembolization for hepatocellular carcinoma. *World J Gastroenterol* 2008; **14**: 5738-5743 [PMID: 18837093 DOI: 10.3748/wjg.14.5738]
23 **Reiner CS**, Gordic S, Puippe G, Morsbach F, Wurnig M, Schaefer N, Veit-Haibach P, Pfammatter T, Alkadhi H. Histogram Analysis of CT Perfusion of Hepatocellular Carcinoma for Predicting Response to Transarterial Radioembolization: Value of Tumor Heterogeneity Assessment. *Cardiovasc Intervent Radiol* 2016; **39**: 400-408 [PMID: 26216725 DOI: 10.1007/s00270-015-1185-1]
24 **Kan Z**, Kobayashi S, Phongkitkarun S, Charnsangavej C. Functional CT quantification of tumor perfusion after transhepatic arterial embolization in a rat model. *Radiology* 2005; **237**: 144-150 [PMID: 16183930 DOI: 10.1148/radiol.2371040526]
25 **Tsushima Y**, Funabasama S, Aoki J, Sanada S, Endo K. Quantitative perfusion map of malignant liver tumors, created from dynamic computed tomography data. *Acad Radiol* 2004; **11**: 215-223 [PMID: 14974597 DOI: 10.1016/S1076-6332(03)00578-6]
26 **Ippolito D**, Fior D, Bonaffini PA, Capraro C, Leni D, Corso R, Sironi S. Quantitative evaluation of CT-perfusion map as indicator of tumor response to transarterial chemoembolization and radiofrequency ablation in HCC patients. *Eur J Radiol* 2014; **83**: 1665-1671 [PMID: 24962900 DOI: 10.1016/j.ejrad.2014.05.040]
27 **Ippolito D**, Bonaffini PA, Ratti L, Antolini L, Corso R, Fazio F, Sironi S. Hepatocellular carcinoma treated with transarterial chemoembolization: dynamic perfusion-CT in the assessment of residual tumor. *World J Gastroenterol* 2010; **16**: 5993-6000 [PMID: 21157976 DOI: 10.3748/wjg.v16.i47.5993]
28 **Syha R**, Grözinger G, Grosse U, Maurer M, Zender L, Horger M, Nikolaou K, Ketelsen D. Parenchymal Blood Volume Assessed by C-Arm-Based Computed Tomography in Immediate Posttreatment Evaluation of Drug-Eluting Bead Transarterial Chemoembolization in Hepatocellular Carcinoma. *Invest Radiol* 2016; **51**: 121-126 [PMID: 26488373 DOI: 10.1097/rli.0000000000000215]
29 **Syha R**, Grözinger G, Grosse U, Maurer M, Zender L, Horger M, Nikolaou K, Ketelsen D. C-arm computed tomography parenchymal blood volume measurement in evaluation of hepatocellular carcinoma before transarterial chemoembolization with drug eluting beads. *Cancer Imaging* 2015; **15**: 22 [PMID: 26715200 DOI: 10.1186/s40644-015-0057-x]
30 **Peynircioğlu B**, Hızal M, Çil B, Deuerling-Zheng Y, Von Roden M, Hazırolan T, Akata D, Özmen M, Balkancı F. Quantitative liver tumor blood volume measurements by a C-arm CT post-processing software before and after hepatic arterial embolization therapy: comparison with MDCT perfusion. *Diagn Interv Radiol* 2015; **21**: 71-77 [PMID: 25538037 DOI: 10.5152/dir.2014.13290]
31 **Mehdizade A**, Somon T, Wetzel S, Kelekis A, Martin JB, Scheidegger JR, Sztajzel R, Lovblad KO, Ruefenacht DA, Delavelle J. Diffusion weighted MR imaging on a low-field open magnet. Comparison with findings at 1.5T in 18 patients with cerebral ischemia. *J Neuroradiol* 2003; **30**: 25-30 [PMID: 12624588]
32 **Igarashi H**. What stroke MRI provides to us. *Rinsho Shinkeigaku* 2007; **47**: 921-924 [PMID: 18210836]
33 **Schellinger PD**, Bryan RN, Caplan LR, Detre JA, Edelman RR, Jaigobin C, Kidwell CS, Mohr JP, Sloan M, Sorensen AG, Warach S. Evidence-based guideline: The role of diffusion and perfusion MRI for the diagnosis of acute ischemic stroke: report of the Therapeutics and Technology Assessment Subcommittee of the American Academy of Neurology. *Neurology* 2010; **75**: 177-185 [PMID: 20625171 DOI: 10.1212/WNL.0b013e3181e7c9dd]
34 **Kele PG**, van der Jagt EJ. Diffusion weighted imaging in the liver. *World J Gastroenterol* 2010; **16**: 1567-1576 [PMID: 20355235 DOI: 10.3748/wjg.v16.i13.1567]
35 **Dijkstra H**, Baron P, Kappert P, Oudkerk M, Sijens PE. Effects of microperfusion in hepatic diffusion weighted imaging. *Eur Radiol* 2012; **22**: 891-899 [PMID: 22080250 DOI: 10.1007/

s00330-011-2313-1]
36 **Chung WS**, Kim MJ, Chung YE, Kim YE, Park MS, Choi JY, Kim KW. Comparison of gadoxetic acid-enhanced dynamic imaging and diffusion-weighted imaging for the preoperative evaluation of colorectal liver metastases. *J Magn Reson Imaging* 2011; **34**: 345-353 [PMID: 21702068 DOI: 10.1002/jmri.22671]
37 **Sandrasegaran K**, Akisik FM, Lin C, Tahir B, Rajan J, Saxena R, Aisen AM. Value of diffusion-weighted MRI for assessing liver fibrosis and cirrhosis. *AJR Am J Roentgenol* 2009; **193**: 1556-1560 [PMID: 19933647 DOI: 10.2214/ajr.09.2436]
38 **Lambregts DM**, Vandecaveye V, Barbaro B, Bakers FC, Lambrecht M, Maas M, Haustermans K, Valentini V, Beets GL, Beets-Tan RG. Diffusion-weighted MRI for selection of complete responders after chemoradiation for locally advanced rectal cancer: a multicenter study. *Ann Surg Oncol* 2011; **18**: 2224-2231 [PMID: 21347783 DOI: 10.1245/s10434-011-1607-5]
39 **Kim SY**, Lee SS, Byun JH, Park SH, Kim JK, Park B, Kim N, Lee MG. Malignant hepatic tumors: short-term reproducibility of apparent diffusion coefficients with breath-hold and respiratory-triggered diffusion-weighted MR imaging. *Radiology* 2010; **255**: 815-823 [PMID: 20501719 DOI: 10.1148/radiol.10091706]
40 **Heo SH**, Jeong YY, Shin SS, Kim JW, Lim HS, Lee JH, Koh YS, Cho CK, Kang HK. Apparent diffusion coefficient value of diffusion-weighted imaging for hepatocellular carcinoma: correlation with the histologic differentiation and the expression of vascular endothelial growth factor. *Korean J Radiol* 2010; **11**: 295-303 [PMID: 20461183 DOI: 10.3348/kjr.2010.11.3.295]
41 **Nasu K**, Kuroki Y, Tsukamoto T, Nakajima H, Mori K, Minami M. Diffusion-weighted imaging of surgically resected hepatocellular carcinoma: imaging characteristics and relationship among signal intensity, apparent diffusion coefficient, and histopathologic grade. *AJR Am J Roentgenol* 2009; **193**: 438-444 [PMID: 19620441 DOI: 10.2214/ajr.08.1424]
42 **Jiang ZX**, Peng WJ, Li WT, Tang F, Liu SY, Qu XD, Wang JH, Lu HF. Effect of b value on monitoring therapeutic response by diffusion-weighted imaging. *World J Gastroenterol* 2008; **14**: 5893-5899 [PMID: 18855990 DOI: 10.3748/wjg.14.5893]
43 **Wybranski C**, Zeile M, Löwenthal D, Fischbach F, Pech M, Röhl FW, Gademann G, Ricke J, Dudeck O. Value of diffusion weighted MR imaging as an early surrogate parameter for evaluation of tumor response to high-dose-rate brachytherapy of colorectal liver metastases. *Radiat Oncol* 2011; **6**: 43 [PMID: 21524305 DOI: 10.1186/1748-717x-6-43]
44 **Bonekamp S**, Jolepalem P, Lazo M, Gulsun MA, Kiraly AP, Kamel IR. Hepatocellular carcinoma: response to TACE assessed with semiautomated volumetric and functional analysis of diffusion-weighted and contrast-enhanced MR imaging data. *Radiology* 2011; **260**: 752-761 [PMID: 21771960 DOI: 10.1148/radiol.11102330]
45 **Yu JS**, Kim JH, Chung JJ, Kim KW. Added value of diffusion-weighted imaging in the MRI assessment of perilesional tumor recurrence after chemoembolization of hepatocellular carcinomas. *J Magn Reson Imaging* 2009; **30**: 153-160 [PMID: 19557734 DOI: 10.1002/jmri.21818]
46 **Kubota K**, Yamanishi T, Itoh S, Murata Y, Miyatake K, Yasunami H, Morio K, Hamada N, Nishioka A, Ogawa Y. Role of diffusion-weighted imaging in evaluating therapeutic efficacy after transcatheter arterial chemoembolization for hepatocellular carcinoma. *Oncol Rep* 2010; **24**: 727-732 [PMID: 20664980 DOI: 10.3892/or_00000914]
47 **Mannelli L**, Kim S, Hajdu CH, Babb JS, Taouli B. Serial diffusion-weighted MRI in patients with hepatocellular carcinoma: Prediction and assessment of response to transarterial chemoembolization. Preliminary experience. *Eur J Radiol* 2013; **82**: 577-582 [PMID: 23246330 DOI: 10.1016/j.ejrad.2012.11.026]
48 **Thoeny HC**, De Keyzer F. Diffusion-weighted MR imaging of native and transplanted kidneys. *Radiology* 2011; **259**: 25-38 [PMID: 21436095 DOI: 10.1148/radiol.10092419]
49 **Agnello F**, Ronot M, Valla DC, Sinkus R, Van Beers BE, Vilgrain V. High-b-value diffusion-weighted MR imaging of benign hepatocellular lesions: quantitative and qualitative analysis. *Radiology* 2012; **262**: 511-519 [PMID: 22143926 DOI: 10.1148/radiol.11110922]
50 **Taouli B**, Tolia AJ, Losada M, Babb JS, Chan ES, Bannan MA, Tobias H. Diffusion-weighted MRI for quantification of liver fibrosis: preliminary experience. *AJR Am J Roentgenol* 2007; **189**: 799-806 [PMID: 17885048 DOI: 10.2214/ajr.07.2086]
51 **Watanabe H**, Kanematsu M, Goshima S, Kajita K, Kawada H, Noda Y, Tatahashi Y, Kawai N, Kondo H, Moriyama N. Characterizing focal hepatic lesions by free-breathing intravoxel incoherent motion MRI at 3.0 T. *Acta Radiol* 2014; **55**: 1166-1173 [PMID: 24316660 DOI: 10.1177/0284185113514966]
52 **Yamada I**, Aung W, Himeno Y, Nakagawa T, Shibuya H. Diffusion coefficients in abdominal organs and hepatic lesions: evaluation with intravoxel incoherent motion echo-planar MR imaging. *Radiology* 1999; **210**: 617-623 [PMID: 10207458 DOI: 10.1148/radiology.210.3.r99fe17617]
53 **Penner AH**, Sprinkart AM, Kukuk GM, Gütgemann I, Gieseke J, Schild HH, Willinek WA, Mürtz P. Intravoxel incoherent motion model-based liver lesion characterisation from three b-value diffusion-weighted MRI. *Eur Radiol* 2013; **23**: 2773-2783 [PMID: 23666233 DOI: 10.1007/s00330-013-2869-z]
54 **Ichikawa S**, Motosugi U, Ichikawa T, Sano K, Morisaka H, Araki T. Intravoxel incoherent motion imaging of focal hepatic lesions. *J Magn Reson Imaging* 2013; **37**: 1371-1376 [PMID: 23172819 DOI: 10.1002/jmri.23930]
55 **Woo S**, Lee JM, Yoon JH, Joo I, Han JK, Choi BI. Intravoxel incoherent motion diffusion-weighted MR imaging of hepatocellular carcinoma: correlation with enhancement degree and histologic grade. *Radiology* 2014; **270**: 758-767 [PMID: 24475811 DOI: 10.1148/radiol.13130444]
56 **Xiao Y**, Pan J, Chen Y, Chen Y, He Z, Zheng X. Intravoxel Incoherent Motion-Magnetic Resonance Imaging as an Early Predictor of Treatment Response to Neoadjuvant Chemotherapy in Locoregionally Advanced Nasopharyngeal Carcinoma. *Medicine* (Baltimore) 2015; **94**: e973 [PMID: 26091468 DOI: 10.1097/md.0000000000000973]
57 **Kim DY**, Kim HS, Goh MJ, Choi CG, Kim SJ. Utility of intravoxel incoherent motion MR imaging for distinguishing recurrent metastatic tumor from treatment effect following gamma knife radiosurgery: initial experience. *AJNR Am J Neuroradiol* 2014; **35**: 2082-2090 [PMID: 24970548 DOI: 10.3174/ajnr.A3995]
58 **Hauser T**, Essig M, Jensen A, Laun FB, Münter M, Maier-Hein KH, Stieltjes B. Prediction of treatment response in head and neck carcinomas using IVIM-DWI: Evaluation of lymph node metastasis. *Eur J Radiol* 2014; **83**: 783-787 [PMID: 24631600 DOI: 10.1016/j.ejrad.2014.02.013]
59 **Hauser T**, Essig M, Jensen A, Gerigk L, Laun FB, Münter M, Simon D, Stieltjes B. Characterization and therapy monitoring of head and neck carcinomas using diffusion-imaging-based intravoxel incoherent motion parameters-preliminary results. *Neuroradiology* 2013; **55**: 527-536 [PMID: 23417120 DOI: 10.1007/s00234-013-1154-9]
60 **Hu YC**, Yan LF, Wu L, Du P, Chen BY, Wang L, Wang SM, Han Y, Tian Q, Yu Y, Xu TY, Wang W, Cui GB. Intravoxel incoherent motion diffusion-weighted MR imaging of gliomas: efficacy in preoperative grading. *Sci Rep* 2014; **4**: 7208 [PMID: 25434593 DOI: 10.1038/srep07208]
61 **Zhang SX**, Jia QJ, Zhang ZP, Liang CH, Chen WB, Qiu QH, Li H. Intravoxel incoherent motion MRI: emerging applications for nasopharyngeal carcinoma at the primary site. *Eur Radiol* 2014; **24**: 1998-2004 [PMID: 24838795 DOI: 10.1007/s00330-014-3203-0]
62 **Marzi S**, Forina C, Marucci L, Giovinazzo G, Giordano C, Piludu F, Landoni V, Spriano G, Vidiri A. Early radiation-induced changes evaluated by intravoxel incoherent motion in the major salivary glands. *J Magn Reson Imaging* 2015; **41**: 974-982 [PMID: 24700435 DOI: 10.1002/jmri.24626]
63 **Kim HS**, Suh CH, Kim N, Choi CG, Kim SJ. Histogram analysis of intravoxel incoherent motion for differentiating recurrent tumor from treatment effect in patients with glioblastoma: initial clinical experience. *AJNR Am J Neuroradiol* 2014; **35**: 490-497 [PMID:

23969343 DOI: 10.3174/ajnr.A3719]
64 **Cui Y**, Zhang C, Li X, Liu H, Yin B, Xu T, Zhang Y, Wang D. Intravoxel Incoherent Motion Diffusion-weighted Magnetic Resonance Imaging for Monitoring the Early Response to ZD6474 from Nasopharyngeal Carcinoma in Nude Mouse. *Sci Rep* 2015; **5**: 16389 [PMID: 26574153 DOI: 10.1038/srep16389]
65 **Ding Y**, Hazle JD, Mohamed AS, Frank SJ, Hobbs BP, Colen RR, Gunn GB, Wang J, Kalpathy-Cramer J, Garden AS, Lai SY, Rosenthal DI, Fuller CD. Intravoxel incoherent motion imaging kinetics during chemoradiotherapy for human papillomavirus-associated squamous cell carcinoma of the oropharynx: preliminary results from a prospective pilot study. *NMR Biomed* 2015; **28**: 1645-1654 [PMID: 26451969 DOI: 10.1002/nbm.3412]
66 **Che S**, Zhao X, Ou Y, Li J, Wang M, Wu B, Zhou C. Role of the Intravoxel Incoherent Motion Diffusion Weighted Imaging in the Pre-treatment Prediction and Early Response Monitoring to Neoadjuvant Chemotherapy in Locally Advanced Breast Cancer. *Medicine* (Baltimore) 2016; **95**: e2420 [PMID: 26825883 DOI: 10.1097/md.0000000000002420]
67 **Gaeta M**, Benedetto C, Minutoli F, D'Angelo T, Amato E, Mazziotti S, Racchiusa S, Mormina E, Blandino A, Pergolizzi S. Use of diffusion-weighted, intravoxel incoherent motion, and dynamic contrast-enhanced MR imaging in the assessment of response to radiotherapy of lytic bone metastases from breast cancer. *Acad Radiol* 2014; **21**: 1286-1293 [PMID: 25088834 DOI: 10.1016/j.acra.2014.05.021]
68 **Joo I**, Lee JM, Han JK, Choi BI. Intravoxel incoherent motion diffusion-weighted MR imaging for monitoring the therapeutic efficacy of the vascular disrupting agent CKD-516 in rabbit VX2 liver tumors. *Radiology* 2014; **272**: 417-426 [PMID: 24697148 DOI: 10.1148/radiol.14131165]
69 **Joo I**, Lee JM, Grimm R, Han JK, Choi BI. Monitoring Vascular Disrupting Therapy in a Rabbit Liver Tumor Model: Relationship between Tumor Perfusion Parameters at IVIM Diffusion-weighted MR Imaging and Those at Dynamic Contrast-enhanced MR Imaging. *Radiology* 2016; **278**: 104-113 [PMID: 26200601 DOI: 10.1148/radiol.2015141974]
70 **Koh DM**. Science to practice: can intravoxel incoherent motion diffusion-weighted MR imaging be used to assess tumor response to antivascular drugs? *Radiology* 2014; **272**: 307-308 [PMID: 25058129 DOI: 10.1148/radiol.14140714]
71 **Guo Z**, Zhang Q, Li X, Jing Z. Intravoxel Incoherent Motion Diffusion Weighted MR Imaging for Monitoring the Instantly Therapeutic Efficacy of Radiofrequency Ablation in Rabbit VX2 Tumors without Evident Links between Conventional Perfusion Weighted Images. *PLoS One* 2015; **10**: e0127964 [PMID: 26020785 DOI: 10.1371/journal.pone.0127964]
72 **Shirota N**, Saito K, Sugimoto K, Takara K, Moriyasu F, Tokuuye K. Intravoxel incoherent motion MRI as a biomarker of sorafenib treatment for advanced hepatocellular carcinoma: a pilot study. *Cancer Imaging* 2016; **16**: 1 [PMID: 26822946 DOI: 10.1186/s40644-016-0059-3]
73 **Granata V**, Fusco R, Catalano O, Filice S, Amato DM, Nasti G, Avallone A, Izzo F, Petrillo A. Early assessment of colorectal cancer patients with liver metastases treated with antiangiogenic drugs: The role of intravoxel incoherent motion in diffusion-weighted imaging. *PLoS One* 2015; **10**: e0142876 [PMID: 26566221 DOI: 10.1371/journal.pone.0142876]
74 **Park YS**, Lee CH, Kim JH, Kim IS, Kiefer B, Seo TS, Kim KA, Park CM. Using intravoxel incoherent motion (IVIM) MR imaging to predict lipiodol uptake in patients with hepatocellular carcinoma following transcatheter arterial chemoembolization: a preliminary result. *Magn Reson Imaging* 2014; **32**: 638-646 [PMID: 24703575 DOI: 10.1016/j.mri.2014.03.003]
75 **Hori M**, Fukunaga I, Masutani Y, Taoka T, Kamagata K, Suzuki Y, Aoki S. Visualizing non-Gaussian diffusion: clinical application of q-space imaging and diffusional kurtosis imaging of the brain and spine. *Magn Reson Med Sci* 2012; **11**: 221-233 [PMID: 23269009 DOI: 10.2463/mrms.11.221]
76 **Rosenkrantz AB**, Padhani AR, Chenevert TL, Koh DM, De Keyzer F, Taouli B, Le Bihan D. Body diffusion kurtosis imaging: Basic principles, applications, and considerations for clinical practice. *J Magn Reson Imaging* 2015; **42**: 1190-1202 [PMID: 26119267 DOI: 10.1002/jmri.24985]
77 **Sun PZ**, Wang Y, Mandeville E, Chan ST, Lo EH, Ji X. Validation of fast diffusion kurtosis MRI for imaging acute ischemia in a rodent model of stroke. *NMR Biomed* 2014; **27**: 1413-1418 [PMID: 25208309 DOI: 10.1002/nbm.3188]
78 **Zhao L**, Wang Y, Jia Y, Zhong S, Sun Y, Zhou Z, Zhang Z, Huang L. Cerebellar microstructural abnormalities in bipolar depression and unipolar depression: A diffusion kurtosis and perfusion imaging study. *J Affect Disord* 2016; **195**: 21-31 [PMID: 26852094 DOI: 10.1016/j.jad.2016.01.042]
79 **Kamiya K**, Kamagata K, Miyajima M, Nakajima M, Hori M, Tsuruta K, Mori H, Kunimatsu A, Arai H, Aoki S, Ohtomo K. Diffusional Kurtosis Imaging in Idiopathic Normal Pressure Hydrocephalus: Correlation with Severity of Cognitive Impairment. *Magn Reson Med Sci* 2016; Epub ahead of print [PMID: 26841854 DOI: 10.2463/mrms.mp.2015-0093]
80 **Yuan L**, Sun M, Chen Y, Long M, Zhao X, Yin J, Yan X, Ji D, Ni H. Non-Gaussian diffusion alterations on diffusion kurtosis imaging in patients with early Alzheimer's disease. *Neurosci Lett* 2016; **616**: 11-18 [PMID: 26797581 DOI: 10.1016/j.neulet.2016.01.021]
81 **Jiang R**, Jiang J, Zhao L, Zhang J, Zhang S, Yao Y, Yang S, Shi J, Shen N, Su C, Zhang J, Zhu W. Diffusion kurtosis imaging can efficiently assess the glioma grade and cellular proliferation. *Oncotarget* 2015; **6**: 42380-42393 [PMID: 26544514 DOI: 10.18632/oncotarget.5675]
82 **Tyagi N**, Riaz N, Hunt M, Wengler K, Hatzoglou V, Young R, Mechalakos J, Lee N. Weekly response assessment of involved lymph nodes to radiotherapy using diffusion-weighted MRI in oropharynx squamous cell carcinoma. *Med Phys* 2016; **43**: 137 [PMID: 26745906 DOI: 10.1118/1.4937791]
83 **Chen Y**, Ren W, Zheng D, Zhong J, Liu X, Yue Q, Liu M, Xiao Y, Chen W, Chan Q, Pan J. Diffusion kurtosis imaging predicts neoadjuvant chemotherapy responses within 4 days in advanced nasopharyngeal carcinoma patients. *J Magn Reson Imaging* 2015; **42**: 1354-1361 [PMID: 25873208 DOI: 10.1002/jmri.24910]
84 **Rosenkrantz AB**, Sigmund EE, Winnick A, Niver BE, Spieler B, Morgan GR, Hajdu CH. Assessment of hepatocellular carcinoma using apparent diffusion coefficient and diffusion kurtosis indices: preliminary experience in fresh liver explants. *Magn Reson Imaging* 2012; **30**: 1534-1540 [PMID: 22819175 DOI: 10.1016/j.mri.2012.04.020]
85 **Filli L**, Wurnig M, Nanz D, Luechinger R, Kenkel D, Boss A. Whole-body diffusion kurtosis imaging: initial experience on non-Gaussian diffusion in various organs. *Invest Radiol* 2014; **49**: 773-778 [PMID: 24979203 DOI: 10.1097/rli.0000000000000082]
86 **Goshima S**, Kanematsu M, Noda Y, Kondo H, Watanabe H, Bae KT. Diffusion kurtosis imaging to assess response to treatment in hypervascular hepatocellular carcinoma. *AJR Am J Roentgenol* 2015; **204**: W543-W549 [PMID: 25905960 DOI: 10.2214/ajr.14.13235]
87 **Martín Noguerol T**, Sánchez-González J, Martínez Barbero JP, García-Figueiras R, Baleato-González S, Luna A. Clinical Imaging of Tumor Metabolism with ^{1}H Magnetic Resonance Spectroscopy. *Magn Reson Imaging Clin N Am* 2016; **24**: 57-86 [PMID: 26613876 DOI: 10.1016/j.mric.2015.09.002]
88 **Kuo YT**, Li CW, Chen CY, Jao J, Wu DK, Liu GC. In vivo proton magnetic resonance spectroscopy of large focal hepatic lesions and metabolite change of hepatocellular carcinoma before and after transcatheter arterial chemoembolization using 3.0-T MR scanner. *J Magn Reson Imaging* 2004; **19**: 598-604 [PMID: 15112309 DOI: 10.1002/jmri.20046]
89 **Wu B**, Peng WJ, Wang PJ, Gu YJ, Li WT, Zhou LP, Tang F, Zhong GM. In vivo 1H magnetic resonance spectroscopy in evaluation of hepatocellular carcinoma and its early response to transcatheter arterial chemoembolization. *Chin Med Sci J* 2006; **21**: 258-264 [PMID: 17249202]
90 **Chen CY**, Li CW, Kuo YT, Jaw TS, Wu DK, Jao JC, Hsu JS, Liu GC. Early response of hepatocellular carcinoma to transcatheter

arterial chemoembolization: choline levels and MR diffusion constants--initial experience. *Radiology* 2006; **239**: 448-456 [PMID: 16569781 DOI: 10.1148/radiol.2392042202]

91 **Bonekamp S**, Shen J, Salibi N, Lai HC, Geschwind J, Kamel IR. Early response of hepatic malignancies to locoregional therapy-value of diffusion-weighted magnetic resonance imaging and proton magnetic resonance spectroscopy. *J Comput Assist Tomogr* 2011; **35**: 167-173 [PMID: 21412085 DOI: 10.1097/RCT.0b013e3182004bfb]

92 **Bian DJ**, Xiao EH, Hu DX, Chen XY, Situ WJ, Yuan SW, Sun JL, Yang LP. Magnetic resonance spectroscopy on hepatocellular carcinoma after transcatheter arterial chemoembolization. *Chin J Cancer* 2010; **29**: 198-201 [PMID: 20109351 DOI: 10.5732/cjc.009.10312]

93 **Sourbron S**. Technical aspects of MR perfusion. *Eur J Radiol* 2010; **76**: 304-313 [PMID: 20363574 DOI: 10.1016/j.ejrad.2010.02.017]

94 **Tofts PS**. Modeling tracer kinetics in dynamic Gd-DTPA MR imaging. *J Magn Reson Imaging* 1997; **7**: 91-101 [PMID: 9039598 DOI: 10.1002/jmri.1880070113]

95 **Huang B**, Wong CS, Whitcher B, Kwong DL, Lai V, Chan Q, Khong PL. Dynamic contrast-enhanced magnetic resonance imaging for characterising nasopharyngeal carcinoma: comparison of semiquantitative and quantitative parameters and correlation with tumour stage. *Eur Radiol* 2013; **23**: 1495-1502 [PMID: 23377545 DOI: 10.1007/s00330-012-2740-7]

96 **Xu H**, Xie JX, Li X, Yang ZH, Zheng ZZ, Wang B, Wang Z. Perfusion-weighted MRI in evaluating the intranodular hemodynamic characteristics of dysplastic nodules and hepatocellular carcinomas in an experimental rat model. *J Magn Reson Imaging* 2008; **27**: 102-109 [PMID: 18022847 DOI: 10.1002/jmri.21188]

97 **Chen X**, Xiao E, Shu D, Yang C, Liang B, He Z, Bian D. Evaluating the therapeutic effect of hepatocellular carcinoma treated with transcatheter arterial chemoembolization by magnetic resonance perfusion imaging. *Eur J Gastroenterol Hepatol* 2014; **26**: 109-113 [PMID: 24284371 DOI: 10.1097/MEG.0b013e328363716e]

98 **Chen BB**, Shih TT. DCE-MRI in hepatocellular carcinoma-clinical and therapeutic image biomarker. *World J Gastroenterol* 2014; **20**: 3125-3134 [PMID: 24695624 DOI: 10.3748/wjg.v20.i12.3125]

99 **Braren R**, Altomonte J, Settles M, Neff F, Esposito I, Ebert O, Schwaiger M, Rummeny E, Steingoetter A. Validation of preclinical multiparametric imaging for prediction of necrosis in hepatocellular carcinoma after embolization. *J Hepatol* 2011; **55**: 1034-1040 [PMID: 21354233 DOI: 10.1016/j.jhep.2011.01.049]

100 **Morgan B**, Utting JF, Higginson A, Thomas AL, Steward WP, Horsfield MA. A simple, reproducible method for monitoring the treatment of tumours using dynamic contrast-enhanced MR imaging. *Br J Cancer* 2006; **94**: 1420-1427 [PMID: 16670720 DOI: 10.1038/sj.bjc.6603140]

101 **Zhao JG**, Feng GS, Kong XQ, Li X, Li MH, Cheng YS. Assessment of hepatocellular carcinoma vascularity before and after transcatheter arterial chemoembolization by using first pass perfusion weighted MR imaging. *World J Gastroenterol* 2004; **10**: 1152-1156 [PMID: 15069716 DOI: 10.3748/wjg.v10.i8.1152]

102 **Zhao JG**, Feng GS, Kong XQ, Li X, Li MH, Cheng YS. Changes of tumor microcirculation after transcatheter arterial chemoembolization: first pass perfusion MR imaging and Chinese ink casting in a rabbit model. *World J Gastroenterol* 2004; **10**: 1415-1420 [PMID: 15133845 DOI: 10.3748/wjg.v10.i10.1415]

103 **Ogawa S**, Lee TM, Kay AR, Tank DW. Brain magnetic resonance imaging with contrast dependent on blood oxygenation. *Proc Natl Acad Sci USA* 1990; **87**: 9868-9872 [PMID: 2124706 DOI: 10.1073/pnas.87.24.9868]

104 **Pauling L**, Coryell CD. The Magnetic Properties and Structure of the Hemochromogens and Related Substances. *Proc Natl Acad Sci USA* 1936; **22**: 159-163 [PMID: 16588065 DOI: 10.1073/pnas.22.3.159]

105 **Wedegärtner U**, Popovych S, Yamamura J, Kooijman H, Adam G. DeltaR2* in fetal sheep brains during hypoxia: MR imaging at 3.0 T versus that at 1.5 T. *Radiology* 2009; **252**: 394-400 [PMID: 19546425 DOI: 10.1148/radiol.2522080844]

106 **Chalouhi GE**, Alison M, Deloison B, Thiam R, Autret G, Balvay D, Cuenod CA, Clément O, Salomon LJ, Siauve N. Fetoplacental oxygenation in an intrauterine growth restriction rat model by using blood oxygen level-dependent MR imaging at 4.7 T. *Radiology* 2013; **269**: 122-129 [PMID: 23696681 DOI: 10.1148/radiol.13121742]

107 **Nissen JC**, Mie MB, Zöllner FG, Haneder S, Schoenberg SO, Michaely HJ. Blood oxygenation level dependent (BOLD)--renal imaging: concepts and applications. *Z Med Phys* 2010; **20**: 88-100 [PMID: 20807689 DOI: 10.1016/j.zemedi.2010.01.003]

108 **Hofmann L**, Simon-Zoula S, Nowak A, Giger A, Vock P, Boesch C, Frey FJ, Vogt B. BOLD-MRI for the assessment of renal oxygenation in humans: acute effect of nephrotoxic xenobiotics. *Kidney Int* 2006; **70**: 144-150 [PMID: 16641929 DOI: 10.1038/sj.ki.5000418]

109 **Chopra S**, Foltz WD, Milosevic MF, Toi A, Bristow RG, Ménard C, Haider MA. Comparing oxygen-sensitive MRI (BOLD R2*) with oxygen electrode measurements: a pilot study in men with prostate cancer. *Int J Radiat Biol* 2009; **85**: 805-813 [PMID: 19728195 DOI: 10.1080/09553000903043059]

110 **Zhao D**, Pacheco-Torres J, Hallac RR, White D, Peschke P, Cerdán S, Mason RP. Dynamic oxygen challenge evaluated by NMR T1 and T2*--insights into tumor oxygenation. *NMR Biomed* 2015; **28**: 937-947 [PMID: 26058575 DOI: 10.1002/nbm.3325]

111 **Belfatto A**, White DA, Zhang Z, Zhang Z, Cerveri P, Baroni G, Mason RP. Mathematical modeling of tumor response to radiation: radio-sensitivity correlation with BOLD, TOLD, ΔR1 and ΔR2* investigated in large Dunning R3327-AT1 rat prostate tumors. *Conf Proc IEEE Eng Med Biol Soc* 2015; **2015**: 3266-3269 [PMID: 26736989 DOI: 10.1109/embc.2015.7319089]

112 **Hallac RR**, Zhou H, Pidikiti R, Song K, Stojadinovic S, Zhao D, Solberg T, Peschke P, Mason RP. Correlations of noninvasive BOLD and TOLD MRI with pO2 and relevance to tumor radiation response. *Magn Reson Med* 2014; **71**: 1863-1873 [PMID: 23813468 DOI: 10.1002/mrm.24846]

113 **Choi JW**, Kim H, Kim HC, Lee Y, Kwon J, Yoo RE, Cho HR, Choi SH, Chung JW. Blood oxygen level-dependent MRI for evaluation of early response of liver tumors to chemoembolization: an animal study. *Anticancer Res* 2013; **33**: 1887-1892 [PMID: 23645735]

114 **Zhang LJ**, Zhang Z, Xu J, Jin N, Luo S, Larson AC, Lu GM. Carbogen gas-challenge blood oxygen level-dependent magnetic resonance imaging in hepatocellular carcinoma: Initial results. *Oncol Lett* 2015; **10**: 2009-2014 [PMID: 26622788 DOI: 10.3892/ol.2015.3526]

115 **Kim HO**, Kim JS, Shin YM, Ryu JS, Lee YS, Lee SG. Evaluation of metabolic characteristics and viability of lipiodolized hepatocellular carcinomas using 18F-FDG PET/CT. *J Nucl Med* 2010; **51**: 1849-1856 [PMID: 21098794 DOI: 10.2967/jnumed.110.079244]

116 **Mocherla B**, Kim J, Roayaie S, Kim S, Machac J, Kostakoglu L. FDG PET/CT imaging to rule out extrahepatic metastases before liver transplantation. *Clin Nucl Med* 2007; **32**: 947-948 [PMID: 18030049 DOI: 10.1097/RLU.0b013e3181598cef]

117 **Kim SH**, Won KS, Choi BW, Jo I, Zeon SK, Chung WJ, Kwon JH. Usefulness of F-18 FDG PET/CT in the Evaluation of Early Treatment Response After Interventional Therapy for Hepatocellular Carcinoma. *Nucl Med Mol Imaging* 2012; **46**: 102-110 [PMID: 24900042 DOI: 10.1007/s13139-012-0138-8]

118 **Zhao M**, Wu PH, Zeng YX, Zhang FJ, Huang JH, Fan WJ, Gu YK, Zhang L, Tan ZB, Lin YE. [Evaluating efficacy of transcatheter arterial chemo-embolization combined with radiofrequency ablation on patients with hepatocellular carcinoma by 18FDG-PET/CT]. *Ai Zheng* 2005; **24**: 1118-1123 [PMID: 16159437]

119 **Han AR**, Gwak GY, Choi MS, Lee JH, Koh KC, Paik SW, Yoo BC. The clinical value of 18F-FDG PET/CT for investigating unexplained serum AFP elevation following interventional therapy for hepatocellular carcinom. *Hepatogastroenterology* 2009; **56**: 1111-1116 [PMID: 19760952]

120 **Chen YK**, Hsieh DS, Liao CS, Bai CH, Su CT, Shen YY, Hsieh JF, Liao AC, Kao CH. Utility of FDG-PET for investigating unexplained serum AFP elevation in patients with suspected hepatocellular carcinoma recurrence. *Anticancer Res* 2005; **25**: 4719-4725 [PMID:

16334166]
121 **Boss A**, Bisdas S, Kolb A, Hofmann M, Ernemann U, Claussen CD, Pfannenberg C, Pichler BJ, Reimold M, Stegger L. Hybrid PET/MRI of intracranial masses: initial experiences and comparison to PET/CT. *J Nucl Med* 2010; **51**: 1198-1205 [PMID: 20660388 DOI: 10.2967/jnumed.110.074773]
122 **Boss A**, Kolb A, Hofmann M, Bisdas S, Nägele T, Ernemann U, Stegger L, Rossi C, Schlemmer HP, Pfannenberg C, Reimold M, Claussen CD, Pichler BJ, Klose U. Diffusion tensor imaging in a human PET/MR hybrid system. *Invest Radiol* 2010; **45**: 270-274 [PMID: 20351651 DOI: 10.1097/RLI.0b013e3181dc3671]
123 **Torigian DA**, Zaidi H, Kwee TC, Saboury B, Udupa JK, Cho ZH, Alavi A. PET/MR imaging: technical aspects and potential clinical applications. *Radiology* 2013; **267**: 26-44 [PMID: 23525716 DOI: 10.1148/radiol.13121038]
124 **Lee G**, I H, Kim SJ, Jeong YJ, Kim IJ, Pak K, Park do Y, Kim GH. Clinical implication of PET/MR imaging in preoperative esophageal cancer staging: comparison with PET/CT, endoscopic ultrasonography, and CT. *J Nucl Med* 2014; **55**: 1242-1247 [PMID: 24868109 DOI: 10.2967/jnumed.114.138974]
125 **Buchbender C**, Heusner TA, Lauenstein TC, Bockisch A, Antoch G. Oncologic PET/MRI, part 1: tumors of the brain, head and neck, chest, abdomen, and pelvis. *J Nucl Med* 2012; **53**: 928-938 [PMID: 22582048 DOI: 10.2967/jnumed.112.105338]
126 **Yu JS**, Chung JJ, Kim JH, Cho ES, Kim DJ, Ahn JH, Kim KW. Detection of small intrahepatic metastases of hepatocellular carcinomas using diffusion-weighted imaging: comparison with conventional dynamic MRI. *Magn Reson Imaging* 2011; **29**: 985-992 [PMID: 21616624 DOI: 10.1016/j.mri.2011.04.010]
127 **Tsouana E**, Stoneham S, Fersht N, Kitchen N, Gaze M, Bomanji J, Fraioli F, Hargrave D, Shankar A. Evaluation of treatment response using integrated 18F-labeled choline positron emission tomography/magnetic resonance imaging in adolescents with intracranial non-germinomatous germ cell tumours. *Pediatr Blood Cancer* 2015; **62**: 1661-1663 [PMID: 25854508 DOI: 10.1002/pbc.25538]
128 **Fowler KJ**, Maughan NM, Laforest R, Saad NE, Sharma A, Olsen J, Speirs CK, Parikh PJ. PET/MRI of Hepatic 90Y Microsphere Deposition Determines Individual Tumor Response. *Cardiovasc Intervent Radiol* 2015; Epub ahead of print [PMID: 26721589 DOI: 10.1007/s00270-015-1285-y]
129 **Lipnick S**, Liu X, Sayre J, Bassett LW, Debruhl N, Thomas MA. Combined DCE-MRI and single-voxel 2D MRS for differentiation between benign and malignant breast lesions. *NMR Biomed* 2010; **23**: 922-930 [PMID: 20878970 DOI: 10.1002/nbm.1511]
130 **Faeghi F**, Baniasadipour B, Jalalshokouhi J. Comparative Investigation of Single Voxel Magnetic Resonance Spectroscopy and Dynamic Contrast Enhancement MR Imaging in Differentiation of Benign and Malignant Breast Lesions in a Sample of Iranian Women. *Asian Pac J Cancer Prev* 2015; **16**: 8335-8338 [PMID: 26745081]

P- Reviewer: Ooi LLPJ, Ramia JM **S- Editor**: Ma YJ
L- Editor: Wang TQ **E- Editor**: Wang CH

World Journal of Gastroenterology

Submit a Manuscript: http://www.wjgnet.com/esps/
Help Desk: http://www.wjgnet.com/esps/helpdesk.aspx
DOI: 10.3748/wjg.v22.i20.4848

World J Gastroenterol 2016 May 28; 22(20): 4848-4859
ISSN 1007-9327 (print) ISSN 2219-2840 (online)

ORIGINAL ARTICLE

Basic Study

Immunological changes in different patient populations with chronic hepatitis C virus infection

Laszlo Szereday, Matyas Meggyes, Melinda Halasz, Julia Szekeres-Bartho, Alajos Par, Gabriella Par

Laszlo Szereday, Matyas Meggyes, Melinda Halasz, Julia Szekeres-Bartho, Department of Medical Microbiology and Immunology, University of Pecs, Clinical Centre, 7624 Pecs, Hungary

Laszlo Szereday, Matyas Meggyes, Melinda Halasz, Julia Szekeres-Bartho, Janos Szentagothai Research Centre, 7624 Pecs, Hungary

Alajos Par, Gabriella Par, First Department of Internal Medicine, University of Pecs, Clinical Centre, 7624 Pecs, Hungary

Author contributions: Szereday L, Meggyes M, Halasz M, Szekeres-Bartho J, Par A and Par G substantially contributed to the conception and design of the study, acquisition, analysis and interpretation of data; all authors drafted the article and made critical revisions related to the intellectual content of the manuscript, and approved final version of the article to be published.

Supported by Grants from Hungarian National Research Fund (OTKA K81454 and OTKA K104960); Liver Research Foundation (Pécs), United European Gastroenterology Federation; Janos Bolyai Research Scholarship of the Hungarian Academy of Sciences to Szereday L.

Institutional review board statement: Written informed consent was obtained from all patients. The study protocol conforms to ethical guidelines of 1975 Declaration of Helsinki. Approval from the Regional Ethics Committee at the Medical School, University of Pécs, was obtained.

Conflict-of-interest statement: All authors do not have any conflict of interest.

Data sharing statement: No additional data are available.

Correspondence to: Laszlo Szereday, MD, PhD, Associate Professor of Microbiology, Department of Medical Microbiology and Immunology, University of Pecs, Clinical Centre, 7624 Pecs, Hungary. szereday.laszlo@pte.hu
Telephone: +36-72-536001
Fax: +36-72-536253

Received: January 12, 2016
Peer-review started: January 15, 2016
First decision: February 18, 2016
Revised: March 5, 2016
Accepted: April 7, 2016
Article in press: April 7, 2016
Published online: May 28, 2016

Abstract

AIM: To investigate killer inhibitory and activating receptor expression by natural killer (NK), natural killer T-like (NKT-like) and CD8+ T lymphocytes in patients with chronic hepatitis C virus (HCV) infection with elevated and with persistently normal alanine aminotransferase (PNALT).

METHODS: The percentage of peripheral blood Treg cells, KIR2DL3, ILT-2, KIR3DL1, CD160, NKG2D, NKG2C expressing NK, T and NKT-like cells, cytokine production and NK cytotoxicity were determined by flow cytometry. Twenty-one patients with chronic HCV infection with elevated alanine aminotransferase, 11 HCV carriers with persistently normal alanine aminotransferase and 15 healthy volunteers were enrolled.

RESULTS: No significant differences were observed in the percentage of total T, NK or NKT-like cells between study groups. Comparing the activating and inhibitory

receptor expression by NK cells obtained from HCV carriers with PNALT and chronic HCV hepatitis patients with elevated alanine aminotransferase, NKG2D activating receptor expression was the only receptor showing a significant difference. NKG2D expression of NK cells was significantly lower in patients with elevated alanine aminotransferase. The expression of CD160, NKG2D and NKG2C activating receptor by CD8+ T cells were significantly lower in patients with chronic HCV hepatitis than in healthy controls and in HCV carriers with PNALT. Plasma TGF-β1 levels inversely correlated with NKG2D expression by NK cells. In vitroTGF-β1 treatment inhibited NK cells cytotoxic activity and downregulated NKG2D expression. CD8+ T cells from HCV carriers with PNALT showed significantly elevated expression of CD160, NKG2D and NKG2C activating receptors compared to chronic HCV patients with elevated alanine aminotransferase. Enhanced expression of inhibitory KIR2DL3 receptor, and decreased ILT-2 expression on NK cells were also found in chronic hepatitis C patients compared to healthy controls.

CONCLUSION: Our study demonstrated a complex dysregulation of activating and inhibitory receptor expression, such as decreased NKG2D and CD160 activating receptor expression and increased KIR2DL3 inhibitory receptor expression by NK and cytotoxic T cells and may provide further mechanism contributing to defective cellular immune functions in chronic hepatitis C. Increased NKG2D receptor expression in HCV patients with persistently normal ALT suggests an important pathway for sustaining NK and CD8 T cell function and a protective role against disease progression.

Key words: Hepatitis C; Natural killer cell; NKG2D; Cytotoxicity; Cytokine

Core tip: The host immune response to hepatitis C virus (HCV) involves both innate and adaptive arms of the immune system. Natural killer (NK) cells are key components of the innate antiviral immune response. To better characterize the immune defects underlying chronic viral persistence, we focus our analysis on killer inhibitory and activating receptor expression in patients with chronic HCV infection with elevated alanine aminotransferase (ALT) and also in patients with HCV carriers with persistently normal ALT. Decreased NKG2D and CD160 activating receptor expression and increased KIR2DL3 inhibitory receptor expression by NK and cytotoxic T cells in patients with chronic hepatitis C contributing to defective cellular immune functions.

Szereday L, Meggyes M, Halasz M, Szekeres-Bartho J, Par A, Par G. Immunological changes in different patient populations with chronic hepatitis C virus infection. *World J Gastroenterol* 2016; 22(20): 4848-4859 Available from: URL: http://www.wjgnet.com/1007-9327/full/v22/i20/4848.htm DOI: http://dx.doi.org/10.3748/wjg.v22.i20.4848

INTRODUCTION

More than 170 million people worldwide are chronically infected by hepatitis C virus (HCV)[1]. Approximately 20% of HCV infected patients resolves acute hepatitis and clears the virus, but most develop life-long infection, making HCV a leading cause of chronic liver disease, cirrhosis and hepatocellular carcinoma[2]. No vaccine is currently available to prevent hepatitis C[3]. The mechanisms favoring persistent infection are still poorly understood.

Approximately 30% of patients with chronic HCV (CHC) infection show persistently normal alanine aminotransferase (ALT) levels and are considered CHC carriers[4].

The host immune response to HCV involves both innate and adaptive arms of the immune system. Natural killer (NK) cells are key components of the innate antiviral immune response. NK cells, a subset of lymphocytes, represent between 5% and 15% of mononuclear cells in the peripheral blood and up to 45% in some organs, such as the liver. The major functional role of NK cells is the defense against tumor cells and lyses of virus-infected cells[5]. However, given their potent cytotoxic and cytokine secretion potential, their activity needs to be tightly regulated. The activation state of an NK cell is determined partly by the integration of activating and inhibitory signals after interaction of surface NK cell receptors, including the highly diverse killer Ig-like receptor (KIR) family, with ligands found on target cells.

Previous results from our laboratory showed an impaired NK activity in chronic hepatitis[6]. Therefore, altered function of NK cells might be one of the mechanisms by which viruses escape the immune system. Activating receptors on NK and T cells might provide not only the machinery to induce proliferation and fight off infection, but also to support maintenance of the cells critically needed under conditions of extended viral infections during CHC.

There is new evidence that NK cells also can be activated to negatively regulate T cell responses because they can produce interleukin-10 (IL-10)[7,8]. Under conditions of continued stimulation - like CHC infection - IL-10 response by NK cells could limit the magnitude of CD8 T cell response and protect from T cell-mediated disease. If the NK cells are not regulated properly, the regulation is lost with detrimental consequences.

Natural killer T-like (NKT-like) cells are a sublineage of T cells that share characteristics of conventional T cells and NK cells and bridge innate and adaptive immunity[9]. The most characteristic immunoregulatory function

of NKT cells is their ability to promptly secrete large amounts of Th1 and Th2 cytokines including interferon-γ (IFN-γ) and IL-4, respectively, upon stimulation[10]. Downstream, this culminates in the activation of different cell types of the innate immune system such as macrophages, NK cells, and dendritic cells as well as effector T cells of the adaptive immune system.

Although shown to mediate immunity against a wide range of pathogenic microbes, including bacteria, fungi, parasites, and viruses, the mechanism(s) by which NKT cells are activated during infection is still unclear. NKT-like cells are abundant in the liver; however, their role in the control of hepatitis C virus infection remains to be determined[11].

CD8+ T cells are important in viral elimination by using direct killing of infected cells and non-cytotoxic mechanisms such as the secretion of antiviral cytokines [IFN-γ or tumor necrosis factor (TNF)-α][12]. Despite the detection of HCV-specific CD8+ T cells in the peripheral blood and the intrahepatic lymphocytic infiltrate in patients with chronic hepatitis C, the virus can persist. This persistence in spite of the presence of these cytotoxic cells is still unexplained and suggests that cell killing is not sufficient to eliminate the virus. Studies in humans have revealed that even strong CD8+ T cell responses in the acute phase of infection may not be adequate to prevent progression to chronicity[13-15]. Several investigators have clearly shown that HCV-specific CD8+ T cells have functional defects during chronic infection, as indicated by impaired IFN-γ production, cytotoxic effector functions, and *in vitro* proliferation[16,17]. While the mechanisms responsible for the dysfunctions of HCV-specific T cells in chronically infected patients remain unclear, recent studies suggest a major contribution of regulatory T cells.

To better characterize the immune defects underlying chronic viral persistence, in this study we focus our analysis on killer inhibitory and activating receptor expression in patients with chronic hepatitis C virus infection with elevated ALT and also in patients with CHC carriers with persistently normal ALT (PNALT) by NK, NKT-like and CD8+ T lymphocytes, given the central role played by these cells in the control of viral infections. Progress in the understanding of antiviral immune responses in CHC carriers with PNALT could elucidate key mechanisms playing a role in the control of viral infection.

MATERIALS AND METHODS

Patients

Persistently normal ALT was defined as ALT < 30 IU/L in men, ALT < 19 IU/L in women measured every 3 mo over an 18-mo period. Patients with Fibroscan result suggesting > F1 liver fibrosis (LS > 7.0 kPa) were excluded from the CHC with PNALT group. Eleven age-matched healthy blood donors served as controls.

All HCV subjects were seronegative for anti-HIV 1, 2 antibodies (ELISA 2.0, Abbott, Wiesbaden, Germany), and HBsAg (Hepanostica Uniform II, Organon Teknika, Oss, The Netherlands), and were positive for both anti-HCV antibody and HCV-RNA. Diagnosis of chronic hepatitis C was established by means of histology in all symptomatic patients, but liver biopsy was not performed in CHC carriers with PNALT.

HCV markers

Anti-HCV antibody was examined using enzyme-linked immunoabsorbent assay (ELISA) (Detect-HCV Ab, Biochem Immunosystem, ITC, Canada). Serum HCV RNA detection and quantification were performed with Roche Cobas Amplicor HCV 2.0 assay (lower limit of detection < 50 IU/mL) and Cobas Amplicor HCV Monitor Assay (Roche Diagnostics) according to the manufacturer's instructions.

Sample preparation

Venous blood samples were collected in heparanized tubes and peripheral blood mononuclear cells (PBMC) were prepared by Ficoll-Paque density gradient centrifugation.

Antibodies and flow cytometry

Separated cells were washed in PBS and incubated for 30 min at room temperature with the monoclonal antibodies. The following monoclonal antibodies were used for these studies: FITC-conjugated anti-CD3, anti-CD8, anti-CD4, PE-conjugated anti-CD25, anti-KIR2DL3 (CD158b), anti-ILT-2 (CD85), anti-NKG2C, anti-CD160, anti-NKG2D, anti-KIR3DL1 (CD158e) and APC-conjugated anti-CD56. After washing the cells in PBS, cells were fixed with 4% paraformaldehyde, stored at 4 ℃, in dark, to be processed for FACS analysis. At least 10000 cells were analyzed on the FACS Calibur flow-cytometer (Becton Dickinson Immunocytometry Systems, Erembodegen, Belgium) after single gating on lymphoid cells for all mAb combinations. The percentage of positive cells was calculated using Cellquest software (Becton Dickinson, San Diego, CA, United States). Figure 1 shows the gating technique used to detect different lymphocyte subpopulations with representative flow cytometric dot plots. The effect of TGF-β1 treatment on NKG2D, CD160 and KIR2DL3 expression by NK cells.

PBMC were separated from heparinized venous blood on Ficoll-Paque gradient. One million cells were treated with recombinant active TGF-β1 protein (1 ng/mL) for 48 h at 37 ℃ in a tissue culture incubator. NKG2D, CD160 and KIR2DL3 expression by NK cells was determined by flow cytometry.

NK and CD8+ T separation and cytometric bead array

Natural killer and CD8+ T cells were separated by MACS Cell Separation Technology (all reagents and instruments from Miltenyi Biotec, Frank Diagnosztika Kft., Budapest, Hungary). PBMCs were first magnetically labeled with CD56 or CD8 MicroBeads

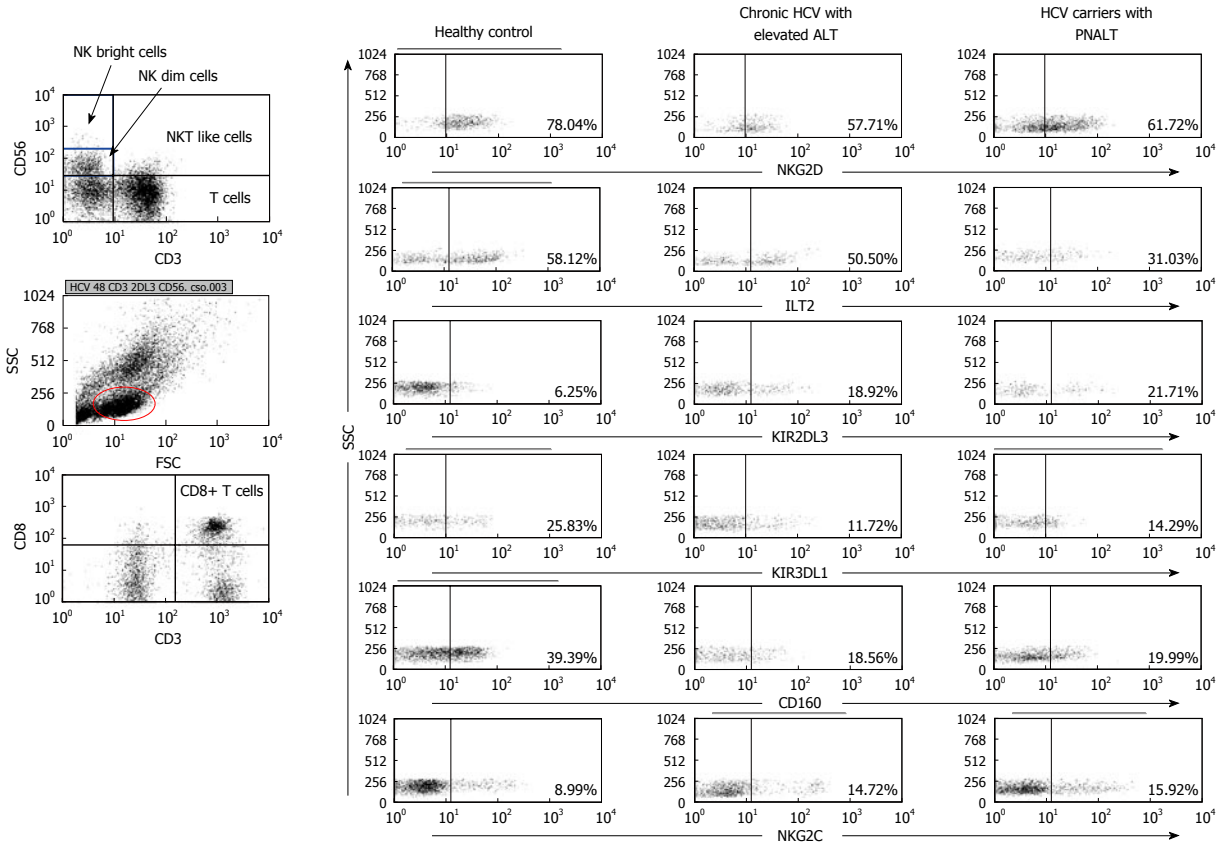

Figure 1 Gating strategy and representative flow cytometric dot plots. Figure 1 shows the gating technique used to detect different lymphocyte subpopulations. For analysis of NK, NK^{dim}, NK^{bright}, NKT-like and CD8+ T cells cells lymphogate was created based on physical characteristics typical of lymphoid cells using forward and side scatter parameters. Representative dot plots show the expression of NKG2D, ILT-2, KIR2DL3, KIR3DL1, CD160 and NKG2C by NK cells in the peripheral blood from patients with chronic HCV with elevated ALT or PNALT and in healthy individuals. HCV: Hepatitis C virus; ALT: Alanine aminotransferase; PNALT: Persistently normal ALT; NK: Natural killer cell.

according to the manufacturer's instructions and CD56+ or CD8+ T cells were positively selected on the cell separation column. In the next step, the magnetic beads bound to the cell surface were enzymatically released from the CD56+ cells, which were then magnetically labeled with CD3 MicroBeads and the CD3+ subpopulation positively selected to compose the CD3+CD56+ T cell population. The remaining fraction of the CD56+ cells, which did not bind the CD3 beads composed the CD3-CD56+ NK cell population. Purity was greater than 95%. CD8+ and CD3-CD56+ cell populations were stimulated with 1 μg/mL of ionomycin and 25 ng/mL of PMA (Sigma-Aldrich, Sigma-Aldrich Kft., Budapest, Hungary) in RPMI 1640 Medium containing 10% fetal bovine serum, penicillin and streptomycin (all from Invitrogen, Csertex Kft., Budapest, Hungary) overnight for cytokine production. The levels of IL-2, IL-4, IL-5, IL-10, IFN-γ and TNF-α were determined from the culture supernatants with cytometric bead array (CBA) (#550749, BD Biosciences, Soft Flow Hungary Kft., Pécs, Hungary) using different capture beads according to the manufacturer's instructions to detect the respective cytokines. Samples were analyzed right after the experiment on a FACS calibur flow cytometer (BD Immunocytometry Systems, Erembodegen, Belgium) calculating the amount of cytokines with CBA Software (BD Biosciences, San Diego, CA, United States).

Cytotoxic assay for NK cell activity

Cytotoxicity was determined as described earlier[18]. Cytotoxic activity of NK cells was evaluated by FACS analysis. Target cells (1×10^6) were pre-stained with the green fluorescent membrane dye PKH67 (Sigma, Hungary) and effector cells were added to 25×10^4 target cells to yield effector to target (E:T) ratios of 12.5:1, 25:1, and 50:1. The tubes were centrifuged for 30 s at 1200 rpm to pellet the effector and target cells together. These cell mixtures were incubated for 4 h at 37 ℃ in 5% CO_2. After incubation the cell mixture was centrifuged at 1200 rpm and stained with propidium iodide (PI, 5 μg/mL, Sigma, Hungary). Dead target cells were identified by simultaneous PKH67 and PI-positivity. Target cells incubated without effector cells were used to assess spontaneous cell death. The percentage of lysed target cells was calculated by subtracting background (spontaneous cell death) expression from experimental samples. Cytotoxicity was expressed as the percentage of lysed target cells in each effector-to-target ratio.

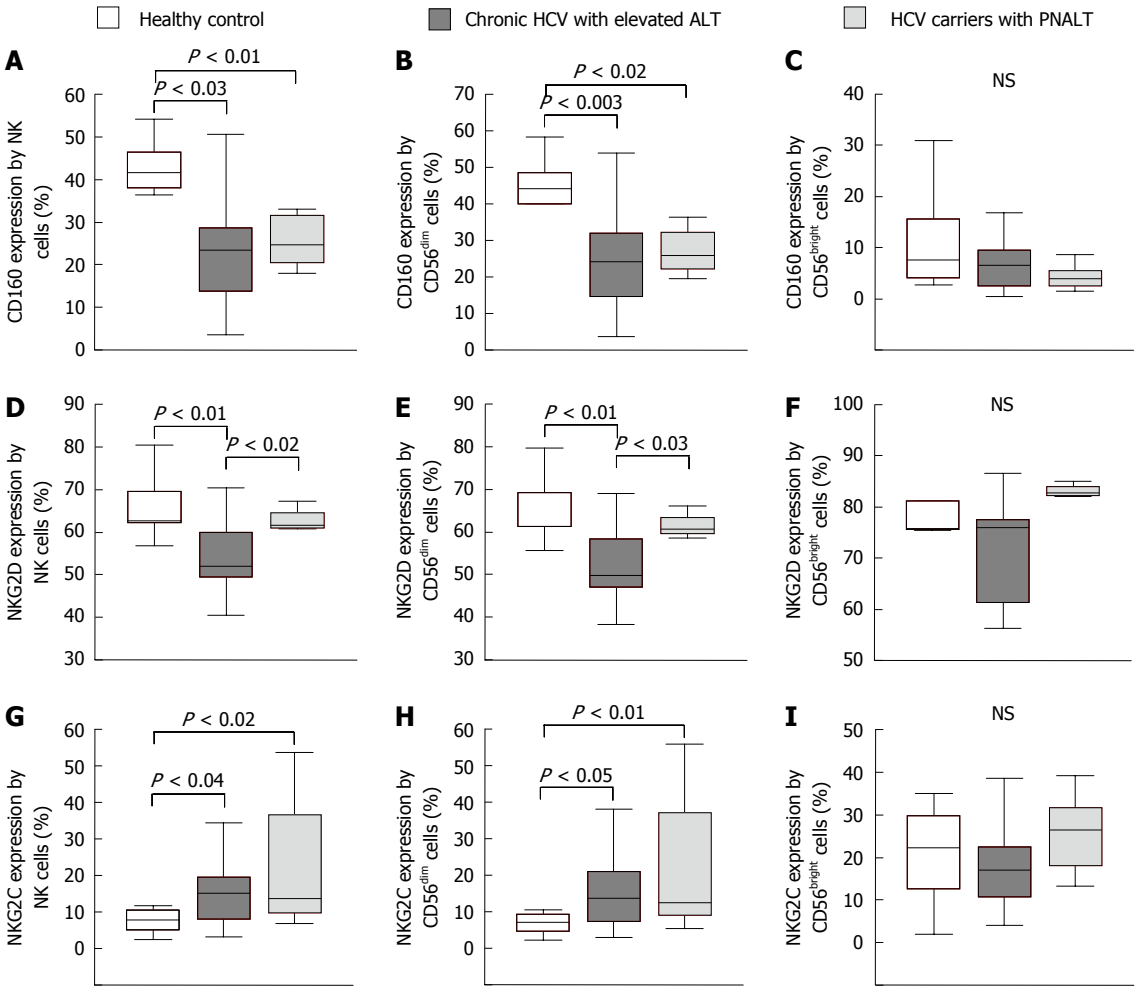

Figure 2 Activating natural killer cell receptor expression by natural killer cells in the peripheral blood from patients with chronic hepatitis C virus with elevated alanine aminotransferase or persistently normal alanine aminotransferase and in healthy individuals. The expression of CD160 (A-C), NKG2D (D-F) and NKG2C (G-I) by NK cells and NK cell subsets in the peripheral blood from patients with chronic HCV with elevated ALT or PNALT and in healthy individuals. The solid bars represent medians; the boxes indicate the interquartile ranges and the lines show the most extreme observations. Differences were considered statistically significant for *P* values ≤ 0.05. HCV: Hepatitis C virus; ALT: Alanine aminotransferase; PNALT: Persistently normal ALT; NK: Natural killer cell.

Effect of TGF-β1 on NK cytotoxicity

PBMC were separated from heparinized venous blood on Ficoll-Paque gradient. One million cells were treated with recombinant active TGF-β1 protein (1 ng/mL) for 48 h at 37 ℃. Following incubation we determined cytotoxicity of NK cells by flow cytometry.

Statistical analysis

Statistical analysis was performed using non-parametric Mann-Whitney *U*-test with statistical software SPSS version 11.0 package (SPSS, Inc. Chicago, IL, United States) (Figures 2-5). Results are expressed as mean value ± standard error of the mean (SEM). Statistical comparisons were made by using one-way ANOVA with Bonferroni correction (Figures 6 and 7). The results were expressed as the mean value ± SEM. Differences were considered significant if the *P* value was equal to or less than 0.05. Correlation between variables was assessed by calculating Spearman rank correlation coefficient. Differences were accepted as significant at a level of $P < 0.05$.

RESULTS

Patients

Twenty one patients with CHC infection with elevated ALT > 2 × ULN (11 males, 10 females, mean age: 57 years; range 38-70 years) and 11 (2 males, 9 females, mean age: 56 years; range 41-63 years) HCV carriers with persistently normal ALT were studied.

Lymphocyte frequency

No significant differences were observed in the percentage of helper (CD4+) or cytotoxic (CD8+) T cells, regulatory (CD4+CD25^{high}) T cells, NK (CD3-CD56+) or NKT-like (CD3+CD56+) cells in peripheral blood of patients with CHC hepatitis with elevated ALT compared to CHC patients with PNALT and also to

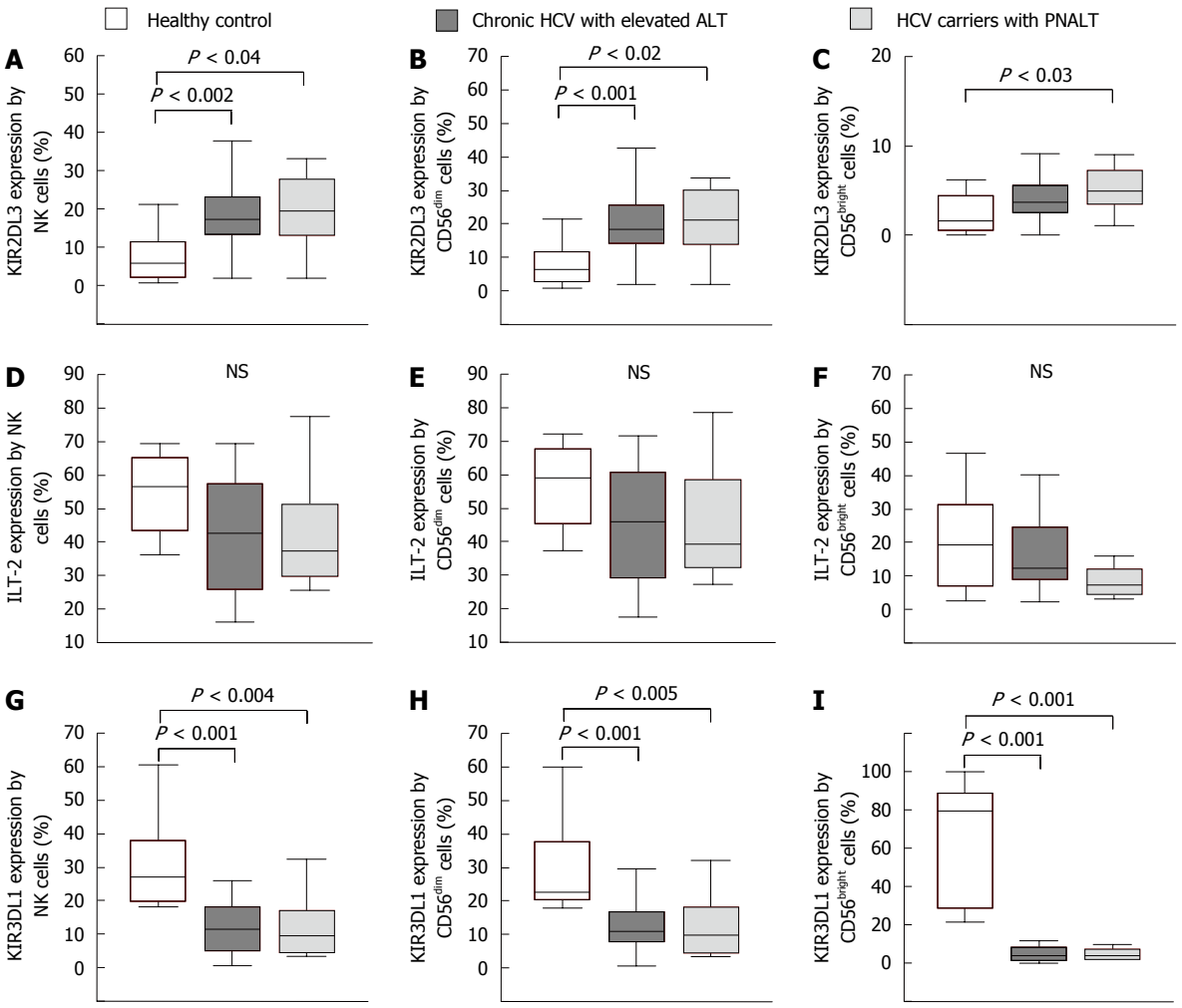

Figure 3 Inhibitory natural killer cell receptor expression by natural killer cells in the peripheral blood from patients with chronic hepatitis C virus with elevated alanine aminotransferase or persistently normal alanine aminotransferase and in healthy individuals. The expression of KIR2DL3 (A-C), ILT-2 (D-F) and KIR3DL1 (G-I) by NK cells and NK cell subsets in the peripheral blood from patients with chronic HCV with elevated ALT or PNALT and in healthy individuals. The solid bars represent medians; the boxes indicate the interquartile ranges and the lines show the most extreme observations. Differences were considered statistically significant for *P* values ≤ 0.05. HCV: Hepatitis C virus; ALT: Alanine aminotransferase; PNALT: Persistently normal ALT; NK: Natural killer cell.

healthy controls (Table 1).

Activating and inhibitory NK cell receptor expression by NK cells in the peripheral blood from patients with CHC with elevated ALT or PNALT and in healthy individuals

The phenotypes and functional activities of various populations of innate effectors have been reported to be impaired in all stages of HCV infection[6,19-21]. The balance of activating and inhibitory signals through the killer activating and the inhibitory receptors control NK cell activity. Since the role of NK cells determining disease inflammatory activity reflected by ALT elevation in chronic hepatitis C is not clear, we investigated different activating and inhibitory NK cell receptor expression by NK cells in patients with CHC with elevated ALT or PNALT.

CD160 and NKG2D activating NK cell receptor expression was significantly lower in patients with CHC infection than in healthy controls (Figure 2A and D). NKG2D expression by NK cells was significantly lower in CHC patients with elevated ALT than in CHC positive patients with PNALT (Figure 2D). Expression of NKG2C was higher in NK cells from patients with CHC infection as compared to healthy controls but significantly lower than CHC carriers (Figure 2G). NK cells can be divided into two populations based on the intensity of the CD56 marker at the cell surface. $CD56^{dim}$ NK cells are the more cytotoxic subset, whereas $CD56^{bright}$ cells are poorly cytotoxic and preferentially secrete cytokines when activated[22]. The majority of NK cells were of the $CD3^{-}CD56^{dim}$ phenotype and our data shows that this cell population represents the above mentioned alterations in activating receptor expression by NK cells (Figure 2B, E and H). In contrast to $CD56^{dim}$ cells, we found no significant difference in the killer activating NK cell receptor expression by $CD56^{bright}$ cells between the investigated groups (Figure 2C, F and I).

An enhanced expression of inhibitory KIR2DL3 receptor on NK cells was found in peripheral blood of patients with CHC infection and also in CHC carriers

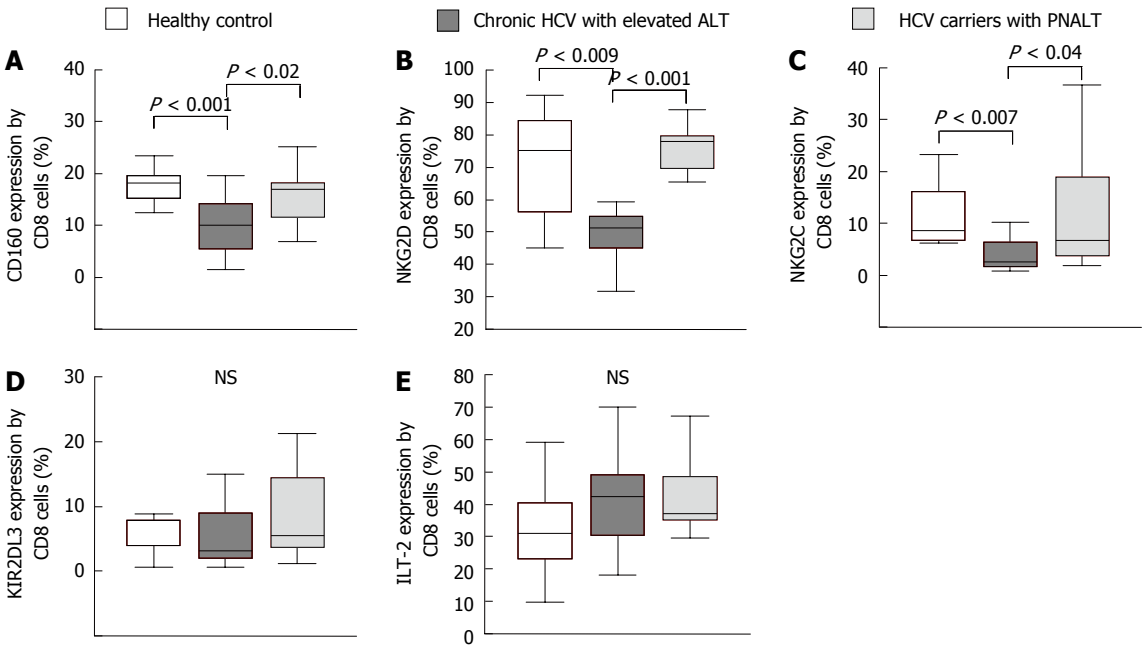

Figure 4 Activating and inhibitory natural killer cell receptor expression by CD8+ T cells in the peripheral blood from patients with chronic hepatitis C virus with elevated alanine aminotransferase or persistently normal alanine aminotransferase and in healthy individuals. The expression of CD160 (A), NKG2D (B), NKG2C (C), KIR2DL3 (D) and ILT-2 (E) by CD8+ T cells in the peripheral blood from patients with chronic HCV with elevated ALT or PNALT and in healthy individuals. The solid bars represent medians; the boxes indicate the interquartile ranges and the lines show the most extreme observations. Differences were considered statistically significant for *P* values ⩽ 0.05. HCV: Hepatitis C virus; ALT: Alanine aminotransferase; PNALT: Persistently normal ALT; NK: Natural killer cell.

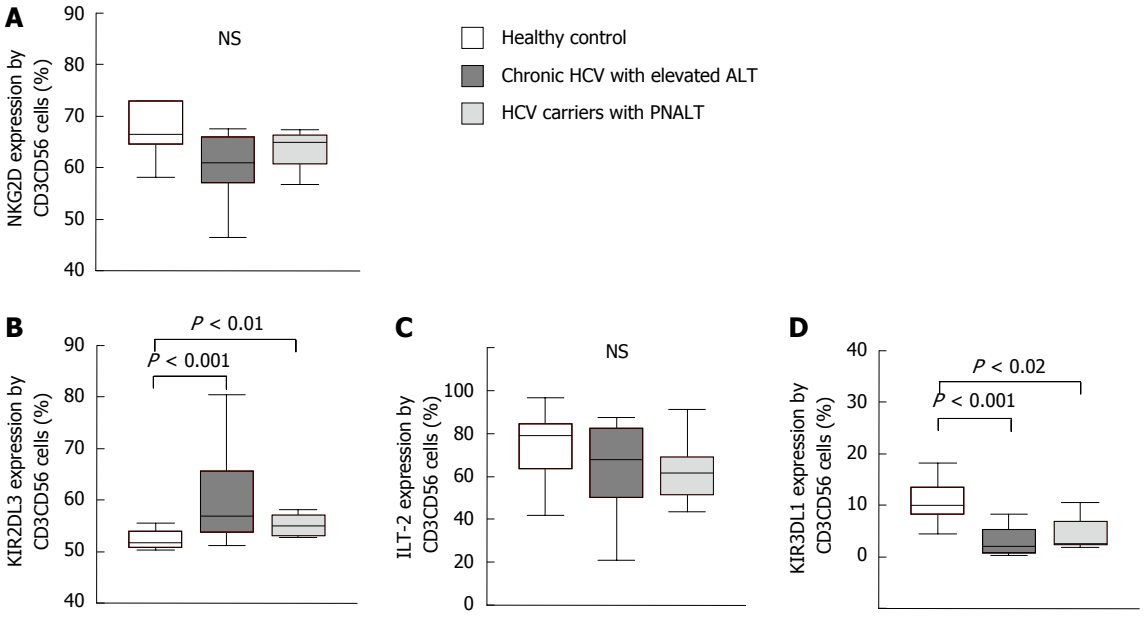

Figure 5 Activating and inhibitory natural killer cell receptor expression by NKT-like cells in the peripheral blood from patients with chronic hepatitis C virus with elevated alanine aminotransferase or persistently normal alanine aminotransferase and in healthy individuals. The expression of NKG2D (A), KIR2DL3 (B), ILT-2 (C) and KIR3DL1 (D) by NKT-like cells in the peripheral blood from patients with chronic HCV with elevated ALT or PNALT and in healthy individuals. The solid bars represent medians; the boxes indicate the interquartile ranges and the lines show the most extreme observations. Differences were considered statistically significant for *P* values ⩽ 0.05. HCV: Hepatitis C virus; ALT: Alanine aminotransferase; PNALT: Persistently normal ALT; NK: Natural killer cell.

with PNALT in comparison to healthy controls (Figure 3A). No significant differences were found between study groups in regarding expression of ILT-2 on NK cells (Figure 3D-F). KIR3DL1 inhibitory NK cell receptor expression was significantly decreased by NK, $CD56^{dim}$ and $CD56^{bright}$ cells in patients with CHC irrespectively of ALT compared to healthy individuals (Figure 3G-I).

Activating and inhibitory receptor expression by CD8+ T cells

Significantly lower percentage of CD160, NKG2D and NKG2C activating receptor expressing CD8+ T cells

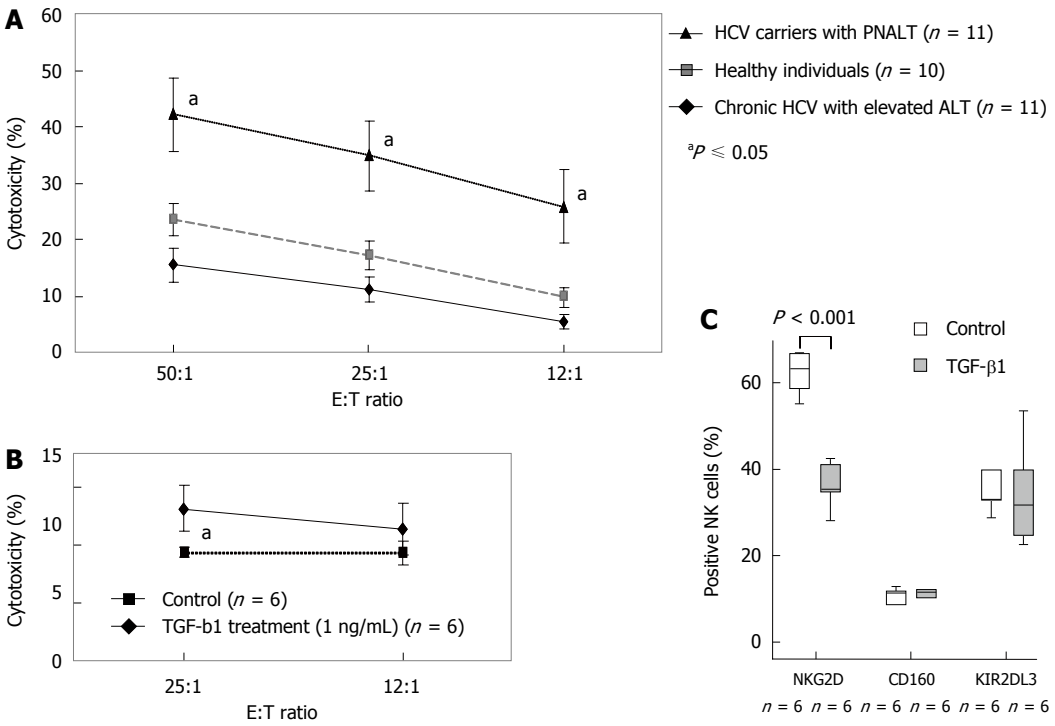

Figure 6 Natural killer cell cytotoxicity against K562 cells in patients with chronic hepatitis C virus with elevated alanine aminotransferase or persistently normal alanine aminotransferase and in healthy individuals and the effect of in vitro TGF-β1 treatment on the cytotoxicity and natural killer cell receptor expression of freshly isolated natural killer cells. A: Cytotoxicity of NK cells isolated from healthy individuals, HCV carriers with PNALT and chronic HCV with elevated ALT. Cytotoxic activity of NK cells as a percentage of lysed cells is indicated in patients with chronic HCV with elevated ALT or PNALT and in healthy individuals at different effector and target cell ratios. Statistical comparisons were made by using one-way ANOVA with Bonferroni correction. The results were expressed as the mean value ± standard error of the mean (SEM). $^aP \leq 0.05$, significant from patients with chronic HCV with elevated ALT and healthy individuals. B: Cytotoxicity of TGF-β treated NK cells isolated from healthy individuals. Cytotoxic activity of NK cells as a percentage of lysed cells is indicated after TGFβ1 treatment (1 ng/mL) at different effector and target cell ratios. C: Expression of NKG2D, KIR2DL3 and CD160 receptors by TGF-β-treated NK cells. Different NK cell receptor expression by NK cells after TGFβ1 treatment (1 ng/mL). Statistical comparisons were made by one-way ANOVA with Bonferroni correction. The solid bars represent medians; the boxes indicate the interquartile ranges and the lines show the most extreme observations. Differences were considered statistically significant for *P* values ≤ 0.05. E: Effector cell; T: Target cell; HCV: Hepatitis C virus; ALT: Alanine aminotransferase; PNALT: Persistently normal ALT; NK: Natural killer cell.

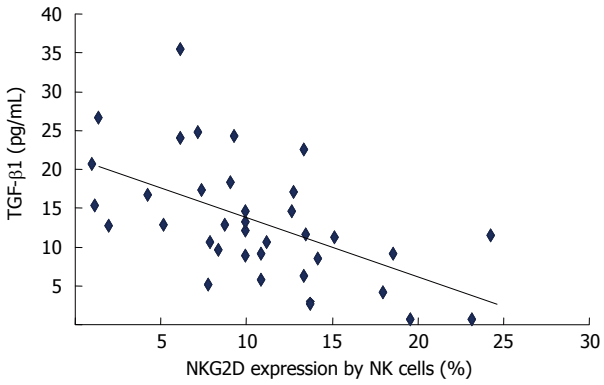

Figure 7 The correlation of plasma transforming growth factor β1 levels with NKG2D expression by natural killer cells in patients with chronic hepatitis C virus hepatitis. Shown is plasma TGF-β1 levels with NKG2D expressed by NK cells. Correlation between variables was assessed by calculating Spearman rank correlation coefficient. NK: Natural killer cell; TGF-β1: Transforming growth factor β1.

were found in patients with CHC hepatitis than in healthy controls and in CHC carriers with PNALT. (Figure 4A-C). We found no difference in the percentage of inhibitory receptor (KIR2DL3 and ILT-2) expression by CD8+ T cells in patients with CHC infection compared to healthy controls (Figure 4D and E).

Activating and inhibitory NK cell receptor expression by NKT-like cells

No significant difference was found between healthy controls and patients with HCV infection with respect to expression of NKG2D on NKT-like cells (Figure 5A). KIR2DL3 inhibitory NK cell receptor expression by NKT-like cells revealed an enhanced proportion of KIR2DL3-expressing cells in peripheral blood of patients with CHC in comparison to healthy controls (Figure 5B).

Regarding expression of ILT-2 inhibitory receptors, we found no difference in the percentage of ILT-2 receptor expressing NKT-like cells in study groups (Figure 5C). KIR3DL1 inhibitory receptor expression -similarly to NK cells- was significantly decreased on NKT-like cells in patients with CHC irrespective of ALT compared to healthy individuals (Figure 5D).

Alteration of cytokine production by NK and CD8+ T cells in CHC infection

NK cells produced significantly higher IL-10, TNF-α and IFN-γ in patients with CHC compared to healthy individuals (Table 2). In addition, IL-2, IL-4, IL-5,

Table 1 Peripheral blood mononuclear cell phenotype characteristics in patients with chronic hepatitis C virus with elevated alanine aminotransferase or persistently normal alanine aminotransferase and in healthy individuals

	Healthy individuals	Chronic HCV with elevated ALT	HCV carriers with PNALT
Percentage of PBL			
CD3+CD4+	29.38 ± 8.11	33.15 ± 9.08	34.46 ± 6.49
CD3+CD4+CD25+	4.27 ± 1.62	4.05 ± 1.57	5.24 ± 1.43
CD3+CD4+CD25^{bright}+	0.52 ± 0.26	0.38 ± 0.26	0.40 ± 0.13
CD3+CD56+	2.99 ± 1.73	5.07 ± 4.15	3.48 ± 2.72
CD3-CD56+	17.34 ± 7.42	16.42 ± 5.26	17.04 ± 7.71
CD3-CD56^{dim}+	16.04 ± 7.36	14.58 ± 5.72	15.92 ± 7.14
CD3-CD56^{bright}+	1.15 ± 0.64	1.75 ± 1.54	1.27 ± 1.01
CD3+CD8+	28.59 ± 4.55	25.27 ± 8.77	24.66 ± 6.14

Statistical comparisons were made by using the ANOVA tests. The results were expressed as the mean value ± SD. HCV: Hepatitis C virus; ALT: Alanine aminotransferase; PNALT: Persistently normal ALT; NK: Natural killer cell.

IL-10, TNF-α and IFN-γ production by NK cells isolated from CHC carriers with PNALT was significantly higher compared to healthy controls (Table 2). PNALT was associated with higher level of IL-4 and TNF-α compared to CHC hepatitis group (Table 2). CHC infection was associated with significantly higher IL-4, IL-5, IL-10 and TNF-α levels produced by CD8+ T cells compared to healthy individuals. Only IL-10 differed significantly between PNALT and elevated ALT group. CD8+ cells of CHC carriers with PNALT produced significantly higher amount of IL-10 compared to CHC hepatitis group (Table 2).

Cytotoxicity of NK cells and the effect of in vitro TGF-β1 treatment

Earlier we demonstrated that TGF-β1 levels significantly higher in patients with chronic hepatitis C with elevated ALT compared to PNALT group and healthy individuals. TGF-β1 levels positively correlated with Knodell histological activity index assessed by liver biopsy. Since impaired NK cell function has been attributed to down-modulation of activating receptors NKG2D *via* secretion of TGF-β1 in lung and colorectal cancer patients, we investigated the effect of TGF-β1 treatment on NK cell cytotoxicity[23].

To determine whether decreased NKG2D expression by NK cells in CHC patients with elevated ALT is potentially related to their increased TGF-β1 levels, we studied the in vitro effect of TGF-β1 treatment on the cytotoxicity of NK cells in response to co-culture with the classical NK cell target K562 cells. NK cells from CHC carriers with PNALT showed significantly higher cytotoxic activity compared to patients with chronic CHC with elevated ALT or healthy individuals (Figure 6A). Treatment of freshly isolated NK cells with TGF-β1 suppressed NK-dependent lysis of K562 cells (13.21 *vs* 9.43, $P < 0.01$) (Figure 6B).

Effect of TGF-β1 on NKG2D expression of freshly isolated NK cells

To investigate if TGF-β1 was responsible for down-modulation of NKG2D, we incubated freshly isolated NK cells obtained from healthy volunteers with 1 ng/mL TGF-β1 for 48 h and analyzed NKG2D expression by FACS. Incubation of NK cells with TGF-β1 significantly down-regulate surface NKG2D expression by NK cells (63.08 *vs* 36.21, $P < 0.01$). In contrast, TGF-β1 did not alter the level of other NK receptors, including the activating NK cell receptor, CD160 (37.47 *vs* 34.04 NS) or the inhibitory NK cell receptor, KIR2DL3 (11.05 *vs* 11.04 NS). These data suggest that TGF-β1 specifically down-modulates NKG2D without affecting other NK receptors.

Together, our data strongly suggest that secretion of TGF-β1 in CHC patients can down-modulate NKG2D expression by NK cells (Figure 6C). Plasma TGF-β1 levels inversely correlated with NKG2D expression by NK cells in CHC infected individuals (Figure 7).

DISCUSSION

Following acute HCV infection a majority of healthy adults will develop persistent viremia. Effective clearance of an acute viral infection typically requires the coordinated function of multiple arms of the immune system, including the innate immune system (interferons, NK and NKT-like cells), as well as the acquired immune response specific to a given pathogen (CD4+ and CD8+ T cells). A functional impairment of NK, NKT-like and CD8 T cells has been reported in CHC infections by several observations, and different mechanisms have been proposed to explain this defective function[5,19-21,24].

Natural killer cell receptors are important regulators of NK and CD8+ T cell functions. Regarding the fact that impaired activities of CD8+ T[6,20] and NK cells[19,21,24] have been reported in patients with chronic hepatitis C infection, we analyzed whether dysregulation of NK cell receptors on these cell might be involved in the inefficient cellular immune response observed in chronic hepatitis C. In this study we analyzed the expression of different activating and inhibitory NK cell receptors in CHC patients with elevated and with persistently normal ALT.

We found that the percentages of NKG2D or CD160 activating receptor positive NK and CD8+ T cells were significantly decreased in CHC patients with elevated ALT compared to healthy individuals. This discrepancy was not found in CHC infected patients with persistently normal ALT. CD8+ T cells from CHC carriers with PNALT showed significantly elevated expression of CD160, NKG2D and NKG2C activating receptors compared to CHC patients with elevated ALT. Comparing the activating and inhibitory receptor expression by NK cells obtained from CHC carriers with PNALT and CHC hepatitis patients with elevated ALT,

Table 2 Cytokine production by natural killer cell and CD8+ T cells in the peripheral blood from patients with chronic hepatitis C virus with elevated alanine aminotransferase or persistently normal alanine aminotransferase and in healthy individuals

	IL-2	IL-4	IL-5	IL-10	TNF-α	IFN-γ
NK cells						
Healthy individuals	400.4 ± 357.4	32.4 ± 23.5	6.3 ± 1.39	5.50 ± 0.23	1301.7 ± 417.3	2739.2 ± 61.2
Chronic HCV with elevated ALT	817.3 ± 316.2	20.2 ± 8.6[c]	27.9 ± 15.6	9.30 ± 1.63[a]	3034.3 ± 649.7[a,c]	3268.6 ± 140.4[a]
HCV carriers with PNALT	1182.3 ± 447.7[e]	169.5 ± 48.1[a]	18.3 ± 5.83[e]	9.70 ± 1.22[a]	4491.6 ± 148.6[b]	3231 ± 77.9[b]
CD8+						
Healthy individuals	1944.5 ± 303.9	26.1 ± 6.9	65.5 ± 20.8	18.2 ± 4.9	1369.0 ± 224.5	2608.4 ± 81.2
Chronic HCV with elevated ALT	2440.5 ± 378.3	276.3 ± 98.1[a]	461.2 ± 213.9[a]	58.3 ± 15.8[a,c]	3247.4 ± 590.8[a]	2721.9 ± 78.7
HCV carriers with PNALT	2502.1 ± 238.5[e]	253.1 ± 95.2[a]	374.8 ± 171.6[a]	258.3 ± 71.9[e]	3895.0 ± 218.3[b]	2719.7 ± 127.0

Concentrations of cytokines are given in picograms per milliliter (mean ± SD). [a]$P < 0.05$, [e]$P < 0.02$, [b]$P < 0.001$, *vs* healthy individuals, significantly different; [c]$P < 0.05$ *vs* symptomatic individuals, significantly different. HCV: Hepatitis C virus; ALT: Alanine aminotransferase; PNALT: Persistently normal ALT; NK: Natural killer cell; IL-2: Interleukin-2; TNF-α: Tumor necrosis factor α; IFN-γ: Interferon-γ.

NKG2D activating receptor expression was the only receptor showing a significant difference. Investigating $CD56^{dim}$ NK cells, NKG2D receptor expression was significantly elevated in persistently normal ALT group compared to CHC hepatitis patients.

Analyzing inhibitory NK cell receptors expressed by CD8+ T, NK or NKT-like cells, we did not find any difference in the expression of KIR2DL3, ILT-2 or KIR3DL1 between patients with CHC infection with elevated ALT and CHC carriers with PNALT. Interestingly KIR3DL1 expression by NK and NKT-like cells was significantly lower in patients with chronic hepatitis C with elevated ALT compared to healthy individuals. On the other hand KIR2DL3 expression by NK and NKT-like cells were significantly increased in patients with CHC infection with elevated ALT and CHC carriers with PNALT compared to healthy individuals.

The mechanisms by which NK and NKT-like cells in hepatitis express KIR2DL3 at considerable high levels remain elusive. One possibility is that the expression levels of NK receptors may be modified by various types of cytokines released under chronically inflamed conditions. Given previous findings that high level of serum TGF-β production were observed in CHC infected patients[25] and that TGF-β can up regulate the expression of inhibitory receptors on NK cells[26] we hypothesized that TGF-β would contribute to the high expression of KIR2DL3 on NK and NKT-like cells in CHC infection. We found that TGF-β1 significantly down-regulated surface NKG2D expression by NK cells, but did not alter the level of other NK receptors, including the activating NK cell receptor CD160 or the inhibitory NK cell receptor KIR2DL3, suggesting that other factors, including the virus itself, play a role in the modulation of activating or inhibitory receptor expression.

The activation status of NK, NKT-like and CD8+ T cells depends on the balance between activating and inhibitory signals delivered by surface receptors. Thus, our present findings of up-regulated expression of inhibitory receptors combined with the concomitant down-regulation of activating receptors synergistically leads to the dominant delivery of inhibitory signals to NK, NKT cells and KIR receptor-positive T cells. This altered receptor expression is reflected by impaired cytotoxic function of NK cells. Our data agree with other studies[27,28], which reported a significant reduction in NK cytotoxic activity in patients with CHC infection, but disagree with several other studies[24,29].

Our results show that NK cells from CHC carriers with PNALT have significantly higher cytotoxic activity compared to patients with CHC with elevated ALT or healthy individuals. Since NKG2D expression by NK cells in PNALT patients was at normal level we hypothesize that further factors may be involved in the regulation of their activity.

The pathogenesis of impaired CD8 response in CHC infection still remains partially understood. To further clarify this issue, in this study, we looked for activating and inhibitory receptor expression by CD8+ T cells. Our results show that CD8 T cell triggering can be hindered by engagement of inhibitory natural killer cell receptors, which are expressed on previously activated CD8 T cells. Although we found no differences in the expression of inhibitory receptor expression by CD8+ T cells between healthy individuals and HCV infected patients, but we found that activating NK receptors are expressed at significantly lower frequencies on CD8+ T cells during CHC infection. These findings suggest that decreased expression of activating NK receptors may play a role in HCV infection, possibly by inhibiting CD8 T-cell triggering.

Other factors such as cytokines may also play an important role during CHC infection[30-32]. IL-10 has largely been appreciated for its direct and indirect inhibitory effects on several T cell responses. IL-10 has been shown to contribute to regulation of immunopathology. The increased production of IL-10 by CD8+ T cells in CHC patients with persistently normal ALT reported in this paper is supposed to be important for limiting CD8 T cell response and contributing to asymptomatic virus carrier state. The NK cells of CHC carriers with PNALT produced significantly higher level of IL-4 and TNF-α, together with high cytotoxic activity compared to patients with CHC infection. We showed that cytokine pattern of NK cells and CD8+ T cells are

shifted towards a virus-permissive profile in patients with CHC infection which may ultimately contribute to HCV chronicity.

A major unresolved issue is the exact role of immune cells in different patient populations with acute and chronic hepatitis C virus infection. Further investigations are needed to clear whether NK, NKT-like and CD8+ T cells expressing various activating and inhibitory receptors could lead to viral clearance.

In conclusion we found complex dysregulation of activating and inhibitory receptor expression, such as decreased NKG2D and CD160 activating receptor expression and increased KIR2DL3 inhibitory receptor expression by NK and cytotoxic T cells in patients with chronic hepatitis C contributing to defective cellular immune functions. NKG2D receptor expression was significantly elevated in CHC infected patients with persistently normal ALT suggesting an important pathway for sustaining NK and CD8 T cell function and its critical role in protection against disease progression.

COMMENTS

Background

The host immune response to hepatitis C virus (HCV) involves both innate and adaptive arms of the immune system. Natural killer (NK) cells are key components of the innate antiviral immune response.

Research frontiers

To better characterize the immune defects underlying chronic viral persistence, the authors focus their analysis on killer inhibitory and activating receptor expression in patients with chronic HCV (CHC) infection with elevated alanine aminotransferase (ALT) and also in patients with CHC carriers with persistently normal ALT.

Innovations and breakthroughs

The authors found complex dysregulation of activating and inhibitory receptor expression by NK and cytotoxic T cells in patients with chronic hepatitis C contributing to defective cellular immune functions.

Applications

The percentage of Treg cells, KIR2DL3, ILT-2, KIR3DL1, CD160, NKG2D, NKG2C expressing NK, T and NKT-like cells, cytokine production and NK cytotoxicity were determined by flow cytometry.

Terminology

Persistently normal ALT was defined as ALT < 30 IU/L in men, ALT < 19 IU/L in women measured every 3 mo over a 18-mo period.

Peer-review

The manuscript described some phenotypical and functional differences in peripheral lymphocyte subsets between CHC patients with high and normal ALT. They describe a different expression in one NK activating receptor that could be related with TGF-β1 regulation. The manuscript is well written and the methodology is properly done.

REFERENCES

1 **Lavanchy D**. Evolving epidemiology of hepatitis C virus. *Clin Microbiol Infect* 2011; **17**: 107-115 [PMID: 21091831 DOI: 10.1111/j.1469-0691.2010.03432.x]

2 **Cohen J**. The scientific challenge of hepatitis C. *Science* 1999; **285**: 26-30 [PMID: 10428695 DOI: 10.1126/science.285.5424.26]

3 **Stoll-Keller F**, Barth H, Fafi-Kremer S, Zeisel MB, Baumert TF. Development of hepatitis C virus vaccines: challenges and progress. *Expert Rev Vaccines* 2009; **8**: 333-345 [PMID: 19249975 DOI: 10.1586/14760584.8.3.333]

4 **Puoti C**, Bellis L, Guarisco R, Dell' Unto O, Spilabotti L, Costanza OM. HCV carriers with normal alanine aminotransferase levels: healthy persons or severely ill patients? Dealing with an everyday clinical problem. *Eur J Intern Med* 2010; **21**: 57-61 [PMID: 20206870 DOI: 10.1016/j.ejim.2009.12.006]

5 **Nattermann J**, Nischalke HD, Hofmeister V, Ahlenstiel G, Zimmermann H, Leifeld L, Weiss EH, Sauerbruch T, Spengler U. The HLA-A2 restricted T cell epitope HCV core 35-44 stabilizes HLA-E expression and inhibits cytolysis mediated by natural killer cells. *Am J Pathol* 2005; **166**: 443-453 [PMID: 15681828 DOI: 10.1016/S0002-9440(10)62267-5]

6 **Pár G**, Rukavina D, Podack ER, Horányi M, Szekeres-Barthó J, Hegedüs G, Paál M, Szereday L, Mózsik G, Pár A. Decrease in CD3-negative-CD8dim(+) and Vdelta2/Vgamma9 TcR+ peripheral blood lymphocyte counts, low perforin expression and the impairment of natural killer cell activity is associated with chronic hepatitis C virus infection. *J Hepatol* 2002; **37**: 514-522 [PMID: 12217606 DOI: 10.1016/S0168-8278(02)00218-0]

7 **Maroof A**, Beattie L, Zubairi S, Svensson M, Stager S, Kaye PM. Posttranscriptional regulation of Il10 gene expression allows natural killer cells to express immunoregulatory function. *Immunity* 2008; **29**: 295-305 [PMID: 18701085 DOI: 10.1016/j.immuni.2008.06.012]

8 **Brockman MA**, Kwon DS, Tighe DP, Pavlik DF, Rosato PC, Sela J, Porichis F, Le Gall S, Waring MT, Moss K, Jessen H, Pereyra F, Kavanagh DG, Walker BD, Kaufmann DE. IL-10 is up-regulated in multiple cell types during viremic HIV infection and reversibly inhibits virus-specific T cells. *Blood* 2009; **114**: 346-356 [PMID: 19365081 DOI: 10.1182/blood-2008-12-191296]

9 **Exley MA**, Koziel MJ. To be or not to be NKT: natural killer T cells in the liver. *Hepatology* 2004; **40**: 1033-1040 [PMID: 15486982 DOI: 10.1002/hep.20433]

10 **Bendelac A**, Savage PB, Teyton L. The biology of NKT cells. *Annu Rev Immunol* 2007; **25**: 297-336 [PMID: 17150027 DOI: 10.1146/annurev.immunol.25.022106.141711]

11 **Ye L**, Wang X, Wang S, Wang Y, Song L, Hou W, Zhou L, Li H, Ho W. CD56+ T cells inhibit hepatitis C virus replication in human hepatocytes. *Hepatology* 2009; **49**: 753-762 [PMID: 19085952 DOI: 10.1002/hep.22715]

12 **Liu C**, Zhu H, Tu Z, Xu YL, Nelson DR. CD8+ T-cell interaction with HCV replicon cells: evidence for both cytokine- and cell-mediated antiviral activity. *Hepatology* 2003; **37**: 1335-1342 [PMID: 12774012 DOI: 10.1053/jhep.2003.50207]

13 **Cox AL**, Mosbruger T, Lauer GM, Pardoll D, Thomas DL, Ray SC. Comprehensive analyses of CD8+ T cell responses during longitudinal study of acute human hepatitis C. *Hepatology* 2005; **42**: 104-112 [PMID: 15962289 DOI: 10.1002/hep.20749]

14 **Urbani S**, Amadei B, Fisicaro P, Tola D, Orlandini A, Sacchelli L, Mori C, Missale G, Ferrari C. Outcome of acute hepatitis C is related to virus-specific CD4 function and maturation of antiviral memory CD8 responses. *Hepatology* 2006; **44**: 126-139 [PMID: 16799989 DOI: 10.1002/hep.21242]

15 **Kaplan DE**, Sugimoto K, Newton K, Valiga ME, Ikeda F, Aytaman A, Nunes FA, Lucey MR, Vance BA, Vonderheide RH, Reddy KR, McKeating JA, Chang KM. Discordant role of CD4 T-cell response relative to neutralizing antibody and CD8 T-cell responses in acute hepatitis C. *Gastroenterology* 2007; **132**: 654-666 [PMID: 17258733 DOI: 10.1053/j.gastro.2006.11.044]

16 **Gruener NH**, Lechner F, Jung MC, Diepolder H, Gerlach T, Lauer G, Walker B, Sullivan J, Phillips R, Pape GR, Klenerman P. Sustained dysfunction of antiviral CD8+ T lymphocytes after infection with hepatitis C virus. *J Virol* 2001; **75**: 5550-5558 [PMID: 11356962 DOI: 10.1128/JVI.75.12.5550-5558.2001]

17 **Wedemeyer H**, He XS, Nascimbeni M, Davis AR, Greenberg HB, Hoofnagle JH, Liang TJ, Alter H, Rehermann B. Impaired effector

function of hepatitis C virus-specific CD8+ T cells in chronic hepatitis C virus infection. *J Immunol* 2002; **169**: 3447-3458 [PMID: 12218168 DOI: 10.4049/jimmunol.169.6.3447]

18 **Kane KL**, Ashton FA, Schmitz JL, Folds JD. Determination of natural killer cell function by flow cytometry. *Clin Diagn Lab Immunol* 1996; **3**: 295-300 [PMID: 8705672]

19 **Golden-Mason L**, Rosen HR. Natural killer cells: multifaceted players with key roles in hepatitis C immunity. *Immunol Rev* 2013; **255**: 68-81 [PMID: 23947348 DOI: 10.1111/imr.12090]

20 **Sung PS**, Racanelli V, Shin EC. CD8(+)T-Cell Responses in Acute Hepatitis C Virus Infection. *Front Immunol* 2014; **5**: 266 [PMID: 24936203 DOI: 10.3389/fimmu.2014.00266]

21 **Golden-Mason L**, Cox AL, Randall JA, Cheng L, Rosen HR. Increased natural killer cell cytotoxicity and NKp30 expression protects against hepatitis C virus infection in high-risk individuals and inhibits replication in vitro. *Hepatology* 2010; **52**: 1581-1589 [PMID: 20812318 DOI: 10.1002/hep.23896]

22 **Farag SS**, Caligiuri MA. Human natural killer cell development and biology. *Blood Rev* 2006; **20**: 123-137 [PMID: 16364519 DOI: 10.1016/j.blre.2005.10.001]

23 **Lee JC**, Lee KM, Kim DW, Heo DS. Elevated TGF-beta1 secretion and down-modulation of NKG2D underlies impaired NK cytotoxicity in cancer patients. *J Immunol* 2004; **172**: 7335-7340 [PMID: 15187109 DOI: 10.4049/jimmunol.172.12.7335]

24 **Golden-Mason L**, Madrigal-Estebas L, McGrath E, Conroy MJ, Ryan EJ, Hegarty JE, O'Farrelly C, Doherty DG. Altered natural killer cell subset distributions in resolved and persistent hepatitis C virus infection following single source exposure. *Gut* 2008; **57**: 1121-1128 [PMID: 18372499 DOI: 10.1136/gut.2007.130963]

25 **Nelson DR**, Gonzalez-Peralta RP, Qian K, Xu Y, Marousis CG, Davis GL, Lau JY. Transforming growth factor-beta 1 in chronic hepatitis C. *J Viral Hepat* 1997; **4**: 29-35 [PMID: 9031062 DOI: 10.1046/j.1365-2893.1997.00124.x]

26 **Bertone S**, Schiavetti F, Bellomo R, Vitale C, Ponte M, Moretta L, Mingari MC. Transforming growth factor-beta-induced expression of CD94/NKG2A inhibitory receptors in human T lymphocytes. *Eur J Immunol* 1999; **29**: 23-29 [PMID: 9933082 DOI: 10.1002/(SICI)1521-4141(199901)29::01<23::AID-IMMU23>3.0.CO;2-Y]

27 **Gonzalez VD**, Falconer K, Björkström NK, Blom KG, Weiland O, Ljunggren HG, Alaeus A, Sandberg JK. Expansion of functionally skewed CD56-negative NK cells in chronic hepatitis C virus infection: correlation with outcome of pegylated IFN-alpha and ribavirin treatment. *J Immunol* 2009; **183**: 6612-6618 [PMID: 19846870 DOI: 10.4049/jimmunol.0901437]

28 **Nattermann J**, Feldmann G, Ahlenstiel G, Langhans B, Sauerbruch T, Spengler U. Surface expression and cytolytic function of natural killer cell receptors is altered in chronic hepatitis C. *Gut* 2006; **55**: 869-877 [PMID: 16322112 DOI: 10.1136/gut.2005.076463]

29 **Morishima C**, Paschal DM, Wang CC, Yoshihara CS, Wood BL, Yeo AE, Emerson SS, Shuhart MC, Gretch DR. Decreased NK cell frequency in chronic hepatitis C does not affect ex vivo cytolytic killing. *Hepatology* 2006; **43**: 573-580 [PMID: 16496327 DOI: 10.1002/hep.21073]

30 **Dustin LB**, Rice CM. Flying under the radar: the immunobiology of hepatitis C. *Annu Rev Immunol* 2007; **25**: 71-99 [PMID: 17067278 DOI: 10.1146/annurev.immunol.25.022106.141602]

31 **Nishitsuji H**, Funami K, Shimizu Y, Ujino S, Sugiyama K, Seya T, Takaku H, Shimotohno K. Hepatitis C virus infection induces inflammatory cytokines and chemokines mediated by the cross talk between hepatocytes and stellate cells. *J Virol* 2013; **87**: 8169-8178 [PMID: 23678168 DOI: 10.1128/JVI.00974-13]

32 **Yue M**, Deng X, Zhai X, Xu K, Kong J, Zhang J, Zhou Z, Yu X, Xu X, Liu Y, Zhu D, Zhang Y. Th1 and Th2 cytokine profiles induced by hepatitis C virus F protein in peripheral blood mononuclear cells from chronic hepatitis C patients. *Immunol Lett* 2013; **152**: 89-95 [PMID: 23680070 DOI: 10.1016/j.imlet.2013.05.002]

P- Reviewer: Larrubia JR, Pandey VN, Picardi A **S- Editor**: Gong ZM
L- Editor: A **E- Editor**: Wang CH

World Journal of Gastroenterology

Submit a Manuscript: http://www.wjgnet.com/esps/
Help Desk: http://www.wjgnet.com/esps/helpdesk.aspx
DOI: 10.3748/wjg.v22.i20.4860

World J Gastroenterol 2016 May 28; 22(20): 4860-4867
ISSN 1007-9327 (print) ISSN 2219-2840 (online)

ORIGINAL ARTICLE

Basic Study

Gastric emptying, postprandial blood pressure, glycaemia and splanchnic flow in Parkinson's disease

Laurence G Trahair, Thomas E Kimber, Katerina Flabouris, Michael Horowitz, Karen L Jones

Laurence G Trahair, Thomas E Kimber, Katerina Flabouris, Michael Horowitz, Karen L Jones, Discipline of Medicine, The University of Adelaide, Adelaide, SA 5000, Australia

Laurence G Trahair, Michael Horowitz, Karen L Jones, NHMRC Centre of Research Excellence in Translating Nutritional Science to Good Health, The University of Adelaide, Adelaide, SA 5000, Australia

Thomas E Kimber, Neurology Unit, Royal Adelaide Hospital, Adelaide, SA 5000, Australia

Author contributions: Trahair LG, Kimber TE, Horowitz M and Jones KL were involved in the conception and design of the study, and drafted of the manuscript; Trahair LG and Kimber TE were also involved in coordination and subject recruitment; Trahair LG and Flabouris K collected data; Trahair LG, Horowitz M and Jones KL performed statistical analysis; all authors interpreted the data; Jones KL had overall responsibility for the study.

Supported by the Royal Adelaide Hospital, No. 13RAH1475; Australian Postgraduate Award and a Dawes scholarship from the Royal Adelaide Hospital (to Trahair LG); and NHMRC Senior Career Development Award (to Jones KL).

Institutional review board statement: The protocol was approved by the Research Ethics Committee, of the Royal Adelaide Hospital (approval number 111223).

Conflict-of-interest statement: Horowitz M has participated in the advisory boards and/or symposia for Novo Nordisk, Sanofi, Novartis, Eli Lilly, Merck Sharp and Dohme, Boehringer Ingelheim, and AstraZeneca and has received honoraria for this activity. None of the other authors has any personal or financial conflict of interest to declare.

Data sharing statement: Participants gave informed consent for data sharing. No additional data are available.

Correspondence to: Dr. Karen L Jones, NHMRC Senior CDA Research Fellow, Professor, Discipline of Medicine, The University of Adelaide, Level 6 Eleanor Harrald Building, Adelaide, SA 5000, Australia. karen.jones@adelaide.edu.au
Telephone: +61-8-82225394
Fax: +61-8-82233870

Received: November 23, 2015
Peer-review started: November 25, 2015
First decision: January 13, 2016
Revised: January 27, 2016
Accepted: February 20, 2016
Article in press: February 22, 2016
Published online: May 28, 2016

Abstract

AIM: To determine gastric emptying, blood pressure, mesenteric artery blood flow, and blood glucose responses to oral glucose in Parkinson's disease.

METHODS: Twenty-one subjects (13 M, 8 F; age 64.2 ± 1.6 years) with mild to moderate Parkinson's disease (Hoehn and Yahr score 1.4 ± 0.1, duration of known disease 6.3 ± 0.9 years) consumed a 75 g glucose drink, labelled with 20 MBq ^{99m}Tc-calcium phytate. Gastric emptying was quantified with scintigraphy, blood pressure and heart rate with an automated device, superior mesenteric artery blood flow by Doppler ultrasonography and blood glucose by

glucometer for 180 min. Autonomic nerve function was evaluated with cardiovascular reflex tests and upper gastrointestinal symptoms by questionnaire.

RESULTS: The mean gastric half-emptying time was 106 ± 9.1 min, gastric emptying was abnormally delayed in 3 subjects (14%). Systolic and diastolic blood pressure fell (P < 0.001) and mesenteric blood flow and blood glucose (P < 0.001 for both) increased, following the drink. Three subjects (14%) had definite autonomic neuropathy and 8 (38%) had postprandial hypotension. There were no significant relationships between changes in blood pressure, heart rate or mesenteric artery blood flow with gastric emptying. Gastric emptying was related to the score for autonomic nerve function (R = 0.55, P < 0.01). There was an inverse relationship between the blood glucose at t = 30 min (R = -0.52, P < 0.05), while the blood glucose at t = 180 min was related directly (R = 0.49, P < 0.05), with gastric emptying.

CONCLUSION: In mild to moderate Parkinson's disease, gastric emptying is related to autonomic dysfunction and a determinant of the glycaemic response to oral glucose.

Key words: Gastric emptying; Hypotension; Parkinson's disease; Blood pressure; Glucose

Core tip: We measured gastric emptying, blood pressure and blood glucose responses to a glucose drink in 21 patients with mild-to-moderate Parkinson's disease. Gastric emptying was shown to be abnormally delayed 3 patients and 40% had postprandial hypotension - a fall in systolic blood pressure > 20 mmHg after the glucose drink. We demonstrated relationships between gastric emptying and autonomic dysfunction, so that slower gastric emptying was associated with greater autonomic dysfunction, as well as relationships between the blood glucose response with gastric emptying.

Trahair LG, Kimber TE, Flabouris K, Horowitz M, Jones KL. Gastric emptying, postprandial blood pressure, glycaemia and splanchnic flow in Parkinson's disease. *World J Gastroenterol* 2016; 22(20): 4860-4867 Available from: URL: http://www.wjgnet.com/1007-9327/full/v22/i20/4860.htm DOI: http://dx.doi.org/10.3748/wjg.v22.i20.4860

INTRODUCTION

While gastrointestinal dysfunction occurs frequently in Parkinson's disease (PD)[1,2], the prevalence of abnormally delayed gastric emptying (GE) remains uncertain because of substantial variations in both the cohorts studied and the methodology used to quantify GE. Delayed GE has been associated with upper gastrointestinal and motor symptoms, as well as impaired absorption of dopaminergic therapy[3,4].

There is little or no information about the potential impact of GE in two other areas: postprandial blood pressure (BP) and glycaemia. Postprandial hypotension (PPH), a fall in systolic BP of ⩾ 20 mmHg within 2 h of a meal[5], was reported for the first time in 1977 in a patient with PD[6] and is a clinically important disorder, predisposing to syncope and falls and being associated with increased mortality[7]. PPH may occur frequently in PD, but information is limited[8]. It has also been suggested that PPH represents an "early" marker of autonomic dysfunction in PD[8,9]. Our studies have established that GE is pivotal to the regulation of postprandial BP- in healthy older subjects and patients with type 2 diabetes, the magnitude of the hypotensive response is greater when GE is relatively faster[10]. When glucose is infused intraduodenally in healthy older subjects at 1, 2 or 3 kcal/min, there is a substantial fall in systolic BP in response to the 2 and 3 kcal/min, but not the 1 kcal/min, load[11]. In contrast to the effect of GE, gastric distension attenuates the fall in BP[12], and consumption of water has been advocated as a treatment for PPH[7]. Only one study has evaluated the impact of GE on BP in PD and found no relationship in a cohort of 12 patients with mild to moderate disease[13]; BP was not a primary outcome in this study. The hypotensive response to a meal may relate to splanchnic blood pooling, as assessed by measurement of superior mesenteric artery (SMA) blood flow using Doppler ultrasound[14].

GE is an important determinant of postprandial glycaemia, which is a major contributor to "overall" glycaemic control in diabetes, as assessed by glycated hemoglobin[15]. Accordingly, in health[16], subjects with impaired glucose tolerance[16,17] and type 2 diabetes[17], when GE is faster, there is a greater initial glycaemic response. While diabetes per se does not appear to increase the propensity to PD[18], type 2 diabetes may be associated with greater impairments in postural stability and gait[19]. PD is associated with impaired insulin signalling in the brain[20] and drugs developed for the management of diabetes, particularly glucagon-like peptide-1 agonists, may have efficacy in treatment[21]. There is no information about the impact of GE on postprandial glycaemia in PD.

The primary aims of this study were to quantify the GE, BP, SMA flow and blood glucose responses to oral glucose in mild to moderate PD and evaluate the relationships of changes in BP and glycaemia with the rate of GE. We hypothesised that there would be a high prevalence of delayed GE, that consumption of glucose would result in a fall in BP and rises in both SMA flow and blood glucose, and that these responses would be related to GE.

Table 1 List of anti-Parkinsonian medications in 21 patients with Parkinson's disease *n* (%)

Drug	Patients
Pramipexole	11 (52)
Levodopa	9 (43)
Levodopa and Carbidopa	8 (38)
Levodopa, Carbidopa and Entacapone	4 (19)
Rasagiline	3 (14)
Amantadine	1 (5)
Apomorphone	1 (5)
Pregabalin	1 (5)
Selegiline	1 (5)

MATERIALS AND METHODS

Subjects

Twenty one subjects with mild to moderate PD were recruited through advertisements placed in a local Parkinson's newsletter, and outpatient referral by a neurologist (TK). Mild to moderate PD was defined as a score ⩽ 2.5 on the modified Hoehn and Yahr scale[22]. Subjects who were unable to move independently, or who had a history of falls, gastrointestinal disease (unrelated to Parkinson's), diabetes, significant respiratory or cardiac disease, alcohol abuse or epilepsy, were excluded. 13 males and 8 females, age 64.2 ± 1.6 years (range: 51-77 years), body mass index (BMI) 25.2 ± 0.8 kg/m^2 (range: 20.3-34.5 kg/m^2) and known duration of PD 6.3 ± 0.9 years (range: 1-16 years), were studied. Two patients were receiving antihypertensive drugs, which were withdrawn for 24 h before the study day. Details of anti-Parkinsonian medication are summarised in Table 1. Four subjects had received deep brain stimulation for the management of their PD.

Protocol

At an initial screening visit 6-65 d before the study day, a medical history and staging of Parkinson's symptoms on the modified Hoehn and Yahr scale were performed by a neurologist (TK)[22] and a questionnaire to asses symptoms referrable to delayed GE completed[23,24].

On the study day, subjects attended the Department of Nuclear Medicine, Positron Emission Tomography and Bone Densitometry at the Royal Adelaide Hospital at 0830h after an overnight fast from solids (14 h) and liquids (12 h). Where possible, subjects were asked to withhold the morning dose of anti-Parkinsonian medication. On arrival, the subject was seated in front of a gamma camera and an IV cannula inserted into the left antecubital vein for blood sampling. An automated cuff was placed around the upper right arm to measure BP and HR. The subject was then allowed to "rest" for approximately 15 min[11]. At *t* = -3 min, the subject consumed a drink comprising 75 g glucose and 5 g 3-O-Methyl-D-gluco-pyranose (3-OMG) (Carbosynth, Berkshire, United Kingdom) dissolved in water (total drink volume 300 mL), labelled with 20 MBq ^{99m}Tc-calcium phytate (Radpharm Scientific, Belconnen, ACT, Australia) within 3 min. GE, BP, SMA blood flow and blood glucose were measured for 180 min following the drink. At *t* = 180 min, the IV cannula was removed and the subject given a meal. Evaluation of autonomic function, using standardised cardiovascular reflex tests[25], was then performed, prior to the subject leaving the laboratory.

The protocol was approved by the Research Ethics Committee of the Royal Adelaide Hospital, and each subject provided written, informed consent prior to their inclusion. All experiments were carried out in accordance with the Declaration of Helsinki.

Measurements

Gastric emptying: Radioisotopic data was acquired for 180 min following consumption of the drink (60 s frames between *t* = 0-60 min, then 180 s frames from *t* = 60-180 min), where *t* = 0 was the time of completion of the drink. Data were corrected for subject movement, radionuclide decay and γ-ray attenuation[26]. A region-of-interest was drawn around the total stomach and gastric emptying curves (expressed as percentage retention over time) derived. The amount of the drink remaining in the total stomach at 15 min intervals between *t* = 0-180 min, as well as the 50% gastric emptying time (T_{50})[26], were calculated. The normal range for the T_{50} of this drink is 43-157 min, based on data in 21 healthy subjects (age 64.8 ± 1.8 years), matched for age (*i.e.,* within 2 years) to each subject with PD[17]. GE was considered to be abnormally fast or slow when the T_{50} was above, or below, this normal range.

Blood pressure and heart rate: BP and HR were measured using an automated BP monitor (DINAMAP ProCare 100, GE Medical Systems, Milwaukee, WI, United States), every 3 min during the "rest" period, and from *t* = 0-180 min. Baseline BP was calculated as an average of the three measurements obtained immediately prior to the consumption of the drink (*i.e.,* *t* = -9, *t* = 6 and *t* = -3 min)[11]. Maximum changes in BP and HR were calculated as the greatest change that occurred from baseline. Subjects were categorised according to the maximum fall in systolic BP following the drink, *i.e.,* those in which the fall was ⩽ 10 mmHg, > 10 mmHg but < 20 mmHg and ⩾ 20 mmHg. PPH was defined as a sustained (> 10 min) fall in systolic BP of ⩾ 20 mmHg[5].

Superior mesenteric artery blood flow: SMA flow was measured using a Logiq™ e ultrasound system (GE Healthcare Technologies, Sydney, NSW, Australia) and a 3.5C broad spectrum 2.5-4 MHz convex linear array transducer. Measurements were obtained immediately prior to the consumption of the drink (*t* = -3 min), every 15 min between *t* = 0-60 min, and then at *t* = 90 min, 120 min and 180 min. Blood flow (mL/min) was calculated automatically using the formula: π ×

$r^2 \times TAMV \times 60$, where R = the radius of the SMA and TAMV is the time-averaged mean velocity[14]. In all subjects two measurements were acquired by the same, experienced investigator (LT) at each time point.

Blood glucose: Venous blood was sampled immediately prior to the consumption of the drink (t = -3 min), every 15 min between t = 0-60 min and then at t = 90 min, 120 min and 180 min. Blood glucose (mmol/L) was determined immediately using a portable glucometer (Medisense Companion 2 m, Medisense Inc. Waltham, MA, United States). Results were classified, according to World Health Organisation criteria, as normal glucose tolerance (NGT) (fasting blood glucose < 6.1 mmol/L, and 2 h < 7.8 mmol/L), impaired fasting glucose (IFG) (fasting blood glucose < 7.0 mmol/L, but > 6.1 mmol/L), impaired glucose tolerance (IGT) (2 h blood glucose < 11.1 mmol/L, but > 7.8 mmol/L), or diabetes (fasting blood glucose ⩾ 7.0 mmol/L and/or 2 h blood glucose ⩾ 11.1 mmol/L)[27].

Upper gastrointestinal symptoms: Upper gastrointestinal symptoms assessed at the screening visit by questionnaire[23], included anorexia, nausea, early satiety, bloating, vomiting, abdominal pain, dysphagia, heart burn and acid regurgitation. Each was scored as: 0 = none, 1 = mild, 2 = moderate or 3 = severe, for a maximum score of 27[23].

Cardiovascular autonomic nerve function: Autonomic nerve function (ANF) was assessed using standardised cardiovascular reflex tests[25]. Parasympathetic function was evaluated by the variation (R-R interval) of the heart rate during deep breathing and the response to standing ("30:15" ratio). Sympathetic function was assessed by the fall in systolic BP in response to standing. Each of the results was scored according to age-adjusted predefined criteria as 0 = normal, 1 = borderline and 2 = abnormal for a total maximum score of 6. A score ⩾ 3 was considered to indicate definite autonomic dysfunction[25,28]. Orthostatic hypotension (OH) was defined as a sustained reduction in systolic BP of > 20 mmHg within 3 min of standing[29].

Statistical analysis: BP and HR were assessed as changes from baseline, whereas GE, SMA flow and blood glucose were analysed as absolute values. The maximum changes from baseline in BP, HR and blood glucose were also calculated. Areas under the curve (AUCs) were calculated for BP, HR, SMA flow and blood glucose using the trapezoidal rule. Changes in each variable over time were evaluated with ANOVA. Pearson's correlation was used to evaluate relationships between variables. Relationships of BP, upper gastrointestinal symptoms and glycaemia with GE were assessed using the GE T_{50}, given the observed overall linear pattern. A P value < 0.05 was considered significant in all analyses. The number of subjects included was based on power calculations derived from our previous study[10]. The statistical analysis was supervised and reviewed by a professional biostatistician. Data are presented as mean ± SE.

RESULTS

The studies were well tolerated and no adverse events were reported. The mean Hoehn and Yahr score was 1.4 ± 0.1 (range: 1-2.5) and duration of known PD 6.3 ± 0.9 years (range: 1-16 years). Three subjects were unwilling, or unable to withhold their morning anti-Parkinson medications because of the risk of significant motor dysfunction. Three subjects had definite autonomic neuropathy, in 10 subjects the score was ⩾ 2; the mean ANF score was 1.8 ± 0.3 (range: 0-5); 5 subjects had OH. Eight subjects had PPH. In another 8, the maximum fall was > 10 mmHg but < 20 mmHg and in 5 subjects the fall was < 10 mmHg. Four of the 5 subjects with OH also had PPH. The mean score for upper gastrointestinal symptoms was 1.5 ± 0.4 (range: 0-5).

Gastric emptying

Gastric emptying of the drink approximated an overall linear pattern. The T_{50} was 106 ± 9.1 min. In three subjects, GE (T_{50}) was abnormally slow; no subject had abnormally rapid GE.

Blood pressure and heart rate

Baseline systolic BP was 116.9 ± 2.4 mmHg. Following the drink, there was a transient modest rise, followed by a fall, in systolic BP (P < 0.001, Figure 1A), which was sustained until the end of the study. The maximum fall was -18.6 ± 2.0 mmHg, occurring at t = 76.5 ± 12.8 min.

Baseline diastolic BP was 69.1 ± 1.6 mmHg. Following the drink, there was a transient initial rise, and then a fall, in diastolic BP (P < 0.001, Figure 1B), with a nadir between t = 30-45 min, which was sustained until the end of the study. The maximum fall in diastolic BP was -15.6 ± 0.9 mmHg, occurring at t = 85.9 ± 11.6 min.

Baseline heart rate was 69.5 ± 2.1 BPM. Following the drink, there was an increase in heart rate (P < 0.001, Figure 1C), which had returned to baseline by approximately t = 60 min. The maximum increase in HR was 9.5 ± 0.7 BPM occurring at 75.6 ± 13.3 min.

Superior mesenteric artery blood flow

Baseline SMA flow was 565.0 ± 62.5 mL/min. Following the drink, there was a prompt increase in SMA flow (P < 0.001, Figure 2), which had returned to baseline by t = 180 min. The maximum SMA flow was 1208.8 ± 123.0 mL/min, occurring at t = 54.8 ± 8.1 min.

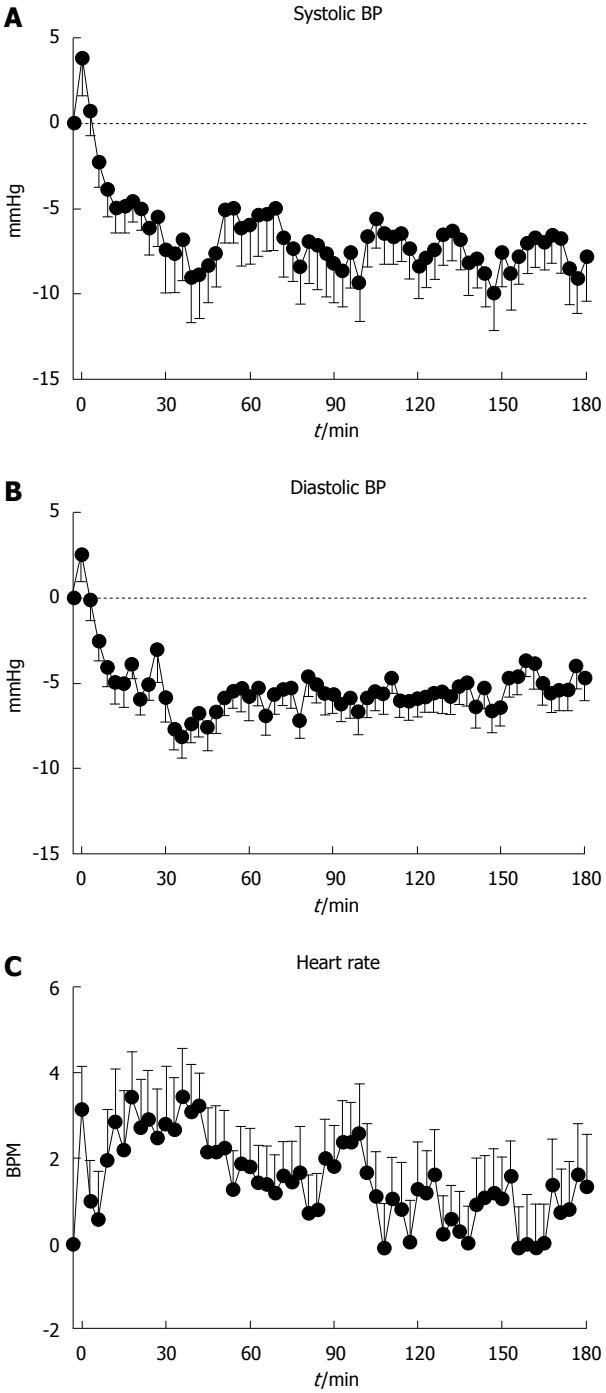

Figure 1 Systolic blood pressure (A), diastolic blood pressure (B) and heart rate (C) immediately before and after 75 g oral glucose load in 21 patients with Parkinson's disease. BP: Blood pressure.

Blood glucose

Baseline blood glucose was 5.6 ± 0.1 mmol/L. Following the drink, there was an increase in blood glucose (P < 0.001, Figure 3), which had returned to baseline by t = 180 min. The maximum blood glucose was 10.2 ± 0.5 mmol/L, occurring at 48.9 ± 4.0 min. Five subjects had IGT, 2 had both IFG and IGT and 1 had "marginal" diabetes (fasting and 2 h blood glucose of 7.1 mmol/L and 11.1 mmol/L, respectively).

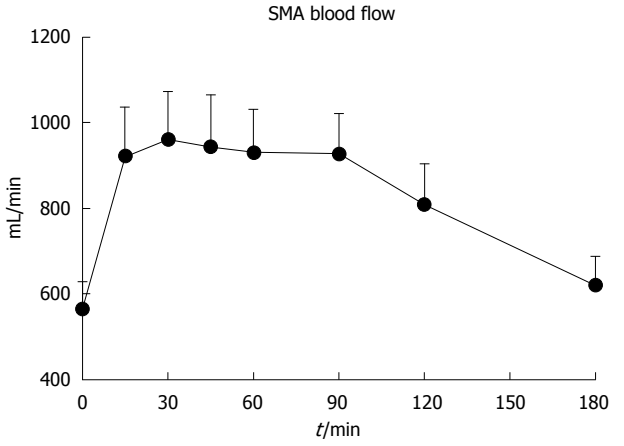

Figure 2 Superior mesenteric artery blood flow immediately before and after 75 g oral glucose load in 21 patients with Parkinson's disease. SMA: Superior mesenteric artery.

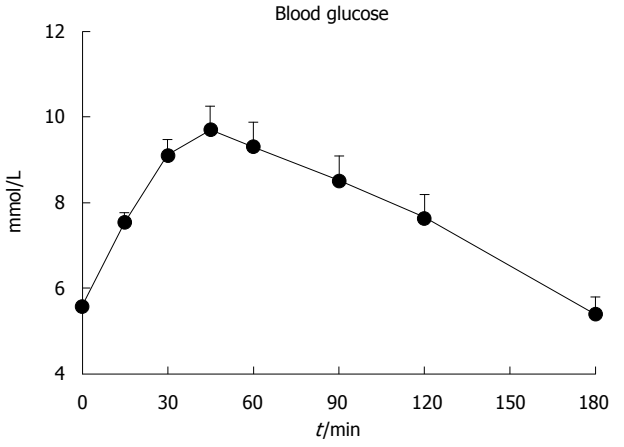

Figure 3 Blood glucose immediately before and after 75 g oral glucose load in 21 patients with Parkinson's disease.

Relationships between variables

There were no significant relationships between the changes in systolic BP, diastolic BP, HR or SMA flow at any time point (absolute values and AUCs). The T_{50} was related directly to the ANF score (R = 0.55, P < 0.01, Figure 4). Upper gastrointestinal symptoms were also related to the score for ANF (R = 0.45, P < 0.05), but not GE.

There was an inverse relationship between the blood glucose at t = 30 min (R = -0.52, P < 0.05, Figure 5), while the blood glucose at t = 180 min (but not 120 min) was related directly (R = 0.49, P < 0.05) to the T_{50}.

There were no significant relationships between T_{50}, Hoehn and Yahr score, duration of disease, or age.

DISCUSSION

Our study has quantified the GE, BP, SMA and glycaemic responses to oral glucose in mild to moderate

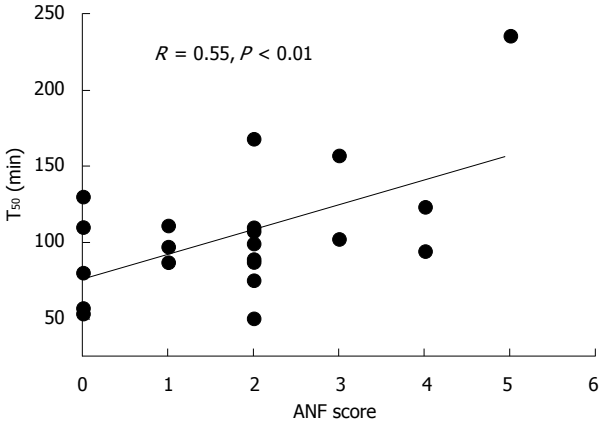

Figure 4 Relationship between gastric half emptying time (GE T_{50}) and autonomic nerve function score (R = 0.55, P < 0.01). ANF: Autonomic nerve function.

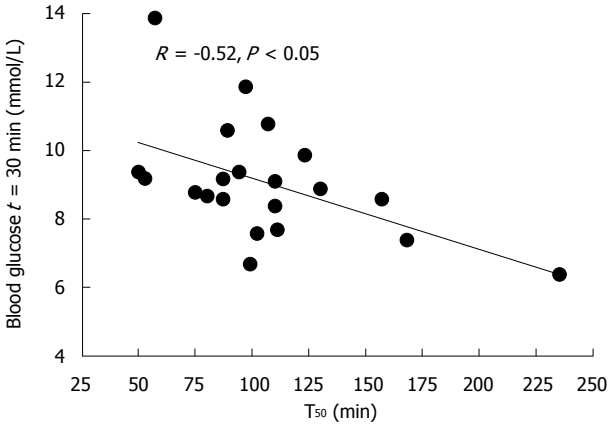

Figure 5 Relationship between the absolute blood glucose at t = 30 min with the gastric half emptying time (GE T_{50}) (R = -0.52, P < 0.05).

PD. In the majority of patients, oral glucose induced a significant fall in systolic BP; *i.e.,* in 16 of 21 patients (76%), this fall was > 10 mmHg and 8 (38%) had PPH. GE of glucose was abnormally delayed in 3 patients (14%), a prevalence lower than we anticipated and slower in those patients with cardiovascular autonomic neuropathy, and gastric emptying was not accelerated in any subject. There was, however, no relationship between the magnitude of the fall in BP with GE. A relationship between the initial glycaemic response to glucose with GE, comparable to that observed in subjects without PD, was demonstrated.

The outcome of studies relating to the prevalence of disordered GE in PD is inconsistent. We measured GE using the "gold-standard" technique of scintigraphy and, while a liquid, rather than a solid, "meal" was used, the precision of solid and high-nutrient liquid meals in the diagnosis of delayed GE appears comparable[30]. It should, however, be recognised that our definition of delayed GE - a T_{50} that was greater than the range observed in healthy subjects, was deliberately stringent, so that more modest gastric motor function cannot be excluded. The observations of a relationship between GE and the severity of autonomic dysfunction and the high prevalence of autonomic dysfunction are not surprising. The pathophysiology of disordered GE in PD is heterogeneous - alpha-synuclein aggregation, abnormalities in the dorsal motor nucleus of the vagus and enteric nervous system, and drugs such as L-dopa may all be important[2]. As with previous studies, there was no significant relationship between GE and the duration of PD[31]. Patients had mild upper gastrointestinal symptoms, possibly in part because the majority were studied off dopaminergic therapy, although symptoms were more common in patients with impaired ANF.

The high prevalence of PPH is comparable to that reported previously - 8 subjects had PPH and the fall in systolic BP was ⩾ 10 mmHg in 16 of 21 (76%) subjects[8]. That the latter may have adverse consequences, even in apparently "asymptomatic" patients[32], dictates the need for greater recognition. We did not observe a relationship between the magnitude of the fall in BP and GE, for which there are a number of potential explanations. Baseline systolic BP was in most cases "normal", which is predictive of a smaller postprandial fall[33]. We have demonstrated in healthy older subjects that the relationship between the fall in BP and the rate of duodenal glucose delivery is non-linear, so that a "threshold" between 1-2 kcal/min must be exceeded to elicit a hypotensive response[11]. In the current study, based on the T_{50}, GE was ⩾ 2 kcal/min in only 4 subjects. Hence, it would be appropriate to re-evaluate this hypothesis further in a larger group of patients. The current study certainly does not exclude the possibility that PD patients with relatively more rapid GE are at increased risk for PPH.

There was an approximate doubling in SMA flow following the glucose drink, as anticipated. In healthy subjects and patients with autonomic failure[34], comparable increases in SMA flow have been observed, but a reduction in BP was only evident in patients with autonomic failure, probably reflecting inadequate sympathetic compensation[34]. The absence of a relationship between BP and SMA flow, may reflect the relatively narrow distribution of the rises in SMA flow, and modest size of the cohort. OH is a frequent manifestation of autonomic involvement in PD and a concordance of PPH and OH in PD has been reported[8], and supported by our study.

The relationship between the initial glycaemic response to the drink and the rate of GE in PD is consistent with observations in health[16], impaired glucose tolerance[16,17], and type 2 diabetes[17] as well as the effect of delayed GE on the absorption of L-dopa in PD[2]. It is now recognised that postprandial glycaemic excursions are a major determinant of overall glycaemic control in type 2 diabetes, assuming increasing importance as glycated hemoglobin normalises[15]. Eight of our 21 subjects (38%) had either impaired glucose tolerance (7 subjects) or

"marginal" diabetes (1 subject); that the blood glucose level at 180 min, but not 120 min, was inversely, rather than directly, related to GE, presumably reflects higher insulin levels achieved earlier, associated with insulin resistance[16]. In healthy subjects an inverse relationship is evidence at 120 min after a 75 g oral glucose load[17]. The recognition that GE is a determinant of glycaemia in PD is not surprising, but potentially important- slower GE, including that induced by dopaminergic therapy, would potentially be advantageous in optimising glycaemic control in type 2 patients with PD. Interestingly, GLP-1 agonists, such as exenatide BD which are undergoing evaluation of their efficacy in the management of PD[21], diminish postprandial glycaemic excursions primarily by slowing GE[35].

In interpreting our observations, it should be recognised that 3 subjects did not withdraw their medication, which may represent a cofounder. We also did not include a control (water) drink because of potential ethical concerns. A normal range for GE allowed the prevalence of disordered GE in PD to be determined - a formal control group was not included because the focus of the present study was on relationships between variables within the Parkinson's group. As discussed, one subject had diabetes, based on fasting and 2 h blood glucose, but these levels were only marginally above the diagnostic cut-offs and this subject was not excluded.

In conclusion, in this unselected population of patients with mild to moderate PD, GE was delayed in only a minority, oral glucose induced a substantial reduction in BP, as well as rises in SMA flow and blood glucose, and GE was an important determinant of the glycaemic, but not the BP, response.

COMMENTS

Background

Delayed gastric emptying is recognised as a sequela of Parkinson's disease (PD), but its prevalence remains uncertain and the potential impact on both postprandial blood pressure and glycaemia have not been evaluated. Postprandial hypotension is known to occur frequently in PD and may be influenced by changes in superior mesenteric artery blood flow.

Research frontiers

Delayed gastric emptying in PD is associated with fluctuations in motor response, upper gastrointestinal symptoms and impaired absorption of dopaminergic therapy. The pathophysiology of postprandial hypotension is poorly defined, but the magnitude of the fall in blood pressure is known to be dependent on the rate of gastric emptying as well as changes in superior mesenteric artery blood flow.

Innovations and breakthroughs

The outcome of studies investigating the prevalence of disordered gastric emptying in PD have been inconsistent, at least in part reflecting variations in the cohorts studied and methodology employed to measure gastric emptying. The authors have measured gastric emptying using the "gold-standard" technique of scintigraphy in a well defined cohort of patients with PD to address these limitations. Furthermore, no study in PD has assessed changes in blood pressure and superior mesenteric artery blood flow following oral glucose.

Applications

The recognition that gastric emptying is a determinant of glycaemia is of importance to the management of glycaemic control in patients with PD who have type 2 diabetes. The authors identified a high prevalence of postprandial hypotension in this population, and given the substantial adverse sequale associated with this condition, this represents an important consideration in the management of PD with likely autonomic involvement.

Terminology

Postprandial hypotension, a fall in systolic blood pressure > 20 mmHg occurring within two hours of a "meal".

Peer-review

This is an excellent manuscript which comprehensively describes a very well-conducted investigation that is clinically relevant.

REFERENCES

1 **Pfeiffer RF**. Gastrointestinal dysfunction in Parkinson's disease. *Lancet Neurol* 2003; **2**: 107-116 [PMID: 12849267]

2 **Marrinan S**, Emmanuel AV, Burn DJ. Delayed gastric emptying in Parkinson's disease. *Mov Disord* 2014; **29**: 23-32 [PMID: 24151126 DOI: 10.1002/mds.25708]

3 **Goetze O**, Nikodem AB, Wiezcorek J, Banasch M, Przuntek H, Mueller T, Schmidt WE, Woitalla D. Predictors of gastric emptying in Parkinson's disease. *Neurogastroenterol Motil* 2006; **18**: 369-375 [PMID: 16629864 DOI: 10.1111/j.1365-2982.2006.00780.x]

4 **Doi H**, Sakakibara R, Sato M, Masaka T, Kishi M, Tateno A, Tateno F, Tsuyusaki Y, Takahashi O. Plasma levodopa peak delay and impaired gastric emptying in Parkinson's disease. *J Neurol Sci* 2012; **319**: 86-88 [PMID: 22632782 DOI: 10.1016/j.jns.2012.05.010]

5 **Jansen RW**, Lipsitz LA. Postprandial hypotension: epidemiology, pathophysiology, and clinical management. *Ann Intern Med* 1995; **122**: 286-295 [PMID: 7825766]

6 **Seyer-Hansen K**. Postprandial hypotension. *Br Med J* 1977; **2**: 1262 [PMID: 589129]

7 **Trahair LG**, Horowitz M, Jones KL. Postprandial hypotension: a systematic review. *J Am Med Dir Assoc* 2014; **15**: 394-409 [PMID: 24630686 DOI: 10.1016/j.jamda.2014.01.011]

8 **Loew F**, Gauthey L, Koerffy A, Herrmann FR, Estade M, Michel JP, Vallotton MB. Postprandial hypotension and orthostatic blood pressure responses in elderly Parkinson's disease patients. *J Hypertens* 1995; **13**: 1291-1297 [PMID: 8984127]

9 **Meco G**, Pratesi L, Bonifati V. Cardiovascular reflexes and autonomic dysfunction in Parkinson's disease. *J Neurol* 1991; **238**: 195-199 [PMID: 1895149]

10 **Jones KL**, Tonkin A, Horowitz M, Wishart JM, Carney BI, Guha S, Green L. Rate of gastric emptying is a determinant of postprandial hypotension in non-insulin-dependent diabetes mellitus. *Clin Sci* (Lond) 1998; **94**: 65-70 [PMID: 9505868]

11 **Vanis L**, Gentilcore D, Rayner CK, Wishart JM, Horowitz M, Feinle-Bisset C, Jones KL. Effects of small intestinal glucose load on blood pressure, splanchnic blood flow, glycemia, and GLP-1 release in healthy older subjects. *Am J Physiol Regul Integr Comp Physiol* 2011; **300**: R1524-R1531 [PMID: 21389332 DOI: 10.1152/ajpregu.00378.2010]

12 **Vanis L**, Gentilcore D, Hausken T, Pilichiewicz AN, Lange K, Rayner CK, Feinle-Bisset C, Meyer JH, Horowitz M, Jones KL. Effects of gastric distension on blood pressure and superior mesenteric artery blood flow responses to intraduodenal glucose in healthy older subjects. *Am J Physiol Regul Integr Comp Physiol* 2010; **299**: R960-R967 [PMID: 20554933 DOI: 10.1152/ajpregu.00235.2010]

13 **Thomaides T**, Karapanayiotides T, Zoukos Y, Haeropoulos C, Kerezoudi E, Demacopoulos N, Floodas G, Papageorgiou E, Armakola F, Thomopoulos Y, Zaloni I. Gastric emptying after semi-solid food in multiple system atrophy and Parkinson disease.

J Neurol 2005; **252**: 1055-1059 [PMID: 15795792 DOI: 10.1007/s00415-005-0815-y]
14 **Perko MJ**. Duplex ultrasound for assessment of superior mesenteric artery blood flow. *Eur J Vasc Endovasc Surg* 2001; **21**: 106-117 [PMID: 11237782]
15 **Monami M**, Lamanna C, Lambertucci L, Longo R, Cocca C, Addante F, Lotti E, Masotti G, Marchionni N, Mannucci E. Fasting and post-prandial glycemia and their correlation with glycated hemoglobin in Type 2 diabetes. *J Endocrinol Invest* 2006; **29**: 619-624 [PMID: 16957410]
16 **Trahair LG**, Horowitz M, Marathe CS, Lange K, Standfield S, Rayner CK, Jones KL. Impact of gastric emptying to the glycemic and insulinemic responses to a 75-g oral glucose load in older subjects with normal and impaired glucose tolerance. *Physiol Rep* 2014; **2**: pii e12204 [PMID: 25413324 DOI: 10.14814/phy2.12204]
17 **Marathe CS**, Horowitz M, Trahair LG, Wishart JM, Bound M, Lange K, Rayner CK, Jones KL. Relationships of Early And Late Glycemic Responses With Gastric Emptying During An Oral Glucose Tolerance Test. *J Clin Endocrinol Metab* 2015; **100**: 3565-3571 [PMID: 26171801 DOI: 10.1210/JC.2015-2482]
18 **Lu L**, Fu DL, Li HQ, Liu AJ, Li JH, Zheng GQ. Diabetes and risk of Parkinson's disease: an updated meta-analysis of case-control studies. *PLoS One* 2014; **9**: e85781 [PMID: 24465703 DOI: 10.1371/journal.pone.0085781]
19 **Kotagal V**, Albin RL, Müller ML, Koeppe RA, Frey KA, Bohnen NI. Diabetes is associated with postural instability and gait difficulty in Parkinson disease. *Parkinsonism Relat Disord* 2013; **19**: 522-526 [PMID: 23462483 DOI: 10.1016/j.parkreldis.2013.01.016]
20 **Lima MM**, Targa AD, Noseda AC, Rodrigues LS, Delattre AM, dos Santos FV, Fortes MH, Maturana MJ, Ferraz AC. Does Parkinson's disease and type-2 diabetes mellitus present common pathophysiological mechanisms and treatments? *CNS Neurol Disord Drug Targets* 2014; **13**: 418-428 [PMID: 24059307]
21 **Hölscher C**. Drugs developed for treatment of diabetes show protective effects in Alzheimer's and Parkinson's diseases. *Sheng Li Xue Bao* 2014; **66**: 497-510 [PMID: 25331995]
22 **Goetz CG**, Poewe W, Rascol O, Sampaio C, Stebbins GT, Counsell C, Giladi N, Holloway RG, Moore CG, Wenning GK, Yahr MD, Seidl L. Movement Disorder Society Task Force report on the Hoehn and Yahr staging scale: status and recommendations. *Mov Disord* 2004; **19**: 1020-1028 [PMID: 15372591 DOI: 10.1002/mds.20213]
23 **Jones KL**, Horowitz M, Carney BI, Wishart JM, Guha S, Green L. Gastric emptying in early noninsulin-dependent diabetes mellitus. *J Nucl Med* 1996; **37**: 1643-1648 [PMID: 8862300]
24 **Horowitz M**, Maddox AF, Wishart JM, Harding PE, Chatterton BE, Shearman DJ. Relationships between oesophageal transit and solid and liquid gastric emptying in diabetes mellitus. *Eur J Nucl Med* 1991; **18**: 229-234 [PMID: 2070801]
25 **Piha SJ**. Cardiovascular autonomic reflex tests: normal responses and age-related reference values. *Clin Physiol* 1991; **11**: 277-290 [PMID: 1893685]
26 **Gentilcore D**, Bryant B, Wishart JM, Morris HA, Horowitz M, Jones KL. Acarbose attenuates the hypotensive response to sucrose and slows gastric emptying in the elderly. *Am J Med* 2005; **118**: 1289 [PMID: 16271921 DOI: 10.1016/j.amjmed.2005.05.019]
27 **Alberti KG**, Zimmet PZ. Definition, diagnosis and classification of diabetes mellitus and its complications. Part 1: diagnosis and classification of diabetes mellitus provisional report of a WHO consultation. *Diabet Med* 1998; **15**: 539-553 [PMID: 9686693]
28 **Ewing DJ**, Clarke BF. Diagnosis and management of diabetic autonomic neuropathy. *Br Med J* (Clin Res Ed) 1982; **285**: 916-918 [PMID: 6811067]
29 **Freeman R**, Wieling W, Axelrod FB, Benditt DG, Benarroch E, Biaggioni I, Cheshire WP, Chelimsky T, Cortelli P, Gibbons CH, Goldstein DS, Hainsworth R, Hilz MJ, Jacob G, Kaufmann H, Jordan J, Lipsitz LA, Levine BD, Low PA, Mathias C, Raj SR, Robertson D, Sandroni P, Schatz IJ, Schondorf R, Stewart JM, van Dijk JG. Consensus statement on the definition of orthostatic hypotension, neurally mediated syncope and the postural tachycardia syndrome. *Auton Neurosci* 2011; **161**: 46-48 [PMID: 21393070 DOI: 10.1016/j.autneu.2011.02.004]
30 **Phillips LK**, Rayner CK, Jones KL, Horowitz M. Measurement of gastric emptying in diabetes. *J Diabetes Complications* 2014; **28**: 894-903 [PMID: 25047170 DOI: 10.1016/j.jdiacomp.2014.06.005]
31 **Hardoff R**, Sula M, Tamir A, Soil A, Front A, Badarna S, Honigman S, Giladi N. Gastric emptying time and gastric motility in patients with Parkinson's disease. *Mov Disord* 2001; **16**: 1041-1047 [PMID: 11748735]
32 **Kohara K**, Jiang Y, Igase M, Takata Y, Fukuoka T, Okura T, Kitami Y, Hiwada K. Postprandial hypotension is associated with asymptomatic cerebrovascular damage in essential hypertensive patients. *Hypertension* 1999; **33**: 565-568 [PMID: 9931166]
33 **Masuo K**, Mikami H, Habara N, Ogihara T. Orthostatic and postprandial blood pressure reduction in patients with essential hypertension. *Clin Exp Pharmacol Physiol* 1991; **18**: 155-161 [PMID: 2054958]
34 **Kooner JS**, Raimbach S, Watson L, Bannister R, Peart S, Mathias CJ. Relationship between splanchnic vasodilation and postprandial hypotension in patients with primary autonomic failure. *J Hypertens Suppl* 1989; **7**: S40-S41 [PMID: 2632742]
35 **Nauck MA**, Niedereichholz U, Ettler R, Holst JJ, Orskov C, Ritzel R, Schmiegel WH. Glucagon-like peptide 1 inhibition of gastric emptying outweighs its insulinotropic effects in healthy humans. *Am J Physiol* 1997; **273**: E981-E988 [PMID: 9374685]

P- Reviewer: Marin T **S- Editor**: Ma YJ **L- Editor**: A
E- Editor: Ma S

World Journal of Gastroenterology

Submit a Manuscript: http://www.wjgnet.com/esps/
Help Desk: http://www.wjgnet.com/esps/helpdesk.aspx
DOI: 10.3748/wjg.v22.i20.4868

World J Gastroenterol 2016 May 28; 22(20): 4868-4880
ISSN 1007-9327 (print) ISSN 2219-2840 (online)

ORIGINAL ARTICLE

Basic Study

Wortmannin influences hypoxia-inducible factor-1 alpha expression and glycolysis in esophageal carcinoma cells

Ling Zeng, Hai-Yun Zhou, Na-Na Tang, Wei-Feng Zhang, Gui-Jun He, Bo Hao, Ya-Dong Feng, Hong Zhu

Ling Zeng, Hai-Yun Zhou, Na-Na Tang, Wei-Feng Zhang, Gui-Jun He, Bo Hao, Ya-Dong Feng, Hong Zhu, Department of Gastroenterology, The First Affiliated Hospital of Nanjing Medical University, Nanjing 210029, Jiangsu Province, China

Author contributions: Zhu H designed the research; Tang NN, Zhang WF and He GJ performed the research; Hao B, Feng YD and Zhu H analyzed the data; Zeng L and Zhou HY wrote the paper.

Supported by the National Natural Science Foundation of China, No. 30800511.

Institutional review board statement: The study was reviewed and approved by The First Affiliated Hospital of Nanjing Medical University Institutional Review Board.

Conflict-of-interest statement: To the best of our knowledge, no conflict of interest exists.

Data sharing statement: Technical appendix, statistical code, and dataset available from the corresponding author at zhuhong1059@126.com. Participants gave informed consent for data sharing. No additional data are available.

Correspondence to: Hong Zhu, MD, PhD, Department of Gastroenterology, The First Affiliated Hospital of Nanjing Medical University, No. 300 Guang Zhou Road, Gulou District, Nanjing 210029, Jiangsu Province, China. zhuhong1059@126.com
Telephone: +86-25-86862684
Fax: +86-25-86862684

Received: October 10, 2015
Peer-review started: October 12, 2015
First decision: March 7, 2016
Revised: March 20, 2016
Accepted: April 15, 2016
Article in press: April 15, 2016
Published online: May 28, 2016

Abstract

AIM: To investigate the influence of phosphatidylinositol-3-kinase protein kinase B (PI3K/AKT)-HIF-1α signaling pathway on glycolysis in esophageal carcinoma cells under hypoxia.

METHODS: Esophageal carcinoma cell lines Eca109 and TE13 were cultured under hypoxia environment, and the protein, mRNA and activity levels of hypoxia inducible factor-1 alpha (HIF-1α), glucose transporter 1, hexokinase-Ⅱ, phosphofructokinase 2 and lactate dehydrogenase-A were determined. Supernatant lactic acid concentrations were also detected. The PI3K/AKT signaling pathway was then inhibited with wortmannin, and the effects of hypoxia on the expression or activities of HIF-1α, associated glycolytic enzymes and lactic acid concentrations were observed. Esophageal carcinoma cells were then transfected with interference plasmid with HIF-1α-targeting siRNA to assess impact of the high expression of HIF-1α on glycolysis.

RESULTS: HIF-1α is highly expressed in the esophageal carcinoma cell lines tested, and with decreasing levels of oxygen, the expression of HIF-1α and the associated glycolytic enzymes and the extracellular lactic acid concentration were enhanced in the esophageal carcinoma cell lines Eca109 and TE13. In both normoxia and hypoxic conditions, the level of glycolytic enzymes

and the secretion of lactic acid were both reduced by wortmannin. The expression and activities of glycolytic enzymes and the lactic acid concentration in cells were reduced by inhibiting HIF-1α, especially the decreasing level of glycolysis was significant under hypoxic conditions.

CONCLUSION: The PI3K/AKT pathway and HIF-1α are both involved in the process of glycolysis in esophageal cancer cells.

Key words: Hypoxia-inducible factor-1 alpha; Hypoxia; Glycolysis; Esophageal neoplasms; Cell metabolism

Core tip: Fluorescence analysis, spectrophotometry, real-time PCR, Western blot and siRNA interference technology were used to investigate the influence of phosphatidylinositol-3-kinase protein kinase B-HIF-1α signaling pathway on glycolysis under hypoxia in esophageal carcinoma cells. The results obtained provide experimental evidence for the mechanism of glycolysis enhanced by hypoxia.

Zeng L, Zhou HY, Tang NN, Zhang WF, He GJ, Hao B, Feng YD, Zhu H. Wortmannin influences hypoxia-inducible factor-1 alpha expression and glycolysis in esophageal carcinoma cells. *World J Gastroenterol* 2016; 22(20): 4868-4880 Available from: URL: http://www.wjgnet.com/1007-9327/full/v22/i20/4868.htm DOI: http://dx.doi.org/10.3748/wjg.v22.i20.4868

INTRODUCTION

Esophageal cancer, as one of the most common malignant tumors in China with a poor prognosis, is characterized by fast invasion and early metastasis with chemotherapy and radiotherapy tolerance. Previous studies have confirmed that tumor hypoxia is an important factor leading to radiotherapy and chemotherapy resistance and that it promotes tumor invasion and metastasis and affects cell energy metabolism[1,2]. Tumor cells always prefer aerobic glycolysis metabolism to obtain energy, and this preference was named Warburg effect[3]. It enhances the ability of tumor cells to metabolize glucose to provide energy sources for their rapid proliferation and growth as well as help with their hypoxia tolerance. Synergies between tumor tissue hypoxia and the Warburg effect may play an important role in the promotion of tumor metastasis and resistance to chemotherapy.

Hypoxia-inducible factor-1 alpha (HIF-1α) is known as a key regulatory factor of tissue adaptation under hypoxia. It is highly expressed in most tumors and metastases and is inseparable from the glycolytic pathway of tumor cells[4]. The PI3K/AKT signaling pathway widely exists in cells, and it is involved in cell growth, proliferation, differentiation and regulatory signal transduction pathways. The pathway is also one of the most closely regulated pathways in cancer cells influencing glucose metabolism, in addition to its participation in the regulation of HIF-1α expression[5-7]. Therefore, we hypothesized that the PI3K/AKT pathway and HIF-1α may play a key role in the synergistic effect of hypoxia and the Warburg effect.

MATERIALS AND METHODS

Materials

Human esophageal carcinoma cell lines TE13 and Eca109 were purchased from the Shanghai Institute of Biochemistry and Cell Biology (Shanghai, China). Interference plasmid with HIF-1α-targeting siRNA was manufactured by the Kejira Corporation (Shanghai, China). Competent *E. coli* TOP10 cells were bought from the Bordi Corporation (Nanjing, China). The antibodies for HIF-1α, AKT, glucose transporter-1 (GLUT-1), lactate dehydrogenase-A (LDHA) and the secondary antibodies were obtained from Santa Cruz Biotechnology. The antibodies for HK-Ⅱ and p-AKT were obtained from Cell Signaling Technology. The GAPDH antibody was purchased from Bioworld. The Takara reverse transcription kit, the SYBR Green quantitative PCR kit, TRIzol and all the primers were obtained from the Shanghai to Betting Biotechnology Co., Ltd. A hypoxic incubator was purchased from Sanyo.

Cell lines

Esophageal carcinoma cell lines TE13 and Eca109 (2×10^5 cells/well) maintained in DMEM with 10% fetal bovine serum were covered with serum-free medium when the cells grew to 60% confluency and starved for 24 h. Three groups of adherent cells in the logarithmic growth phase were placed into the hypoxia incubator (5% CO_2, 1% O_2 and 94% N_2), and the cells were incubated for 6 h, 12 h, 24 h and 48 h. A corresponding blank control was also set up.

Cell transfection and colony selection

Two pairs of HIF-1α-siRNA oligonucleotide fragments were designed and synthesized according to the human HIF-1α gene sequence (GenBank No. NM001530). The sequences were 5′-GATCCCGAGGAAGAACTATGAACATAATTCAAGAGATTATGTTCATAGTTCTTCCTCTTTTTGGAT-3′ (sense strand) and 5′-AGCTATCCAAAAAGAGGAAGAACTATGAACATAATCTCTTGAATTATGTTCATAGTTCTTCCTCGG-3′ (antisense strand) for sequence one, and 5′-GATCCCGACTGATGACCAGCAACTTGATTCAAGAGATCAAGTTGCTGGTCATCAGTCTTTTTGGAT-3′ (sense strand) and 5′-AGCTATCCAAAAAGACTGATGACCAGCAACTTGATCTCTTGAATCAAGTTGCTGGTCATCAGTCGG-3′ (antisense strand) for sequence two.

To construct a plasmid on the basis of the pGCsi vector manual, TOP10 cells were amplified and agarose gel electrophoresis was performed to acquire the plasmids, which were named pGCsi-HIF-1 and pGCsi-HIF-2. They were routinely used to transfect the cell lines Eca109 and TE13. The cell transfection efficiencies were determined based on the green fluorescence as detected by fluorescence microscopy, and finally, the pGCsi-HIF-1 plasmid was selected as the follow-up interference plasmid. The plasmid pGCsi-HIF-1 and its negative control plasmids were transfected. The cell clones were batched and picked after four weeks. The results of RT-PCR and Western blot were combined. The plasmid pGCsi-HIF-1 and corresponding negative control plasmids were named TE13/shRNA, TE13/Neo, Eca109/shRNA and Eca109/Neo.

Drug effectiveness

Wortmannin at an experimental concentration of 2 μmol/L was incubated with the cells in a hypoxia incubator (1% O_2) for 12 h and the control group was cultured for the same time under normoxia.

Western blot analysis

Western blot analysis was performed to detect the protein expression of HIF-1α and the associated glycolysis genes. The proteins were conventionally extracted, transferred to membranes and incubated. The corresponding primary antibody concentrations were as follows: HIF-1α (1:500), HK-Ⅱ (1:1000), GLUT-1 (1:200), LDHA (1:200) and β-actin (1:4000). The secondary antibodies conjugated with HRP were goat anti-mouse (1:4000), goat anti-rabbit (1:4000) and rabbit anti-goat (1:5000). The signal was developed using ECL chemiluminescence.

Quantitative real-time PCR

To extract and purify the total RNA, TRIzol-blue reagent was used to extract the cells pretreated in each group according to the instructions of the TRIzol Kit. Then, 1 μg of total RNA was reverse transcribed with the RevertAid™ First Strand cDNA Synthesis Kit. The mRNA levels were determined by qRT-PCR using the Bio-Rad MJ Mini Opticon.

Activities of enzymes

The cells (5×10^5 cells/well) were washed twice in PBS and 500 μL of PBA was added after trypsin digestion. Sonication and centrifugation (10000 r/min) for 10 min were used to acquire the supernatant, and then the activities of LDH and HK were detected by colorimetry according to the kit instructions.

Spectrophotometry

Spectrophotometry was performed to detect the concentration of lactic acid in the supernatant of the nutrient solution.

Statistical analysis

Statistical analyses were performed using SPSS 18.0 software. Gray value analysis was performed with Tanon Gis software, and the ratio of the target band to the internal reference band represented the protein expression levels of the target gene. The differences in the expression of HIF-1α and the associated glycolytic enzymes, the activities of HK and LDH and the lactic acid concentration among the multiple groups were analyzed using an *F* test, and indicators between the two groups were compared using Student's *t*-test or *t*-test. $P < 0.05$ was considered statistically significant.

RESULTS

Influence of oxygen concentration on the protein levels of HIF-1α and the associated glycolytic enzymes in esophageal cancer cells

Under hypoxic condition (1% O_2), the protein expression of HIF-1α in esophageal carcinoma cell lines increased gradually with time. After 12 h of hypoxia, its expression peaked and then maintained a high level. Then, it began to decrease after 48 h. The protein expression of GLUT-1 and HK-Ⅱ also elevated gradually after incubation under hypoxic conditions and reached its peak at a time between 12 and 24 h, whereas the protein change of LDHA did not follow a similar trend (Figure 1).

Influence of oxygen concentration on the lactic acid concentration in the supernatant of esophageal carcinoma cells

The lactic acid concentration in the supernatant of the cells increased in an upward trend with lower oxygen concentrations. When the culture time for the esophageal carcinoma cell lines (TE13 and Eca109) under hypoxia was extended for 6-48 h, the lactic acid concentration peaked at 12 h and was then maintained at that level or decreased slightly (Figure 2).

Effect of wortmannin on the mRNA expression of glycolytic enzymes in esophageal carcinoma cells

mRNA expression: Compared with a normoxic environment, the mRNA expression of HIF-1α and HK-Ⅱ under hypoxic conditions increased significantly in the esophageal carcinoma cell lines Eca109 and TE13. In both normoxic and hypoxic conditions, the mRNA expression of the enzymes in the group pretreated with wortmannin decreased slightly compared with that in the group without pretreatment ($P < 0.05$), but the differences among each group for GLUT-1 and LDHA at the mRNA level were not significant ($P > 0.05$) (Figure 3).

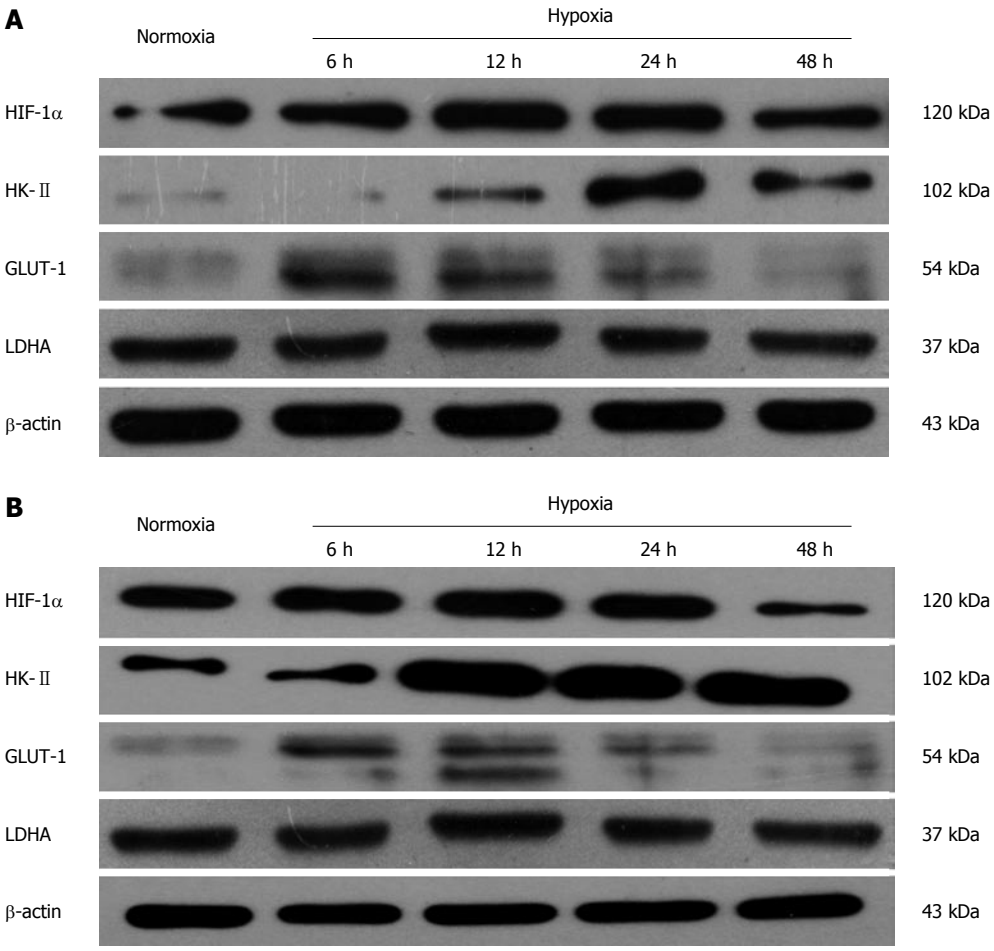

Figure 1 Expression of hypoxia inducible factor-1 alpha and glycolysis enzymes at different time points of hypoxia in Eca109 cells (A) or in TE13 cells (B). HIF-1α: Hypoxia inducible factor-1 alpha; HK-Ⅱ: Hexokinase Ⅱ; GLUT-1: Glucose transporter-1; LDHA: Lactate dehydrogenase-A.

Protein expression: Compared with groups not pretreated with wortmannin, the protein expression of HIF-1α in the pretreated esophageal carcinoma cell lines Eca109 and TE13 incubated under normoxic and hypoxic conditions was inhibited markedly ($P < 0.05$), and the protein expression of the hypoxic group was higher than that of the normoxic group ($P < 0.01$). Because the expression of HIF-1α was repressed most when a culture time of 12 h was used, we chose that time for the subsequent experiments.

The protein expression of HK-Ⅱ and GLUT-1 under normoxia or hypoxia in the groups pretreated with wortmannin was significantly reduced compared with those groups not pretreated ($P < 0.05$ between each of the groups). In the condition of hypoxia, the protein expression of LDHA among each group increased compared with the normal oxygen environment ($P < 0.05$). However, the difference between the group pretreated with wortmannin and the group not pretreated was not statistically significant ($P > 0.05$) (Figure 4).

Enzyme activities and lactic acid concentration

By detecting the activities of LDH and HK-Ⅱ in the esophageal carcinoma cell lines Eca109 and TE13 incubated for 12 h under normoxia and hypoxia, we found that the activities of LDH and HK in the groups pretreated with wortmannin all obviously declined compared with those in the group without pretreatment ($P < 0.05$) (Figure 5A). In the normoxic and hypoxic environments, the lactic acid concentrations in the pretreated group decreased markedly compared with those in the group without pretreatment ($P < 0.05$) (Figure 5B).

Impact on the mRNA expression of glycolytic enzymes after inhibiting the expression of HIF-1α in esophageal carcinoma cells

mRNA expression: Compared with the esophageal carcinoma cells of the untransfected group and the empty vector group, the mRNA expression of GLUT-1 and HK-Ⅱ in the Eca109/siRNA group obviously decreased ($P < 0.05$) (Figure 6). However, the decline in the mRNA expression of LDHA was too small to be significant. The expression of the associated genes in the untransfected group and the empty vector group under hypoxia were enhanced slightly, and the difference was considered statistically significant ($P < 0.05$).

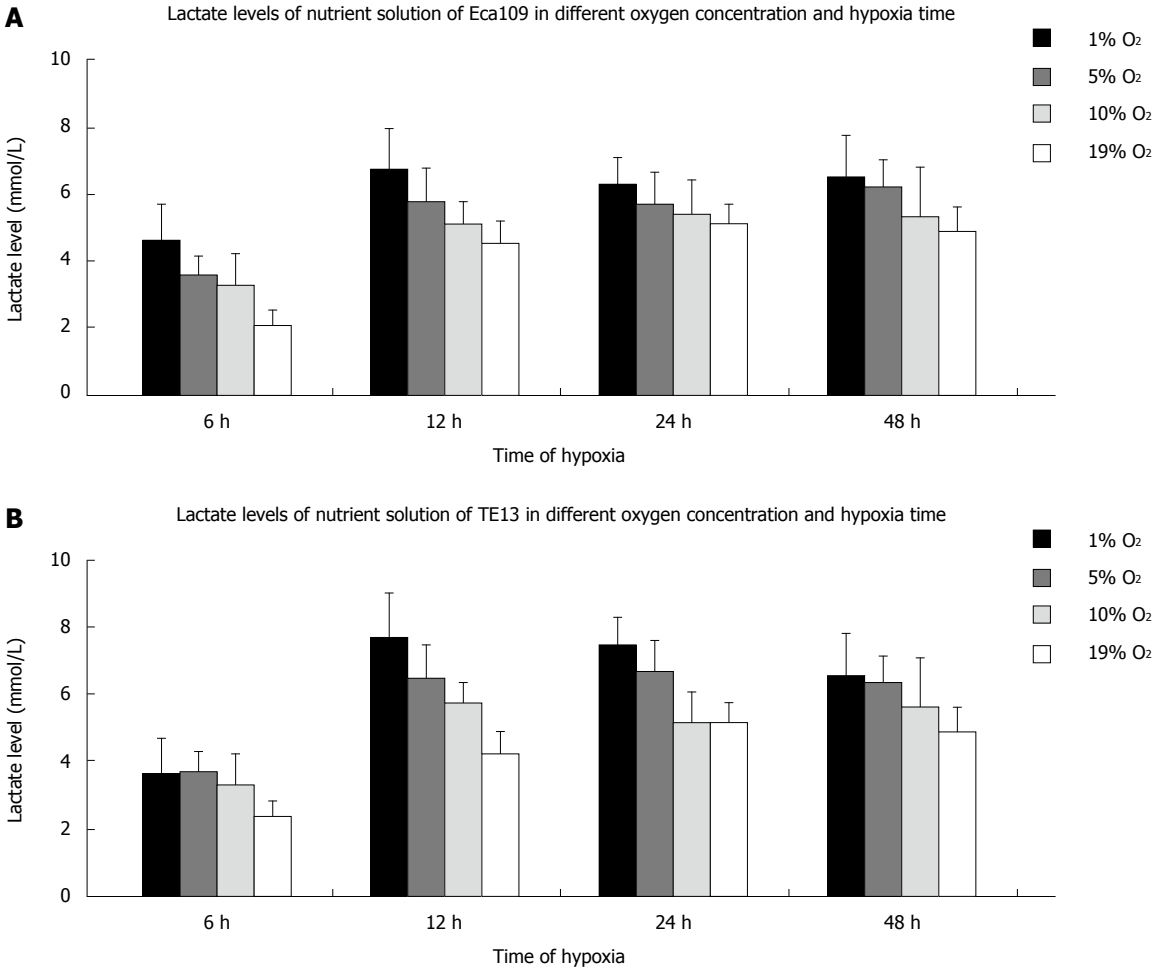

Figure 2 Lactic levels in culture medium of Eca109 cells (A) or TE13 cells (B) in different oxygen environments and at different time points as revealed by photocolorimetric method.

Protein expression: Compared with the TE13 and Eca109 groups, the protein expression of HIF-1α in the TE13/siRNA and Eca109/siRNA groups were clearly reduced, and hypoxia could not correct this phenomenon. Regardless of the oxygen concentration used for culturing, the expression of GLUT-1 and HK-Ⅱ at the protein level in the TE13/siRNA and Eca109/siRNA groups was obviously weaker than that in the control group ($P < 0.05$). However, the expression of LDHA in the group of TE13 and Eca109 under hypoxia was up-regulated significantly compared with that of the normal oxygen group ($P < 0.05$), but mildly declined after inhibiting HIF-1α compared to the cells that were not silenced. The results were not statistically significant ($P > 0.05$) (Figure 7).

Enzymatic activities and lactic acid concentration

The activities of LDH and HK-Ⅱ under normoxia or hypoxia in the Eca109/siRNA and TE13/siRNA groups obviously decreased compared with those of the untransfected and empty vector groups ($P < 0.05$), and the activities of the enzymes under hypoxia increased slightly in the untransfected and empty vector groups ($P > 0.05$) (Figure 8). Moreover, compared with the untransfected group in the normoxia and hypoxia environments, the lactic acid concentrations in the Eca109/siRNA and TE13/siRNA groups were clearly reduced ($P < 0.05$) (Table 1).

DISCUSSION

Hypoxia is one of the basic characteristics of solid tumor microenvironments. On one hand, hypoxia results from the increase in oxygen consumption caused by the rapid proliferation of malignant tumors. On the other hand, the abnormality of the vascular structure and function of tumors leads to a decrease in the blood and oxygen supply, which could also be an important factor further adding to the risk of hypoxia in tumors[8-10]. When tumor size is greater than 1 mm^3, there were a considerable number of tumor cells in a hypoxic state. Hypoxia in tumors is not only the consequence of pathophysiology but also an important initiating factor of malignant transformation and even metastasis in the development of tumors. Research has confirmed that hypoxia can promote oncogenes to produce functionally acquired mutations to cause high expression of the gene itself. It has also been found

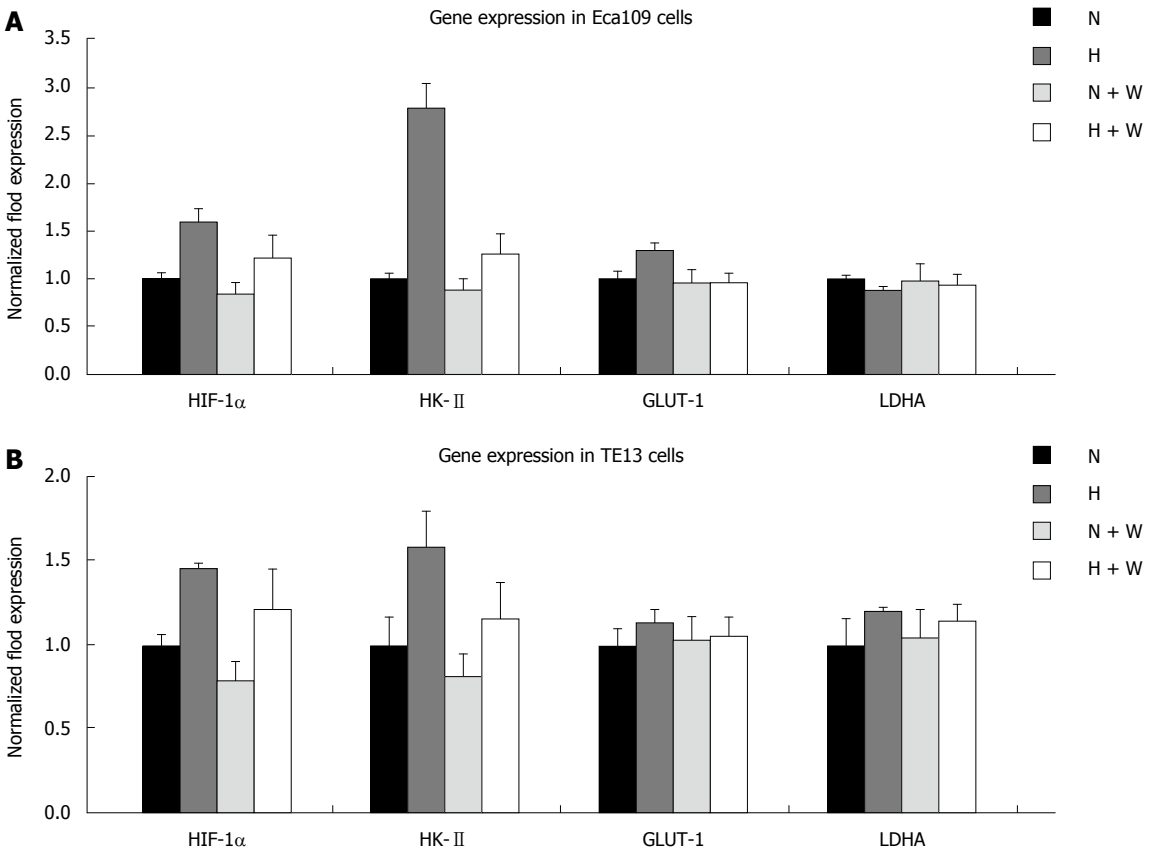

Figure 3 Quantitative real-time PCR analysis of the gene expression of hypoxia inducible factor-1 alpha and glycolysis (*n* = 3). HIF-1α: Hypoxia inducible factor-1 alpha; HK-Ⅱ: Hexokinase Ⅱ; GLUT-1: Glucose transporter-1; LDHA: Lactate dehydrogenase-A.

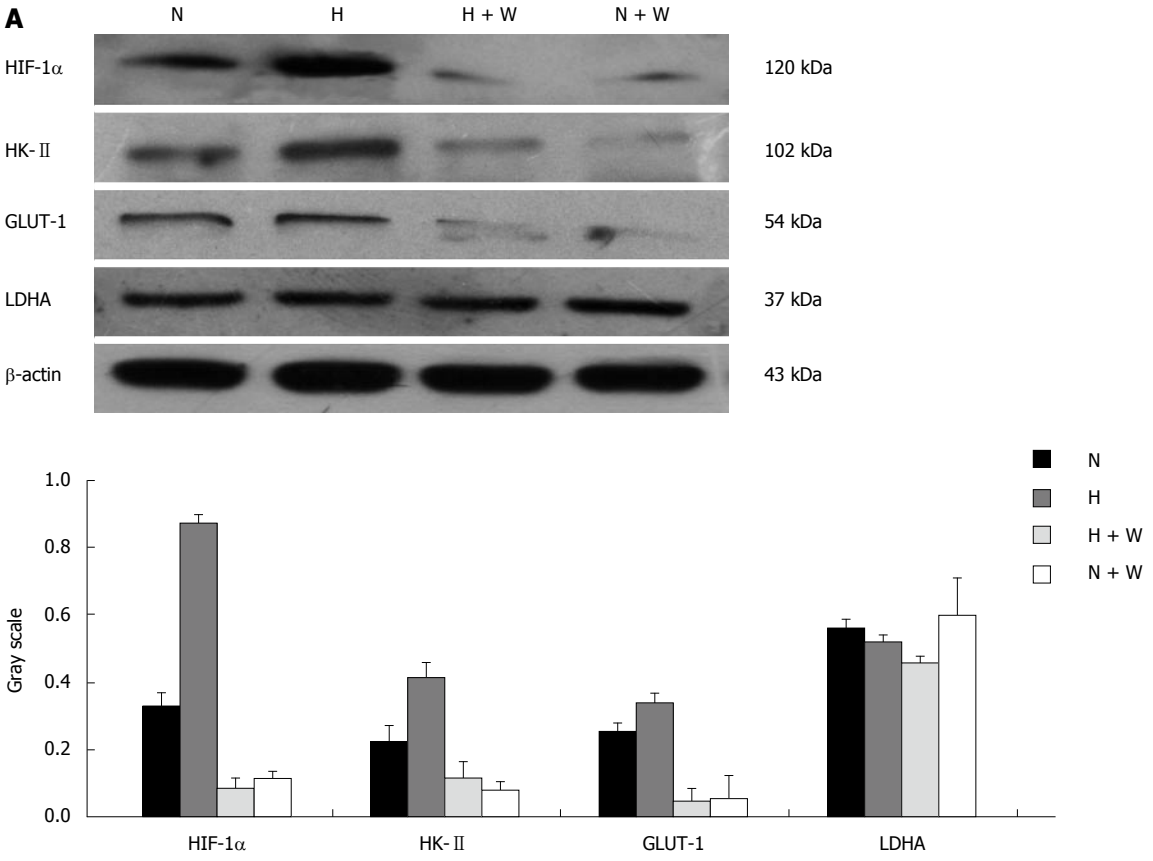

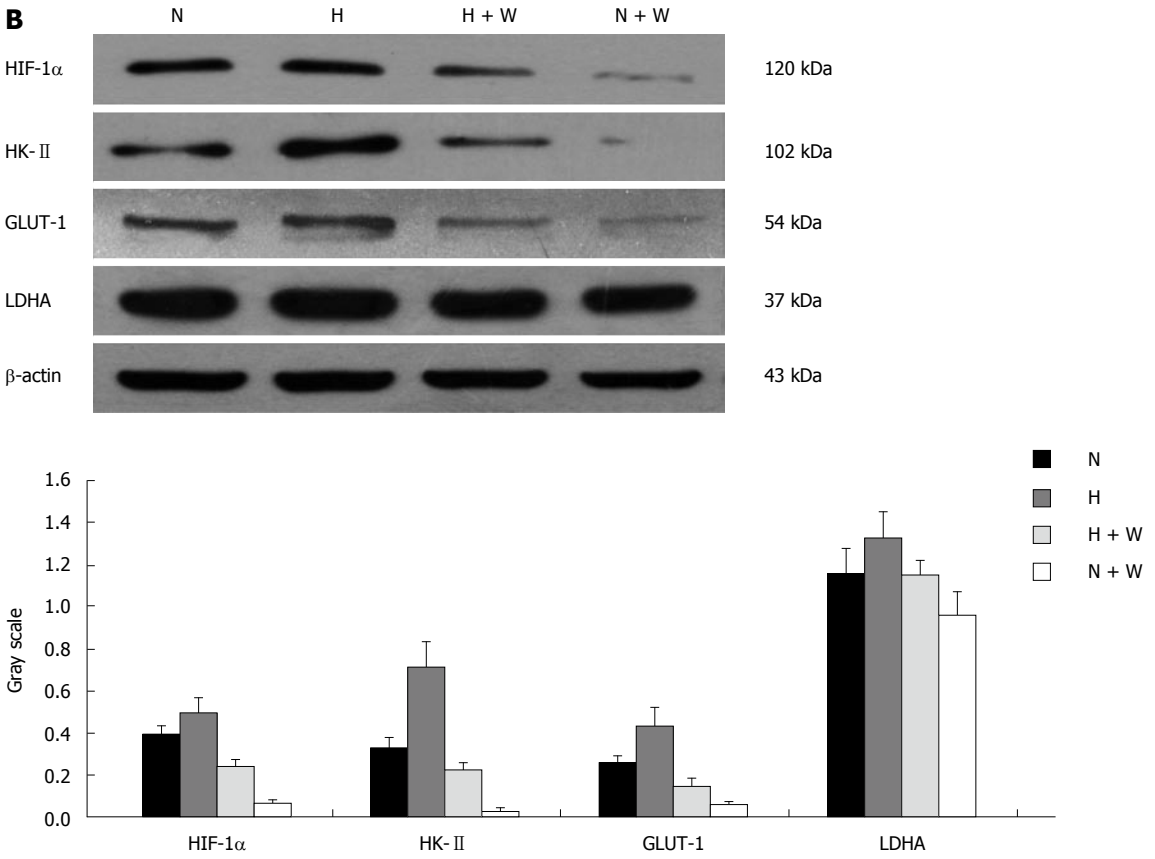

Figure 4 Effect of wortmannin on hypoxia inducible factor-1 alpha and glycolysis protein in Eca109 cells (*n* = 3) (A) and in TE13 cells (B) (*n* = 3). HIF-1α: Hypoxia inducible factor-1 alpha; HIF-1α: Hypoxia inducible factor-1 alpha; HK-Ⅱ: Hexokinase Ⅱ; GLUT-1: Glucose transporter-1; LDHA: Lactate dehydrogenase-A.

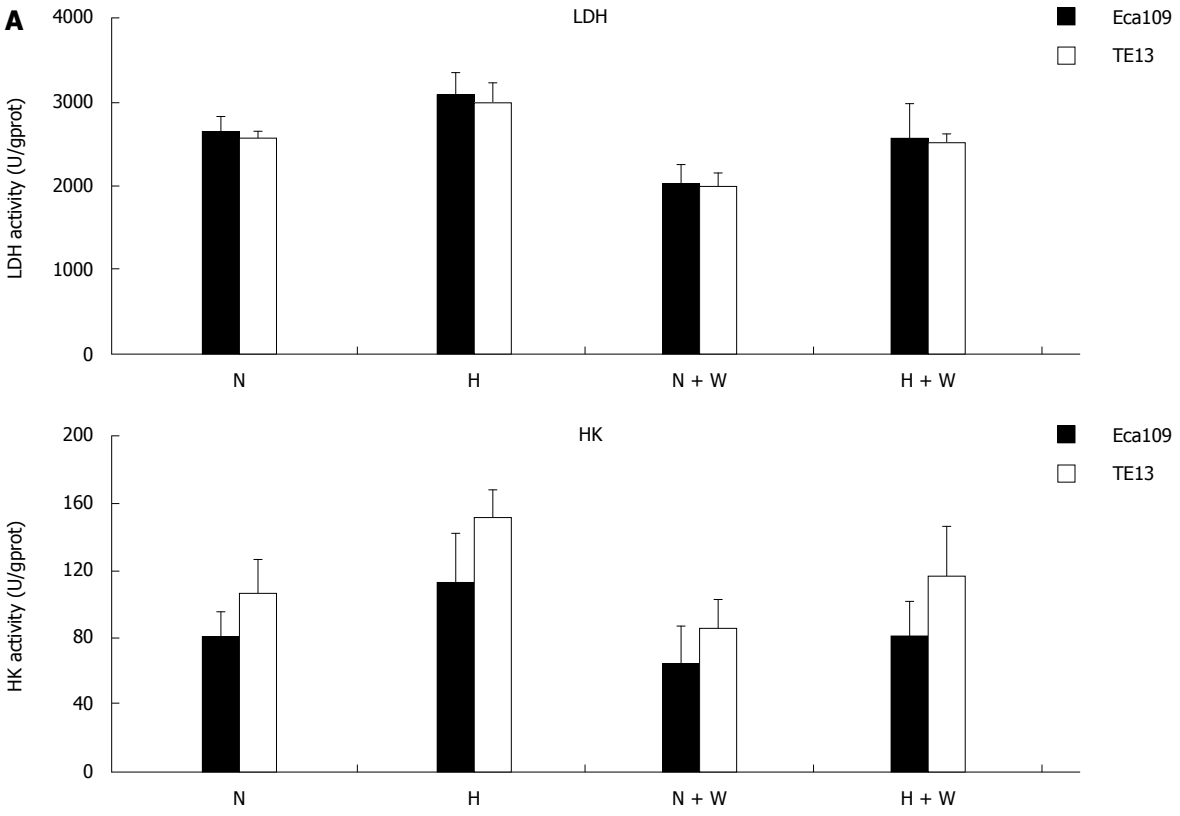

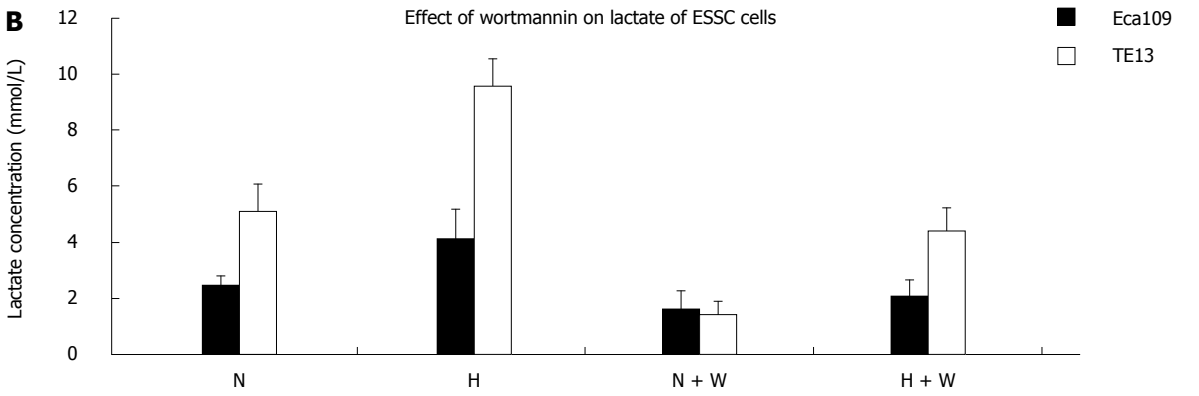

Figure 5 Spectrophotometry analysis of the activities of lactate dehydrogenase and hexokinase (*n* = 3) (A) or the supernatant lactic acid concentration in nutrient solution (*n* = 3) (B). HK: Hexokinase; LDH: Lactate dehydrogenase.

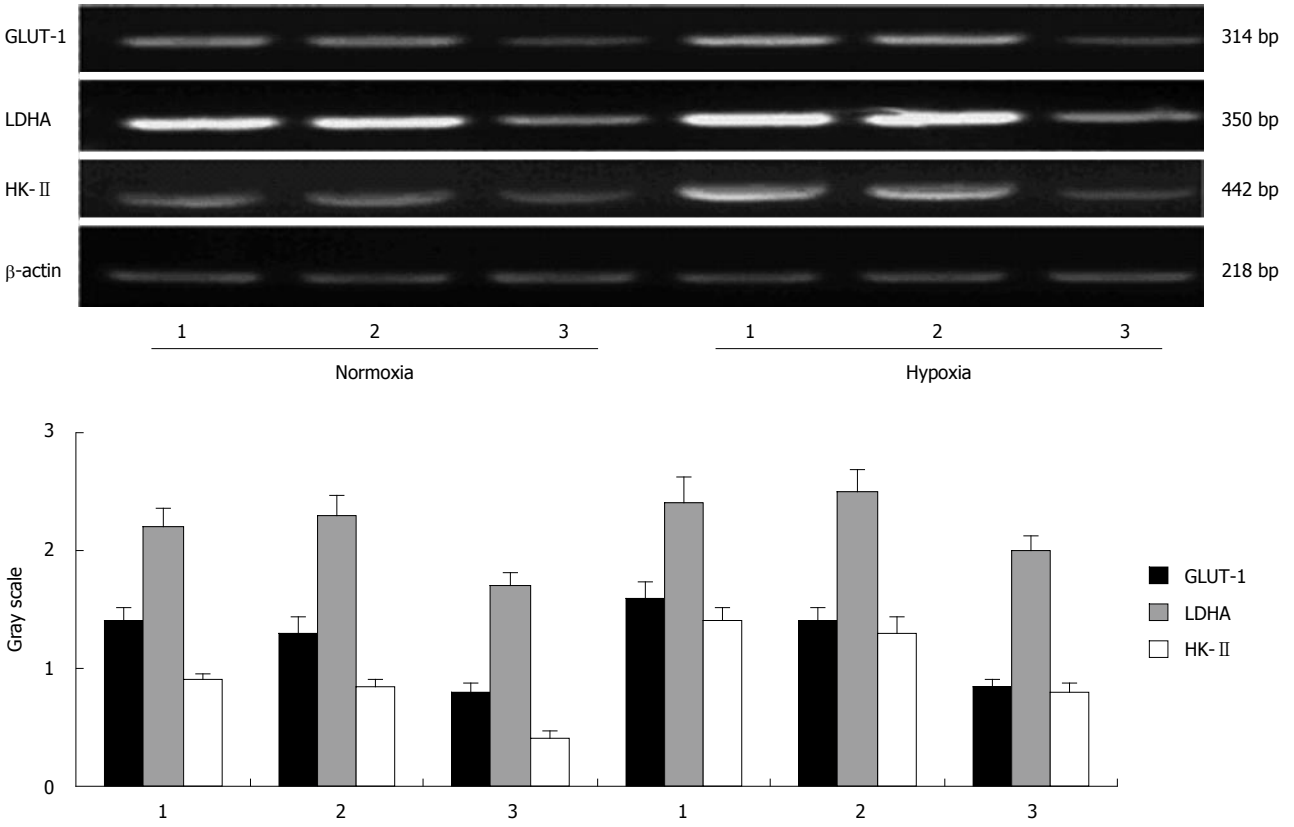

Figure 6 mRNA expression of glycolysis enzymes after hypoxia inducible factor-1 alpha inhibition (*n* = 3). 1: Eca109; 2: Eca109/neo; 3: Eca109/siRNA. HIF-1α: Hypoxia inducible factor-1 alpha; HK-Ⅱ: Hexokinase Ⅱ; GLUT-1: Glucose transporter-1; LDHA: Lactate dehydrogenase-A.

that the corresponding proteins, apart from the tumor suppressor genes, have functionally lacking mutations that down-regulate the expression of genes or weaken the activities of products. In addition, hypoxia can also promote the functionally lacking mutations of the gene associated with DNA repair to improve the mutation frequency of oncogenes and tumor suppressor genes; thus, it is involved in malignant transformations in tumor genesis[11,12]. Furthermore, hypoxia participates in the processes of invasion, metastasis, angiogenesis, immune evasion, and radiotherapy and chemotherapy resistance to affect prognosis[13,14]. Most normal tissues always use aerobic oxidation for energy metabolism in an anaerobic environment, and the glycolytic pathway started to mobilize only when the oxygen supply was insufficient. However, tumor cells prefer glycolysis to gain energy to meet their needs, regardless of the oxygen condition, which is known as the Warburg effect[3]. It is more convenient for tumor cells to gain energy for metabolism and survive under hypoxic conditions, which helps in the acquisition of hypoxia tolerance. The radiotherapy and chemotherapy resistance caused by low metabolic rates during hypoxia helps some tumor cells survive, which could be a source of tumor recurrence[15].

HIF-1 is a transcription factor that widely exists in

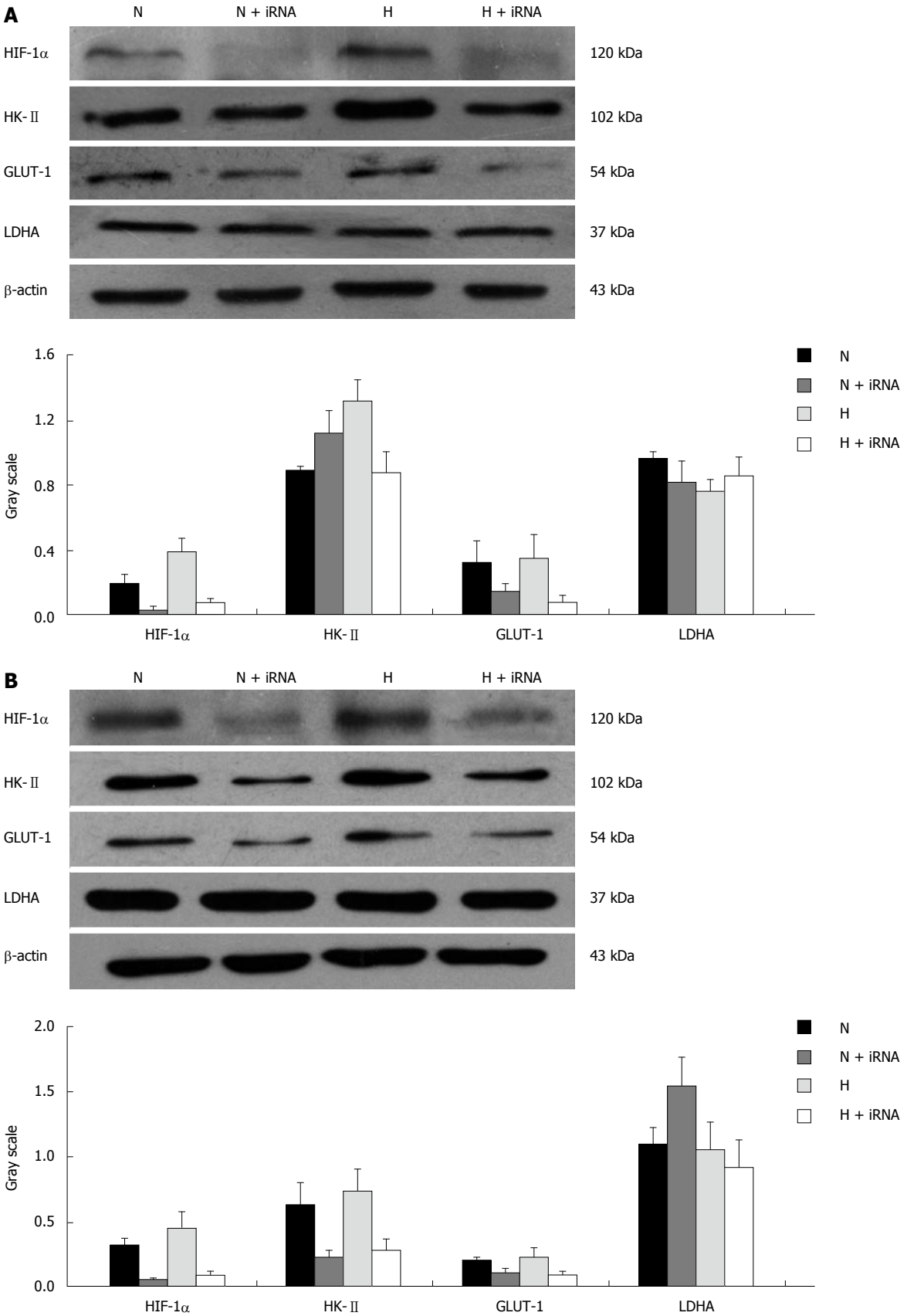

Figure 7 Protein expression of glycolysis enzymes. A: In Eca109 cells after HIF-1α inhibition (n = 3). N: Eca109 + 19% O_2; N + iRNA: Eca109/siRNA + 19% O_2; H: Eca109 + 1% O_2; H + iRNA: Eca109/siRNA + 1% O_2. B: In TE13 cells after HIF-1α inhibition (n = 3). N: TE13 + 19% O_2; N + iRNA: TE13/siRNA + 19% O_2; H: TE13 + 1% O_2; H + iRNA: TE13/siRNA + 1% O_2. HIF-1α: Hypoxia inducible factor-1 alpha; HK-Ⅱ: Hexokinase Ⅱ; GLUT-1: Glucose transporter-1; LDHA: Lactate dehydrogenase-A.

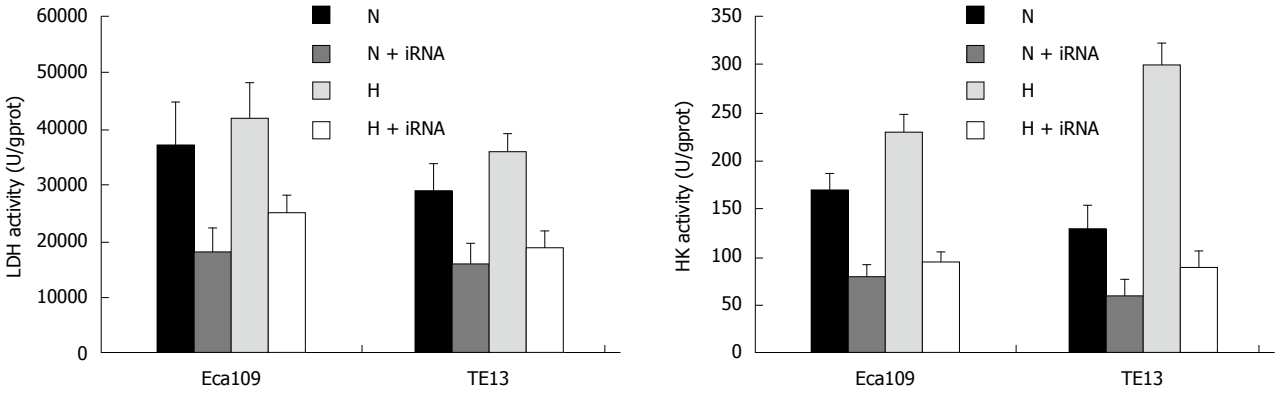

Figure 8 Western blot analysis of the activities of glycolysis enzymes after hypoxia inducible factor-1 alpha inhibition. HIF-1α: Hypoxia inducible factor-1 alpha; HK-Ⅱ: Hexokinase Ⅱ; GLUT-1: Glucose transporter-1; LDHA: Lactate dehydrogenase-A.

Table 1 The changes of supernatant lactic acid concentrations after restraining the expression of hypoxia inducible factor-1 alpha (n = 3)

	TE13		Eca109	
	TE13	TE13/siRNA	Eca109	Eca109/siRNA
A (19% O_2)	3.333 ± 0.833	1.933 ± 0.569[c]	4.867 ± 0.551	1.367 ± 0.346[c]
B (1% O_2)	6.433 ± 1.059[a]	1.567 ± 0.416	8.067 ± 1.160[a]	1.767 ± 1.242[a]

[a]$P < 0.05$, *vs* group A; [c]$P < 0.05$, *vs* non-interference group.

mammals and humans under hypoxic conditions and is a key player in the body's ability to adapt to hypoxia by promoting the expression of hypoxia-induced genes to elicit the specific response to hypoxia of tissues. HIF-1 consisted of HIF-1α and HIF-1β subunits. HIF-1α is not only peculiar to HIF-1 but also the oxygen regulator unit. The hypoxia-inducible genes regulated by HIF are involved in angiogenesis, erythropoiesis, energy metabolism, apoptosis, proliferation and other cellular processes. Previous studies have found that the related glycolytic genes regulated by HIF-1 include the GLUT-1, lactate dehydrogenase A (LDHA), phosphofructokinase 2 (PFK2), aldolase A, enolase 1, phosphoglycerate kinase 1 and glyceraldehyde-3-phosphate dehydrogenase coding genes. HIF-1 induced the expression of the above genes to enhance glycolysis to meet the needs of energy metabolism when the process of oxidative phosphorylation was inhibited by the condition of hypoxia[16-18].

The role of external hypoxia in initiating glycolysis and promoting its progression in tumor cells was previously uncertain. Past studies have investigated breast cancer cell lines MDA-mb-4 and MCF-7, which are highly and lowly malignant, respectively, cultured under normal oxygen conditions and found that the expression of HIF-1α and glycolytic enzymes and the level of glycolysis in MDA-mb-4 were greater in strength than those of MCF-7. Moreover, it is interesting that compared with the expression in normoxic environments, the expression of the genes in the breast cancer cell line MCF-7 under hypoxia was markedly elevated. However, there was no obvious change in MDA-mb-435, which suggested that the enhanced glycolysis in tumor cells was not caused by a single factor and that the environment and other factors were also involved in the process[19]. Renal carcinoma cell line RCC4, which has high expression of HIF-1α, was chosen for study because of its lack of the Von Hippel-Lindau gene (*vH-L* gene), which resulted in the blocked degradation of HIF-1α. In contrast with the level of glycolysis in normoxia and hypoxia conditions, no significant differences between these two conditions were found, but the level of glycolysis under normoxic conditions obviously decreased and increased clearly under hypoxic condition after restoring the regulatory ability of HIF-1α through the transfection of the *vH-L* gene in the RCC4 cell line[20]. It prompted the idea that the added HIF-1α protein accumulated or abnormally induced in cells might be the main factor in the regulatory process of glycolysis in tumor cells, and blocking HIF-1α might be an effective means of suppressing the glycolytic pathway in tumor cells.

Research has shown that most tumor tissues and their metastases have high expression of HIF-1α, and this is closely related to the glycolytic pathway of tumor cells[4]. We also confirmed the high expression of HIF-1α in esophageal cancer tissues in our previous studies[21,22]. To define the influence of hypoxia on the glycolytic level of esophageal carcinoma cells, we observed the changes in the expression of HIF-1α, the associated glycolytic proteins, such as GLUT-1, HK-Ⅱ, and LDHA, and the lactic acid content under different oxygen concentrations. The results showed that the expression of the proteins and the lactic acid concentration changed obviously under hypoxic conditions, and this suggests that the external oxygen concentration plays a regulatory role in glycolysis of esophageal carcinoma cells. Although there was a high glycolysis level under normal oxygen pressure in esophageal tumors, the glycolytic level could be further enhanced with a decrease in the external oxygen concentration. The enhanced glycolysis caused by hypoxia and the change in the genetic signaling

pathways by itself both evolved to the advantages of the Warburg effect. However, experiments also showed that HIF-1α and the associated glycolytic proteins, such as GLUT-1, HK-Ⅱ and LDHA, had a certain correlation in the enhanced process of glycolysis induced by hypoxia and played an important role in the pathophysiological mechanisms of promoting glycolysis, which was found to be enhanced in esophageal carcinoma cells. In addition to the involvement of glucose transport and glycolysis, the relevant proteins of glycolysis in tumor cells also included the glycolysis products, such as carbonic anhydrase (CA) and monocarboxylate transporters (MCTs). Studies have already confirmed that the *CAIX* and *MCT4* gene promoter sequences are the binding sites for HIF-1α, which can promote the transmembrane transport of lactic acid and hydrogen ions by enhancing the expression and activity of CAIX and MCT4 and ensure the smooth progress of glycolysis[23-26]. This finding suggests that HIF-1α, as a key factor in the process of regulating tumor glycolysis, may be involved in the enhanced glycolysis process of tumor cells through glucose transport, glycolysis activation and lactic acid transport.

To further confirm the impact of the high expression of HIF-1α on the process of glycolysis in esophageal tumors, we inhibited HIF-1α successfully in the cell lines Eca109 and TE13 using siRNA interference technology to observe the changes in the lactic acid concentration and the expression of the related glycolytic enzymes in the extracellular nutrient solution under different oxygen concentrations. The results showed that the mRNA and protein expression of GLUT-1 and HK-Ⅱ was down-regulated, and the lactic acid secretion reduced significantly, which was consistent with the trends found when HIF-1α was restrained, and compared with the control group under hypoxia, the expression was still at a low level, although the expression increased mildly when cultured under hypoxia. Thus, we speculate that the regulation of HIF-1α in the glycolysis of esophageal carcinomas depends on the activation of its downstream glycolytic enzymes. However, it is worth noting that the protein expression of LDHA changed slightly when HIF-1α was inhibited, and it also suggests that the regulation of LDHA was not only confined within the role of HIF-1α. When integrated with the literature, the regulation of glucose metabolism in tumors should be the consequence of a combination of multiple factors and multi-links with hypoxia. It also may be that HIF-1α is in a prominent position in the regulatory process, but not all of the glycolysis in esophageal cancers results from this single factor.

The PI3K/AKT signaling pathway is currently attracting much attention in cancer research, and it has been found that PI3K/AKT signaling is disordered in most human tumors and has been closely associated with proliferation, apoptosis, angiogenesis, invasion, metastasis, chemotherapy and radiotherapy resistance. The pathway plays an important role in adapting to the hypoxia environment and participates in the regulation of the HIF-1α singling pathway. A previous study reported that epidermal growth factor (EGF), fibroblast growth factor 2 and insulin-like growth factor 1 could induce the protein expression of HIF-1α by activating the PI3K/AKT signaling pathway and the corresponding tyrosine kinase receptors under normal oxygen pressure[7]. The mechanism of hypoxia tolerance activated by the PI3K/AKT pathway is widespread in mammalian cells, where HIF-1α exerts a critical intermediary role[27].

Based on the speculation that the PI3K/AKT signaling pathway might affect glycolysis in esophageal cancer cells, wortmannin, a specific ATP uncompetitive irreversible inhibitor of PI3K, with a half inhibitory concentration of 0.004 microns, was first extracted from the fungus *Penicillium wortmannin* in 1957. This compound was used to block the PI3K/AKT signaling pathway in the cell lines Eca109 and TE13. Wortmannin binds to PI3K gamma and causes the irreversible modification of lysine 833, while is the active site of PI3K[28]. Wortmannin at high concentrations also had different inhibitory effects on the PIKK family, such as mTOR, DNA-PK, ATM and ATR[29,30]. The results confirmed that the glycolytic level in esophageal cancer cells declined once the PI3K pathway was inhibited, regardless of whether the external oxygen supply was sufficient or not, and it was accompanied by a decrease in the expression of HIF-1α and the associated glycolytic proteins. This was not corrected effectively by culturing under hypoxia. Moreover, we found that the influence of wortmannin on the protein expression of the enzymes of glycolysis was different; the protein expression of GLUT-1 was down-regulated, whereas the mRNA expression did not change much by using wortmannin, which suggests that the regulatory effect of wortmannin on GLUT-1 might act at the protein level. In addition, the results also showed that the activities of HK-Ⅱ and LDH in cells and the secretion of lactic acid were restrained by adding wortmannin, and it could be elevated at different levels after treatment with hypoxia. Therefore, we surmise that the impact of the PI3K/AKT signaling pathway on glycolysis in esophageal tumors involves multiple steps and many factors, including the expression of key protein factors and the regulation of activities of different glycolytic enzymes. This suggests that the PI3K/AKT signaling pathway is involved into the process of glycolysis in esophageal carcinoma.

In summary, the level of glycolysis in esophageal carcinomas could be affected by hypoxic environment and is closely associated with the expression of HIF-1α. The PI3K/AKT pathway and HIF-1α are both involved in glycolysis in esophageal cancer cells, and LDHA, HK-Ⅱ and GLUT-1 might cause downstream effects. The regulation of glycolysis under hypoxic conditions could be achieved by activating the PI3K/AKT pathway through EGF and HIF-1α, and the ex-

pression level of glycolysis decreased markedly when the PI3K/AKT pathway was inhibited, which may be of potential therapeutic value in the future. This study will contribute to an effective treatment strategy for tumor cells under hypoxic environments and provide strong evidence and new thoughts on the diagnosis and treatment of cancers. It also provides direction on the development of new antitumor drugs and thus gives more reasonable and individualized therapeutic schedules to cancer patients in the clinic.

COMMENTS

Background

Esophageal cancer is the sixth leading cause of cancer-related death in China. Although recent developments in therapeutic strategies have helped cure many patients with early-stage disease, the prognosis of patients with advanced disease and metastasis remains poor.

Research frontiers

Tumor hypoxia is an important factor leading to radiotherapy and chemotherapy resistance and promotes tumor invasion and metastasis. It also involves cell energy metabolism. Hypoxia-inducible factor-1 alpha (HIF-1α) is a key regulatory factor of tissue adaptation under hypoxia and is highly expressed in most tumors and metastases. It is also inseparable from the glycolytic pathway of tumor cells. The PI3K/AKT signaling pathway widely exists in cells and is involved in cell growth, proliferation, differentiation and regulatory signal transduction pathways. It is also one of the most closely regulatory pathways of the glucose metabolism of cancer cells besides participating in the regulation of HIF-1α expression.

Innovations and breakthroughs

The authors investigated the signaling pathway of glycolysis from the perspective of hypoxia tolerance in esophageal tumor cells based on HIF-1α and analyzed multiple related glycolytic genes through the PI3K/AKT-HIF-1α pathway to obtain more information regarding the molecular regulatory mechanism of esophageal cancers.

Applications

The findings of this study indicated that the PI3K/AKT pathway and HIF-1α are both involved in the process of glycolysis in esophageal cancer cells, and the regulation of glycolysis in the hypoxia condition could be achieved by activating the PI3K/AKT pathway through EGF and HIF-1α. The expression level of glycolytic enzymes decreased markedly when the PI3K/AKT pathway was inhibited.

Terminology

The study adopted mature and reliable laboratory methods, such as fluorescence analysis, spectrophotometry, real time PCR, Western blot and siRNA interference technology.

Peer-review

Poor prognosis of esophageal cancer is a well-known fact and early diagnosis of this disease is so important. This is a well-written paper.

REFERENCES

1 **Li Y**, Fu L, Li JB, Qin Y, Zeng TT, Zhou J, Zeng ZL, Chen J, Cao TT, Ban X, Qian C, Cai Z, Xie D, Huang P, Guan XY. Increased expression of EIF5A2, via hypoxia or gene amplification, contributes to metastasis and angiogenesis of esophageal squamous cell carcinoma. *Gastroenterology* 2014; **146**: 1701-1713.e9 [PMID: 24561231 DOI: 10.1053/j.gastro.2014.02.029]

2 **Bayer C**, Vaupel P. Acute versus chronic hypoxia in tumors: Controversial data concerning time frames and biological consequences. *Strahlenther Onkol* 2012; **188**: 616-627 [PMID: 22454045 DOI: 10.1007/s00066-012-0085-4]

3 **Warburg O**. On the origin of cancer cells. *Science* 1956; **123**: 309-314 [PMID: 13298683 DOI: 10.1126/science.123.3191.309]

4 **Lum JJ**, Bui T, Gruber M, Gordan JD, DeBerardinis RJ, Covello KL, Simon MC, Thompson CB. The transcription factor HIF-1alpha plays a critical role in the growth factor-dependent regulation of both aerobic and anaerobic glycolysis. *Genes Dev* 2007; **21**: 1037-1049 [PMID: 17437992]

5 **Luo J**, Manning BD, Cantley LC. Targeting the PI3K-Akt pathway in human cancer: rationale and promise. *Cancer Cell* 2003; **4**: 257-262 [PMID: 14585353 DOI: 10.1016/s-1535-6108(03)00248-4]

6 **Xia S**, Yu SY, Yuan XL, Xu SP. [Effects of hypoxia on expression of P-glycoprotein and multidrug resistance protein in human lung adenocarcinoma A549 cell line]. *Zhonghua Yi Xue Zazhi* 2004; **84**: 663-666 [PMID: 15130309]

7 **Shi YH**, Wang YX, Bingle L, Gong LH, Heng WJ, Li Y, Fang WG. In vitro study of HIF-1 activation and VEGF release by bFGF in the T47D breast cancer cell line under normoxic conditions: involvement of PI-3K/Akt and MEK1/ERK pathways. *J Pathol* 2005; **205**: 530-536 [PMID: 15714461 DOI: 10.1002/path.1734]

8 **Sutherland RM**. Tumor hypoxia and gene expression--implications for malignant progression and therapy. *Acta Oncol* 1998; **37**: 567-574 [PMID: 9860315]

9 **Carmeliet P**, Jain RK. Angiogenesis in cancer and other diseases. *Nature* 2000; **407**: 249-257 [DOI: 10.1038/35025220]

10 **Dachs GU**, Tozer GM. Hypoxia modulated gene expression: angiogenesis, metastasis and therapeutic exploitation. *Eur J Cancer* 2000; **36**: 1649-1660 [PMID: 10959051]

11 **Wykoff CC**, Beasley NJ, Watson PH, Turner KJ, Pastorek J, Sibtain A, Wilson GD, Turley H, Talks KL, Maxwell PH, Pugh CW, Ratcliffe PJ, Harris AL. Hypoxia-inducible expression of tumor-associated carbonic anhydrases. *Cancer Res* 2000; **60**: 7075-7083 [PMID: 11156414]

12 **Meiron M**, Anunu R, Scheinman EJ, Hashmueli S, Levi BZ. New isoforms of VEGF are translated from alternative initiation CUG codons located in its 5'UTR. *Biochem Biophys Res Commun* 2001; **282**: 1053-1060 [PMID: 11352659]

13 **Bertout JA**, Patel SA, Simon MC. The impact of O2 availability on human cancer. *Nat Rev Cancer* 2008; **8**: 967-975 [PMID: 18987634 DOI: 10.1038/nrc2540]

14 **Semenza GL**. Molecular mechanisms mediating metastasis of hypoxic breast cancer cells. *Trends Mol Med* 2012; **18**: 534-543 [PMID: 22921864 DOI: 10.1016/j.molmed.2012.08.001]

15 **Biaglow JE**, Cerniglia G, Tuttle S, Bakanauskas V, Stevens C, McKenna G. Effect of oncogene transformation of rat embryo cells on cellular oxygen consumption and glycolysis. *Biochem Biophys Res Commun* 1997; **235**: 739-742 [PMID: 9207231]

16 **Yu ZT**, Zhao HF, Shang XB. [Expression of hypoxia-inducible factor-1alpha and vessel endothelial growth factor in esophageal squamous cell carcinoma and clinico-pathological significance thereof]. *Zhonghua Yi Xue Zazhi* 2008; **88**: 2465-2469 [PMID: 19080625]

17 **Elson DA**, Ryan HE, Snow JW, Johnson R, Arbeit JM. Coordinate up-regulation of hypoxia inducible factor (HIF)-1alpha and HIF-1 target genes during multi-stage epidermal carcinogenesis and wound healing. *Cancer Res* 2000; **60**: 6189-6195 [PMID: 11085544]

18 **Ashrafian H**. Cancer's sweet tooth: the Janus effect of glucose metabolism in tumorigenesis. *Lancet* 2006; **367**: 618-621 [PMID: 16488806]

19 **Robey IF**, Lien AD, Welsh SJ, Baggett BK, Gillies RJ. Hypoxia-inducible factor-1alpha and the glycolytic phenotype in tumors. *Neoplasia* 2005; **7**: 324-330 [PMID: 15967109 DOI: 10.1593/neo.04430]

20 **Semenza GL**. HIF-1 mediates the Warburg effect in clear cell renal carcinoma. *J Bioenerg Biomembr* 2007; **39**: 231-234 [PMID: 17551816]

21 **Du YP**, Shi RH, Xiao B, Zhu H. Expression and significance of hypoxia-inducible factor-1 alpha in esophageal squamous cancer

cell line EC-109. *World Chinese Journal of Digestology* 2006; **14**: 1247-1251

22 **Jing SW**, Wang YD, Kuroda M, Su JW, Sun GG, Liu Q, Cheng YJ, Yang CR. HIF-1α contributes to hypoxia-induced invasion and metastasis of esophageal carcinoma via inhibiting E-cadherin and promoting MMP-2 expression. *Acta Med Okayama* 2012; **66**: 399-407 [PMID: 23093058]

23 **Kwon JE**, Jung WH, Koo JS. Expression of glycolysis-related proteins in solid papillary carcinoma of the breast according to basement membrane status. *Yonsei Med J* 2014; **55**: 576-583 [PMID: 24719122 DOI: 10.3349/ymj.2014.55.3.576]

24 **Ullah MS**, Davies AJ, Halestrap AP. The plasma membrane lactate transporter MCT4, but not MCT1, is up-regulated by hypoxia through a HIF-1alpha-dependent mechanism. *J Biol Chem* 2006; **281**: 9030-9037 [PMID: 16452478]

25 **Rosafio K**, Pellerin L. Oxygen tension controls the expression of the monocarboxylate transporter MCT4 in cultured mouse cortical astrocytes via a hypoxia-inducible factor-1α-mediated transcriptional regulation. *Glia* 2014; **62**: 477-490 [PMID: 24375723 DOI: 10.1002/glia.22618]

26 **Jamali S**, Klier M, Ames S, Barros LF, McKenna R, Deitmer JW, Becker HM. Hypoxia-induced carbonic anhydrase IX facilitates lactate flux in human breast cancer cells by non-catalytic function. *Sci Rep* 2015; **5**: 13605 [PMID: 26337752 DOI: 10.1038/srep13605]

27 **Kitajima Y**, Miyazaki K. The Critical Impact of HIF-1a on Gastric Cancer Biology. *Cancers* (Basel) 2013; **5**: 15-26 [PMID: 24216696 DOI: 10.3390/cancers5010015]

28 **Walker EH**, Pacold ME, Perisic O, Stephens L, Hawkins PT, Wymann MP, Williams RL. Structural determinants of phosphoinositide 3-kinase inhibition by wortmannin, LY294002, quercetin, myricetin, and staurosporine. *Mol Cell* 2000; **6**: 909-919 [PMID: 11090628]

29 **Brunn GJ**, Williams J, Sabers C, Wiederrecht G, Lawrence JC, Abraham RT. Direct inhibition of the signaling functions of the mammalian target of rapamycin by the phosphoinositide 3-kinase inhibitors, wortmannin and LY294002. *EMBO J* 1996; **15**: 5256-5267 [PMID: 8895571]

30 **Sarkaria JN**, Tibbetts RS, Busby EC, Kennedy AP, Hill DE, Abraham RT. Inhibition of phosphoinositide 3-kinase related kinases by the radiosensitizing agent wortmannin. *Cancer Res* 1998; **58**: 4375-4382 [PMID: 9766667]

P- Reviewer: Dinc T, Inamori M **S- Editor**: Ma YJ
L- Editor: Wang TQ **E- Editor**: Ma S

World Journal of Gastroenterology

Submit a Manuscript: http://www.wjgnet.com/esps/
Help Desk: http://www.wjgnet.com/esps/helpdesk.aspx
DOI: 10.3748/wjg.v22.i20.4881

World J Gastroenterol 2016 May 28; 22(20): 4881-4890
ISSN 1007-9327 (print) ISSN 2219-2840 (online)

ORIGINAL ARTICLE

Basic Study

miR-29a up-regulation in AR42J cells contributes to apoptosis *via* targeting *TNFRSF1A* gene

Qiang Fu, Tao Qin, Lin Chen, Chuan-Jiang Liu, Xu Zhang, Yu-Zhu Wang, Ming-Xing Hu, Hao-Yuan Chu, Hong-Wei Zhang

Qiang Fu, Tao Qin, Lin Chen, Chuan-Jiang Liu, Xu Zhang, Yu-Zhu Wang, Ming-Xing Hu, Hao-Yuan Chu, Hong-Wei Zhang, Department of Hepatobiliary Pancreatic Surgery, People's Hospital of Zhengzhou University, School of Medicine, Zhengzhou University, Zhengzhou 450003, Henan Province, China

Author contributions: Fu Q and Chen L performed the majority of experiments; Qin T and Zhang HW designed the research and provided financial support for this work; Liu CJ conducted the experimental analysis; Wang YZ and Hu MX provided vital reagents and were involved in editing the manuscript; Zhang X and Chu HY analyzed sequencing data and developed analysis tools; Fu Q, Qin T and Chen L wrote the paper.

Institutional review board statement: This study was reviewed and approved by the Ethics Committee of People's Hospital of Zhengzhou University.

Institutional animal care and use committee statement: All procedures involving animals were reviewed and approved by the Ethics Committee of People's Hospital of Zhengzhou University.

Conflict-of-interest statement: We declare that we have no financial and personal relationships with other people or organizations that can inappropriately influence our work, and there is no professional or other personal interest of any nature or kind in any products, service and/ or company that could be construed as influencing the position presented in, or the review of, the manuscript entitled "miR-29a up-regulation in the AR42J cells contributes to apoptosis via targeting the TNFRSF1A gene".

Data sharing statement: No additional data are available.

Correspondence to: Hong-Wei Zhang, MD, PhD, Professor, Chief, Department of Hepatobiliary Pancreatic Surgery, People's Hospital of Zhengzhou University, School of Medicine, Zhengzhou University, No. 7 Weiwu Road, Zhengzhou 450003, Henan Province, China. hwzhang666@126.com
Telephone: +86-371-65580368
Fax: +86-371-65580368

Received: January 8, 2016
Peer-review started: January 9, 2016
First decision: February 18, 2016
Revised: February 29, 2016
Accepted: March 18, 2016
Article in press: March 18, 2016
Published online: May 28, 2016

Abstract

AIM: To investigate the expression of miR-29a in rat acute pancreatitis and its functional role in AR42J cell apoptosis.

METHODS: Twelve SD rats were divided into a control group and an acute edematous pancreatitis (AEP) group randomly. AEP was induced by intraperitoneal injection of L-arginine (150 mg/kg) in the AEP group and equal volume of 0.9% NaCl was injected in the control group. The apoptosis of acinar cells in pancreatic tissue was determined by TUNEL assay. miRNA chip assay was performed to examine the expression of miRNAs in two groups. Besides, to further explore the role of miR-29a in apoptosis *in vitro*, recombinant rat TNF-α (50 ng/mL) was administered to treat the rat pancreatic acinar cell line AR42J for inducing AR42J cell apoptosis. Quantitative real-time PCR (qRT-PCR) was adopted to measure miR-29a expression. Then, miRNA mimic, miRNA antisense oligonucleotide (AMO) and control vector were used to transfect AR42J cells. The expression of miR-29a was confirmed by qRT-PCR and

the apoptosis rate of AR42J cells was detected by flow cytometry analysis. Western blot was used to detect the expression of activated caspase3. Moreover, we used bioinformatics software and luciferase assay to test whether TNFRSF1A was the target gene of miR-29a. After transfection, qRT-PCR and Western blot was used to detect the expression of TNFRSF1A in AR42J cells after transfection.

RESULTS: The expression of miR-29a was much higher in the AEP group compared with the control group as displayed by the miRNA chip assay. After inducing apoptosis of AR42J cells *in vitro*, the expression of miR-29a was significantly increased by 1.49 ± 0.04 times in comparison with the control group. As revealed by qRT-PCR assay, the expression of miR-29a was 2.68 ± 0.56 times higher in the miR-29a mimic group relative to the control vector group, accompanied with an obviously increased acinar cell apoptosis rate (42.83 ± 1.25 *vs* 24.97 ± 0.15, $P < 0.05$). Moreover, the expression of miR-29a in the miRNA AMO group was 0.46 ± 0.05 times lower than the control vector group, and the cell apoptosis rate was much lower accordingly (17.27 ± 1.36 *vs* 24.97 ± 0.15, $P < 0.05$). The results of bioinformatics software and luciferase assay showed that TNFRSF1A might be a target gene of miR-29a. *TNFRSF1A* expression was up-regulated in the miR-29a mimic group, while the miR-29a AMO group showed the reverse trend.

CONCLUSION: miR-29a might promote the apoptosis of AR42J cells *via* up-regulating the expression of its target gene *TNFRSF1A*.

Key words: Acute edematous pancreatitis; miR-29a; Apoptosis; AR42J; Target gene; *TNFRSF1A*

Core tip: Apoptosis is a self-protection mechanism in acute pancreatitis. miRNAs are short non-coding RNAs and play important roles in regulating gene expression in multiple cellular processes, such as apoptosis. Here, our group studied the role of miR-29a in pancreatic acinar cell apoptosis. The pancreatic acinar cells showed a tendency to apoptosis when the expression of miR-29a elevated, while the apoptosis rate exhibited the opposite trend by down-regulating the expression of miR-29a. Moreover, we found TNFRSF1A, which encode TNFR1 protein, was a target gene of miR-29a. Our results demonstrated that miR-29a could promote the apoptosis of pancreatic acinar cells *via* up-regulating the expression of *TNFRSF1A* gene in acute pancreatitis.

Fu Q, Qin T, Chen L, Liu CJ, Zhang X, Wang YZ, Hu MX, Chu HY, Zhang HW. miR-29a up-regulation in AR42J cells contributes to apoptosis *via* targeting *TNFRSF1A* gene. *World J Gastroenterol* 2016; 22(20): 4881-4890 Available from: URL: http://www.wjgnet.com/1007-9327/full/v22/i20/4881.htm DOI: http://dx.doi.org/10.3748/wjg.v22.i20.4881

INTRODUCTION

Tumor necrosis factor (TNF)-α is a pleiotropic cytokine that plays a crucial role in angiogenesis, inflammation, proliferation and apoptotic cell death[1]. TNF-α is involved in the development of pancreatitis, and mediates apoptosis in acinar cell suspensions *in vitro* as well as in an *in vivo* model of pancreatitis. Pancreatic acinar cells produce, release, and respond to TNF-α[2], which acts by binding to its two receptors, TNF-R1 and TNF-R2, on the cell surface. TNF-R1, which is the major signaling receptor for TNF-α, is expressed on all cell types. Both soluble and membrane-bound forms of the cytokine can activate TNFR1. The binding of TNF to TNFR1 results in immediate nuclear factor-κB (NF-κB) activation and subsequent apoptosis[3,4].

MicroRNAs (miRNAs) are short non-coding RNAs involved in multiple cellular processes including development, proliferation, differentiation, apoptosis and metabolism[5]. Most studies on miRNAs have focused on the repression of their target genes by binding to complementary sites, causing target mRNAs degradation and/or translational repression[6-9]. In recent years, it had been demonstrated that miRNAs could up-regulate the expression of their target genes. Vasudevan *et al*[10] demonstrated that human miRNA369-3 directs association of the proteins with AREs (AU-rich elements) to activate translation, while let-7 and the synthetic miRNA miRNAcxcr4 induced upregulation of target genes. miR-29a has been extensively demonstrated to play an important role in apoptosis[11-15]. Using miRNA microarray analysis, we found that miR-29a was elevated in a rat model of AEP *in vivo*. TNFRSF1A, which encodes the TNFR1 protein, was predicted to be the target gene of miR-29a with the aid of three online programs (TargetScan, miRanda and TarBase). Our results demonstrated that miR-29a is elevated significantly in AEP *in vivo*. The rate of apoptosis and TNFRSF1A expression increased significantly in AR42J cells following upregulation of miR-29a expression.

MATERIALS AND METHODS

Animal care

All animal experiments were approved by the Animal Research Ethics Committee of People's Hospital of Zhengzhou University, Zhengzhou, China. Surgery was performed under chloral hydrate anesthesia and all efforts were made to minimize animal suffering.

In vivo AEP model

Twelve male SD rats (250-300 g) were divided into two groups randomly ($n = 6$). All rats were anesthetized with 10% chloral hydrate (300 mg/kg,

Table 1 Sequences of miR-29a mimic and antisense oligonucleotide

	Base sequence
miR-29a mimic	ACCCCTTAGAGGATGACTGATTTCTTTTGGTGTTCAGAGTCAATAGAATTTTCTAGCACCATCTGAAATCGGTTATAATGATTGGGGA
miR-29a AMO	ACTGATTTCTTTTGGTGTTCAG

i.p.). 150 mg/kg L-arginine (Sigma, United States) was injected intraperitoneally to establish the AEP model *in vivo*. The rats in the control group were injected with equivalent saline. After 12 h the pancreas of the rats was removed.

TUNEL assay

The apoptosis of acinar cells in pancreatic tissue was determined by terminal-deoxynucleotidyl-transferase-mediated dUTP nick-end labeling (TUNEL) assay by using the *in situ* cell death detection kit (Promega, China). According to the manufacturer's instructions, the tissue was fixed in 10% buffered formaldehyde, embedded in paraffin, and 4-μm sections were adhered to glass slides. After dewaxing and rehydration, the sections were incubated with TUNEL reaction mixture at 37 ℃ for 1 h. Finally, the sections were analyzed under a fluorescence microscope (Olympus, Tokyo, Japan). TUNEL-positive cells displayed brown fluorescence.

miRNA microarray

Total RNA of pancreas tissue was extracted using TRIzol. miRNA microarray analysis was applied to detect the differential expression of miRNAs in pancreas tissue between the two groups.

miR-29a mimic and antisense oligonucleotide construct

The mimic and antisense oligonucleotide of miR-29a, which were designed and synthesized chemically with the help of Genechem Bio Company (Shanghai, China), were inserted into a lentiviral vector carrying the green fluorescent protein (*GFP*) gene. The sequences of miR-29a mimic and AMO are presented in Table 1.

Cell culture and lentiviral transfection

The AR42J cell line (rat pancreatic acinar cell, Institute of Shanghai Cell Biology, Shanghai, China) was cultured in DMEM-F12 medium (Gibco, United States) containing 20% fetal bovine serum (FBS) (Gibco, United States) in a humidified incubator at 37 ℃ with an atmosphere of 5% CO_2. The AR42J cells (1×10^6 cells/well) were seeded in 6-well plates 24 h before transfection and infected at an MOI of 50 with 10 μg/mL of polybrene for 12 h. After 12 h, the transfection liquid was removed and 2 mL normal medium was added for continued culturing. Seventy-two hours after transfection, green fluorescence was observed under a fluorescence microscope.

Induction of apoptosis and amylase assay

AR42J cells at 1×10^6/well were seeded into 6-well plates. After 24 h, the medium was removed and DMEM-F12 medium containing 50 ng/mL recombinant rat TNF-α (Peprotech, United States) was added. Twelve hours later, the supernatant was collected and centrifuged at 1000 rpm for 5 min and then used to detect the level of amylase using an amylase kit (Jiancheng Bio, Nanjing, China) according to the manufacturer's instructions. The control group was incubated with DMEM-F12 medium only.

Western blot analysis

Total protein from the cultured AR42J cells was extracted with RIPA lysis buffer (150 mmol/L NaCl, 50 mmol/L Tris–HCl (pH 7.4), 1% NP-40, 1 μg/mL leupeptin, 1 mmol/L deoxycholic acid and 1 mmol/L EDTA) containing 1 mmol/L phenylmethylsulfonyl fluoride, according to the manufacturer's instructions (Beyotime Bio, Wuhan, China). Proteins (40 μg) from each sample were loaded and separated on a 12% SDS polyacrylamide gel. Proteins were then electrophoretically transferred onto PVDF membranes (Millipore, Bedford, MA, United States), which were then incubated with diluted anti-rat monoclonal activated caspase3 antibody at 1/1000 (CST, United States), anti-rat TNFR1 at 1/200 (SANTA CRUZ Bio, United States) or anti-β-actin at 1/1000 (CST, United States) at 4 ℃ overnight. On the following day, membranes were incubated with an HRP secondary antibody (1:5000) at 37 ℃ for 2 h and then signals were visualized with an electrochemiluminescence kit (Pierce, Rockford, IL, United States).

Flow cytometry analysis of apoptosis

AR42J cells were seeded into 6-well plates (5×10^5/well) and incubated with DMEM-F12 medium containing 50 ng/mL recombinant rat TNF-α for 24 h. Cells were harvested, washed twice with 1 × PBS and then stained using an annexin V-APC apoptosis kit (KeyGEN Bio, Nanjing, China) according to the manufacturer's instructions. All flow cytometric analyses were carried using a FACS Caliber flow cytometer (San Jose, CA, United States).

Target prediction

Three online programs, TargetScan (http://www.targetscan.org), miRanda (http://www.microrna.org/microrna/home.do), and TarBase (http://diana.cslab.ece.ntua.gr/tarbase), were used in combination for predicting the target genes of miR-29a.

Luciferase reporter assay

HEK 293T cells (Institute of Shanghai Cell Biology, Shanghai, China) were cultured in DMEM medium

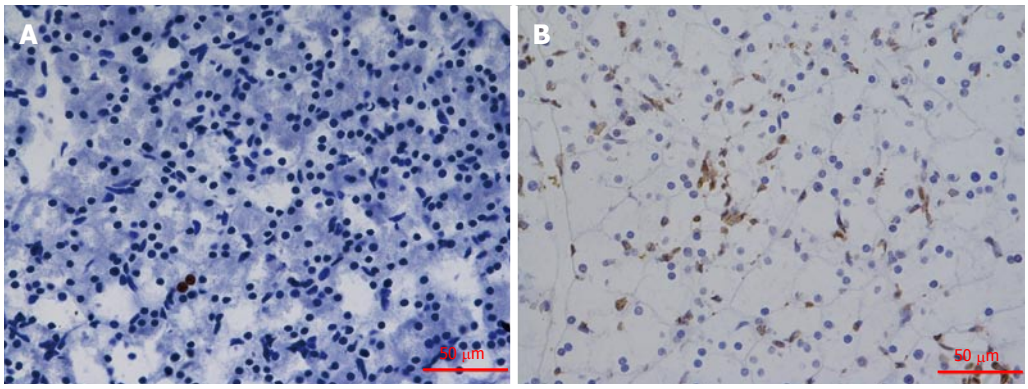

Figure 1 TUNEL staining of pancreatic tissue (× 400). TUNEL-positive cells displayed brown fluorescence. A: TUNEL staining was detected in control rats; B: The tissue of the L-arginine treated rats. The apoptosis increased significantly in Figure 1B.

(Gibco, United States) containing 10% FBS (Gibco, United States) in a humidified incubator at 37 ℃ under 5% CO_2. HEK 293T cells were seeded in 24-well plates 24 h before transfection with 100 ng psiCHECK^{TM}-2 vector (RiboBio, Guangzhou, China) containing the wild-type TNFRSF1A 3'UTR (designated TNFRSF1A 3'UTR-WT) or the TNFRSF1A mutant (designated TNFRSF1A 3'UTR -Mut) together with 50 nmol/L miR-29a miRNA mimic; a non-target control was used in the control group. Luciferase activity was measured 48 h after transfection. Lipofectamine 2000 transfection reagent (Invitrogen, United States) was used for co-transfection of RNA oligonucleotides and plasmids.

Quantitative real-time RT-PCR

Total RNA was isolated using Trizol (Invitrogen, United States) and then reverse-transcribed into cDNA with PrimeScript RT Master Mix (Takara, Japan) according to the manufacturer's instructions. Quantitative real-time PCR was performed using the SYBR Premix Ex Taq^{TM} kit (Takara, Japan). Specific primer sequences are listed as follows: 5'-GTGCTGTTGCCTCTGGTTATCT-3' (forward) and 5'-GAGACAGGATGACTGAAGCGTG-3' (reverse) for *TNFRSF1A*; 5'-TTCAACGGCACAGTCAAGG-3' (forward) and 5'-CTCAGCACCAGCATCACC-3' (reverse) for *GAPDH*. The primers for miR-29a and U6 were synthesized by Guangzhou RiboBio Co. Ltd. (China). Expression of *TNFRSF1A*, relative to *GAPDH* and expression of miR-29a, relative to U6, were determined using the $2^{-\Delta\Delta CT}$ method.

Statistical analysis

The results are expressed as mean ± SD from at least three separate experiments. Statistical analyses were performed using SPSS 13.0 software and comparisons were made using Student's *t*-test and one-way ANOVA. $P < 0.05$ was considered statistically significant.

RESULTS

TUNEL assay

Apoptosis of pancreatic acinar cells was determined by TUNEL assay (Figure 1). The results of TUNEL assays showed that the apoptosis of pancreatic acinar cells increased significantly in the L-arginine group compared with that in the control group ($P < 0.05$).

miR-29a expression in the AEP model in vivo

miRNA-microarray analysis of the miRNAs in the rat pancreas was performed to compare the expression of miRNAs between the control and AEP groups. Numerous miRNAs were significantly different in the AEP group compared with the control group (Figure 2). The expression level of miR-29a was much higher in the AEP group compared with the control group ($P < 0.01$).

AR42J cell apoptosis in vitro

As shown in Figure 3A, the level of amylase in the experimental group increased significantly compared with that in the control group at 12 h after exposure of AR42J cells to the TNF-α ($P = 0.042$). Activated caspase 3 was detected by Western blot analysis as described. Caspase 3 expression increased obviously after the AR42J cells were exposed to TNF-α for 12 h. The apoptosis rate was significantly higher (6.26-fold) in the experimental group compared with that in the control group ($P = 0.026$; Figure 3C). These results demonstrated that the AEP model was successfully established *in vitro*.

Expression of miR-29a is increased in vitro

The expression level of miR-29a was confirmed by quantitative real-time RT-PCR. As shown in Figure 4, the level of miR-29a was significantly higher (1.49-fold) in the experimental group compared with that in the control group after AR42J cells were exposed to TNF-α for 3 h ($P = 0.034$).

miR-29a expression after lentiviral transfection

The lentiviral vector carrying the miR-29a mimic or AMO was transfected into the AR42J cells as described. After 72 h, the cells were evaluated for expression of green fluorescence under a fluorescence

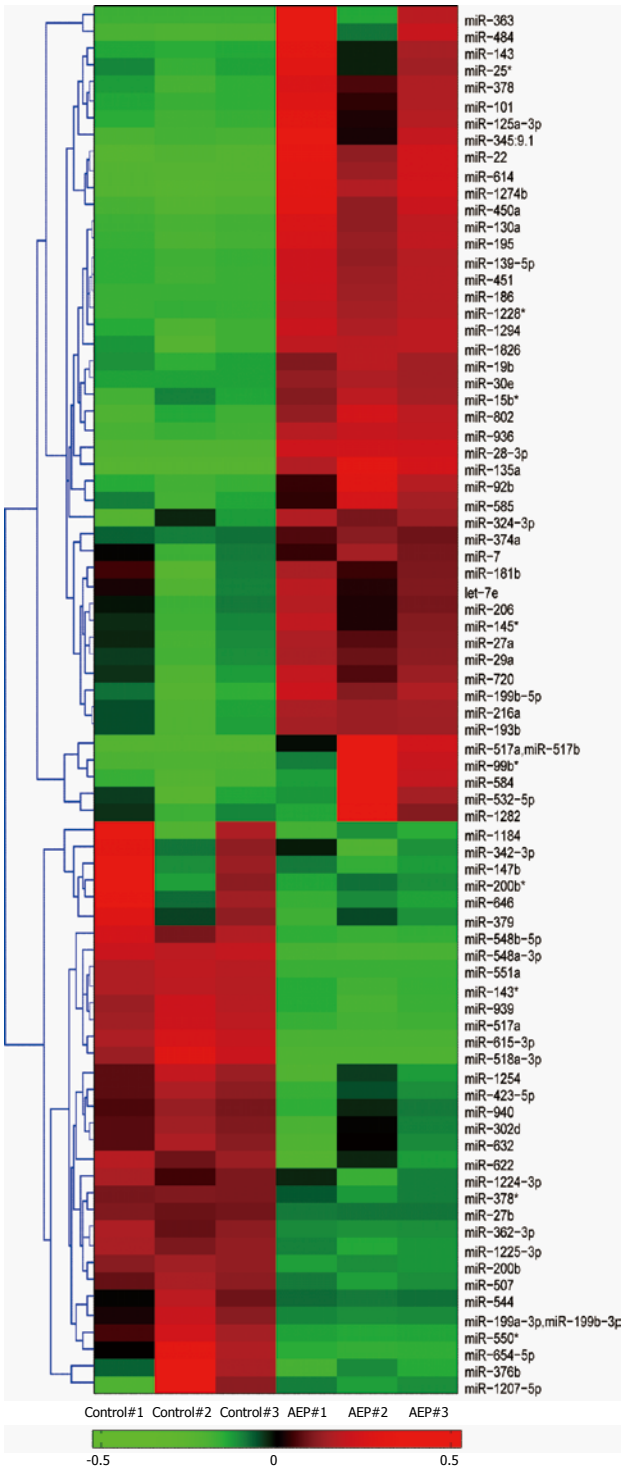

Figure 2 Hierarchically clustered heat map illustrating the changes in miRNA expression profiles between the acute edematous pancreatitis groups and control groups. The significantly expressed miRNA clusters were identified using the Student's *t*-test. The red and green sections represent an increase and a decrease in miRNA expression, respectively, between control group and AEP group. The expression of miR-29a was significantly up-regulated in the AEP group compared with the control group. AEP: Acute edematous pancreatitis.

microscope. As shown in Figure 5A, most of the AR42J cells expressed green fluorescence, which indicated that the AR42J cells were successfully transfected by the lentivirus, from which protein was successfully expressed. miR-29a expression by lentivirus-transfected AR42J cells was analyzed by qRT-PCR. Cells transfected with the miR-2a mimic expressed significantly increased miR-29a levels (P = 0.018; Figure 5B), while cells transfected with the miR-29a AMO expressed lower miR-29a levels (P = 0.020; Figure 5B) compared with the vehicle groups.

Induction of apoptosis after transfection

After lentiviral transfection, the AR42J cells were exposed to TNF-α and the level of amylase in the supernatant was detected as described, suggesting that the AEP model was established successfully (Figure 6A). To investigate the proapoptotic activity of miR-29a, we detected the rate of apoptosis and activated caspase 3 expression in AR42J cells after the AEP model was established *in vitro*. Interestingly, compared with the vehicle group, upregulation of miR-29a increased the expression of activated caspase 3, while the miR-29a AMO group showed a lower level of activated caspase 3 (Figure 6B). The apoptosis rate in the miR-29a mimic group (42.83 ± 1.25%) was significantly higher than that in the vehicle group (24.97 ± 0.15%) (P = 0.030; Figure 6C). In contrast, the apoptosis rate in the miR-29a AMO group (17.27 ± 1.36%) was significantly lower than that in the vehicle group (P = 0.025; Figure 6C).

TNFRSF1A is regulated by miR-29a

By using three online programs (TargetScan, miRanda and TarBase), we predicted that TNFRSF1A was the target gene of miR-29a. As shown in Figure 7, the 3′ UTR of *TNFRSF1A* contains a putative target site for miR-29a. To obtain direct evidence in support of this prediction, the 3′UTR of the rat TNFRSF1A gene was cloned into the *Xba* Ⅰ -site of the pGL3-luciferase reporter vector, which was then used to test its capacity to serve as the direct functional target of miR-29a; the construct was designated pGL3-TNFRSF1A-WT. In parallel, another luciferase reporter construct was prepared in which the putative miR-29a targeting region was specifically mutated and predicted to abolish miR-29a binding; this construct was designated pGL-TNFRSF1A-Mut. Transient transfection of HEK293T cells with pGL-TNFRSF1A-wt and miR-29a led to a significant decrease in luciferase activity compared to that in the control group (P = 0.0018). The activity of the mutant reporter construct, however, was unaffected by co-transfection with miR-29a (P = 0.626).

Expression of TNFRSF1A after transfection

To examine the effect of miR-29a on TNFRSF1A expression, AR42J cells were transfected with a miR-29a mimic or an AMO. TNFRSF1A mRNA levels were analyzed by qRT-PCR. As shown in Figure 8A, the expression of TNFRSF1A was significantly higher (1.86-fold) in the miR-29a mimic group compared with the vehicle group (P = 0.022), while the expression

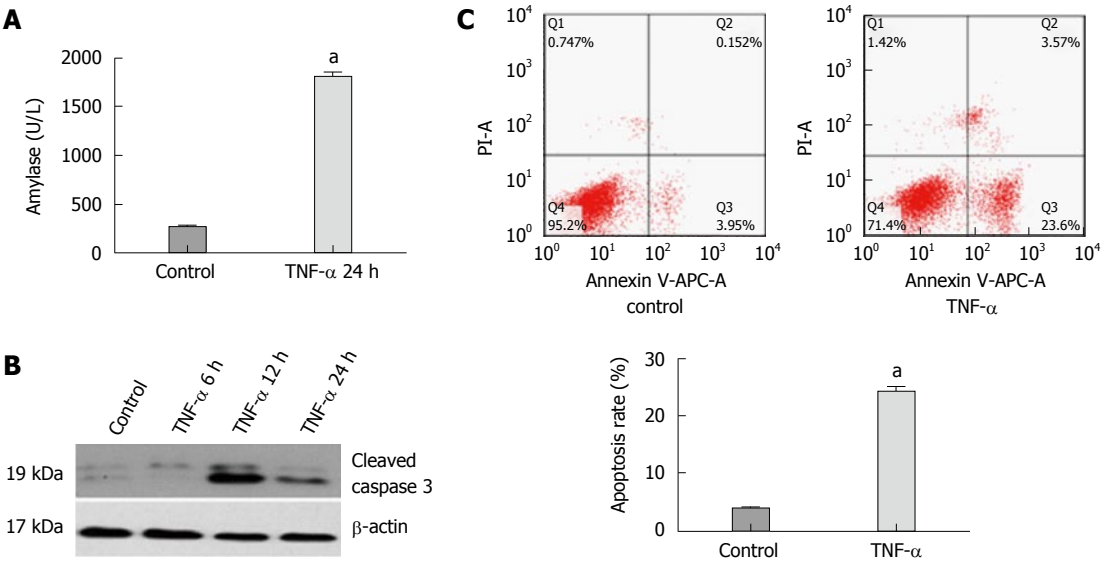

Figure 3 Expression of amylase, activated caspase 3 protein, apoptosis rate of AR42J cells and miR-29a level increase in the experimental group compared with the control group. A: The expression of amylase analysis in the supernatant; B: Western blot analysis of activated caspase 3 in AR42J cells; C: The apoptosis rate of AR42J cells after the treatment with TNF-α for 24 h. Date were obtained from three independent experiments in triplicate and are shown as the mean ± SD. $^{a}P < 0.05$ *vs* control group.

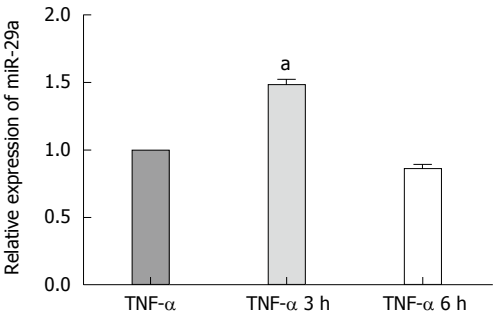

Figure 4 Quantitative real-time PCR analysis of miR-29a in AR42J cells at 3 h and 6 h. The expression of miR-29a was normalized to U6 expression using $2^{-\Delta\Delta ct}$. Data were obtained from three independent experiments in triplicate and are shown as the mean ± SD. $^{a}P < 0.05$ *vs* control group.

was significantly lower (0.61-fold) in the miR-29a AMO group ($P = 0.048$). In parallel, we analyzed the expression of TNFR1 protein in the miR-29a mimic and AMO groups. The miR-29a mimic group expressed higher levels of TNFR1 protein compared with the vehicle group, while the levels were lower in the miR-29a AMO group (Figure 8B).

DISCUSSION

AP is a common clinical condition with high morbidity and mortality, and its incidence increases over recent years[16,17]. There are two patterns of pancreatic acinar cells death: necrosis and apoptosis. Apoptosis is a physiological and programmed form of cell death. The stereotypical and characteristic morphology of apoptosis includes cell shrinkage, retention of organelles and nuclear chromatin condensation, which occurs in response to stimuli[18]. The relationship between apoptosis and AP had been extensively investigated and it has been demonstrated that the severity of AP is inversely related to the rate of apoptosis and correlates directly with the extent of necrosis[19,20]. The feature of the AP model which is induced by L-arginine is reproducible and dose-dependent. In this study, we successfully induced AEP with L-arginine (150 mg/kg) *in vivo* and the result of TUNEL assays confirmed that apoptosis occurred in pancreatic acinar cells.

The AR42J cell line used in this study possessed the properties of exocrine digestive enzymes[21]. There are many advantages of AR42J cells for the investigation of signaling mechanism in the pancreas, such as the ease of cell line culture maintenance, high transduction efficiency and responsiveness to many agonists[22]. The AR42J cell line had been used extensively to establish the AP model *in vitro*. Chanthaphavong *et al*[23] demonstrated that TNF-α induced apoptosis of several cell lines. Furthermore, a recent study showed that TNF-α activated the NF-κB pathway and induced the expression of proinflammatory mediators in pancreatic acinar cells[24]. The results of our study demonstrated that rat recombinant TNF-α cytokine was used successfully to establish the AEP model *in vitro*.

miRNAs are short non-coding RNAs that play an important role in regulating gene expression in multiple cellular processes including apoptosis, metabolism, proliferation, differentiation and development[5]. To date, over 15000 mature miRNAs have been identified in 133 species[25]. In recent years, it has been demonstrated that miRNAs can upregulate the target genes. Vasudevan *et al*[10] showed that human miRNA369-3 directed association of the proteins with AREs to activate translation, and let-7 and the synthetic miRNA miRNAcxcr4 could induce up-regulation of target genes.

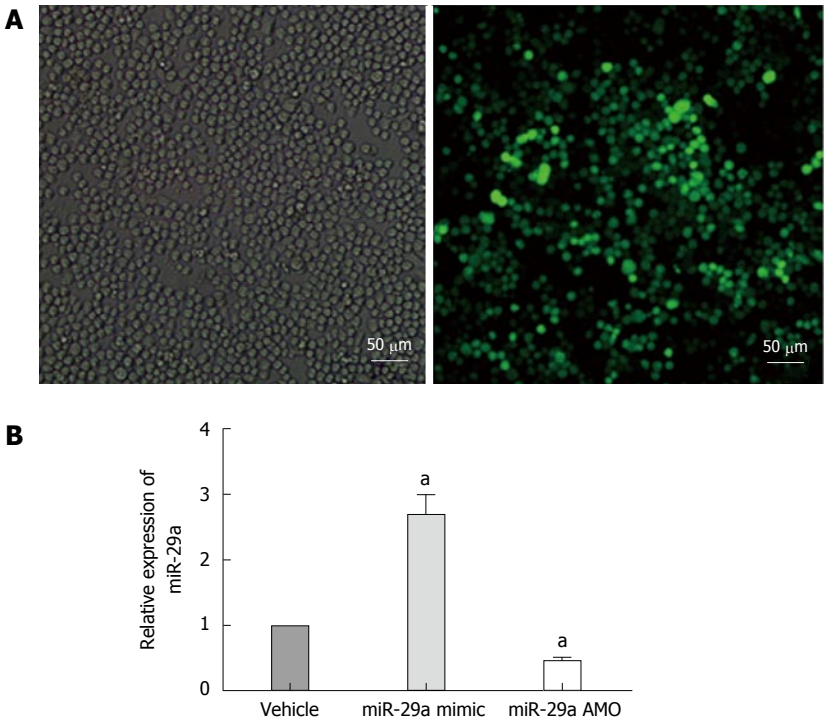

Figure 5 Lentiviral transfection and miRNA expression after transfection. A: Cells were infected with 50 MOI of lentivirus, and imaged 72 h post-transfection. Comparison of bright field filter view to FITC filter view (GFP-expression cells) for the same fields of cells showed about 90% infection efficiency by 72 h; B: Quantitative real-time PCR analysis of miR-29a expression in the AR42J cells after transfection. Date are shown as a ratio of mi-29a mimic and AMO groups to vehicle groups using the $2^{-\Delta\Delta ct}$. Data are representative of three independent experiments. $^{a}P < 0.05$ *vs* vehicle group.

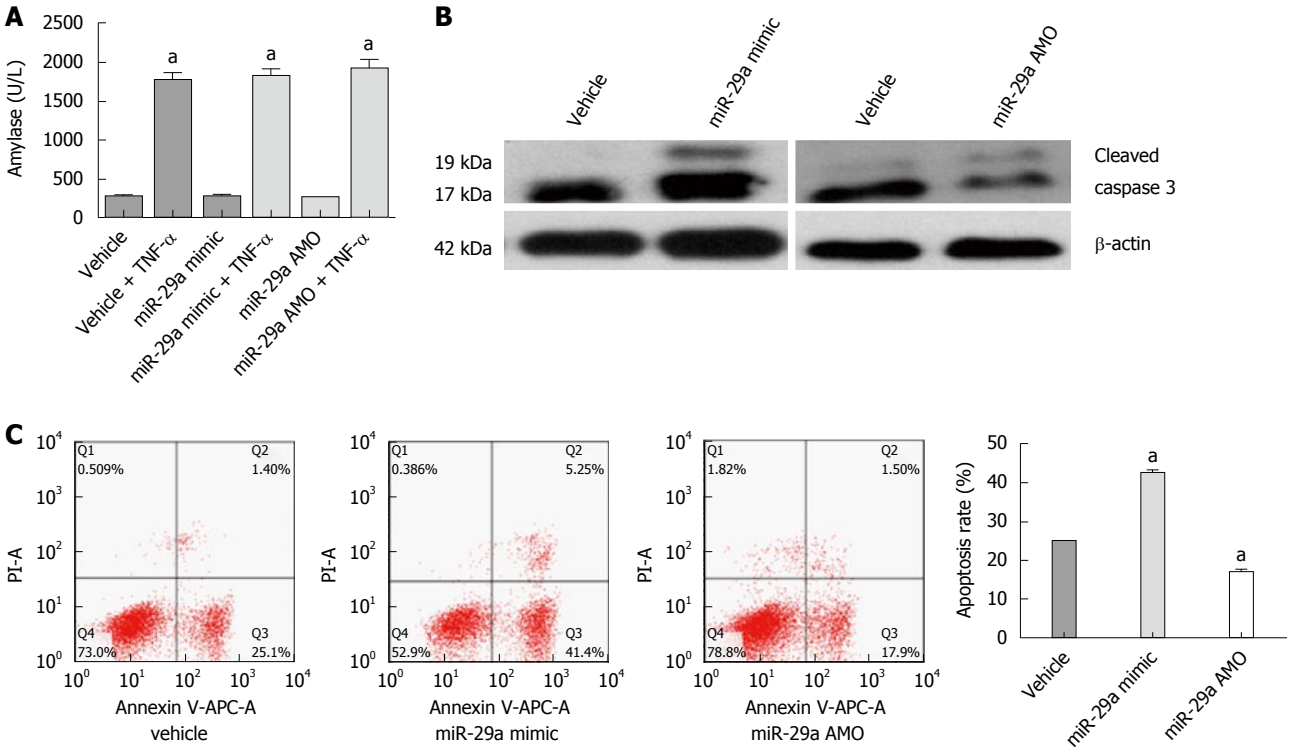

Figure 6 miR-29a promotes the apoptosis of the AR42J cells. A: The amylase analysis in the supernatant increased obviously; B: Western blot analysis of activated caspase 3 in AR42J cells; C: The apoptosis rate of AR42J cells was determined by FACS analysis. Data are representative of mean ± SD from three independent experiments performed in triplicate. $^{a}P < 0.05$ *vs* control or vehicle group.

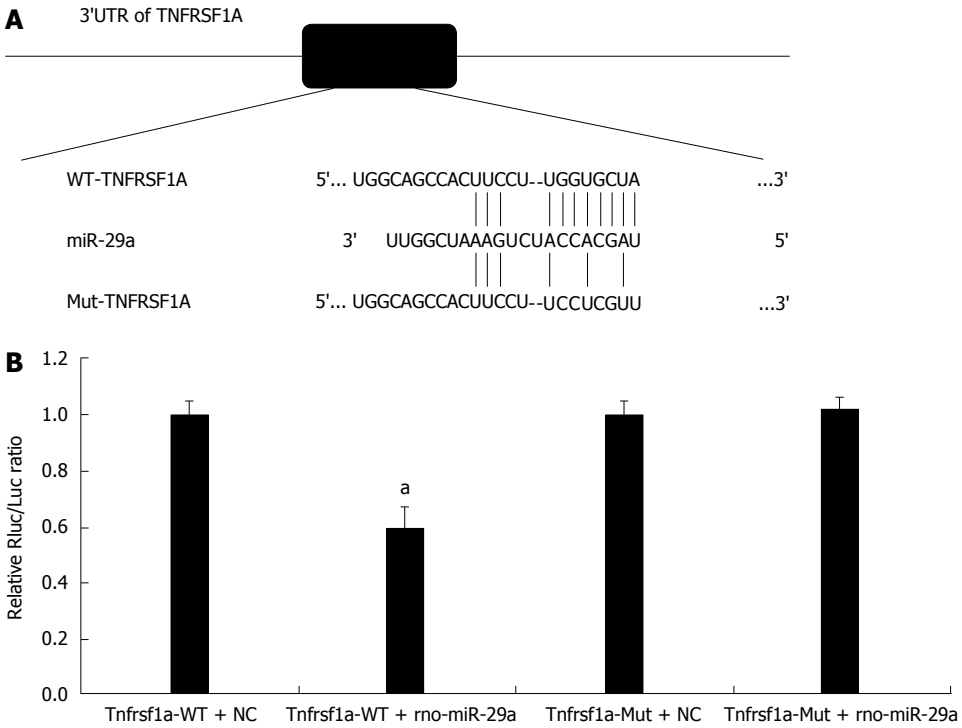

Figure 7 miR-29a targets *TNFRSF1A*. A: The predicted miR-29a binding sites within the 3'UTR of *TNFRSF1A* and mutant version generated by site mutagenesis are shown; B: Luciferase activity was determined 48 h after transfection. The ratio of normalized sensor to control luciferase activity is shown. Data are shown as the mean ± SD and were obtained from three independent experiments performed in triplicate ($^aP < 0.05$ *vs* control miR-transfected cells).

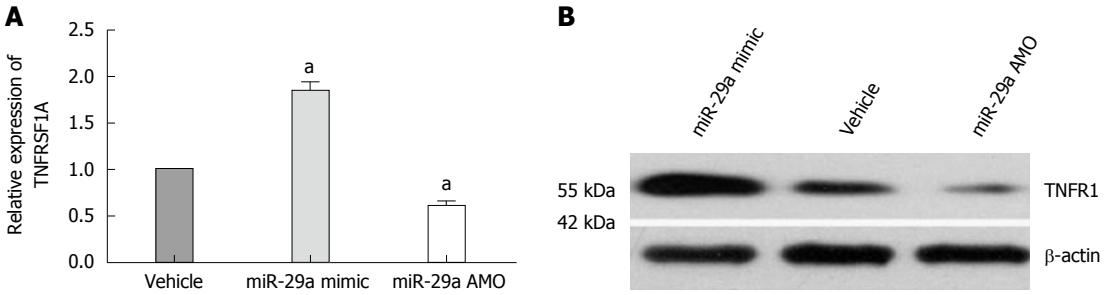

Figure 8 miR-29a promotes *TNFRSF1A* gene expression. A: Quantitative real-time RT-PCR analysis of TNFRSF1A expression in AR42J cells after transfection. Date are shown as a ratio of miR-29a mimic and AMO groups to vehicle group using the $2^{-\Delta\Delta ct}$. Data are representative of three independent experiments ($^aP < 0.05$ *vs* vehicle group); B: Western blot analysis of TNFR1 protein in AR42J cells after transfection.

miR-29a has been extensively demonstrated to promote cell apoptosis *via* suppressing survival genes. Direct repression of CDC42 and p85α by miR-29a can result in the activation of p53 and induction of apoptosis[11]. MCL1, which encodes an anti-apoptotic Bcl-2 family protein, is also the target gene of miR-29a. By repressing MCL-1, miR-29a sensitizes cholangicarcinoma and ALT$^+$ ALCL cells to apoptosis[14]. The results of our miRNA microarray and qRT-PCR analyses revealed that miR-29a is elevated in the AEP model *in vivo* and *in vitro*. miR-29a mimic and AMO were designed to investigate the function of miR-29a. This technology utilizes non-natural synthetic nucleic acids, which bind to the unique sequence of the target mRNAs in a gene-specific manner and has the same effects as the endogenous miRNAs[26,27]. Our result showed that AR42J cells showed a tendency to apoptosis in the miR-29 mimic group, while the apoptosis rate was significantly decreased in the miR-29a AMO group in the AEP model *in vivo*. *TNFRSF1A*, which encodes the TNFR1 protein, was predicted to be the target gene of miR-29a with the help of three online programs (TargetScan, miRanda and TarBase). TNF-R1, which is the major signaling receptor for TNF-α, is expressed on all cell types. Both soluble and membrane-bound forms of the cytokine can activate TNFR1. The binding of TNF-α to TNFR1 results in immediate NF-κB activation and subsequent apoptosis[3,4]. Our study demonstrated that miR-29a mediated up-regulation of the *TNFRSF1A* gene. AR42J cells transfected with the miR-29a mimic expressed higher levels of *TNFRSF1A* mRNA and TNFR1 protein, while the miR-29a AMO group exhibited the opposite trend. miR-29a promotes the expression of *TNFRSF1A*

gene and its regulation mechanism is not binding to and degrading *TNFRSF1A* gene as the the result of luciferase assay in HEK 293T cells. We hypothesized that the combination of miR-29a and TNFRSF1A gene might guide some protein factors, which promote the transcription and translation of genes in pancreatic acinar cells, bind to the target gene. Further investigations need to be performed.

In summary, miR-29a is elevated significantly in AEP, indicating that miR-29a might promote pancreatic acinar cell apoptosis by enhancing expression of *TNFRSF1A* gene.

COMMENTS

Background

Apoptosis is a self-protective mechanism in acute pancreatitis. miRNAs are short non-coding RNAs involved in multiple cellular processes including development, proliferation, differentiation, metabolism and apoptosis.

Research frontiers

It has been reported that miR-29a plays an important role in apoptosis, but little is known about the effect of miR-29a on apoptosis in acute pancreatitis and its regulatory mechanisms.

Innovations and breakthroughs

In this study, the authors demonstrated that miR-29a is elevated significantly in acute edematous pancreatitis. The rate of apoptosis and TNFRSF1A expression increased significantly in AR42J cells following upregulation of miR-29a expression. miR-29a promotes pancreatic acinar cell apoptosis by enhancing expression of *TNFRSF1A* gene directly.

Applications

The study results suggest that miR-29a promotes pancreatic acinar cell apoptosis by enhancing expression of *TNFRSF1A* gene directly in acute pancreatitis, and these findings may provide a theoretical basis for the prevention and treatment of acute pancreatitis.

Terminology

MicroRNAs (miRNAs) are a set of 21- to 24- nucleotide(nt), endogenous, non-coding, regulatory RNA molecules that contribute to modulating the expression levels of specific proteins based on base pairing with their target mRNA molecules.

Peer-review

Authors demonstrated that miR-29a, which has been demonstrated to play an important role in apoptosis, is elevated significantly in acute edematous pancreatitis. The data are interesting and the experiments are well organized. Those findings give novel information on the pathogenesis of acute pancreatitis.

REFERENCES

1 **Ghezzi P**, Cerami A. Tumor necrosis factor as a pharmacological target. *Mol Biotechnol* 2005; **31**: 239-244 [PMID: 16230774 DOI: 10.1385/1-59259-771-8:001]

2 **Gukovskaya AS**, Gukovsky I, Zaninovic V, Song M, Sandoval D, Gukovsky S, Pandol SJ. Pancreatic acinar cells produce, release, and respond to tumor necrosis factor-alpha. Role in regulating cell death and pancreatitis. *J Clin Invest* 1997; **100**: 1853-1862 [PMID: 9312187 DOI: 10.1172/JCI119714]

3 **Wajant H**, Pfizenmaier K, Scheurich P. Tumor necrosis factor signaling. *Cell Death Differ* 2003; **10**: 45-65 [PMID: 12655295 DOI: 10.1038/sj.cdd.4401189]

4 **Borghini S**, Fiore M, Di Duca M, Caroli F, Finetti M, Santamaria G, Ferlito F, Bua F, Picco P, Obici L, Martini A, Gattorno M, Ceccherini I. Candidate genes in patients with autoinflammatory syndrome resembling tumor necrosis factor receptor-associated periodic syndrome without mutations in the TNFRSF1A gene. *J Rheumatol* 2011; **38**: 1378-1384 [PMID: 21459945 DOI: 10.3899/jrheum.101260]

5 **Bartel DP**. MicroRNAs: target recognition and regulatory functions. *Cell* 2009; **136**: 215-233 [PMID: 19167326 DOI: 10.1016/j]

6 **Bartel DP**. MicroRNAs: genomics, biogenesis, mechanism, and function. *Cell* 2004; **116**: 281-297 [PMID: 14744438 DOI: 10.1016/Soo92-8674(04)00045-5]

7 **Giraldez AJ**, Mishima Y, Rihel J, Grocock RJ, Van Dongen S, Inoue K, Enright AJ, Schier AF. Zebrafish MiR-430 promotes deadenylation and clearance of maternal mRNAs. *Science* 2006; **312**: 75-79 [PMID: 16484454 DOI: 10.1126/science.1122689]

8 **Wu L**, Fan J, Belasco JG. MicroRNAs direct rapid deadenylation of mRNA. *Proc Natl Acad Sci USA* 2006; **103**: 4034-4039 [PMID: 16495412 DOI: 10.1073/pnas.0510928103]

9 **Petersen CP**, Bordeleau ME, Pelletier J, Sharp PA. Short RNAs repress translation after initiation in mammalian cells. *Mol Cell* 2006; **21**: 533-542 [PMID: 16483934 DOI: 10.1016/j.molcel.2006.01.031]

10 **Vasudevan S**, Tong Y, Steitz JA. Switching from repression to activation: microRNAs can up-regulate translation. *Science* 2007; **318**: 1931-1934 [PMID: 18048652 DOI: 10.1126/science.1149460]

11 **Park SY**, Lee JH, Ha M, Nam JW, Kim VN. miR-29 miRNAs activate p53 by targeting p85 alpha and CDC42. *Nat Struct Mol Biol* 2009; **16**: 23-29 [PMID: 19079265 DOI: 10.1038/nsmb.1533]

12 **Xiong Y**, Fang JH, Yun JP, Yang J, Zhang Y, Jia WH, Zhuang SM. Effects of microRNA-29 on apoptosis, tumorigenicity, and prognosis of hepatocellular carcinoma. *Hepatology* 2010; **51**: 836-845 [PMID: 20041405 DOI: 10.1002/hep.23380]

13 **Bargaje R**, Gupta S, Sarkeshik A, Park R, Xu T, Sarkar M, Halimani M, Roy SS, Yates J, Pillai B. Identification of novel targets for miR-29a using miRNA proteomics. *PLoS One* 2012; **7**: e43243 [PMID: 22952654 DOI: 10.1371/journal.pone.0043243]

14 **Desjobert C**, Renalier MH, Bergalet J, Dejean E, Joseph N, Kruczynski A, Soulier J, Espinos E, Meggetto F, Cavaillé J, Delsol G, Lamant L. MiR-29a down-regulation in ALK-positive anaplastic large cell lymphomas contributes to apoptosis blockade through MCL-1 overexpression. *Blood* 2011; **117**: 6627-6637 [PMID: 21471522 DOI: 10.1182/blood-2010-09-301994]

15 **Mott JL**, Kurita S, Cazanave SC, Bronk SF, Werneburg NW, Fernandez-Zapico ME. Transcriptional suppression of mir-29b-1/mir-29a promoter by c-Myc, hedgehog, and NF-kappaB. *J Cell Biochem* 2010; **110**: 1155-1164 [PMID: 20564213 DOI: 10.1002/jcb.22630]

16 **Vaz J**, Akbarshahi H, Andersson R. Controversial role of toll-like receptors in acute pancreatitis. *World J Gastroenterol* 2013; **19**: 616-630 [PMID: 23431068 DOI: 10.3748/wjg.v19.i5.616]

17 **Kylänpää L**, Rakonczay Z, O'Reilly DA. The clinical course of acute pancreatitis and the inflammatory mediators that drive it. *Int J Inflam* 2012; **2012**: 360685 [PMID: 23304633 DOI: 10.1155/2012/360685]

18 **Mareninova OA**, Sung KF, Hong P, Lugea A, Pandol SJ, Gukovsky I, Gukovskaya AS. Cell death in pancreatitis: caspases protect from necrotizing pancreatitis. *J Biol Chem* 2006; **281**: 3370-3381 [PMID: 16339139 DOI: 10.1074/jbc.M511276200]

19 **Bhatia M**. Apoptosis versus necrosis in acute pancreatitis. *Am J Physiol Gastrointest Liver Physiol* 2004; **286**: G189-G196 [PMID: 14715516 DOI: 10.1152/ajpgi.00304.2003]

20 **Gukovskaya AS**, Pandol SJ. Cell death pathways in pancreatitis and pancreatic cancer. *Pancreatology* 2004; **4**: 567-586 [PMID: 15550766 DOI: 10.1159/000082182]

21 **Sato H**, Siow RC, Bartlett S, Taketani S, Ishii T, Bannai S, Mann GE. Expression of stress proteins heme oxygenase-1 and -2 in acute pancreatitis and pancreatic islet betaTC3 and acinar AR42J cells. *FEBS Lett* 1997; **405**: 219-223 [PMID: 9089294 DOI: 10.1016/S0014-5793(97)00191-9]

22 **Twait E**, Williard DE, Samuel I. Dominant negative p38 mitogen-activated protein kinase expression inhibits NF-kappaB activation in AR42J cells. *Pancreatology* 2010; **10**: 119-128 [PMID: 20453549

DOI: 10.1159/000290656]
23 **Chanthaphavong RS**, Loughran PA, Lee TY, Scott MJ, Billiar TR. A role for cGMP in inducible nitric-oxide synthase (iNOS)-induced tumor necrosis factor (TNF) α-converting enzyme (TACE/ADAM17) activation, translocation, and TNF receptor 1 (TNFR1) shedding in hepatocytes. *J Biol Chem* 2012; **287**: 35887-35898 [PMID: 22898814 DOI: 10.1074/jbc.M112.365171]
24 **Satoh A**, Gukovskaya AS, Nieto JM, Cheng JH, Gukovsky I, Reeve JR, Shimosegawa T, Pandol SJ. PKC-delta and -epsilon regulate NF-kappaB activation induced by cholecystokinin and TNF-alpha in pancreatic acinar cells. *Am J Physiol Gastrointest Liver Physiol* 2004; **287**: G582-G591 [PMID: 15117677 DOI: 10.1152/ajpgi.00087.2004]
25 **Bentwich I**, Avniel A, Karov Y, Aharonov R, Gilad S, Barad O, Barzilai A, Einat P, Einav U, Meiri E, Sharon E, Spector Y, Bentwich Z. Identification of hundreds of conserved and nonconserved human microRNAs. *Nat Genet* 2005; **37**: 766-770 [PMID: 15965474 DOI: 10.1038/ng1590]
26 **Wang Z**. The guideline of the design and validation of MiRNA mimics. *Methods Mol Biol* 2011; **676**: 211-223 [PMID: 20931400 DOI: 10.1007/978-1-60761-863-8_15]
27 **Hammond SM**. MicroRNA therapeutics: a new niche for antisense nucleic acids. *Trends Mol Med* 2006; **12**: 99-101 [PMID: 16473043 DOI: 10.1016/j.molmed.2006.01.004]

P- Reviewer: Shimizu Y, Soria F **S- Editor**: Qi Y
L- Editor: Wang TQ **E- Editor**: Wang CH

World Journal of Gastroenterology

Submit a Manuscript: http://www.wjgnet.com/esps/
Help Desk: http://www.wjgnet.com/esps/helpdesk.aspx
DOI: 10.3748/wjg.v22.i20.4891

World J Gastroenterol 2016 May 28; 22(20): 4891-4900
ISSN 1007-9327 (print) ISSN 2219-2840 (online)

ORIGINAL ARTICLE

Retrospective Cohort Study

Rectal cancer staging: Multidetector-row computed tomography diagnostic accuracy in assessment of mesorectal fascia invasion

Davide Ippolito, Silvia Girolama Drago, Cammillo Talei Franzesi, Davide Fior, Sandro Sironi

Davide Ippolito, Silvia Girolama Drago, Cammillo Talei Franzesi, Davide Fior, Sandro Sironi, School of Medicine, University of Milano-Bicocca, Milan, 20900 Monza (MB), Italy

Davide Ippolito, Silvia Girolama Drago, Cammillo Talei Franzesi, Davide Fior, Sandro Sironi, Department of Diagnostic Radiology, H. San Gerardo Hospital, Milan, 20900 Monza (MB), Italy

Author contributions: Ippolito D was guarantor of integrity of entire study and conception the study; Ippolito D and Drago SG contributed to study design, acquisition, data analysis/interpretation and statistical analysis; Ippolito D, Drago SG and Franzesi CT contributed to study design, and clinical studies; Franzesi CT and Fior D contributed to literature research; Drago SG contributed to manuscript preparation; Ippolito D and Sironi S contributed to manuscript definition of intellectual content; Ippolito D and Franzesi CT contributed to manuscript editing; all authors contributed to manuscript revision/review; Ippolito D made manuscript final version approval.

Institutional review board statement: The study was reviewed and approved by the H. San Gerardo Institutional Review Board.

Informed consent statement: Every patient gave his informed consent, as required by our Institution.

Conflict-of-interest statement: All the authors are aware of the content of the manuscript and have no conflict of interest.

Data sharing statement: No additional data are available.

Correspondence to: Davide Ippolito, MD, Department of Diagnostic Radiology, H. San Gerardo Hospital, Via Pergolesi 33, Milan, 20900 Monza (MB), Italy. davide.atena@tiscalinet.it
Telephone: +39-02-64488265
Fax: +39-02-64488299

Received: January 28, 2016
Peer-review started: January 30, 2016
First decision: March 7, 2016
Revised: March 24, 2016
Accepted: April 7, 2016
Article in press: April 7, 2016
Published online: May 28, 2016

Abstract

AIM: To assess the diagnostic accuracy of multidetector-row computed tomography (MDCT) as compared with conventional magnetic resonance imaging (MRI), in identifying mesorectal fascia (MRF) invasion in rectal cancer patients.

METHODS: Ninety-one patients with biopsy proven rectal adenocarcinoma referred for thoracic and abdominal CT staging were enrolled in this study. The contrast-enhanced MDCT scans were performed on a 256 row scanner (ICT, Philips) with the following acquisition parameters: tube voltage 120 KV, tube current 150-300 mAs. Imaging data were reviewed as axial and as multiplanar reconstructions (MPRs) images along the rectal tumor axis. MRI study, performed on 1.5 T with dedicated phased array multicoil, included multiplanar T2 and axial T1 sequences and diffusion weighted images (DWI). Axial and MPR CT images independently were compared to MRI and MRF involvement was determined. Diagnostic accuracy of both modalities was compared and statistically analyzed.

RESULTS: According to MRI, the MRF was involved in 51 patients and not involved in 40 patients. DWI allowed to recognize the tumor as a focal mass with high signal intensity on high b-value images, compared with the signal of the normal adjacent rectal wall or with the lower tissue signal intensity background. The number of patients correctly staged by the native axial CT images was 71 out of 91 (41 with involved MRF; 30 with not involved MRF), while by using the MPR 80 patients were correctly staged (45 with involved MRF; 35 with not involved MRF). Local tumor staging suggested by MDCT agreed with those of MRI, obtaining for CT axial images sensitivity and specificity of 80.4% and 75%, positive predictive value (PPV) 80.4%, negative predictive value (NPV) 75% and accuracy 78%; while performing MPR the sensitivity and specificity increased to 88% and 87.5%, PPV was 90%, NPV 85.36% and accuracy 88%. MPR images showed higher diagnostic accuracy, in terms of MRF involvement, than native axial images, as compared to the reference magnetic resonance images. The difference in accuracy was statistically significant (P = 0.02).

CONCLUSION: New generation CT scanner, using high resolution MPR images, represents a reliable diagnostic tool in assessment of loco-regional and whole body staging of advanced rectal cancer, especially in patients with MRI contraindications.

Key words: Magnetic resonance; Multi detector computed tomography; Rectal cancer; Mesorectal fascia; Multiplanar reconstructions

Core tip: The introduction of new generation of multidetector-row computed tomography (MDCT) scanner allowed thin-collimation scanning and high spatial resolution, resulting in improved multiplanar reconstructions (MPRs) and could be potentially useful, in a single examination, for local staging and distant metastases evaluation in rectal cancer patients. On these basis in our study we assessed the accuracy of high row number MDCT for the prediction of tumor invasion of the mesorectal fascia, being MRI findings as reference standard, and whether the addition of high-resolution MPR images can provide greater accuracy.

Ippolito D, Drago SG, Franzesi CT, Fior D, Sironi S. Rectal cancer staging: Multidetector-row computed tomography diagnostic accuracy in assessment of mesorectal fascia invasion. *World J Gastroenterol* 2016; 22(20): 4891-4900 Available from: URL: http://www.wjgnet.com/1007-9327/full/v22/i20/4891.htm DOI: http://dx.doi.org/10.3748/wjg.v22.i20.4891

INTRODUCTION

Treatment options in rectal cancer patients, such as total mesorectal excision (TME) and preoperative neoadjuvant radiochemotherapy in advanced tumor stages[1,2], have greatly increased the importance of accurate preoperative staging to provide information about tumor location, size, configuration, and local infiltration[3]. One of the most important features of local rectal cancer staging is the assessment of the circumferential resection margin (CRM)[1] and relationship of the tumor to the mesorectal fascia (MRF), which actually defines the surgical CRM in TME surgery[4-6].

Magnetic resonance imaging (MRI) is today considered the "state-of-the-art" investigation for preoperative evaluation of pelvic malignant disease due to the method's multiplanar capabilities and its ability to visualize the rectum, the mesorectal fat and the MRF, urinary bladder and internal genitalia with high soft tissue contrast[7].

Although many studies have described the accuracy of computed tomography (CT) for predicting the depth of bowel wall and lymph node invasion[8-11], only few of them have addressed the problems of predicting tumor infiltration of the MRF with new generation of multidetector-row CT (MDCT). The current role of CT in the evaluation of patients with rectal cancer is controversial[3]. In a single examination, CT can assess the entire abdomen, pelvis and chest, allowing for local staging and distant metastases evaluation[12-15]. MRI is an integral part of the diagnostic work-up of patients with rectal cancer due to its proven efficacy to determine the tumor relationship to the MRF[4]. However, MRI does have the downside of limited availability, relatively long image acquisition time and high cost[4]. Moreover, not all patients can undergo MRI because of claustrophobia or the presence of metal in patients' bodies. In addition, another important factor in the preoperative assessment of primary rectal cancer is the frequent presence of distant disease at the time of diagnosis. Modern CT techniques are better suited than MRI to search for the local tumor extent and distant metastases in the same imaging session[16,17]. These considerations on one hand, and improved spatial resolution of new MDCT scanner on the other hand, have revived the discussion whether to use CT or MRI for rectal cancer staging[4,17]. The introduction of MDCT allowed thin-collimation scanning and high spatial resolution[1], resulting in improved multiplanar reconstructions (MPR)[3,17]. MPR images can be potentially useful for local staging in rectal cancer as they can be aligned parallel or perpendicular to the axis of the tumor similar to MR imaging. The aim of the present study was to evaluate the accuracy of high row number MDCT for the prediction of tumor invasion of the MRF being MRI findings as reference standard, and whether the addition of high-resolution MPR images can provide greater accuracy.

MATERIALS AND METHODS

Patients

One hundred and thirty-one patients with biopsy-

proven adenocarcinoma of the rectum and distal margin of the tumor within 15 cm from the anal verge were enrolled in this retrospective study.

The standard workup for patients with a rectal cancer includes a pelvic MRI for the assessment of loco-regional staging and MDCT study to determine the whole body staging.

For this reason the inclusion criteria were: (1) a biopsy proven rectal cancer (0-15 cm from anal verge according to endoluminal biopsy); (2) availability of MRI study of lower abdomen; (3) availability of contrast enhanced MDCT of the chest and abdomen examinations; and (4) both MRI and CT images performed before application of any neo-adjuvant therapy or surgery.

Exclusion criteria were: (1) previous neo-adjuvant therapy for rectal cancer; (2) contraindications to MRI examination; (3) contraindications to contrast enhanced CT imaging (*e.g.*, intolerance/allergy to iodine contrast medium); (4) insufficient MR imaging quality (*e.g.*, movement artifact) and insufficient CT imaging quality (*e.g.*, owing to metal implants); and (5) absence of one of the two diagnostic tools between MRI and CT .

Forty patients were excluded from this study: 2 patients had hip prostheses (important beam hardening artifacts reduced CT images quality); 6 patients were excluded due to movement-related artifacts in MR study; 19 patients had only MRI evaluation and 13 had a CT evaluation alone (patients in which the local MRI staging was performed in another Hospital).

A final cohort of 91 patients (65 male and 26 female, with a mean age of 69 years - range 30 to 89 years) satisfied the inclusion criteria and were enrolled in this study.

The mean interval time between the MRI and CT examination was 37 d (range 0-79 d).

The approval for this study was obtained by the ethical approval committee at our Institution.

CT imaging technique

All MDCT examinations were carried out without luminal rectal contrast media or air insufflation. All CT studies were performed on a 256-slice CT system (Brilliance iCT, Philips Medical Systems, Best, the Netherlands) with the following scan parameters: thickness 2 mm; increment 1 mm; collimation 128 × 0.625; pitch 0.915; rotation time 0.4 s; FOV 350; matrix 512 × 512. The scan images were acquired before and after the intravenous bolus injection of non-ionic iodinated contrast material (Xenetix 350; Guerbet, Aulnay, France), according to the body weight, at a rate of 3.5 mL/s, using a double-syringe injector (Medrad Stellant, Pittsburgh, PA, United States) and 18-gauge catheter positioned into the antecubital vein. Bolus tracking software was used to set individual acquisition times for the arterial, portal and equilibrium phases. Contrast material enhancement was automatically calculated by placing the region of interest cursor over the abdominal aorta, and the level of the trigger threshold was set to increase to 120 HU.

Thirteen seconds after the trigger threshold had been reached, arterial phase CT data acquisition began automatically. The portal venous and equilibrium phases were acquired after 60 and 140 s, respectively, after the trigger threshold had been reached.

Examinations were performed during one breath-hold from the thorax to the anus.

None of the patients received a contrast enema or bowel relaxation.

MRI technique

MRI imaging examination was performed for tumor staging before starting the treatment or surgery.

All MRI examinations were performed with a 1.5-T system (Achieva Plus; Philips, The Netherlands) in combination with a five-channel phased-array body coil.

After a planning scan, axial and sagittal T2 weighted turbo spin-echo (T2WI-TSE) images covering entire length of the rectum were acquired and used to plan high resolution scans.

Scan protocol consisted of axial TSE T1 weighted axial sequence turbo spin-echo (TSE) (slice thickness: 3 mm; slice: 20; gap: 3 mm; TR: 612 ms; TE: 14 ms; flip angle: 90°; FOV: 180; RFOV: 85; matrix: 272 × 320; NSA: 4; time: 4.43 min); sagittal TSE T2 sequence (slice thickness: 3 mm; slice: 32; gap: 0 mm; TR: 5501 ms; TE: 85 ms; flip angle: 90°; FOV: 220; RFOV: 105; matrix: 276 × 200; NSA: 4; time: 4.40 min); axial TSE T2 sequence (slice thickness: 3.5 mm; slice: 18; gap: 3.5 mm; TR: 4750 ms; TE: 120 ms; flip angle: 90°; FOV: 180; RFOV: 85; matrix: 256 × 256; NSA: 4; time: 3.05 min); coronal TSE T2 sequence (slice thickness: 3 mm; slice: 20; gap: 0.5 mm; TR: 5058 ms; TE: 125 ms; flip angle: 90°; FOV: 180; RFOV: 100; matrix: 256 × 256; NSA: 4; time: 3.47 min). The axial and coronal oblique images were performed orthogonal and parallel, respectively, to the long axis of the rectal cancer.

Afterwards diffusion weighted images with background body signal suppression (DWIBS) using a Multi-slice Spin Echo Eco-planar Single Shot (SE-EPI-SSh) sequence were obtained; DWIBS were combined with a short time inversion recovery (STIR) pre-pulse for fat saturation. The DWIBS sequences were acquired in a pure axial plane in order to avoid distortion artifacts, with *b*-value 0 and 1000 s/mm^2 with following parameters: slice thickness: 6 mm; slice: 12; gap: 6 mm; TR: 3000 ms; TE: 74 ms; flip angle: 90°; *b*-value: 0 and 700 s/mm^2; FOV: 380; RFOV: 80; matrix: 240 × 256; NSA: 4; time: 1.30 min; SENSE factor: 1.5. According to recent literature no contrast enhanced dynamic or steady state T1 weighted or fat suppressed

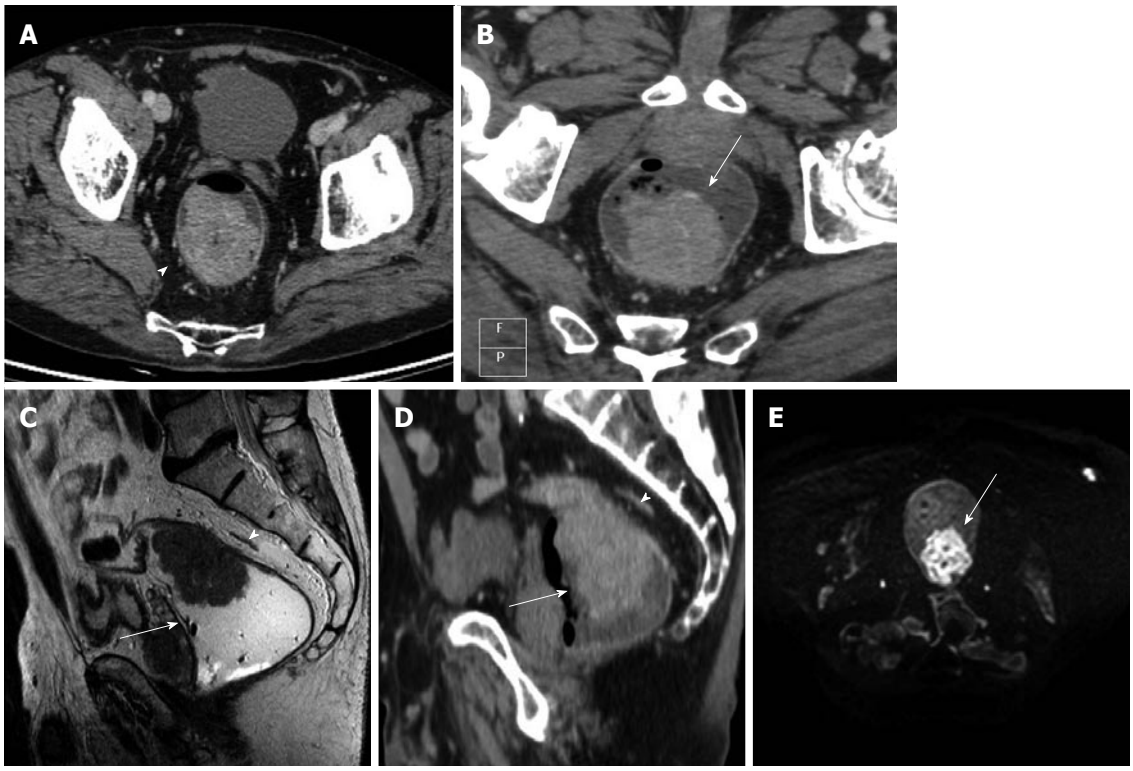

Figure 1 Images obtained in a 54 years-old man with middle-high rectal cancer. A: The pure axial contrast enhanced computed tomography (CE-CT) image shows a tumor, as a intraluminal polypoid mass, with spiculated configuration margin and spread through the mesorectal fat. The tumour does not involve the mesorectal fascia (MRF) (arrowhead); B: Multiplanar reconstruction (MPR) MDCT images, along the axial plane of tumour axis, shows the presence of the tumor (arrow) with no involvement of the MRF; C: T2 (TSE) MRI image of the same patient (sagittal plane), shows the tumor as a polypoid mass (arrow), along the posterior burden of the rectum infiltrating through the muscularis propria into the mesorectal fat without MRF involvement (arrowhead); D: CE-CT MPR image (sagittal slice), at the same level shows the tumour as a polypoid mass inside the rectal lumen infiltrating the mesorectal fat without MRF involvement (arrowhead); E: DWIBS image (*b*-value 1000), the tumor presents high signal, due to restricted water diffusion; the normal rectal wall or the surrounding tissues have a lower signal intensity in comparison with the polypoid mass. The mesorectal (arrow) fascia is not detectable.

sequences were used[18,19].

All these sequences were obtained in free breathing. The total examination time was approximately 30 min. Patients did not undergo any preparation such as bowel cleaning or spasmolytic medication before the MR examinations. Luminal distention was achieved with rectal administration of a small amount (almost 100 mL) of sonography transmission gel to distend the rectal lumen.

CT image analysis

In order to obtain an optimal contrast enhancement, the images of the pelvis were observed in the portal-venous contrast enhanced phase. Multiplanar CT reconstructions were performed from the same radiologist, (blinded to pathological evaluation, clinical and MRI patient data), that analyzed all the CT images and orientated MPR images axial plane along the tumor axis.

According to recent guidelines about clinical management of rectal cancer patients with MRI (recommendations from ESGAR, 2012)[18], sagittal reconstructions are used to determine the longitudinal tumor axis in order to angle the axial and coronal planes as perpendicular and parallel to the tumor axis as possible, respectively. MPR CT images were performed following the same recommendations to obtain axial and oblique coronal planes similar to MRI imaging.

After iv contrast injection the tumor was seen as an intraluminal polypoid mass (Figure 1) or as asymmetric or circumferential mural thickening (> 6 mm)[20] with or without luminal narrowing (with abrupt transition from normal to abnormally thick-walled rectum) and smooth outer bowel margins. In some cases strands of the soft tissue extending from serosal surface into perirectal fat was observed (Figure 1).

The MRF was seen as a thin, curvilinear structure surrounding the mesorectal fat with similar density to muscle adjacent to the rectum[1,21] (Figures 2 and 3). The main outcome parameter was the involvement of MRF defined as a visible fat line between the tumor and the MRF (Figure 3).

All CT axial images were observed first, in order to determine the tumor extension and direct involvement of the MRF; few days after (0-6 d), the same evaluation was done with MPR images.

MRI analysis

For each patient a radiologist with 10 years of experience in abdominal imaging analyzed T2-weighted

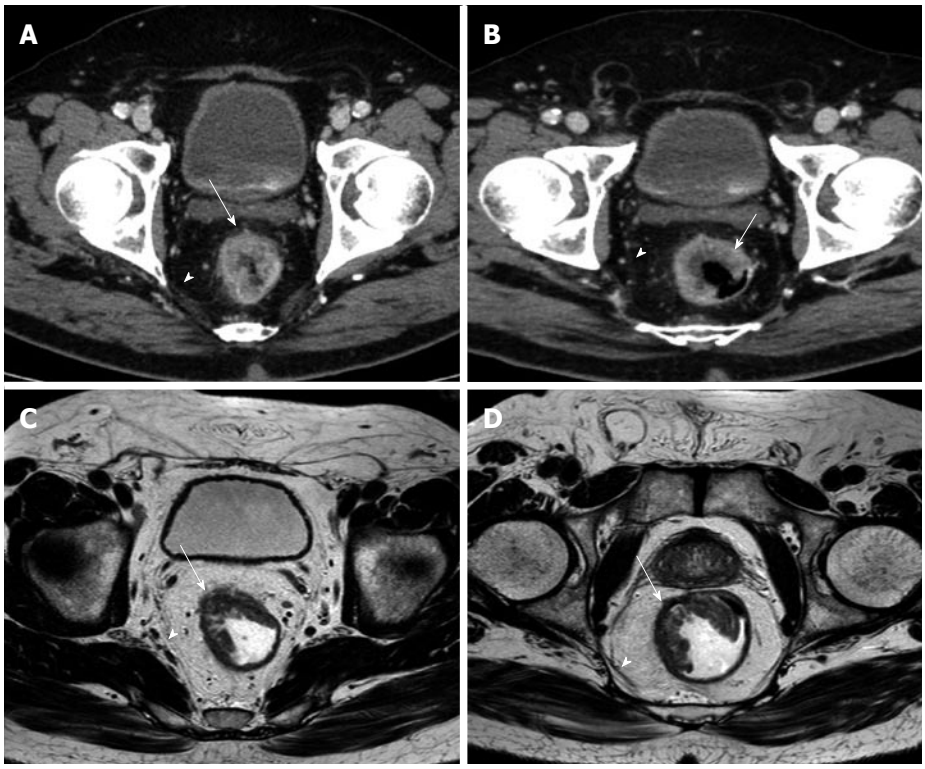

Figure 2 Images obtained in a 64 years-old man with middle rectal cancer. A: Axial contrast enhanced computed tomography (CE-CT) image shows the tumour as an irregular mural thickening of the anterior rectal wall with possible infiltration into the perirectal fat. The mesorectal fascia is seen as a thin line (arrowhead) surrounding the mesorectal fat and is not involved by the tumor (arrow); B: Multiplanar reconstruction (MPR) para-axial CE CT image of the same patient shows the tumour as an irregular mural thickening of the anterior rectal wall (arrow) with no infiltration into the perirectal fat. The mesorectal fascia (arrowhead) is better defined in MPR para-axial CT image; C: T2 (TSE) MRI image of the same patient shows the tumour as a lesion of the anterior rectal wall, slightly hyperintense compared to the muscle, that extends through the hypo-intense muscle layer into the perirectal fat (arrow) and without mesorectal fascia involvement (arrowhead); D: Orthogonal axial high-resolution T2-weighted MR image of the same patient shows an intraluminal mass (arrows) confined to the intact, hypo-intense muscularis propria (the proper muscle layer is shown as a low intensity band (*). The mesorectal fascia (arrowhead).

sequences and DWIBS images in order to detect and correctly localize the primary lesion. The presence of the tumor was diagnosed on T2-weighted sequences. Rectal cancer typically appeared hypointense as compared to the surrounding fat, and slightly hyperintense as compared to the muscles.

The mesorectal fascia was seen as a thin hypo-intense line surrounding the mesorectal fat[1].

DWIBS images were analyzed in order to obtain information about microscopic structures of biologic tissue through water proton mobility and to achieve a possible tool to monitor the response of tumor tissue after therapy[22].

These images were of diagnostic quality and adequate to identify the tumor region. When the anatomic details were unclear due to the low signal-to-noise (SNR) on DWIBS images, they were matched to T2WI images of same planes. The diagnostic criterion on DWI was defined as a focal mass with high signal intensity (SI) on b1000 DW, compared with the signal of the normal adjacent rectal wall or background of lower SI tissue[22].

During images analysis, the radiologist was blinded to clinical patient data and pathological evaluation.

Multiplanar T2 weighted sequences and axial T1 weighted sequences images were evaluated in order to assess the presence of the tumor, the involvement of the MRF and the adjacent structures.

Statistical analysis

All statistical analysis was performed using commercially available software (Med Calc, Med calc software 11.0, Mariakerke Belgium). The McNemar test was used to compare axial and MPR CT images with those of MRI imaging, which was considered as the reference standard, in order to determine the involvement of the MRF.

The sensitivity, specificity, positive predictive value (PPV), negative predictive value (NPV) and accuracy of axial and MPR images were assessed and the obtained data were then compared. Overall accuracy, sensitivity and specificity of the prediction of involvement of the MRF were calculated using cross-tabulation statistics.

RESULTS

In the native axial CT imaging analysis the MRF was involved by the tumor in 51 patients, while on MPR images the involvement of the MRF was observed in 50 patients. At MR image evaluation, the involvement of the MRF by the rectal cancer was observed in 51 patients.

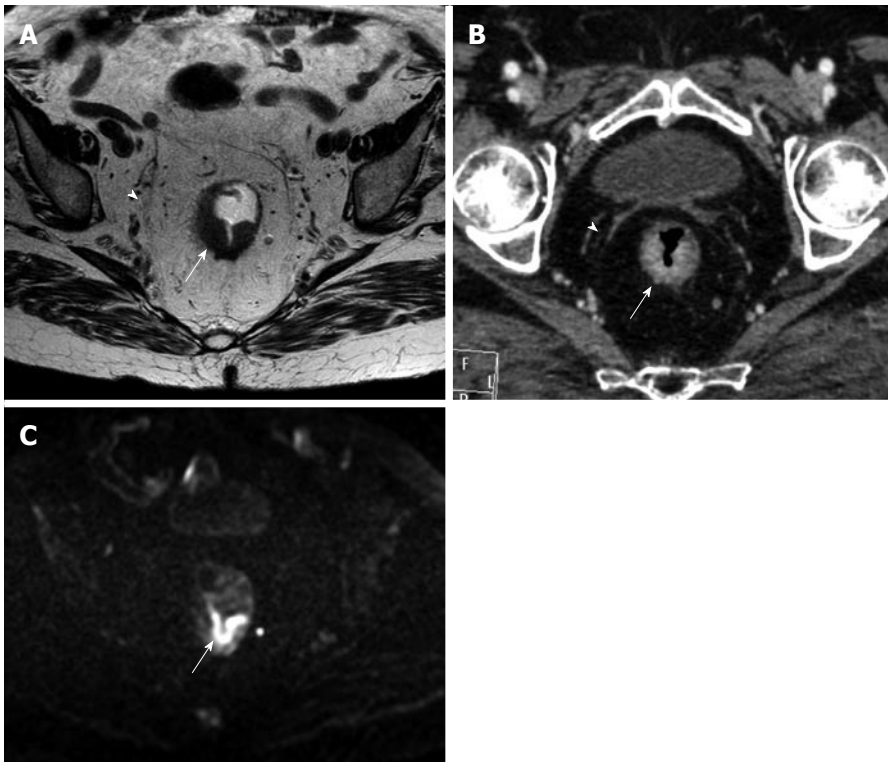

Figure 3 Images obtained in an 86 year-old woman with middle rectal cancer. A: Orthogonal axial high-resolution T2-weighted MR image shows the tumor as a thickening (arrow) along the posterior aspect of the rectum, infiltrating through the muscularis propria (the band of proper muscle layer (*) is destroyed) into the mesorectal fat. The mesorectal fascia is seen as a thin hypointense line (arrowhead) surrounding the mesorectal fat; B: Multiplanar reconstruction (MPR) para-axial contrast enhanced computed tomography image of the same patient shows the tumour as an irregular mural thickening of the posterior rectal wall with spiculations extending into the peri-rectal fat. The mesorectal fascia is well defined and not involved (arrowhead); C: DWIBS image (*b*-value 1000), the tumor (arrow) is clearly recognizable as high signal in comparison with the lower signal intensity of the normal rectal wall.

Table 1 Summarizing table of number of patient correctly staged with multiplanar reconstruction and axial computed tomography images in comparison of magnetic resonance imaging

Image analysis	TN[1]	FN[2]	TP[3]	FP[4]	TOT[5]
CT-axial	30	10	41	10	91
CT-MPR	35	6	45	5	91
MRI	40		51		91

[1]TN: True negative. Number of patients in which the MRF was correctly considered not involved with axial and MPR imaging according to MRI; [2]FN: False negative. Number of patients in which the MRF was wrongly not considered involved with axial and MPR imaging, but it was with MRI; [3]TP: True positive. Number of patients in which the MRF was correctly considered involved with axial and MPR imaging according to MRI; [4]FP: False positive. Number of patients in which the MRF was wrongly considered involved with axial and MPR imaging, but it wasn't with MRI; [5]TOT: Total of patients. CT: Computed tomography; MPR: Multiplanar reconstruction; MRI: Magnetic resonance imaging.

DWIBS allowed to recognize the tumor as a focal mass with high signal intensity on high b-value images, compared with the signal of the normal adjacent rectal wall or with the lower tissue signal intensity background (Figures 1, 3 and 4).

The overall correlation of MPR and native axial findings with the MR images demonstrated (Table 1) that the number of patients correctly staged by evaluating the native axial images was 71 out of 91 patients (41 true positive, TP; 30 true negative, TN), while by using the MPR a total of 80 patients were correctly staged (45 TP and 35 TN) (Figure 4).

The number of false negative (FN) for axial and MPR was respectively 10 FN and 6 FN. The results obtained in our series of patients show an overall good diagnostic value of CT technique: considering the native axial CT images, the overall sensitivity and specificity were respectively 80.4% and 75%, PPV was 80.4%, NPV 75% and Accuracy was 78%. While analyzing the MPR images the sensitivity raised up to 88% and specificity up to 87.5%, PPV was 90%, NPV 85.36% and accuracy raise up to 88% (Table 2). The difference in performance between axial and MPR images was not statistically significant, in terms of sensitivity and specificity (McNemar test with $P = 0.22$ and $P = 0.13$ respectively) (Table 3), but considering the overall diagnostic accuracy, in terms of MRF involvement, the MPR images demonstrated to be superior ($P = 0.02$) in comparison with native axial images alone, as compared to the reference MR images (Table 4).

DISCUSSION

To date, only few studies[1,4,16,17,21,23,24] analyzed the role

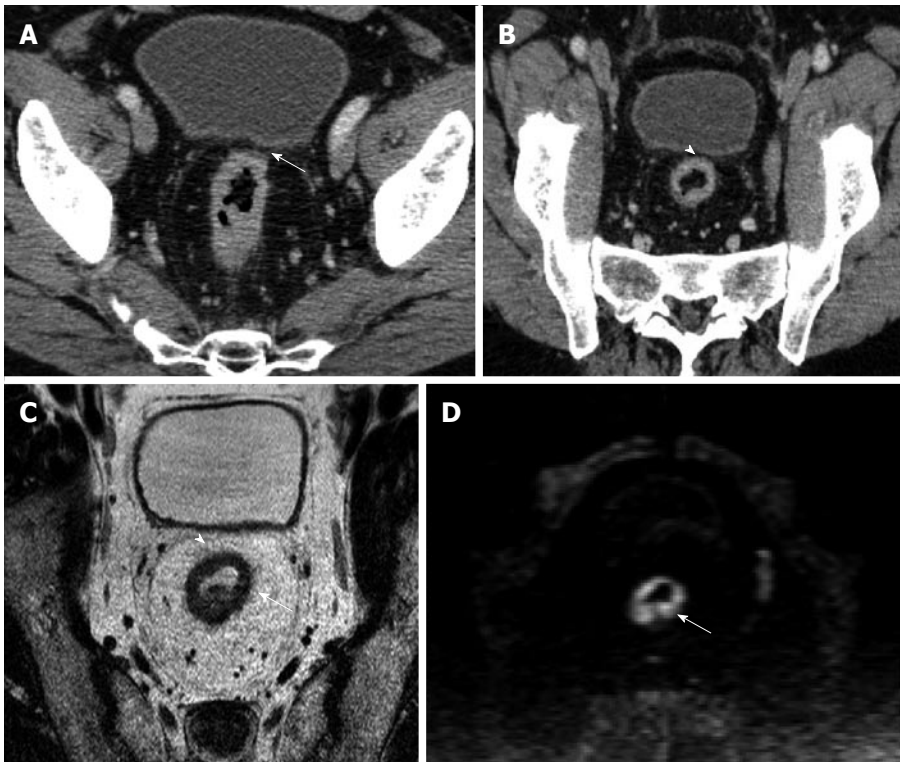

Figure 4 Images obtained in a 68 years-old man with high rectal cancer. A: Axial computed tomography (CT) image shows a tumor as a circumferential thickening in the bowel wall; in the anterior wall (arrow) the tumor seems to involve the mesorectal fascia (MRF); B: Multiplanar reconstruction CT images shows a visible fat line between the tumor and the MRF (arrowhead); C: Axial T2-weighted magnetic resonance image shows a rectal wall involvement by the tumor but also a wide fat pad between the tumor and the free MRF; D: DWIBS image (*b*-value 1000), the tumor is depicted as a high signal circumferential thickening of the bowel wall, in comparison with the lower signal intensity of surrounding tissue.

Table 2 Summarizing table of sensitivity, specificity, positive predictive value, negative predicting value and accuracy of axial and multiplanar reconstruction computed tomography images in correctly identify the involvement of the mesorectal fascia in comparison of magnetic resonance imaging

Axial CT images				
Sensitivity	Specificity	PPV	NPV	Accuracy
80.40%	75%	80.4%	75%	78%
MPR CT images				
Sensitivity	Specificity	PPV	NPV	Accuracy
88%	87.5%	90%	85.36%	88%

CT: Computed tomography; PPV: Positive predictive value; NPV: Negative predicting value; MRF: Mesorectal fascia; MRI: Magnetic resonance imaging.

Table 3 Summarizing table of McNemar test calculation to determine the statistical significant of sensitivity and specificity between axial and multiplanar reconstruction computed tomography images in comparison to magnetic resonance imaging

	Axial- subjects	Axial+ subjects	Total of subjects with MRI+
Sensitivity[1] (P = 0.22)			
MPR- subjects	5	1	6
MPR+ subjects	5	40	45
Total subjects of MRI+	10	41	51[n]
	AXIAL- subjects	AXIAL+ subjects	Total of subjects with MRI-
Specificity[2] (P = 0.13)			
MPR- subjects	29	6	35
MPR+ subject	1	4	5
Total of subjects with MRI-	30	10	40[n]

McNemar test: 2 × 2 contingency table, which tabulates the outcomes of the two tests (axia CT and MPR images) on a sample of n subjects (respectively 51 who were positive with MRI and 40 who were negative). [1]P = 0.22, two tails, not statistically significant; [2]P = 0.13, two tails, not statistically significant. CT: Computed tomography; MRI: Magnetic resonance imaging.

of MDCT as possible and reliable imaging technique in assessment of MRF invasion by rectal cancer. According to recent literature[25], the appropriate angulation of the axial plane orthogonal to the tumor is essential in primary tumor staging, since incorrect plane obliquity leads to a pseudospiculated appearance that may lead to overstaging (Figures 2 and 4). Placement of the orthogonal plane is based on the definition of the tumor on sagittal T2-weighted images.

DWIBS are usually performed in pre-operative rectal cancer staging[22,25] in order to improve the detection and localization of rectal tumors, especially when the tumor is difficult to visualize with other sequences[25]. While these sequences have no role in the assessment of mesorectal fascia involvement, due to the intrinsic limitations of MRF visualization

Table 4 Summarizing table of McNemar test calculation to determine the statistical significant of accuracy between axial and multiplanar reconstruction computed tomography images in comparison to magnetic resonance imaging

	Uncorrect subjects staged with AX/MPR CT images	Correct subjects staged with AX/MPR CT images	Total of correct subjects staged with MRI
Accuracy[1] ($P = 0.02$)			
Uncorrect subjects staged with MPR/AX	9	2	11
Correct subjects staged with MPR/AX	11	69	80
Total of correct subjects staged with MRI	20	71	91

McNemar test: 2 × 2 contingency table, which tabulates the outcomes of the two tests (axial CT and MPR images) on a sample of n subjects (91 correct staged with MRI). [1]$P = 0.02$, two tails, statistically significant. MPR: Multiplanar reconstruction; MRI: Magnetic resonance imaging; CT: Computed tomography.

at high b-values. While the DWIBS are frequently employed in restaging of rectal cancer patients, due to the possibilities to offer information about structures of biologic tissue through water proton mobility, and suggested as a possible tool to monitor the response of tumor tissue after therapy[22,25].

Several problems frequently arise during this critical initial step, due to motion artifacts, small tumor size, low contrast between the tumor and the rectal wall on fast relaxation fast spin-echo (FSE) T2-weighted images, redundancy and tortuosity of the rectum. In addition, nodes along the pelvic sidewall and superior rectal vessels may fall outside the FOV of axial high-resolution images.

In this setting the clinical use of MDCT images combined with MPR along the different axis of rectal lumen, permits to overcoming some of these limitations, having also the possibility to include a large FOV and modify the different perpendicular axial plane in a less time consuming analysis in order to evaluate the tumor axis (also in case of tortuosity and redundancy of the rectum), the MRF involvement and distant lymph-nodes sites. Moreover the new generation multidetector row CT scanner permits to increase the spatial resolution, offering high detailed images combined with short acquisition time and avoiding or reducing possible motion artifacts. Unfortunately, for small size rectal tumor, there's a lower contrast between the tumor and the rectal wall using CT images compared to MR images, especially if combined with use of DWIBS.

A recent survey of United Kingdom practice has revealed that less than 50% of patients were offered MR staging and up to 80% of patients who do not undergo MR staging have a CT examination[1]. The results obtained in this study may help to establish MDCT as an effective diagnostic technique in the evaluation of preoperative local staging of rectal cancer[3].

In our study we compared the diagnostic capability of MDCT images, with new generation of multi-row scanner, in the prediction of MRF involvement by rectal cancer, by evaluating native axial images and MPRs, as compared with MR images as reference standard[1,4,16,23]. In our series of patients a good diagnostic quality was achieved for both series of CT images, obtaining an accuracy of 78% for pure axial images and 88% for MPR (difference statistically significant, $P = 0.02$), while the sensitivity of pure axial images was 80.4% and these results arise to 88% with MPR. Previous studies reported high accuracy rates for CT[3,17,21], however, most patients in these early series had advanced disease[3,26]. In more recent reports, a less satisfactory results have been obtained, with accuracy rates ranging between 41% and 82%[3,4,16,24] in rectal cancer. Those results, probably, were related to the limited spatial collimation and insufficient reconstructions increments used in CT-protocol (*i.e.*, thickening from 5 to 10 mm, no MPRs)[4,16,25] as well as the absence of standardized contrast agent injection protocol. Therefore, the spatial resolution of the scans was too low to make any reliable predictions on margin involvement, especially if compare with MR protocol (assumed with 3 mm thickness and with different orientation of the axial plane)[16,23,27]. In comparison with previous studies we obtained an higher PPV (90%); this result could be explained by the use of thinner slices (2 mm), increasing consequently the spatial resolution, close to MR images protocol (3 mm). The employed protocol, 2 mm thickness and 1 mm of increment, offers reliable results comparable with MR images, especially with the use of MPR.

Our findings are more similar to those of Shina[1] that found an accuracy rate in predicting the involvement of mesorectal fascia in comparison with histopathology of 96.5% and 91.2% on MPR and axial images, respectively. Multiplanar reconstructions images in addiction to axial images significantly improve the diagnostic accuracy in image interpretation ($P = 0.02$), even if the difference of sensitivity and specificity between axial images and MPR not reach the statistical significant ($P > 0.05$). In the study of Matsuoka[28] the accuracy of MDCT (4 slices, 5 mm thickness) and MRI was assessed using the histopatology as gold standard, with equal results between CT and MRI in the preoperative local staging of rectal carcinoma. In our series of patients the NPV of MDCT was 75% for axial images and 85.36% for MPRs, with specificity of 75% and 87.5% respectively.

One of the limitations of this study is represented by the use of MRI as reference standard, rather than histology, although this comparison is virtually impossible since patients with a MRF involvement are currently treated with long courses of chemoradiation therapy[4,29]. In addiction we did not perform any luminal distention on CT images and this could

explaining some discrepancies of finally rectal cancer findings, between CT and MRI analysis. Another limitation of CT images is represented by the fact that in patients with small amounts of peri-rectal fat, the identification of the true extramural extension is more challenging due to smaller tissue interfaces, causing a higher rate of mistakes in assessment of involvement of the MRF. In our series, we did not considered the BMI of the patient as well as the amount of peri-rectal fat, in order to obtain a reliable data about sensitivity of CT images, in daily current clinical practice.

Moreover, as well known, CT-images do not allow accurate differentiation of different bowel layers, as compared with MRI, but the involvement of the MRF represents the main aim of rectal cancer imaging, since the MRF involvement determines the distinction between primary resectable and locally advanced tumors[1].

In conclusion, despite these limitations the CT imaging of rectal cancer patients with new generation MDCT scanner, demonstrated high sensitivity and high accuracy in assessment of MRF involvement, especially with the use of MPRs, and would become a potential one-step imaging tool. CT imaging could be useful as making decision therapy process during a whole-body staging workup, allowing accurate distant rectal staging and local involvement of the MRF in a single examination.

COMMENTS

Background

Treatment options in rectal cancer are total mesorectal excision (TME) or preoperative neoadjuvant radiochemotherapy in patients with locally advanced rectal cancer (LARC). One of the most important features of local rectal cancer staging is the assessment of the tumor relationship with the mesorectal fascia (MRF), which defines the circumferential resection margin (CRM) in TME surgery. To date MR imaging investigation is used for local staging and to identifying patients who may benefit from preoperative chemotherapy-radiation therapy (patients in which the MRF and the CRM could be involved by the tumor). However not all patients can undergo MRI because of claustrophobia or the presence of metal in patients' bodies; moreover MRI has the downside of limited availability, relatively long image acquisition time and high cost. Another important factor in the preoperative assessment of primary rectal cancer is the frequent presence of distant disease at the time of diagnosis, which are assessed, routinely, with CT. For these reasons, the use of MDCT for local staging and distant metastases evaluation could offer high detailed images combined with low cost and short acquisition time.

Research frontiers

New generation of high row number MDCT scans allow thin-collimation, high spatial resolution and better multiplanar reconstructions (MPRs). MPR images can be aligned parallel or perpendicular to the axis of the tumor similar to MR imaging and can be useful for predicting tumor infiltration of the MRF in local staging of rectal cancer. Therefore MDCT can assess in a single examination, the entire abdomen, pelvis and chest, allowing for local staging and distant metastases evaluation.

Innovations and breakthroughs

Considering the variability among the results in previous studies, the actual evidence suggests that old CT protocol, having a limited spatial collimation, an insufficient reconstructions increments and poor MPRs, could not be used for local staging in rectal cancer. New generation MDCT scanner used in modern clinical practice, with high sensitivity and high accuracy in assessment of MRF involvement, would become a potential one-step imaging tool for distant rectal cancer staging and local involvement of the MRF.

Applications

The importance of this work relies on the possibility to offer, in a single step examination, a new diagnostic approach (performed with new generation MDCT,) that allows the non-invasive evaluation of MRF involvement in local rectal staging, as well as the assessment of distant metastases using high detailed images of the entire abdomen, pelvis and chest. Moreover in this manuscript the authors compared and commented our results with those of previous literature on this field by using the two different techniques modalities (*i.e.*, CT and MRI).

Terminology

TME is a surgical technique that entails en bloc resection of the primary tumor and the mesorectum by means of dissection along the mesorectal fascial plane or the CRM. MDCT are new generation of CT with high number of detector, which allow to obtain high spatial resolution images with thinner collimation. MPR is multiplanar reconstructions of the images are images obtained after a post-processing of native axial CT images. Thanks to high collimation of MDCT, all pure axial images can be orientated along different planes (*i.e.*, coronal, sagittal, and oblique axis). MRF is mesorectal fascia, surrounds the mesorectal fat around the rectum. The mesorectal fascia runs along the anterior aspect of the sacrum, where it fuses with the presacral fascia, and then laterally on either side of the rectum. Anteriorly in males, it forms a dense band of connective tissue posterior to the seminal vesicle and prostate gland (the Denonvilliers fascia). The MRF is critical for surgical planning in TME. On T2-weighted images appears as a thin hypointense line surrounding the meserectal fat. On CT images is depicted as a thin line surrounding the mesorectal fat with similar density to the muscles.

Peer-review

Congratulations for the article. Often in daily clinic are situations where you can not perform an MRI either clinical or resource problems. Having information like that concludes this article endorse the decisions of physicians to such situations and allow proper staging of patients.

REFERENCES

1 **Sinha R**, Verma R, Rajesh A, Richards CJ. Diagnostic value of multidetector row CT in rectal cancer staging: comparison of multiplanar and axial images with histopathology. *Clin Radiol* 2006; **61**: 924-931 [PMID: 17018304 DOI: 10.1016/j.crad.2006.03.019]

2 **Quirke P**, Durdey P, Dixon MF, Williams NS. Local recurrence of rectal adenocarcinoma due to inadequate surgical resection. Histopathological study of lateral tumour spread and surgical excision. *Lancet* 1986; **2**: 996-999 [PMID: 2430152 DOI: 10.1016/S0140-6736(86)92612-7]

3 **Kulinna C**, Eibel R, Matzek W, Bonel H, Aust D, Strauss T, Reiser M, Scheidler J. Staging of rectal cancer: diagnostic potential of multiplanar reconstructions with MDCT. *AJR Am J Roentgenol* 2004; **183**: 421-427 [PMID: 15269036 DOI: 10.2214/ajr.183.2.1830421]

4 **Vliegen R**, Dresen R, Beets G, Daniels-Gooszen A, Kessels A, van Engelshoven J, Beets-Tan R. The accuracy of Multi-detector row CT for the assessment of tumor invasion of the mesorectal fascia in primary rectal cancer. *Abdom Imaging* 2008; **33**: 604-610 [PMID: 18175167 DOI: 10.1007/s00261-007-9341-y]

5 **Quirke P**, Dixon MF. The prediction of local recurrence in rectal adenocarcinoma by histopathological examination. *Int J Colorectal Dis* 1988; **3**: 127-131 [PMID: 3045231 DOI: 10.1007/BF01645318]

6 **Nagtegaal ID**, Marijnen CA, Kranenbarg EK, van de Velde CJ, van Krieken JH. Circumferential margin involvement is still an important predictor of local recurrence in rectal carcinoma: not one millimeter but two millimeters is the limit. *Am J Surg Pathol* 2002; **26**: 350-357 [PMID: 11859207 DOI: 10.1097/00000478-200203000-00009]

7 **Blomqvist L**, Holm T, Nyrén S, Svanström R, Ulvskog Y, Iselius L. MR imaging and computed tomography in patients with rectal

tumours clinically judged as locally advanced. *Clin Radiol* 2002; **57**: 211-218 [PMID: 11952317 DOI: 10.1053/crad.2001.0736]

8 **Beets-Tan RG**, Beets GL, Borstlap AC, Oei TK, Teune TM, von Meyenfeldt MF, van Engelshoven JM. Preoperative assessment of local tumor extent in advanced rectal cancer: CT or high-resolution MRI? *Abdom Imaging* 2000; **25**: 533-541 [PMID: 10931993 DOI: 10.1007/s002610000086]

9 **Hadfield MB**, Nicholson AA, MacDonald AW, Farouk R, Lee PW, Duthie GS, Monson JR. Preoperative staging of rectal carcinoma by magnetic resonance imaging with a pelvic phased-array coil. *Br J Surg* 1997; **84**: 529-531 [PMID: 9112909]

10 **Heriot AG**, Grundy A, Kumar D. Preoperative staging of rectal carcinoma. *Br J Surg* 1999; **86**: 17-28 [PMID: 10027354 DOI: 10.1046/j.1365-2168.1999.00996.x]

11 **Goldman S**, Arvidsson H, Norming U, Lagerstedt U, Magnusson I, Frisell J. Transrectal ultrasound and computed tomography in preoperative staging of lower rectal adenocarcinoma. *Gastrointest Radiol* 1991; **16**: 259-263 [PMID: 1879647 DOI: 10.1007/BF01887361]

12 **Heo SH**, Kim JW, Shin SS, Jeong YY, Kang HK. Multimodal imaging evaluation in staging of rectal cancer. *World J Gastroenterol* 2014; **20**: 4244-4255 [PMID: 24764662 DOI: 10.3748/wjg.v20.i15.4244]

13 **Dewhurst C**, Rosen MP, Blake MA, Baker ME, Cash BD, Fidler JL, Greene FL, Hindman NM, Jones B, Katz DS, Lalani T, Miller FH, Small WC, Sudakoff GS, Tulchinsky M, Yaghmai V, Yee J. ACR Appropriateness Criteria pretreatment staging of colorectal cancer. *J Am Coll Radiol* 2012; **9**: 775-781 [PMID: 23122343 DOI: 10.1016/j.jacr.2012.07.025]

14 **Bipat S**, Glas AS, Slors FJ, Zwinderman AH, Bossuyt PM, Stoker J. Rectal cancer: local staging and assessment of lymph node involvement with endoluminal US, CT, and MR imaging--a meta-analysis. *Radiology* 2004; **232**: 773-783 [PMID: 15273331 DOI: 10.1148/radiol.2323031368]

15 **Samee A**, Selvasekar CR. Current trends in staging rectal cancer. *World J Gastroenterol* 2011; **17**: 828-834 [PMID: 21412492 DOI: 10.3748/wjg.v17.i7.828]

16 **Wolberink SV**, Beets-Tan RG, de Haas-Kock DF, van de Jagt EJ, Span MM, Wiggers T. Multislice CT as a primary screening tool for the prediction of an involved mesorectal fascia and distant metastases in primary rectal cancer: a multicenter study. *Dis Colon Rectum* 2009; **52**: 928-934 [PMID: 19502858 DOI: 10.1007/DCR.0b013e318194f923]

17 **Ahmetoğlu A**, Cansu A, Baki D, Kul S, Cobanoğlu U, Alhan E, Ozdemir F. MDCT with multiplanar reconstruction in the preoperative local staging of rectal tumor. *Abdom Imaging* 2011; **36**: 31-37 [PMID: 19949791 DOI: 10.1007/s00261-009-9591-y]

18 **Beets-Tan RG**, Lambregts DM, Maas M, Bipat S, Barbaro B, Caseiro-Alves F, Curvo-Semedo L, Fenlon HM, Gollub MJ, Gourtsoyianni S, Halligan S, Hoeffel C, Kim SH, Laghi A, Maier A, Rafaelsen SR, Stoker J, Taylor SA, Torkzad MR, Blomqvist L. Magnetic resonance imaging for the clinical management of rectal cancer patients: recommendations from the 2012 European Society of Gastrointestinal and Abdominal Radiology (ESGAR) consensus meeting. *Eur Radiol* 2013; **23**: 2522-2531 [PMID: 23743687 DOI: 10.1007/s00330-013-2864-4]

19 **van de Velde CJ**, Boelens PG, Borras JM, Coebergh JW, Cervantes A, Blomqvist L, Beets-Tan RG, van den Broek CB, Brown G, Van Cutsem E, Espin E, Haustermans K, Glimelius B, Iversen LH, van Krieken JH, Marijnen CA, Henning G, Gore-Booth J, Meldolesi E, Mroczkowski P, Nagtegaal I, Naredi P, Ortiz H, Påhlman L, Quirke P, Rödel C, Roth A, Rutten H, Schmoll HJ, Smith JJ, Tanis PJ, Taylor C, Wibe A, Wiggers T, Gambacorta MA, Aristei C, Valentini V. EURECCA colorectal: multidisciplinary management: European consensus conference colon & amp; rectum. *Eur J Cancer* 2014; **50**: 1.e1-1.e34 [PMID: 24183379 DOI: 10.1016/j.ejca.2013.06.048]

20 **Raman SP**, Chen Y, Fishman EK. Evolution of imaging in rectal cancer: multimodality imaging with MDCT, MRI, and PET. *J Gastrointest Oncol* 2015; **6**: 172-184 [PMID: 25830037 DOI: 10.3978/j.issn.2078-6891.2014.108]

21 **Dar RA**, Chowdri NA, Parray FQ, Shaheen F, Wani SH, Mushtaque M. Pre-operative staging of rectal cancer using multi-detector row computed tomography with multiplanar reformations: single center experience. *Indian J Cancer* 2014; **51**: 170-175 [PMID: 25104203 DOI: 10.4103/0019-509X.138292]

22 **Monguzzi L**, Ippolito D, Bernasconi DP, Trattenero C, Galimberti S, Sironi S. Locally advanced rectal cancer: value of ADC mapping in prediction of tumor response to radiochemotherapy. *Eur J Radiol* 2013; **82**: 234-240 [PMID: 23122748 DOI: 10.1016/j.ejrad.2012.09.027]

23 **Wolberink SV**, Beets-Tan RG, de Haas-Kock DF, Span MM, van de Jagt EJ, van de Velde CJ, Wiggers T. Conventional CT for the prediction of an involved circumferential resection margin in primary rectal cancer. *Dig Dis* 2007; **25**: 80-85 [PMID: 17384512 DOI: 10.1159/000099174]

24 **Maizlin ZV**, Brown JA, So G, Brown C, Phang TP, Walker ML, Kirby JM, Vora P, Tiwari P. Can CT replace MRI in preoperative assessment of the circumferential resection margin in rectal cancer? *Dis Colon Rectum* 2010; **53**: 308-314 [PMID: 20173478 DOI: 10.1007/DCR.0b013e3181c5321e]

25 **Kaur H**, Choi H, You YN, Rauch GM, Jensen CT, Hou P, Chang GJ, Skibber JM, Ernst RD. MR imaging for preoperative evaluation of primary rectal cancer: practical considerations. *Radiographics* 2014; **32**: 389-409 [PMID: 22411939 DOI: 10.1148/rg.322115122]

26 **Maier A**, Fuchsjäger M. Preoperative staging of rectal cancer. *Eur J Radiol* 2003; **47**: 89-97 [PMID: 12880989]

27 **Taylor A**, Slater A, Mapstone N, Taylor S, Halligan S. Staging rectal cancer: MRI compared to MDCT. *Abdom Imaging* 2012; **32**: 323-327 [PMID: 16967240 DOI: 10.1007/s00261-006-9081-4]

28 **Matsuoka H**, Nakamura A, Masaki T, Sugiyama M, Takahara T, Hachiya J, Atomi Y. A prospective comparison between multidetector-row computed tomography and magnetic resonance imaging in the preoperative evaluation of rectal carcinoma. *Am J Surg* 2003; **185**: 556-559 [PMID: 12781885 DOI: 10.1016/S0002-9610(03)00067-9]

29 **Aljebreen AM**, Azzam NA, Alzubaidi AM, Alsharqawi MS, Altraiki TA, Alharbi OR, Almadi MA. The accuracy of multi-detector row computerized tomography in staging rectal cancer compared to endoscopic ultrasound. *Saudi J Gastroenterol* 2013; **19**: 108-112 [PMID: 23680707 DOI: 10.4103/1319-3767.111950]

P- Reviewer: Palacios-Eito A, Razek AA **S- Editor**: Yu J
L- Editor: A **E- Editor**: Wang CH

World Journal of Gastroenterology

Submit a Manuscript: http://www.wjgnet.com/esps/
Help Desk: http://www.wjgnet.com/esps/helpdesk.aspx
DOI: 10.3748/wjg.v22.i20.4901

World J Gastroenterol 2016 May 28; 22(20): 4901-4907
ISSN 1007-9327 (print) ISSN 2219-2840 (online)

ORIGINAL ARTICLE

Retrospective Study

Clinical and *ABCB11* profiles in Korean infants with progressive familial intrahepatic cholestasis

Ji Sook Park, Jae Sung Ko, Jeong Kee Seo, Jin Soo Moon, Sung Sup Park

Ji Sook Park, Jae Sung Ko, Jeong Kee Seo, Jin Soo Moon, Department of Pediatrics, Seoul National University College of Medicine, Seoul 110-799, South Korea

Sung Sup Park, Department of Laboratory Medicine, Seoul National University College of Medicine, Seoul 110-799, South Korea

Ji Sook Park, Department of Pediatrics, Gyeongsang National University School of Medicine, Jinju, Gyeongnam 660-702, South Korea

Author contributions: Ko JS and Moon JS designed the study; Park SS performed the genetic analyses; Park JS and Seo JK collected and analyzed the clinical data and wrote the paper.

Institutional review board statement: This study was carried out after obtaining the clearance from the ethical board of the hospital (GNUH 2015-09-004-001).

Conflict-of-interest statement: There was no conflict of interest among the authors.

Correspondence to: Jeong Kee Seo, MD, PhD, Department of Pediatrics, Seoul National University College of Medicine, Daehak-ro, Jongno-gu, Seoul 110-799, South Korea. jkseo@snu.ac.kr
Telephone: +82-2-20723778
Fax: +82-2-20723917

Received: January 19, 2016
Peer-review started: January 20, 2016
First decision: February 18, 2016
Revised: February 29, 2016
Accepted: March 14, 2016
Article in press: March 14, 2016
Published online: May 28, 2016

Abstract

AIM: To investigate clinical profiles and mutations of *ABCB11* in Koreans with progressive familial intrahepatic cholestasis 2 and review the differences between Koreans and others.

METHODS: Of 47 patients with neonatal cholestasis, five infants had chronic intrahepatic cholestasis with normal γ-glutamyl transpeptidase. Direct sequencing analyses of *ABCB11*, including exons and introns, were performed from peripheral blood.

RESULTS: Living donor-liver transplantation was performed in four patients because of rapidly progressive hepatic failure and hepatocellular carcinoma. Three missense mutations were found in two patients: compound heterozygous 677C>T (S226L)/3007G>A (G1003R) and heterozygous 2296G>A (G766R). The mutations were located near and in the transmembranous space.

CONCLUSION: Alterations in the transmembrane of the bile salt export pump in the Korean infants were different from those previously reported in Chinese, Japanese, Taiwanese, and European patients.

Key words: Hepatocellular carcinoma; Progressive familial intrahepatic cholestasis; *ABCB11*; Bile salt export pump

Core tip: Reports of progressive familial intrahepatic cholestasis (PFIC) mutations in Asian countries have been less than those in Western countries because of time consuming and expensive diagnostic tools. Recently, reports on mutations of *ABCB11* in Asian patients with PFIC have been increasing. In this study, the authors report mutations of *ABCB11* in Korean infants with PFIC2 and compare Korean mutations with previously reported mutations.

Park JS, Ko JS, Seo JK, Moon JS, Park SS. Clinical and *ABCB11* profiles in Korean infants with progressive familial intrahepatic cholestasis. *World J Gastroenterol* 2016; 22(20): 4901-4907 Available from: URL: http://www.wjgnet.com/1007-9327/full/v22/i20/4901.htm DOI: http://dx.doi.org/10.3748/wjg.v22.i20.4901

INTRODUCTION

Progressive familial intrahepatic cholestasis (PFIC) is an autosomal recessive disorder that manifests as cholestasis during the neonatal period due to defective bile secretion. PFIC is divided into types 1, 2, and 3 according to their different clinical manifestations and genetics. In PFIC1 and PFIC2, cholestasis develops during the neonatal period, and γ-glutamyl transpeptidase (GGT) is within normal limits. PFIC3 develops later than PFIC1 and PFIC2, and features a positive prenatal history of maternal cholestasis. Generally, cholestasis with elevated GGT is associated with PFIC3 rather than PFIC1 and PFIC2. Persistent or repetitive cholestasis develops within 1 year of age and rapidly progresses to liver cirrhosis and hepatic failure in patients with PFIC. Mutations of biliary transporters associated with PFIC have been discovered, which can aid in understanding the diagnosis and pathogenesis. The genes are *ATP8B1, ABCB11,* and *ABCB4,* which encode familial intrahepatic cholestasis 1 protein (FIC1), bile salt export pump (BSEP), and multidrug resistance protein 3 (MDR3) in PFIC1, 2, and 3, respectively.

ABCB11 is located on chromosome 2q24. It encodes BSEP, which plays a role in the secretion of conjugated bile acids, including taurocholates. BSEP defect can cause cholestasis with a normal range of GGT because of a bile secretion defect[1]. Over 82 different *ABCB11* mutations have been reported[2,3]. Of them, E297G and D482G account for 30% of BSEP mutations in European patients with PFIC2. In Asia, mutations of BSEP in Chinese, Japanese, and Taiwanese patients with PFIC2 were reported[4-7].

To the best of our knowledge, there have been fewer reports of *ABCB11* (BSEP) mutations in Asians with PFIC2 than in Europeans[2,4-7]. Because PFIC2 features rapid progression to liver cirrhosis and hepatic failure within the first decade, rapid diagnosis, management, and prediction of prognosis are important. In the present study, the authors investigated clinical profiles of Korean infants with PFIC and performed a mutation analysis on the *ABCB11* gene. The authors obtained clearance from the ethical board of the hospital (GNUH 2015-09-004-001).

MATERIALS AND METHODS

Patients

Between 2005 and 2006, 47 patients visited the Department of Pediatrics in Seoul National University Children's Hospital for neonatal cholestasis. Examinations included abdominal ultrasonography, duodenal intubation, a hepatobiliary scan, and liver biopsy. Inborn error of metabolism, total parenteral nutrition, drug related cholestasis, congenital infection, and cholestasis secondary to sepsis were excluded. PFIC was suspected based on intrahepatic cholestasis with normal ranged GGT or on the results of the genetic analyses. None had a family history of PFIC.

Genetic analyses

Genetic analyses were performed for diagnosis with parental consent. Direct sequencing analysis of *ABCB11* was done using peripheral blood. Exons and flanking intron sequences of the *ABCB11* gene (NC_000002.10) were amplified by polymerase chain reaction (PCR) from total genomic DNA. PCR products were purified by ExoSAP-IT (USB, Cleveland, OH, United States) and subjected to DNA sequencing using the BigDye v3.1 Terminator Chemistry (PE Applied Biosystems, Foster City, CA, United States), followed by separation on an ABI 3100 DNA sequencer (PE Applied Biosystems). Sequence data were analyzed manually and were assembled with the Seqscape v2.5 (PE Applied Biosystems). As reference control, the *ABCB11* genomic sequence was obtained from http://pharmacogenetics.ucsf.edu/set1/BSEPrefseq.html.

RESULTS

Among the 47 patients with cholestatic jaundice presented during the 2-year period, extrahepatic biliary atresia was diagnosed in eleven, congenital infection with TORCH in four, neonatal intrahepatic cholestasis caused by citrin deficiency in three, arthrogryposis, renal dysfunction, cholestasis (ARC) syndrome in two, neonatal Dubin-Johnson syndrome in two, Alagille syndrome in one, and non-syndromic bile duct paucity in one[8]. PFIC was suspected in five patients with intrahepatic cholestasis and normal GGT. Table 1 summarizes the clinical and laboratory findings of the patients. The chief complaint was cholestatic jaundice in all patients, and onset of the symptom ranged from 20 d to 9 mo after birth. Gallstone was developed in patient 1 and 2, and hepatocellular carcinoma (HCC) was developed in patient 1 (Figure 1). Hepatic pathologic examinations were performed

Table 1 Clinical, laboratory findings and mutations of five infants with progressive familial intrahepatic cholestasis

Patient	Sex	Age of symptom onset	Age at LTx	Associated sign	AST/ALT (IU/L) (0-37/0-41)	T/D. bil (mg/dL) (0-1.2/0-0.5)	GGT (IU/L) (6-71)	AFP (ng/mL) (0-7.0)	Mutations of *ABCB11*
1	F	20 d	24 mo	Gallstone, HCC	602/242	11.3/7.9	29	3070	S226L/ G1003R
2	F	9 mo	10 yr	Gallstone	178/242	8.2/5.2	25	< 5	G776R
3	M	5 d	6 mo	-	416/93	35.1/14	25	21500	No
4	M	1 mo	3.5 mo	-	1467/250	44.5/25.1	50	-	No
5	M	2 mo	-	-	951/677	14.3/8.0	52	770000	No

LTx: Liver transplantation; T/D.bil: Total bilirubin/direct bilirubin; GGT: γ-glutamyl transpeptidase (normal values in brackets; Laboratory values were obtained at initial visits of five cases).

Figure 1 Radiologic hepatic evaluations in patient 1 and 2. A: Abdominal computed tomography of patient 1 revealed two contrast-enhanced hepatic masses (arrows) at 21 mo of age; B: Gallstone and its posterior shadow (circle) were observed on liver ultrasonography in patient 2.

in all patients. Various degrees of periportal fibrosis and inflammatory cell infiltration, canalicular and cytoplasmic bile pigments, cholestasis, and bile ductular dilatation and proliferation were noted in all hepatic specimens of the patients. HCC was confirmed from an excised liver in patient 1 (Figure 2). Living donor liver transplantations were performed in four patients due to hepatic failure between 2.5 mo and 10 years after their initial visits. Three of the 10 alleles examined showed mutations: compound heterozygous 677C>T (S226L)/3007G>T (G1003R) in patient 1 and heterozygous 2296G>A (G776R) in patient 2 (Figure 3). Three of the five patients showed no mutation of *ABCB11*. The PolyPhen program (http://genetics.bwh.harvard.edu/pph2) predicted that S226L is probably benign with a score of 0.175, but the SIFT program (http://sift.jcvi.org) predicted that S226L deleteriously affects protein function. G1003R and G776R were predicted to be probably damaging with scores of 1.000 by the PolyPhen-2 program and to affect deleteriously protein functions. 3007G/T (G1003R) was a novel mutation of *ABCB11*.

DISCUSSION

Three mutations were found in two patients with the PFIC phenotype: 677C>T in exon 8 (S226L) and 3007G>A in exon 23 (G1003R) in patient 1 and 2296G>A in exon 19 (G766R) in patient 2 (Figure 3). Patients with mutations presented with chronic intrahepatic cholestasis with normal GGT from the infantile period, rapidly declining liver functions, gallstone without intravascular hemolysis, and HCC (Table 1, Figures 1-3).

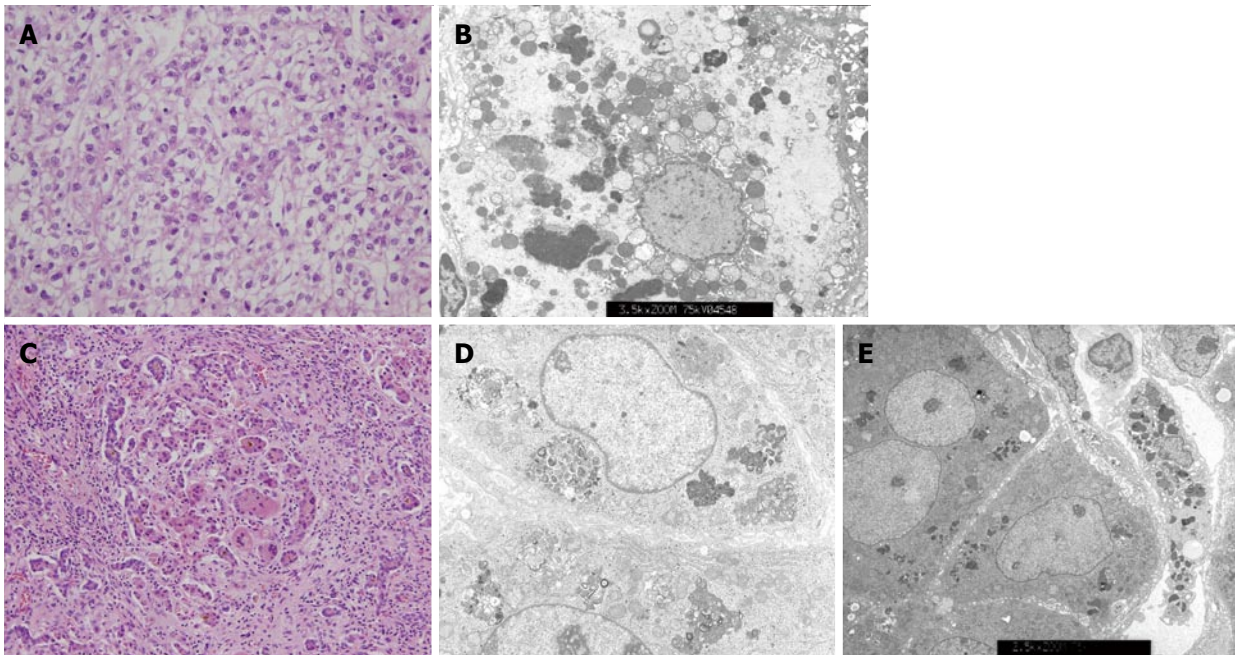

Figure 2 Liver histologic features from infants with chronic intrahepatic cholestasis with normal ranges of γ-glutamyl transpeptidase. A: Hepatocellular carcinoma was confirmed by liver specimen at hepatectomy taken from patient 1 at 24 mo of age. Cellular atypia with trabecular and acinar type was shown. Microvascular invasion was not identified; hematoxylin-eosin stain, original magnification × 400; B: Electron microscopic examination of liver specimen from patient 2 shows many globular or curly appearance electron dense materials in the cytoplasm with original magnification of × 3.5k; C: Liver biopsy at hepatectomy taken at 6 months of age from patient 3 shows periportal fibrosis, inflammatory cell infiltration, intracanalicular bile plugs, giant cell formation, and bile ductular proliferation; hematoxylin-eosin stain, original magnification × 200; D: Electron microscopic examination of liver specimen from patient 4 at 3.5 mo of age reveals amorphous and coarse granular bile pigments in the dilated bile canaliculi. Original magnification × 5.0k; E: Electron microscopic examination of liver specimen from patient 5 shows aggregated bile pigments in the cytoplasm. Original magnification × 2.5k.

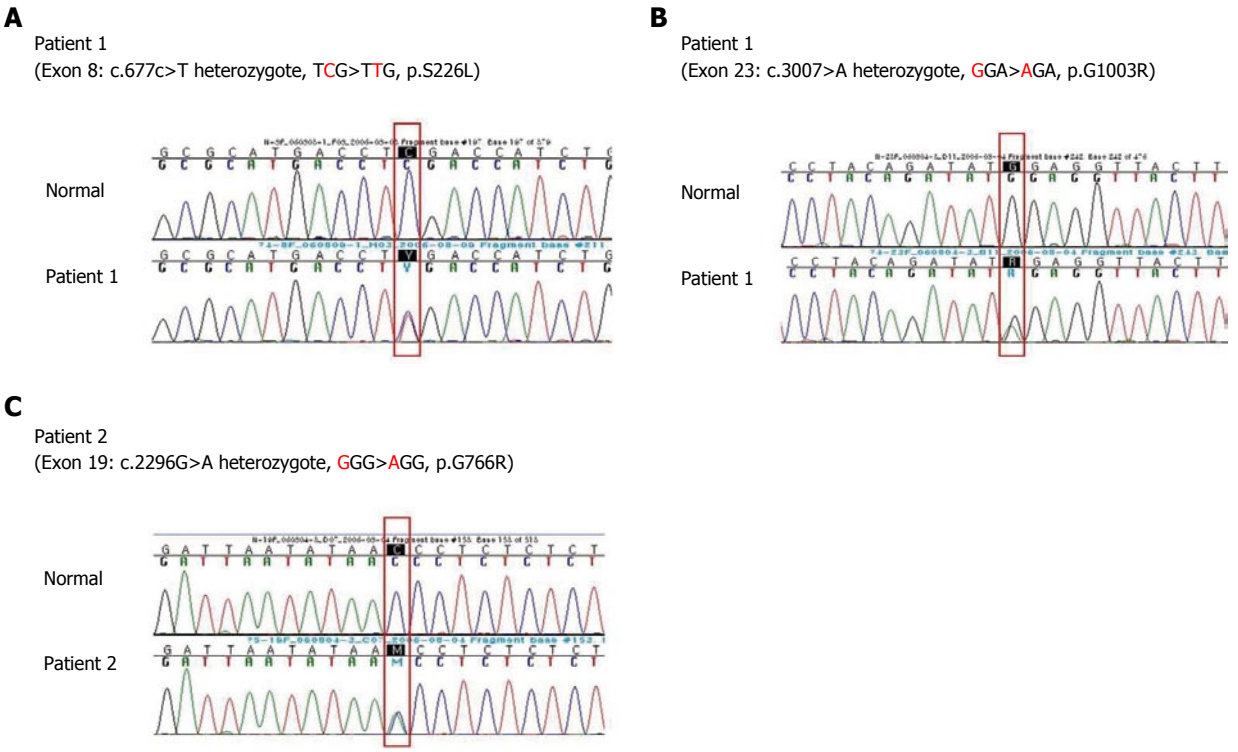

Figure 3 Direct sequencing analysis of the *ABCB11* genes demonstrating (A) heterozygous C to T substitution in exon 8 predicting a missense mutation at amino acid position 226(p.S226L) (B) heterozygous G to A in exon 23 predicting a missense mutation at amino acid position 1003 (p.G1003R), and (C) heterozygous G to A in exon 19 predicting a missense mutation at amino acid position 776(p.G776R), (A) and (B) were detected in *ABCB11* gene of patient 1 and (C) was detected in patient 2.

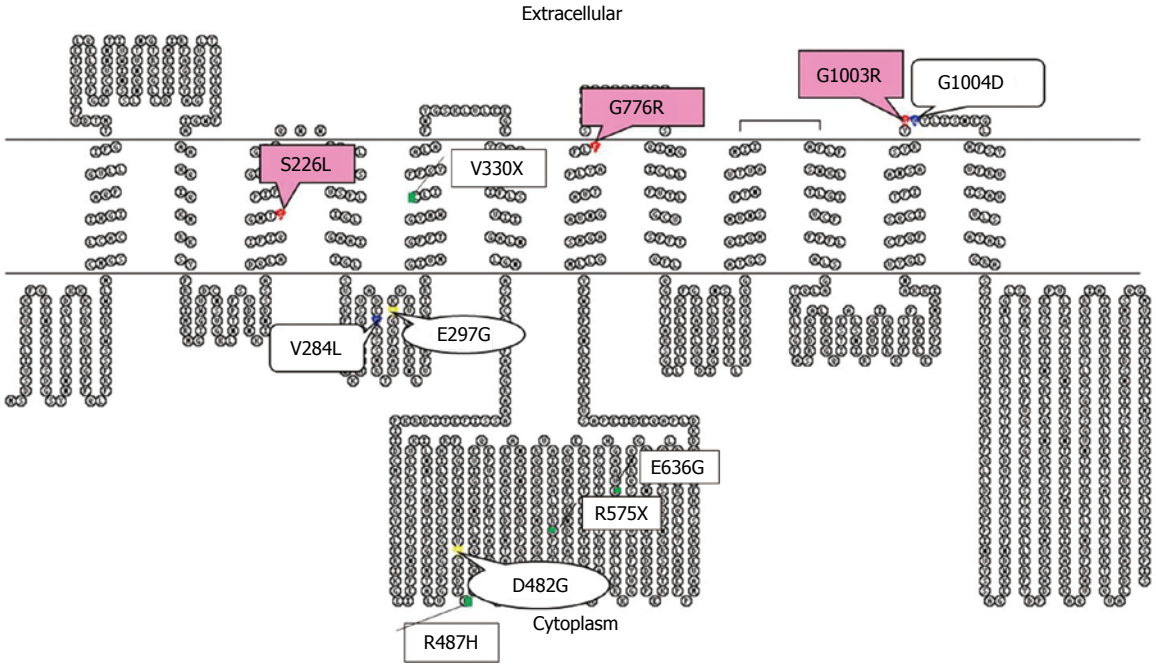

Figure 4 Putative secondary structure of bile salt export pump generated with the TOPO program (http://www.sacs.ucsf.edu/TOPO-run/wtopo.pl). Mutations are represented in red for mutations in patient 1 and 2, green for Japanese, blue for Taiwanese, and yellow for common European mutations. Bile salt export pump alterations in the present study were located at and near the transmembranous space, which was different from most of the mutations from Chinese, Japanese, Taiwanese, and European patients[2,5,7,12].

PFICs are developed by mutations of bile transporters, and the incidence of the mutation has not yet been established[9]. In addition, its incidence might be underestimated in Korea because diagnosis in a patient with suspected PFIC is often time consuming and expensive because of clinical methods such as clinical courses, laboratory findings, pathologic examination, and genetic analysis. Differentiation between PFIC1 and PFIC2 is difficult based on clinical manifestations and pathologic findings because of their marked clinical overlap[1]. PFIC1 patients usually present with more diverse extrahepatic symptoms, including diarrhea, than patients with PFIC2[10]. The patients did not show diarrhea or pruritus, but patient 1 did develop gallstones and HCC.

To the best our knowledge, Asian reports on PFIC2 are relatively lacking in comparison to Western reports[2,4-7]. However, reports on mutations of BSEP in Asian patients with PFIC2 are increasing by denaturing high performance liquid chromatography, high-resolution melting analysis, and direct sequencing. The reported Asian BSEP mutations were as follows: R575X, E636G, R487H, and V330X in Japanese patients; 1 bp deletion (position 1145), V284L, and G1004D in Taiwanese patients; and 20 mutations, including A167T, in Chinese patients[4,7,11,12]. Of the hundreds of BSEP mutations, E297G and D482G were the most common mutations in European patients[13]. Most of the previously reported mutations in Chinese and Europeans are located in the canalicular cytoplasm[2,4,12]. However, three different missense mutations (S226L, G1003R, and G775R) in the present study were located at and near the transmembranous (TM) part of BSEP (Figure 4). The TM alterations of BSEP in Korean infants might be due to ethnic differences. Further study, however, is needed because the number of mutations in the Korean patients with PFIC2 was low.

There was no mutation of *ABCB11* in patient 3, 4, and 5. TPJ2 mutations can also cause a PFIC2 like phenotype and further genetic analyses of TPJ2 are necessary[14]. Patient 5 showed elevated GGT levels and decreased serum total bilirubin in a relatively short clinical course. Therefore, the possibilities of PFIC1 and PFIC2 are less, but careful follow-ups are essential with the possibility of benign recurrent intrahepatic cholestasis.

Compound heterozygotes of 677C>T (S226L) and 3007G>A (G1003R) in patient 1, and one missense mutation of 2296G>A (G766R) in patient 2 were noted (Figure 3). The mutations were predicted to be damaging or deleterious to BSEP, based on the clinical course of the patients and the results of PolyPhen-2 and SIFT program. Unfortunately, the authors could not perform genetic analyses of *ABCB11* of the parents.

HCC developed in patient 1 (Figures 2 and 3A). Knisely *et al*[15] reported BSEP dysfunctions in 10 patients who presented with HCC under the age of 5 years. Chronic intrahepatic bile acids or suppressed DNA ligase by protein dysfunctions were suggested previously[16,17], but specific factors contributing to the development of HCC have not been evident. Cholangiocarcinoma and hepatoblastoma in patients with PFIC2 has also been reported[18,19]. The level of serum alpha fetoprotein (AFP) are high in > 60%

of patients with HCC and hepatoblastoma, and AFP increased markedly to 204000 ng/mL at 21 mo of age in patient 1. In patient 5, a significantly high level of AFP was noted on the first laboratory examination. There was no evidence of hepatic mass on liver ultrasonography (USG) and inborn errors of metabolism on laboratory examination. The level of AFP was decreased to 530000 ng/mL after 1 mo. The decline of AFP and no occurrence of hepatic mass on liver USG could rule out the development of hepatic tumor in patient 5. Therefore, the increment of serum AFP and hepatic imaging can be useful modalities for early detection of hepatic tumors in a patient with PFIC2.

Various degrees of periportal fibrosis, inflammatory cell infiltrates, intracytoplasmic and intracanalicular cholestasis, giant cell transformation, and bile ductular proliferation on the pathologic examinations were noted in the present study (Figure 2). Bile duct paucity or bile ductular proliferation was not a typical finding in patients with PFIC, but pathologic findings might depend on the clinical moment when the biopsy was performed. Pathologic examinations in the present study did not show typical findings for PFIC because our hepatic specimens were obtained at the time of liver transplantation, except in patient 5. Pathologic differentiation from PFIC1 to PFIC2 depends on the severity of the aforementioned findings and characters of canalicular bile salts. Coarse granular bile salts can suggest PFIC1, while amorphous and filiform bile salts under electron microscopic examination can suggest PFIC2[1]. However, pathologic differentiation seems to depend significantly on clinical moments for biopsy and experience or skill of the pathologist.

In conclusion, the present study is the first report on Korean infants with PFIC, including early onset HCC, living donor liver transplantations, and novel mutation and ethnic differences of *ABCB11*. We tentatively suggest the suspicion of PFIC1 or PFIC2 when children are suffering from chronic intrahepatic cholestasis with normal GGT and without other associated anomalies from their infantile periods, regardless of family history. Early genetic analysis for PFIC1 or PFIC2 might be helpful to diagnose, predict prognosis, and make an early treatment plan.

COMMENTS

Background

Because progressive familial intrahepatic cholestasis (PFIC)2 features rapid progression to liver cirrhosis and hepatic failure within the first decade, rapid diagnosis, management, and prediction of prognosis are important. The authors investigated the clinical profiles of Korean infants with PFIC, performed mutation analysis on the *ABCB11* gene, and reviewed the differences between Korean and other previous mutations.

Research frontiers

In the present study, a novel mutation of *ABCB11* in Korean infants with PFIC2 and the sites of amino acid alterations were different from those previously identified in Europeans.

Innovations and breakthroughs

The authors report a rare PFIC2 in Korean patients and its genetic novel mutations. These mutations affected amino acid substitutions of BSEP, and the sites were different from previous reports. The number of mutations, however, was low.

Applications

The described novel mutations of *ABCB11* in Korean infants with PFIC2 might be helpful to understand racial differences in the future. However, further study is warranted, including a larger single nucleotide polymorphism database of Koreans.

Peer-review

There were concerns about the number of mutations in Korean infants with PFIC2. However, the focus of the manuscript is potentially interesting, and the present report is significant because of the rarity in character of PFIC2, especially in Asian groups.

REFERENCES

1 **Harris MJ**, Le Couteur DG, Arias IM. Progressive familial intrahepatic cholestasis: genetic disorders of biliary transporters. *J Gastroenterol Hepatol* 2005; **20**: 807-817 [PMID: 15946126 DOI: 10.1111/j.1400-1746.2005.03743.x]

2 **Strautnieks SS**, Byrne JA, Pawlikowska L, Cebecauerová D, Rayner A, Dutton L, Meier Y, Antoniou A, Stieger B, Arnell H, Ozçay F, Al-Hussaini HF, Bassas AF, Verkade HJ, Fischler B, Németh A, Kotalová R, Shneider BL, Cielecka-Kuszyk J, McClean P, Whitington PF, Sokal E, Jirsa M, Wali SH, Jankowska I, Pawłowska J, Mieli-Vergani G, Knisely AS, Bull LN, Thompson RJ. Severe bile salt export pump deficiency: 82 different ABCB11 mutations in 109 families. *Gastroenterology* 2008; **134**: 1203-1214 [PMID: 18395098 DOI: 10.1053/j.gastro.2008.01.038]

3 **Francalanci P**, Giovannoni I, Candusso M, Bellacchio E, Callea F. Bile salt export pump deficiency: A de novo mutation in a child compound heterozygous for ABCB11. Laboratory investigation to study pathogenic role and transmission of two novel ABCB11 mutations. *Hepatol Res* 2013; **43**: 315-319 [PMID: 23437912 DOI: 10.1111/j.1872-034X.2012.01061.x]

4 **Hu G**, He P, Liu Z, Chen Q, Zheng B, Zhang Q. Diagnosis of ABCB11 gene mutations in children with intrahepatic cholestasis using high resolution melting analysis and direct sequencing. *Mol Med Rep* 2014; **10**: 1264-1274 [PMID: 24969679 DOI: 10.3892/mmr.2014.2349]

5 **Chen HL**, Liu YJ, Su YN, Wang NY, Wu SH, Ni YH, Hsu HY, Wu TC, Chang MH. Diagnosis of BSEP/ABCB11 mutations in Asian patients with cholestasis using denaturing high performance liquid chromatography. *J Pediatr* 2008; **153**: 825-832 [PMID: 18692205 DOI: 10.1016/j.jpeds.2008.06.034]

6 **Chen ST**, Chen HL, Su YN, Liu YJ, Ni YH, Hsu HY, Chu CS, Wang NY, Chang MH. Prenatal diagnosis of progressive familial intrahepatic cholestasis type 2. *J Gastroenterol Hepatol* 2008; **23**: 1390-1393 [PMID: 18853996 DOI: 10.1111/j.1440-1746.2008.05432.x]

7 **Goto K**, Sugiyama K, Sugiura T, Ando T, Mizutani F, Terabe K, Ban K, Togari H. Bile salt export pump gene mutations in two Japanese patients with progressive familial intrahepatic cholestasis. *J Pediatr Gastroenterol Nutr* 2003; **36**: 647-650 [PMID: 12717091]

8 **Ko JS**, Song JH, Park SS, Seo JK. Neonatal intrahepatic cholestasis caused by citrin deficiency in Korean infants. *J Korean Med Sci* 2007; **22**: 952-956 [PMID: 18162705 DOI: 10.3346/jkms.2007.22.6.952]

9 **Jansen PL**, Strautnieks SS, Jacquemin E, Hadchouel M, Sokal EM, Hooiveld GJ, Koning JH, De Jager-Krikken A, Kuipers F, Stellaard F, Bijleveld CM, Gouw A, Van Goor H, Thompson RJ, Müller M. Hepatocanalicular bile salt export pump deficiency in patients with progressive familial intrahepatic cholestasis. *Gastroenterology* 1999; **117**: 1370-1379 [PMID: 10579978]

10 **Alissa FT**, Jaffe R, Shneider BL. Update on progressive familial intrahepatic cholestasis. *J Pediatr Gastroenterol Nutr* 2008; **46**:

241-252 [PMID: 18376240 DOI: 10.1097/MPG.0b013e3181596060]
11 **Chen HL**, Chang PS, Hsu HC, Ni YH, Hsu HY, Lee JH, Jeng YM, Shau WY, Chang MH. FIC1 and BSEP defects in Taiwanese patients with chronic intrahepatic cholestasis with low gamma-glutamyltranspeptidase levels. *J Pediatr* 2002; **140**: 119-124 [PMID: 11815775 DOI: 10.1067/mpd.2002.119993]
12 **Liu LY**, Wang ZL, Wang XH, Zhu QR, Wang JS. ABCB11 gene mutations in Chinese children with progressive intrahepatic cholestasis and low gamma glutamyltransferase. *Liver Int* 2010; **30**: 809-815 [PMID: 19845854 DOI: 10.1111/j.1478-3231.2009.02112.x]
13 **Hayashi H**, Takada T, Suzuki H, Akita H, Sugiyama Y. Two common PFIC2 mutations are associated with the impaired membrane trafficking of BSEP/ABCB11. *Hepatology* 2005; **41**: 916-924 [PMID: 15791618 DOI: 10.1002/hep.20627]
14 **Carlton VE**, Pawlikowska L, Bull LN. Molecular basis of intrahepatic cholestasis. *Ann Med* 2004; **36**: 606-617 [PMID: 15768832 DOI: 10.1080/07853890410018916]
15 **Knisely AS**, Strautnieks SS, Meier Y, Stieger B, Byrne JA, Portmann BC, Bull LN, Pawlikowska L, Bilezikçi B, Ozçay F, László A, Tiszlavicz L, Moore L, Raftos J, Arnell H, Fischler B, Németh A, Papadogiannakis N, Cielecka-Kuszyk J, Jankowska I, Pawłowska J, Melín-Aldana H, Emerick KM, Whitington PF, Mieli-Vergani G, Thompson RJ. Hepatocellular carcinoma in ten children under five years of age with bile salt export pump deficiency. *Hepatology* 2006; **44**: 478-486 [PMID: 16871584 DOI: 10.1002/hep.21287]
16 **Bernstein H**, Bernstein C, Payne CM, Dvorakova K, Garewal H. Bile acids as carcinogens in human gastrointestinal cancers. *Mutat Res* 2005; **589**: 47-65 [PMID: 15652226 DOI: 10.1016/j.mrrev.2004.08.001]
17 **Prieto-Alamo MJ**, Laval F. Deficient DNA-ligase activity in the metabolic disease tyrosinemia type I. *Proc Natl Acad Sci USA* 1998; **95**: 12614-12618 [PMID: 9770534]
18 **Scheimann AO**, Strautnieks SS, Knisely AS, Byrne JA, Thompson RJ, Finegold MJ. Mutations in bile salt export pump (ABCB11) in two children with progressive familial intrahepatic cholestasis and cholangiocarcinoma. *J Pediatr* 2007; **150**: 556-559 [PMID: 17452236 DOI: 10.1016/j.jpeds.2007.02.030]
19 **Richter A**, Grabhorn E, Schulz A, Schaefer HJ, Burdelski M, Ganschow R. Hepatoblastoma in a child with progressive familial intrahepatic cholestasis. *Pediatr Transplant* 2005; **9**: 805-808 [PMID: 16269056 DOI: 10.1111/j.1399-3046.2005.00380.x]

P- Reviewer: Kamimura K, Vij M, Wang JS **S- Editor**: Ma YJ
L- Editor: Filipodia **E- Editor**: Wang CH

World Journal of Gastroenterology

Submit a Manuscript: http://www.wjgnet.com/esps/
Help Desk: http://www.wjgnet.com/esps/helpdesk.aspx
DOI: 10.3748/wjg.v22.i20.4908

World J Gastroenterol 2016 May 28; 22(20): 4908-4917
ISSN 1007-9327 (print) ISSN 2219-2840 (online)

ORIGINAL ARTICLE

Retrospective Study

Primary hepatic epithelioid angiomyolipoma: A malignant potential tumor which should be recognized

Jie Liu, Cheng-Wu Zhang, De-Fei Hong, Ran Tao, Yuan Chen, Min-Jie Shang, Yu-Hua Zhang

Jie Liu, Cheng-Wu Zhang, De-Fei Hong, Ran Tao, Min-Jie Shang, Yu-Hua Zhang, Department of Hepatopancreatobiliary Surgery and Minimally Invasive Surgery, Zhejiang Provincial People's Hospital, Hangzhou 310014, Zhejiang Province, China

Yuan Chen, Department of Pathology, Zhejiang Provincial People's Hospital, Hangzhou 310014, Zhejiang Province, China

Author contributions: Liu J and Zhang CW contributed equally to this work; Liu J collected and analyzed the data, and drafted the manuscript; Zhang CW designed and supervised the study; Tao R revised the manuscript; Chen Y was responsible for pathological analysis; Shang MJ and Zhang YH provided analytical oversight; and Hong DF provided academic support; all authors have read and approved the final version to be published.

Institutional review board statement: The study was reviewed and approved by the Zhejiang Provincial People's Hospital Institutional Review Board.

Informed consent statement: The study participant provided informed written consent for this study.

Conflict-of-interest statement: We declare that we have no financial or personal relationships with other people or organizations that can inappropriately influence our work, and there is no professional or other personal interest of any nature or kind in any product, service and/or company that could be construed as influencing the position presented in, or the review of, the manuscript entitled "Primary hepatic epithelioid angiomyolipoma: A malignant potential tumor which should be recognized".

Data sharing statement: Technical appendix, statistical code, and dataset available from the corresponding author at zcw1989@sina.com. Participants gave informed consent for data sharing.

Correspondence to: Cheng-Wu Zhang, MD, Department of Hepatopancreatobiliary Surgery and Minimally Invasive Surgery, Zhejiang Provincial People's Hospital, 158 Shangtang Road, Hangzhou 310014, Zhejiang Province, China. zcw1989@sina.com
Telephone: +86-571-85893419
Fax: +86-571-85131448

Received: January 20, 2016
Peer-review started: January 22, 2016
First decision: March 7, 2016
Revised: March 20, 2016
Accepted: March 30, 2016
Article in press: March 30, 2016
Published online: May 28, 2016

Abstract

AIM: To improve the clinical diagnosis and recognition of hepatic epithelioid angiomyolipoma (HEAML).

METHODS: Four cases of primary HEAML were confirmed based on the pathology archive system in our hospital from January 2009 to November 2015. The general state, clinical symptoms, imaging manifestations, histological results and immunohistochemistry of these patients were retrospectively reviewed and analyzed. Studies of HEAML published in the last 15 years were collected from PubMed and MEDLINE to summarize the clinical symptoms, imaging characteristics, pathological features and management of HEAML.

RESULTS: Four cases of primary HEAML were retrieved from our archives. These included three female patients and one male patient, with a mean age of 41.8 ± 11.5 years (ranging from 31 to 56 years). The mean

tumor size was 7.3 ± 5.5 cm (ranging from 3.0 to 15 cm). In the contrast-enhanced imaging, the tumor was obviously enhanced in the arterial phase, but enhanced continuously or exhibited a slow-density masse during the venous and delayed phases. Histologically, the tumors mainly consisted of epithelioid cells that comprised approximately 95% of the total neoplastic mass. Although no metastases occurred in our patients, pathological studies revealed necrosis, mitotic figures and liver invasion in two patients, which indicates aggressive behavior. Immunohistochemical staining revealed that human melanoma black 45 (HMB-45) and Melan-A were positive in 4 cases. We only identified 81 cases with primary HEAML, including our present patients, from 26 articles available from PubMed and MEDLINE. The majority of the papers were published as case reports. Only 5 (5/75, 6%) cases were associated with tuberous sclerosis complex (TSC). More than half (35/66) were discovered incidentally upon physical examination. Approximately 65% (22/34) of the patients were misdiagnosed with HCC or other tumors before surgery. Approximately 10% (8/81) of the patients with HEAML had recurrence or metastasis after surgery, which was a very high and alarming rate.

CONCLUSION: HEAML is a very rare primary hepatic tumor that is often misdiagnosed before surgery. Patients should be followed closely after surgery because of its malignant potential.

Key words: Epithelioid angiomyolipoma; Imaging; Liver; Immunohistochemical staining; Human melanoma black 45

Core tip: Hepatic epithelioid angiomyolipoma (HEAML) is very rare tumor that is often misdiagnosed because of atypical symptoms and imaging manifestation. The diagnosis can be made based upon characteristic pathological and immunohistochemical criteria. Traditionally, it is thought to be a benign tumor and is therefore largely ignored. Thus, it is important to improve the recognition of HEAML. This is the first article to analyze the clinicopathological data and imaging results of HEAML comprehensively by combining our four patients with other cases reported worldwide. In fact, HEAML has malignant potential and should be followed closely after surgery.

Liu J, Zhang CW, Hong DF, Tao R, Chen Y, Shang MJ, Zhang YH. Primary hepatic epithelioid angiomyolipoma: A malignant potential tumor which should be recognized. *World J Gastroenterol* 2016; 22(20): 4908-4917 Available from: URL: http://www.wjgnet.com/1007-9327/full/v22/i20/4908.htm DOI: http://dx.doi.org/10.3748/wjg.v22.i20.4908

INTRODUCTION

Angiomyolipoma (AML) is a kind of solid tumor that contains varying proportions of fat, smooth muscle cells, and blood vessels. Depending upon the dominant cell type, AML can be subcategorized into epithelioid, spindle, and intermediate forms. The former are perivascular epithelioid cells (PECs), including AML, lymphangiomyomatosis, and clear cell "sugar" tumor of the lungs[1]. Epithelioid angiomyolipoma (EAML) is a rare and special type of angiomyolipoma that most commonly occurs in the kidney, lung, heart, mediastinum, retroperitoneum, and vagina. Hepatic EAML (HEAML) was first reported by Yamasaki *et al*[2], and so far no more than 80 cases have been reported worldwide. HEAML, which was generally considered benign in the past, has malignant potential according to these reports[3]. There are no unique clinical symptoms of HEAML, which leads to confusion with other types of hepatic tumors easily[4]. Therefore, it has a very high rate of misdiagnosis. Here, we retrospectively reviewed the clinicopathological features of HEAML patients based on PubMed and MEDLINE data, including our four patients, who were finally diagnosed with HEAML through pathology and immunohistochemistry. The aim of our study was to improve the rate of accurate preoperative diagnosis and the degree of recognition of this rare tumor.

MATERIALS AND METHODS

Four cases of primary HEAML were confirmed based on the pathology archive system in our hospital from January 2009 to November 2015. The general state, clinical symptoms, imaging manifestations, histological results and immunohistochemistry of these patients were retrospectively reviewed. Important histological parameters including the diameter of the main tumor, the number of tumor nodules, cytological atypia, coagulative necrosis, mitotic count, liver invasion and vascular invasion were collected. Immunohistochemical staining for HMB-45, Melan-A, smooth muscle actin (SMA), HepPar-1, S-100, CK and fetoprotein (AFP) was repeated to verify the diagnosis. Follow-up data were obtained from the clinical records.

Articles about primary HEAML (excluding PEComa) were collected from January 2000 to November 2015 from PubMed and MEDLINE, and non-English publications were included. Clinical data were retrieved from the articles including sex, tumor size, case number, location of tumor, clinical presentation, preoperative diagnosis, association with TSC, treatment and prognosis.

SPSS (version 15.0 for Windows) software was used for statistical analyses. The results are presented as the mean ± SD or median.

Table 1 Clinicopathologic data of 4 cases of hepatic epithelioid angiomyolipoma

Case	Sex/age	Size (cm)	Location of tumor in the liver	Clinical presentation	Fat	Details of imaging findings	Preoperative diagnosis	Pathologic features					
								Satellite tumor	Cytologic atypia	Mitotic count	Coagulative necrosis	LI	VI
1	M/34	15.0	L	Abdominal pain and fever	No	Arterial phase enhancement and washout at portovenous phase (CT)	HCC	+	+	+	+	+	-
2	F/46	3.5	L	None	No	Arterial phase enhancement and washout at portovenous phase (CT)	HCC	-	-	-	-	-	
3	F/31	3.0	R	None	No	Arterial phase enhancement and washout at portovenous phase (CT)	HCC	-	+	+	+	+	-
4	F/56	7.5	L	None	No	Arterial phase enhancement and no delayed washout at portovenous phase (MRI)	HCA	-	-	-	-	-	-

LI: Liver invasion; VI: Vascular invasion; HCC: Hepatocellular cancer; HCA: Hepatocellular adenoma. Size of the main tumor nodule.

RESULTS

The clinicopathological features of the 4 cases are summarized in Table 1. All 4 cases received surgical resection. The pathological and histological diagnosis of HEAML was verified in all 4 cases. Three patients were female and one patient was male. The mean age was 41.8 ± 11.5 years (ranging from 31 to 56 years). The male patient was rushed to the emergency room because of upper abdominal pain and fever, whereas the other 3 patients presented with liver masses on ultrasound but without symptoms or signs upon physical examination. The medical histories of all four patients were normal. Tests for the hepatitis C virus antibody and hepatitis B virus surface antigen were all negative, and there was no evidence of tuberous sclerosis. The results of the liver function test, routine blood test, serum AFP and carbohydrate antigen199 (CA199) were normal for our 4 patients with the exception of the male patient, who had elevated alkaline phosphatase; however, this patient tested negative for bacterial infection, and a fever caused by the tumor was considered first. All of the cases presented with intraparenchymal tumors, and the mean tumor diameter was 7.3 ± 5.5 cm (ranging from 3.0 to 15 cm). In the three female patients, the tumor presented as a single lesion. One tumor was located in the right lobe, while the other two tumors were located in the left lobe. In contrast, the male patient presented with three tumor lesions in bilateral liver lobes. Detailed imaging results were available for the four patients. Dynamic contrast-enhanced imaging showed two different presentations. The computed tomography scan of the male patient showed multiple low-density masses in the plain phase (Figure 1A), with the biggest lesion, measuring 15.0 cm × 12.0 cm × 10.0 cm in size, in the left hepatic lobe. In the arterial phase, strong contrast enhancement with low density in the center was observed (Figure 1B). The tumors had almost washed out the contrast agent except for a weak contrast-enhanced effect in the center that was perhaps induced by arterioportal venous shunting in the portal phase (Figure 1C). In the delayed phase, the tumors exhibited low density in comparison with the liver tissue (Figure 1D). The imaging of patients 2 and 3 showed similar manifestations. However, for patient 4, the foci had showed boundaries and high signal in T2WI (Figure 2A) but low signal in the plain phase (Figure 2B). A significantly and uniformly enhanced mass during the arterial phase was observed (Figure 2C). However, different from other cases, this mass was enhanced continuously during the venous and delayed phases (Figure 2D). Based on the available clinical findings, a preoperative diagnosis of hepatocellular adenoma (HCA) or HCC was made. None of the cases presented with extrahepatic metastasis, and they were diagnosed as primary liver tumors with no evidence of other organ involvement. Extended left lobectomy and laparoscopic hepatectomy were performed, respectively, because of the uncertain nature.

With respect to the pathological findings, gross examination revealed that the external surface of the mass was smooth and brownish in color. Sections revealed well-circumscribed, non-encapsulated tumors. The largest tumor was multiloculated with amorphous

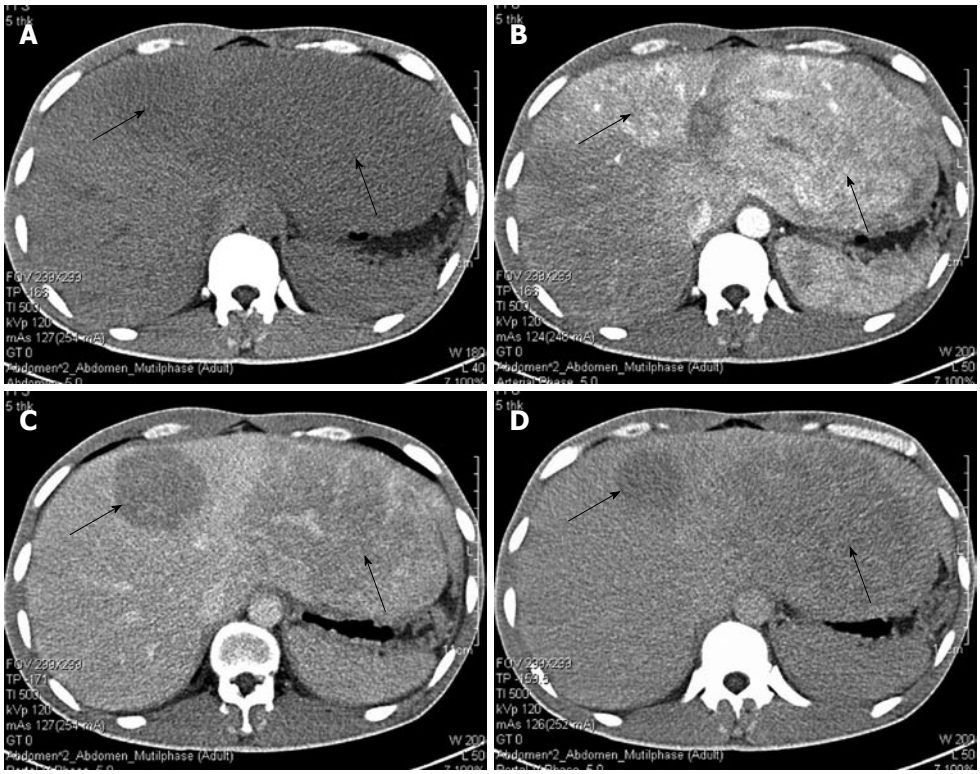

Figure 1 Computed tomography manifestation of the male patient. A: Low-density masses in the plain phase (black arrows); B: In the arterial phase, a strong contrast-enhancing effect with low-density in center was observed; C: In the portal phase, tumors had almost washed out the contrast agent, but a weak contrast-enhancing effect was sustained; D: Low-density masses in the delayed phase.

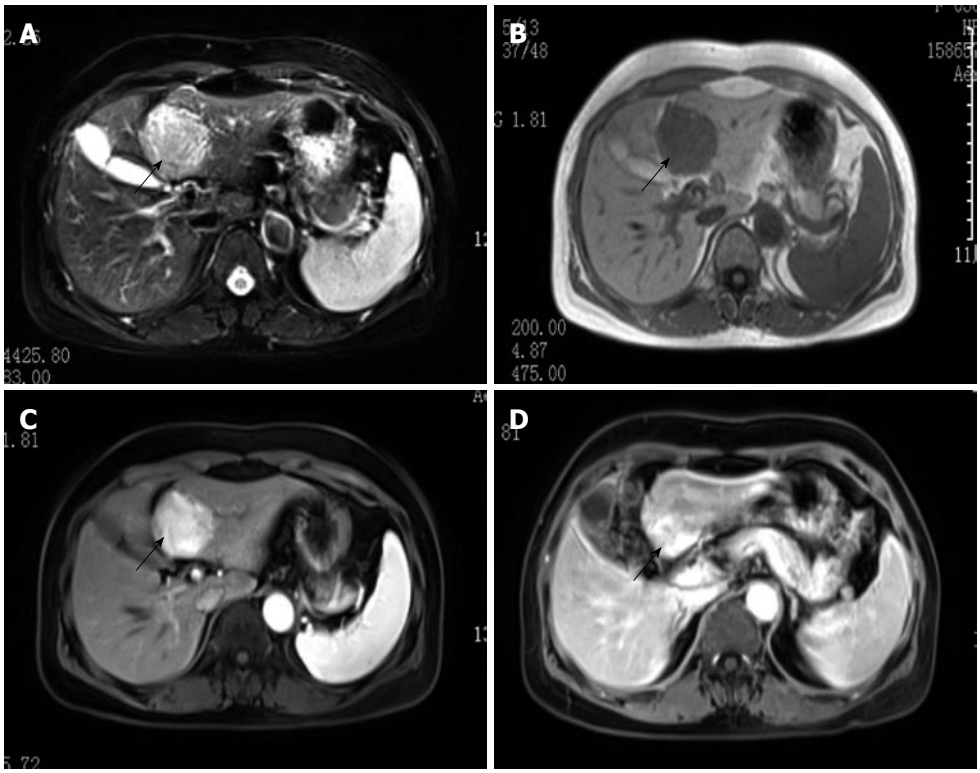

Figure 2 Magnetic resonance imaging manifestation of the female patient. The tumor had clear boundaries and showed high signal on T2WI (A, black arrow) and low signal in the plain phase (B); Hyperenhancement in the arterial phase (C) and delayed phase (D).

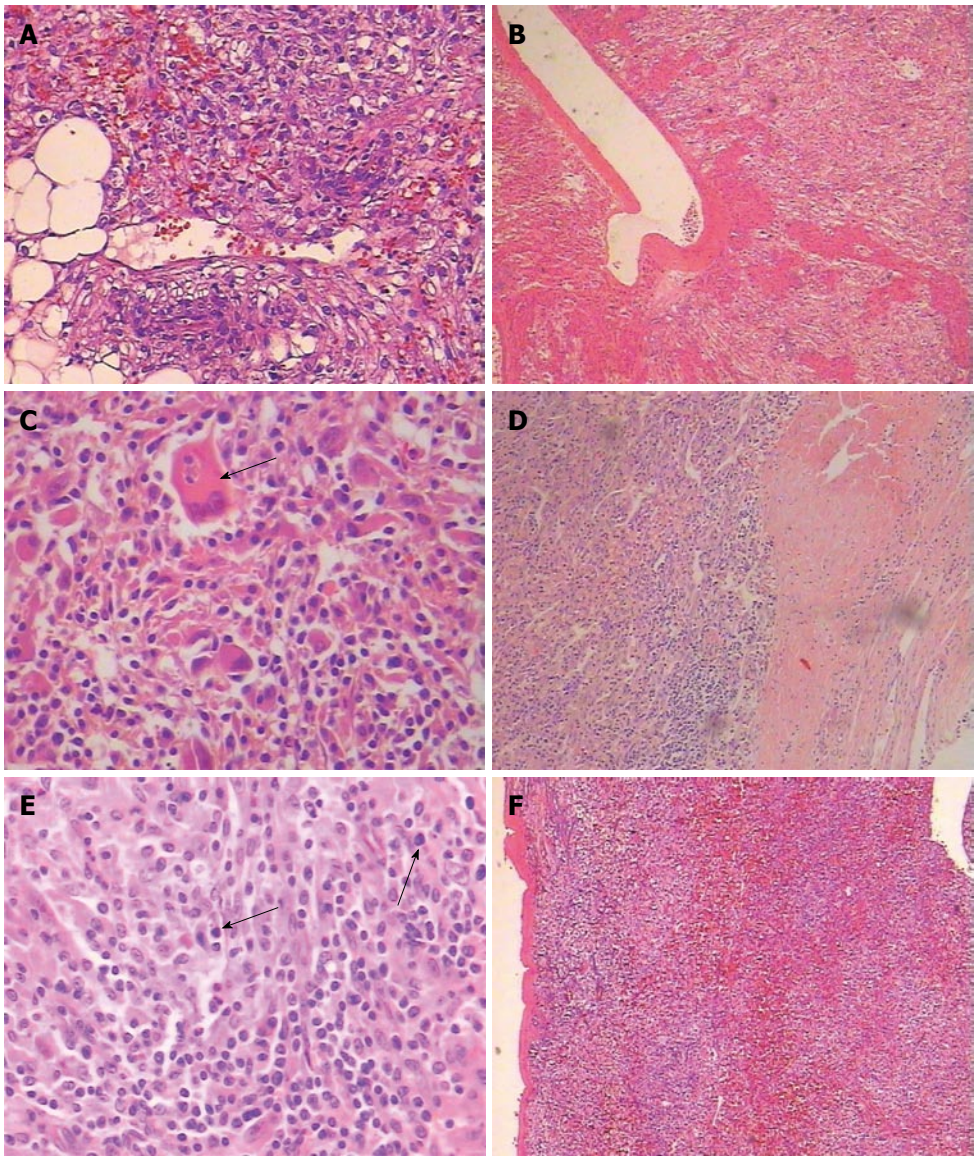

Figure 3 Histology of hepatic epithelioid angiomyolipoma. A: The tumor comprised of sheets of large polygonal cells with abundant granular eosinophilic cytoplasm (HE, × 200); B: The tumor cells were arranged radial around blood vessels (HE, × 40); Microscopic features signifying aggressive behavior were observed: C: Cytologic atypia (black arrow) (HE, × 200); D: Coagulative necrosis (HE, × 40); E: Increased mitotic count (black arrow) (HE, × 200); F: Tumors mainly consisted of epitheli¬oid cells that comprised approximately 95% of the total neoplastic mass (HE, × 40).

necrotic tissue and hemorrhagic fluid. The male patient had the other two satellite tumor nodules whose size was 1 cm and 2 cm, respectively. Microscopically, the tumor was comprised of sheets of large polygonal cells with abundant granular eosinophilic cytoplasm in areas with typical features of HEAML (Figure 3A). A radial arrangement around blood vessels was observed (Figure 3B). Microscopic features including cytologic atypia (Figure 3C), coagulative necrosis (Figure 3D) and increased mitotic count (Figure 3E) were observed in two cases, which indicates aggressive behavior. All tumors mainly consisted of epithelioid cells that comprised approximately 95% of the total neoplastic mass (Figure 3F). Tumors also contained a few spindle myoid cells, mature fat, and thick-walled vasculature. Immunohistochemical analysis revealed that 4 patients were positive for the melanocytic markers HMB-45 (Figure 4A), Melan-A (Figure 4B), SMA (Figure 4C) and VIM (Figure 4D), but negative for S-100 (Figure 4E), CK (Figure 4F), AFP (Figure 4G) and HepPar-1 (Figure 4H). The diagnosis was corrected to HEAML based on the above evidence. The median follow-up period was 30 months (ranging from 2 to 72 mo). All patients were alive with no evidence of recurrence at the time of review.

Our search of PubMed and MEDLINE confirmed a total of 81 cases (including our four cases) with primary HEAML from 26 articles[2,3,5-27] (Table 2). The majority of the cases were single case reports with the exception of 6 publications that reported more than 5 cases per article. Even so, those articles only focused on the pathological or imaging presentations. These limited results reflect the overall poor recognition of HEAML. Summarizing these available reports is

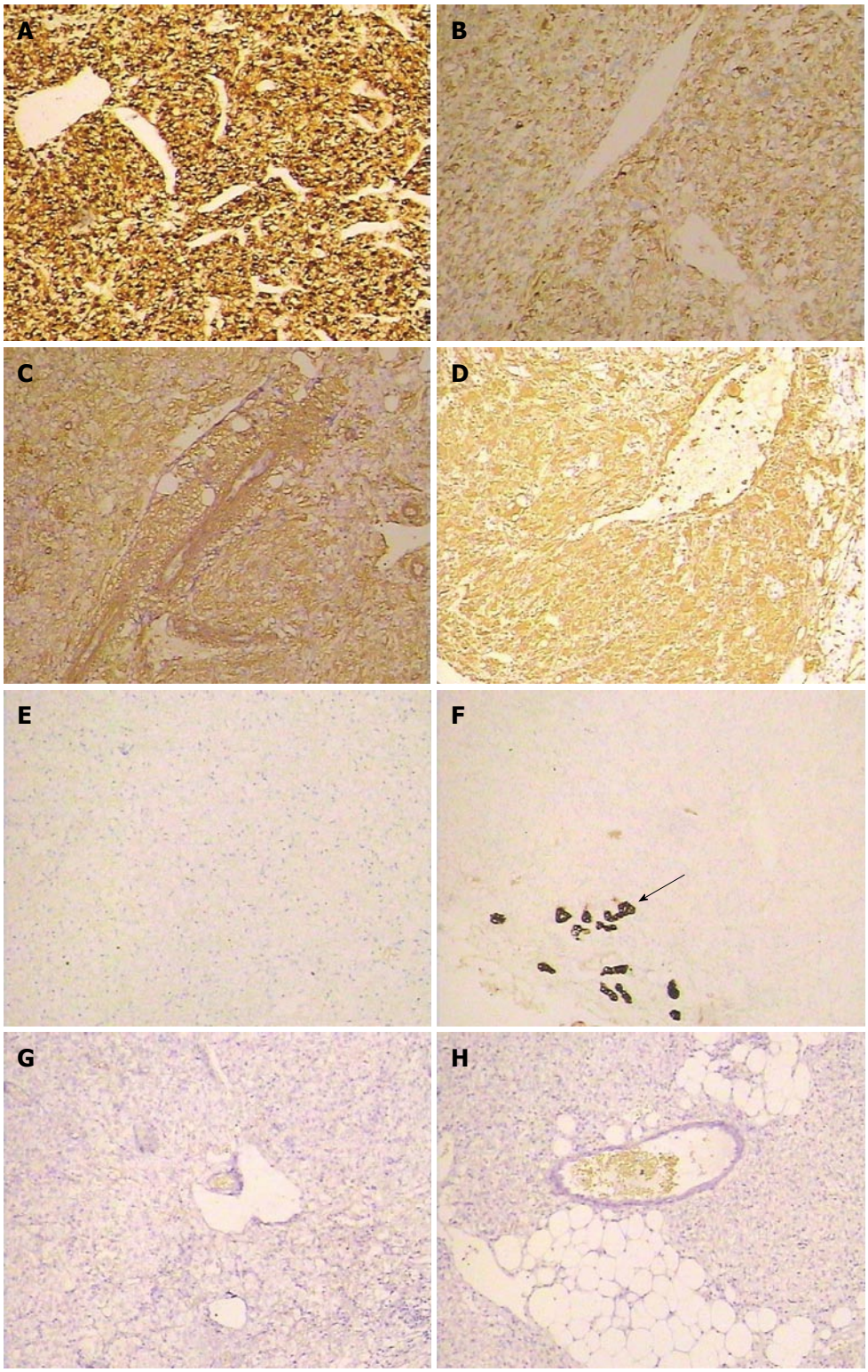

Figure 4 Immunohistochemical staining of hepatic epithelioid angiomyolipoma. The tumor cells were positive for melanocytic markers HMB-45 (A, × 40), Melan-A (B, × 40), SMA (C, × 40), and VIM (D, × 40), but negative for S-100 (E, × 40), CK (the arrow indicates the bile duct epithelium) (F, × 40), AFP (G, × 40), and Herpar-1 (H, × 40).

necessary to further promote the diagnosis of HEAML.

DISCUSSION

In all series of HEAML, more women suffered from HEAML than men, at a ratio of 5:1. Although some patients with HEAML had atypical gastrointestinal symptoms, including abdominal pain or distension, discomfort and vomiting, more than half (35/66, 53%) of the cases were discovered incidentally upon

Table 2 Summary of available reports of hepatic epithelioid angiomyolipoma from PubMed and MEDLINE

Year	Authors	Number (F/M)	Size (cm)	Location (L/R)	Clinical symptoms (*n*)	Diagnosis before surgery (*n*)	TSC (*n*)	Treatment	Recurrence/ metastasis (*n*)
2015	Our study	3/1	3.0-15.0	3/1	Abdominal pain and fever (1) No symptoms (3)	HCC (3) HCA (1)	None	Surgery	None
2014	Dai *et al*[24]	3/2	2.5-7.0	2/3	Abdominal pain (2) None (3)	HCC (4) FNH (1)	None	Surgery	None
2014	Tajima *et al*[25]	0/1	10.5	0/1	Abdominal pain	Hepatic AML	None	Surgery	None
2014	Zhou *et al*[27]	1/0	30.0	1/0	Abdominal discomfort	NA	None	Surgery	None
2014	Xu *et al*[26]	22/3	3.0-20.0	12/13	Abdominal pain (10) Abdominal distention (3) No symptoms (15)	HCC or other tumor	1	Surgery	2
2013	Occhionorelli *et al*[22]	1/0	8.0	1/0	Abdominal pain	NA	NA	Surgery	None
2013	Zhao *et al*[23]	3/2	0.6-9.7	2/3	No symptoms	NA	None	Surgery	NA
2013	Saito *et al*[21]	0/1	1.2	1/0	No symptoms	HCC	None	Surgery	None
2013	Lo *et al*[20]	5/0	1.2-25.0	1/4	Abdominal distention (1) Abdominal discomfort (1) Epigastralgia (1) None (2)	HCC (1) HCA (2) AML Liver tumor with uncertain nature	None	Surgery	None
2013	Ji *et al*[19]	6/0	5.0-9.5	5/1	None (5) Abdominal pain (1)	AML	None	Surgery and biopsy	NA
2012	Limaiem *et al*[18]	0/1	8.2	1/0	Abdominal pain	HCC	None	Surgery	None
2012	Agaimy *et al*[16]	1/0	2.0	1/0	Nausea	Metastatic adenocarcinoma or carcinoid	None	Surgery	None
2012	Xie *et al*[17]	1/0	3.4	0/1	Dyspnea	HCC	1	Biopsy	None
2010	Wen *et al*[15]	0/1	4.1	1/0	None	HCC	NA	Surgery	NA
2009	Leenman *et al*[13]	1/0	6.0	1/0	Abdominal pain	NA	NA	Surgery	NA
2009	Xu *et al*[14]	10/0	1.5-10.0	6/6	NA	NA	1	Surgery	2
2009	Alatasis *et al*[12]	1/0	11.0	Multiple	None	HCC	1	Biopsy	NA
2008	Deng *et al*[11]	0/1	18.0	0/1	Abdominal pain	AML	None	Surgery	1
2007	Khalbuss *et al*[10]	1/0	12.0	1/0	Abdominal pain	Adenoma or hamartoma	1	Surgery	None
2006	Rouquie *et al*[9]	1/0	7.0	1/0	None	NA	None	Surgery	None
2004	Tryggvason *et al*[8]	1/0	6.0	1/0	Abdominal pain	NA	None	Surgery	None
2004	Mizuguchi *et al*[7]	1/0	NA	0/1	None	AML	NA	Surgery	1
2000	Savastano *et al*[6]	1/0	1.2	1/0	NA	NA	NA	Surgery	None
2000	Flemming *et al*[5]	3/0	1.0-20.0	2/2	NA	HCC	None	Surgery (2) Biopsy (1)	1
2000	Yamasaki *et al*[2]	1/0	2.0	0/1	None	NA	None	Surgery	None
2000	Dalle *et al*[3]	1/0	15.0	0/1	Nausea and loss of appetite	HCC	NA	Biopsy	1

F/M: Female/male; L/R: Left/right; TSC: Tuberous sclerosis complex; HCC: Hepatocellular cancer; HCA: Hepatocellular adenoma; FNH: Focal nodular hyperplasia; AML: Angiomyolipoma; NA: Not available.

physical examination based on the available data and were similar to three female patients in our research. One of our patients had a fever due to the central necrosis in the large size of the tumor. Rupture and hemorrhage were reported as the first symptoms in a few cases[22,25]. Abnormal liver function was frequently observed in patients with larger tumor size. Tumor size varied considerably, with lesions ranging from a few millimeters to as large as 30 cm having been reported. In general, bigger tumors have greater malignant potential. There was no difference regarding the location of the tumor in either the left or right lobe (44:39). Some reports showed that 26%-32% of AML patients had associated TSC[28,29]; however, interestingly, this ratio was less than 5% in China[26]. Among 75 patients who had valid data, only 5 (5/75, 6%) were associated with TSC, which was similar to the domestic study. All four cases in our report were solitary tumors without TSC. It was confirmed that approximately 50% of TSC patients had AML, but approximately 80% of the patients with AML were sporadic cases, which were not related to TSC.

HEAML always presents with less typical imaging manifestations, especially when smooth muscle and vascular components dominated in tumor as seen in the less fat types, which leads to confusion with other hepatic tumors easily and making a correct diagnosis very difficult before surgery. In dynamic enhanced CT or magnetic resonance imaging, multiple manifestations of HEAML were observed[21,23,24]. Most were obviously enhanced in the early arterial phase but showed low density in the portal venous phase and delayed phase, which has been confirmed by our research and by previous reports in the literature. Similar imaging signs could be observed in other hypervascular hepatic lesions, just like HCC. It is very

difficult to discriminate between HEAML and HCC; 60% of patients with HEAML were misdiagnosed with HCC before surgery in 81 cases. According to the pathology, the so-called "false capsule" of HEAML, different from the real capsule of HCC, was just formed by the compression of the surrounding liver tissues, and had no histological structure in fact. Although the excretion of the contrast medium was relatively slow on the imaging in HEAML, this difference was not enough to distinguish the HCC or HEAML, especially in large tumors with central necrosis or hemorrhage. Focal nodular hyperplasia (FNH) always showed a central scar, which is a characteristic sign and could be an important basis in the differential diagnosis. In addition, FNH presented delayed enhancement on enhancement scans, which was also different from most HEAML. One patient in our study was diagnosed with hepatic adenoma during hospitalization because of enhancement in all phases on enhancement scans. Other fat rich tumors such as lipoma show almost no enhancement on imaging scans because of poor blood supply.

Pathology is the only definite diagnostic criteria. The gross observation of HEAML is not characteristic; most are solitary but multifocal tumors, such as cystic degeneration, have been reported in several case reports. Its morphological features under the microscope were revealed by Xu *et al*[26] by analyzing 25 cases of HEAML. It was characterized by marked cytological atypia; relatively rare mitotic figures; radial distribution of tumor cells around the thin-walled blood vessels or muscular vessels; and the presence of common multinucleated giant cells and large ganglion-like tumor cells. Although the presence of epithelioid cells is important for the diagnosis of EAML, the ratio is still under debate. Aydin *et al*[29] thought that it could be defined as an EAML if epithelioid cell components were greater than 10%, but most scholars believed that this standard was too low and should be as high as 50%, or even more than 90%. In our patients, the epithelial cells of EAML reached more than 95%. Apparently, more cases and follow-up results are needed to reach a unanimous conclusion.

Renal EAML has malignant potential and may metastasize to the lymph node, liver, lung, or bone in approximately one-third of cases. Poor outcome is considered when necrosis, mitotic figures, or a plastic nucleus are observed in pathological studies. Nese *et al*[30] showed that a carcinoma-like growth pattern and extrarenal extension and/or renal vein involvement were significant independent prognostic factors in a multivariate analysis. Brimo *et al*[31] summarized the pathological characteristics of renal EAML progression: (1) $\geqslant$ 2 mitotic figures per 10 high-power field; (2) atypical mitotic figures; (3) $\geqslant$ 70% of atypical epithelioid cells; and (4) necrosis. The presence of 3 or more features was highly predictive of malignant behavior. Faraji *et al*[32] also showed that marked cytological atypia and extensive tumor necrosis were related to the progression of EAML. Although HEAML is considered to be a benign tumor in several series of case reports, 8 cases of malignant HEAML have been reported[3,5,7,11,14,26], and there is a lack of evidence to determine whether the same prognostic parameters of renal EAML are applicable to HEAML.

As a member of the PEComa family, the immunological phenotype of HEAML has the characteristics of bidirectional differentiation of melanoma cells and smooth muscle cells. The tumor cell is positive for the expression of cell markers including MART-1, HMB45, Melan A and SMA, but negative for all epithelial markers including EMA and S-100. This is the most important criterion for the differential diagnosis of HEAML. Those tumor cells are also negative for typical markers of HCC, including AEP, HepPar 1 and canalicular polyclonal CEA. HEAML is sometimes misdiagnosed as malignant melanoma because of the differentiation of melanocytes; however, primary hepatic melanoma is very rare, and the tumor cells are positive for S-100 but negative for smooth muscle cell markers based on immunohistochemical analysis.

Based on previous reports, surgery is the only effective way to cure HEAML; however, biopsies were also used in a few cases with the risk of tumor growth and metastasis. In one case, the tumor volume increased from 760.8 cm^3 to 1967.8 cm^3, a 2.6-fold increase during the 102 d after HEAML was diagnosed by biopsy[7]. A metastatic mass in the right lower quadrant and portal vein thrombosis were suspected in another biopsy case. Approximately 10% (8/81) of patients with HEAML had recurrence or metastasis after surgery, which was a very high and alarming rate. Although no recurrence or metastasis occurred in our study, pathological studies still show necrosis, mitotic figures and liver invasion in two patients, which indicates aggressive behavior. To be vigilant, although the majority of AMLs always are considered as benign tumors for their biological behavior, the potential risk of malignant changes of HEAML needs to be noticed and should be followed rigorously after surgery.

COMMENTS

Background

Hepatic angiomyolipoma (HAML) is a rare benign tumor that belongs to a family of tumors that have collectively been called "PEComa". As a specific form, the hepatic epithelioid angiomyolipoma (HEAML) has malignant potential and is often misdiagnosed because of atypical symptoms and imaging manifestations. Characteristic pathological and immunohistochemical features are the diagnostic criteria. Therefore, it is important to improve the recognition of HEAML.

Research frontiers

In the past15 years, there have been scattered reports of HEAML, and the majority of those were case reports. In addition, those articles only focused on the pathology or imaging aspects, respectively. Therefore, more cases need to be collected and summarized, and more attention should be paid to this disease.

Innovations and breakthroughs

This is the first study to summary the clinical symptoms, imaging manifestations and pathological features of HEAML by retrospectively analyzing 81 cases from 26 articles, including our four patients, to improve the recognition of HEAML and reduce the misdiagnosis of this disease.

Applications

By understanding the characteristics of the clinical symptoms, imaging manifestations and pathological features of HEAML, this study could help us to improve confidence in the diagnosis of HEAML, especially in the differential diagnosis with other solid tumors in the liver, such as hepatic cellular cancer and adenoma.

Peer-review

In this manuscript, the authors analyze and summarize the clinical symptoms, imaging manifestations and pathological features of patients with HEAML by collecting all 81 cases to improve the rate of accurate diagnosis. No similar report has been published before. It will be helpful for scholars to obtain knowledge of this disease.

REFERENCES

1 **Hornick JL**, Fletcher CD. PEComa: what do we know so far? *Histopathology* 2006; **48**: 75-82 [PMID: 16359539 DOI: 10.1111/j.1365-2559.2005.02316.x]

2 **Yamasaki S**, Tanaka S, Fujii H, Matsumoto T, Okuda C, Watanabe G, Suda K. Monotypic epithelioid angiomyolipoma of the liver. *Histopathology* 2000; **36**: 451-456 [PMID: 10792487]

3 **Dalle I**, Sciot R, de Vos R, Aerts R, van Damme B, Desmet V, Roskams T. Malignant angiomyolipoma of the liver: a hitherto unreported variant. *Histopathology* 2000; **36**: 443-450 [PMID: 10792486]

4 **Park HK**, Zhang S, Wong MK, Kim HL. Clinical presentation of epithelioid angiomyolipoma. *Int J Urol* 2007; **14**: 21-25 [PMID: 17199855 DOI: 10.1111/j.1442-2042.2006.01665.x]

5 **Flemming P**, Lehmann U, Becker T, Klempnauer J, Kreipe H. Common and epithelioid variants of hepatic angiomyolipoma exhibit clonal growth and share a distinctive immunophenotype. *Hepatology* 2000; **32**: 213-217 [PMID: 10915726 DOI: 10.1053/jhep.2000.9142]

6 **Savastano S**, Piotto M, Mencarelli R, Spanio P, Rubaltelli L. [A monotypic variant of hepatic angiomyolipoma completely composed of perivascular epithelioid cells. A case]. *Radiol Med* 2000; **100**: 79-81 [PMID: 11109461]

7 **Mizuguchi T**, Katsuramaki T, Nobuoka T, Nishikage A, Oshima H, Kawasaki H, Kimura S, Satoh M, Hirata K. Growth of hepatic angiomyolipoma indicating malignant potential. *J Gastroenterol Hepatol* 2004; **19**: 1328-1330 [PMID: 15482547 DOI: 10.1111/j.1440-1746.2004.03583.x]

8 **Tryggvason G**, Blöndal S, Goldin RD, Albrechtsen J, Björnsson J, Jónasson JG. Epithelioid angiomyolipoma of the liver: case report and review of the literature. *APMIS* 2004; **112**: 612-616 [PMID: 15601311 DOI: 10.1111/j.1600-0463.2004.apm1120909.x]

9 **Rouquie D**, Eggenspieler P, Algayres JP, Béchade D, Camparo P, Baranger B. [Malignant-like angiomyolipoma of the liver: report of one case and review of the literature]. *Ann Chir* 2006; **131**: 338-341 [PMID: 16386232 DOI: 10.1016/j.anchir.2005.11.014]

10 **Khalbuss WE**, Fischer G, Bazooband A. Imprint cytology of epithelioid hepatic angiomyolipoma: mimicry of hepatocellular carcinoma. *Acta Cytol* 2007; **51**: 670-672 [PMID: 17718152]

11 **Deng YF**, Lin Q, Zhang SH, Ling YM, He JK, Chen XF. Malignant angiomyolipoma in the liver: a case report with pathological and molecular analysis. *Pathol Res Pract* 2008; **204**: 911-918 [PMID: 18723294 DOI: 10.1016/j.prp.2008.06.007]

12 **Alatassi H**, Sahoo S. Epithelioid angiomyolipoma of the liver with striking giant cell component: fine-needle aspiration biopsy findings of a rare neoplasm. *Diagn Cytopathol* 2009; **37**: 192-194 [PMID: 19156824 DOI: 10.1002/dc.20979]

13 **Leenman EE**, Mukhina MS, Nasyrov AR. [Monophasic angiomyolipoma (PEComa) of the liver]. *Arkh Patol* 2009; **71**: 44-46 [PMID: 20131508]

14 **Xu PJ**, Shan Y, Yan FH, Ji Y, Ding Y, Zhou ML. Epithelioid angiomyolipoma of the liver: cross-sectional imaging findings of 10 immunohistochemically-verified cases. *World J Gastroenterol* 2009; **15**: 4576-4581 [PMID: 19777618 DOI: 10.3748/wjg.15.4576]

15 **Wen MC**, Jan YJ, Li MC, Wang J, Lin A. Monotypic epithelioid angiomyolipoma of the liver with TFE3 expression. *Pathology* 2010; **42**: 300-302 [PMID: 20350230 DOI: 10.3109/00313021003631254]

16 **Agaimy A**, Vassos N, Croner RS, Strobel D, Lell M. Hepatic angiomyolipoma: a series of six cases with emphasis on pathological-radiological correlations and unusual variants diagnosed by core needle biopsy. *Int J Clin Exp Pathol* 2012; **5**: 512-521 [PMID: 22949933]

17 **Xie L**, Jessurun J, Manivel JC, Pambuccian SE. Hepatic epithelioid angiomyolipoma with trabecular growth pattern: a mimic of hepatocellular carcinoma on fine needle aspiration cytology. *Diagn Cytopathol* 2012; **40**: 639-650 [PMID: 21563318 DOI: 10.1002/dc.21703]

18 **Limaiem F**, Korbi S, Lahmar A, Bouraoui S, Aloui S, Jedidi S, Miloudi N, Mzabi-Regaya S. A misleading hepatic tumour: epithelioid angiomyolipoma. *Acta Gastroenterol Belg* 2012; **75**: 443-445 [PMID: 23402089]

19 **Ji JS**, Lu CY, Wang ZF, Xu M, Song JJ. Epithelioid angiomyolipoma of the liver: CT and MRI features. *Abdom Imaging* 2013; **38**: 309-314 [PMID: 22610058 DOI: 10.1007/s00261-012-9911-5]

20 **Lo RC**. Epithelioid angiomyolipoma of the liver: a clinicopathologic study of 5 cases. *Ann Diagn Pathol* 2013; **17**: 412-415 [PMID: 23786777 DOI: 10.1016/j.anndiagpath.2013.04.009]

21 **Saito Y**, Shimada M, Utsunomiya T, Morine Y, Imura S, Ikemoto T, Mori H, Hanaoka J, Sugimoto K, Iwahashi S, Yamada S, Asanoma M, Ishibashi H. Hepatic epithelioid angiomyolipoma with arterioportal venous shunting mimicking hepatocellular carcinoma: report of a case. *J Med Invest* 2013; **60**: 262-266 [PMID: 24190045]

22 **Occhionorelli S**, Dellachiesa L, Stano R, Cappellari L, Tartarini D, Severi S, Palini GM, Pansini GC, Vasquez G. Spontaneous rupture of a hepatic epithelioid angiomyolipoma: damage control surgery. A case report. *G Chir* 2013; **34**: 320-322 [PMID: 24342160]

23 **Zhao Y**, Ouyang H, Wang X, Ye F, Liang J. MRI manifestations of liver epithelioid and nonepithelioid angiomyolipoma. *J Magn Reson Imaging* 2014; **39**: 1502-1508 [PMID: 24129971 DOI: 10.1002/jmri.24291]

24 **Dai CL**, Xue LP, Li YM. Multi-slice computed tomography manifestations of hepatic epithelioid angiomyolipoma. *World J Gastroenterol* 2014; **20**: 3364-3368 [PMID: 24696616 DOI: 10.3748/wjg.v20.i12.3364]

25 **Tajima S**, Suzuki A, Suzumura K. Ruptured hepatic epithelioid angiomyolipoma: a case report and literature review. *Case Rep Oncol* 2014; **7**: 369-375 [PMID: 24987358 DOI: 10.1159/000363690]

26 **Xu H**, Wang H, Zhang X, Li G. [Hepatic epithelioid angiomyolipoma: a clinicopathologic analysis of 25 cases]. *Zhonghua Bing Li Xue Zazhi* 2014; **43**: 685-689 [PMID: 25567596]

27 **Zhou Y**, Chen F, Jiang W, Meng Q, Wang F. Hepatic epithelioid angiomyolipoma with an unusual pathologic appearance: expanding the morphologic spectrum. *Int J Clin Exp Pathol* 2014; **7**: 6364-6369 [PMID: 25337292]

28 **Parfitt JR**, Bella AJ, Izawa JI, Wehrli BM. Malignant neoplasm of perivascular epithelioid cells of the liver. *Arch Pathol Lab Med* 2006; **130**: 1219-1222 [PMID: 16879028 DOI: 10.1043/1543-2165(2006)130[1219:MNOPEC]2.0.CO;2]

29 **Aydin H**, Magi-Galluzzi C, Lane BR, Sercia L, Lopez JI, Rini BI, Zhou M. Renal angiomyolipoma: clinicopathologic study of 194 cases with emphasis on the epithelioid histology and tuberous sclerosis association. *Am J Surg Pathol* 2009; **33**: 289-297 [PMID: 18852677 DOI: 10.1097/PAS.0b013e31817ed7a6]

30 **Nese N**, Martignoni G, Fletcher CD, Gupta R, Pan CC, Kim H, Ro JY, Hwang IS, Sato K, Bonetti F, Pea M, Amin MB, Hes O,

Svec A, Kida M, Vankalakunti M, Berel D, Rogatko A, Gown AM, Amin MB. Pure epithelioid PEComas (so-called epithelioid angiomyolipoma) of the kidney: A clinicopathologic study of 41 cases: detailed assessment of morphology and risk stratification. *Am J Surg Pathol* 2011; **35**: 161-176 [PMID: 21263237 DOI: 10.1097/PAS.0b013e318206f2a9]

31 **Brimo F**, Robinson B, Guo C, Zhou M, Latour M, Epstein JI. Renal epithelioid angiomyolipoma with atypia: a series of 40 cases with emphasis on clinicopathologic prognostic indicators of malignancy. *Am J Surg Pathol* 2010; **34**: 715-722 [PMID: 20410812 DOI: 10.1097/PAS.0b013e3181d90370]

32 **Faraji H**, Nguyen BN, Mai KT. Renal epithelioid angiomyolipoma: a study of six cases and a meta-analytic study. Development of criteria for screening the entity with prognostic significance. *Histopathology* 2009; **55**: 525-534 [PMID: 19912358 DOI: 10.1111/j.1365-2559.2009.03420.x]

P- Reviewer: Berkane S, Leber B **S- Editor**: Ma YJ
L- Editor: Wang TQ **E- Editor**: Ma S

World Journal of Gastroenterology

Submit a Manuscript: http://www.wjgnet.com/esps/
Help Desk: http://www.wjgnet.com/esps/helpdesk.aspx
DOI: 10.3748/wjg.v22.i20.4918

World J Gastroenterol 2016 May 28; 22(20): 4918-4925
ISSN 1007-9327 (print) ISSN 2219-2840 (online)

ORIGINAL ARTICLE

Observational Study

Efficacy of peroral endoscopic myotomy *vs* other achalasia treatments in improving esophageal function

Madhusudhan R Sanaka, Umar Hayat, Prashanthi N Thota, Ramprasad Jegadeesan, Monica Ray, Scott L Gabbard, Neha Wadhwa, Rocio Lopez, Mark E Baker, Sudish Murthy, Siva Raja

Madhusudhan R Sanaka, Umar Hayat, Prashanthi N Thota, Ramprasad Jegadeesan, Monica Ray, Scott L Gabbard, Neha Wadhwa, Rocio Lopez, Department of Gastroenterology, Q3 Cleveland Clinic, Cleveland, OH 44195, United States

Mark E Baker, Department of Radiology, Cleveland Clinic, Cleveland, OH 44195, United States

Sudish Murthy, Siva Raja, Department of Cardiothoracic Surgery, Cleveland Clinic, Cleveland, OH 44195, United States

Author contributions: Sanaka MR designed the study, acquired data and wrote the manuscript; Hayat U, Thota PN, Jegadeesan R, Ray M, Gabbard SL, Wadhwa N, Baker ME, Murthy S and Raja S contributed equally to the study, acquired the data and reviewed the manuscript; Lopez R designed the study, analyzed the data and reviewed the manuscript; All authors approved the final manuscript.

Institutional review board statement: This study was reviewed and approved by Cleveland Clinic Institutional Review Board.

Informed consent statement: All patients provided written informed consent prior to their treatments.

Conflict-of-interest statement: There are no conflicts of interest to report.

Data sharing statement: No additional data are available.

Correspondence to: Madhusudhan R Sanaka, MD, FACG, FASGE, Department of Gastroenterology, Q3 Cleveland Clinic, 9500 Euclid Ave, Cleveland, OH 44195, United States. sanakam@ccf.org
Telephone: +1-216-4443423
Fax: +1-216-4446284

Received: February 14, 2016
Peer-review started: February 14, 2016
First decision: March 21, 2016
Revised: March 26, 2016
Accepted: April 7, 2016
Article in press: April 7, 2016
Published online: May 28, 2016

Abstract

AIM: To assess and compare the esophageal function after peroral endoscopic myotomy (POEM) *vs* other conventional treatments in achalasia.

METHODS: Chart review of all achalasia patients who underwent POEM, laparoscopic Heller myotomy (LHM) or pneumatic dilation (PD) at our institution between January 2012 and March 2015 was performed. Patient demographics, type of achalasia, prior treatments, pre- and post-treatment timed barium swallow (TBE) and high-resolution esophageal manometry (HREM) findings were compared between the three treatment groups. Patients who had both pre- and 2 mo post-treatment TBE or HREM were included in the final analysis. TBE parameters compared were barium column height, width and volume of barium remaining at 1 and 5 min. HREM parameters compared were basal lower esophageal sphincter (LES) pressures and LES-integrated relaxation pressures (IRP). Data are presented as mean ± SD, median [25th, 75th percentiles] or frequency (percent). Analysis of variance, Kruskal-Wallis test, Pearsons χ^2 test and Fishers Exact tests were used for analysis.

RESULTS: A total of 200 achalasia patients were included of which 36 underwent POEM, 22 underwent PD and 142 underwent LHM. POEM patients were older (55.4 ± 16.8 years *vs* 46.5 ± 15.7 years, $P = 0.013$) and had higher BMI than LHM (29.1 ± 5.9 kg/m^2 *vs* 26 ± 5.1 kg/m^2, $P = 0.012$). More number of patients in POEM and PD groups had undergone prior treatments compared to LHM group (72.2% *vs* 68.2% *vs* 44.3% respectively, $P = 0.003$). At 2 mo post-treatment, all TBE parameters including barium column height, width and volume remaining at 1 and 5 min improved significantly in all three treatment groups ($P = 0.01$ to $P < 0.001$) except the column height at 1 min in PD group ($P = 0.11$) . At 2 mo post-treatment, there was significant improvement in basal LES pressure and LES-IRP in both LHM (40.5 mmHg *vs* 14.5 mmHg and 24 mmHg *vs* 7.1 mmHg respectively, $P < 0.001$) and POEM groups (38.7 mmHg *vs* 11.4 mmHg and 23.6 mmHg *vs* 6.6 mmHg respectively, $P < 0.001$). However, when the efficacy of three treatments were compared to each other in terms of improvement in TBE or HREM parameters at 2 mo, there was no significant difference ($P > 0.05$).

CONCLUSION: POEM, PD and LHM were all effective in improving esophageal function in achalasia at short-term. There was no difference in efficacy between the three treatments.

Key words: Achalasia; Dysphagia; Heller myotomy; Peroral endoscopic myotomy; Manometry; Pneumatic dilation

Core tip: This study evaluated and compared the efficacy of peroral endoscopic myotomy with laparoscopic Heller myotomy and pneumatic dilation in improving esophageal function in achalasia. Esophageal function was objectively assessed by timed barium esophagram and high resolution manometry at 2 mo follow-up. The results demonstrate that all three treatment modalities are effective in improving esophageal function at short term follow-up and there was no difference in efficacy between the three treatment modalities.

Sanaka MR, Hayat U, Thota PN, Jegadeesan R, Ray M, Gabbard SL, Wadhwa N, Lopez R, Baker ME, Murthy S, Raja S. Efficacy of peroral endoscopic myotomy *vs* other achalasia treatments in improving esophageal function. *World J Gastroenterol* 2016; 22(20): 4918-4925 Available from: URL: http://www.wjgnet.com/1007-9327/full/v22/i20/4918.htm DOI: http://dx.doi.org/10.3748/wjg.v22.i20.4918

INTRODUCTION

Achalasia is a rare primary esophageal motility disorder, with an incidence of about 1 per 100000 per year[1]. The disease is characterized by aperistalsis of the esophageal body and impaired relaxation of the lower esophageal sphincter (LES), caused by progressive destruction and degeneration of neurons in the myenteric plexus. Typical symptoms of achalasia are dysphagia, regurgitation of undigested food, retrosternal pain, and weight loss. The disease is irreversible and all the current treatments of achalasia are aimed at palliation of symptoms[2]. Established treatment options include disruption of the LES by endoscopic pneumatic dilation (PD) and laparoscopic Heller myotomy (LHM). Both treatments are considered the "standard of care" and have similar excellent short-term results, as demonstrated in a large, randomized, controlled trial[3]. Because of submucosal fibrosis after treatment and the natural course of the disease, symptoms can recur, leading to a need for retreatment in some patients. LHM has been shown to provide more durable long-term symptom relief than PD and is considered the preferred treatment[4]. Recently, peroral endoscopic myotomy (POEM) is emerging as an alternative to LHM. POEM has the advantages of minimal invasiveness of an endoscopic procedure and the precision of a surgical myotomy[5].

Both PD and LHM improve parameters of objective esophageal function, such as LES pressures on high resolution esophageal manometry (HREM), esophageal emptying on timed barium esophagram (TBE) and esophagogastric junction (EGJ) distensibility[6]. Objective improvement in these parameters regardless of symptoms is predictive of long-term favorable response. For example, patients with LES-Integrated relaxation pressures (IRP) of > 10 mmHg after treatment were shown to have a significantly higher risk for retreatment during follow-up[7-9]. Vaezi *et al*[10] have shown that patients with incomplete esophageal emptying after PD on TBE had a 90% risk for treatment failure within 1 year, whereas the treatment success rate remained about 90% in patients with complete emptying. Therefore, these parameters are useful not only to objectively determine esophageal function post-treatment, but also for predicting the need for retreatments.

Since POEM is relatively new, only short- and intermediate-term treatment success rates are available. There were several studies that showed objective improvement in esophageal function assessed by HREM and TBE findings after POEM[11-15]. Bhayani *et al*[16], reported that improvement in HREM parameters after POEM was comparable to LHM. To date, there are several studies comparing the improvement in esophageal function between either PD and LHM or POEM and LHM. However, there are no studies comparing the outcomes between all three treatment modalities. Hence, the aim of this study was to compare objective improvement in esophageal function among achalasia patients who underwent POEM, LHM and PD at our institution.

MATERIALS AND METHODS

This study was approved by the Institutional Review Board at the Cleveland Clinic. We reviewed medical records of all adult achalasia patients who underwent one of the three treatment modalities at our institution between January 2012 and March 2015. A written informed consent was obtained from all patients prior to the treatments. Patient demographics, type of achalasia, prior treatments, pre- and 2-mo post-treatment TBE and HREM parameters were compared between the three treatment groups. All patients undergoing either POEM or LHM had TBE and HREM performed before and at two months post-treatment as part of our standard clinical practice. Most of the patients who underwent PD had TBE and HREM performed before and TBE alone performed at two months post-treatment.

LHM procedure

In our patients, LHM was performed with anterior approach and thoracic esophagus was mobilized and full-thickness myotomy was performed along distal 4-6 cm of esophagus and was extended 2-3 cm on to the gastric wall. Subsequently a partial anterior fundoplication (Dor fundoplicaiton) was performed. Patients underwent barium swallow study next day to exclude perforation and liquid diet was initiated and gradually advanced over the next few days.

PD procedure

A standard upper endoscopy was performed under sedation by monitored anesthesia care and esophagus was cleared of any residual food debris. A guidewire was placed into the antrum and under fluoroscopic guidance, and a Rigiflex balloon (Boston Scientific, MA, United States) of either 30 mm or 35 mm diameter was passed and positioned across the gastroesophageal junction and inflated for few seconds until the "waist" was obliterated. A 30 mm balloon was used when patients underwent PD for the first time, and a 35 mm balloon was used for patients undergoing subsequent PD. All patients underwent a barium swallow post-procedure to exclude a perforation and were discharged home on clear liquid diet with gradual advancement of diet.

POEM procedure

All POEM procedures were performed under general anesthesia in an operating room using standard steps as described by Inoue *et al*[5]. The steps were (1) creation of a submucosal tunnel starting approximately 12 cm proximal to the LES and extending distally to about 2-4 cm into the stomach side. The submucosal tunnel was usually created on anterior esophageal wall except in post-Heller patients in whom it was created on the posterior esophageal wall; (2) Myotomy of the circular muscle fibers starting 3-4 cm distally from the first incision and 2-4 cm into the stomach wall; and (3) Closure of the entry site of the submucosal tunnel by using endoscopic clips. Next day, patients underwent a soluble contrast swallow radiograph to exclude transmural perforations. If swallow study is unremarkable, patients were started on clear liquid diet, discharged home and were advised to advance diet gradually over the next 1-2 wk.

HREM procedure

HREM was performed by using the following protocol: a 36-channel, solid-state catheter system with high-fidelity circumferential sensors at 1-cm intervals was advanced through the nasal canal (Sierra Scientific Instruments Inc., Los Angeles, CA, United States). Pressure data of ten, 5 mL swallows of water were recorded and analyzed by using a dedicated computerized analysis system. All relevant parameters were analyzed according to the Chicago classification. Diagnostic criteria for achalasia were incomplete relaxation of LES (IRP > 15 mmHg) and aperistalsis of the esophageal body. Achalasia was classified into type I, if there was 100% peristasis without esophageal pressurization, type II if there was pan-esophageal pressurization > 30 mmHg in $\geqslant$ 20% of swallows and as type III when there were premature contractions in $\geqslant$ 20% of swallows.

TBE procedure

Patients were instructed to drink the maximum volume of dilute barium sulfate contrast (45% weight in volume) that they could tolerate without regurgitation or aspiration (mostly between 100 and 250 mL) over a period of 30 to 45 s. With the patient in upright position, radiographs of the esophagus were taken at 1 and 5 min after the last swallow. Height and width of the barium column were measured using a calibrated ruler. Estimated esophageal barium volume was calculated as a simple cylinder (πr^2 × height of barium column, r = barium width divided by 2).

Statistical analysis

Data are presented as mean ± SD, median (25^{th}, 75^{th} percentiles) or frequency (percent). A univariable analysis was performed to assess differences between treatment groups. Analysis of variance (ANOVA) or the non-parametric Kruskal-Wallis tests were used for continuous or ordinal variables and Pearson's chi-square tests were used for categorical factors. When the overall test suggested a difference between at least 2 of the groups, post-hoc comparisons were done at a significance level of 0.017 (0.05/3 tests) to adjust for multiple comparisons. In addition, analysis of covariance was performed to assess the association between treatment and outcomes while adjusting for possible confounders. For each outcome, a logarithm transformation ln[(y-1) + min(y)] was modeled as the dependent variable with age at time of treatment, body mass index (BMI) and having had previous treatments

Table 1 Patient characteristics *n* (%)

Factor	PD (*n* = 22)		LHM (*n* = 142)		POEM (*n* = 36)		*P* value
	n	Summary	*n*	Summary	*n*	Summary	
Age at diagnosis (yr)	22	47.5 ± 17.0	142	45.8 ± 15.6	36	52.6 ± 17.2	0.078[a]
Age at current treatment (yr)	22	50.3 ± 17.9	142	46.5 ± 15.7[3]	36	55.4 ± 16.8[2]	0.013[a]
Gender	22		142		36		0.19[c]
Female		11 (50.0)		71 (50.0)		12 (33.3)	
Male		11 (50.0)		71 (50.0)		24 (66.7)	
Ethnicity	22		141		36		0.85[d]
White		17 (77.3)		118 (83.7)		31 (86.1)	
Black		4 (18.2)		19 (13.5)		4 (11.1)	
Other		1 (4.5)		4 (2.8)		1 (2.8)	
BMI (kg/m^2)	22	27.1 ± 6.9	142	26.0 ± 5.1[3]	36	29.1 ± 5.9[2]	0.012[a]
Achalasia sub-type	14		120		34		0.023[d]
Subtype 1		5 (35.7)		30 (25.0)		13 (38.2)	
Subtype 2		6 (42.9)		82 (68.3)		18 (52.9)	
Subtype 3		2 (14.3)		1 (0.83)		3 (8.8)	
Achalasia variant		1 (7.1)		7 (5.8)		0 (0.0)	
Prior treatments							
Received any prior treatment	22	15 (68.2)	140	62 (44.3)[3]	36	26 (72.2)[2]	0.003[c]
Months from last to current treatment	14	17.7 [2.3, 87.5]	54	6.3 [3.2,28.5]	25	14.7 [6.4,20.2]	0.29[b]
Botulinium toxin injection	22	1 (4.5)	140	16 (11.4)	36	8 (22.2)	0.11[c]
PD	22	9 (40.9)[2]	140	19 (13.6)[1,3]	36	11 (30.6)[2]	0.002[c]
LHM	22	7 (31.8)[2]	140	1 (0.71)[1,3]	36	10 (27.8)[2]	< 0.001[c]
Botulinum toxin injection and regular endoscopic balloon dilation	22	2 (9.1)	140	1 (0.71)	36	0 (0.0)	0.050[d]
Regular endoscopic balloon dilation	22	3 (13.6)	140	34 (24.3)[3]	36	2 (5.6)[2]	0.031[c]

[1]Significantly different from PD; [2]Significantly different from LHM; [3]Significantly different from POEM. Values presented as Mean ± SD, Median [P25, P75] or N (column %). *P*-value: a = ANOVA, b = Kruskal-Wallis test, c = Pearson's χ^2 test, d = Fisher's Exact test. PD: Pneumatic dilation; LHM: Laparoscopic Heller myotomy; POEM: Peroral endoscopic myotomy.

as the independent variables. No adjustments were done for type of achalasia because (1) it was missing for > 15% of patients and (2) it is a 5 level variable. All analyses were performed using SAS version 9.4 (The SAS Institute, Cary, NC, United States) and a *P*-value < 0.05 was considered statistically significant. The statistical methods of this study were reviewed by Rocio Lopez, MS, Biostatistician from Department of Biostatistics, Cleveland Clinic, Cleveland, OH, United States.

RESULTS

A total of 200 achalasia patients were included of which 36 underwent POEM, 22 underwent PD and 142 underwent LHM. Baseline patient characteristics are summarized in Table 1. Patients who underwent POEM were significantly older compared to LHM patients (55.4 years *vs* 46.5 years, *P* = 0.013). POEM patients also had higher BMI compared to LHM patients (29.1 kg/m^2 *vs* 26 kg/m^2, *P* = 0.012). PD and POEM patients have had more prior treatments performed compared to LHM patients (68%, 72% and 44%, *P* = 0.003).

Pre-treatment and 2-mo post-treatment TBE and HREM findings in the three treatment groups are summarized in Tables 2 and 3. There was no significant difference in pre-treatment TBE and HREM parameters in all three treatments groups (*P* > 0.05). Post-treatment, there was significant improvement in TBE and HREM parameters in all three treatment groups. Both basal LES and LES-IRP pressures improved significantly after both POEM and LHM (*P* < 0.05). HREM was not routinely performed in all PD patients post-treatment and hence that data is not available. Actual LES-IRP at 2 mo decreased to less than 10 mmHg in 66/92 patients (71.7%) in LHM group, 19/26 patients (73.1%) in POEM group and 0/3 patients (0%) in PD group (*P* not significant). TBE parameters such as barium column height, width and volume remaining at both 1 min and 5 min improved significantly in all the three treatment groups (*P* < 0.05) except column height at 1 min in TBE group (*P* = 0.11). Actual barium column height at 5 min on TBE at 2 mo decreased by more than 50% in 73/131 patients (55.7%) in LHM group, 16/34 patients (47.1%) in POEM group and 7/20 patients (35%) in PD group (*P* not significant). Eckardt symptom scores improved significantly in both POEM and LHM patients (although only 7 patients had these available both pre- and post-treatment in LHM group). Eckardt scores were not available in PD group.

Details of multivariate analysis assessing pre- and post-treatment differences in HREM and TBE parameters in all three treatment groups are shown in Table 4. The degree of improvement in TBE parameters did not significantly differ among the three treatment groups (*P* > 0.05). Similarly, there was no significant difference in improvement in HREM parameters between the POEM and LHM groups (*P* > 0.05). Only 3 patients in the PD group had HREM testing done pre- and post-treatment, hence this group was not included

Table 2 High-resolution esophageal manometry and timed barium swallow findings: Univariable analysis

Factor	PD (*n* = 22)		LHM (*n* = 142)		POEM (*n* = 36)		*P* value
	n	Summary	*n*	Summary	*n*	Summary	
Pre-treatment							
Eckardt score	2	7.0 (7.0, 7.0)	9	6.0 (5.0, 7.0)	36	6.5 (5.0, 8.0)	0.77
HREM							
Basal mean pressure (mmHg)	2	31.9 (10.6, 53.2)	86	40.5 (27.2, 51.7)	24	38.7 (27.0, 48.7)	0.89
LES-IRP pressure (mmHg)	3	29.1 (12.0, 34.5)	92	24.0 (17.5, 34.4)	26	23.6 (20.2, 33.4)	0.92
TBE							
Height in 1 min (cm)	22	10.2 (7.0, 13.6)	133	9.5 (7.2, 15.0)	34	9.8 (4.0, 14.5)	0.43
Width in 1 min (cm)	22	3.4 (2.5, 4.0)	133	3.0 (2.5, 4.0)	34	3.4 (2.0, 4.4)	0.93
Volume remaining at 1 min (cc)	22	67.3 (44.0, 126.2)	133	71.6 (41.1, 131.9)	34	52.8 (37.7, 119.2)	0.44
Height in 5 min (cm)	20	6.5 (4.0, 10.5)	131	8.0 (5.0, 12.5)	34	5.3 (2.5, 10.0)	0.063
Width at 5 min (cm)	20	2.7 (2.0, 3.6)	131	2.5 (2.0, 3.7)	34	2.5 (1.5, 4.0)	0.83
Volume remaining at 5 min (cc)	20	40.8 (15.5, 73.1)	131	49.1 (15.7, 91.6)	34	25.4 (11.3, 62.8)	0.12
2-mo post-treatment							
Eckardt score	4	4.5 (2.0, 6.0)	50	1.00 (0.00, 2.0)	36	1.00 (0.00, 2.0)	0.073
HREM							
Basal mean pressure (mmHg)	2	22.0 (18.8, 25.1)	86	14.5 (7.6, 22.7)	24	11.4 (8.2, 20.2)	0.32
LES-IRP pressure (mmHg)	3	10.8 (10.5, 19.4)	92	7.1 (3.9, 10.7)	26	6.6 (3.3, 11.1)	0.18
TBE							
Height in 1 min (cm)	22	8.0 (5.8, 11.0)	133	6.7 (4.5, 10.2)	34	6.3 (2.1, 9.5)	0.39
Width in 1 min (cm)	22	2.0 (1.5, 2.5)	133	2.0 (1.2, 2.5)	34	1.6 (0.50, 2.5)	0.28
Volume remaining at 1 min (cc)	22	25.4 (14.1, 41.7)	133	20.4 (6.0, 49.8)	34	12.8 (0.79, 47.7)	0.31
Height in 5 min (cm)	20	2.2 (0.00, 6.5)	131	2.5 (0.00, 6.2)	34	2.3 (0.00, 6.9)	0.94
Width at 5 min (cm)	20	1.05 (0.00, 2.6)	131	1.00 (0.00, 2.1)	34	0.50 (0.00, 2.0)	0.97
Volume remaining at 5 min (cc)	20	4.1 (0.00, 30.2)	131	2.7 (0.00, 21.2)	34	0.54 (0.00, 18.8)	0.98
Post - pre treatment difference							
Eckardt score	-	-	7	-6.0 (-8.0, -2.0)	36	-6.0 (-7.0, -4.0)	0.75
HREM							
Post-Pre basal mean pressure (mmHg)	2	-10.0 (-34.4, 14.5)	86	-25.1 (-36.8, -12.1)	24	-19.6 (-43.1, -11.9)	0.78
Post-Pre LES-IRP pressure (mmHg)	3	-9.7 (-23.7, -1.5)	92	-15.2 (-26.4, -8.3)	26	-14.2 (-24.5, -7.8)	0.60
TBE							
Post-Pre height at 1 min (cm)	22	-0.90 (-5.5, 1.9)	133	-2.5 (-7.0, 0.30)	34	-2.8 (-8.5, 1.5)	0.73
Post-Pre width at 1 min (cm)	22	-1.4 (-2.0, -0.30)	133	-1.00 (-2.0, -0.20)	34	-1.5 (-2.1, 0.00)	0.79
Post-Pre volume at 1 min (cc)	22	-40.2 (-81.2, -14.1)	133	-35.8 (-101.8, -10.4)	34	-29.5 (-100.7, -0.29)	0.74
Post-Pre height at 5 min (cm)	20	-0.75 (-5.4, 0.05)	131	-4.7 (-10.0, 0.00)	34	-2.0 (-7.5, 1.9)	0.069
Post-Pre width at 5 min (cm)	20	-0.90 (-2.3, 0.00)	131	-1.5 (-2.2, -0.20)	34	-1.00 (-2.4, 0.00)	0.86
Post-Pre volume at 5 min (cc)	20	-14.0 (-45.9, -2.6)	131	-31.3 (-66.1, -5.5)	34	-17.0 (-37.7, 0.00)	0.14

Values presented as Median (P25, P75) with Kruskal-Wallis tests. PD: Pneumatic dilation; LHM: Laparoscopic Heller myotomy: POEM: Peroral endoscopic myotomy; HREM: High resolution esophageal manometry; TBE: Timed barium esophagram; LES: Lower esophageal sphincter; IRP: Integrated relaxation pressure.

in the multivariate analysis on HREM.

DISCUSSION

Our study showed that all three treatment modalities for achalasia namely PD, LHM and POEM were effective in improving esophageal function evaluated at 2 mo post-treatment. All three treatments resulted in significant improvement in esophageal emptying on TBE. Both POEM and LHM led to significant decrease in LES pressures on HREM. More importantly, this is the first study that demonstrates efficacy of all three treatments and that there was no significant difference in efficacy between the three treatments on short term follow-up.

Pre and post-treatment physiologic evaluation of esophageal function in achalasia by HREM is very important to assess the improvement after treatment and also to predict long term response. HREM parameters such as LES-IRP were shown to correlate with symptom scores of achalasia[17,18]. Several studies in achalasia patients treated with PD and LHM have shown that the HREM parameters also predict long term need for retreatment[6-9,19]. As such LES-IRP of greater than 10 mmHg after treatment was predictive of requiring retreatment on follow-up. In our study, LES-IRP decreased significantly after treatment in all three treatment modalities (although only 3 patients in PD group had HREM post-treatment). Post-treatment LES-IRP was only 7.1 mmHg and 6.6 mmHg in LHM and POEM groups respectively, and hence we predict our patients would have excellent long term efficacy. Teitelbaum *et al*[12] have shown that decreased LES-IRP at 2 mo after POEM persisted at 1 year as well, which supports our long-term prediction in our POEM and LHM groups.

Table 3 Improvement in high resolution esophageal manomtery and timed barium esophagram parameters in each treatment group

Factor	*n*	PD (*n* = 22) Pre-Treatment	Post-treatment	*P* value
HREM[1]				
TBE				
Height at 1 min (cm)	22	10.2 (7.0, 13.6)	8.0 (5.8, 11.0)	0.11
Width at 1 min (cm)	22	3.4 (2.5, 4.0)	2.0 (1.5, 2.5)	< 0.001
Volume at 1 min (cc)	22	67.3 (44.0, 126.2)	25.4 (14.1, 41.7)	< 0.001
Height at 5 min (cm)	20	6.5 (4.0, 10.5)	2.2 (0.00, 6.5)	0.026
Width at 5 min (cm)	20	2.7 (2.0, 3.6)	1.05 (0.00, 2.6)	< 0.001
Volume at 5 min (cc)	20	40.8 (15.5, 73.1)	4.1 (0.00, 30.2)	0.001
		LHM (*n* = 142)		
Factor				
HREM				
Basal mean pressure (mmHg)	86	40.5 (27.2, 51.7)	14.5 (7.6, 22.7)	< 0.001
LES-IRP pressure (mmHg)	92	24.0 (17.5, 34.4)	7.1 (3.9, 10.7)	< 0.001
TBE				
Height at 1 min (cm)	133	9.5 (7.2, 15.0)	6.7 (4.5, 10.2)	< 0.001
Width at 1 min (cm)	133	3.0 (2.5, 4.0)	2.0 (1.2, 2.5)	< 0.001
Volume at 1 min (cc)	133	71.6 (41.1, 131.9)	20.4 (6.0, 49.8)	< 0.001
Height at 5 min (cm)	131	8.0 (5.0, 12.5)	2.5 (0.00, 6.2)	< 0.001
Width at 5 min (cm)	131	2.5 (2.0, 3.7)	1.00 (0.00, 2.1)	< 0.001
Volume at 5 min (cc)	131	49.1 (15.7, 91.6)	2.7 (0.00, 21.2)	< 0.001
		POEM (*n* = 36)		
Factor				
Eckardt score	36	6.5 (5.0, 8.0)	1.00 (0.00, 2.0)	< 0.001
HREM				
Basal mean pressure (mmHg)	24	38.7 (27.0, 48.7)	11.4 (8.2, 20.2)	< 0.001
LES-IRP pressure (mmHg)	26	23.6 (20.2, 33.4)	6.6 (3.3, 11.1)	< 0.001
TBE				
Height at 1 min (cm)	34	9.8 (4.0, 14.5)	6.3 (2.1, 9.5)	0.01
Width at 1 min (cm)	34	3.4 (2.0, 4.4)	1.6 (0.50, 2.5)	< 0.001
Volume at 1 min (cc)	34	52.8 (37.7, 119.2)	12.8 (0.79, 47.7)	< 0.001
Height at 5 min (cm)	34	5.3 (2.5, 10.0)	2.3 (0.00, 6.9)	0.017
Width at 5 min (cm)	34	2.5 (1.5, 4.0)	0.50 (0.00, 2.0)	< 0.001
Volume at 5 min (cc)	34	25.4 (11.3, 62.8)	0.54 (0.00, 18.8)	0.003

[1]HREM data not available in PD group. Values presented as Median (P25, P75) with Wilcoxon signed rank test. PD: Pneumatic dilation; LHM: Laparoscopic Heller myotomy; POEM: Peroral endoscopic myotomy; HREM: High resolution esophageal manometry; TBE: Timed barium esophagram; LES: Lower esophageal sphincter; IRP: Integrated relaxation pressure.

Esophageal emptying assessed by a TBE is a complementary test to HREM for functional assessment of esophageal physiology. Similar to LES-IRP, post-treatment improvement in esophageal emptying is a predictor of the need for retreatment in achalasia[3,10]. Vaezi *et al*[10] have shown that successful esophageal emptying, defined as at least 50% reduction of barium column after treatment, was associated with long-term remission of symptoms. In that study, patients with sub-optimal esophageal emptying after PD required retreatments on long-term follow-up. In our study, barium column height decreased by more than 50% in all three treatments groups at 2 mo follow-up, reinforcing the efficacy of all three treatments. In our POEM patients, Eckardt scores improved significantly paralleling the improvement in LES pressures. However, we suspect to have had similar decrease in Eckardt scores in LHM and PD groups if they were available, since LES pressures decreased significantly in those patients as well. There was also no significant difference in esophageal emptying between the three treatment groups, reinforcing comparable efficacy of all three treatment modalities.

In our study, there were some notable differences in patient characteristics among PD, LHM and POEM groups. Patients in POEM and PD treatments groups were older, had higher BMI, and more likely to have received prior treatments. This is likely due to the selection bias of a particular treatment modality for different patients at our institution. Usually younger patients and fit surgical candidates were offered LHM due to its well established long term durability record. Older and somewhat less ideal surgical candidates were preferentially offered either PD or POEM. Initially the following subsets of patients were considered for POEM: (1) Obese patients, patients with upper abdominal surgical scars *i.e.*, hostile abdomen and those with prior failed LHM, in whom LHM is technically difficult or less desirable; and (2) patients over 60 years of age (not younger patients since long term cumulative effects of gastroesophageal reflux disease (GERD) after POEM are not yet known). However, we do not believe that this selection bias should have affected the results of our study significantly.

Table 4 High resolution esophageal manomtery and Timed barium esophagram findings: Adjusted analysis[1]

Outcome	PD	LHM	POEM	*P* value
Eckardt score	[2]	-5.7 (-6.7, -4.5)	-5.6 (-6.1, -5.2)	0.94
HREM				
Post-Pre basal mean pressure (mm Hg)	[2]	-27.5 (-30.3, -24.5)	-33.1 (-38.0, -27.6)	0.084
Post-Pre LES-IRP pressure (mm Hg)	[2]	-20.1 (-22.2, -17.9)	-20.9 (-24.7, -16.5)	0.76
TBE				
Post-Pre height at 1 min (cm)	-2.7 (-5.1, -0.05)	-4.6 (-5.5, -3.7)	-5.4 (-7.1, -3.5)	0.21
Post-Pre width at 1 min (cm)	-1.4 (-1.9, -0.77)	-1.3 (-1.5, -1.03)	-1.7 (-2.2, -1.2)	0.28
Post-Pre volume at 1 min (cc)	-81.8 (-112.4, -44.3)	-79.3 (-92.7, -64.8)	-95.6 (-119.4, -67.6)	0.58
Post-Pre height at 5 min (cm)	-5.8 (-7.7, -3.7)	-6.0 (-6.8, -5.2)	-5.8 (-7.3, -4.1)	0.95
Post-Pre width at 5 min (cm)	-1.6 (-2.4, -0.74)	-1.5 (-1.8, -1.1)	-1.9 (-2.5, -1.3)	0.47
Post-Pre volume at 5 min (cc)	-68.2 (-89.9, -43.5)	-51.2 (-60.9, -41.0)	-64.6 (-82.0, -45.3)	0.28

[1]ANOVA analysis was used to obtain adjusted means. A logarithm transformation of each outcome [ln(y -1 + min(y)] was modeled as the outcome variable with age at time of treatment, BMI and having had previous treatments as the independent variables. 2Data not available Only 3 patients in PD group had HREM testing done both pre- and post-treatment, hence this group was not included in the models. Values presented as mean (95%CI). PD: Pneumatic dilation; LHM: Laparoscopic Heller myotomy; POEM: Peroral endoscopic myotomy; HREM: High resolution esophageal manomtery; TBE: Timed barium esophagram; LES: Lower esophageal sphincter; IRP: Integrated relaxation pressure.

There are some limitations in our study including its retrospective design and only short-term follow-up. The details of patients' symptoms such as Eckardt scores were not available in all our patients except in the POEM group. Only 3/22 patients had HREM after treatment in the PD group. Details about GERD, a common adverse effect of any achalasia treatment, were not available and hence were not included in this study. It is also beyond the scope of this paper and we acknowledge it as one of the limitations of our study. Evaluation of esophagogastric junction (EGJ) distensibility by EndoFlip is another parameter being used for assessing esophageal physiology and is a useful predictor of treatment outcomes[6]. EGJ distensibility was however, not assessed in our patients. The main strength of our study lies in the real world scenario of treating patients with established achalasia and a large number of patients in the study. All patients had multi-disciplinary clinical evaluation by gastroenterologists, thoracic surgeons and radiologists, along with TBE and HREM before and after treatment. This is also the first study which compared the efficacy of all three standard treatments of achalasia in a large number of patients.

In conclusion, this study shows that all three treatments of achalasia namely POEM, LHM and PD lead to improvement in esophageal function as assessed by HREM and TBE in the short-term. These results support the selection of any of the three treatment modalities based on patient characteristics and availability of local expertise to perform these procedures. Larger, prospective studies with homogeneous patient populations and longer follow-up are required to compare the efficacy of these treatment modalities in achalasia.

ACKNOWLEDGMENTS

This study was submitted in an abstract form to Digestive Disease Week, May 2016 at San Diego, CA, United States.

COMMENTS

Background

Achalasia is a primary esophageal motility disorder characterized by esophageal aperistalsis and impaired relaxation of lower esophageal sphincter. Standard treatments are palliative and include laparoscopic Heller myotomy (HLM) and endoscopic pneumatic dilation (PD). Recently peroral endoscopic myotomy is rapidly emerging as a standard treatment as well. This study evaluated and compared the efficacy of peroral endoscopic myotomy *vs* other standard treatments of achalasia in improving esophageal function.

Research frontiers

Peroral endoscopic myotomy is gaining popularity due to its minimal invasiveness of an endoscopic procedure and high precision of a surgical myotomy. There are several studies comparing peroral endoscopic myotomy with either PD or HLM. This study compared the efficacy of all three treatment modalities in improving esophageal function. The study findings help the peers in appropriate selection of each treatment modality based on local expertise and availability.

Innovations and breakthroughs

Recent innovations in the achalasia include emergence of peroral endoscopic myotomy as a standard treatment modality. Several studies have shown its effectives in palliation of symptoms comparable to other treatments such as PD and HLM. This study evaluated and compared the efficacy of all three standard treatments in improving esophageal function objectively by timed barium esophagram and high resolution esophageal manometry. Peroral endoscopic myotomy was effective and was comparable to other treatments in improving esophageal function in the short term in patients with achalasia.

Applications

This study results suggested that perooral endoscopic myotomy is effective not only in proving symptoms but also objective esophageal function in achalasia similar to PD and HLM. Furthermore, the study findings have practical implications in the sense that selection of one of the three treatment modalities may be done based on local expertise and patient choice.

Terminology

Achalasia is rare primary esophageal disorder characterized by esophageal peristasis and impaired relaxation of lower esophageal sphincter. Treatment of achalasia is aimed at palliation of symptoms by disruption of lower esophageal sphincter. Standard treatments include endoscopic PD, HLM and recently

emerging incisionless peroral endoscopic myotomy.

Peer-review

There is paucity of data comparing the efficacy of all three treatment modalities of achalasia namely HLM, PD and peroral endoscopic myotomy in improving objective esophageal function. This study showed that all three treatments modalities are effective and comparable in the short term. These findings have important practical implications in the treatment of patients with achalasia.

REFERENCES

1 **Podas T**, Eaden J, Mayberry M, Mayberry J. Achalasia: a critical review of epidemiological studies. *Am J Gastroenterol* 1998; **93**: 2345-2347 [PMID: 9860390]

2 **Vaezi MF**, Pandolfino JE, Vela MF. ACG clinical guideline: diagnosis and management of achalasia. *Am J Gastroenterol* 2013; **108**: 1238-1249; quiz 1250 [PMID: 23877351 DOI: 10.1038/ajg.2013.196]

3 **Boeckxstaens GE**, Annese V, des Varannes SB, Chaussade S, Costantini M, Cuttitta A, Elizalde JI, Fumagalli U, Gaudric M, Rohof WO, Smout AJ, Tack J, Zwinderman AH, Zaninotto G, Busch OR. Pneumatic dilation versus laparoscopic Heller's myotomy for idiopathic achalasia. *N Engl J Med* 2011; **364**: 1807-1816 [PMID: 21561346 DOI: 10.1056/NEJMoa1010502]

4 **Yaghoobi M**, Mayrand S, Martel M, Roshan-Afshar I, Bijarchi R, Barkun A. Laparoscopic Heller's myotomy versus pneumatic dilation in the treatment of idiopathic achalasia: a meta-analysis of randomized, controlled trials. *Gastrointest Endosc* 2013; **78**: 468-475 [PMID: 23684149 DOI: 10.1016/j.gie.2013.03.1335]

5 **Inoue H**, Minami H, Kobayashi Y, Sato Y, Kaga M, Suzuki M, Satodate H, Odaka N, Itoh H, Kudo S. Peroral endoscopic myotomy (POEM) for esophageal achalasia. *Endoscopy* 2010; **42**: 265-271 [PMID: 20354937 DOI: 10.1055/s-0029-1244080]

6 **Rohof WO**, Hirsch DP, Kessing BF, Boeckxstaens GE. Efficacy of treatment for patients with achalasia depends on the distensibility of the esophagogastric junction. *Gastroenterology* 2012; **143**: 328-335 [PMID: 22562023 DOI: 10.1053/j.gastro.2012.04.048]

7 **Zaninotto G**, Costantini M, Rizzetto C, Zanatta L, Guirroli E, Portale G, Nicoletti L, Cavallin F, Battaglia G, Ruol A, Ancona E. Four hundred laparoscopic myotomies for esophageal achalasia: a single centre experience. *Ann Surg* 2008; **248**: 986-993 [PMID: 19092343 DOI: 10.1097/SLA.0b013e3181907bdd]

8 **Eckardt VF**, Gockel I, Bernhard G. Pneumatic dilation for achalasia: late results of a prospective follow up investigation. *Gut* 2004; **53**: 629-633 [PMID: 15082578]

9 **Hulselmans M**, Vanuytsel T, Degreef T, Sifrim D, Coosemans W, Lerut T, Tack J. Long-term outcome of pneumatic dilation in the treatment of achalasia. *Clin Gastroenterol Hepatol* 2010; **8**: 30-35 [PMID: 19782766 DOI: .10.1016/j.cgh.2009.09.020]

10 **Vaezi MF**, Baker ME, Achkar E, Richter JE. Timed barium oesophagram: better predictor of long term success after pneumatic dilation in achalasia than symptom assessment. *Gut* 2002; **50**: 765-770 [PMID: 12010876]

11 **Verlaan T**, Rohof WO, Bredenoord AJ, Eberl S, Rösch T, Fockens P. Effect of peroral endoscopic myotomy on esophagogastric junction physiology in patients with achalasia. *Gastrointest Endosc* 2013; **78**: 39-44 [PMID: 23453184 DOI: 10.1016/j.gie.2013.01.006]

12 **Teitelbaum EN**, Soper NJ, Santos BF, Arafat FO, Pandolfino JE, Kahrilas PJ, Hirano I, Hungness ES. Symptomatic and physiologic outcomes one year after peroral esophageal myotomy (POEM) for treatment of achalasia. *Surg Endosc* 2014; **28**: 3359-3365 [PMID: 24939164 DOI: 10.1007/s00464-014-3628-1]

13 **Lu B**, Li M, Hu Y, Xu Y, Zhang S, Cai LJ. Effect of peroral esophageal myotomy for achalasia treatment: A Chinese study. *World J Gastroenterol* 2015; **21**: 5622-5629 [PMID: 25987787 DOI: 10.3748/wjg.v21.i18.5622]

14 **Inoue H**, Sato H, Ikeda H, Onimaru M, Sato C, Minami H, Yokomichi H, Kobayashi Y, Grimes KL, Kudo SE. Per-Oral Endoscopic Myotomy: A Series of 500 Patients. *J Am Coll Surg* 2015; **221**: 256-264 [PMID: 26206634 DOI: 10.1016/j.jamcollsurg.2015.03.057]

15 **Familiari P**, Gigante G, Marchese M, Boskoski I, Tringali A, Perri V, Costamagna G. Peroral Endoscopic Myotomy for Esophageal Achalasia: Outcomes of the First 100 Patients With Short-term Follow-up. *Ann Surg* 2016; **263**: 82-87 [PMID: 25361224 DOI: 10.1097/SLA.0000000000000992]

16 **Bhayani NH**, Kurian AA, Dunst CM, Sharata AM, Rieder E, Swanstrom LL. A comparative study on comprehensive, objective outcomes of laparoscopic Heller myotomy with per-oral endoscopic myotomy (POEM) for achalasia. *Ann Surg* 2014; **259**: 1098-1103 [PMID: 24169175 DOI: 10.1097/SLA.0000000000000268]

17 **Yaghoobi M**, Mikaeli J, Montazeri G, Nouri N, Sohrabi MR, Malekzadeh R. Correlation between clinical severity score and the lower esophageal sphincter relaxation pressure in idiopathic achalasia. *Am J Gastroenterol* 2003; **98**: 278-283 [PMID: 12591041]

18 **Tang Y**, Xie C, Wang M, Jiang L, Shi R, Lin L. Association of High-Resolution Manometry Metrics with the Symptoms of Achalasia and the Symptomatic Outcomes of Peroral Esophageal Myotomy. *PLoS One* 2015; **10**: e0139385 [PMID: 26421919 DOI: 10.1371/journal.pone.0139385]

19 **Alderliesten J**, Conchillo JM, Leeuwenburgh I, Steyerberg EW, Kuipers EJ. Predictors for outcome of failure of balloon dilatation in patients with achalasia. *Gut* 2011; **60**: 10-16 [PMID: 21068135 DOI: 10.1136/gut.2010.211409]

P- Reviewer: Castro FJ, Osawa S **S- Editor**: Qi Y **L- Editor**: A **E- Editor**: Wang CH

World Journal of Gastroenterology

Submit a Manuscript: http://www.wjgnet.com/esps/
Help Desk: http://www.wjgnet.com/esps/helpdesk.aspx
DOI: 10.3748/wjg.v22.i20.4926

World J Gastroenterol 2016 May 28; 22(20): 4926-4935
ISSN 1007-9327 (print) ISSN 2219-2840 (online)

ORIGINAL ARTICLE

Prospective Study

Acoustic radiation force impulse imaging for assessing liver fibrosis in alcoholic liver disease

Anita Kiani, Vanessa Brun, Fabrice Lainé, Bruno Turlin, Jeff Morcet, Sophie Michalak, Antonia Le Gruyer, Ludivine Legros, Edouard Bardou-Jacquet, Yves Gandon, Romain Moirand

Anita Kiani, Vanessa Brun, Yves Gandon, Department of Abdominal Imaging, Rennes University Hospital, 35033 Rennes, France

Fabrice Lainé, Jeff Morcet, Clinical Inverstigation Center, CIC INSERM 1414, Rennes University Hospital, 35033 Rennes, France

Fabrice Lainé, Antonia Le Gruyer, Ludivine Legros, Edouard Bardou-Jacquet, Romain Moirand, Department of Hepatology, Rennes University Hospital, 35033 Rennes, France

Bruno Turlin, Department of Pathology, Rennes University Hospital Rennes, 35033 Rennes, France

Sophie Michalak, Department of Pathology, Angers University Hospital, 49100 Angers, France

Romain Moirand, Department of Addictology, Rennes University Hospital, 35033 Rennes, France

Romain Moirand, Department of Research INSERM UMR 991, Rennes 1 Medicine University, 35000 Rennes, France

Author contributions: Kiani A, Lainé F and Moirand R designed the research; Kiani A, Brun V, Lainé F, Turlin B, Michalak S, Le Gruyer A, Legros L, Bardou-Jacquet E and Moirand R performed the research; Kiani A, Brun V, Lainé F, Morcet J, Gandon Y and Moirand R analyzed the data; Morcet J contributed to statistical analysis; Kiani A, Brun V, Lainé F, Morcet J, Bardou-Jacquet E nd Moirand R wrote the paper.

Institutional review board statement: The local ethics committee approved this study.

Clinical trial registration statement: This study is registered at https://clinicaltrials.gov/ct2/show/NCT01789008?term=NCT01789008&rank=1. The registration identification number is NCT01789008.

Informed consent statement: All study participants, or their legal guardian, provided informed written consent prior to study enrollment.

Conflict-of-interest statement: The authors of this manuscript have no conflicts of interest to disclose.

Data sharing statement: No additional data are available.

Correspondence to: Anita Kiani, MD, Department of Abdominal Imaging, Rennes University Hospital, CHU Rennes, 2 rue H. Le Guilloux, 35033 Rennes, France. anita.kiani@chu-rennes.fr
Telephone: +33-2-99284309
Fax: +33-2-99284364

Received: February 10, 2016
Peer-review started: February 10, 2016
First decision: March 8, 2016
Revised: March 26, 2016
Accepted: April 7, 2016
Article in press: April 7, 2016
Published online: May 28, 2016

Abstract

AIM: To evaluate the performance of elastography by ultrasound with acoustic radiation force impulse (ARFI) in determining fibrosis stage in patients with alcoholic liver disease (ALD) undergoing alcoholic detoxification in relation to biopsy.

METHODS: Eighty-three patients with ALD undergoing detoxification were prospectively enrolled. Each patient underwent ARFI imaging and a liver biopsy on

the same day. Fibrosis was staged according to the METAVIR scoring system. The median of 10 valid ARFI measurements was calculated for each patient.

RESULTS: Sixty-nine males and thirteen females (one patient excluded due to insufficient biopsy size) were assessed with a mean alcohol consumption of 132.4 ± 128.8 standard drinks per week and mean cumulative year duration of 17.6 ± 9.5 years. Sensitivity and specificity were respectively 82.4% (0.70-0.95) and 83.3% (0.73-0.94) (AUROC = 0.87) for F ⩾ 2 with a cut-off value of 1.63m/s; 82.4% (0.64-1.00) and 78.5% (0.69-0.89) (AUROC = 0.86) for F ⩾ 3 with a cut-off value of 1.84m/s; and 92.3% (0.78-1.00] and 81.6% (0.72-0.90) (AUROC = 0.89) for F = 4 with a cut-off value of 1.94 m/s.

CONCLUSION: ARFI is an accurate, non-invasive and easy method for assessing liver fibrosis in patients with ALD undergoing alcoholic detoxification.

Key words: Alcoholic liver disease; Elastography; Non-invasive; Acoustic radiation force impulse; Fibrosis

Core tip: The aim of this study was to evaluate the performance of elastography by ultrasound with acoustic radiation force impulse (ARFI) in determining fibrosis stage in patients with alcoholic liver disease (ALD) undergoing alcoholic detoxification. Compared to biopsy, ARFI is an accurate, non-invasive and easy method for assessing liver fibrosis in patients with ALD undergoing alcoholic detoxification, with a good sensitivity and specificity.

Kiani A, Brun V, Lainé F, Turlin B, Morcet J, Michalak S, Le Gruyer A, Legros L, Bardou-Jacquet E, Gandon Y, Moirand R. Acoustic radiation force impulse imaging for assessing liver fibrosis in alcoholic liver disease. *World J Gastroenterol* 2016; 22(20): 4926-4935 Available from: URL: http://www.wjgnet.com/1007-9327/full/v22/i20/4926.htm DOI: http://dx.doi.org/10.3748/wjg.v22.i20.4926

INTRODUCTION

Chronic alcohol abuse is a major public health problem worldwide. Alcoholic liver disease (ALD) is one of the most common complications and a leading cause of alcohol-related death, due to liver cirrhosis and its complications. In 2004, 3.8% of all global deaths and 4.6% of global disability-adjusted life-years were attributable to alcohol consumption. The treatment of alcoholic liver disease generates substantial costs for the healthcare system[1].

Three histological lesions characterise ALD: steatosis, steatohepatitis and fibrosis. There are different stages of fibrosis, the last of which is cirrhosis. In ALD, it is important to know the fibrosis stage in order to guide management decisions and estimate prognosis. The appropriate intervention strategies can prevent serious long-term outcomes[2]. Patients with cirrhosis run a greater risk of complications (portal hypertension, hepatocellular carcinoma, ascites, *etc.*) and need closer follow-up. Informing patients of their cirrhosis could also provide an incentive to stop alcohol consumption. However, patients with severe fibrosis or cirrhosis are completely clinically asymptomatic for a long period of time and can be difficult to diagnose.

Liver biopsy is the gold standard for assessment of liver fibrosis, evaluating fibrosis, steatosis and the necroinflammatory stage at the same time. However, biopsy is an invasive procedure associated with morbidity and minor complications (local discomfort at the biopsy site, pain and transient hypotension due to a vasovagal reaction) reported in 5%-20% of cases and major complications (bleeding and peritonitis) in 0.3%-0.6% of cases. The mortality rate is 0.01%-0.3%[3]. Moreover, there are other considerations such as contraindications (ascites, intrahepatic biliary duct dilation, coagulation disorders), insufficient sampling and inter-observer variability. A 1-d hospital stay is also necessary, leading to significant costs.

This led to the development of alternative non-invasive methods for assessing hepatic fibrosis in alcoholic liver disease. Serum markers alone or in combination with specific algorithms have been used for the non-invasive assessment of liver fibrosis. Examples include Fibrotest®, Forns index and APRI[4-6]. The limitations of these tests are the influence of comorbid conditions and a lack of liver specificity. Another method involves measuring the elasticity of liver tissue (liver stiffness) which is markedly influenced by the stage of fibrosis. The most popular method for measuring liver stiffness is transient elastography (TE) by Fibroscan®, which has been validated for hepatitis C liver disease patients. Some authors have even combined TE and serum markers[7].

A new ultrasound technique has recently emerged: acoustic radiation force impulse (ARFI) elastography. ARFI could be of great utility in the measurement of liver fibrosis in alcoholic liver disease. This non-invasive method has the particular advantage of combining conventional ultrasound and liver stiffness measurement. Ultrasound is the primary imaging technique used worldwide to evaluate diffuse hepatic diseases. Acoustic radiation force is a phenomenon associated with the propagation of acoustic waves in attenuating media. The device generates a short-duration (262 ms) acoustic pulse by ultrasound. This pulse creates mechanical excitation and displacement of tissue. The deformation induced by the acoustic pulse is followed by a relaxation process after which the tissue returns to its original configuration, generating a shear wave. The speed of this wave is cal-

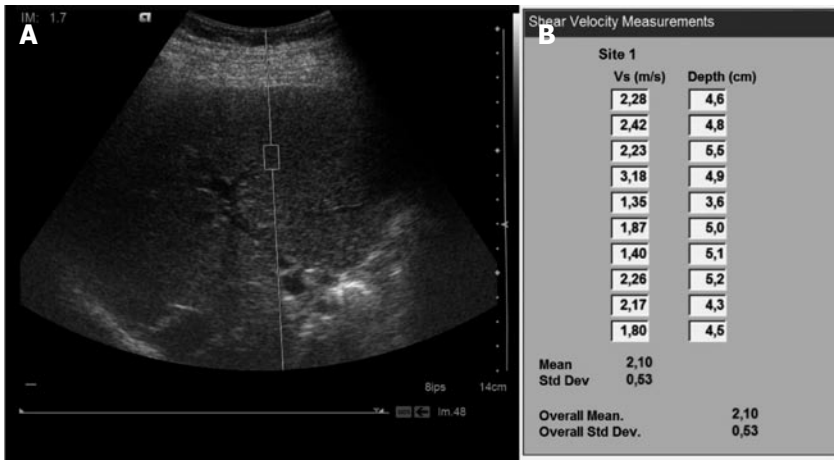

Figure 1 Image of liver stiffness measurement by acoustic radiation force impulse in patients with alcoholic liver disease. A: Acoustic radiation force impulse examination of a patient; B: Ten values with associated depths.

culated, providing a quantitative measurement. The shear wave speed of the tissue can be reconstructed as soft tissues are elastic and deformed more easily than rigid tissue.

In the past few years, ARFI has started to be assessed in comparison to biopsy, TE and biological markers. These studies mainly involved hepatitis B, hepatitis C and non-alcoholic steatohepatitis (NASH).

The aim of our prospective study was to evaluate the performance of ARFI in determining fibrosis stage in patients with alcoholic liver disease in relation to biopsy.

MATERIALS AND METHODS

Subjects

The local ethics committee approved this study. All patients gave written informed consent prior to enrolment. This study is an ancillary single-centre study of a larger, ongoing, multi-centre trial on validation of non-invasive fibrosis tests in ALD. Clinical Trials Identifier: NCT01789008.

From February 2013 to June 2015, the study was offered to all patients referred to the University Hospital of Rennes, France, who were admitted to the addiction treatment unit in the liver disease department for detoxification with an indication of liver biopsy for alcoholic liver disease. The inclusion criteria were: patients over 18 years old, hospitalisation for alcoholic detoxification, high-risk alcohol consumption (more than 210 g of alcohol per week for men and 140 g of alcohol per week for women) for a cumulative period of more than 5 years, a rise in serum aspartate transferase (AST) greater than 1.5 the upper limit of the normal range, associated with a rise in gamma-glutamyl transferase (GGT) and not explained by another cause of liver disease. When patients had features of metabolic syndrome or were obese, liver disease was felt to be principally due to alcohol consumption when the AST/alanine amino transferase (ALT) ratio was greater than one, and GGT was markedly high, and when the abnormalities decreased with alcohol withdrawal. Non-inclusion criteria were: cirrhosis already known or obvious due to clinical and biological signs (ascites, increased prothrombin time or oesophageal varices), other causes of hepatic disease (viral, autoimmune or cholestatic disease) or contraindication to biopsy. The interval between alcohol cessation and the procedure was not more than 10 d. Eighty-three patients were prospectively enrolled.

ARFI elastography

ARFI imaging was performed with a Siemens Acuson S2000TM ultrasound system (Siemens AG, Erlangen, Germany), with software version VB10D and a 4C1 curved ultrasound probe. The region of interest (ROI) of 10 mm length and 5 mm width was placed while performing B-mode imaging in the right lobe of the liver at a maximum depth of 8 cm, avoiding large vessels, biliary ducts and potential lesions (Figure 1). The operator applied the minimum pressure required to take the image.

Patients were in fasted state. None had cardiac disease. They were in the supine position with the right arm in maximum abduction and were asked to stop normal breathing for a moment and not inhale or exhale deeply. The aim was to minimise breathing motion and avoid inhaling/exhaling, which are known influencing factors[8]. The probe was placed between and parallel to the seventh to tenth intercostal space.

Ten valid acquisitions were obtained for each patient, in the same intercostal space but with different locations and at different depths. Each acquisition period was about 10-15 s long. The median of all 10 acquisitions was calculated and considered as indicative of fibrosis severity. The results were expressed in m/s. For each measurement, the depth of the box was given. Measurements were obtained at a depth of 1 cm from the liver capsule down to a maximum depth of 8 cm below the transducer. If the measurement was

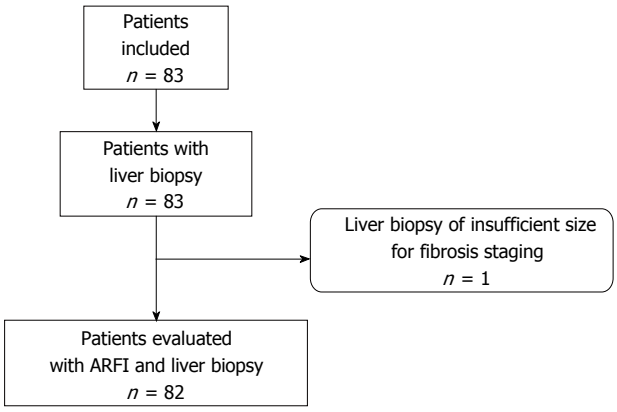

Figure 2 Patient flowchart. ARFI: Acoustic radiation force impulse.

technically evaluated as non-reliable by the device, X.XX was displayed on the screen. Reliable, successful liver stiffness measurements were defined as the median of 10 valid measurements with a success rate ⩾ 60% (based on TE).

The operator was blinded for all patient characteristics including clinical, biological and histological data.

Abdominal ultrasound

Liver and abdominal ultrasound imaging was performed at the same time for all patients using the same device and probe as for the ARFI examination. We recorded the right liver lobe size (right liver arrow), the distance between the skin and the superficial liver capsule, the liver structure and any focal liver lesion.

Liver biopsy

Liver biopsy was performed under percutaneous ultrasound guidance after ARFI acquisition on the same day. The liver samples were fixed and for each patient three slides were stained with hematoxylin-eosin and Sirius red. To avoid sampling errors, specimens under 15 mm long were excluded. A senior pathologist, blinded to clinical, histological, biological and ARFI data, assessed the liver biopsies according to the METAVIR scoring system[9]. Fibrosis was staged from 0 to 4 determined according to the METAVIR score: F = fibrosis. F0: no fibrosis; F1: portal fibrosis without septa (minimal fibrosis); F2: portal fibrosis with rare septa (moderate fibrosis); F3: numerous septa without cirrhosis (severe fibrosis); and F4: cirrhosis. Perisinusoidal fibrosis was evaluated according to Brunt's score[10].

Clinical and biological parameters

Biological parameters were measured prior to liver biopsy and ARFI. These included: prothrombin, alkaline phosphatase, albumin, γ-globulin, platelets, AST, ALT, γ-glutamyl transferase, iron and ferritin. Other parameters were age, sex, body mass index (BMI) and hypertension.

Statistical analysis

Groups of patients were formed according to fibrosis stage and data were expressed as mean ± SD if normally distributed and median (range) if not normally distributed. Comparisons between groups were made using *t*-tests for normally distributed variables, Mann Whitney *U* test for non-normally distributed variables and the χ^2 test or Fisher's exact test for categorical variables. Spearman's analysis was used to determine any correlations. Optimal cut-off values for fibrosis stages F ⩾ 2, F ⩾ 3 and F = 4 were determined by optimisation of Youden's index from the AUROC curve analysis. Sensitivity, specificity, negative predictive value (NPV) and positive predictive value (PPV) were also calculated. The variables tested in the univariate analysis were ARFI, effects of prothrombin, alkaline phosphatase, albumin, γ-globulin, platelets, AST, ALT, γ-glutamyl transferase, iron, ferritin, age, sex, BMI and hypertension ($P < 0.2$). Multivariate ordinal logistic regression analysis using fibrosis stage (in three classes: F0-F1/F2/F3-F4) as the outcome variable was used to assess the strength of the relationship with ARFI even after adjustments for other factors associated with fibrosis progression or confusion factors. A P value of < 0.05 was considered statistically significant. An algorithm was developed using the clustering method. Statistical analyses were performed using SAS V9.4 software (SAS Institute, United States).

RESULTS

Eighty-two patients (69 males and 13 females) were evaluated in the analysis. One enrolled patient was excluded due to insufficient biopsy size (Figure 2). The mean age of the patients was 43.8 ± 10 years and the mean BMI was 22.9 ± 4.3 kg/m^2. Mean alcohol consumption was 132.4 ± 128.8 standard drinks (defined as 10 g of pure alcohol per standard drink in France) per week with a mean cumulative year duration of 17.6 ± 9.5 years. Mean biopsy size was 30.7 ± 10.5 mm. Patient characteristics and fibrosis stages are summarised in Tables 1 and 2 respectively. Successful liver stiffness measurements (10 valid measurements) were obtained in 100% of patients measured with ARFI imaging.

The median values for ARFI imaging according to fibrosis stage are described in Table 2 (mean of medians ± SD). The results showed a significant and strong correlation between ARFI measurements and the histological fibrosis stage ($P < 0.0001$) (Figure 3). Analyses to determine the optimal ARFI cut-off values were performed according to stages of clinical interest, for F ⩾ 2, ⩾ F3 and F = 4. AUROC values were respectively 0.87, 0.86 and 0.89 (Figure 4). Sensitivity, specificity, PPV and NPV are shown in Table 3 according to the cut-off values.

Table 1 Clinical and biochemical characteristics of patients with alcoholic liver disease

Characteristic	Normal values	Patients included (n = 82)
Sex (male/female)	NA	69/13
Age (yr)	NA	43.8 ± 10
Body mass index (kg/m^2)	NA	22.9 ± 4.3
AST (IU/L)	0-35	62.0 (44-98)
ALT (IU/L)	0-35	67.0 (40-105)
γ-glutamyl transpeptidase (IU/L)	5-36	316.0 (141-654)
γ-globulin (g/L)	7-15	8.7 (7.4-10.4)
Alkaline phosphatase (IU/L)	30-120	90.5 (66-121)
Prothrombin (%)	70-130	101.2 ± 12.4
Platelets (× 10^9/L)	180-390	191.5 ± 71.7
Iron (μmol/L)	18-22	16.2 ± 8.1
Ferritin (μg/L)	Male: 30-300	478.0 (310.5-787.5)
	Female: 20-150	404.0 (216.0-783.0)
Albumin (g/L)	40-60	39.0 ± 4.9

Kolmogorow Smirnow analysis was performed, followed by parametric or non-parametric tests. Mean ± SD or median (25th-75th interquartile ranges) was used respectively. AST: Aspartate transaminase; ALT: Alanine transaminase; IU: International unit.

Table 2 Number of patients and mean values of acoustic radiation force impulsepredicting for assessing liver stiffness according to the different fibrosis stages

Fibrosis stage	Number of patients	ARFI (m/s)
F0	13	1.25 ± 0.31
F1	35	1.40 ± 0.36
F2	17	1.86 ± 0.42
F3	4	1.83 ± 0.47
F4	13	2.25 ± 0.36
P value		< 0.0001

ARFI: Acoustic radiation force impulsepredicting.

Significant variables in univariate analyses (P < 0.2) as described previously were entered into the multivariate model (Table 4). The proportional odds assumption was verified (P = 0.76) and the coefficient of determination (R²) was 61%. Age ⩾ 50 [OR = 4.73 (1.43-15.66)] and γ-globulin ⩾ 10 g/L [OR = 9.67 (2.19-42.63)] were independently associated with fibrosis stage. Moreover, the relationship between fibrosis and ARFI was still significant [40.71 (9.94-166.7)] after adjusting for those additional parameters.

The correlation between the mean and median of the 10 values was excellent with a Spearman correlation coefficient of 0.98 (P < 0.001).

Medians were calculated using a different number of values (2-9) to determine whether or not there was a need for 10 values. The values were taken in order. Spearman's correlation coefficient is 0.98 between the median of 10 and 6 values (P < 0.0001).

DISCUSSION

This study demonstrates that ARFI imaging could be used for the assessment of liver fibrosis in ALD. We suggest that a median of 1.63 m/s could be used as an ARFI diagnostic threshold for diagnosing significant liver fibrosis (F ⩾ 2) with sensitivity and specificity of respectively 82.4% and 83.3% (AUROC = 0.87). Moreover, the threshold of 1.94 m/s provided a diagnosis of cirrhosis with a sensitivity of 92.3% and specificity of 81.6%.

Table 3 Diagnostic performance of acoustic radiation force impulse for the different liver fibrosis stages

Diagnostic parameters	F ⩾ 2	F ⩾ 3	F = 4
ARFI cut-off (m/s)	1.63	1.84	1.94
Sensitivity (%)	82.4 (0.70-0.95)	82.4 (0.64-1.00)	92.3 (0.78-1.00)
Specificity (%)	83.3 (0.73-0.94)	78.5 (0.69-0.89)	81.6 (0.72-0.90)
Area under curve (AUROC)	0.87	0.86	0.89
PPV (%)	77.8 (0.64-0.91)	50.0 (0.31-0.69)	48.0 (0.28-0.68)
NPV (%)	87.0 (0.77-0.97)	94.4 (0.88-1.00)	98.2 (0.95-1.00)

ARFI: Acoustic radiation force impulse; PPV: Positive predictive value; NPV: Negative predictive value.

Table 4 Univariate and multivariate ordinal regression analyses

Characteristic	Univariate analysis OR (95%) P value	Multivariate analysis OR (95%) R^2 = 0.61; STPOA[1]: 0.76
ARFI	29.06 [8.59-98.33] P < 0.0001	40.71 [9.94-166.7] P < 0.0001
Sex		
Female	1	
Male	2.43 [0.79-7.42] P = 0.12	
Age		
< 50 yr	1	1
⩾ 50 yr	4.01 [1.55-10.39] P = 0.004	4.73 [1.43-15.66] P = 0.01
Body mass index	1.07 [0.97-1.18] P = 0.19	
AST	1.00 [0.992-1.01] P = 0.98	
ALT	0.99 [0.98-0.999] P = 0.04	
γ-glutamyl transpeptidase	1.00 [1.000-1.002] P = 0.05	
γ-globulin		
< 10	1	1
⩾ 10	7.42 [2.34-23.56] P = 0.003	9.67 [2.19-42.63] P = 0.004
Alkaline phosphatase	1.01 [1.001-1.012] P = 0.02	
Prothrombin	0.002 [0.001-0.06] P = 0.001	
Platelets	1.00 [0.99-1.01] P = 0.93	
Iron	1.03 [0.97-1.08] P = 0.33	
Ferritin	1.001 [1.000-1.002] P = 0.06	
Albumin	0.90 [0.82-1.00] P = 0.05	

[1]Score test for the proportional odds assumption.

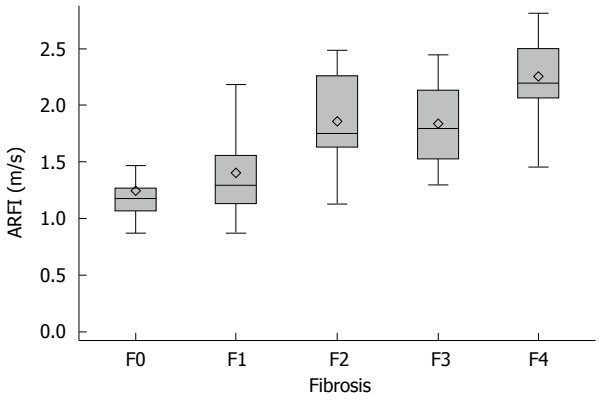

Figure 3 Relationship between acoustic radiation force impulse predicting values and histological fibrosis stages. The relationship was significant between the velocity of the sheer wave (median of 10 ARFI values) and the fibrosis stage (assessed by the METAVIR score on biopsies) in all 82 patients ($P < 0.0001$). The box represents the interquartile range, the horizontal line in the box indicates the median value and the diamond indicates the mean value. The horizontal lines above and below the box indicate the maximum and minimum values.

In alcoholic liver disease, the identification of cirrhosis (F4) is important for optimal patient care. The follow-up schedule includes endoscopy every 3-4 years, ultrasonography every 6 mo, hepatitis vaccination and contraindication to certain drugs. The identification of stage ⩾ F2 is less important clinically than in viral hepatitis but can lead to closer medical surveillance of fibrosis with ARFI, and even serve as an incentive for detoxification. For both stages, the AUROC curve value was close to 1, indicating good diagnostic accuracy[11].

To date, the predominant and most reliable non-invasive method for the diagnosis of liver fibrosis in alcoholic liver disease is transient elastography (TE)[12]. Compared to TE, ARFI has several advantages. First, B-mode evaluation of the liver (and other organs such as the spleen) is possible with the same device and can therefore be incorporated into routine ultrasound protocols, thereby reducing costs. The use of B-mode can also determine optimal ROI placement, preserving structures such as lesions, large blood vessels, biliary ducts or even heterogeneous areas. Second and probably most importantly is the liver stiffness measurement success rate of 100%, which was reported both in the literature and in our study, whereas in some studies TE has a success rate of under 70%[13,14]. This is a major strength of the ARFI method compared to TE. Third, ARFI imaging can be performed in some cases where TE is not possible[15]. Bota *et al*[16] demonstrated that the presence of ascites did not influence the ARFI measurement reliability rate, whereas TE cannot be performed in the case of ascites. TE is unreliable for overweight and obese patients whereas ARFI can be performed to a maximum depth of 8 cm. Published data also suggest that ARFI may not be influenced by steatosis grade, unlike TE[14,17,18]. This is a clear advantage in our population, as steatosis is often associated with ALD[19]. ARFI is also a good

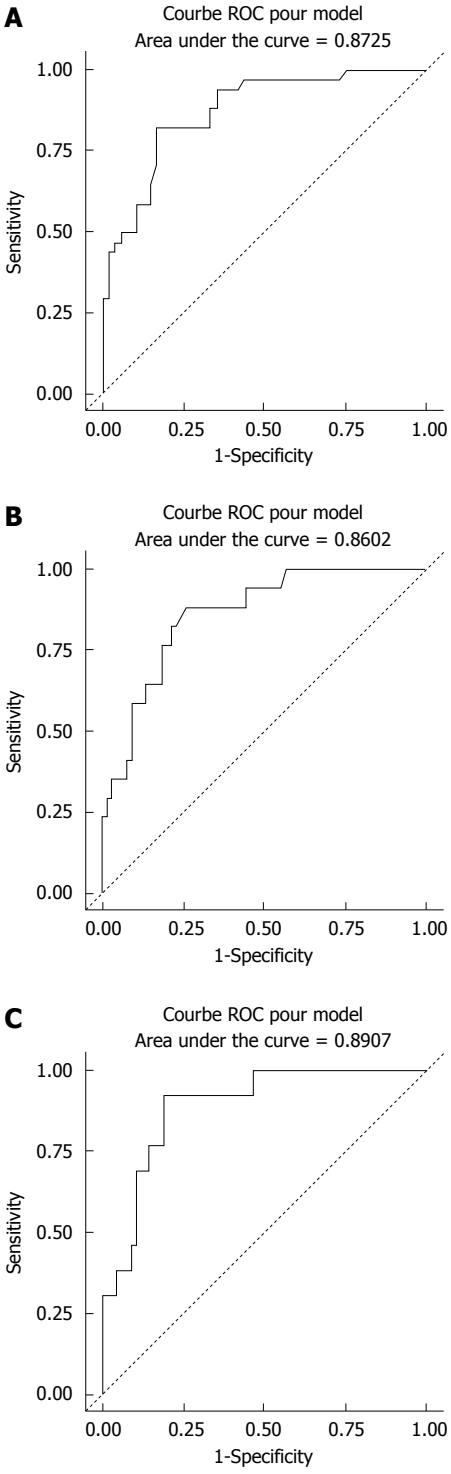

Figure 4 Receiver operating characteristic curves of acoustic radiation force impulse predicting liver fibrosis in patients with alcoholic liver disease. A: ROC curve for F ⩾ 2; B: ROC curve for F ⩾ 3; C: ROC curve for F = 4.

alternative for patients with contraindications to biopsy or TE. The ARFI measurement area size of 1 cm (compared to 4 cm for TE) can easily be offset by the possibility of several measurements in different parts of the liver.

Recently, studies have also started to evaluate ARFI on hepatitis B, hepatitis C and NASH[20-23]. ARFI has good intra-operator and inter-operator

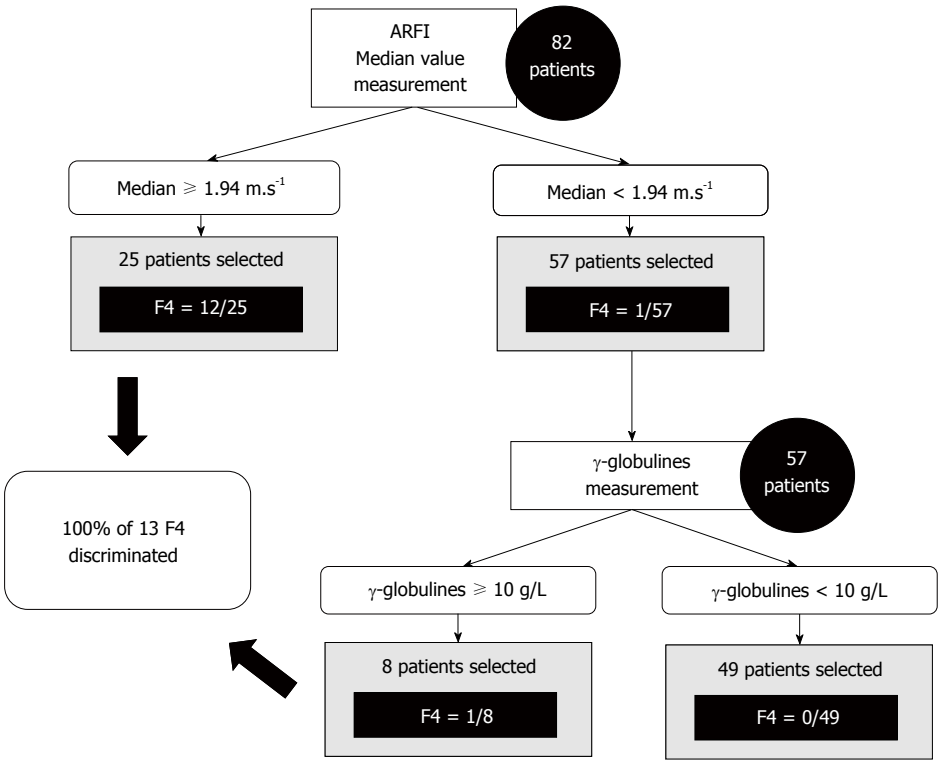

Figure 5 Decision tree for acoustic radiation force impulse predicting as a screening test for F = 4.

reproducibility, as described in the Bota *et al*[24] study, with an intraclass correlation coefficient (ICC) of 0.90 and 0.81 for intra- and inter-operator reproducibility respectively. The cut-off values reported in the literature are different, however. In hepatitis B, hepatitis C and NASH, cut-off values in m/s for F = 4 were respectively 1.84 for Dong *et al*[18] 1.55 for Sporea *et al*[21] and 1.9 for Yoneda *et al*[25]. These differences suggest that ARFI values differ depending on the disease, as shown in the meta-analysis by Nierhoff *et al*[23]. There is therefore a need to define cut-off values for each diffuse liver disease. To our knowledge, there is only one other study, by Zhang *et al*[26] evaluating the performance of ARFI imaging for the assessment of liver fibrosis in patients with ALD in comparison to biopsy, with an AUROC value of 0.89 for F = 4. However, the study populations are very different. In their international multi-centre study, Sporea *et al*[21] showed that the cut-off values predictive of fibrosis stages differ between European and Asian populations. This could explain why the cut-off values are respectively 1.27 and 1.65 for F ⩾ 2 and F = 4 in the Chinese study by Zhang and 1.63 and 1.94 in our study, using the same ultrasound device.

Our study showed good sensitivity and specificity, as described previously. But the excellent negative predictive value of ARFI (98.2% for F = 4) can open the possibility of using ultrasound elastography as a screening test rather than a diagnostic test. A decision tree of clinical value is proposed in Figure 5. Other larger studies are clearly needed to confirm these results.

Our study included patients undergoing alcoholic detoxification. Bardou-Jacquet *et al*[27] recently suggested that the alcohol consumption greatly influences TE and by extension liver stiffness, but could be a useful tool in the follow-up of patient as an indicator of alcohol consumption beyond the sole fibrosis evaluation. Fibrosis evaluation made on patients undergoing detoxification is the most common clinical situation. So, ARFI values may also be influenced by alcohol consumption and alcohol cessation. This may explain some mismatches between ARFI and biopsies.

In our study, ARFI was performed according to guidelines. In certain debatable conditions, the neutral condition was chosen. For example, according to the literature and the device provider's instructions, 10 measurements were taken and the median value was calculated, as for TE, with the patient gently holding their breath. Ten measurements were taken for each patient in our study, and the median was calculated for each one. Karlas *et al*[28] reported that deep inhalation on measurements could increase values by an average of 13%, while Horster *et al*[29] and Goertz *et al*[8] reported no difference. In our study, the patients were therefore asked to stop normal breathing for a moment. As previous studies reported that ARFI results could be influenced by food intake, we decided to perform ARFI in a fasted state[30]. An interlobar difference was found in the literature[31]. Our measurements were therefore taken in the right liver lobe in the intercostal space. This location was chosen for several reasons. First, operator pressure on the liver may produce false positives due to direct

probe compression, which occurs when measurements are taken in the left liver lobe. The measurements were taken in the intercostal spaces so that the ribs limit this compressive effect. Moreover, the operator exerted minimal pressure. Heartbeat artefacts could falsify the measurements when performed in the left lobe. Second, the aim was to use the same location as the biopsy. ARFI imaging was performed prior to liver biopsy to prevent the interaction of artefacts (such as from haematoma).

However, some findings are discordant with the results of the biopsy, which is considered the gold standard. One reason may be that ARFI produces mean values for a large area in the right liver lobe whereas liver biopsy involves taking a sample. The specimen obtained represents only 1/50000 of the total liver volume and it is well known that fibrosis has an uneven distribution within the liver[32]. In order to be comparable and reliable, multiple biopsies from different locations in the right liver lobe should be taken to gain an accurate comparison with the ARFI values obtained in different locations in the right liver lobe in the same intercostal space[33,34]. This requirement is ethically disputable. Another solution would be to compare ARFI values and hepatic explant findings.

In the literature, many factors have been reported to influence ARFI values, including sex, BMI, age, ethnicity, fasted state, depth of ROI, inflammation grade, obstructive cholestasis and certain other biological markers (alanine transaminase, platelets, prothrombin time, albumin, hyaluronic acid, cholesterol, γ-globulin)[18,21,28,30,35-41]. In our study, in the multivariate analysis, statistically significant correlations were only found for γ-globulin and age. This suggests that liver stiffness and hence fibrosis stage should be interpreted in view of the biological and clinical findings.

Millonig *et al*[42] suggested that liver stiffness is a direct function of central venous pressure and Goertz *et al*[8] reported that heart dysfunction may impair ARFI accuracy. None of the patients analysed in our study had heart failure.

In the literature, the median of the values is reported as being more accurate than the mean, and is used by convention. In our study we also calculated the mean of the 10 values for each patient. The correlation between the mean and median was almost perfect with a correlation factor of 0.98. This suggests that the mean of ten values could have been used instead of the median on our cohort of patients. Larger studies are needed to confirm this observation.

Another disputable point is the number of 10 values chosen for the median calculation. In many articles, the recommended number is 10. However, even if ARFI is a fast technique, obtaining ten values takes time. Therefore, in our study we analysed medians calculated from 2 to 9 values (the first values) and compared them to the median of 10 values. It would appear that a number of 6 values is sufficient to determine an accurate median with an excellent correlation coefficient of 0.98.

In addition to the benefits of ARFI as a non-invasive technique, our study has numerous strengths. This was a prospective study of a homogeneous population of alcoholic liver disease patients, with a delay no more than 10 d between the procedures and the beginning of alcohol withdrawal. The clinician, operator and pathologist were blinded to the results. Fibrosis was assessed by biopsy. The mean biopsy size was 30.7 ± 10.5 mm with the majority larger than 25 mm. Factors reported to influence ARFI results in the literature were taken into consideration and generally included in the multivariate analysis. Guidelines on the ARFI technique were summarised and applied to the measurements for each patient. To our knowledge, only one other study evaluating the performance of ARFI in predicting liver fibrosis in ALD has been published, but concerned a different ethnic population.

There were also limitations to our study. One is sample size. Larger studies or meta-analyses are needed to confirm the ARFI threshold in ALD. The comparison with TE was not done and would also be useful. The literature suggests that liver stiffness is influenced by inflammation[43,44]. Inflammation was only assessed and confirmed by transaminase levels in our study and not by histology. Correlation with steatosis grade was not assessed, but published data suggest that moderate/severe steatosis is not a significant error factor for ARFI elastography[14,18].

ARFI is an accurate, non-invasive and easy method for assessing liver fibrosis in patients with ALD. This imaging technique can be easily incorporated into routine patient care. Cut-off values are suggested and require further confirmation in larger studies. A comparison with TE and supersonic shear-wave elastography (Aixplorer Supersonic®) would be interesting for a complete live liver assessment.

ACKNOWLEDGMENTS

We received support from the national clinical research program for public hospitals of France. Thanks to Tracey Westcott for the language help.

COMMENTS

Background

Acoustic radiation force impulse (ARFI) elastography has the particular advantage of combining conventional ultrasound and liver stiffness measurement. ARFI imaging is an accurate, non-invasive and easy method for assessing liver fibrosis in patients with hepatitis B and C. The aim of this study was to evaluate the performance of ARFI in determining fibrosis stage in patients with alcoholic liver disease (ALD).

Research frontiers

Liver biopsy is the gold standard for assessment of liver fibrosis. However, biopsy is an invasive procedure. This study suggests that ARFI imaging, a non-invasive method, could be used for the assessment of liver fibrosis in ALD.

Innovations and breakthroughs

The study showed the algorithm between ARFI and biochemical parameters for the prediction of presence of cirrhosis. Sensibility and specificity of ARFI were good. The investigation was carried out within European population of patients with ALD undergoing alcoholic detoxification.

Applications

This study is helpful for further research in Acoustic Radiation Force Impulse imaging among patients undergoing alcoholic detoxification.

Peer-review

The study showed the interesting algorithm between ARFI and biochemical parameters for the prediction of presence of cirrhosis. Interestingly, the investigation was carried out within European population of patients with ALD undergoing alcoholic detoxification. The paper makes original contribution and it is clinically exhaustive. The manuscript is well written, seems accurate and well organized. The authors clearly presented any doubts concerning the investigation conducted by them.

REFERENCES

1 **Rehm J**, Mathers C, Popova S, Thavorncharoensap M, Teerawattananon Y, Patra J. Global burden of disease and injury and economic cost attributable to alcohol use and alcohol-use disorders. *The Lancet* 2009; **373**: 2223-2233 [DOI: 10.1016/S0140-6736(09)60746-7]

2 **Mueller S**, Seitz HK, Rausch V. Non-invasive diagnosis of alcoholic liver disease. *World J Gastroenterol* 2014; **20**: 14626-14641 [PMID: 25356026 DOI: 10.3748/wjg.v20.i40.14626]

3 **Myers RP**, Fong A, Shaheen AA. Utilization rates, complications and costs of percutaneous liver biopsy: a population-based study including 4275 biopsies. *Liver Int* 2008; **28**: 705-712 [PMID: 18433397 DOI: 10.1111/j.1478-3231.2008.01691.x]

4 **Imbert-Bismut F**, Ratziu V, Pieroni L, Charlotte F, Benhamou Y, Poynard T. Biochemical markers of liver fibrosis in patients with hepatitis C virus infection: a prospective study. *Lancet* 2001; **357**: 1069-1075 [PMID: 11297957 DOI: 10.1016/S0140-6736(00)04258-6]

5 **Forns X**, Ampurdanès S, Llovet JM, Aponte J, Quintó L, Martínez-Bauer E, Bruguera M, Sánchez-Tapias JM, Rodés J. Identification of chronic hepatitis C patients without hepatic fibrosis by a simple predictive model. *Hepatology* 2002; **36**: 986-992 [PMID: 12297848 DOI: 10.1053/jhep.2002.36128]

6 **Wai CT**, Greenson JK, Fontana RJ, Kalbfleisch JD, Marrero JA, Conjeevaram HS, Lok AS. A simple noninvasive index can predict both significant fibrosis and cirrhosis in patients with chronic hepatitis C. *Hepatology* 2003; **38**: 518-526 [PMID: 12883497 DOI: 10.1053/jhep.2003.50346]

7 **Lee HJ**, Seo YS, Kim DJ, Kang HS, An H, Kim JH, Cheong JY, Yim HJ, Yeon JE, Lee HS, Byun KS, Cho SW, Kim DJ, Um SH, Kim CD, Ryu HS. Application of the HALF index obviates the need for liver biopsy in half of all patients with chronic hepatitis B. *J Gastroenterol Hepatol* 2011; **26**: 987-995 [PMID: 21198828 DOI: 10.1111/j.1440-1746.2010.06609.x]

8 **Goertz RS**, Egger C, Neurath MF, Strobel D. Impact of food intake, ultrasound transducer, breathing maneuvers and body position on acoustic radiation force impulse (ARFI) elastometry of the liver. *Ultraschall Med* 2012; **33**: 380-385 [PMID: 22723037 DOI: 10.1055/s-0032-1312816]

9 **Bedossa P**, Poynard T. An algorithm for the grading of activity in chronic hepatitis C. The METAVIR Cooperative Study Group. *Hepatology* 1996; **24**: 289-293 [PMID: 8690394 DOI: 10.1002/hep.510240201]

10 **Brunt EM**, Janney CG, Di Bisceglie AM, Neuschwander-Tetri BA, Bacon BR. Nonalcoholic steatohepatitis: a proposal for grading and staging the histological lesions. *Am J Gastroenterol* 1999; **94**: 2467-2474 [PMID: 10484010 DOI: 10.1111/j.1572-0241.1999.01377.x]

11 **Swets JA**. Measuring the accuracy of diagnostic systems. *Science* 1988; **240**: 1285-1293 [PMID: 3287615 DOI: 10.1126/science.3287615]

12 **Fernandez M**, Trépo E, Degré D, Gustot T, Verset L, Demetter P, Devière J, Adler M, Moreno C. Transient elastography using Fibroscan is the most reliable noninvasive method for the diagnosis of advanced fibrosis and cirrhosis in alcoholic liver disease. *Eur J Gastroenterol Hepatol* 2015; **27**: 1074-1079 [PMID: 26011235 DOI: 10.1097/MEG.0000000000000392]

13 **Castéra L**, Foucher J, Bernard PH, Carvalho F, Allaix D, Merrouche W, Couzigou P, de Lédinghen V. Pitfalls of liver stiffness measurement: a 5-year prospective study of 13,369 examinations. *Hepatology* 2010; **51**: 828-835 [PMID: 20063276 DOI: 10.1002/hep.23425]

14 **Bota S**, Herkner H, Sporea I, Salzl P, Sirli R, Neghina AM, Peck-Radosavljevic M. Meta-analysis: ARFI elastography versus transient elastography for the evaluation of liver fibrosis. *Liver Int* 2013; **33**: 1138-1147 [PMID: 23859217 DOI: 10.1111/liv.12240]

15 **Foucher J**, Castéra L, Bernard PH, Adhoute X, Laharie D, Bertet J, Couzigou P, de Lédinghen V. Prevalence and factors associated with failure of liver stiffness measurement using FibroScan in a prospective study of 2114 examinations. *Eur J Gastroenterol Hepatol* 2006; **18**: 411-412 [PMID: 16538113]

16 **Bota S**, Sporea I, Sirli R, Popescu A, Danila M, Jurchis A, Gradinaru-Tascau O. Factors associated with the impossibility to obtain reliable liver stiffness measurements by means of Acoustic Radiation Force Impulse (ARFI) elastography--analysis of a cohort of 1,031 subjects. *Eur J Radiol* 2014; **83**: 268-272 [PMID: 24360231 DOI: 10.1016/j.ejrad.2013.11.019]

17 **Mueller S**, Millonig G, Sarovska L, Friedrich S, Reimann FM, Pritsch M, Eisele S, Stickel F, Longerich T, Schirmacher P, Seitz HK. Increased liver stiffness in alcoholic liver disease: differentiating fibrosis from steatohepatitis. *World J Gastroenterol* 2010; **16**: 966-972 [PMID: 20180235 DOI: 10.3748/wjg.v16.i8.966]

18 **Dong DR**, Hao MN, Li C, Peng Z, Liu X, Wang GP, Ma AL. Acoustic radiation force impulse elastography, FibroScan®, Forns' index and their combination in the assessment of liver fibrosis in patients with chronic hepatitis B, and the impact of inflammatory activity and steatosis on these diagnostic methods. *Mol Med Rep* 2015; **11**: 4174-4182 [PMID: 25651500 DOI: 10.3892/mmr.2015.3299]

19 **Brunt PW**, Kew MC, Scheuer PJ, Sherlock S. Studies in alcoholic liver disease in Britain. I. Clinical and pathological patterns related to natural history. *Gut* 1974; **15**: 52-58 [PMID: 4362373]

20 **Sporea I**, Sirli R, Bota S, Popescu A, Sendroiu M, Jurchis A. Comparative study concerning the value of acoustic radiation force impulse elastography (ARFI) in comparison with transient elastography (TE) for the assessment of liver fibrosis in patients with chronic hepatitis B and C. *Ultrasound Med Biol* 2012; **38**: 1310-1316 [PMID: 22698510 DOI: 10.1016/j.ultrasmedbio.2012.03.011]

21 **Sporea I**, Bota S, Peck-Radosavljevic M, Sirli R, Tanaka H, Iijima H, Badea R, Lupsor M, Fierbinteanu-Braticevici C, Petrisor A, Saito H, Ebinuma H, Friedrich-Rust M, Sarrazin C, Takahashi H, Ono N, Piscaglia F, Borghi A, D'Onofrio M, Gallotti A, Ferlitsch A, Popescu A, Danila M. Acoustic Radiation Force Impulse elastography for fibrosis evaluation in patients with chronic hepatitis C: an international multicenter study. *Eur J Radiol* 2012; **81**: 4112-4118 [PMID: 23000186 DOI: 10.1016/j.ejrad.2012.08.018]

22 **Fierbinteanu Braticevici C**, Sporea I, Panaitescu E, Tribus L. Value of acoustic radiation force impulse imaging elastography for non-invasive evaluation of patients with nonalcoholic fatty liver disease. *Ultrasound Med Biol* 2013; **39**: 1942-1950 [PMID: 23932277 DOI: 10.1016/j.ultrasmedbio.2013.04.019]

23 **Nierhoff J**, Chávez Ortiz AA, Herrmann E, Zeuzem S, Friedrich-Rust M. The efficiency of acoustic radiation force impulse imaging for the staging of liver fibrosis: a meta-analysis. *Eur Radiol* 2013; **23**: 3040-3053 [PMID: 23801420 DOI: 10.1007/s00330-013-2927-6]

24 **Bota S**, Sporea I, Sirli R, Popescu A, Danila M, Costachescu D. Intra- and interoperator reproducibility of acoustic radiation force impulse (ARFI) elastography--preliminary results. *Ultrasound Med Biol* 2012; **38**: 1103-1108 [PMID: 22579536 DOI: 10.1016/j.ultrasm

edbio.2012.02.032]
25 **Yoneda M**, Suzuki K, Kato S, Fujita K, Nozaki Y, Hosono K, Saito S, Nakajima A. Nonalcoholic fatty liver disease: US-based acoustic radiation force impulse elastography. *Radiology* 2010; **256**: 640-647 [PMID: 20529989 DOI: 10.1148/radiol.10091662]
26 **Zhang D**, Li P, Chen M, Liu L, Liu Y, Zhao Y, Wang R. Non-invasive assessment of liver fibrosis in patients with alcoholic liver disease using acoustic radiation force impulse elastography. *Abdom Imaging* 2015; **40**: 723-729 [PMID: 24811766 DOI: 10.1007/s00261-014-0154-5]
27 **Bardou-Jacquet E**, Legros L, Soro D, Latournerie M, Guillygomarc'h A, Le Lan C, Brissot P, Guyader D, Moirand R. Effect of alcohol consumption on liver stiffness measured by transient elastography. *World J Gastroenterol* 2013; **19**: 516-522 [PMID: 23382630 DOI: 10.3748/wjg.v19.i4.516]
28 **Karlas T**, Pfrepper C, Wiegand J, Wittekind C, Neuschulz M, Mössner J, Berg T, Tröltzsch M, Keim V. Acoustic radiation force impulse imaging (ARFI) for non-invasive detection of liver fibrosis: examination standards and evaluation of interlobe differences in healthy subjects and chronic liver disease. *Scand J Gastroenterol* 2011; **46**: 1458-1467 [PMID: 21916815 DOI: 10.3109/00365521.2011.610004]
29 **Horster S**, Mandel P, Zachoval R, Clevert DA. Comparing acoustic radiation force impulse imaging to transient elastography to assess liver stiffness in healthy volunteers with and without valsalva manoeuvre. *Clin Hemorheol Microcirc* 2010; **46**: 159-168 [PMID: 21135491 DOI: 10.3233/CH-2010-1342]
30 **Popescu A**, Bota S, Sporea I, Sirli R, Danila M, Racean S, Suseanu D, Gradinaru O, Ivascu Siegfried C. The influence of food intake on liver stiffness values assessed by acoustic radiation force impulse elastography-preliminary results. *Ultrasound Med Biol* 2013; **39**: 579-584 [PMID: 23415282 DOI: 10.1016/j.ultrasmedbio.2012.11.013]
31 **D'Onofrio M**, Gallotti A, Mucelli RP. Tissue quantification with acoustic radiation force impulse imaging: Measurement repeatability and normal values in the healthy liver. *AJR Am J Roentgenol* 2010; **195**: 132-136 [PMID: 20566806 DOI: 10.2214/AJR.09.3923]
32 **Cholongitas E**, Senzolo M, Standish R, Marelli L, Quaglia A, Patch D, Dhillon AP, Burroughs AK. A systematic review of the quality of liver biopsy specimens. *Am J Clin Pathol* 2006; **125**: 710-721 [PMID: 16707372 DOI: 10.1309/W3XCNT4HKFBN2G0B]
33 **Bedossa P**, Dargère D, Paradis V. Sampling variability of liver fibrosis in chronic hepatitis C. *Hepatology* 2003; **38**: 1449-1457 [PMID: 14647056 DOI: 10.1016/j.hep.2003.09.022]
34 **Maharaj B**, Maharaj RJ, Leary WP, Cooppan RM, Naran AD, Pirie D, Pudifin DJ. Sampling variability and its influence on the diagnostic yield of percutaneous needle biopsy of the liver. *Lancet* 1986; **1**: 523-525 [PMID: 2869260]
35 **Liao LY**, Kuo KL, Chiang HS, Lin CZ, Lin YP, Lin CL. Acoustic radiation force impulse elastography of the liver in healthy patients: test location, reference range and influence of gender and body mass index. *Ultrasound Med Biol* 2015; **41**: 698-704 [PMID: 25638317 DOI: 10.1016/j.ultrasmedbio.2014.09.030]
36 **Rifai K**, Cornberg J, Mederacke I, Bahr MJ, Wedemeyer H, Malinski P, Bantel H, Boozari B, Potthoff A, Manns MP, Gebel M. Clinical feasibility of liver elastography by acoustic radiation force impulse imaging (ARFI). *Dig Liver Dis* 2011; **43**: 491-497 [PMID: 21439919 DOI: 10.1016/j.dld.2011.02.011]
37 **Zhang D**, Chen M, Wang R, Liu Y, Zhang D, Liu L, Zhou G. Comparison of acoustic radiation force impulse imaging and transient elastography for non-invasive assessment of liver fibrosis in patients with chronic hepatitis B. *Ultrasound Med Biol* 2015; **41**: 7-14 [PMID: 25308941 DOI: 10.1016/j.ultrasmedbio.2014.07.018]
38 **Attia D**, Pischke S, Negm AA, Rifai K, Manns MP, Gebel MJ, Lankisch TO, Potthoff A. Changes in liver stiffness using acoustic radiation force impulse imaging in patients with obstructive cholestasis and cholangitis. *Dig Liver Dis* 2014; **46**: 625-631 [PMID: 24666759 DOI: 10.1016/j.dld.2014.02.020]
39 **Pfeifer L**, Strobel D, Neurath MF, Wildner D. Liver stiffness assessed by acoustic radiation force impulse (ARFI) technology is considerably increased in patients with cholestasis. *Ultraschall Med* 2014; **35**: 364-367 [PMID: 24824763 DOI: 10.1055/s-0034-1366057]
40 **Nishikawa T**, Hashimoto S, Kawabe N, Harata M, Nitta Y, Murao M, Nakano T, Mizuno Y, Shimazaki H, Kan T, Nakaoka K, Takagawa Y, Ohki M, Ichino N, Osakabe K, Yoshioka K. Factors correlating with acoustic radiation force impulse elastography in chronic hepatitis C. *World J Gastroenterol* 2014; **20**: 1289-1297 [PMID: 24574802 DOI: 10.3748/wjg.v20.i5.1289]
41 **Raghuwanshi B**, Jain N, Jain M. Normal values in healthy liver in central India by acoustic radiation force impulse imaging. *J Clin Diagn Res* 2013; **7**: 2498-2501 [PMID: 24392382 DOI: 10.7860/JCDR/2013/7479.3589]
42 **Millonig G**, Friedrich S, Adolf S, Fonouni H, Golriz M, Mehrabi A, Stiefel P, Pöschl G, Büchler MW, Seitz HK, Mueller S. Liver stiffness is directly influenced by central venous pressure. *J Hepatol* 2010; **52**: 206-210 [PMID: 20022130 DOI: 10.1016/j.jhep.2009.11.018]
43 **Arena U**, Vizzutti F, Corti G, Ambu S, Stasi C, Bresci S, Moscarella S, Boddi V, Petrarca A, Laffi G, Marra F, Pinzani M. Acute viral hepatitis increases liver stiffness values measured by transient elastography. *Hepatology* 2008; **47**: 380-384 [PMID: 18095306 DOI: 10.1002/hep.22007]
44 **Palmeri ML**, Wang MH, Rouze NC, Abdelmalek MF, Guy CD, Moser B, Diehl AM, Nightingale KR. Noninvasive evaluation of hepatic fibrosis using acoustic radiation force-based shear stiffness in patients with nonalcoholic fatty liver disease. *J Hepatol* 2011; **55**: 666-672 [PMID: 21256907 DOI: 10.1016/j.jhep.2010.12.019]

P- Reviewer: Domagalski K, Kayadibi H **S- Editor**: Qi Y
L- Editor: A **E- Editor**: Wang CH

World Journal of Gastroenterology

Submit a Manuscript: http://www.wjgnet.com/esps/
Help Desk: http://www.wjgnet.com/esps/helpdesk.aspx
DOI: 10.3748/wjg.v22.i20.4936

World J Gastroenterol 2016 May 28; 22(20): 4936-4945
ISSN 1007-9327 (print) ISSN 2219-2840 (online)

ORIGINAL ARTICLE

Prospective Study

Longitudinal molecular characterization of endoscopic specimens from colorectal lesions

Petra Minarikova, Lucie Benesova, Tereza Halkova, Barbora Belsanova, Stepan Suchanek, Jiri Cyrany, Inna Tuckova, Jan Bures, Miroslav Zavoral, Marek Minarik

Petra Minarikova, Stepan Suchanek, Miroslav Zavoral, Inna Tuckova, Marek Minarik, Department of Internal Medicine, 1st Faculty of Medicine of Charles University and Military University Hospital, CZ 16902 Prague, Czech Republic

Lucie Benesova, Tereza Halkova, Barbora Belsanova, Marek Minarik, Genomac Research Institute, Centre for Applied Genomics of Solid Tumors, CZ 16100 Prague, Czech Republic

Jiri Cyrany, Jan Bures, 2nd Department of Internal Medicine - Gastroenterology, Charles University, Faculty of Medicine at Hradec Kralove, University Teaching Hospital, CZ 50005 Hradec Kralove, Czech Republic

Author contributions: Minarikova P, Benesova L and Minarik M designed the study; Halkova T, Belsanova B and Cyrany J performed the research; Benesova L, Halkova T and Suchanek S analyzed the data; Minarikova P, Benesova L and Minarik M wrote the paper; Bures J and Zavoral M revised the manuscript for final submission.

Supported by Internal Grant Agency of the Czech Ministry of Health, No. NT 14383.

Institutional review board statement: The study was reviewed and approved by the Institutional Review Board of the Military University Hospital, Prague.

Informed consent statement: All study participants provided informed written consent prior to study enrollment.

Conflict-of-interest statement: All authors declare no conflict of interest.

Data sharing statement: Technical and clinical data is available from the corresponding author at mminarik@email.com. Participants have consented to use of their data for further research and other non-commercial purposes.

Correspondence to: Marek Minarik, PhD, Director, Genomac Research Institute, Centre for Applied Genomics of Solid Tumors, CZ 16100 Prague, Czech Republic. mminarik@email.com
Telephone: +420-226203530
Fax: +420-226203542

Received: February 24, 2016
Peer-review started: February 29, 2016
First decision: March 21, 2016
Revised: April 9, 2016
Accepted: May 4, 2016
Article in press: May 4, 2016
Published online: May 28, 2016

Abstract

AIM: To compare molecular profiles of proximal colon, distal colon and rectum in large adenomas, early and late carcinomas. To assess feasibility of testing directed at molecular markers from this study in routine clinical practice.

METHODS: A prospective 3-year study has resulted in the acquisition of samples from 159 large adenomas and 138 carcinomas along with associated clinical parameters including localization, grade and histological type for adenomas and localization and stage for carcinomas. A complex molecular phenotyping has been performed using multiplex ligation-dependent probe amplification technique for the evaluation of CpG-island

methylator phenotype (CIMP), PCR fragment analysis for detection of microsatellite instability and denaturing capillary electrophoresis for sensitive detection of somatic mutations in *KRAS*, *BRAF*, *TP53* and *APC* genes.

RESULTS: Molecular types according to previously introduced Jass classification have been evaluated for large adenomas and early and late carcinomas. An increase in CIMP+ type, eventually accompanied with *KRAS* mutations, was notable between large adenomas and early carcinomas. As expected, the longitudinal observations revealed a correlation of the CIMP+/*BRAF*+ type with proximal location.

CONCLUSION: Prospective molecular classification of tissue specimens is feasible in routine endoscopy practice. Increased frequency of some molecular types corresponds to the developmental stages of colorectal tumors. As expected, a clear distinction is notable for tumors located in proximal colon supposedly arising from the serrated (methylation) pathway.

Key words: Colorectal cancer; CpG-island methylator phenotype; DNA; Microsatellite instability; *BRAF*

Core tip: The results indicate that molecular subtyping from endoscopic biopsies is feasible in routine gastroenterology practice to evaluate a patient's prognosis. Subtyping based on Jass classification can be used to evaluate molecular mechanisms of adenoma-carcinoma transition.

Minarikova P, Benesova L, Halkova T, Belsanova B, Suchanek S, Cyrany J, Tuckova I, Bures J, Zavoral M, Minarik M. Longitudinal molecular characterization of endoscopic specimens from colorectal lesions. *World J Gastroenterol* 2016; 22(20): 4936-4945 Available from: URL: http://www.wjgnet.com/1007-9327/full/v22/i20/4936.htm DOI: http://dx.doi.org/10.3748/wjg.v22.i20.4936

INTRODUCTION

The variability in clinical manifestation of colorectal cancer as well as considerable differences in outcome between some colorectal cancer patients has prompted wide-ranging research into the molecular basis of the disease[1]. The main effort has been directed at mechanisms underlying initiation and progression of colorectal neoplasia from normal colonic mucosa as well as factors defining therapy response and the overall patient's survival[2-5].

There is historic evidence suggesting that more than two-thirds of colorectal cancers begin as colorectal adenomas[6]. The size of adenoma is considered a fundamental risk factor and is directly associated with histological characteristics such as the amount of villosity and dysplasia. Aberrant activation of (proto)oncogenes in key signaling pathways has long been a subject of study in colorectal cancer research. Among others, mutations in two major (proto)oncogenes, *KRAS* and *BRAF*, are frequently found in both carcinomas as well as in adenomas[7]. In 1990, *KRAS* mutations were contributed to the shorter overall survival of colorectal cancer patients[8]. The prognostic value was later restricted only to specific *KRAS* mutation types (Exon 1, codon 12, but not codon 13 mutations)[9]. Later it was discovered that mutations in *KRAS* as well as *NRAS* (both members of a common subgroup, RAS-family) are the major causes of therapy resistance in colorectal tumors treated by monoclonal antiEGFR inhibitors[10,11]. Accordingly, the current NCCA guidelines include recommendations for predictive RAS-testing as a standard of care for colorectal carcinomas[12].

Since 1990, three distinct molecular pathways underlying the malignant transformation of advanced adenomatous polyps into cancerous lesions have been studied[13]. The different pathways are based on independent genomic events leading to the loss of key cellular regulatory mechanisms causing proliferation, invasion and metastasis. The resulting molecular subtypes are denoted by either chromosomal instability (CIN), microsatellite instability (MSI) or CpG-island methylator phenotype (CIMP)[14,15]. The subtypes are typically characterized by disruptions on the DNA level including mutations and allelic losses of major tumor suppressors in CIN[16], mutations of mismatch DNA repair genes in MSI[17] (also referred to as the replication of positive phenotype, RER+) and aberrant methylation of promoter regions of tumor suppressors in CIMP[18]. Over the past decade, clinical associations of these subtypes have been intensively studied. The majority of colorectal carcinomas bear signs of the CIN subtype, most notably somatic mutations of *APC* and *TP53* tumor suppressors and associated losses of alleles at 5q and 17p chromosomal locations [observed as a loss of heterozygosity (LOH)][19]. The CIN type is closely following the fundamental genetic model of colorectal tumorigenesis[20]. While the individual mutations and allelic losses of *APC* and *TP53* tumor suppressors bear no direct prognostic value[21], the "CIN high" phenotype derived from a combination of several markers (mutations and LOH) indicates poor survival compared to the "CIN low" or MSI phenotypes[22].

The CIMP phenotype is on the molecular level notably distinct from the CIN and may also be complemented by MSI[23,24] as a result of *MLH1* promoter methylation[25]. There is sufficient evidence that evaluation of CIMP together with *BRAF* mutation and combined with a presence or absence of MSI gives a strong indication of a patient's survival prognosis. Tumors bearing the CIMP+/*BRAF*+ phenotype exhibit

Table 1 Patient characteristics

Adenomas	94
Gender	
Women	39
Aged	34-98 (median 67.7)
Men	55
Aged	40-89 (median 68.0)
Localization	
Proximal colon	37
Distal colon	42
Rectum	15
Histology	
Tubular	47
Tubulovilous	39
Vilous	4
Serrated	4
Dysplasia	
Low-grade	78
High-grade	16
Carcinomas	127
Gender	
Women	44
Aged	34-98 (median 70.2)
Men	83
Aged	42-90 (median 68.5)
Localization	
Proximal colon	50
Distal colon	38
Rectum	39
Stage	
Early (Ⅰ and Ⅱ)	66
Advanced (Ⅲ and Ⅳ)	61

shorter disease-free survival[26]. Typically arising from serrated lesions and more frequent in the proximal colon (caecum and ascendens) they are the result of a specific molecular process and exhibit a distinct biological behavior[27]. In turn, a concurrent presence of MSI dramatically improves the prognosis of patients with CIMP+/*BRAF*+ tumors[28] as the MSI unstable tumors are less likely to spread to lymph nodes and to develop distant metastases[29]. Aside from the prognostic importance, there is also an ongoing discussion on the importance of CIMP/MSI/*BRAF* phenotyping for prediction of response to chemotherapy treatment[30].

In early 2015, two retrospective studies published a relationship between specific molecular subtypes and the survival of colorectal cancer patients on large patient cohorts[31,32]. Utilizing the knowledge of the above described molecular pathways, the specific molecular types were evaluated based on MSI and CIMP phenotyping in combination with the mutation status of *KRAS* and *BRAF*, as previously suggested by Jass[33]. A significant difference in survival for the different molecular types was indeed confirmed by both studies aimed at patients in stages Ⅲ and Ⅳ, respectively. The five molecular subtypes, now universally referred to as Type Ⅰ-Ⅴ, and a group consisting of the rest, marked as Others, were also characterized by their most likely longitudinal localization and the prevailing gender and age of the patients. Based on the studies mentioned above[31-33], Type 1 is characterized by CIMP+, *BRAF*+, MSI, proximal localization and good prognosis; Type 2 by CIMP+, *BRAF*+, microsatellite stability (MSS) or MSI-Low (MSI-L), proximal localization and poor prognosis; Type 3 by CIMP-, *KRAS*+, MSS or MSI-L, proximal localization and poor prognosis; Type 4 by CIMP-, *KRAS*- and *BRAF*-, MSS or MSI-L, distal localization and median prognosis; Type 5 by CIMP-, *KRAS*- and *BRAF*-, MSI, proximal localization and good prognosis.

While the original Jass characterization gave a unique complex view on the alternative pathways of molecular carcinogenesis, it has, most importantly, now been verified to represent a viable tool in clinical management of the disease. It is, therefore, eminent to adapt appropriate procedures for methodology as well as logistics of testing procedures in current clinical practice. While most studies traditionally rely on molecular testing directed at FFPE sections from resected tissue, endoscopic biopsies as well as endoscopically removed malignant polyps are also more recently being routinely used[34].

Longitudinal clinicopathological heterogeneity of colorectal cancer has been reported as early as 2002[35]. Biological diversity stemming from embryonic origins may be responsible for different mechanisms of tumorigenesis in proximal and distal colon and rectum resulting in different manifestation, response to therapy and the overall prognosis[36]. In this work, we present data from molecular phenotyping and mutation analysis of tissue samples acquired during colonoscopy. We present molecular profiling of colorectal carcinomas as well as of their precursor lesions, large adenomatous polyps. We evaluate molecular profiles at proximal, distal and rectal tumor localizations and assess overall feasibility and clinical utility of such molecular classification in routine endoscopy practice.

MATERIALS AND METHODS

Study population

The prospective study design was reviewed and certified by the Scientific and Ethics boards of the Military University Hospital. All patients admitted into the study have signed an informed consent. Patients were treated at the endoscopy unit and consecutive samples were collected during a 2-year prospective study. Tissue samples were obtained either as endoscopic biopsies or by endoscopic polypectomy (EPE) or endoscopic mucosal resection (EMR). The inclusion criteria was based solely on primary morphology evaluations by the endoscopist. The large adenomas (AA) were assigned as being any size greater than 1 cm[6]. Stage Ⅰ and Ⅱ carcinomas were jointly assigned as early carcinomas (EC) and Stage Ⅲ and Ⅳ were assigned as late

Table 2 Overview of the molecular testing results *n* (%)

Marker	Localization	Advanced adenoma[1]	Early carcinoma[2]	Late carcinoma[3]
MSI	Proximal	0 (0)	5 (20)	7 (24.14)
	Distal	0 (0)	0 (0)	0 (0)
	Rectum	0 (0)	0 (0)	0 (0)
CIMP	Proximal	13 (30.95)	15 (65.22)	16 (59.25)
	Distal	7 (16.28)	10 (45.45)	6 (35.29)
	Rectum	2 (13.33)	11 (50.22)	8 (47.06)
BRAF	Proximal	7 (10.94)	4 (17.39)	7 (24.14)
	Distal	1 (1.49)	0 (0.00)	0 (0.00)
	Rectum	4 (17.39)	1 (4.20)	2 (11.11)
KRAS	Proximal	25 (35.71)	11 (44.00)	15 (51.72)
	Distal	28 (43.08)	11 (44.00)	4 (23.53)
	Rectum	12 (50.00)	10 (41.67)	7 (38.88)
APC	Proximal	24 (35.82)	5 (20.83)	5 (17.24)
	Distal	22 (34.38)	8 (34.78)	6 (37.5)
	Rectum	9 (37.50)	7 (29.17)	8 (44.44)
TP53	Proximal	5 (7.46)	8 (33.33)	8 (27.59)
	Distal	2 (3.13)	8 (34.78)	8 (50.00)
	Rectum	1 (4.17)	11 (45.83)	10 (55.55)

[1]> 1 cm; [2]Stage Ⅰ or Ⅱ; [3]Stage Ⅲ or Ⅳ.

carcinomas (LC). The description of patients from this study is listed in Table 1.

Tumor characteristics

In order to follow a prospective strategy of all evaluations, we have decided to use adenomatous polyp size beyond 10 mm as the only inclusion criteria that allows immediate decision about molecular testing during the endoscopy procedure. DNA from fresh biopsies or FFPE sections was extracted following a standard histopathology evaluation to ensure adequacy (viability, quantity, tumor cell fraction) for the testing. On FFPE sections, tumor-positive areas were clearly marked by a pathologist prior to microdissection. DNA was extracted from fresh and FFPE specimens using a standard spin-column procedure using a commercial kit (JETquick Tissue DNA spin, GENOMED G.m.b.H, Loehne, DE).

Microsatellite instability testing

Microsatellite instability was evaluated using MSI Analysis System, Version 1.2 (Promega corporation, Madison, WI, United States). The multiplex PCR kit produces fluorescently labelled amplicons of five nearly monomorphic mononucleotide markers (BAT-25, BAT-26, NR-21, NR-24 and MONO-27) and two additional polymorphic markers (Penta C and Penta D) for specimen identification[37]. PCR amplicons were resolved on a 16-capillary sequencer (ABI PRISM 3100, Applied Biosystems, Foster City, CA, United States) according to the manufacturers protocol. The data was evaluated by GeneMarker software (Softgenetics, State College, PA). Only samples exhibiting unstable alleles at 2 or more markers were assigned as MSI, otherwise the assignment was MSI-L (1 marker instable) or MSS (no unstable markers detected).

CpG island methylator phenotype testing

The CIMP phenotype evaluation was based on multiplex ligation-dependent probe amplification technique (MLPA) utilizing a non-bisulfite conversion approach. A commercial MLPA kit was used (SALSA MLPA ME042 CIMP, MRC Holland, NL) and the MLPA data was evaluated by GeneMarker software using an appropriate MLPA CIMP panel (available for download from the Softgenetics website). The investigated genes were as suggested by Ogino[38]. A CIMP-high phenotype was assigned to a sample showing any of the MLPA probes methylated for at least 6 out of 8 evaluated genes (*RUNX3*, *CACNA1G*, *IGF2*, *MLH1*, *NEUROG1*, *CRABP1*, *SOCS1* and *CDKN2A*)[39].

KRAS, BRAF, APC and TP53 mutation testing

Somatic mutation testing in *KRAS, BRAF, APC* and *TP53* genes was performed by denaturing capillary electrophoresis (DCE) using a previously described protocol[40-43]. The technique is based on a principle of differential denaturation of wildtype and mutant alleles, similar to the high-resolution melting technique[44]. In brief, the target sequences harboring the mutation sites were amplified using GC-clamping at one of the primers and a fluorescence label at the other primer. The PCR amplification program was concluded by a heteroduplex formation step in which the product mixture was heated for 8 min at 95 ℃, then kept at 65 ℃ for 30 min and finally cooled at 0.1 ℃/s down to 15 ℃. Each amplicon was then subjected to capillary electrophoresis separation at optimized separating temperature leading to the resolution of homo- and hetero- duplex forms in case of a mutation presence. In order to speed up the screening process, amplicons with similar separating temperatures were analyzed in different capillaries during the same run. The target amplicons included exons 2, 3 and 4 of *KRAS* gene, the V600E mutation (exon 15) of *BRAF* gene[41], codon span 1250-1550 (mutation cluster region) of *APC* gene[42,45] and exons 5 to 8 of *TP53* gene[43]. According to the Catalog of somatic mutations in cancer (COSMIC) this testing panel should detect more than 88% of somatic mutations in the studied genes[46].

RESULTS

Over the 2-year duration of the project, a total of 6080 colonoscopies were performed yielding 297 tissue specimens. The set included 159 large AA, 74 EC and 64 LC (see Methods for details of the AA/EC/LC assignment).

The success rates for DNA extractions were 96.3% (104/108) for fresh tissue and 93.7% (177/189) for FFPE sections. The amounts of extracted DNA were typically between 500-1000 μL volumes of 5-10 ng/μL. A complete set of results consisting of MSI, CIMP, *BRAF*, *KRAS*, *APC* and *TP53* data was obtained for 246 out of 281 extracted DNA samples (87.6%). The

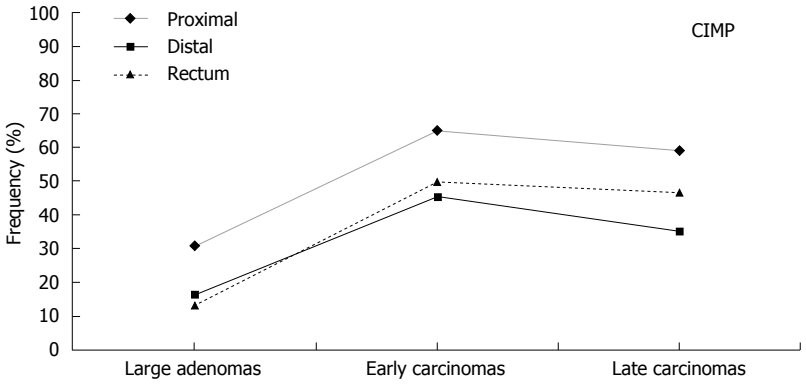

Figure 1 Longitudinal frequency of CpG-island methylator phenotype phenotype in different tumor types. CIMP: CpG-island methylator phenotype.

incomplete molecular profiles were largely due to failed CIMP examination in FFPE mainly as a results of low amounts or low quality of DNA. Results for individual markers obtained for each tumor subtype at proximal, distal and rectal localizations are listed in Table 2.

CIMP, BRAF and MSI

The distribution of CIMP+ phenotypes for the three evaluated tumor types along the proximal and distal colon and rectum is shown in Figure 1. In all three types the CIMP+ frequency in proximal colon is 15% higher than in distal colon or rectum. In all three sections there is a 2-3 fold jump in frequency between large adenomas and early carcinomas while only a relatively small change (< 10%) between early and late carcinomas.

The *BRAF* mutations were found in 12 of 154 large adenomas (7.8%), 5 of 74 (6.8%) early carcinomas and in 9 of 64 (14.1%) advanced carcinomas. A CIMP+/*BRAF*+ combination was mostly found in proximal colon with frequency gradually increasing with the tumor progression from 5.3% (2/38) in large adenomas to 13% (3/23) and 26% (7/27) in early and late carcinomas, respectively.

In agreement with previous reports MSI has only been found in early and late cancers, but not in adenomatous tissue[47]. In carcinomas, MSI was detected only in the proximal localization at 16.0% in early cancers (4/25) and 24.1% in late cancers (7/29). MSI was accompanied by CIMP+ phenotype in 81.2% (9/11) and 88.9% (8/9) of CIMP+ carcinoma had *MLH1* promoter methylation.

APC, KRAS and TP53

Mutations in *APC*, *KRAS* and *TP53* were observed in all tumor groups across proximal and distal colon as well as in the rectum. Similarly to a recently published study[25], we have found a higher frequency of *APC* and *KRAS* mutations in CIMP+ carcinomas with a presence of *MLH1* methylation when compared to CIMP+ without *MLH1* methylation. The difference was 20%; 2/10 *vs* 33.3%; 9/27 for *APC* (P = 0.74) and 21.4%; 3/14 *vs* 59.3%; 16/27 for *KRAS* (P = 0.031). Regardless of the tumor localization, *TP53* mutation rates showed a significant increase from large adenomas (5.1%; 8/155) to early and late carcinomas (36.5%; 27/74 for early and 41.3%; 26/63 for late, $P < 0.001$, $\chi^2 = 49.928$). Also in an agreement with previous findings[48] *TP53* mutations were detected more frequently in the group of CIMP- carcinomas compared to the CIMP+ carcinomas (39.6%; 38/96 *vs* 27.1%; 13/48), but the result was not statistically significant.

DISCUSSION

Principal contributions of various pre-analytical factors to the success of molecular genetic testing from FFPE sections have long been studied[49]. Among others, the principal importance of the quality of the formalin solution (buffered to neutral pH) and the duration of fixation has been recognized[50]. The negative effects of fixation are intensified for small volume samples, typically acquired by endoscopic biopsies. At the same time, upon extraction, the small biopsy specimens often yield low amounts of DNA limiting the extent of the molecular testing. For complex molecular profiling, such as the subtyping performed in this study, a prioritization of the individual tests, as already practiced in molecular testing of other cancer types[51], is clearly a necessity for future routine use.

Most cases of inconclusive results in this study were, indeed, due to the low DNA quality or amount. A dedicated mutation technology typically based on single-plex PCR usually requires only minute amounts of DNA. The MSI detection approach utilizing a multiplex PCR followed by capillary electrophoresis is also low to medium in the demand of DNA. On the other hand, CIMP evaluation by MLPA requires by far the highest amounts of input DNA. With a very limited availability of other reliable CIMP-detection techniques, this is clearly the limiting factor.

Assignment of Jass molecular subtypes

According to the original work of Jass[33] and the recent publications by Phipps *et al*[32] and Sinicrope

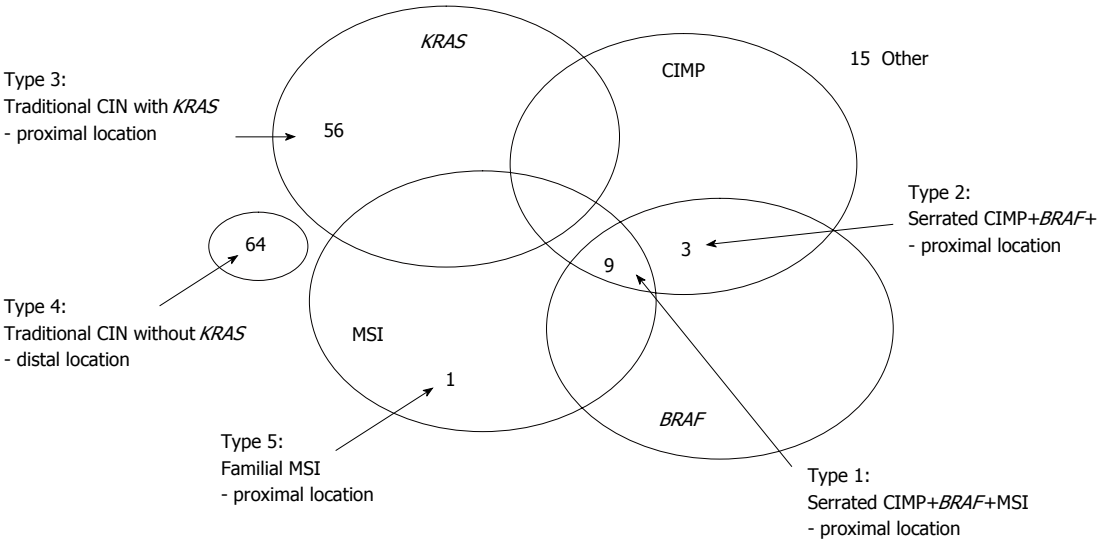

Figure 2 Molecular classification of colorectal carcinomas (all stages) using classification according to Jass and others[30-32]. MSI: Microsatellite instability; CIN: Chromosomal instability; CIMP: CpG-island methylator phenotype.

et al[31], we have applied their principles to our data to assign the molecular subtypes. The classification is based on a combined evaluation of CIMP/MSI/*BRAF*/*KRAS* testing. The resulting spectrum of molecular subtypes for carcinomas in our study is presented in Figure 2. Even with the smaller size of our prospective group, the relative distribution among the 6 different groups (Types 1-5 and Others) corresponds to the data presented in those large retrospective cohorts. The Type 4 and Type 3, both characteristic of the CIN pathway, were the most frequent at 43.2% and 37.8%, respectively, followed by Types 1 and 2, resulting from the CIMP-serrated pathway, at 6.0% and 2.0%, respectively.

The probability of developing future advanced adenomas or cancers increases with the size of adenoma and can range from 1.5% to 7.7% for sizes below 5 mm, 3% to 15.9% for sizes between 5 and 20 mm and 7% to 19.3% for adenomas over 20 mm in size[6]. We have evaluated the Jass-types separately for the groups of large adenomas, early carcinomas and late carcinomas to visualize the degree of molecular irregularities along the tumor progression route. The evaluation workflows for all groups are shown in Figure 3.

A notable change in the distribution patterns of the molecular types can be observed between large adenomas and early carcinomas. The main difference appears to be a result of an increase in CIMP+/*BRAF*- phenotypes from large adenomas (13.8%, 13/94) to early carcinomas (50.0%, 31/62). When explored further, an additional increase in a *KRAS* positive subgroup can be noticed. Accordingly, the rate of CIMP+/*BRAF*-/*KRAS*+ increases from 10.6% (10/94) in large adenomas to 30.6% (19/62) in early carcinomas. At the same time, this increase is complemented by the decrease of CIMP-/*BRAF*-/*KRAS*+ from 49.0% (38/94) in large adenomas to 16.1% (10/62) in early carcinomas, but also partially by the decrease in CIMP-/*BRAF*-/*KRAS*- from 39.3% (37/94) in large adenomas to 30.6% (19/66) in early carcinomas. In other words, methylation, partially accompanied by *KRAS* mutation, takes place during malignant transformation of at least some colorectal tumors during the transition from large adenomas to early carcinomas.

In addition to the Jass types an interesting molecular subgroup has recently been identified including carcinomas with CIMP+ phenotype with unmethylated *MLH1* harboring *KRAS* mutations[25]. We have identified high frequency of *KRAS* mutations in the CIMP+/unmethylated *MLH1*- group within early carcinomas (10/17; 58.8%) as well as late carcinomas (6/10; 60%). According to the previous reports such cancers arise mainly from *KRAS*-mutated traditional serrated adenomas and exhibit poor prognosis. This is in contrast to the CIMP- carcinomas.

Characterization of molecular types according to location

Combined with the information on mutator pathways a full longitudinal image of the colorectal cancer landscape can be elucidated[52]. Data from our study have confirmed the predominant manifestation of the CIMP-associated Type 1 and Type 3 in the proximal colon. At the same time, tumors bearing the CIN characteristics are evenly distributed throughout the colon and rectum. It is clear that further research will lead to more molecular tests to be performed routinely in the diagnosis and therapy of colorectal neoplasia. The molecular subtyping of adenomas and carcinomas using the Jass classification may lead to the discovery of molecular markers specific for the malignant conversion of colonic tissue from precursor lesions to malignant tumors. Such markers would be viable tools to complement endoscopic screening and the diagnosis of colorectal cancer patients.

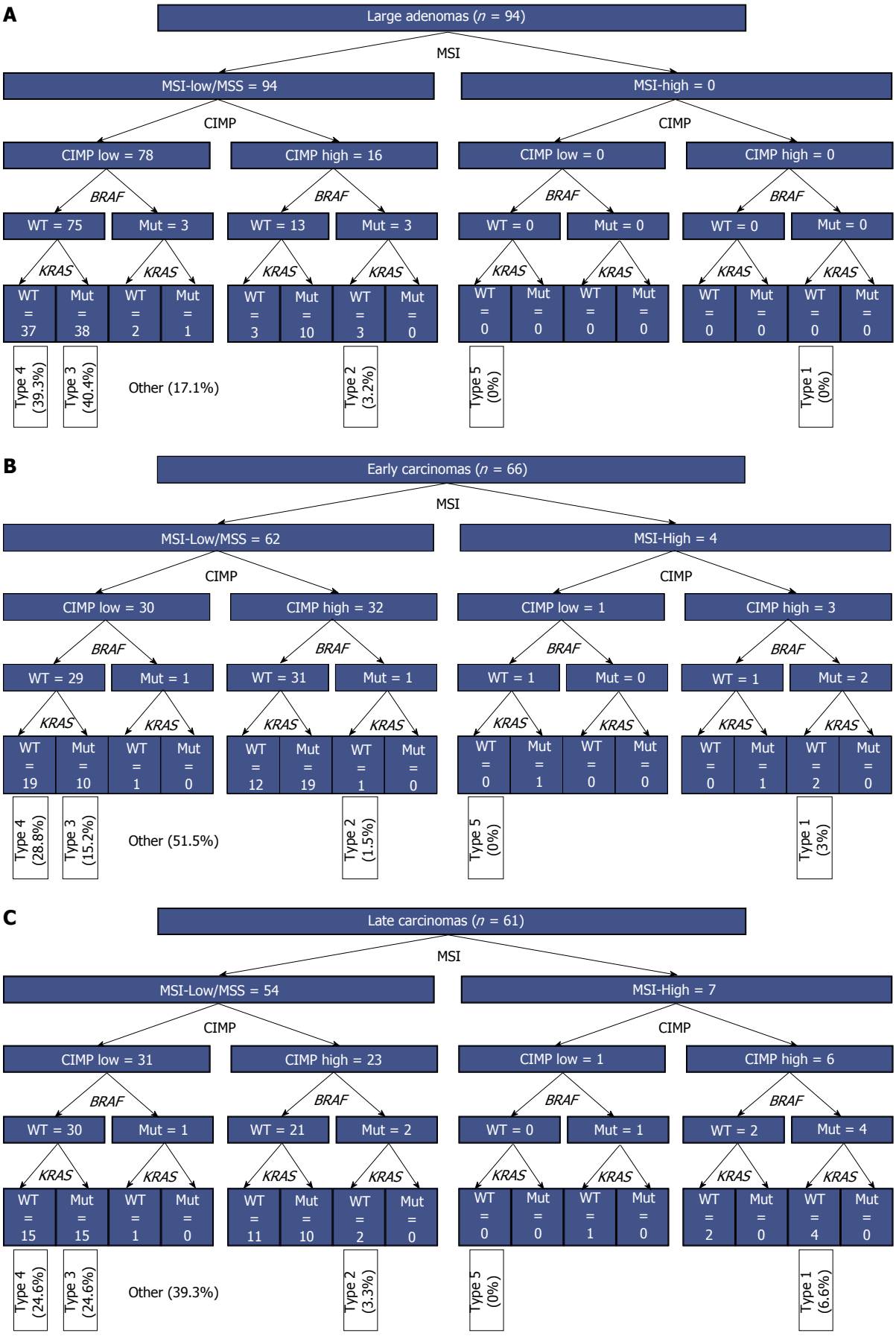

Figure 3 Evaluation workflows for assignment of Jass types in large adenomas (A), early carcinomas (B) and late carcinomas (C).

COMMENTS

Background

Recent advances in molecular profiling have resulted in definition of molecular types of colorectal cancer based on genetic and epigenetic aberrations. Resulting from separate developmental pathways the different types are associated with distinct prognostic features, which can be utilized in clinical practice.

Research frontiers

In a prospective study, endoscopic specimens from colorectal carcinomas as well as pre-malignant lesions were subjected to molecular profiling directed at evaluation of microsatellite instability (MSI) and CpG-island methylator phenotype (CIMP) status in combination with somatic mutations of *KRAS, BRAF, TP53* and *APC* genes.

Innovations and breakthroughs

The distribution of molecular types was evaluated for precursor lesions (large adenomas) and for early and late carcinomas with respect to their localization in proximal colon, distal colon and rectum.

Applications

The study demonstrates feasibility of molecular profiling in routine gastroenterology practice. The study results further suggest distinct molecular changes occurring during the malignant transition from large adenoma to early carcinoma, in particular DNA methylation affecting *KRAS*-mutated tumors.

Terminology

Somatic aberrations: Changes in DNA composition (base sequence or methylation) occurring within cells as a result of external factors and not the inheritance. CIMP: A molecular subtype characterized by methylation at certain positions within the DNA sequence. MSI: A molecular subtype characterized by unequal numbers of repetitions of short DNA sequences obtained for different cells within a tissue. The MSI occurs due to somatic aberrations in genes securing a proper function of the DNA repair system. Promoter methylation of *MLH1* gene is a frequent cause of MSI.

Peer-review

The authors studied molecular profiles of proximal and distal colon and rectum in colorectal adenomas and carcinomas that were obtained by routine endoscopic biopsy. They analyzed CIMP, MSI and mutations of *KRAS* and *BRAF*, and then classified into molecular subtypes in colorectal tumors. Most importantly, longitudinal molecular characterization was clearly shown in colorectal tumors based on CIMP/MSI/*BRAF*/*KRAS* classification. This approach to the molecular classification of colorectal cancer should accelerate understanding of causation, have an impact on clinical management, and facilitate the development of new ways to prevent and treat colorectal cancer.

REFERENCES

1 **Markowitz SD**, Bertagnolli MM. Molecular origins of cancer: Molecular basis of colorectal cancer. *N Engl J Med* 2009; **361**: 2449-2460 [PMID: 20018966 DOI: 10.1056/NEJMra0804588]

2 **Vogelstein B**, Fearon ER, Hamilton SR, Kern SE, Preisinger AC, Leppert M, Nakamura Y, White R, Smits AM, Bos JL. Genetic alterations during colorectal-tumor development. *N Engl J Med* 1988; **319**: 525-532 [PMID: 2841597]

3 **Konishi M**, Kikuchi-Yanoshita R, Tanaka K, Muraoka M, Onda A, Okumura Y, Kishi N, Iwama T, Mori T, Koike M, Ushio K, Chiba M, Nomizu S, Konishi F, Utsunomiya J, Miyaki M. Molecular nature of colon tumors in hereditary nonpolyposis colon cancer, familial polyposis, and sporadic colon cancer. *Gastroenterology* 1996; **111**: 307-317 [PMID: 8690195]

4 **Jass JR**. Towards a molecular classification of colorectal cancer. *Int J Colorectal Dis* 1999; **14**: 194-200 [PMID: 10647627]

5 **Kim JC**, Cho YK, Roh SA, Yu CS, Gong G, Jang SJ, Kim SY, Kim YS. Individual tumorigenesis pathways of sporadic colorectal adenocarcinomas are associated with the biological behavior of tumors. *Cancer Sci* 2008; **99**: 1348-1354 [PMID: 18422752 DOI: 10.1111/j.1349-7006.2008.00819.x]

6 **Rex DK**, Kahi CJ, Levin B, Smith RA, Bond JH, Brooks D, Burt RW, Byers T, Fletcher RH, Hyman N, Johnson D, Kirk L, Lieberman DA, Levin TR, O'Brien MJ, Simmang C, Thorson AG, Winawer SJ. Guidelines for colonoscopy surveillance after cancer resection: a consensus update by the American Cancer Society and the US Multi-Society Task Force on Colorectal Cancer. *Gastroenterology* 2006; **130**: 1865-1871 [PMID: 16697749]

7 **Yang S**, Farraye FA, Mack C, Posnik O, O'Brien MJ. BRAF and KRAS Mutations in hyperplastic polyps and serrated adenomas of the colorectum: relationship to histology and CpG island methylation status. *Am J Surg Pathol* 2004; **28**: 1452-1459 [PMID: 15489648]

8 **Andreyev HJ**, Norman AR, Cunningham D, Oates JR, Clarke PA. Kirsten ras mutations in patients with colorectal cancer: the multicenter "RASCAL" study. *J Natl Cancer Inst* 1998; **90**: 675-684 [PMID: 9586664]

9 **Imamura Y**, Morikawa T, Liao X, Lochhead P, Kuchiba A, Yamauchi M, Qian ZR, Nishihara R, Meyerhardt JA, Haigis KM, Fuchs CS, Ogino S. Specific mutations in KRAS codons 12 and 13, and patient prognosis in 1075 BRAF wild-type colorectal cancers. *Clin Cancer Res* 2012; **18**: 4753-4763 [PMID: 22753589 DOI: 10.1158/1078-0432.CCR-11-3210]

10 **Riely GJ**, Ladanyi M. KRAS mutations: an old oncogene becomes a new predictive biomarker. *J Mol Diagn* 2008; **10**: 493-495 [PMID: 18832458 DOI: 10.2353/jmoldx.2008.080105]

11 **Karapetis CS**, Khambata-Ford S, Jonker DJ, O'Callaghan CJ, Tu D, Tebbutt NC, Simes RJ, Chalchal H, Shapiro JD, Robitaille S, Price TJ, Shepherd L, Au HJ, Langer C, Moore MJ, Zalcberg JR. K-ras mutations and benefit from cetuximab in advanced colorectal cancer. *N Engl J Med* 2008; **359**: 1757-1765 [PMID: 18946061 DOI: 10.1056/NEJMoa0804385]

12 NCCN (National Comprehensive Cancer Network) Recent Updates to NCCN Clinical Practice Guidelines In Oncology. Available from: URL: http://www.nccn.org/professionals/physician_gls/recently_updated.asp

13 **Tomlinson I**, Ilyas M, Johnson V, Davies A, Clark G, Talbot I, Bodmer W. A comparison of the genetic pathways involved in the pathogenesis of three types of colorectal cancer. *J Pathol* 1998; **184**: 148-152 [PMID: 9602705]

14 **Ogino S**, Goel A. Molecular classification and correlates in colorectal cancer. *J Mol Diagn* 2008; **10**: 13-27 [PMID: 18165277 DOI: 10.2353/jmoldx.2008.070082]

15 **Worthley DL**, Leggett BA. Colorectal cancer: molecular features and clinical opportunities. *Clin Biochem Rev* 2010; **31**: 31-38 [PMID: 20498827]

16 **Pino MS**, Chung DC. The chromosomal instability pathway in colon cancer. *Gastroenterology* 2010; **138**: 2059-2072 [PMID: 20420946 DOI: 10.1053/j.gastro.2009.12.065]

17 **Fujiwara T**, Stolker JM, Watanabe T, Rashid A, Longo P, Eshleman JR, Booker S, Lynch HT, Jass JR, Green JS, Kim H, Jen J, Vogelstein B, Hamilton SR. Accumulated clonal genetic alterations in familial and sporadic colorectal carcinomas with widespread instability in microsatellite sequences. *Am J Pathol* 1998; **153**: 1063-1078 [PMID: 9777938]

18 **Curtin K**, Slattery ML, Samowitz WS. CpG island methylation in colorectal cancer: past, present and future. *Patholog Res Int* 2011; **2011**: 902674 [PMID: 21559209 DOI: 10.4061/2011/902674]

19 **Drost J**, van Jaarsveld RH, Ponsioen B, Zimberlin C, van Boxtel R, Buijs A, Sachs N, Overmeer RM, Offerhaus GJ, Begthel H, Korving J, van de Wetering M, Schwank G, Logtenberg M, Cuppen E, Snippert HJ, Medema JP, Kops GJ, Clevers H. Sequential cancer mutations in cultured human intestinal stem cells. *Nature* 2015; **521**: 43-47 [PMID: 25924068 DOI: 10.1038/nature14415]

20 **Fearon ER**, Vogelstein B. A genetic model for colorectal tumorigenesis. *Cell* 1990; **61**: 759-767 [PMID: 2188735]

21 **Dix BR**, Robbins P, Soong R, Jenner D, House AK, Iacopetta BJ. The common molecular genetic alterations in Dukes' B and C colorectal carcinomas are not short-term prognostic indicators of

survival. *Int J Cancer* 1994; **59**: 747-751 [PMID: 7989112]
22 **Watanabe T**, Kobunai T, Yamamoto Y, Matsuda K, Ishihara S, Nozawa K, Yamada H, Hayama T, Inoue E, Tamura J, Iinuma H, Akiyoshi T, Muto T. Chromosomal instability (CIN) phenotype, CIN high or CIN low, predicts survival for colorectal cancer. *J Clin Oncol* 2012; **30**: 2256-2264 [PMID: 22547595 DOI: 10.1200/JCO.2011.38.6490]
23 **Cheng YW**, Pincas H, Bacolod MD, Schemmann G, Giardina SF, Huang J, Barral S, Idrees K, Khan SA, Zeng Z, Rosenberg S, Notterman DA, Ott J, Paty P, Barany F. CpG island methylator phenotype associates with low-degree chromosomal abnormalities in colorectal cancer. *Clin Cancer Res* 2008; **14**: 6005-6013 [PMID: 18829479 DOI: 10.1158/1078-0432.CCR-08-0216]
24 **Kang GH**. Four molecular subtypes of colorectal cancer and their precursor lesions. *Arch Pathol Lab Med* 2011; **135**: 698-703 [PMID: 21631262 DOI: 10.1043/2010-0523-RA.1]
25 **Kim JH**, Bae JM, Cho NY, Kang GH. Distinct features between MLH1-methylated and unmethylated colorectal carcinomas with the CpG island methylator phenotype: implications in the serrated neoplasia pathway. *Oncotarget* 2016; Epub ahead of print [PMID: 26883113 DOI: 10.18632/oncotarget.7374]
26 **Samadder NJ**, Vierkant RA, Tillmans LS, Wang AH, Weisenberger DJ, Laird PW, Lynch CF, Anderson KE, French AJ, Haile RW, Potter JD, Slager SL, Smyrk TC, Thibodeau SN, Cerhan JR, Limburg PJ. Associations between colorectal cancer molecular markers and pathways with clinicopathologic features in older women. *Gastroenterology* 2013; **145**: 348-356.e1-2 [PMID: 23665275 DOI: 10.1053/j.gastro.2013.05.001]
27 **Bettington M**, Walker N, Clouston A, Brown I, Leggett B, Whitehall V. The serrated pathway to colorectal carcinoma: current concepts and challenges. *Histopathology* 2013; **62**: 367-386 [PMID: 23339363 DOI: 10.1111/his.12055]
28 **Lochhead P**, Kuchiba A, Imamura Y, Liao X, Yamauchi M, Nishihara R, Qian ZR, Morikawa T, Shen J, Meyerhardt JA, Fuchs CS, Ogino S. Microsatellite instability and BRAF mutation testing in colorectal cancer prognostication. *J Natl Cancer Inst* 2013; **105**: 1151-1156 [PMID: 23878352 DOI: 10.1093/jnci/djt173]
29 **Popat S**, Hubner R, Houlston RS. Systematic review of microsatellite instability and colorectal cancer prognosis. *J Clin Oncol* 2005; **23**: 609-618 [PMID: 15659508]
30 **Shiovitz S**, Bertagnolli MM, Renfro LA, Nam E, Foster NR, Dzieciatkowski S, Luo Y, Lao VV, Monnat RJ, Emond MJ, Maizels N, Niedzwiecki D, Goldberg RM, Saltz LB, Venook A, Warren RS, Grady WM; Alliance for Clinical Trials in Oncology. CpG island methylator phenotype is associated with response to adjuvant irinotecan-based therapy for stage III colon cancer. *Gastroenterology* 2014; **147**: 637-645 [PMID: 24859205 DOI: 10.1053/j.gastro.2014.05.009]
31 **Sinicrope FA**, Shi Q, Smyrk TC, Thibodeau SN, Dienstmann R, Guinney J, Bot BM, Tejpar S, Delorenzi M, Goldberg RM, Mahoney M, Sargent DJ, Alberts SR. Molecular markers identify subtypes of stage III colon cancer associated with patient outcomes. *Gastroenterology* 2015; **148**: 88-99 [PMID: 25305506 DOI: 10.1053/j.gastro.2014.09.041]
32 **Phipps AI**, Limburg PJ, Baron JA, Burnett-Hartman AN, Weisenberger DJ, Laird PW, Sinicrope FA, Rosty C, Buchanan DD, Potter JD, Newcomb PA. Association between molecular subtypes of colorectal cancer and patient survival. *Gastroenterology* 2015; **148**: 77-87.e2 [PMID: 25280443 DOI: 10.1053/j.gastro.2014.09.038]
33 **Jass JR**. Classification of colorectal cancer based on correlation of clinical, morphological and molecular features. *Histopathology* 2007; **50**: 113-130 [PMID: 17204026]
34 **Krol LC**, 't Hart NA, Methorst N, Knol AJ, Prinsen C, Boers JE. Concordance in KRAS and BRAF mutations in endoscopic biopsy samples and resection specimens of colorectal adenocarcinoma. *Eur J Cancer* 2012; **48**: 1108-1115 [PMID: 22446020 DOI: 10.1016/j.ejca.2012.02.054]
35 **Iacopetta B**. Are there two sides to colorectal cancer? *Int J Cancer* 2002; **101**: 403-408 [PMID: 12216066]
36 **Minoo P**, Zlobec I, Peterson M, Terracciano L, Lugli A. Characterization of rectal, proximal and distal colon cancers based on clinicopathological, molecular and protein profiles. *Int J Oncol* 2010; **37**: 707-718 [PMID: 20664940]
37 **Murphy KM**, Zhang S, Geiger T, Hafez MJ, Bacher J, Berg KD, Eshleman JR. Comparison of the microsatellite instability analysis system and the Bethesda panel for the determination of microsatellite instability in colorectal cancers. *J Mol Diagn* 2006; **8**: 305-311 [PMID: 16825502]
38 **Ogino S**, Kawasaki T, Kirkner GJ, Kraft P, Loda M, Fuchs CS. Evaluation of markers for CpG island methylator phenotype (CIMP) in colorectal cancer by a large population-based sample. *J Mol Diagn* 2007; **9**: 305-314 [PMID: 17591929]
39 **Ogino S**, Nosho K, Kirkner GJ, Kawasaki T, Meyerhardt JA, Loda M, Giovannucci EL, Fuchs CS. CpG island methylator phenotype, microsatellite instability, BRAF mutation and clinical outcome in colon cancer. *Gut* 2009; **58**: 90-96 [PMID: 18832519 DOI: 10.1136/gut.2008.155473]
40 **Salek C**, Benesova L, Zavoral M, Nosek V, Kasperova L, Ryska M, Strnad R, Traboulsi E, Minarik M. Evaluation of clinical relevance of examining K-ras, p16 and p53 mutations along with allelic losses at 9p and 18q in EUS-guided fine needle aspiration samples of patients with chronic pancreatitis and pancreatic cancer. *World J Gastroenterol* 2007; **13**: 3714-3720 [PMID: 17659731 DOI: 10.3748/wjg.v13.i27.3714]
41 **Hinselwood DC**, Abrahamsen TW, Ekstrøm PO. BRAF mutation detection and identification by cycling temperature capillary electrophoresis. *Electrophoresis* 2005; **26**: 2553-2561 [PMID: 15948220]
42 **Minarik M**, Minarikova L, Hrabikova M, Minarikova P, Hrabal P, Zavoral M. Application of cycling gradient capillary electrophoresis to detection of APC, K-ras, and DCC point mutations in patients with sporadic colorectal tumors. *Electrophoresis* 2004; **25**: 1016-1021 [PMID: 15095442]
43 **Kristensen AT**, Bjørheim J, Ekstrøm PO. Detection of mutations in exon 8 of TP53 by temperature gradient 96-capillary array electrophoresis. *Biotechniques* 2002; **33**: 650-653 [PMID: 12238774]
44 **Simi L**, Pratesi N, Vignoli M, Sestini R, Cianchi F, Valanzano R, Nobili S, Mini E, Pazzagli M, Orlando C. High-resolution melting analysis for rapid detection of KRAS, BRAF, and PIK3CA gene mutations in colorectal cancer. *Am J Clin Pathol* 2008; **130**: 247-253 [PMID: 18628094 DOI: 10.1309/LWDY1AXHXUULNVHQ]
45 **Miyoshi Y**, Nagase H, Ando H, Horii A, Ichii S, Nakatsuru S, Aoki T, Miki Y, Mori T, Nakamura Y. Somatic mutations of the APC gene in colorectal tumors: mutation cluster region in the APC gene. *Hum Mol Genet* 1992; **1**: 229-233 [PMID: 1338904]
46 **Forbes SA**, Beare D, Gunasekaran P, Leung K, Bindal N, Boutselakis H, Ding M, Bamford S, Cole C, Ward S, Kok CY, Jia M, De T, Teague JW, Stratton MR, McDermott U, Campbell PJ. COSMIC: exploring the world's knowledge of somatic mutations in human cancer. *Nucleic Acids Res* 2015; **43**: D805-D811 [PMID: 25355519 DOI: 10.1093/nar/gku1075]
47 **Young J**, Leggett B, Gustafson C, Ward M, Searle J, Thomas L, Buttenshaw R, Chenevix-Trench G. Genomic instability occurs in colorectal carcinomas but not in adenomas. *Hum Mutat* 1993; **2**: 351-354 [PMID: 8257987]
48 **Toyota M**, Ohe-Toyota M, Ahuja N, Issa JP. Distinct genetic profiles in colorectal tumors with or without the CpG island methylator phenotype. *Proc Natl Acad Sci USA* 2000; **97**: 710-715 [PMID: 10639144]
49 **Hicks DG**, Boyce BF. The challenge and importance of standardizing pre-analytical variables in surgical pathology specimens for clinical care and translational research. *Biotech Histochem* 2012; **87**: 14-17 [PMID: 21732745 DOI: 10.3109/10520295.2011.591832]
50 **Cree IA**, Deans Z, Ligtenberg MJ, Normanno N, Edsjö A, Rouleau E, Solé F, Thunnissen E, Timens W, Schuuring E, Dequeker E, Murray S, Dietel M, Groenen P, Van Krieken JH; European Society of Pathology Task Force on Quality Assurance in Molecular Pathology; Royal College of Pathologists. Guidance for laboratories performing

molecular pathology for cancer patients. *J Clin Pathol* 2014; **67**: 923-931 [PMID: 25012948 DOI: 10.1136/jclinpath-2014-202404]

51 **Rafael OC**, Aziz M, Raftopoulos H, Vele OE, Xu W, Sugrue C. Molecular testing in lung cancer: fine-needle aspiration specimen adequacy and test prioritization prior to the CAP/IASLC/AMP Molecular Testing Guideline publication. *Cancer Cytopathol* 2014; **122**: 454-458 [PMID: 24723383 DOI: 10.1002/cncy.21426]

52 **Sugai T**, Habano W, Jiao YF, Tsukahara M, Takeda Y, Otsuka K, Nakamura S. Analysis of molecular alterations in left- and right-sided colorectal carcinomas reveals distinct pathways of carcinogenesis: proposal for new molecular profile of colorectal carcinomas. *J Mol Diagn* 2006; **8**: 193-201 [PMID: 16645205]

P- Reviewer: Akiyama Y, Tanimoto MA **S- Editor**: Ma YJ
L- Editor: A **E- Editor**: Wang CH

World Journal of Gastroenterology

Submit a Manuscript: http://www.wjgnet.com/esps/
Help Desk: http://www.wjgnet.com/esps/helpdesk.aspx
DOI: 10.3748/wjg.v22.i20.4946

World J Gastroenterol 2016 May 28; 22(20): 4946-4957
ISSN 1007-9327 (print) ISSN 2219-2840 (online)

SYSTEMATIC REVIEWS

Colorectal cancer screening in countries of European Council outside of the EU-28

Emma Altobelli, Francesco D'Aloisio, Paolo Matteo Angeletti

Emma Altobelli, Francesco D'Aloisio, Paolo Matteo Angeletti, Department of Life, Health and Environmental Sciences, University of L'Aquila, 67100 L'Aquila, Italy

Emma Altobelli, Epidemiology and Biostatistics Unit, AUSL Teramo, University of L'Aquila, 67100 L'Aquila, Italy

Author contributions: Altobelli E contributed to this paper with conception and design of the study, literature review, drafting and critical revision and editing; D'Aloisio F participated to literature search and participated in writing the paper; Angeletti PM participated to literature search, acquired the data and participated in writing the paper; all authors have approved the final version of manuscript.

Conflict-of-interest statement: The authors declared no conflict of interest.

Correspondence to: Dr. Emma Altobelli, Professor, Department of Life, Health and Environmental Sciences, University of L'Aquila, Piazzale Salvatore Tommasi 1, 67100 L'Aquila, Coppito (Aq), Italy.
emma.altobelli@cc.univaq.it
Telephone: +39-86-2434666
Fax: +39-86-2433425

Received: March 6, 2016
Peer-review started: March 7, 2016
First decision: April 1, 2016
Revised: April 13, 2016
Accepted: May 4, 2016
Article in press: May 4, 2016
Published online: May 28, 2016

Abstract

AIM: To provide an update on colorectal cancer (CRC) screening programmes in non-European Union (EU)-28 Council of Europe member states as of December 2015.

METHODS: The mission of the Council of Europe is to protect and promote human rights in its 47 member countries. Its 19 non-EU member states are Albania, Andorra, Armenia, Azerbaijan, Bosnia and Herzegovina, Republika Srpska, Georgia, Iceland, Liechtenstein, Republic of Moldova, Monaco, Montenegro, Norway, Russian Federation, San Marino, Serbia, Switzerland, FYR of Macedonia, Turkey, and Ukraine (EU-19). The main data source were GLOBOCAN, IARC, WHO, EUCAN, NORDCAN, ENCR, volume X of the CI5, the ministerial and Public Health Agency websites of the individual countries, PubMed, EMBASE, registries of some websites and the www.cochranelibrary.com, Scopus, www.clinicaltrials.gov, www.clinicaltrialsregister.eu, Research gate, Google and data extracted from screening programme results.

RESULTS: Our results show that epidemiological data quality varies broadly between EU-28 and EU-19 countries. In terms of incidence, only 30% of EU-19 countries rank high in data quality as opposed to 86% of EU-28 states. The same applies to mortality data, since 52% of EU-19 countries as against all EU-28 countries are found in the high ranks. Assessment of the method of collection of incidence data showed that only 32% of EU-19 countries are found in the top three quality classes as against 89% of EU-28 countries. For the mortality data, 63% of EU-19 countries are found in the highest ranks as opposed to all EU-28 member states. Interestingly, comparison of neighbouring countries offering regional screening shows, for instance, that incidence and mortality rates are respectively 38.9 and 13.0 in Norway and 29.2 and

10.9 in Sweden, whereas in Finland, where a national organised programme is available, they are respectively 23.5 and 9.3.

CONCLUSION: Cancer screening should be viewed as a key health care tool, also because investing in screening protects the weakest in the population, decreases the social burden of cancer, and reduces all types of health care costs, including those for radical surgery, long-term hospitalisation, and chemotherapy.

Key words: Colorectal cancer; Screening; EU-28; EU-19; European Union; Early detection; European Council

Core tip: In the WHO Europe Region, colorectal cancer (CRC) is the first tumour with 471000 new cases per year and a mortality rate of 28.2 per 100000 population. Large-scale studies have found a reduction in mortality due to the adoption of population-based screening programmes. A 2010 European Parliament resolution called for the adoption of prevention programmes. As a result, some member states have begun enacting programmes, others are organising strategies for CRC screening implementation, and others still are moving from pilot projects to national-scale programmes. The present systematic review provides an update on CRC screening programmes in non EU-28 European Council States.

Altobelli E, D'Aloisio F, Angeletti PM. Colorectal cancer screening in countries of European Council outside of the EU-28. *World J Gastroenterol* 2016; 22(20): 4946-4957 Available from: URL: http://www.wjgnet.com/1007-9327/full/v22/i20/4946.htm DOI: http://dx.doi.org/10.3748/wjg.v22.i20.4946

INTRODUCTION

Although cervical, breast and colorectal cancer are the only tumours for which screening has proven efficacy and cost-effectiveness, in several European countries screening implementation is fraught with difficulties. This is especially true of programmes regarding colorectal cancer (CRC)[1-3], a highly common malignancy. According to GLOBOCAN data[3], 1.36 million new cases affecting 17.2 per 100000 population (746000 men and 614000 women) are diagnosed in the world each year, and 693000 people (373000 men and 320000 women) die from CRC, accounting for a yearly mortality rate of 8.4 per 100000.In the World Health Organisation (WHO) Europe Region, CRC is the first tumour by incidence, with 471000 new cases each year and a mean mortality rate of 28.2 per 100000 population[4]. In the European Union (EU-28), its mean incidence rate is 31.3 per 100000 population, with 345000 new cases per year and an incidence per 100000 population of 39.5 for men 39.5 and 24.4 for women. The mean CRC incidence rates for men and women in the WHO Europe Region are 35.6 and 22.6 per 100000 population, respectively. In addition, with 228000 deaths per year and a mortality rate of 12.3 per 100000 population, CRC is the second cause of cancer death after lung cancer for men and women in the region[4]. The mean mortality rates per 100000 population in EU-28 countries and the WHO Europe Region are respectively 15.2 and 15.7 for men and 9.0 and 9.7 for women[4].

CRC incidence is quite variable in EU-28 countries, and is higher in central and northern member states than in eastern ones. However, the lower rates found in eastern Europe are higher than the world mean[3]. This has prompted the Council of Europe to recommend the priority activation of CRC screening programmes[5]. According to a 2008 European Commission report on the diffusion of CRC screening programmes in the EU, only 12 of the then 22 member states had population-based screening programmes; the others were recommended to provide to their citizens equal access to cancer prevention[6].

Crucially, more than 95% of CRC cases could benefit from surgical treatment if diagnosed early[7]. Several large-scale studies have found a considerable reduction in mortality due to the adoption of population-based screening programmes[8,9].

The first European guidelines on CRC screening and the quality of CRC diagnosis were issued in 2010[10]. A European Parliament resolution of 6 May 2010 asked the Commission to promote the adoption of prevention programmes by any means and to encourage member states to allocate further resources to primary prevention and early diagnosis through screening[11]. As a result, some member states have begun enacting programmes, others are organising strategies for CRC screening implementation[3], and others still are moving from pilot projects to national-scale programmes[12-16].

The aim of the present systematic review is to provide an update on CRC screening programmes in non EU-28 European Council member states as of December 2015.

MATERIALS AND METHODS

Council of Europe member countries

The Council of Europe is a supranational institution founded in 1949 by the Treaty of London. Its mission is to protect and promote human rights in member countries. There are 47 member countries and a number of states with observer status. All EU-28 States are members (Austria, Belgium, Bulgaria, Croatia, Cyprus, Czech Republic, Denmark, Estonia, Finland, France, Germany, Greece, Hungary, Ireland, Italy, Latvia, Lithuania, Luxembourg, Malta, Poland, Portugal, Romania, Slovakia, Slovenia, Spain, Sweden, the Netherlands, and the United Kingdom). The other

Table 1 Number of cases and standardized colorectal cancer burden in women and men in EU-19, 2012 (Adapted from Ferlay *et al*[4])

Country	WOMAN						MAN					
	Incidence		5-yr prevalence		Mortality		Incidence		5-yr prevalence		Mortality	
	Cases	ASR (W)	Cases	%	Cases	ASR (W)	Cases	ASR (W)	Cases	%	Cases	ASR (W)
Albania	167	7.9	501	39.9	90	4.0	175	9.0	526	42.0	97	4.8
Andorra	NR											
Armenia	4.4	17.0	939	68.6	281	9.7	426	22.8	855	77.1	261	13.4
Azerbaijan	346	6.4	209	4.0	755	19.8	313	7.1	661	18.5	187	4.3
Bosnia and Herzegovina	489	13.3	1427	84.8	327	7.7	620	20.7	1811	119.1	422	12.7
Georgia	300	7.5	608	31.3	173	4.0	305	9.9	631	38.3	177	5.5
Iceland	79	28.3	238	183.6	21	5.8	78	28.9	232	177.5	27	9.3
Liechtenstein	NR											
Republic of Moldova	716	23.0	1736	111.0	409	12.6	799	36.0	1963	143.2	491	22.0
Monaco	NR											
Montenegro	107	21.1	314	118.7	67	12.0	157	36.2	465	187.3	95	20.7
Norway	1947	35.8	5665	279.6	779	12.1	1966	42.6	5839	289.8	727	14.3
Russian Fed	33183	21.8	78454	119.1	21791	12.7	26745	30.0	63572	116.4	18116	19.9
San Marino	NR											
Serbia	2143	23.3	6281	151.4	1213	11.5	3370	43.4	9919	248.8	1922	22.8
Switzerland	2167	23.6	6522	193.8	718	6.4	2707	36.3	8340	259.9	1668	12.8
FYR Macedonia'	366	20.5	1070	124.0	213	10.8	421	28.4	1256	147.3	239	15.5
Turkey	5041	13.1	10690	38.2	3030	7.8	6889	20.6	14982	54.7	4128	12.6
Ukraine	9780	19.9	23110	109.6	5704	10.8	6269	29.9	22120	127.8	5929	18.8
EU-28	151920	24.4	417252	189.0	69087	9.0	193426	39.5	535845	257.8	82959	15.2

EU-28: Countries members of European Union; NR: Not Reported; ASR (W): Per 100000.

19 countries (hereafter EU-19) are in the European area: Albania, Andorra, Armenia, Azerbaijan, Bosnia and Herzegovina, Republika Srpska, Georgia, Iceland, Liechtenstein, Republic of Moldova, Monaco, Montenegro, Norway, Russian Federation, San Marino, Serbia, Switzerland, FYR of Macedonia, Turkey, and Ukraine.

Sources of EU-19 epidemiological data: Search strategy

The main data source was the GLOBOCAN 2012 website of the International Agency for Research on Cancer (IARC), which provides access to several databases that enable assessing the impact of CRC in 184 countries or territories in the world[4].

Additional sources were the WHO, EUCAN and NORDCAN, the European Network of Cancer Registries (ENCR), volume X of the CI5, and the ministerial and Public Health Agency websites of the individual countries. The PubMed search used "Early Detection of Cancer" or "Colorectal Cancer screening" AND "state name" for each of the 19 countries. A MeSH search was conducted using the same criteria. The EMBASE did not provide further relevant results. The registries of some websites and the www.cochranelibrary.com, Scopus, www.clinicaltrials.gov, www.clinicaltrialsregister.eu, Research gate, and Google databases were also consulted. Other data were extracted from screening programme results.

Statistical analysis

Incidence and mortality data, their age-standardised rates per 100000 population (ASR-W), and 5-year prevalence estimates for 2012 are reported by gender in Table 1. The quality of incidence and mortality data of EU-19 and EU-28 based on Data Sources and Methods[17] is compared in Table 2. The information regarding screening programmes in EU-19 is shown in Table 3. Finally mean income, total population, the existence of any registries, the availability of early detection tests at the public primary health care level, and the ranking of CRC incidence and mortality in EU-19 countries are reported in Table 4. The distribution of screening programmes (organised, spontaneous, unknown) in EU-28 and EU-19 countries is shown in Figure 1.

RESULTS

The results of the present systematic review are listed by physical geographical area as well as disaggregated by state. The incidence and mortality data are reported as ASR-W per 100000 population.

Northern Europe

The only North European countries that are not also EU-28 members are Iceland and Norway. The United Kingdom and Northern Ireland, Ireland, Finland, Denmark, Estonia, and Latvia offer organised national screening programmes and Sweden an organised regional programme; only Lithuania adopts spontaneous screening (Figure 1).

Iceland: The incidence rate of CRC in Iceland is 28.9 and 28.3 in men and women, respectively, with

Table 2 Quality assessment of Epidemiological data source and methods according to Mathers *et al*[17]

Data source			
EU-19 Incidence A: Iceland Norway, Ukraine B: Serbia, Switzerland C: Turkey D: Bosnia Herzegovina, Russian Federation E: - F: - G: Albania, Armenia, Azerbaijan, FYR Macedonia, Georgia, Montenegro, Republic of Moldova	EU-19 Mortality 1: Iceland, Republic of Moldova 2: Azerbaijan, Norway, Russian Federation, Serbia, Switzerland 3: Albania, Armenia, FYR Macedonia 4: - 5: Bosnia Herzegovina 6: Georgia, Montenegro, Turkey	EU-28 Incidence A: Austria, Belgium, Bulgaria, Croatia, Czech Republic, Denmark, Estonia, Ireland, Latvia, Lithuania, Malta, Sweden, Slovenia,Slovakia, The Netherlands, United Kingdom, Finland, France (Martinique) B: France, Germany, Italy, Spain C: Portugal, Poland D: Luxembourg, France (La Reunion) E: Romania F: - G: Greece, Hungary, France (Guadalupe), France (Guiana)	EU-28 Mortality 1: Estonia, Hungary, Ireland, Latvia, Lithuania, Malta, Slovenia, Slovakia, Romania, United Kingdom, Finland 2: Austria, Belgium, Bulgaria, Croatia, Czech Republic, Denmark, France, Germany, Italy, Luxembourg, Spain, Sweden, The Netherlands, France (Guadalupe), (La Reunion), France (Martinique), France (Guiana) 3: Greece, Portugal, Poland 4: - 5: - 6: -
Methods			
EU-19 Incidence 1: Iceland, Norway 2: Bosnia Herzegovina, Ukraine 3: Turkey, Switzerland 4: Albania, FYR Macedonia, Republic of Moldova, Serbia 5: Armenia, Azerbaijan, Georgia 6: Turkey 7: - 8: - 9: Montenegro	EU-28 Mortality 1: Albania, FYR Macedonia, Iceland, Norway, Republic of Moldova, Serbia, Switzerland 2: Armenia, Azerbaijan, Bosnia Herzegovina, Georgia, Ukraine 3: - 4: - 5: Turkey 6: Montenegro	EU-19 Incidence 1: Austria, Bulgaria, Croatia, Czech Republic, Denmark, Estonia, Finland, Germany, Ireland, Latvia, Lithuania, Malta, Slovakia, Slovenia, Sweden The Netherlands, United Kingdom, France (La Reunion), France (Martinique) 2: Belgium, Cyprus 3: France (metropolitan) , Germany, Italy, Poland, Spain 4: Greece, Hungary, Luxembourg, Portugal 5: Romania, France (Guadalupe), 6: - 7: - 8: - 9: -	EU-28 Mortality 1: Austria. Bulgaria, Croatia, Czech Republic, Denmark, Estonia, Finland, France (metropolitan) Germany, Greece, Hungary, Ireland, Italy, Latvia, Lithuania, Luxembourg, Malta, Poland, Portugal, Slovakia, Slovenia, Spain, Sweden, The Netherlands, United Kingdom, France (Martinique) 2: Belgium, Cyprus, France (Guadalupe) 3: Greece, Portugal, Poland 4: - 5: France (La Reunion) 6: -

Comparison between EU-19 and EU-28 countries, as defined in the main text. -: No country classified in that category.

a mortality rate of 9.3 for men and 5.8 for women (Table 1).The national cancer registry, linked to the NORDCAN project, covers the whole population and provides high-quality data (Table 2). Iceland has no active organised CRC screening programme (Table 3). The decision to adopt one, made in 2008[18], was postponed due to the economic crisis. According to a recent congress communication[19], a programme offering screening with the iFOBT at 2-year intervals to 55 to 75 year olds is due to start soon (Table 3). Until then, only spontaneous screening with the iFOBT will be available at the level of public primary health care (Table 4). CRC is the third most common tumour in both genders in the country and the fourth and second cause of cancer death in Iceland (Table 4).

Norway: In this country the incidence of CRC is 42.6 among men and 35.8 among women, with a mortality rate - 12.1 in men and 14.3 in women (Table 1). High data quality is ensured by a national cancer registry linked to the NORDCAN that covers the whole population (Table 2). A pilot study offering the iFOBT at 2-year intervals was activated in 2012 in the Ostfold region[20]. In a randomised controlled study (NORCCAPP) conduced in the Oslo and Telemark areas in 1999-2001 the population was assigned to three groups that were tested with the iFOBT, received the iFOBT + sigmoidoscopy, or were just asked to report if they had had a diagnosis of CRC in the course of the study[21] (Table 3). CRC is the second most common tumour in both sexes and the second cause of cancer death for both sexes in Norway (Table 4).

Balkan countries

Several of these countries are EU-19 States: Albania, Republika Srpska, Bosnia and Herzegovina, Montenegro, and Serbia. Slovenia and Croatia are EU-28 Member states offering organised screening programmes (Figure 1).

Albania: Albania has a low CRC incidence rate, 9.0 among men and 7.9 among women, and an equally low mortality rate, respectively 4.8 and 4.0 (Table 1). Hospital-based disease registries provide non-excellent data quality (Table 2). Neither spontaneous nor organised screening is available[22]. The most recent data are for 2011. A 2015 paper[23] that first measured the frequency of gastrointestinal polypoid lesions in the Albanian population stressed the absence of a screening programme. According to the

Table 3 Distribution of colorectal cancer screening programmes in EU-19 as of December 2015

Country	Program			Test	Screening interval (yr)	Age (yr)	Program start	Pop target	Level of participation (%)
	Type	Status	Region						
Federation of Bosnia and Heregovina[22]	Spontaneous Organised	NatW	All country	FOBT	-	> 50	-	-	-
Republika Srpska[22]	Spontaneous	NatW	All country	FOBT	-	> 50	-	-	-
Georgia[51]	Organised	NatW	Tblisi	gFOBT	2	50-69	-	25388	53
			OutsideTblisi	gFOBT	2	50-69	-	71364	84
Iceland[18]	Programmed as organised	NatW	All country	FOBT	2	55-75[19]	-	86000[19]	
Iceland[19]	Spontaneous	NatW	All country	Colonoscopy		50-59			30
Monaco[35]	PB	Natw	All country	iFOBT (from 2015) gFOBT	2	50-80	2006	16000[35]	60
Montenegro[22,28]	None	-	-	-	-	-	-	-	-
Montenegro[28]	Not PB	PilotStudy	Danilograv, municipality of Podgorica	iFOBT	-	50-74	2010-2011	4500	33.3
Norway[20]	PB	Pilot Study	Østfold, Akershus and Buskerud	iFOBT	2		2012		
Norway[21]	PB	Pilot Study RCT	Oslo and Telemark in 1999-2001 NORCAPP	FOBT and FOBT + Sigmoidoscopy	-	55-64	1999-2000	13823	64.8
Russian Fed[42]	PB	Pilot Study	Sant Petersburb, all 18 town district	iFOBT		48-75	November 15	20000	
Russian Fed[43]	NPB	Pilot Study	Kazan, Tatarstan Republic	FOBT, DRE, questionnaire	-		2010	1071	
San Marino[36,37]	PB	Natw	All country	iFOBT	2	50-79	2009		65[37]
Serbia[31]	PB	Natw	All country	iFOBT	2	50-74		789330	58.38
Switzerland[32]	Spontaneous	NatW	All country	FOBT or Colonoscopy	2, 10	50-80	2013	13170	22
Switzerland[33]	PB	Pilot Study RCT	Glarus, Vallée du Joux Uri	FOBT and or Colonoscopy	-	50-80	2001	20000	
Switzerland[34]	PB	Pilot Study, NRCT	Vaud	iFOBT or Colonoscopy		50-69	2015		
Turkey[44]	Organised Spontaneous	NatW		FOBT		50-69	2009	11681513	30[44]
Ukraine[46,54]	PB	NatW		Not available	Not available	Not available	2002-2006		Not available

gFOBT: Guaiac test; iFOBT: Immunological test; FOBT: Not specified if gFOBT or iFOBT; DRE: Digital rectal exam; NPB: Not population-based.

WHO report[24], neither the FOBT nor colonoscopy are available at the level of public primary health care (Table 4).

Bosnia and Herzegovina, Republika Srpska: In the Federation of Bosnia and Herzegovina the incidence of CRC is 20.7 among men and 13.3 among women, with a mortality rate of 12.7 in men and 7.7 in women. Data quality is not excellent (Table 2). According to Giordano *et al*[22], spontaneous and organised screening based on the FOBT is available for those aged more than 50 years. However, Buturovic reports that in the Konjic area colonoscopy is not available[25]. As shown in Table 4, the WHO has no data on the availability of screening tests (FOBT, colonoscopy) at the level of public primary health care[26]. The tumour represents the third and second most common cancer and the second and third cause of death in the country (Table 4).

In the Republika Srpska only spontaneous screening is available to subjects older than 50 years[22]. Again, there is no clear information on screening programmes.

FYR Macedonia: In this country CRC incidence is moderately high in men (28.4) as well as women (20.5) (Table 1) and mortality rates of 15.5 and 10.8, respectively. Data quality is mediocre (Table 2). There seem to be no organised screening programmes, even though the iFOBT is available at the public primary health care level[27] (Table 4). CRC is the third most common tumour in the country for both sexes and the second cause of cancer death (Table 4).

Montenegro: The incidence of CRC in Montenegro is 36.2 among men and 21.1 among women, with a mortality rate of 20.7 in men and 12.0 in women. Data quality is poor (Table 2). A population-based screening programme using the iFOBT and involving subjects aged 50 to 74 years was conducted from February 2010 to March 2011 in Danilograv municipality (Podgorica)[28], while neither organised nor opportunistic screening is available in the other areas[22]. According

Table 4 National cancer profiles

Country	Income[1]	Total population	Cancer registry	Availability at public primary health care levels of early detection tests		Ranking CRC incidence[2]		Ranking CRC mortality[2]	
				Faecal occult blood test	Bowel cancer screening by exam or colonoscopy	Man	Woman	Man	Woman
North Europe									
Iceland[2]	High	326000	National, population-based	-	-	3rd	3rd	2nd	4th
Norway[2]	High	4994000	National, population-based	Yes	-	2nd	2nd	3rd	2nd
Central Europe									
Liechtenstein[3]	High non OECD	36925	NA	-	-	2nd	3rd	NR	NR
Monaco	High non OECD	38000	Hospital-based	Yes	Yes	NR	NR	NR	NR
Switzerland[3]	High	7997000	Sub-national population-based[a]	Yes	Yes	2nd	2nd	3rd	3rd
South Europe									
Andorra	High non OECD	78000	Hospital-based	Yes	Yes	NR	NR	NR	NR
San Marino	High non OECD	31000	National population-based	Yes	Yes	NR	NR	NR	NR
Balcanian countries									
Albania[3]	Upper middle	3162000	Sub-national, hospital-based	-	-	> 5th	5th	> 5th	5th
Bosnia and Herzegovina[3]	Upper middle	3834000	NA	-	-	3rd	2nd	2nd	3rd
Montenegro[3]	Upper middle	621000	NA	-	-	2nd	2nd	2nd	3rd
Serbia[3]	Upper middle	9553000	Sub-national	Yes	Yes	2nd	2nd	2nd	3rd
FYR of Macedonia[3]	Upper middle	2106000	National	Yes	-	3rd	3rd	2nd	2nd
Eastern Europe									
Republic of Moldova[3]	Lower middle	3514000	National, hospital-based	Yes	Yes	2nd	2nd	2nd	2nd
Russian Fed[3]	High non OECD	143000000	Sub-national, population-based[b]	Yes	Yes	3rd	2nd	3rd	2nd
Turkey[3]	Upper middle	73997000	Sub-national population-based[c]	Yes	Yes	4th	3rd	4th	3rd
Ukraine[3]	Lower middle	45530000	National, population-based	-	-	2nd	2nd	2nd	2nd
Caucasican countries									
Armenia[3]	Lower middle	2969000	National, hospital-based	Yes	-	5th	3rd	4th	2nd
Azerbaijan[3]	Upper middle	9309000	NA	Yes	-	4th	4th	5th	5th
Georgia[3]	Lower middle	4358000	Sub-national population-based	-	-	5th	> 5th	5th	> 5th

OECD (Organization for Economic Co-operation and Development): [1]It referred to pro capita Gross National Income (current US$) as indicated by World Bank: High income $382742014; High Income non OECD: $18939; Upper middle $79012014; Lower middle $2012; [2]Incidence and mortality between different cancers for country: data from http://www.who.int/cancer/country-profiles/en/adapted for each country; [3]Data available from: http://assets.krebsliga.ch/downloads/fl2014.pdf; [a]Registry in Zurich, Vaud, Valais, Ticino, St Gall-Appenzell, Neuchâtel, Graubünden and Glarus, Geneva, Basel; [b]Registry in Saint Petersburg; [c]Registry in Trabzon, Izmir, Erdine, Antalya. Information about registry existence are available from Ref. [46]. NA: Not available; NR: Not reported; CRC: Colorectal cancer.

to WHO data (Table 4), early detection tests are not available at the public primary health care level[29]. CRC ranks respectively as the second and third cause of cancer death in Montenegro (Table 4).

Serbia: At 43.3 in men and 23.3 in women, the incidence of CRC in Serbia is fairly high and the tumour is the second most common malignancy in both sexes. The mortality rates are 28.8 in men and 11.5 in women, and CRC is respectively the second and third cause of cancer death in the country. Data quality is good (Table 2). In 2013 Serbia implemented a national screening programme by extending a programmes that had been active in Vozdovac, Subotica and Zrenjanin since 2005[30]. The current programme is offered to 50 to 74 year olds without evidence of CRC and uses the iFOBT. Its results are available online. The rate of participation as of 30 September 2015 was 58.38%[31].

Central Europe

France, Poland, Hungary, and the Netherlands offer national organised programmes, and Belgium a regional programme. Austria, Germany, the Czech Republic, Slovakia, and Luxembourg provide for spontaneous screening (Figure 1). The other countries

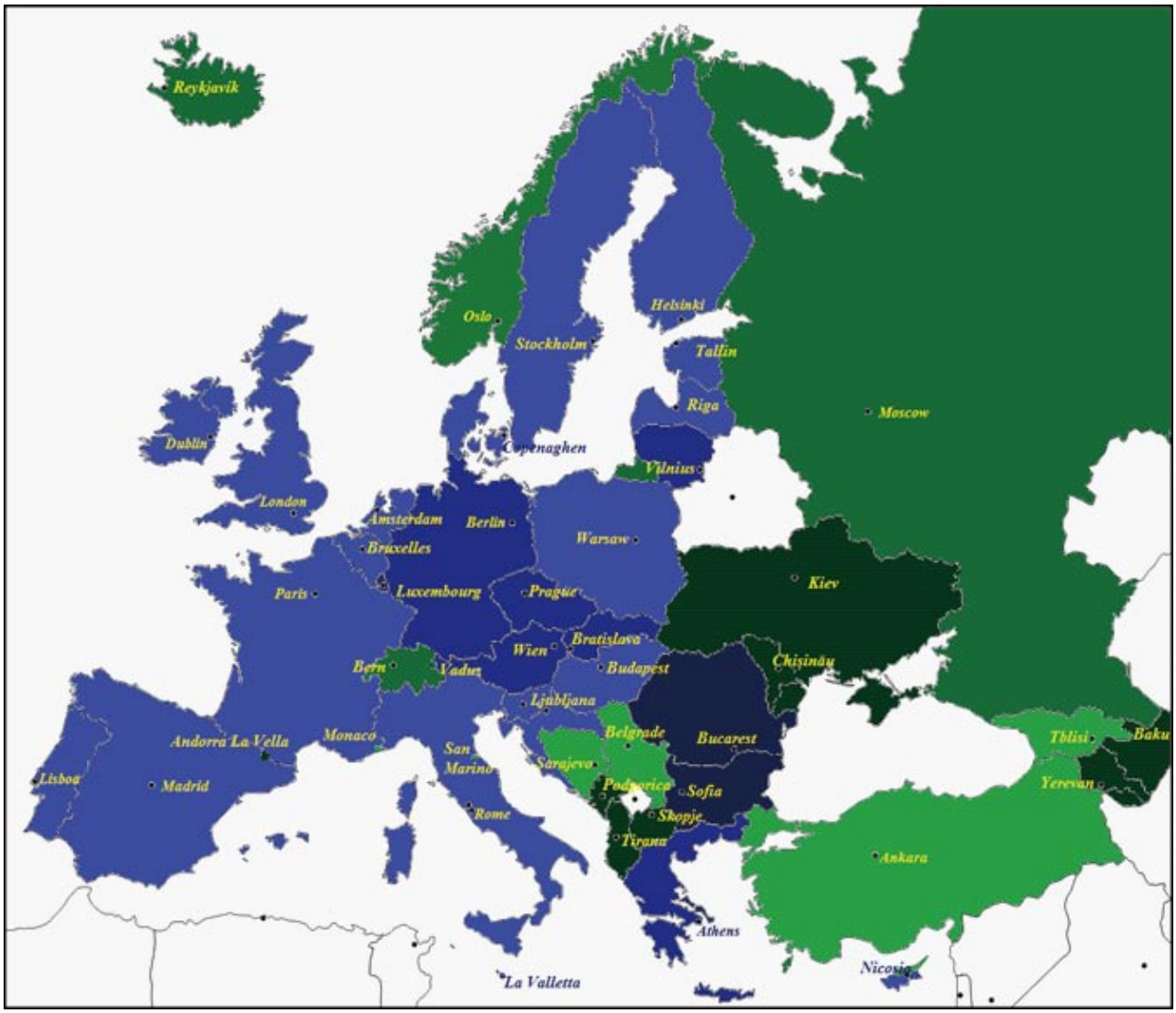

EU-28 Countries with organised screening

	ASW-R	Inc.	Mort.
Belgium[r]	36.7	11.8
Croatia	32.9	18.7
Cyprus	24.5	6.9
Denmark	40.5	14.5
Estonia	27.2	12.3
Finland	23.5	8.3
France	30.0	10.2
Hungary	42.3	20.8
Ireland	34.9	12.2
Italy	33.9	10.8
Latvia	23.7	19.9
Malta	31.9	12.2
Netherlands	40.2	13.4
Poland	27.0	14.5
Portugal[r]	31.7	13.6
Slovenia	37.0	16.2
Spain	33.1	12.3
Sweden[r]	29.2	10.9
United Kingdom	30.2	10.7

EU-28 Countries with spontaneous screening

	ASW-R	Inc.	Mort.
Austria	26.0	9.9
Czech Republic	38.9	15.4
Luxembourg	31.5	11.2
Lithuania	23.4	13.7
Germany	30.9	10.4
Greece	13.5	7.5
Slovakia	42.7	18.0

EU-28 Countries with unknown screening status

	ASW-R	Inc.	Mort.
Bulgaria	31.5	16.0
Romania	26.4	13.4

EU-19 Country with spontaneous screening

	ASW-R	Inc.	Mort.
Iceland	28.4	7.4
Russia	24.5	15.2
Switzerland	29.4	9.3

EU-19 Countries with organised screening

	ASW-R	Inc.	Mort.
Bosnia[r]	16.6	9.8
Georgia	8.5	4.6
Monaco	NA	NA
Norway[r]	38.9	13.0
San marino	NA	NA
Sebia	32.6	16.6
Turkey[r]	16.6	10.0

EU-19 Countries with unknown screening status

	ASW-R	Inc.	Mort.
Albania	8.4	4.4
Andorra	NA	NA
Armenia	19.3	11.1
Azerbaj	6.7	4.1
Liechtstenstein	NA	NA
Monteneg	28.2	15.9
Macedonia	24.3	13.0
Moldova	28.3	16.5
Ukraine	23.4	13.7

Figure 1 Comparison between EU-28 and EU-19 according to distribution of screening programmes. Inc: Incidence; Mort:. Mortality; [r]: Regional screening; NA: Not available.

in the area are Switzerland, Liechtenstein, and the Principality of Monaco.

Switzerland: The incidence rate of CRC is 36.3 in men and 23.3 in women; CRC is the second most common neoplasm in the country (Table 4). With a mortality rate of 28.8 in men and 6.4 in women, CRC ranks as the third cause of cancer death in both sexes (Table 4). Data quality is good and in line with that of neighbouring countries (Italy, France, and Germany). Since 2002, the Swiss Federal Statistical Office has been conducting a telephone survey, the Swiss Health Interview Survey (SHIS). In 2007, it assessed for the first time the date and reason for the use of the iFOBT and/or colonoscopy and asked detailed questions on screening[32]. The 2007 results found a rate of participation of 18.9% for both methods. In 2012 participation rose to 22.2% (P = 0.036)[33]; colonoscopy rose from 8.2% in 2007 to 15% (P < 0.001) and the iFOBT fell from 13% to 9.8% (P = 0.002). In 2007 the prevalence of CRC screening among respondents was 24.5% among higher-income respondents (> $6000 a month) and 10.5% in those with a low income (< $2000); the 2012 survey found a similar difference (respectively 28.6% and 16.0%). There was no association with education or occupation[32]. Since 1 July 2013 the test (colonoscopy every 10 years and iFOBT every 2 years) is partially covered by the mandatory insurance for those aged 50 to 69 years. In Uri Canton an organised programme is offered to 50-80 year olds without a past or current history of CRC. The programme was introduced in 2000 and the results of the first round have been published[33]; the patient could choose among colonoscopy, sigmoidoscopy, and iFOBT + sigmoidoscopy, and more than 70% opted for colonoscopy. Another programme in Vaud Canton offers screening to individuals aged 50 to 69 years having no risk factors or a past or current history of CRC; they can choose between the iFOBT every 2 years and colonoscopy every 10 years; the excess is paid for by the Cantonal administration, the remaining expenses are sustained by the patient. The programme is co-ordinated by the Fondation Vaudoise pour le Dépistage du Cancer[34].

Liechtenstein: In this tiny state the incidence data are provided by the National Bureau of Statistics. CRC is the second most common cancer in men and the third in women. No data are available on CRC screening programmes, neither through institutional websites nor through the WHO (Table 4).

Principality of Monaco: Official incidence and mortality data validated by the WHO are not available for this city-state, but they are probably similar to those of France. The Centre Monégasque de Dépistage has been coordinating the CRC screening campaign since 2006. The programme uses the iFOBT. Subjects receiving a letter of invitation can choose between picking up the examination kit at their general practitioner (GP) or at the screening centre. Those with a positive test are referred to the Centre Hospitalier Princesse Grace, where digestive endoscopy is performed to establish the cause of the bleeding. The service is offered to residents and foreign workers aged 50-80 years. Participation is about 60%. In March every year, the Blue March is organised in France and the Principality to promote CRC awareness and focus the attention of the population on the value of CRC prevention[35].

Southern Europe

In this region, Italy, Spain, Malta, and Cyprus offer national organised programmes, and Portugal a regional organised programme. In Greece screening is spontaneous (Figure 1). There are also two tiny states, Andorra and San Marino.

San Marino: Official incidence and mortality data are not available; however, since San Marino is nestled in the Italian region of Emilia-Romagna, they should be similar to those of Italy. A national programme, offered to individuals aged 50 to 75 years and managed by the Screening Centre of the Istituto per la Sicurezza Sociale, has been in place since 2009. The test is delivered home by mail and the recipient is asked to take it to the relevant Health Centre. Failure to do so in three months results in a reminder. Subjects with a positive test are referred to the State Hospital for a second-level examination, usually colonoscopy[36]. Participation rates (65%) have been illustrated at a press conference and are encouraging[37].

Andorra: WHO incidence and mortality data are not available, but they can reasonably be considered to resemble those of Cataluña. According to the 2014 WHO report - Cancer Country Profiles, CRC screening with the iFOBT and colonoscopy are generally available at the public primary health care level in this small Pyrenean state[38] (Table 4). However, unlike the case of breast cancer, the institutional website provides no information on CRC prevention.

Eastern Europe

In this area, Romania and Bulgaria do not offer organised screening (Figure 1). The other states in the region include the Republic of Moldova, the Russian Federation, Turkey and Ukraine.

Republic of Moldova: In this country CRC is the second most common neoplasm in men and women alike (Table 4) with an incidence of 36.0 and 23.0 respectively. The mortality rate is 22.0 and 12.6, respectively; CRC is the second cause of cancer mortality in the country (Table 4). The literature provides

no information on screening programmes, but the FOBT and colonoscopy are both available at the public primary health care level[39] (Table 4).

Russian Federation: CRC is the third tumour by incidence and mortality among men (respectively 30.0 and 19.9) and the second among women (respectively 21.8 and 11.5) (Tables 1 and 4). Data quality is mediocre (Table 2). No national screening programmes are in place[40]. The poor awareness regarding CRC involves a high rate of late diagnoses (25.6% in stage Ⅳ *vs* 18.8% in the United States) despite the fact that the iFOBT and colonoscopy are largely available at the public primary health care level[41] (Table 4). A screening campaign launched in November 2015 in the Saint Petersburg area, which hosts the sole cancer registry in the Federation[42], follows an earlier, small-scale programme set up in the Kazan region[43] (Table 3).

Turkey: In Turkey CRC incidence is 20.6 and 13.1 in men and women, respectively (Table 1). The mortality rate is 12.6 and 10.8, respectively (Table 1). Data quality is mediocre (Table 2). The national Cancer Control Department has been promoting cancer prevention campaigns since 2003. In 2009 there were no active population-based programmes, but merely some sporadic pilot studies[44]. However, a KETEM centre per province (including 2 in Istanbul and 3 in Ankara) supervise the execution of cancer screening (breast and cervical cancer) according with national guidelines; CRC was added in 2009. Screening is not covered by Social Security provisions and is sustained by the Health Ministry only for older and poorer people. Screening is largely spontaneous, but some centres like Ankara have started population-based programmes[44] (Table 3). In the future, GPs will be given the task of encouraging patients to pursue early CRC detection[44]. Both the FOBT and colonoscopy are available at the public primary health care level, as reported by the WHO country cancer profile[45]. CRC is the third and fourth cause of cancer death in the country (Table 4).

Ukraine: In Ukraine, the incidence rate of CRC is 29.9 in men and 19.9 in women and the tumour ranks second as a cause of cancer death. The mortality rate is 18.8 in men and 10.8 in women. Data quality is excellent (Table 2). According to the cancer registry, the 2002-2006 cancer plan included prevention programmes for cervical, breast, colorectum, prostate, skin, and oral cavity[46]. Based on WHO data, screening tests are not available at the public primary health care level[47] (Table 4).

Caucasian countries

These states lie on the extreme eastern boundary of Europe, where the Caucasus traditionally represents the geographical border with the Middle East.

Armenia: In Armenia CRC is the fifth most common tumour among men (22.8) and the third among women (17.0); it is the fourth cause of cancer death among men (13.4) and the second among women (9.7) (Tables 1 and 4). Data quality is fairly poor (Table 2). The literature supplies no information on screening, but the FOBT is available at the level of public primary health care[48].

Azerbaijan: In Azerbaijan CRC incidence is fairly low in both sexes (7.1 in men and 6.4 in women) and is the fourth most common tumour. CRC mortality is lower in men (4.3) than in women (19.8) and the tumour is the fifth cause of cancer death in the country (Tables 1 and 4). Data quality is poor (Table 2). Although there are no published data on screening, the WHO report indicates that the FOBT is available at the public primary health care level[49].

Georgia: In this country CRC incidence is low: 9.9 in men and 7.5 in women. The mortality figures are 5.5 in men and 4.0 in women. Data quality is poor (Table 2). Even though according to the WHO reports neither the FOBT nor colonoscopy is available for first-level screening[50], the literature and the official websites mention a CRC screening campaign and report its results[51]. These data are summarised in Table 2.

DISCUSSION

Improvements in the health status of populations and the progressive increase in life expectancy call for the promotion and diffusion of healthy lifestyles, to reduce the impact of non-communicable diseases; in particular, cancer entails an extremely high social and psychological burden. The chief mission of the Council of Europe is to promote and protect human rights in member states by issuing orientation papers and guidelines. In particular, art. 11 of the Social Charter, "The Right to Protection of Health", explicitly mentions the promotion of the health of the citizens of member states[52] and art. 3 of the Convention on Human Rights and Biomedicine makes reference to equal and appropriate access to health care[53].

Interestingly, comparison of neighbouring countries offering regional screening shows, for instance, that incidence and mortality rates are 38.9 and 13.0 in Norway and 29.2 and 10.9 in Sweden, whereas in Finland, where a national organised programme is available, they are respectively 23.5 and 9.3[54].

Epidemiological data quality varies broadly between EU-28 and EU-19 countries. In terms of incidence, only 30% of EU-19 countries rank high in data quality (A, B and C), as opposed to 86% of EU-28 states. The same applies to mortality data: 52%of EU-19 countries as against all EU-28 countries are found in the high ranks

(1, 2, or 3) (Table 2).

Assessment of the method of collection of incidence data showed that only 32% of EU-19 countries were found in the top three quality classes (A, B and C) as against 89% of EU-28 countries. For the mortality data, 63% of EU-19 countries were found in the highest ranks as opposed to all EU-28 member states (Table 2). The continuous improvement in the quality of epidemiological data collection critically supports public health decision-making, in that it represents the phenomena studied in an increasingly accurate manner in all geographical areas. This is all the more important at a time when the European continent is besieged by problems such as the economic downturn, climate change, international tensions and, last but definitely not least, the management of strong migration flows. The economic crisis has hampered the activation of large-scale screening programmes in countries, like Iceland[19], where the recession has had a devastating impact, involving their postponement. In other emerging states and areas, like Serbia[30,31], Georgia[51], and Saint Petersburg[42], population-based programmes have been implemented despite the crisis, making cancer prevention a priority, also to reduce social inequality. Clearly, it is critical to stimulate awareness of the importance of cancer prevention through screening.

In a recent British study, Moffat *et al*[55] found that awareness is crucial where cancer and its early detection are concerned. The authors measured CRC symptom knowledge before and after an awareness campaign directed at lower-income subjects, and showed that the campaign improved the knowledge of suspicious symptoms. Notably, the campaign also increased screening requests to GPs. Another key finding was a greater awareness of CRC among the elderly, suggesting that differential campaigns are not required for different age classes. Large-scale campaigns like the Blue March, organised in France and Monaco Principality, should therefore be encouraged[35].

The absence of organised screening increases the social burden of cancer, delaying the adoption of treatments of proven efficacy that induce as little disability as possible. The situation is especially clear in economically and technologically advanced countries like Switzerland, where a significantly lower demand for testing has been found among low-income than high-income citizens. Conceivably, the problem is even more severe in countries where early detection testing is not provided by the national health care system and is predominantly out of pocket, compounding the vulnerability of the poorer groups in the population. State funding is a problem in several countries, like Turkey, where dedicated cancer screening centres are found in each province and are theoretically easier to reach. In fact, however, the fact that most people have to pay for their tests, since only the poorest and oldest benefit from state help, prevents access by large swathes of the population. It should be stressed that the activation of organised screening programmes is not a net cost to emerging countries[56], but is actually cost-effective[57,58], also considering that early tumour detection considerably reduces subsequent social and health costs[43].

The situation of these countries contrasts with the one characterising small states like Monaco Principality and San Marino, where the tiny population enables a more effective organisation of health care, including prevention. Monaco Principality deserves high praise for extending screening benefits to foreign workers[35].

Screening professionals and activity

Finally, gastroenterologists play an important role in CRC screening. They should not view early detection testing as a practice undermining their expertise, but as a resource that adds to their specialist training[59]. The same applies to clinical pathologists: in some countries, like Russia, their training is predominantly oriented to necroscopy[40]: diagnosing living patients is therefore a challenge for all health care figures. The epidemiologist also has a critical role in local screening co-ordination, patient flow organisation, data management, and data transmission to cancer registries, to improve cancer knowledge and treatment in the various districts. GPs are an essential link in the prevention chain, since they have the task of raising the awareness of those who are at risk and of stimulating those who would benefit from screening to undergo testing, without alarming them. In Turkey, for instance, GPs have the task of directing patients to screening[44]. Patient associations and health care professionals should also work to increase the awareness of institutions and law-makers towards screening and its benefits.

In conclusion, cancer screening should be viewed as a key health care tool, also because investing in screening protects the weakest in the population, decreases the social burden of cancer, and reduces all types of health care costs, including those for radical surgery, long-term hospitalisation, and chemotherapy. Finally, screening for those at risk should be stimulated, offered without charge, and adequately publicised irrespective of the health care system organisation in place.

COMMENTS

Background

Although colorectal cancer (CRC) is a tumour for which screening has proven efficacy and cost-effectiveness, in several European countries screening implementation is fraught with difficulties. CRC incidence is quite variable among European countries, and the lower rates found in eastern Europe are higher than the world mean.

Research frontiers

The Council of Europe has recommended the priority activation of CRC screening programmes. According to a 2008 European Commission report on the diffusion of CRC screening programmes in the EU, only 12 of the then 22

member states had population-based screening programmes; the others were recommended to provide to their citizens equal access to cancer prevention.

Innovations and breakthroughs

The present paper provides a systematic review of the screening programmes that are active in the non-EU 28 members of the Council of Europe, using data collected from institutional websites and from the literature. Besides reviewing the epidemiological data (incidence, 5-year prevalence, and mortality), it undertakes a critical examination of their quality and provides key information on colorectal cancer and the prevention strategies adopted in each country.

Applications

The absence of organised screening increases the social burden of cancer, delaying the adoption of treatments of proven efficacy that induce as little disability as possible. Conceivably, the problem is even more severe in countries where early detection testing is not provided by the national health care service and is predominantly out of pocket, compounding the vulnerability of the poorer groups in the population. Notably, the activation of organised screening programmes in emerging countries would actually be cost-effective, also considering that early tumour detection considerably reduces subsequent social and health costs.

Terminology

Fecal occult blood (FOB) refers to blood in the feces that is not visibly apparent. A fecal occult blood test (FOBT) checks for hidden (occult) blood in the stool (feces); immunochemical test (iFOBT) is based on human hemoglobin antibodies.

Peer-review

This review paper covers recent topics in CRC screening, and is concisely written. The information given is helpful to promote the further advance in the field.

REFERENCES

1 **Altobelli E**, Lattanzi A. Cervical carcinoma in the European Union: an update on disease burden, screening program state of activation, and coverage as of March 2014. *Int J Gynecol Cancer* 2015; **25**: 474-483 [PMID: 25695550 DOI: 10.1097/IGC.0000000000000374]

2 **Altobelli E**, Lattanzi A. Breast cancer in European Union: an update of screening programmes as of March 2014 (review). *Int J Oncol* 2014; **45**: 1785-1792 [PMID: 25174328 DOI: 10.3892/ijo.2014.2632]

3 **Altobelli E**, Lattanzi A, Paduano R, Varassi G, di Orio F. Colorectal cancer prevention in Europe: burden of disease and status of screening programs. *Prev Med* 2014; **62**: 132-141 [PMID: 24530610 DOI: 10.1016/j.ypmed.2014.02.010]

4 **Ferlay J**, Soerjomataram I, Dikshit R, Eser S, Mathers C, Rebelo M, Parkin DM, Forman D, Bray F. Cancer incidence and mortality worldwide: sources, methods and major patterns in GLOBOCAN 2012. *Int J Cancer* 2015; **136**: E359-E386 [PMID: 25220842 DOI: 10.1002/ijc.29210]

5 European Council, 2003. L 327/34 council recommendation of 2 December 2003 on cancer screening (2003/878/EC). Off J Eur Union, 2003

6 European Commission, 2008. Report from the Commission to the Council, the European Parliament, the European Economic and Social Committee and the Committee of the Regions Implementation of the Council Recommendation of 2 December 2003 on Cancer Screening (2003/878/EC) Brussels, 22.12.2008 COM(2008) 882 Final

7 **Pawa N**, Arulampalam T, Norton JD. Screening for colorectal cancer: established and emerging modalities. *Nat Rev Gastroenterol Hepatol* 2011; **8**: 711-722 [PMID: 22045159 DOI: 10.1038/nrgastro.2011.205]

8 **Burt RW**. Colorectal cancer screening. *Curr Opin Gastroenterol* 2010; **26**: 466-470 [PMID: 20664346 DOI: 10.1097/MOG.0b013e32833d1733]

9 **Gupta AK**, Brenner DE, Turgeon DK. Early detection of colon cancer: new tests on the horizon. *Mol Diagn Ther* 2008; **12**: 77-85 [PMID: 18422372]

10 **Von Karsa L**, Segnan N, Patnick J. European Guidelines for Quality Assurance in Colorectal Cancer Screening. Publications Office of the European Union, 2010 [DOI: 10.2772/15379]

11 European Commission, 2010. P7_TA(2010) 0152 - Commission Communication on Action Against Cancer: European Partnership. European Parliament Resolution of 6 May 2010 on the Commission Communication on Action Against Cancer: European Partnership, 2010

12 **Benson VS**, Atkin WS, Green J, Nadel MR, Patnick J, Smith RA, Villain P. Toward standardizing and reporting colorectal cancer screening indicators on an international level: The International Colorectal Cancer Screening Network. *Int J Cancer* 2012; **130**: 2961-2973 [PMID: 21792895 DOI: 10.1002/ijc.26310]

13 **Brenner H**, Hoffmeister M, Haug U. Should colorectal cancer screening start at the same age in European countries? Contributions from descriptive epidemiology. *Br J Cancer* 2008; **99**: 532-535 [PMID: 18628760 DOI: 10.1038/sj.bjc.6604488]

14 **Center MM**, Jemal A, Smith RA, Ward E. Worldwide variations in colorectal cancer. *CA Cancer J Clin* 2009; **59**: 366-378 [PMID: 19897840 DOI: 10.3322/caac.20038]

15 **Swan H**, Siddiqui AA, Myers RE. International colorectal cancer screening programs: population contact strategies, testing methods and screening rates. *Pract Gastroenterol* 2012; **36**: 20-29

16 **Zavoral M**, Suchanek S, Zavada F, Dusek L, Muzik J, Seifert B, Fric P. Colorectal cancer screening in Europe. *World J Gastroenterol* 2009; **15**: 5907-5915 [PMID: 20014454 DOI: 10.3748/wjg.15.5907]

17 **Mathers CD**, Fat DM, Inoue M, Rao C, Lopez AD. Counting the dead and what they died from: an assessment of the global status of cause of death data. *Bull World Health Organ* 2005; **83**: 171-177 [PMID: 15798840]

18 Available from: URL: http://healthcaredelivery.cancer.gov/icsn/colorectal/screening.html#iceland

19 **Guðlaugsdóttir S**. Implementing colorectal cancer screening program in Iceland. In: WEO Barcelona October 2015 proceedings of WEO Colorectal Cancer Screening Meeting. Barcelona, Spain. Available from: URL: https://www.researchgate.net/publication/283569319_

20 Cancer registry of Norway. Available from: URL: http://www.kreftregisteret.no/en/Cancer-prevention/Screening-for-colorectal-cancer/

21 **Hoff G**, Grotmol T, Skovlund E, Bretthauer M. Risk of colorectal cancer seven years after flexible sigmoidoscopy screening: randomised controlled trial. *BMJ* 2009; **338**: b1846 [PMID: 19483252 DOI: 10.1136/bmj.b1846]

22 **Giordano L**, Bisanti L, Salamina G, Ancelle Park R, Sancho-Garnier H, Espinas J, Berling C, Rennert G, Castagno R, Dotti M, Jaramillo L, Segnan N. The EUROMED CANCER network: state-of-art of cancer screening programmes in non-EU Mediterranean countries. *Eur J Public Health* 2016; **26**: 83-89 [PMID: 26072520 DOI: 10.1093/eurpub/ckv107]

23 **Cekodhima G**, Alimehmeti I, Cekodhima A, Belishta O. Gastrointestinal polypoid lesions: the Albanian reality. *RRJMHS* 2015; **4**: 33-37

24 WHO cancer country profile. Available from: URL: http://www.who.int/cancer/country-profiles/alb_en.pdf?ua=1

25 **Buturovic S**. Colonoscopy as a method of choice in the diagnosis of colorectal cancer. *Acta Inform Med* 2014; **22**: 164-166 [PMID: 25132707 DOI: 10.5455/aim.2014.22.164-166]

26 WHO cancer country profile. Available from: URL: http://www.who.int/cancer/country-profiles/bih_en.pdf?ua=1

27 WHO cancer country profile. Available from: URL: http://www.who.int/cancer/country-profiles/mkd_en.pdf?ua=1

28 **Panic N**, Rösch T, Smolovic B, Radunovic M, Bulajic M, Pavlovic-Markovic A, Krivokapic Z, Djuranovic S, Ille T, Bulajic M. Colorectal cancer screening in a low-incidence area: general invitation versus family risk targeting: a comparative study from Montenegro. *Eur J Gastroenterol Hepatol* 2015; **27**: 1222-1225 [PMID: 26067224 DOI: 10.1097/MEG.0000000000000415]

29 WHO cancer country profile. Available from: URL: http://www.who.int/cancer/country-profiles/mne_en.pdf?ua=1
30 **Official Gazette of RS.** No. 107/05, 72/09: Article 16, paragraph 2 of the Law on Health Care Law, 88/10, 99.10, 57/11, 119/12 and 45/13) and Article 42, paragraph 1 of the Law on Government ("Official Gazette of RS", No. 55/05, 71/05 - correction, 101/07, 65/08, 16/11, 68/12 - US and 72/12). Available from: URL: http://www.skriningsrbija.rs/files/File/English/REGULATION_ON_THE_NATIONAL_PROGRAM_FOR_EARLY_DETECTION_OF_COLORECTAL_CANCER.pdf
31 Cancer registry of Serbia. Available from: URL: http://www.skriningsrbija.rs/eng/colorectal-cancer-screening/statistics/
32 **Fedewa SA**, Cullati S, Bouchardy C, Welle I, Burton-Jeangros C, Manor O, Courvoisier DS, Guessous I. Colorectal Cancer Screening in Switzerland: Cross-Sectional Trends (2007-2012) in Socioeconomic Disparities. *PLoS One* 2015; **10**: e0131205 [PMID: 26147803 DOI: 10.1371/journal.pone.0131205]
33 **Marbet UA**, Bauerfeind P, Brunner J, Dorta G, Valloton JJ, Delcò F. Colonoscopy is the preferred colorectal cancer screening method in a population-based program. *Endoscopy* 2008; **40**: 650-655 [PMID: 18609465 DOI: 10.1055/s-2008-1077350]
34 **Auer R**, Selby K, Bulliard JL, Nichita C, Dorta G, Ducros C, Cornuz J. [Shared decision making in the colorectal cancer screening program in the canton of Vaud]. *Rev Med Suisse* 2015; **11**: 2209-2215 [PMID: 26742350]
35 The Monaco Health Screening Centre. Available from: URL: http://en.gouv.mc/Policy-Practice/Social-Affairs-and-Health/An-exemplary-Public-Health-system/Monaco-Health-Screening-Centre
36 Istituto per la sicurezza sociale di San Marino. Available from: URL: http://www.iss.sm/on-line/home/menudestra/screening-prevenzione.html
37 Screening del tumore al colon-retto: San Marino è meglio dell' Italia. Il giornale di San Marino 10/06/2014. Available from: URL: http://giornalesm.com/screening-del-tumore-al-colon-retto-san-marino-e-meglio-dellitalia/
38 WHO cancer country profile. Available from: URL: http://www.who.int/cancer/country-profiles/and_en.pdf?ua=1
39 WHO cancer country profile. Available from: URL: http://www.who.int/cancer/country-profiles/mda_en.pdf?ua=1
40 **Goss PE**, Strasser-Weippl K, Lee-Bychkovsky BL, Fan L, Li J, Chavarri-Guerra Y, Liedke PE, Pramesh CS, Badovinac-Crnjevic T, Sheikine Y, Chen Z, Qiao YL, Shao Z, Wu YL, Fan D, Chow LW, Wang J, Zhang Q, Yu S, Shen G, He J, Purushotham A, Sullivan R, Badwe R, Banavali SD, Nair R, Kumar L, Parikh P, Subramanian S, Chaturvedi P, Iyer S, Shastri SS, Digumarti R, Soto-Perez-de-Celis E, Adilbay D, Semiglazov V, Orlov S, Kaidarova D, Tsimafeyeu I, Tatishchev S, Danishevskiy KD, Hurlbert M, Vail C, St Louis J, Chan A. Challenges to effective cancer control in China, India, and Russia. *Lancet Oncol* 2014; **15**: 489-538 [PMID: 24731404 DOI: 10.1016/S1470-2045(14)70029-4]
41 WHO cancer country profile. Available from: URL: http://www.who.int/cancer/country-profiles/rus_en.pdf?ua=1
42 Available from: URL: http://globenewswire.com/news-release/2015/11/09/785009/0/en/Colorectal-screening-project-to-start-in-Russia-with-Biohit-Oyj-s-ColonView-test.html
43 **Starostina MA**, Afanasjeva ZA, Hasanov RSh, Borisov DA, Nagumanov EV, Gordeev MG. Screening for colorectal cancer in Tatarstan Republic. *Onco Surgery* 2014; **6**: 40-45
44 **Tatar M**, Tatar F. Colorectal cancer in Turkey: current situation and challenges for the future. *Eur J Health Econ* 2010; **10** Suppl 1: S99-105 [PMID: 20012668 DOI: 10.1007/s10198-009-0197-7]
45 WHO cancer country profile. Available from: URL: http://www.who.int/cancer/country-profiles/tur_en.pdf?ua=1
46 **Forman D**, Bray F, Brewster DH, Gombe Mbalawa C, Kohler B, Piñeros M, Steliarova-Foucher E. Swaminathan R, Ferlay J, editors. Cancer Incidence in Five Continents Vol. X IARC Scientific Publication No. 164
47 WHO cancer country profile. Available from: URL: http://www.who.int/cancer/country-profiles/ukr_en.pdf?ua=1
48 WHO cancer country profile. Available from: URL: http://www.who.int/cancer/country-profiles/arm_en.pdf?ua=1
49 WHO cancer country profile. Available from: URL: http://www.who.int/cancer/country-profiles/aze_en.pdf?ua=1
50 WHO cancer country profile. Available from: URL: http://www.who.int/cancer/country-profiles/geo_en.pdf?ua=1
51 **Davies P**, Jugell L. Capacity assessment and recommendations of cancer screening in Geogia, Tblisi. Available from: URL: http://www.ecca.info/fileadmin/user_upload/Reports/UNFPA_Cancer_Screening_in_Georgia.pdf
52 Charter of fundamental rights of the European union. Official Journal of the European Communities 2000/C 364/01. Available from: URL: http://www.europarl.europa.eu/charter/pdf/text_en.pdf
53 Convention for the protection of Human Rights and Dignity of the Human Being with regard to the Application of Biology and Medicine: Convention on Human Rights and Biomedicine. ETS No. 164. Available from: URL: http://www.coe.int/it/web/conventions/full-list/-/conventions/treaty/164
54 **Schreuders EH**, Ruco A, Rabeneck L, Schoen RE, Sung JJ, Young GP, Kuipers EJ. Colorectal cancer screening: a global overview of existing programmes. *Gut* 2015; **64**: 1637-1649 [PMID: 26041752 DOI: 10.1136/gutjnl-2014-309086]
55 **Moffat J**, Bentley A, Ironmonger L, Boughey A, Radford G, Duffy S. The impact of national cancer awareness campaigns for bowel and lung cancer symptoms on sociodemographic inequalities in immediate key symptom awareness and GP attendances. *Br J Cancer* 2015; **112** Suppl 1: S14-S21 [PMID: 25734383 DOI: 10.1038/bjc.2015.31]
56 **Ginsberg GM**, Lauer JA, Zelle S, Baeten S, Baltussen R. Cost effectiveness of strategies to combat breast, cervical, and colorectal cancer in sub-Saharan Africa and South East Asia: mathematical modelling study. *BMJ* 2012; **344**: e614 [PMID: 22389347 DOI: 10.1136/bmj.e614]
57 **Lansdorp-Vogelaar I**, Knudsen AB, Brenner H. Cost-effectiveness of colorectal cancer screening. *Epidemiol Rev* 2011; **33**: 88-100 [PMID: 21633092 DOI: 10.1093/epirev/mxr004]
58 **Pignone M**, Saha S, Hoerger T, Mandelblatt J. Cost-effectiveness analyses of colorectal cancer screening: a systematic review for the U.S. Preventive Services Task Force. *Ann Intern Med* 2002; **137**: 96-104 [PMID: 12118964 DOI: 10.7326/0003-4819-137-2-200207160-00007]
59 **Stanford SB**, Lee S, Masaquel C, Lee RH. Achieving competence in colonoscopy: Milestones and the need for a new endoscopic curriculum in gastroenterology training. *World J Gastrointest Endosc* 2015; **7**: 1279-1286 [PMID: 26675559 DOI: 10.4253/wjge.v7.i18.1279]

P- Reviewer: Nishiyama M **S- Editor**: Yu J **L- Editor**: A
E- Editor: Ma S

World Journal of Gastroenterology

Submit a Manuscript: http://www.wjgnet.com/esps/
Help Desk: http://www.wjgnet.com/esps/helpdesk.aspx
DOI: 10.3748/wjg.v22.i20.4958

World J Gastroenterol 2016 May 28; 22(20): 4958-4962
ISSN 1007-9327 (print) ISSN 2219-2840 (online)

CASE REPORT

Idiopathic abdominal cocoon syndrome with unilateral abdominal cryptorchidism and greater omentum hypoplasia in a young case of small bowel obstruction

Xiang Fei, Hai-Rui Yang, Peng-Fei Yu, Hai-Bo Sheng, Guo-Li Gu

Xiang Fei, Hai-Rui Yang, Peng-Fei Yu, Guo-Li Gu, Department of General Surgery, the Air Force General Hospital, Chinese PLA, Beijing 100142, China

Hai-Bo Sheng, Department of Urinary Surgery, the Air Force General Hospital, Chinese PLA, Beijing 100142, China

Author contributions: Gu GL designed the research; Gu GL, Yang HR, Sheng HB and Fei X performed the research; Fei X and Yu PF collected and analyzed the data; Gu GL and Fei X wrote the paper; and Gu GL revised the paper.

Supported by Major Projects of Chinese PLA "13th Five-Year Plan" Logistics Research Subject, No. AKJ15J003.

Institutional review board statement: This work has been carried out in accordance with the Declaration of Helsinki (2000) of the World Medical Association. This study was approved ethically by Ethics Committee of the Air Force General Hospital, PLA.

Informed consent statement: The patient involved in this study gave his written informed consent authorizing use and disclosure of his protected health information.

Conflict-of-interest statement: All the authors have no conflicts of interests to declare.

Correspondence to: Dr. Guo-Li Gu, Associate Professor, Deputy Director, Department of General Surgery, the Air Force General Hospital, Chinese PLA, No.30, Fucheng Road, Haidian District, Beijing 100142, China. kzggl@163.com
Telephone: +86-10-66928303
Fax: +86-10-66928303

Received: February 14, 2016
Peer-review started: February 14, 2016
First decision: March 7, 2016
Revised: March 15, 2016
Accepted: April 7, 2016
Article in press: April 7, 2016
Published online: May 28, 2016

Abstract

Abdominal cocoon syndrome (ACS) is a rare cause of intestinal obstruction due to total or partial encapsulation of the small intestine by a fibrocollagenous membrane. Idiopathic ACS with abdominal cryptorchidism and greater omentum hypoplasia is even rarer clinically. We successfully treated a 26-year-old male case of small bowel obstruction with acute peritonitis. He was finally diagnosed with idiopathic ACS with unilateral abdominal cryptorchidism and greater omentum hypoplasia during exploratory laparotomy. He then underwent enterolysis, cryptorchidectomy, and appendectomy. He recovered gradually from the operations and early postoperative inflammatory ileus. There has been no recurrence of intestinal obstruction since the operation, and he is still in follow-up. We analyzed his clinical data and retrospectively reviewed the literature, and our findings may be helpful for the clinical diagnosis and treatment on ACS.

Key words: Abdominal cocoon syndrome; Abdominal cryptorchidism; Intestinal obstruction; Diagnosis; Treatment

Core tip: Abdominal cocoon syndrome (ACS) is a rare abdominal disease where a portion or all of the abdominal organs are wrapped in a dense membrane-like fibrous tissue. Intestinal obstruction is the main

clinical manifestation of ACS. Because of its rarity and lack of characteristic symptoms, ACS is fairly difficult to diagnose pre-operatively. Surgeons should be aware of this disease when confronted with a case of intestinal obstruction whose abdominal radiography shows intestinal loop aggregation cluster. Accompanying cryptorchidism is possible, and a careful physical examination and operative exploration for the undescended testicle should be performed. Postoperative care and dietary guidance are very important to the rehabilitation of ACS patients. Postoperative re-adhesion and early postoperative inflammatory ileus easily occur after extensive enterolysis.

Fei X, Yang HR, Yu PF, Sheng HB, Gu GL. Idiopathic abdominal cocoon syndrome with unilateral abdominal cryptorchidism and greater omentum hypoplasia in a young case of small bowel obstruction. *World J Gastroenterol* 2016; 22(20): 4958-4962 Available from: URL: http://www.wjgnet.com/1007-9327/full/v22/i20/4958.htm DOI: http://dx.doi.org/10.3748/wjg.v22.i20.4958

INTRODUCTION

Abdominal cocoon syndrome (ACS) is a rare abdominal disease where a portion or all of the abdominal organs are wrapped in dense membrane-like fibrous tissue. It was first reported in 1978 and is also known as idiopathic sclerosing peritonitis, primary sclerosing peritonitis, and sclerosing encapsulating peritonitis[1,2]. The etiology and epidemiological characteristics of idiopathic ACS remain unknown. Intestinal obstruction is the main clinical manifestation of ACS. Usually, ACS is chanced upon during abdominal surgery. Because of its rarity and lack of characteristic symptoms, ACS is fairly difficult to diagnose prior to the operation.

We successfully treated a young male with intestinal obstruction secondary to idiopathic ACS with unilateral abdominal cryptorchidism and greater omentum hypoplasia.

CASE REPORT

A 26-year-old male patient was admitted to the emergency department with complaints of abdominal pain, nausea, and vomiting for about 10 h on November 25, 2014. Although this patient had a history of overeating before hospitalization, he did not have a history of chronic systemic disease or abdominal trauma. Upon physical examination, there was asymmetrical distension and general tenderness with heightened intestinal sounds, especially prominent in the right middle abdomen. The right testicle was not palpable in the scrotum. The laboratory examinations showed normal peripheral leukocyte counts (7.98 × 10^9/L), but the ratio of neutrophils was slightly elevated to 75.1%. Abdominal radiography detected the dilated intestine with air-fluid levels in the right middle abdomen (Figure 1). Abdominal computed tomography detected dilated small intestinal loops containing air-fluid levels clustered in the middle abdomen that were surrounded by a thick and sac-like membrane (Figure 2). The widespread adhesions between the peritoneum and small intestine were found during exploratory laparotomy. With further exploration, a cocoon-like fibrous structure was identified in the middle abdomen that surrounded the majority of small intestine (Figure 3). The right undescended testicle had softened and adhered tightly to the fibrous membrane near the appendix. The greater omentum was hypoplastic. When the cocoon-like fibrous membrane was opened, the small intestinal segments were dilated due to obstruction, but they were otherwise normal in structure. The obstruction was caused by fibrous bands of irregular thickness inside the cocoon-like fibrous membrane. The operation was completed after total excision of the fibrous membrane and removal of the adhesions. The released small intestinal segments were rearranged and coated with sodium hyaluronate. At the same time, the right undescended testicle and appendix were resected. Postoperative pathologic examination showed that the testis with interstitial fibrosis had no spermatogonium, primary spermatocyte, secondary spermatocyte, spermatid, or spermatozoon present in the seminiferous tubules (Figure 4).

Figure 1 Abdominal radiography. The dilated intestine with air-fluid levels was prominent in the right middle abdomen.

Patient recovery during postoperative week one went well, but he suffered early postoperative inflammatory ileus (EPII) performance with intermittent abdominal pain and vomiting on postoperative day 12. After a series of symptomatic treatments for about 5 d, including fasting, gastrointestinal decompression, inhibiting secretion of digestive juices by octreotide, nutritional support, and maintaining balance of electrolytes; he recovered gradually and was discharged on December

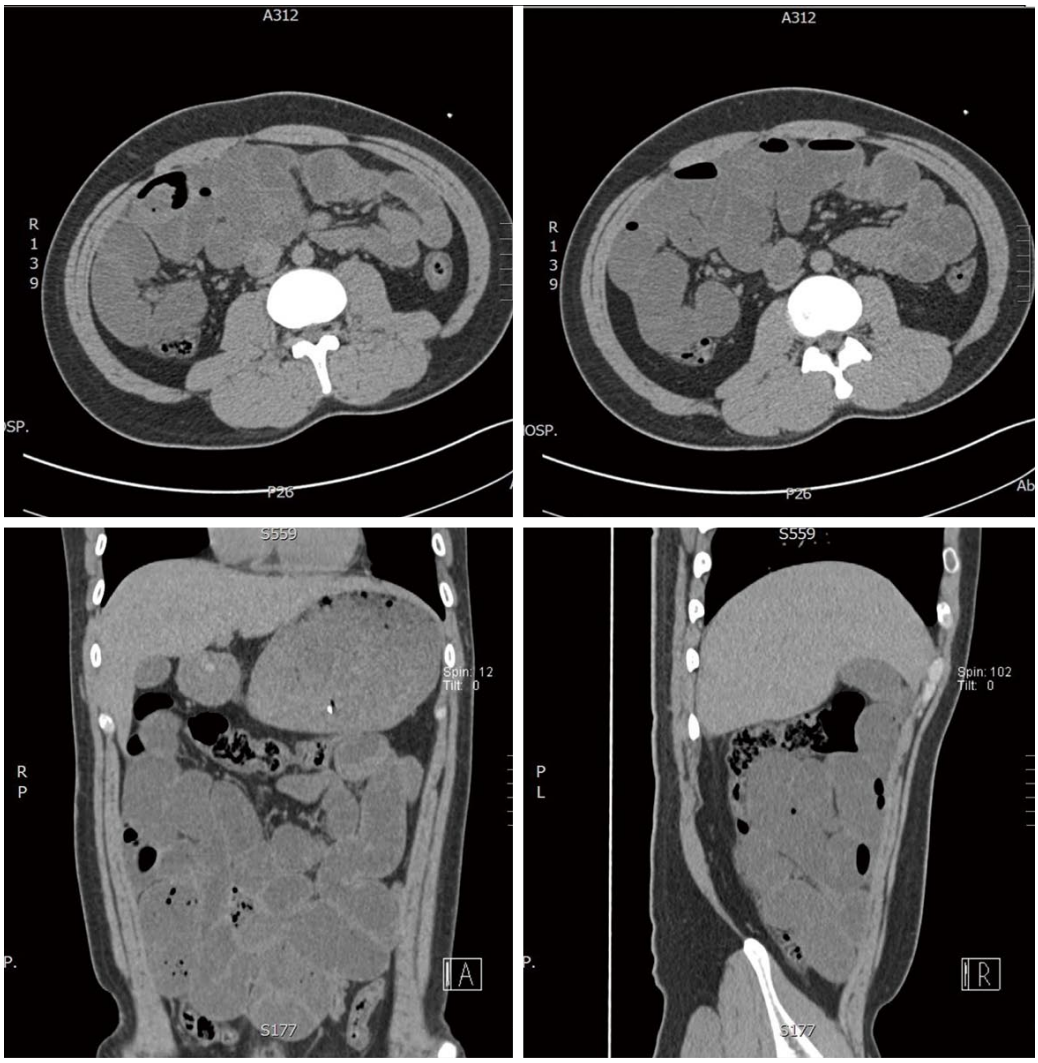

Figure 2 Abdominal computed tomography scans. Dilated small intestinal loops containing air-fluid levels were clustered in the right middle abdomen and surrounded by a sac-like membrane.

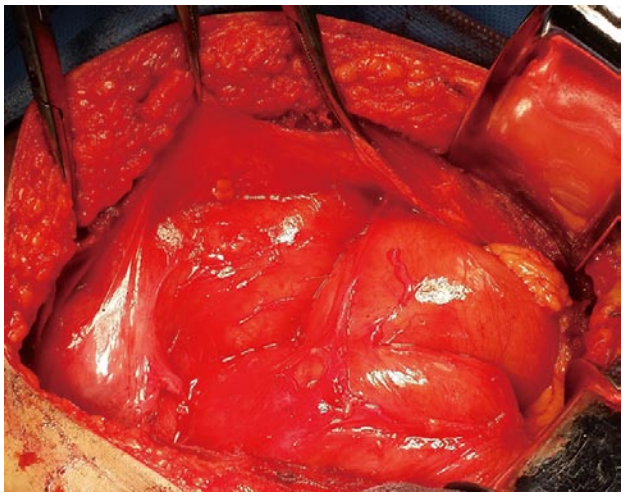

Figure 3 Intraoperative findings. Dilated small intestine was surrounded by a capsular structure in the right middle abdomen, which had a regular surface composed of natural fibrous membranes.

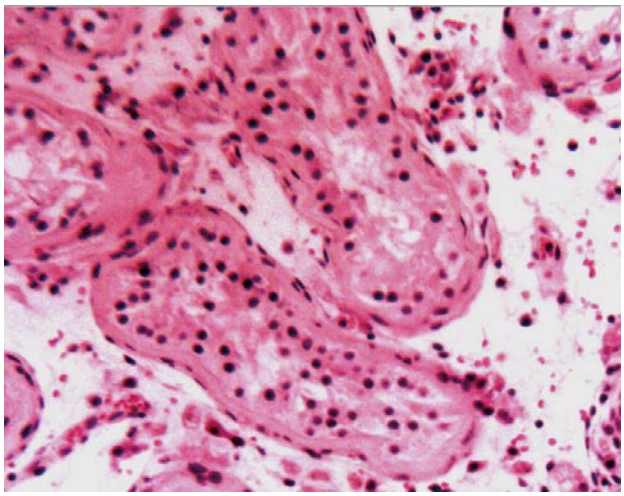

Figure 4 Pathologic examination (HE × 200). The testis with interstitial fibrosis had no spermatogonium, primary spermatocyte, secondary spermatocyte, spermatid, or spermatozoon in the seminiferous tubules.

20 2014. The intestinal obstruction has not recurred, and he is still undergoing follow-up.

DISCUSSION

According to whether its etiology is explicit or not, ACS can be divided into two subtypes: primary (idiopathic) and secondary[3]. Usually, secondary ACS results in chronic asymptomatic peritonitis, such as endometriosis, retrograde menstruation, peritoneal dialysis, and abdominal tuberculosis[4]. Although idiopathic ACS is rare clinically, patients with idiopathic ACS are often accompanied by the absence of the greater omentum and cryptorchidism, suggesting that genetic factors may play a role in the etiology of idiopathic ACS. Our case developed intestinal obstruction and peritonitis without any other known risk factors; but the typical fibrous membrane surrounding the small intestine with greater omentum hypoplasia and undescended testicle confirmed that the diagnosis of idiopathic ACS is correct.

Although ACS is a rare cause of intestinal obstruction, we should vigilantly remember this disease when faced with a case of intestinal obstruction whose abdominal radiography shows intestinal loop aggregation into a cluster[5,6]. When ACS is suspected, accompanying cryptorchidism should be suspected, and a careful physical examination and operative exploration for the undescended testicle should be performed. How to deal with the undescended testicle remains controversial[7,8]. Because surgical options of the undescended testicle interfere with patient fertility and have a high risk of seminoma, it is necessary to fully communicate with the patient about this matter before the operation is performed. As for the appendix, we think appendectomy may be a good option for patients with ACS, because the occurrence of postoperative abdominal adhesions is inevitable, and it will be very difficult to perform appendectomy in these postoperative patients if appendicitis or other appendical diseases occurs[9]. The surgeon should pay attention to reserve the vital intestine and possibly the ileocecal valve and to avoid resecting the "cocoon", as tumor results in short bowel syndrome.

As to the patients with ACS, postoperative care and dietary guidance are very important to their rehabilitation. Postoperative re-adhesion and EPII occur easily after the extensive dissection of the enterolysis[10]. Therefore, we should encourage patients to get out of bed early in order to promote intestinal peristalsis recovery and to avoid recurrence of intestinal obstruction. The patients' diet should be gradually restored since their gastrointestinal function recovery is manifested as exhaust and defecation. The whole process of diet restoring maybe take about 10 d to 2 wk, beginning from liquid diet and progressing to semi-liquid diet, soft diet, and finally to general diet. Our case's discharge time was delayed for about 7 d by EPII because of improper self-eating.

COMMENTS

Case characteristics

Patient was admitted to the emergency department with complaints of abdominal pain, nausea, and vomiting for about 10 h.

Clinical diagnosis

Upon physical examination, there was asymmetrical distension and general tenderness with heightened intestinal sounds, which were especially prominent in the right middle abdomen.

Differential diagnosis

Abdominal computed tomography detected dilated small intestinal loops containing air-fluid levels clustered in the middle abdomen that were surrounded by a thick and sac-like membrane.

Laboratory diagnosis

During exploratory surgery, a cocoon-like fibrous structure surrounding the majority of the small intestine was identified in the middle abdomen.

Imaging diagnosis

Abdominal computed tomography detected dilated small intestinal loops containing air-fluid levels clustered in the middle abdomen that were surrounded by a thick and sac-like membrane.

Pathological diagnosis

Pathologic examination showed that the testis with interstitial fibrosis had no spermatogonium, primary spermatocyte, secondary spermatocyte, spermatid, or spermatozoon in the seminiferous tubules.

Treatment

The patient underwent a series of operations, firstly exploratory laparotomy, and then enterolysis, cryptorchidectomy, and appendectomy.

Term explanation

Abdominal cocoon syndrome (ACS) is a rare cause of intestinal obstruction due to total or partial encapsulation of the small intestine by a fibrocollagenous membrane.

Experiences and lessons

When encountering a suspected case of ACS, the surgeon must be aware of the possibility of accompanying cryptorchidism. Then, a careful physical examination and operative exploration for the undescended testicle should be performed. Postoperative care and dietary guidance are very important to their rehabilitation.

Peer-review

This manuscript is a very interesting case report of a rare disease, ACS. Here, the patient presented with a small bowel obstruction with acute peritonitis. ACS is a rare disease where a portion of or all of the abdominal organs are wrapped in dense membrane-like fibrous tissue.

REFERENCES

1 **Uzunoglu Y**, Altintoprak F, Yalkin O, Gunduz Y, Cakmak G, Ozkan OV, Celebi F. Rare etiology of mechanical intestinal obstruction: Abdominal cocoon syndrome. *World J Clin Cases* 2014; **2**: 728-731 [PMID: 25405199 DOI: 10.12998/wjcc.v2.i11.728]

2 **Akbulut S**. Accurate definition and management of idiopathic sclerosing encapsulating peritonitis. *World J Gastroenterol* 2015; **21**: 675-687 [PMID: 25593498 DOI: 10.3748/wjg.v21.i2.675]

3 **Sohail MZ**, Hasan S, Dala-Ali B, Ali S, Hashmi MA. Multiple abdominal cocoons: an unusual presentation of intestinal obstruction and a diagnostic dilemma. *Case Rep Surg* 2015; **2015**: 282368 [PMID: 25893128 DOI: 10.1155/2015/282368]

4 **Kaur S**, Doley RP, Chabbhra M, Kapoor R, Wig J. Post trauma

abdominal cocoon. *Int J Surg Case Rep* 2015; **7C**: 64-65 [PMID: 25590647 DOI: 10.1016/j.ijscr.2014.10.081]

5 **Karan A**, Özdemir M, Bostancı MT, Bostancı EB. Idiopathic abdominal cocoon syndrome: Preoperative diagnosis with computed tomography. *Turk J Gastroenterol* 2015; **26**: 193-194 [PMID: 25835123 DOI: 10.5152/tjg.2015.7312]

6 **Frost JH**, Price EE. Abdominal cocoon: idiopathic sclerosing encapsulating peritonitis. *BMJ Case Rep* 2015; **2015**: pii: bcr2014207524 [PMID: 25612756 DOI: 10.1136/bcr-2014-207524]

7 **Solmaz A**, Tokoçin M, Arıcı S, Yiğitbaş H, Yavuz E, Gülçiçek OB, Erçetin C, Çelebi F. Abdominal cocoon syndrome is a rare cause of mechanical intestinal obstructions: a report of two cases. *Am J Case Rep* 2015; **16**: 77-80 [PMID: 25671606 DOI: 10.12659/AJCR.892658]

8 **Awe JA**. Abdominal cocoon syndrome (idiopathic sclerosing encapsulating peritonitis): how easy is its diagnosis preoperatively? A case report. *Case Rep Surg* 2013; **2013**: 604061 [PMID: 23738183 DOI: 10.1155/2013/604061]

9 **Acar T**, Kokulu İ, Acar N, Tavusbay C, Hacıyanlı M. Idiopathic encapsulating sclerosing peritonitis. *Ulus Cerrahi Derg* 2015; **31**: 241-243 [PMID: 26668535 DOI: 10.5152/UCD.2015.2786]

10 **Jayant M**, Kaushik R. Abdominal cocoon in a young man. *World J Emerg Med* 2014; **5**: 234-236 [PMID: 25225591 DOI: 10.5847/wjem.j.1920-8642.2014.03.014]

P- Reviewer: Peters JH, Yamada A **S- Editor**: Qi Y
L- Editor: Filipodia **E- Editor**: Zhang DN

Published by **Baishideng Publishing Group Inc**
8226 Regency Drive, Pleasanton, CA 94588, USA
Telephone: +1-925-223-8242
Fax: +1-925-223-8243
E-mail: bpgoffice@wjgnet.com
Help Desk: http://www.wjgnet.com/esps/helpdesk.aspx
http://www.wjgnet.com

ISSN 1007-9327